# 1. Introduction

## 1.1. The immune system

In the late 18th century the English physician Edward Jenner showed that inoculation of healthy individuals with cowpox could protect them against the fatal infectious disease of smallpox. Since Jenner, who phrased the term, the inoculation of healthy individuals with attenuated strains of disease-causing agents (or components of those) to provide protection from disease is called vaccination. Therewith, he was the inventor of the first vaccine and is generally regarded as the father of the scientific discipline immunology (Murphy, 2012). To understand the mode of action of smallpox vaccine and hence also the basic of the therapeutic approach underlying the presented work the immune system has to be introduced.

Our immune system protects us against infectious diseases caused by viruses, bacteria, pathogenic fungi and parasites. Moreover, there is convincing evidence that the immune system substantially contributes to clear arising transformed and malignant cells from the body and hence providing protection from non-infectious disease. The immune system is basically composed of two arms of defense: innate and adoptive immunity. They are communicating and interacting with each other, but show distinct response patterns. Innate immunity displays an orchestra of first line defense mechanisms. It shows low specificity and is immediately available to combat a broad range of invading pathogens. Innate cellular immune responses are carried out by macrophages, dendritic cells (DCs), mast cells, granulocytes and natural killer cells. The protective effect of vaccines, however, is mainly attributed to adaptive immunity. Based on its ability to specifically recognize distinct pathogens and to form an immunological memory it can mediate life-long protection against the respective pathogen. B and T lymphocytes are the major effector cells of adaptive immunity. Through a highly specialized repertoire of receptors (B- and T cell receptors), displaying an enormous plasticity, they are able to distinguish between foreign (non-self) and self-antigens. Virtually, any substance being recognized and responded to by the immune system is referred to as an antigen. Upon recognition of their specific antigen naïve B and T lymphocytes with a matching receptor undergo clonal expansion and massive proliferation. Through differentiation into antibody secreting plasma-cells B cells mediate humoral immunity. T lymphocytes develop in different types of effector cells and facilitate cellular adoptive immunity. Although, adoptive immune responses are delayed due to the aforementioned recognition and expansion process compared to innate immune responses, it possesses the unique trait to from immunological memory. Therewith, it can respond more efficient upon re-infection with the same pathogen and provide its host with life-long protection (Murphy, 2012).

As immunology has evolved to a complex field since Jenner's days only aspects which are relevant for the presented work can be highlighted in more detail.

### 1.1.1. The processing and presentation of antigens are crucial requirements for the recognition of pathogens and tumors

#### 1.1.1.1. MHC molecules – versatile tools for antigen presentation

Major histocompatibility complex (MHC) transgenic mice serve as an experimental model system in this work. Therefore, it is important to understand the structure and genetic organization of MHC molecules and genes. Additionally, the molecular structure and amino acid sequence of MHC molecules is providing information which peptide epitopes are likely to be presented. This in turn is important to predict possible epitopes which might be processed from the antigens we chose as targets in our experimental approach.

The major histocompatibility complex is large gene cluster which is located on chromosome 6 in humans and chromosome 17 in mice. It contains more than 200 genes coding for MHC molecules and components of the antigen-presenting machinery. The human MHC genes are called human leukocyte antigen genes (short HLA genes) whereas the murine homologues are referred to as H-2 genes. MHC molecules form complexes with peptides (derived from e.g. antigens) inside the cell and then are transported to the cell surface for presentation, where they can be recognized by T cells. There are two classes of classical MHC molecules with distinct peptide presentation patterns.

MHC class I molecules are basically presenting peptides which were processed in the cytosol. They consist of two protein chains, a heavy α-chain and a smaller chain, called the $\beta_2$-microglobluin, which are non-covalently associated. It should be noted here, that the genes encoding for the $\beta_2$-microglobluin and the invariant chain are located outside the MHC locus (in humans chromosomes 15 and 5, respectively and in mice chromosome 2 and 18). The α-chain forms three distinct domains. The $\alpha_3$ domain spans the plasma membrane, whereas the $\alpha_1$ and the $\alpha_2$ domains form the peptide binding cleft (see figure 1.1). A presented peptide is bound to the cleft in an elongated conformation and the binding is stabilized on both ends of the peptide via intermolecular interactions (H-bonds and ionic interactions) independent of the peptide's sequence. These interactions, however, limit the length of bound peptides to generally 8 to 10 amino acids. In addition, there are key-peptide interaction sites inside the MHC molecule's binding cleft which preferentially bind to certain amino acid residues inside the peptide. Therewith, they determine parts of the amino acid sequence of peptides which can be presented by the respective MHC class I molecule. Because these interactions also strengthen the binding of the peptide to the cleft, the peptide residues involved are referred to as anchor residues.

The MHC class II molecules deliver peptides which are originating from the vesicular system. Their three-dimensional structure appears similar to that of MHC class I molecules and they are also composed of a non-covalent bi-molecular complex with an α- and a β-chain. Differently from class I molecules, both chains have the same length and form to domains. The $\alpha_2$ and $\beta_2$ domains span the membrane and the $\alpha_1$ and $\beta_2$ domains constitute the peptide-binding cleft (see figure 1.1). Whereas the peptide-binding groove of the MHC class I molecules shows a closed conformation with the bound peptide

buried deep within the molecule, the cleft of MHC class II molecules is not closed at its ends. Conclusively, the ends of the peptides are not essential for the binding and the presented peptides can be much longer than for class I molecules, which is typically between 13 (at least) to 17 amino acids. The interaction with the MHC molecule is facilitated by a core of generally 9 amino acids inside the bound peptide. The amino acids 1, 4, 6, and 9 provide the anchor residues within this so called core sequence.

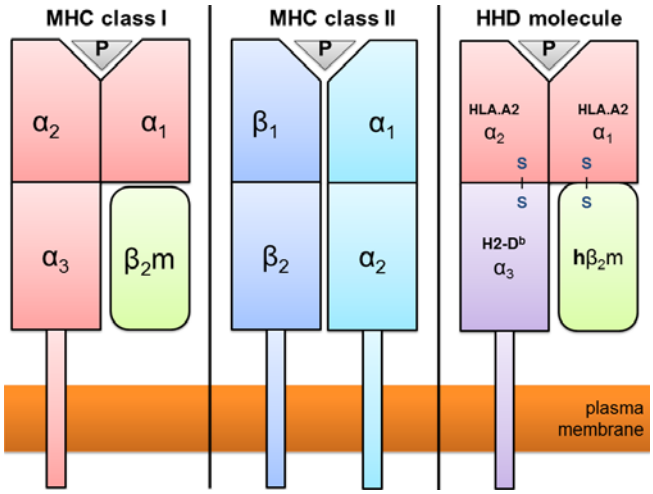


**Figure 1.1**: **Schematic structure of MHC class I and class II molecules and the chimeric MHC class I molecule HHD**. $\alpha_x$: α-chain-domain x, $\beta_x$: β-chain-domain x, $\beta_2$m: $\beta_2$-microglobulin, P: presented peptide, h: human, HLA.A2: HLA.A*0201, S-S: disulfide bonds

The expression pattern of MHC class I and II molecules throughout the organism is different. MHC class I molecules are expressed by almost all cells of the body except red blood cells. In contrast MHC class II molecules are normally expressed on cells of the immune system, which are dendritic cells, macrophages, B cells and T cells and thymic cortical epithelial cells. The latter play an important role in the establishment of central tolerance which will be discussed later. Importantly, T cells of mice do not express MHC class II molecules.

The peptide-binding clefts are highly polymorph which is attributed to the fact that the MHC locus is polygenic as well as polymorphic. In humans there are three genes for the MHC class I α-chain described, namely HLA-A, B- and C. For MHC class II there are also three α-chain and β-chain sets (HLA-DR, -DP, and -DQ) with an additional β-chain gene whose gene product is able to bind the HLA-DRα chain. For each of the MHC genes there are varying numbers of alleles found throughout the human population. Up to date there are 8000 different alleles for MHC class I and roughly 2000 MHC class II alleles described (Robinson et al., 2013).The fact that each individual is heterozygous for the whole MHC locus and that the MHC haplotypes are co-dominant additionally increases the diversity between individuals of the same species. The ‘MHC isoforms’ originating from the many varying MHC alleles differ from one another in up to 20 amino acids accounting for distinct peptide binding preferences of each respective isoform. The majority of the amino acid differences is particularly located in parts of the proteins that constitute the peptide binding clefts leading to the circumstance that each of the MHC class I or class II isoforms priorities a specific set of anchor residues termed sequence motifs.

The identification of the aforementioned sequence motifs was an achievement of the pioneering work of Rammensee and colleagues (Falk, Rotzschke, Stevanovic, Jung, & Rammensee, 1991). MHC molecule chains are loosely associated unless an adequate peptide is stably bound. MHC:peptide complexes are indeed so stable that they can be co-purified from cells. Denaturation of MHC molecules releases the bound peptides (called “elution of peptides” by Rammensee) whose sequence can be consequently identified via mass spectrometry. On the basis of the gathered sequence findings Rammensee and colleagues developed algorithms for the prediction of short peptides within a longer polypeptide or protein sequence that might be presented by a respective MHC molecule. We used the following online tools to predict possible MHC peptide binders inside our target antigens’ sequences:

- the database SYFPHEITI ((Rammensee, Bachmann, Emmerich, Bachor, & Stevanovic, 1999), Ver. 1.0, last update August 27$^{th}$ 2012, access via: http://www.syfpeithi.de/),
- the servers NetMHC (Net MHC 3.4. Server, http://www.cbs.dtu.dk/services/NetMHC/, (Lundegaard, Lund, & Nielsen, 2008)), and
- NetMHCIIpan (NetMHCIIpan 3.0 Server, http://www.cbs.dtu.dk/services/NetMHCIIpan/, (Karosiene et al., 2013)).

We decided to work with long peptide target antigen sequences (30 to 35 amino acids) which were longer than minimal epitopes for several reasons. One reason is the high polymorphism of the HLA alleles. Within long peptides small peptide ligands for several HLA alleles can be comprised. Therewith, we increase the number of HLA isoforms which can present the targeted antigen. Another aspect arguing for long peptides is the fact that we ensure proper antigen processing by professional antigen presenting cells, which will be elucidated in the following sections (see section 1.1.1.3).

#### 1.1.1.2. Murine MHC molecules and HLA transgenic mice – a model system to identify epitopes presented in a human MHC context

The MHC locus of mice is similarly organized as in humans. Mice have two MHC class I α-chain genes (H-2K and H-2B) and two pairs of MHC calls II α- and β-chains, called H-2A and H-2E. The polymorphism of inbred laboratory strains, however, is strongly restricted. In fact mice of the very same inbred strain all carry the exactly identical MHC haplotypes. This is why respective haplotypes are referred to with additional superscript letters behind the MHC molecule’s name (e.g. H-2A$^{b}$). C57BL/6 mice, the inbred strain used for our work and genetic background for HLA transgenic mice, have the MHC haplotype b (IMGT Information System®, (Lefranc et al., 2009), http://www.imgt.org/ IMGTrepertoireMHC/ Polymorphism/ haplotypes/ mouse/ MHC/ Mu_haplotypes.html).

The HLA transgenic mouse model employed in this work displays a chimeric MHC class I molecule, the HHD molecule. It is a chimera carrying the human $\alpha_1$ and $\alpha_2$ domain (and therewith epitope

binding specificity) from HLA.A*0201 (short HLA.A2) fused to the $\alpha_3$ domain of murine H-2D$^b$ for a better surface expression. This modified α-chain is covalently linked (via a 15 aa linker) to human $\beta_2$-microglobulin for a higher stability of the complex (see figure 1.1, (Pascolo et al., 1997)).

The HLA class I and II transgenic (tg) mice used in our work were generated by crossing of different H-2-deficient and HLA transgenic mouse strains.

The strain introducing the H-2 class I knockout (KO) and the chimeric HHD molecule, is called HHD tg H-2D$^{b-/-}$ $\beta_2$m$^{-/-}$ double KO. It was also generated in multi-step intercrossing process. The H-2D$^b$ gene was knocked out by homologous recombination (Pascolo et al., 1997) in embryonic stem (ES) cells. The resulting mice were crossed with $\beta_2$m$^{-/-}$ KO mice, which were generated through KO via homologous recombination in ES cells (Koller, Marrack, Kappler, & Smithies, 1990). The HHD molecule was introduced into C57BL/6 X SJL recipients via transgenesis. Resulting animals were crossed with H-2D$^{b-/-}$ $\beta_2$m$^{-/-}$ double KO mice. Introduction of the HHD transgene partially restored the CD8$^+$ T cell repertoire (5,5 % of T lymphocytes instead of 20-30 % in normal animals), which is lacking completely in H-2D$^{b-/-}$ $\beta_2$m$^{-/-}$ double KO mice. Moreover, these mice do not show any H-2 class I molecule surface expression and a diversified CD8$^+$ T cell receptor repertoire (Pascolo et al., 1997).

HLA-DR1-tg H-2 class-II-KO (H-2A β°) mice brought the murine MHC class II KO and HLA class II transgenes into the system. HLA-DR1 tg mice were generated via FVB/N oocytes injection of HLA-DR1*0101 and HLA-DRB1*0101 tg constructs (Altmann et al., 1995). Resulting animals were crossed with H-2A$_\beta^{o/o}$ mice. These mice in term were generated by disruption of the H-2A β-chain locus via homologous recombination on ES cell line D3, carrying a mutations in the H-2E α-chain promoter (Cosgrove et al., 1991). This mutation prevents expression of the H-2E α-chain and therewith the surface expression of the whole H-2E protein. The H-2 class-II-KO (H-2A β°) mice show a near-complete lack of CD4$^+$ T cells in spleens and lymph nodes.

HHD tg H-2D$^{b-/-}$ $\beta_2$m$^{-/-}$ double KO were intercrossed with HLA-DR1-tg H-2 class-II-KO to obtain HHD/HLA-DR1 double transgenic (dtg) H-2 class I/II KO mice (Pajot et al., 2004), which will be referred to throughout this work as A2.DR1 dtg mice. A2.DR1 dtg mice show no surface expression of murine H-2 class I and II molecules, but instead they express HHD (high) and HLA.DR1 (intermediate) molecules. The number of peripheral CD8$^+$ T cells is similarly low as in the HHD tg H-2D$^{b-/-}$ $\beta_2$m$^{-/-}$ double KO accounting for 2-3 % of total splenocytes. CD4$^+$ T cells represent 13-14 % of the total splenocyte population.

We employed the A2.DR1 dtg mice for our experiments in order to identify mutated tumor epitopes within tumor antigen derived long peptides, which are possibly presented in a human MHC context.

### 1.1.1.3. Antigen processing

The knowledge of how antigens are processed to suitable peptide fragments for presentation on MHC molecules is steadily becoming more complex (Neefjes, Jongsma, Paul, & Bakke, 2011). This is why only the basic mechanisms will be adumbrated in this section.

Newly synthesized MHC class I molecules fold and assemble correctly in the lumen of the endoplasmic reticulum (ER). As MHC class I molecules mainly present cytosolic peptides, these have to be transported into the ER. There is constant turn-over of cytosolic proteins (self-proteins or proteins originating from (intracellular) pathogens) in the cytoplasm which serves as source for peptides prone to presentation. The degradation of proteins (often tagged with ubiquitin – the signal for degradation) is basically carried out by a large, multicatalytic protease complex composed of the cylindrical 20S catalytic core and two 19S regulatory caps (one on each end), called the proteasome. Some of the constitutively expressed catalytic subunits (β1, β2, β5) of the 20S core can be replaced by alternative subunits (LMP2, LMP7, MECL-1). Their genes are encoded in the MHC locus and are inducible by IFN-γ. A proteasome carrying these inducible catalytic subunits is called the immunoproteasome. The immunoproteasome preferentially cleaves proteins after potential anchor residues suitable for MHC class I molecules and its activity can be increased by binding of PA28 (proteasome-activator complex). Peptide fragments produced by the proteasome are transported via the ATP-dependent peptide transporter complex TAP (transporters associated with antigen processing) into the ER, where they can be further trimmed by aminopeptidases to a suitable length for MHC loading. In the ER, newly synthesized MHC class I α-chain molecules are stabilized by the chaperon calnexin until they are assembled with the $\beta_2$-microglobulin. Then they are passed over to the peptide-loading-complex of chaperons and chaperon-like molecules (e.g. tapasin) binding to the TAP transporter. The loading of peptide releases the MHC class I molecule from the loading complex. Loaded peptide:MHC class I complexes are transported via the Golgi apparatus to the plasma membrane, where they can present antigens to $CD8^+$ T cells (see figure 1.2 A (Murphy, 2012)).

Like class I molecules (and all other cell-surface glycoporteins) the MHC class II chains are translocated into the ER, where they are assembled. To prevent binding of peptides inside the ER lumen to the freshly folded MHC class II chains, they from a trimer with the MHC class II-associated invariant chain protein Ii (CD74). A part of the Ii protein chains is thereby lying inside the peptide-binding cleft and therewith blocking it from randomly binding ER peptides. The MHC class II α:β-Ii complex is delivered from the ER to the low-pH-endosomal compartment, a process which is also mediated by the Ii protein. Inside endosomes the Ii protein gets cleaved by proteases like cathepsin L and S until only a short fragment is left. This fragment, which is still blocking the peptide binding cleft, is called CLIP (class II-associated invariant chain peptide). The endosomal compartment is also providing the peptides which are prone to bind to the MHC class II molecules. Extracellular proteins are internalized into endocytotic vesicles via phago- and/or pinocytotic processes. Inside the cell endosomes become increasingly acidic. This leads to the activation of proteases (like the before mentioned cathepsins) breaking down extracellular and

pathogenic proteins. The latter can be also derived from pathogens which are replicating within the intracellular vesicles. On their way to the cell surface MHC class II containing endosomes can fuse with endocytosed peptides filled vesicles. Consecutively, the MHC class II like molecule HLA-DM, which binds and stabilizes the MHC class II:CLIP complex, catalyzes the exchange of CLIP with other (e.g. pathogenic) peptides. Loaded MHC class II:peptide complexes are then transported to the plasma membrane, where they can present their cargo to $CD4^+$ T cells (see figure 1.2 B (Murphy, 2012)).

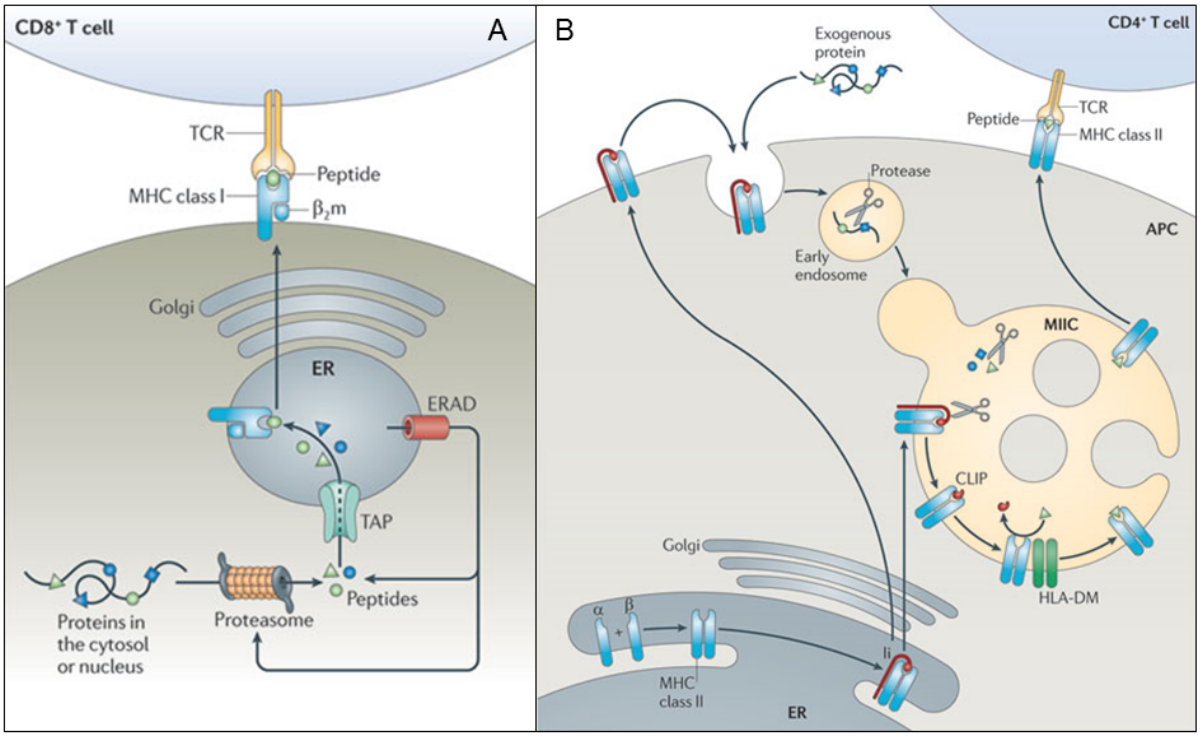


**Figure 1.2**: **The classical MHC class I and class II antigen presentation pathways**. (**A**) **MHC class I presentation pathway**. TAP: transporter associated with antigen-presentation, ER: endoplasmic reticulum, $\beta_2$m: $\beta_2$-microglobulin, ERAD: ER-associated protein degradation, TCR: T cell receptor. (**B**) **MHC class II presentation pathway**. Ii: invariant chain, MIIC: MHC class II compartment, CLIP: class II-associated invariant chain peptide, HLA-DM: chaperone, APC: antigen-presenting cell. This figure is taken from (Neefjes et al., 2011).

Besides the two classical mechanisms of antigen processing there are other pathways which allow the presentation of cytosolic antigens by MHC class II molecules and *vice versa* the presentation of extracellular antigens by MHC class I molecules. The loading of cytosol-derived peptides onto MHC class II molecules could be facilitated by a phenomenon called autophagy. It is an auto-digestive process, which is important for intracellular homeostasis by removal of misfolded proteins, damaged organelles and by providing molecules for cellular remodeling during conditions of cellular stress. Old and damaged cytosolic components (also pathogens) are thereby recycled within acidic organelles, called autophagosomes. Autophagosomes, as part of the lysosomal compartment, can provide (self-) peptides for the presentation on MHC class II molecules (Crotzer & Blum, 2010).

The second case, the presentation of peptides from extracellular sources by MHC class I molecules, is particularly important in the context of this work. This process, called cross-presentation, is

believed to be the major mechanism by which tumor antigens are presented to the immune system (Kurts, Robinson, & Knolle, 2010). The ability to cross-present is basically restricted to cells of the immune system, more precisely to professional antigen-presenting cells. Predominantly dendritic cells, and to a far lesser extent macrophages and B cells have the ability to cross-present. Although the effects of cross-presentations are known for more than 25 years, a clear mechanistic background is not yet revealed. However, it was solved that extracellular material is taken up by antigen-presenting cells through receptor-mediated endocytosis. It was shown that endosomes showing low (but steady) proteolytic activity and relatively high pH leads to the accumulation of antigen, possibly giving them more time to exit into the cytoplasm and therewith entering the MHC class I loading pathway (Accapezzato et al., 2005; Delamarre, Pack, Chang, Mellman, & Trombetta, 2005). After entering the cytosol the fate of these antigens could be proteasome and TAP-dependent (Kovacsovics-Bankowski & Rock, 1995). This is the reason why this suggested route of cross-presentation is referred to as the cytoslic pathway. The vacuolar pathway is proposed as an alternative. Therein, internalized pathogens/antigens are more completely broken down by endosomal proteases for the loading onto MHC class I molecules which were recycled from the extracellular membrane (Fehres, Unger, Garcia-Vallejo, & van Kooyk, 2014; Merzougui, Kratzer, Saveanu, & van Endert, 2011). There are evidences for both pathways but the picture as a whole remains ambiguous.

Of special relevance for this work, it was shown that (synthetic) long peptides can more efficiently enter the cross-presentation pathway than respective whole proteins (H. Zhang et al., 2009). This is indicating that antigen presentation in the setting of a long peptide vaccine is basically mediated through cross-presentation. Dendritic cells are the most potent cross-presenting cells and display many more essential functions in the initiation of an adoptive immune response upon infection but also upon vaccination.

### 1.1.2. Dendritic cells – masterminds of vaccination success

Dendritic cells are professional antigen presenting cells (APC) and have an outstanding role because of their ability to activate naïve T lymphocytes. DCs can originate from both myeloid and lymphoid progenitors in the bone marrow. They migrate via the blood stream from the BM to tissues all throughout the body and to secondary lymphoid organs. There are two main classes of DCs, called the conventional (or myeloid) DCs and the plasmocytoid DCs. Conventional DCs can be further subdivided and diverse subsets are described in mice and humans. In our context particularly important are subsets of conventional DCs. This is why the importance of DCs in initiation of an adoptive immune response will be discussed in the context of conventional DCs.

Tissue resident conventional DCs have an immature phenotype associated with low levels of expression of co-stimulatory (like B7 molecules) and of MHC molecules. Immature DCs are very active in ingesting antigens by receptor-mediated phagocytosis and engulfment of large volumes of the

surrounding fluids through macropinocytosis. The most important receptors involved in phagocytosis are: Fc receptors, C-type lectins (e.g. the mannose receptor), and dectin-1 (recognizing fungi-derived carbohydrates). Moreover, DCs express Toll-like receptors (TLRs) which serve to recognize pathogen-associated molecular patterns (PAMPs) and danger signals. Some cell-surface proteins of DCs act as entry receptors for viruses rendering DCs susceptible for infection by a number of those. This magnitude of antigen sampling mechanisms allows DCs to present virtually any type of antigen, derived from fungi, parasites, viruses, bacteria and tumors. Furthermore, DCs can also use all of the antigen-presenting pathways listed above. Upon stimulation of TLRs significant changes in DC behavior are initiated. Antigens are more efficiently processed and alteration in the pattern of expressed chemokine receptors leads to the migration of DCs to lymphoid tissue, most importantly LNs. On their way (via the CCR7-CCL21-axis) they further mature and by the time they arrive in lymphoid tissues they are fully matured. This means they stopped taking up antigens and express high levels MHC class I and II molecules, which present epitopes from processed pathogens. In addition, mature DCs strongly express surface co-stimulatory molecules CD80 (B7.1) and CD86 (B7.2) and produce chemokines (CCL18) which attract naïve T lymphocytes (Murphy, 2012).

In case of virus infections but also in terms of tumor antigen presentation the antigen has to be cross-presented to prime naïve $CD8^+$ T cells to become fully activated cytotoxic T lymphocytes (CTLs). Dendritic cells, resident in draining LNs and expressing the surface marker CD24, CD8α and CD103 (αE integrin), are the most potent cross-presenting cells in mice (Bedoui et al., 2009; Heath & Carbone, 2009). In humans the CD141 (BDCA-3) positive DCs seem to cross-present most efficiently (Haniffa et al., 2012). Generally, the initiation of a $CD8^+$ T cell response to antigen which is not produced by the APC itself and therefore has to be cross-presented is known as cross-priming.

In the first step of cross-priming tissue DCs deliver antigen form peripheral tissues to the secondary lymphoid organs and hand it over to resident ($CD8\alpha^+$) DCs (Allan et al., 2006). Moreover, the DCs need to receive the above mentioned danger signals from TLR ligation by PAMPs. Ligation of TLR3 (ligand poly(I:C) sequences) and TLR9 (ligand CpG sequences) was shown to enhance cross-presentation effectively in mice (Maurer et al., 2002; Schulz et al., 2005). Next, antigen-specific $CD4^+$ T helper ($T_H$) cells are recruited. The $T_H$ cells alter the DCs to a transient state in which they can effectively program CTLs for sustained effector functions and memory formation. This trait of $T_H$ cells is called DC licensing and is mediated by CD40 (expressed on the DC) - CD40L (CD154, expressed by the $T_H$ cell) interaction (C. M. Smith et al., 2004). Now the licensed, cross-presenting DC is ready for CTL programming. Naïve $CD8^+$ T cells are most probably attracted to the DCs by CCR5-ligands (CCR5 is expressed on naïve CTLs). Next to transmission of signal II (CD80/86-CD28 interaction) and TCR receptor ligation other actions seem to be necessary for proper CTL programming. CD70 (a member of the TNF receptor family molecules) seems to increase the survival through interaction with CD27 on CTL side (Keller, Xiao, Peperzak, Naik, & Borst, 2009). Possibly down-regulation of PD-1 ligands on DC side also promotes acquisition of active CTL function (Keir, Freeman, & Sharpe, 2007). Definitely, IL-2 is

needed during priming to ensure CTL survival (Williams, Tyznik, & Bevan, 2006). Which cell in this trio is providing the IL-2 is not clear; the $T_H$ cells (as indicated in 1.3 A) would just be self-evident (see figure 1.3, cross-priming is reviewed in (Kurts et al., 2010)).

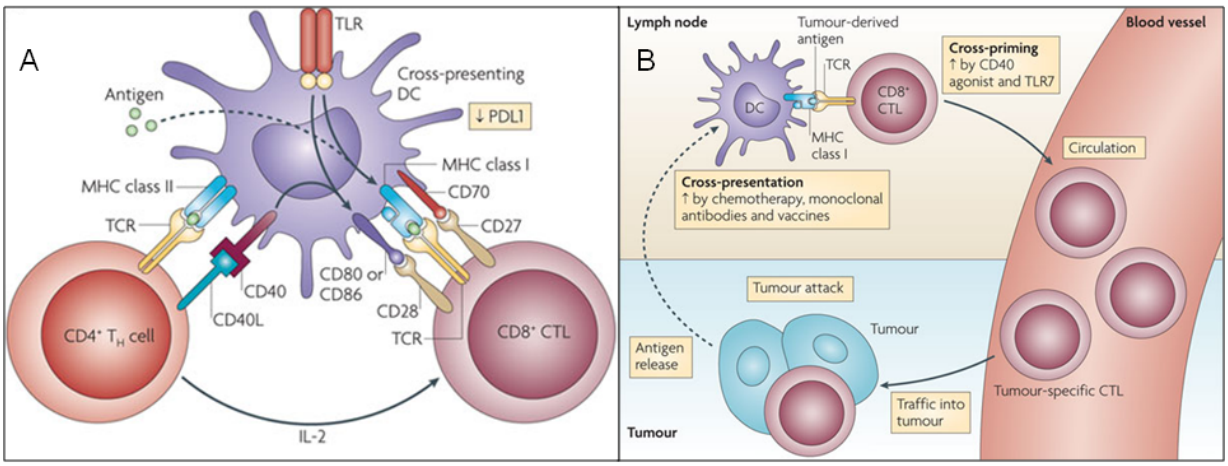


**Figure 1.3**: (**A**): **Molecular mechanisms of classical cross-priming**. Dendritic cells (DC) present endocytosed and processed antigen loaded on MHC class II molecules to $CD4^+$ T helper cells ($T_H$) and cross-present it through MHC class I molecules to $CD8^+$ cytotoxic T cells (CTL). $CD4^+$ T cells can stimulate CTLs by secreting interleukin-2 (IL-2) and license DCs via CD40L (ligand) – CD40 interactions. DCs react to licensing with up-regulation of co-stimulatory molecules (CD70, CD80, CD86) and down-regulation of inhibitor molecules (PD-L1: programmed cell death ligand). Toll-like receptor (TLR) ligations can further boost activation and cross-presentation capacity of DCs. (**B**) **Cross-presentation and DCs as critical components in anti-tumor immunity**. Tumor-antigens are released from the tumor or introduced through vaccination are cross-presented by DCs, which can be boosted by chemotherapy or antibodies. For a successful cross-priming of CTLs, however, danger signals (TLR7 e.g.) or co-stimulation (CD40) is required. After priming CTLs are thought to enter to the blood stream, expand and circulate to the tumor. This figure is taken from (Kurts et al., 2010).

Conclusively, DCs are key players in mediating anti-tumor immune responses as they are able to cross-present and prime CTLs (see figure 1.3 B). This route of antigen-processing and T cell response initiation after anti-cancer vaccination with synthetic peptides is suggested by Melief and colleagues. Tumor-antigen comprising peptides used for vaccination and applied subcutaneously are taken up by tissue-resident DCs, which migrate to the vaccination-draining LN, where they probably present the tumor-antigens by cross-presentation (Melief, 2008; Melief & van der Burg, 2008). From this knowledge we have drawn tow conclusions for the design of our vaccine. First we should include an adjuvant which is potent to initiate cross-priming, like the TLR9 ligand and danger signal CpG (shown to be especially potent in mice). Second, as $CD4^+$ T helper cells are required for proper licensing of DCs, T helper cell epitopes should be included in our vaccine.

### 1.1.3. T cell development in the thymus works hand-in-hand with the establishment of central tolerance

Mature naïve $CD4^+$ and $CD8^+$ T cells, which are fully activated by antigen-presenting DCs to display effector functions as described in the previous chapter, originate from the thymus. In the thymus they develop from progenitor cells in an orchestrated multi-step process through interactions with thymic epithelial cell and other immune cells residing in the thymus to result in a T cell population with a highly diverse and self-tolerant T cell receptor repertoire (TCR).

In the classical model common lymphoid progenitor cells (CLP) originate from hematopoietic stem cells (HCS), which can give rise to all cellular progenies of the adaptive and innate immune system (Kondo, Weissman, & Akashi, 1997). More recently, a second pathway comes up in which HSCs first give rise to multi-potent progenitors (MPPs). Some MPPs express lymphoid-specific genes and are therefore termed lymphoid-primed MPPs (LMPP) or early lymphoid progenitors (ELP). CPLs are not originating from MPPs and together with the LMPPs they form the pool of thymic seeding progenitors (TSP). Most probably, these cells can leave the bone marrow and migrate to the thymus under the guidance of certain chemokines (e.g. CCR7) and adhesion molecules (e.g. PSGL1: P-selectin glycoprotein ligand 1). In the thymus they progress upon encounter with the thymic epithelium to early thymic progenitors (ETP) (alternative model is reviewed (Love & Bhandoola, 2011; Rothenberg, 2014). ETPs are partially uncommitted and still have the potential to give rise to myeloid cells, NK cells, DCs, and rarely B cells (Koch & Radtke, 2011). They do not express any T cell lineage marker (like CD3, CD4 and CD8) and are therefore referred to as $CD8^-CD4^-$ double negative (DN) cells. Although progressing in T cell lineage commitment they do not express the co-receptors until TCR α-chain rearrangement. But the DN phase can be subdivide into 4 different DN differentiation stages according to the expression of the markers CD44 (adhesion molecule) and CD25 (IL-2 receptor α-chain) (Murphy, 2012).

ETPs represent the first DN stage (DN1) and are $CD44^+CD25^-$. They reside in the cortico-meduallary junction were they start proliferating due to the onset of Notch-signaling upon interaction with most probably stromal cells. When they migrate further into the cortex towards the sub-capsular zone they encounter cortical thymic epithelial cells (cTECS), which together with fibroblasts drive progression to the DN2 stage. This is characterized by up-regulation of CD25 and onset of rearrangement of the TCR β-, γ- and δ-chain loci. The rearrangement of the TCR chain and expression of CD3 finally commits DN cells to the T cell lineage. TCR β-, γ- and δ-chain rearrangement continues throughout the DN3 stage accompanied by down-regulation of CD44. The end of the DN3 stage is an important checkpoint. Cells which successfully rearranged TCR γ- and δ-chain (a minority of roughly 20 % of DN cells) are close to finalize differentiation and are prone to leave the thymus as $γ{:}δ^+CD3^+$ ($CD4^-CD8^-$) T cells. Cells showing an unproductive rearrangement of the β-chain locus get stuck in the DN3 stage and soon die, whereas cells with a successfully rearranged TCR β-chain down-regulate CD25 and progress to the DN4 stage. These T cells are now committed to the α:β lineage. Importantly, upon a productive rearrangement of the β-chain locus during the DN3 stage the β-chain pairs with a surrogate pre-T-cell receptor α-chain (pre-T-cell-α), which together make up the pre-T cells receptor (pre-TCR). The pre-TCR assembles with CD3 and the pre-TCR:CD3 complex is able to constitutively signal, which leads to an arrest of further β-chain rearrangement (allelic exclusion) and proliferation during the DN4 stage. DN4 ($CD44^-CD25^-$) cells migrate to the outer cortex, where they start expressing both, CD4 and CD8 molecules, and therewith passing on to the double positive stage (DP). During the DP stage they stop proliferation and the TCR α-chain locus is rearranged. Successfully rearranged α-chains replace the pre-TCR-α-chain. Interestingly, the somatic recombination of the TCR α-chain locus does not underlie allelic exclusion and it is possible that both

alleles are productively rearranged, giving rise to two different TCRs upon assembly with the β-chain (Murphy, 2012).

At the end of the DP stage, after assembly of the successful rearranged TCR α-chain with the β-chain, the fate of the pre-mature T cells depends on interaction of the α:β-TCR with peptide:MHC complexes expressed by thymic resident cells.

The first TRC dependent selection process, directly at the DP stage, is called positive selection and takes place in the cortex of the thymus. TCRs seem to carry an inherent specificity of either MHC class I or MHC class II molecules, which could be mediated by certain amino acid residues in the V domains in α- and β-chains of the TCR interacting with MHC molecules. CD4 and CD8 co-receptors in turn interact with invariant sites of the MHC molecules and the lineage decision for $CD4^+$ or $CD8^+$ T cells is made depending on the strength of the signaling form the respective co-receptor (Murphy, 2012). Cortical thymic epithelial cells (cTECs) present self-antigen to double positive T cells. cTECs are able to express MHC molecules of both classes and they possess unique features to process self-peptides (thymoproteasome, cathepsin L) (Murata et al., 2007; Nakagawa et al., 1998). This way they are able to produce and present so called “private antigens”, which are self-antigens that differ from self-antigens produced by other APCs. Positive selection in turn is driven by the interaction of self-peptide:MHC complexes on cTECs with TCRs and co-receptors of DP cells. As a matter of fact, DP cells which fail to interact with self-peptide:MHC complexes die, a phenomenon called death by neglect. Only about 10-30 % of DP cells survive positive selection. The presentation of “private self-antigens” appears to be critical for the versatility of the T cell repertoire, as it was shown that a defective thymoproteasome leads to a crippled $CD8^+$ TCR repertoire with a higher affinity for self-antigens (Klein, Kyewski, Allen, & Hogquist, 2014). Additionally, there is increasing evidence of DP cell depletion in the thymic cortex due to negative selection, which is crucially dependent on dendritic cells presenting ubiquitous self-antigen (McCaughtry, Baldwin, Wilken, & Hogquist, 2008).

Positively selected single positive (SP) cells rapidly migrate from the cortex to the thymic medulla. In the medulla SP cells whose TCRs bind too strongly to self-peptide:MHC complexes undergo apoptosis, a process called negative selection. Negative selection is mainly mediated by medullar thymic epithelial cells (mTECs) and certain subsets of DCs. Also B cells are situated in the medulla, which display self-antigen presenting capacity, but how they contribute to negative selections remains to be solved (Frommer & Waisman, 2010). mTECs have the unique trait to ectopically express almost all ‘peripheral’ tissue-restricted antigens (TRAs) in a mosaic pattern, meaning each TRA is only expressed by 1-3 % of mTECS at any given time. This so called promiscuous gene expression is attributed to the activity of the molecular regulator AIRE (autoimmune regulator), which can turn on silent gene loci (Mathis & Benoist, 2009). Like cTECs, mTECs can also present self-antigen on MHC class II complexes and autophagy is suggested as a possible process of endogenous MHC class II loading. In the medulla three subsets of dendritic cells contribute to negative selection (Li, Park, Foss, & Goldschneider, 2009; L. Wu & Shortman,

2005). Resident conventional DCs (cDCs) preferentially seed the medulla and sample their presented self-antigens in the thymic microenvironment, whereas migratory mDCs are thought to transport peripherally collected and captured blood-borne self-antigens into the thymus. The migratory population of plasmacytoid DCs (pDCs) most probably samples its self-antigen cargo solely in the periphery and as pDCs' antigen-presenting capacity is poor it remains to be solved how they contribute to central tolerance. After undergoing the listed developmental and selective steps 1-3 % of the progenitor cells which originally entered the thymus leave it as mature naïve single positive T cells and constitute the T cell repertoire.

These observations lead to the development of the affinity model of thymic selection (see figure 1.4 C). T cells require weak interactions of their TCR with self-peptide:MHC complexes to protect them from death through neglect during positive selection. Too strong interactions, however, lead to negative selection (also referred to as clonal deletion) by apoptosis. Moreover, differentiation of regulatory T cells ($T_{reg}$) seems to occur optimal within an window of affinity between positive and negative selection (Klein et al., 2014).

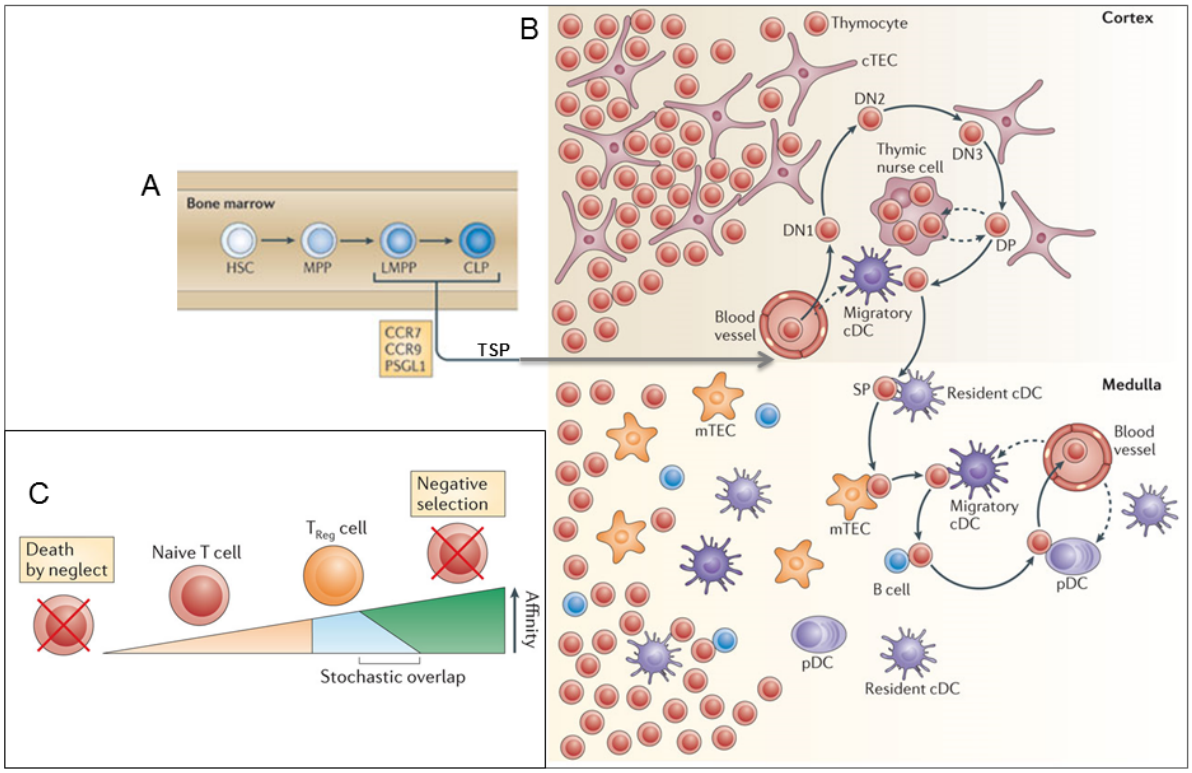


**Figure 1.4**: (**A**) **Early developmental stages of bone marrow progenitors of T cells**. LMMP (lymphoid-primed multi-potent progenitor) and CLPs (common lymphoid progenitor) are thymic seeding progenitors (TSP) which migrate from the bone marrow to the thymus. HSC: hematopoietic stem cell, MMP: multi-potent-progenitor, CCR7/9: CC-chemokine receptor 7/9, PSGL1: P-selectin glycoprotein ligand 1. This figure is adapted from (Love & Bhandoola, 2011). (**B**) **Stromal cell interactions at different stages of T cell development in the thymus.** DN: double negative, DP: double positive, mTEC: medullar thymic epithelial cells, cTEC: cortical thymic epithelial cells, cDC: conventional dendritic cells, pDC: plasmocytoid dendritic cells. This figure is adapted from (Klein et al., 2014). (**C**): **The affinity model of T cell selection**. This figure is taken from (Klein et al., 2014).

Redirection of auto-reactive $CD4^+$ T cells into the $T_{reg}$ linage is called clonal deviation. It was shown, that there is no clear demarcation between clonal deviation and clonal deletion, neither between the decision of differentiation to $CD4^+$ conventional T cells or $T_{reg}$ cells (Wirnsberger, Hinterberger, & Klein, 2011). This is why, the natural TCR repertoires of these two $CD4^+$ T cell populations show some overlap (Pacholczyk & Kern, 2008). Klein and Kyewski suggest the following scenario: Although the different antigen-presenting cells in the medulla all seem to have the ability to promote clonal deletion and deviation (Klein & Jovanovic, 2011), thymic DCs and mTECs most probably display not entirely overlapping pools of presented self-antigens (MHC-ligandomes) during negative selection and induction of central tolerance. This could lead in term to the occasional escape of an auto-reactive naïve effector T cells, specific for a rarely presented self-antigen, into the periphery. $T_{reg}$ cells with the same antigen-specificity counterbalance the activity of self-reactive effector T cells by dominant regulatory mechanisms (Klein et al., 2014). Indeed, the suppression of auto-reactive T cells by $T_{reg}$ cells in the periphery is a crucial prerequisite of peripheral tolerance (Wing & Sakaguchi, 2010).

Several conclusions can be drawn from effects of central tolerance for the development of a vaccine. Central tolerance is able to purge the T cell repertoire from the majority of auto-reactive T cells. If an auto-reactive T cell can escape to the periphery, the second save-guard mechanism of suppression by regulatory T cells prevents autoimmunity. At this point some facts have to be anticipated: most of the tumor antigens are shared with normal tissue. As we shall see later, it is indeed possible to detect and induce immune responses against shared tumor antigens. However, they are often hampered, partially because of the existence of regulatory T cells and partially because TCRs of auto-reactive T cells are prone to show a lower affinity due to central tolerogenic processes. Moreover, there is the risk of induction of autoimmunity when tolerance against these shared tumor antigens is broken. To target mutated tumor antigens, which are not shared with normal tissue, has the potential to circumvent all of the mentioned issues.

### 1.1.4. Activation of naïve T cells leads to differentiation into effector T cells

Most of the major mechanisms underlying T cell activation were already discussed in chapter 1.1.2. in the context of cross-priming by dendritic cells. Therefore, the common mechanisms for $CD4^+$ and $CD8^+$ T cell activation will be only briefly discussed at that point.

The initial contact between DCs and T cells is mediated by unspecific binding of adhesion molecules, most importantly LFA-1 and CD2 on the TC side and ICAM-1, ICAM-2, and CD58 on DCs. In case a naïve T cell recognizes its specific ligand present on MHC molecules, TCR signaling induces a stronger binding of LFA-1 to its ligands ICAM-1 and ICAM-2 through conformational changes. This leads to a clustering of adhesion molecules, TCRs and co-receptors, and co-stimulatory (either activating or inhibiting) molecules forming a stable junctions between the two cells called the immunological synapse or supra-molecular activation cluster (SMAC) (Grakoui et al., 1999).

The full activation of naïve T cells depends on three signals. The first signal are the stimuli, which result from the engagement of the TCR with its specific peptide:MHC-complex. This includes the CD3 signaling complex transmitting the TCR signal downstream and ligation of the respective co-receptors with the MHC molecules (MHC class II with the CD4 and MHC class I with the CD8 co-receptor) (Salmond, Filby, Qureshi, Caserta, & Zamoyska, 2009).

The second signal comes from co-stimulatory molecules, which are critical for T cell survival and expansion. Generally, the APC is expressing ligands of co-stimulatory receptors which are exposed on the T cell surface. The most important stimulatory receptor, as already mentioned, is CD28 binding B7-molcules. Co-simulation by CD28 leads to the up-regulation of the IL-2 receptor α-chain (CD25) on the T cell, which upon association with the β- and γ- receptor chains is rendering the IL-2 receptor highly sensitive for IL-2 (Zhou et al., 2002). IL-2 is the key growth factor for T cell survival in general and for T cells undergoing clonal expansion specifically. Furthermore, IL-2 can trigger its own synthesis in an autocrine loop. Other well characterized co-stimulatory receptors expressed by T cells are ICOS (CD278, Inducible T cell co-stimulator, belongs to the CD28 superfamily) and the two TNF receptor family members 4-1BB (CD137) and OX40 (CD134). Their corresponding ligands expressed by DCs are ICOSL (ICOS ligand, B7-H2), 4-1BBL (4-1BB ligand) and OX40L (OX40 ligand TRAF2: TNF receptor-associated factor 2), respectively (Croft, 2003; Dong et al., 2001). Next to the activating co-stimulatory signals there are also several inhibitory receptors expressed on T cells, which can down-modulate or even inhibit complete activation. The two most prominent representatives are CTL-4 and PD-1 (see section 1.1.2.). CTLA-4 (cytotoxic T lymphocyte antigen 4, CD125) is structurally related to CD28 and competes with CD28 for binding of B7 molecules. Signaling through CTLA-4 can reduce the sensitivity of the T cells receptor and restrict IL-2 production. Negative co-stimulatory signals are important to prevent immoderate immune responses and maintain self-tolerance (Greenwald, Freeman, & Sharpe, 2005).

The “signal 2” molecules, inhibitory as well as stimulatory, are prominent targets and tools for the manipulation of T cell responses in the context of immunotherapy against cancer and some of them we will encounter later also in conjunction with vaccine strategies. Furthermore, in many immunological experimental approaches, strong proliferation of T cells can be induced *in vitro* by agonistic antibodies binding to CD3 (like e.g. OKT3) and CD28.

Cytokines, which are secreted by the antigen presenting cells and can direct naïve T cell differentiation into different effector T cells subsets during activation, are constituents of signal 3 (Murphy, 2012). As we shall see in the following paragraphs, signal 3 is of especial relevance for differentiation of $CD4^+$ T cells.

Summed up, the activation of naïve T cells leads to differentiation into distinct effector T cell subsets. The activation generally takes place in secondary lymphoid organs, predominantly in infection site draining lymph nodes. After clonal expansion the effector T cells reenter the circulation and migrate, guided by adhesion molecules and chemokines, to sites of infection, where they unfold their effector

functions. Whereas cytotoxic T cells can operate directly by contact-mediated killing of infected cells and indirectly by secretion of cytokines, helper T cells act basically indirect through the secretion of cytokines. After the infection is cleared, the vast majority of the expanded T cell populations dies during the so called contraction phase. 5 - 10 % of the effector T cells, however, survive and give rise to memory formation. They change once again their phenotype and populate a pool of different memory T cell subsets, which can provide the host with lifelong protection. Upon reencounter with the same pathogen that caused the initial immune response, they rapidly elicit recall responses (Arens & Schoenberger, 2010; Murphy, 2012).

### 1.1.5. $CD8^+$ T cells – accurate and efficient serial killers

When a fully differentiated and activated cytotoxic $CD8^+$ T cell finds a virus infected target cell at the infection side (or a tumor cell), again the first contact after TCR antigen:MHC-complex engagement is made by the up-regulated adhesion molecules CD2 and LFA1. They can bind to ICAM and CD58 on infected cells. After initial contact is made an immunological synapse is formed. Importantly, activated CTLs no longer need stimuli from co-receptor molecules, which are anyway generally not expressed by target cells unless the target cell is an infected macrophage or dendritic cell. Signaling through the immunological synapse leads to cytoskeletal reorientation that focuses exocytosis to site of contact and triggers synthesis of new cytotoxic proteins. The site-directed secretion of cytotoxic effector proteins into the narrow space formed by the immunological synapse between the two interaction partners is essential to avoid killing of neighboring uninfected cells and therewith bystander tissue damage (Bossi et al., 2002). The cytotoxic cargo of CTLs is stored in modified lysosomes, cytotoxic granules, and is released in a calcium-dependent manner. The glycoprotein CD107a (LAMP-1: lysosomal associated membrane protein-1) in the membranes of lysosomes can serve as a marker for degranulation of cytotoxic granules and provides information about the cytolytic activity of CTLs (Aktas, Kucuksezer, Bilgic, Erten, & Deniz, 2009). The main effector molecules inside the cytotoxic granules are perforin and granzymes, which are both required for effective killing. Perforin is a pore-forming protein which enables the entry of granzymes, a family of serine proteases, into the target cells. Granzyme B in turn triggers apoptosis through activation of caspase 3. The remnants of apoptotic cells are cleared by macrophages (Chowdhury & Lieberman, 2008).

The interaction between a target cell and a CTL is rather short and after having killed its target CTLs can directly proceed to the next virus infected cell. Another mechanism, by which CTLs can kill, is the expression of FasL and ligation of Fas (CD95) on target cells, which undergo apoptosis upon Fas signaling (Arens & Schoenberger, 2010).

Beside their cytotoxic activity CTLs can also release cytokines, like IFN-γ and TNF-α. IFN-γ can directly inhibit viral replication and leads to the up-regulation of the antigen-presenting machinery by enhancing transcription. IFN-γ also recruits macrophages to the site of infection and can activate them to up-regulate their intrinsic armory to eliminate pathogens inside their intracellular vesicles. TNF-α

synergizes with IFN-γ in activation of macrophages and kills target cells through binding of TNFR-1 (which can initiate apoptosis signals by its death receptor domain) (Slifka & Whitton, 2000).

### 1.1.6. $CD4^+$ T cells – indispensible helpers

In comparison to CTLs $CD4^+$ T cells can differentiate into several different subsets upon activation. Four major T helper cell populations are well characterized namely $T_H1$, $T_H2$, $T_H17$, and $T_{reg}$ cells. Several potential lineages, like $T_H3$, $T_{FH}$ (follicular T helper cells), $T_R1$ and others are described but their mode of action and route of differentiation is not fully understood. This is partially attributed to a high plasticity between the different lineages, especially at early developmental stages. Also the environments in which these T cell subsets are primed and display their functions seem to contribute to their phenotype (Zhu & Paul, 2010). Due to the complexity, only the established lineages will be discussed further, focusing on $T_H1$ cells and $T_{reg}$ cells as they seem to contribute substantially to the observations made in the presented work.

Crucial for the sequestered differentiation from a common naïve $CD4^+$ T cell progenitor is the cytokine milieu (signal 3) during the priming phase at early infection. IFN-γ and IL-2, secreted by innate immune cells, favor the differentiation into $T_H1$ cells by activating STAT1 and STAT4 (STAT: signal transducing activators of transcription). STAT family members are important transcription factors, signaling thought the JAK-STAT pathway, for the cytokine-induced differentiation of $CD4^+$ T cells lineages. In $T_H1$ cells STAT1 (activated by IFN-γ) induces the expression of the master transcription factor of the $T_H1$ lineage T-bet. T-bet, in turn, switches on the genes for the IFN-γ and IL-12 receptors. IL-12 activates STAT4, which drives expansion by proliferation and lineage commitment (O'Shea & Paul, 2010). The signal 3 cytokine combinations as well as the master transcriptional regulators for the other T helper cell lineages are listed in table 1.1.

**Table 1.1**: **Major $CD4^+$ T helper cell subsets: important factors for differentiation and effector functions** (References used: (Murphy, 2012; Zhu & Paul, 2010; Zorn et al., 2006)

| **$CD4^+$ T cell subset** | **$T_H1$ cells** | **$T_H2$ cells** | **$T_H17$ cells** | **$iT_{reg}$ cells** |
|---|---|---|---|---|
| **Signal 3 cytokine cocktail** | IL-12, IFN-γ | IL-4 | TGF-β, IL-6 | TGF-β, IL-2 |
| **STAT family members** | STAT1, STAT4 | STAT6 | STAT3 | STAT3, STAT5 |
| **Master transcription factor** | T-bet | GATA3 | RORγT | FoxP3 |
| **Important effector cytokines** | IL-2, IFN-γ, TNF-α | IL-4, IL-5, Il-10, IL-13 | IL-6, IL-17A, IL-17F | TGF-β, IL-10 |

Each differentiated effector T helper cell subset displays a distinct array of functions. All subsets have in common that their effector functions are (mostly) mediated through the release of cytokines. $T_H17$ cells promote inflammation indirectly by secreting IL-17 cytokines which act on local tissue cells. Tissue fibroblasts and epithelial cells secrete chemokines which trigger neutrophil responses protecting the host against extracellular bacteria and fungi (Weaver, Hatton, Mangan, & Harrington, 2007). $T_H2$ cells are important for parasite defense, particularly infections with helminthes. They drive responses of eosinophils and mast cells and switch B cells to secret IgE isotype antibodies, indicating that $T_H2$ cells are also

involved in allergic reactions (Yazdanbakhsh, Kremsner, & van Ree, 2002). Inducible regulatory T cells ($iT_{reg}$ cells) differentiate from naïve CD4 T cells in the presence of IL-2 and TGF-β and the absence of other inflammatory cytokines. Their mode of action will be discussed in the following chapter together with the actions of natural $T_{reg}$ cells.

$T_H1$ cells produce large amounts of IFN-γ, which is coupled to their main function to activate macrophages. When a $T_H1$ cell recognizes a macrophage, infected with an intracellular pathogen, via TCR antigen:MHC recognition an immunological synapse is formed between the two cells and the $T_H1$ cell starts producing effector cytokines. The newly synthesized cytokines are released at the site of contact between the cells. First, $T_H1$ cells sensitize the macrophage to respond to IFN-γ through CD40L (expressed on $T_H1$ cells) - CD40 (expressed on macrophages) interactions. TNF-α and LT-α (lymphotoxin-alpha) can substitute CD40 signaling though TNFR-1 stimulation, which seems to be important for macrophage viability. IFN-γ, as described for CTLs, mediates activation of macrophages and causes up-regulation of the macrophages' intrinsic microbicidal mechanisms to eliminate the intracellular pathogens. $T_H1$ cells can also directly kill infected macrophages by up-regulation of FasL. By secreting IL-2 they can induce proliferation of other effector T cells to increase their number at the site of infection (Murphy, 2012; Zhu & Paul, 2008).

Last but not least one more property of $CD4^+$ T helper cell subsets may be mentioned: cytotoxicity of $CD4^+$ T cells. It is described for humans and mice that $CD4^+$ T cells can acquire a cytolytic phenotype under certain conditions. It is usually associated with chronic viral infections and conditions of chronic antigen stimulation (e.g. HCMV in humans (Zaunders et al., 2004) and LCMV in mice (Jellison, Kim, & Welsh, 2005)). It seems rational to speculate that cytolytic $CD4^+$ T cells may be important in context of virus infections, in which the virus is able to circumvent CTL recognition (Marshall & Swain, 2011) and in virus-driven tumors (EBV, (Paludan et al., 2002)). But it has also been described that under lymphopenic conditions cytolytic T helper cells (ThCTLs) can eradicate melanoma in mice (Quezada et al., 2010). Interestingly, in $\beta_2$-microglobulin KO mice ThCTLs seem to compensate the lack of NK cells and CTLs (which in turn is attributed to severely hampered MHC class I expression in these animals, see section about HLA tg mice) (Muller et al., 1992). ThCTLs can kill MHC class II antigen-presenting targets in a CTL cytolytic manner by secreting cytotoxic granules carrying granzymes and perforin. Moreover, degranulation can also be detected by CD107a. ThCTLs display a $T_H1$ like cytokine secretion pattern, as they are able to secret combinations of IFN-γ, TNF-α and IL-2 (Casazza et al., 2006). Importantly, they do not develop under $T_H1$ polarizing conditions and it is not clear yet whether the ThCTL phenotype is stable (review in (Marshall & Swain, 2011)).

### 1.1.7. Regulatory T cells – Janus faced helpers

$CD25^+CD4^+$ regulatory T cells account for 5 – 10 % of the total $CD4^+$ T cell population (Wing & Sakaguchi, 2010). As it already became clear in previous passages the $T_{reg}$ cell pool is populated by to sources: thymic derived natural $T_{reg}$ ($nT_{reg}$) and peripheral induced $T_{reg}$ cells ($iT_{reg}$). Up to date there are no

clear markers defined to distinguish $iT_{reg}$s and $nT_{reg}$s and their exact relative proportion remains to be determined. Estimations employing the markers Helios and NRP1, which are described to be enriched within the $nT_{reg}$ population, suggest for a proportion of 70 – 90 % of $nT_{reg}$ cells (Thornton et al., 2010; Yadav et al., 2012).

The master transcriptional regulator for $T_{reg}$ cell development is Foxp3 (forkhead box P3), which drives the expression of many genes associated with the suppressive phenotype of this $CD4^+$ T cell population. As it became clear already, this phenotype is thought to correlate with a distinct TCR repertoire with an increased affinity to self-antigens compared to conventional $CD4^+$ T cells (see affinity model section 1.1.3). Furthermore, $T_{reg}$ cells express high levels of CD25, the IL-2 receptor α-chain, which leads to the formation of the high-affinity IL-2 receptor (Sakaguchi, 2004). Indeed, the homeostasis of $T_{reg}$ cells, more than any other TC subset, critically depends on IL-2. As it was recently elucidated, $T_{reg}$ cells are neither homogenous nor static and there are now functional subsets identified (see figure 1.5). 'Central' $T_{reg}$ cells are comparable to naïve conventional $CD4^+$ T cells. They express the lymphoid homing receptors CCR7 and CD62L and are hence are found in the circulation and secondary lymphoid organs. 'Effector' $T_{reg}$ cells show enhanced function and signs of recent antigen encounter. They down-regulate the expression of CCR7 and CD62L and up-regulate CD44, CD103 and KLRG1 (killer cell lectin-like receptor subfamily T member-1). This expression pattern indicates that they are rather found in peripheral tissue sites than in the circulation and secondary lymphoid organs. In humans these two subsets are described as resting $Foxp3^{low}CD45RA^{hi}CD25^{low}$ and effector $FoxP3^{hi}CD45RA^{low}CD25^{hi}$ $T_{reg}$ cells respectively (Miyara et al., 2009). So far it is not clear whether these two populations are stable or whether they can convert into each other. The last subset, the tissue resident $T_{reg}$ cells, is very heterogeneous because these cells are polarized by the environment they reside in (see figure 1.5). They are thought to be especially important in maintaining peripheral tolerance at the respective tissue site and therefore show long-term residence in non-lymphoid tissues ($T_{reg}$ cell subsets recently reviewed in (Liston & Gray, 2014)).

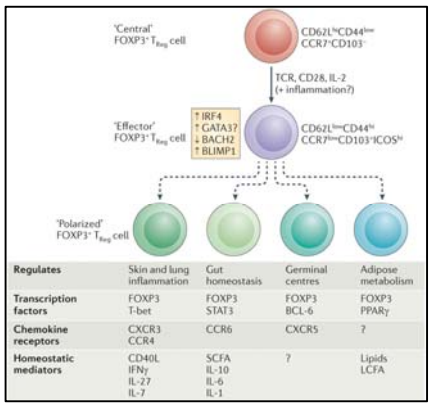


**Figure 1.5**: **The activation and differentiation of $T_{reg}$ cells**. Central $T_{reg}$ cells displaying a naïve phenotype are thought to differentiate into effector $T_{reg}$ cells which can get polarized to specific tissue-resident populations. BACH2: BTB and CNC homologue, BLIMP1: B-lymphocyte-induced maturation protein 1, IRF4: interferon regulatory factor 4, BCL-6: C cell lymphoma 6, CCR: CC-chemokine receptor, CXCR: CXC-chemokine receptor, GATA3: GATA-binding 3, ICOS: inducible T cell co-stimulator, LCFA: long-chain fatty acid, PPARγ: peroxisome proliferator-activated receptor-γ; SCFA: short-chain-fatty acid. This figure is taken from (Liston & Gray, 2014).

The major role of regulatory T cells in immunity is to sustain peripheral tolerance and to prevent potentially damaging immunopathology at the end of an infection. Misbalance in $T_{reg}$ cell homeostasis can lead on the one hand to autoimmunity (in case of decreased $T_{reg}$ functions, e.g. type 1 diabetes, inflammatory bowel disease (IBD), asthma) and on the other hand immoderate $T_{reg}$ cell activity can cause immune suppression. Immune suppression through recruitment of $T_{reg}$ cells is a substantial tumor escape mechanism and is critical in the context of the presented work.

$T_{reg}$ cells possess a magnitude of different effector mechanisms which contribute to their suppressive phenotype. These mechanisms can be grouped into four basic modes of action (reviewed in (Vignali, Collison, & Workman, 2008)). First to mention is the release of inhibitory cytokines, most importantly IL-10, TGF-β and IL-35. Contact-depend cytolysis mediated by granzymes (A and B) and perforin is another immunosuppressive mechanism by which $T_{reg}$ cells can induce apoptosis of natural killer (NK) cells, B cells, and conventional T cells. In this context, the direct killing of tumor-reactive NK cells and CTLs by $T_{reg}$ cells was shown to be perforin and granzyme B dependent in mice (Cao et al., 2007). The third mode of action comprises mechanisms which inhibit effector cells by means of metabolic disruption. There is evidence that $T_{reg}$ cells can consume large amounts of IL-2 in a given microenvironment trough their high-affinity IL-2 receptor (CD25) and therewith deprive surrounding effector T cells from IL-2, which leads to apoptosis (Pandiyan, Zheng, Ishihara, Reed, & Lenardo, 2007). Moreover, $T_{reg}$ cells can express the ectoenzymes CD39 and CD73 (ectonucleoside triphosphate diphsphohydrolase 1 and 5'-nucleotidase, respectively) on their cell surfaces which together can catalyze the hydrolysis of ATP, ADP and, AMP to adenosine (Deaglio et al., 2007). Extracellular adenosine suppresses effector T cell activity by stimulating the adenosine receptor 2A ($A_{2A}R$) and can lead to the induction of a tolerogenic phenotype of DCs (Challier, Bruniquel, Sewell, & Laugel, 2013). In addition $T_{reg}$ cells seem to be able to transfer the second messenger cAMP via gap junctions into effector T cells which leads to direct inhibition (Bopp et al., 2007). The last mechanism of $T_{reg}$ cell suppression is the targeting of dendritic cells. $T_{reg}$ cells thereby interfere with DC maturation and function. Through the constitutive expression of CTLA-4 they can perturb the CD28-CD80/CD86 co-stimulatory axis (Qureshi et al., 2011). Binding of CTLA-4 to CD80/CD86 leads to their down-regulation and the production of the immunosuppressive molecule IDO (indoleamine 2,3-dioxygeanse) (Mellor & Munn, 2004). By expressing LAG3 (lymphocyte activation gene 3), a CD4 homologue, $T_{reg}$ cells can bind to MHC class II expressed on DCs and prevent activation (Liang et al., 2008).

### 1.1.8. T cell memory - Versatility for long-lasting protection

After the acute phase of the infection 5 to 10 % of the expanded effector T cell population, depending on the infectious agent, can give rise to memory T cells. According to mouse studies, it is generally believed that this pool of cells contains precursors of antigen-specific long-lived memory T cells, which can drive efficient protective immune responses upon re-exposure with the same pathogen (Wherry & Ahmed, 2004). In an adult individual memory T cells are the most abundant lymphocyte population in

the body. They constitute 35 % of the circulating T cell pool and between 80 - 90 % of all tissue-resident T cells, indicating that the majority of memory T cells are residing in different peripheral tissue sites.

In humans memory T cells can be first of all distinguished by the expression of the CD45RO isoform instead of expressing the CD45RA isoform as naïve T cells do. $CD45RO^{+}CD45RA^{-}$ memory T cells can be further categorized by functions and phenotypes. The expression of the lymph-node homing receptor CCR7 subdivides circulating memory T cells into $CD45RA^{-}CCR7^{+}$ central memory T cells ($T_{CM}$) and $CD45RA^{-}CCR7^{-}$ effector memory T cells ($T_{EM}$) (Sallusto, Lenig, Forster, Lipp, & Lanzavecchia, 1999). Due to expression of lymphoid homing receptors (CCR7, CD62L) $T_{CM}$ cells preferentially reside in the peripheral lymphoid organs, basically the lymph nodes. Upon antigen encounter they show a higher proliferative capacity than $T_{EM}$ cells, but lack immediate effector functions. Instead, they produce vast amounts of effector cytokines, predominantly IL-2 (see table 1.2), are effective in stimulating DCs and they are eventually able to differentiate into $T_{EM}$ cells (progression model for the generation of memory T cell subsets, (Farber, Yudanin, & Restifo, 2014; Sallusto, Geginat, & Lanzavecchia, 2004)). $T_{EM}$ cells express receptors for migration to sites of infections and peripheral tissues (e.g. CCR5, CCR3), where they can directly display their effector functions upon antigen re-encounter. They produce effector cytokines IFN-γ, TNF-α and IL-2 or other effector molecules (e.g. perforin) and are key mediators of the memory T cell response against re-infections and cancer (Pages et al., 2005).

Recently, a new memory T cell subset was identified in the peripheral blood of mice and humans, which shows 'stem-cell-like' capacities and is therefore called stem cell memory T cells ($T_{SCM}$) (Gattinoni et al., 2011; Y. Zhang, Joe, Hexner, Zhu, & Emerson, 2005). They appear "naive" as they are CD45RA but not CD45RO positive. Moreover, they express, amongst others, CD127 (IL-7 receptor α-chain), high levels of co-stimulatory molecules CD27 and CD28 and lymphoid homing receptors CCR7 and CD62L. $T_{SCM}$ cells have a high proliferative and self-renewing potential. Moreover, they are described to be 'multi-potent', because they can further differentiate into other (memory) T cell subsets. Importantly, in the field of cancer immunotherapy this T cell subsets is discussed as valuable new tool for adoptive T cell therapies (Gattinoni, Klebanoff, & Restifo, 2012).

**Table 1.2: Major phenotypic and functional properties of human circulating and tissue-resident memory T cell subsets.** Expression levels of recall cytokines: +: low, ++: medium, +++: high. This table is adapted from (Farber et al., 2014)

| | Circulating memory T cells | | | Tissue-resident memory T cells | |
|---|---|---|---|---|---|
| | $T_{SCM}$ cells | $T_{CM}$ cells | $T_{EM}$ cells | $T_{RM}$ cells | $CD103^{+}$ $T_{RM}$ cells |
| **CD45RA** | + | - | - | - | - |
| **CCR7** | + | + | - | - | - |
| **CD69** | - | - | - | + | + |
| **CD103** | - | - | - | - | + |
| **IL-2** | +++ | +++ | ++ | +/- | +/- |
| **IFN-γ** | + | ++ | +++ | +++ | +++ |
| **TNF-α** | + | ++ | +++ | +++ | +++ |

Also only within past several years, another research focus was set on tissue-resident memory T cells ($T_{RM}$). They are not circulating and instead reside in peripheral tissue sides, like the lungs, skin, and the bone marrow (Clark et al., 2012; Teijaro et al., 2011). As shown in table 1.2 they distinguish from circulating memory T cell sub-populations through the expression of the early activation marker CD69 (although in humans $T_{EM}$ cells found in spleen and LN are also described to express CD69). CD103 (the epithelial cell-binding αEβ7 intergrin) expression by $T_{RM}$ cells seems to be specific for certain tissues (skin, lungs and BM in mice), indicating tissue-specific signatures in the phenotypes of $T_{RM}$ cells. $T_{RM}$ cells are probably highly compartmentalized tissue-specific populations tailored to protect the host against typical pathogens invading the respective tissue type and are shown to rapidly respond to their antigens upon re-encounter in a multi-functional manner (reviewed in (Farber et al., 2014)).

## 1.2. Cancer

Due tremendous medical achievements and increasing health standards all over the world the landscape of leading causes of death changed dramatically throughout the last century. In developed countries infectious diseases have been replaced by other causes of death, namely cardiovascular diseases followed right away by caner. According to the German “Kerbsatlas” (DKFZ, 2012) cancer is the second most common cause of death for both genders in Germany. Worldwide cancer accounted for 8.2 million deaths in 2012 (WHO 2014, Globocan 2012, IARC) and the WHO is estimating that annual cancer cases will rise from 14 million in 2012 to 22 within in the next two decades. Strikingly, the WHO further denotes that 60 % of world’s total new annual cases will occur in less developed countries (Africa, Asia, Central and South America).

Cancer is often referred to as a disease of advanced age. An indeed the incidences of most cancer entities increase with age. Taking into consideration that the mentioned medical progress also accounts for a steadily increasing life expectancy cancer became a growing major public health problem (Jemal et al., 2011; Soerjomataram et al., 2012).

It almost appears cynical, now that mankind mostly defeated one of its major tormentors, infectious diseases like the plague or small pox, it has to struggle with yet another ancient enemy, who was hiding behind the previous one until its time came. And obviously this enemy has more manifold weapons and more inventive strategies to combat the attempts to defeat it. Siddhartha Mukherjee is explicitly right by calling cancer “the emperor of all maladies” in the title of his biography about this disease.

Several characteristics distinguish cancer from other diseases and are causative for substantial treatment difficulties. Cancer is in fact a general term for a large group of diseases comprising the formation of neoplasms or malignant tumors originating from any part of the body (WHO 2014). Tumors are formed by abnormal cells that grow unlimited beyond their normal boundaries. In that way they can invade adjacent tissue and spread to other organs, a process referred to as metastasis. An overwhelming burden of metastasis is the major cause of death from cancer (WHO 2014). In other terms cancer is an abnormal version of the body’s own self. To define the traits which distinguish cancerous cells from normal tissue and mechanisms underlying the formation of abnormalities are considered to be the key for successful treatment of cancer. And indeed, throughout the last decades the fog is lifting and cancer might be best defined on a molecular level as a disease of genes. Malignant transformation of normal to abnormal cells is underlying an accumulation of genetic alterations in a multi-step process.

Hanahan and Weinberg formulated in the year 2000 the hallmarks of cancer (Hanahan & Weinberg, 2000) describing six major capabilities which cells are acquiring during the malignant transformation process. The hallmarks are: sustained proliferative signaling, evading growth suppression, resisting cell death, enabling replicative immortality, inducing angiogenesis and activating invasion and

metastasis. In 2011 they added two more emerging hallmarks to the list (Hanahan & Weinberg, 2011), which are deregulation of cellular energetics and circumvention of immune destruction. They are further connecting lines of evidence to two “enabling characteristics” which all hallmarks of cancer underlie. The first characteristic is genomic instability and accumulation of mutations, which are accounting for each other and accelerating the acquisition of a malignant phenotype. The second characteristic is inflammation which is fostering the hallmarks. Obviously, cancer is closely interwoven with functions of the immune system and this complex interplay will be discussed in the next section. During the last decade another malicious characteristic of cancer was revealed. Tumors are able to recruit non-transformed cells in their surrounding and reprogram them to create favorable conditions for tumor growth. Therewith, these corrupted normal cells create a “tumor microenvironment” that contributes to the acquisition of the hallmark traits.

Due to its complexity only some of the important features of cancer can be discussed circumstantially in the context of the presented work. Choosing the examples of colorectal and pancreatic cancer unique molecular patterns will be highlighted which we consider to be potential opportunities for targeted therapy.

Besides lung cancer and gender specific cancers (like breast and prostate) colorectal cancer belongs to the most prevalent cancer types in the world (Figure 1.6). Pancreatic cancer is less common but more fatal. Interestingly, for the most common subtypes of these tumor entities, pancreatic adenocarcinoma and colorectal adenocarcinoma, fairly similar multistep processes of tumorigenesis are suggested. Moreover, somatic mutations in the oncogene *Kras* and the tumor suppressor *Tp53* seem to be crucial for both processes.

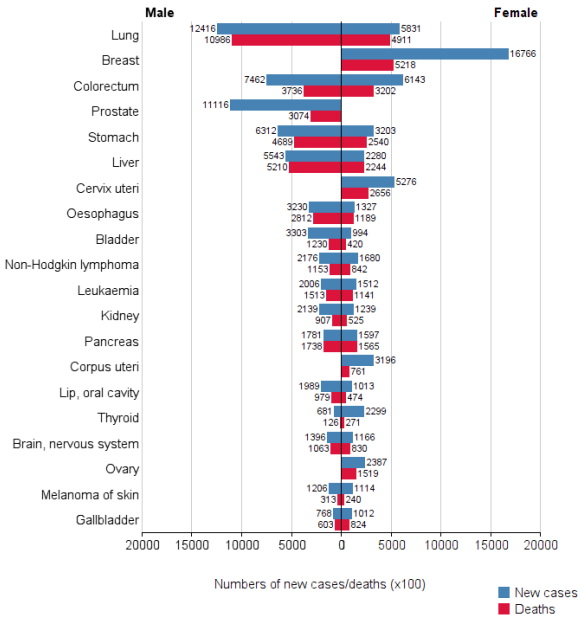


**Figure 1.6**: Dual multi-bar chart of **cancer incidence and mortality** of the top 20 most common cancer entities in whole world population according to gender in the year 2012 (WHO 2014, GLOBOCAN 2012).

### 1.2.1. Mutations in oncogenes and tumor suppressor genes

As indicated above one of the major achievements of the last century in cancer research was to define cancer as a genetic disease. Human cancers are genetically instable showing aneuploidy (changes in chromosomal numbers), translocations, inversions and deletions of parts of chromosomes or whole chromosomes (Lengauer, Kinzler, & Vogelstein, 1998). This can lead to phenomena like gene amplifications and loss of heterozygosity (LOH). Chromosomal translocation for instance can create oncogenes by fusion of two genes. The most famous example is the oncogene *BCR-ABL* on the Philadelphia chromosome in chronic myeloid leukemia (CML) (Rowley, 1973). Gene amplification of a non-mutated gene can cause an oncogenic phenotype simply by heavily increased copy number-caused over-expression (10 to 100 copies are possible). LOH or "homozygous deletion" generally affects tumor suppressor genes. One allele of a tumor suppressor gets lost due to chromosomal deletion and the second one carries an inactivating point mutation which is resulting in complete loss of tumor suppressive activity. Indeed, point mutations make up the vast majority of genetic alterations throughout human cancers and most probably these small alterations are causative for the more profound chromosomal aberrations by inactivating major components of DNA repair mechanisms. It is believed that cancer cells can only cope with this massive genetic chaos because of defects in DNA maintenance pathways which would normally trigger cells death due to severe DNA damage (Vogelstein et al., 2013).

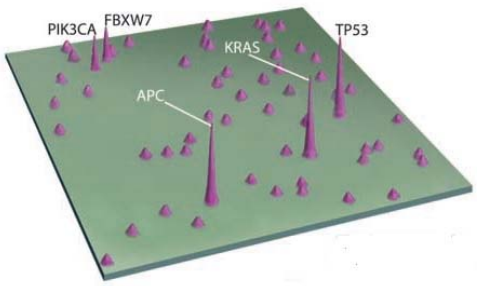


**Figure 1.7**: **Two-dimensional map of a CRC genome landscape**. "Mountain" genes (*Kras*, *APC*, *Tp53*) are mutated in a large number of tumors, whereas "hill" genes are mutated infrequently. This figure is taken from (Wood et al., 2007).

Revolutionary progress in sequencing technologies throughout the last ten years made it possible to detect somatic point mutations in a high-throughput manner by sequencing the exomes or whole genomes of numerous tumors of different cancer types. Through analysis of these data, B. Vogelstein and colleagues introduced the picture of a cancer genome landscape with mutated gene-mountains and hills as shown for colorectal cancer in figure 1.7 (Wood et al., 2007). Hills represent genes which are infrequently mutated and mountains stand for genes which are altered in a high percentage of tumors. The genes accounting for the mountains (roughly 140 up to date) can promote or drive tumorigenesis in case of being mutated. This is why mutations altering driver gene functions are also referred to as driver mutations. Infrequently mutated genes carry accordingly passenger mutations, because their altered

activity does not provide a selective growth advantages for the tumor. A tumor typically comprises two to eight driver mutations and corresponding driver genes can be classified in 12 signaling pathways regulating the three major cellular processes of differentiation, survival and genome integrity (Vogelstein et al., 2013).

In 2013 Campbell, Stratton and colleagues made the effort to analyze whole genome sequencing data from more than 7'000 cancers to gain insight into the processes leading to somatic mutations (Alexandrov et al., 2013). They could identify 20 distinct combinations of mutation types which they termed mutational signatures and some of which were present in many cancer classes and other were unique for single cancer entities. The origin of many signatures remained hidden, whereas some could be linked to the age of the cancer patient at diagnosis and others were associated with defects in DNA maintenance or exposure to mutagens. Moreover, cancers which are known to be caused by environmental exposure to mutagens, like tobacco smoke in lung cancer and UV light exposure in skin cancer, show among the highest numbers of somatic mutations as can be seen in figure 1.8 (Pfeifer, 2010; Vogelstein et al., 2013). Also cancers with known defects in the DNA mismatch repair machinery (Pena-Diaz et al., 2012), like colorectal cancer, acquire a high numbers of somatic mutations.

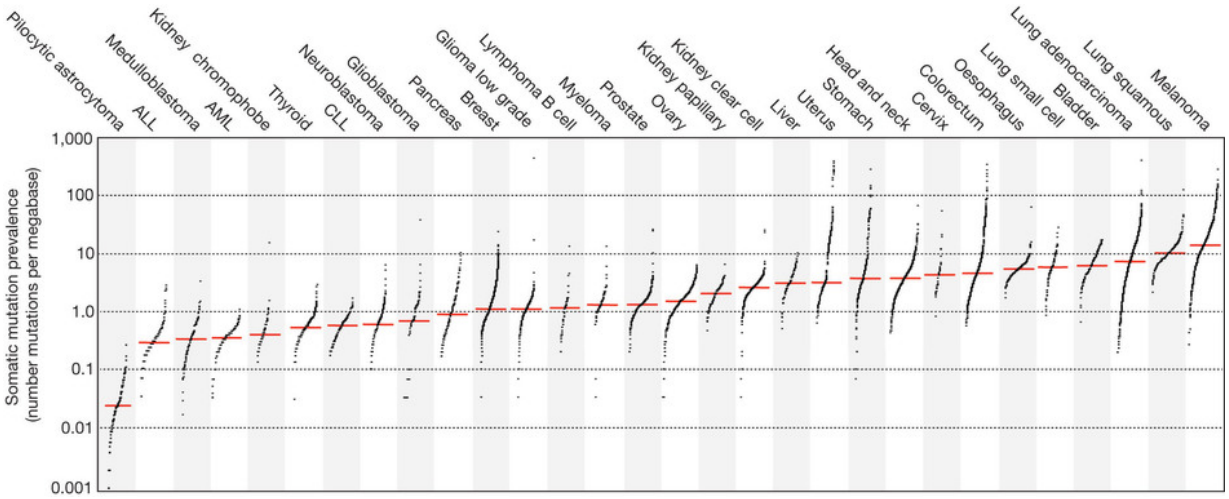


**Figure 1.8**: **Prevalence of somatic mutations in different human tumor entities**. Every dot represents one tumor sample and the red lines the median numbers of mutations found in the respective cancer type (ALL: acute lymphoblastic leukemia, AML: acute myeloid leukemia, CLL: chronic lymphocytic leukemia). This figure is adapted from (Alexandrov et al., 2013).

In this context cancer development can be also regarded as an evolutionary progress underlying the Darwinian principles: increasing genetic and phenotypic diversity through acquisition of inheritable genetic variations (e.g. a new mutation passed from one individual cancer cell clone to its progenies) and ensuing selection (e.g. through the immune system or chemotherapy) (Stratton, Campbell, & Futreal, 2009). This process is considered to be the leading course of the observed complex genetic diversity of cancer which is manifested in intra-tumor, inter-metastatic, intra-metastatic and of course inter-patient heterogeneity. C. Swanton nicely demonstrated intra-tumor heterogeneity and branched evolution for renal cell cancer by multi-region sequencing of different primary tumor regions and metastasis from

individual patients (Gerlinger et al., 2012). According to his results Swanton suggests a trunk-branch model of intra-tumor heterogeneity in which the developing tumor is considered as a growing tree with different levels of complexity. Simplified, the first level of complexity, the trunk of the tree, comprises ubiquitous, founding driver mutations. The following levels, the sprouting branches representing different regions within one tumor, harbor heterogeneous ("private") mutations. These mutations are rather passenger mutations which may become important under distinct selective pressure (e.g. chemotherapy, lack of nutrients) and then provide a fitness benefit for those clones. Moreover, there is the possibility that under changing environmental conditions passenger mutations could either replace driver mutations from the trunk of the tree or become additional driver mutations (Swanton, 2012; Yap, Gerlinger, Futreal, Pusztai, & Swanton, 2012). Total replacement of trunk driver mutations is possible but seems be a rather rare event. Therefore, Swanton further speculates that trunk driver mutations may present more robust therapeutic targets. We share Swanton's rating concerning the therapeutic potential of early driver mutations. This is why we decided to target mutated genes which are known drivers for colorectal and pancreatic tumorigenesis.

### 1.2.2. *Kras* and *Braf* – two prototypical oncogenes

The first gene proved to have a tumorigenic activity was a viral gene called *v-Src* (found in the chicken Rous' sarcoma virus) coding for a tyrosine kinase. Genes with the potential to transform cells and therewith contribute to development of cancer were termed oncogenes. For the two researches J.M. Bishop and H.E. Varmus in the late seventies of the last century it was puzzling to find a homolog of the *Src* oncogene as a fixed constituent in the normal genome of vertebrate cells (Oppermann, Levinson, Varmus, Levintow, & Bishop, 1979; Sheiness & Bishop, 1979). They concluded that the virus must have kidnapped the vertebrate's c-Src gene earlier in evolution. As the human *c-Src* obviously displayed no oncogenic activity but an altered, mutated viral version did, they termed c-Src a proto-oncogene (Stehelin, Varmus, Bishop, & Vogt, 1976).

Conclusively, mutations can activate proto-oncogenes to become cancer-promoting oncogenes which are constitutively active or displaying an altered activity compared to their wild-type (wt) counterparts. This is why a mutated oncogene is often compared to a stuck accelerator in a car. Generally, one allele with an activating somatic mutation is sufficient to unfold an oncogenic effect. Next to mutations also chromosomal translocations or gene amplification can activate oncogenes, as mentioned before. Sometimes, due to chromosomal translocation, a proto-oncogene is rearranged in juxtaposition to enhancer and other activating promoter elements which account for an increased transcriptional activity. Proto-oncogenes typically encode for genes that are central players in control of cell proliferation, apoptosis or both. According to their physiological function they can be broadly grouped into classes: transcription factors, chromatin remodelers, growth factor receptors, signal transducers, and apoptosis regulators (Croce, 2008).

Actually, gene products of oncogenes are often protein kinases in central signaling pathways with an altered, hyperactive activity. In this regard, the two oncoproteins, Kras and Braf, on which this work is focusing on in means of a targeted immunological anti-cancer approach, are prototypical oncogenes.

The *Kras* gene (originally named *v-Ki-ras2*, for Kirsten rat sarcoma viral oncogene homolog) encodes for a small GTPase and was one of the first identified proto-oncogenes (Ellis et al., 1981; McGrath et al., 1983). *Kras* is the most important isoform of the *ras* family of small GTPases in the context of cancer. Ras proteins are crucial molecular switches which couple receptor activation to downstream signaling pathways (nicely review in context of hyperactive mutated *Ras* in (Schubbert, Shannon, & Bollag, 2007)). These pathways regulate proliferation, differentiation and survival, highlighting ras proteins as important regulators of cell fate. Ras proteins cycle between a GDP-bound inactive and a GTP-bound active state. The transition between the two states is strictly regulated by GAPs (GTPase activating proteins) which are able to influence ras intrinsic GTPase activity. Most somatic missense mutations found in oncogenic Kras are activating mutations which impair the hydrolysis form GTP to GDP (GTPase activity) and lead to the resistance to GAPs, resulting in accumulation of active, GTP-bound Kras. As pointed out in figure 1.9 A the hot-spot mutations sites within the *Kras* gene are located at positions G12, G13, and Q61 in the G domain. Pioneering studies from the 1980s showed that mutations at position G12 are most prevalent (Burmer & Loeb, 1989) and account for both impaired intrinsic GTPase activity and resistance to GAPs. Moreover, certain G12 amino acid substitutions seem to be of different quality, as it was shown *in vitro* that G12V and G12R displayed stronger transforming phenotypes compared to G12S and G12D substitutions (Seeburg, Colby, Capon, Goeddel, & Levinson, 1984).

The link between oncogenic Kras and our working hypothesis is the idea that mutations in oncogenes distinguish cancer cells from normal cells. Hence, oncogenic Kras could make cancer cells visible and attackable by T cells, if mutated oncogene-derived epitopes are presented by the tumor cell. Indeed, Kras is a suitable candidate to target, as mutations are found in ~ 30 % of human cancers with an especially high incidence for the tumor entities we are interested in. According to the COSMIC database for somatic mutations in cancer (from the Sanger Institute, *COSMIC v69 Release*, http://cancer.sanger.ac.uk/cancergenome/projects/cosmic/, (Bamford et al., 2004)) *Kras* mutations are found in 70 % of pancreatic cancers and in 36 % of adenocarcinomas of the colon.

Our second oncogenic target is a direct signaling interaction partner of Kras. As shown in figure 1.9 C the 'Raf-mitogen-activated-signal regulated kinas-kinase (MEK)-extracellular signal-regulated kinase (ERK)', short Raf-MEK-ERK-pathway, is one of the most important downstream effector pathways regulated by ras proteins and as a MAP-kinase pathway involved in cell proliferation, survival and differentiation (reviewed in (Roberts & Der, 2007)). The *Braf* gene codes for a serine/threonine-protein kinase, which gets activated through interaction with Ras-GTP to phosphorylate downstream targets (e.g. MEK). Somatic missense mutations predominantly occur in the kinase domain of Braf (see figure 1.9 B), whereat the V600E substitution is accounting for ~ 80 % of all mutations found (Davies et al., 2002). The

amino acid V600 is situated in the activation loop of the kinase domain and the gain-of-function substitution to glutamic acid renders oncogenic Braf constitutively active, independent from activation through Ras. *Braf* mutations are most frequent in melanoma (incidence of 43 %) and are found in 10.7 % and 1.4 % of adenocarcinomas of the large intestine and the pancreas, respectively (COSMIC database *v69 Release*). Recently, targeted therapy of oncogenic Braf caused a little sensation as the small molecule inhibitor vemurafenib was approved the first drug for Braf V600E mutated metastatic melanoma by the FDA and the European Union (Bollag et al., 2012).

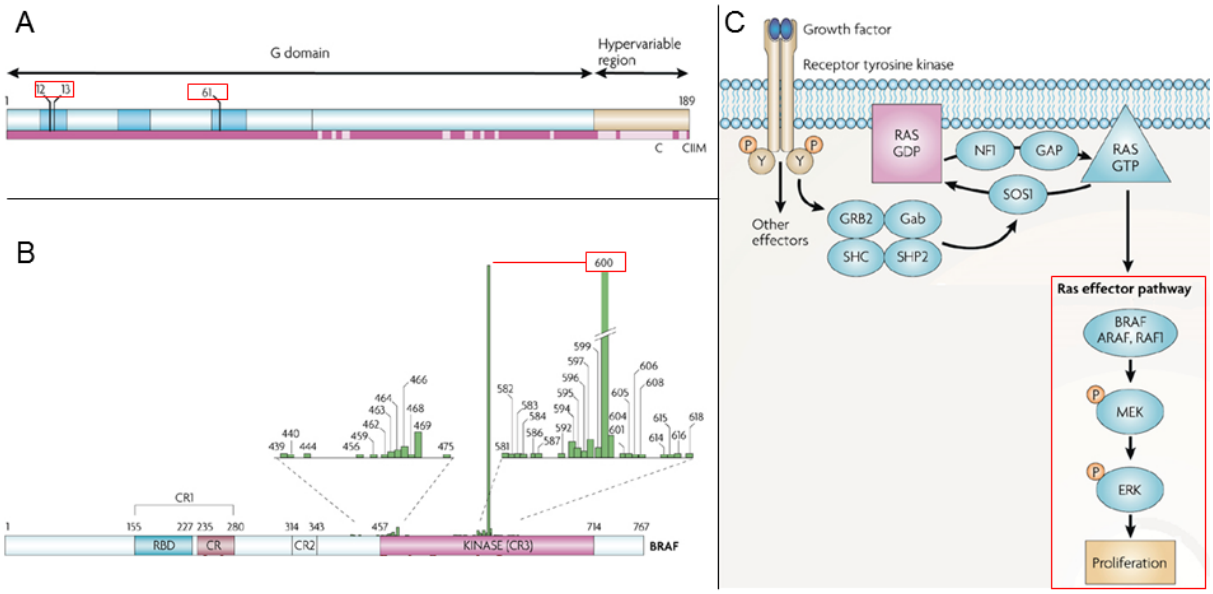


**Figure 1.9**: **Domain structure of Kras and Braf and their physiological connection**. **(A) Domain structure of Kras** (isoform KRAS4A): The G domain contains the phosphate binding loop (P loop) which binds the γ-phosphate of guanosine triphosphate (GTP) and the switches I and II regulate the binding of Kras effectors and regulators. The hyper-variable region at the C-terminus comprises a key cysteine (C) CAAX motif (here CIIM) which is facilitating membrane location by being post-transcriptional modified through farnesylation (CIIM) and palmitoylation (C). The degree of homology with other ras family members is highlighted in the box at the bottom of the sketch, wherein conserved residues are displayed in magenta and variable residues in pink. Hot-spot mutations site are found at positions 12, 13 and 61 (red boxes). **(B) Domain structure and cancer mutations of Braf**. Green bars show locations of somatic mutations found in human tumors. The lengths of the bars represent the relative proportion of mutations at a certain residue. Mutations at residue V600 (red box) are found in over 90 % of tumors. RDB: Ras-binding domain, CR: cysteine-rich domain, CR2: serine- and threonine-rich regulatory domain, CR3: catalytic kinase domain. **(C) Simplified Ras/Braf signaling pathway**. Upon growth factor binding the receptor complex gets activated which can contain the adaptor proteins SHC (SH2-containing protein), GRB2 (growth-factor-receptor bound protein 2) and Gab (GRB2-associated binding). This complex can recruit SHP2 and SOS1 (son of sevenless homolog 1). SOS1 increases Ras-GTP levels by catalyzing the nucleotide exchange on Ras. Signaling is terminated through binding of GAP (GTPase-activating protein) / NF1 (neurofibromin) which accelerates the conversion of Ras-GTP to Ras-GDP (guanosine diphosphate). From all possible signaling pathways only the Braf-MEK-ERK cascade (a MAP kinase pathway) is sketched which often determines proliferation. MEK: mitogen-activated and extracellular-signal regulated kinase kinase, ERK: extracellular signal-regulated kinas, P: phosphate, Y: receptor tyrosine. This figure is adapted from (Schubbert et al., 2007)

### 1.2.3. *Tp53* – the ultimate tumor suppressor gene and guardian of the genome

Next to proto-oncogenes the human genome contains another group of genes whose activity can prevent cancer development. They were first categorized as growth-suppressing genes, so called tumor-suppressor genes. The first tumor-suppressor gene was identified in a rare childhood tumor, the retinoblastoma, and was accordingly called retinoblastoma (*Rb*) (Hollingsworth, Hensey, & Lee, 1993). It

was shown that both alleles of the gene have to be defect for retinoblastoma formation. Thus, compared to oncogenes, mutations in tumor suppressor genes abrogate or reduce their activity. To stay with the car metaphor: a mutated tumor suppressor is comparable to a dysfunctional brake. As pointed out for *Rb,* to abrogate tumor suppressor function the maternal and the paternal alleles have to be inactivated. In general this is achieved by loss of one allele through chromosomal deletion and an inactivating mutation in the remaining allele. Another mechanism is the phenomenon of haplo-insufficiency, meaning if one allele is lost the remaining one cannot compensate for the missing activity of the other (Santarosa & Ashworth, 2004).

An additional possibility how tumor suppressor genes can lose their function leads to the tumor suppressor *Tp53* which we chose to be one target in the presented work. Classically, *Tp53* can be inactivated by combined mutation and deletion as found for the inherited Li-Fraumeni syndrome. In many cancer cells, however, only one *Tp53* allele is mutated and the other is unaltered (Srivastava, Zou, Pirollo, Blattner, & Chang, 1990). Indeed, one mutant *Tp53* allele can exert a dominant negative effect by hampering wt p53 function. Mutated p53 proteins prevents the binding of wt p53 to the promoter regions of its target genes (Willis, Jung, Wakefield, & Chen, 2004), indicating that the *Tp53* gene encodes for a transcription factor. But p53 is not just a transcription factor; it is the crucial transcription factor regulating a manifold of processes which protect the cell from malignant transformation and to list all of its functions would go beyond the scope of this work. In a nutshell, p53 senses signals of genotoxic stress (DNA damage) and can regulate specific cellular responses. It activates DNA repair mechanisms, can lead to cells cycle arrest and senescence and in case of fatal DNA damage it induces apoptosis. All of these processes protect the cell from malignant transformation and led to the fact that p53 was referred to as the "guardian of the genome" (Lane, 1992). Recent studies, however, linked mutant p53 to further cellular processes associated with cancer by displaying gain-of-function (GOF) properties. These processes comprise the maintenance of stem cells, invasion, metastasis and interaction with the tumor microenvironment (reviewed in (Bieging, Mello, & Attardi, 2014) and (Solomon, Madar, & Rotter, 2011)).

As it already became clear, also the guardian of the genome's kryptonite are single nucleotide mutations, of which 80 % are found in the DNA-binding domain (DBD) clustering at six hot-spot mutation sites. As shown in figure 1.10 mutations can be qualitatively grouped into structural mutations, which alter the three-dimensional structure, and contact mutations, which interfere with DNA interaction (Cho, Gorina, Jeffrey, & Pavletich, 1994).

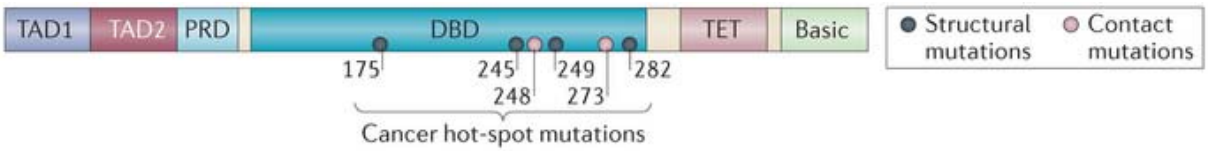


**Figure 1.10**: **Domain structure of the p53 protein with hot-spot mutation sites indicated**. TAD: transcriptional activation domain, PRD: proline-rich domain, DBD: DNA binding domain, TET: tetramerization domain, Basic: carboxy-terminal region rich in basic residues. This figure is adapted from (Bieging et al., 2014)

As for the oncogenes *Kras* and *Braf* we postulate that also mutated p53 sequences can serve as immunological targets for cancer therapy. In fact, mutated p53 is found in 50 % of all human cancers, which makes it the most frequently mutated cancer associated gene. Facilitating the IARC TP53 Database ((Petitjean et al., 2007), latest version R17, November 2013) we identified the most prevalent amino-acid substitutions found at the hotspot mutation sites of *Tp53* for CRC and pancreatic carcinoma. Interestingly, some of the chosen amino acid substitutions, namely R175H, G245S, R248W, R248Q, R273H (reviewed in (Bieging et al., 2014)), were linked to the GOF capacity of mutant *Tp53*.

### 1.2.4. Pancreatic Cancer

As sketched above pancreatic cancer is one of the most common cancer entities and it is still one of the most fatal cancers with an overall 5-year survival rate of only < 5 %. Several risk factors have been associated with pancreatic cancer. 20 % of cases can be attributed to cigarette smoking and it was shown that tumors from smokers accumulated more mutations than those of non-smokers. Similar to colorectal cancer there are dietary risk factors: high-fat diet as well as diets high in red meat and low in vegetables and fibers. Moreover, pancreatic cancer is more frequent in case of obesity, diabetes mellitus, chronic pancreatitis and male gender. The risk for pancreatic cancer increases with age and an earlier onset than 50 years of age is pointing towards a familial disposition. Indeed, 5 to 10 % of patients have a family history. Germline mutations in *BRCA2* (breast cancer 2, early onset), an important DNA-binding protein in the Faconi DNA repair pathways, and *CDKN2A* (cyclin-dependent kinase inhibitor 2A, coding for the p16 protein also known as Ink4A (inhibitor of cyclin-dependent kinase 4)), a cell cycle regulator, are correlated with inherited susceptibility to pancreatic cancer (reviewed in (Vincent, Herman, Schulick, Hruban, & Goggins, 2011)).

Basically, three distinct precursor lesions can give rise to ductal pancreatic adenocarcinoma. The best characterized precursor lesions are pancreatic intraepithelial neoplasias (PanIN) arising through noninvasive epithelial proliferations within in the smaller pancreatic ducts and accounting for 16-45 % of non-invasive pancreatic lesions. Equally frequent are intraductal papillary mucinous neoplasms (IPMN, ~ 50 % of resected pancreatic lesion), found in the larger pancreatic ducts often producing large amount of mucin. Less common mucinous cystic neoplasms (MCN, 16 % of pre-invasive lesion) are large mucin-producing lesions with a distinctive “ovarian-type” stroma typically encountered in women (reviewed in (Lennon et al., 2014)).

On the basis of genetic alterations and histological analysis of PanIN precursor lesions and invasive tumors a progression model for pancreatic adenocarcinomas is suggested. The progression from minimally dysplastic epithelium (PanIN grade 1A and 1B) to more severe dysplasia (PanIN-2 and PanIN-3) finally resulting in invasive carcinoma (Hruban et al., 2001) is paralleled genetically through accumulation of major driver mutations. As indicated in figure 1.11 activating mutations in the oncogenes *ERBB2* (coding for the Her/2neu protein – human epidermal growth factor 2) and *EGFR* (epidermal growth factor receptor) as well as in *Kras* (Kanda et al., 2012) are considered as the earliest genetic

events already occurring during a pre-neoplastic state and minimal neoplasia. In the following steps of pancreatic carcinogenesis tumor suppressor genes get inactivated through mutations and chromosomal events, starting with inactivating mutations of *CDKN2A* (coding for the Ink4A protein) in an early neoplastic state. While progressing to high-grade neoplasia finally resulting in invasive carcinoma *Tp53*, *SMAD4/DPC4* (deleted in pancreatic cancer, locus 4) and *BRCA2* are inactivated in the depicted order by mutations and LOH (progression model reviewed in (Bardeesy & DePinho, 2002) and (Hidalgo, 2010)). Moreover, the genetic alterations documented in invasive adenocarcinomas not only occur in PanIN lesions but are also partially found in IPMNs and MCNs.

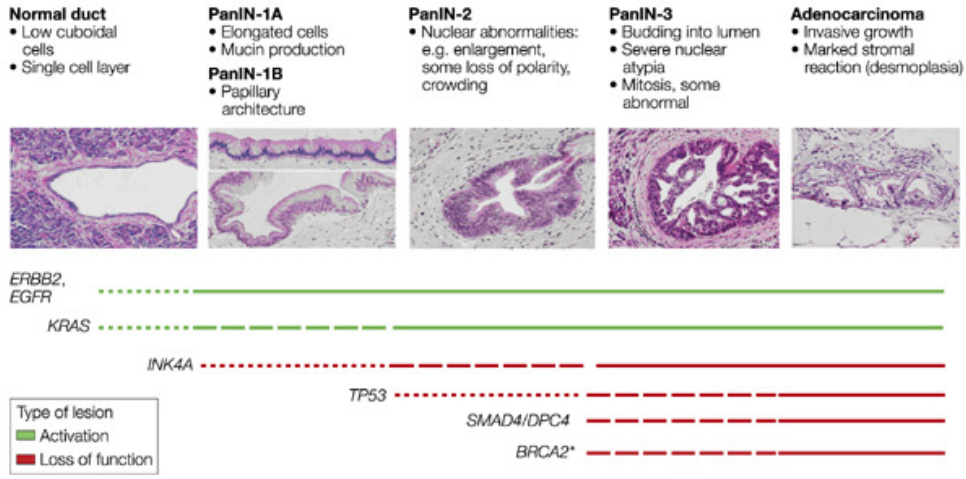


**Figure 1.11**: **Progression model of pancreatic cancer**. The stages and onsets of histo-pathologic and genetic alterations are displayed. The thickness of the lines corresponds to the frequency of the respective genetic mutation. This figure is adapted from (Bardeesy & DePinho, 2002)

Attributed to the circumstances that there are so far no reliable early detection strategies and that this disease is basically free of symptoms until a metastasized state, patients are diagnosed too late for a successful therapeutic intervention. The standard of care for local or resectable disease (10 % of cases) is chemotherapy with gemcitabine in an adjuvant prior and/or neoadjuvant setting post surgery. Locally advanced/unresectable and metastatic disease account for about 90 % of patients at diagnosis and the median survival are up to 20 and 4-6 month, respectively (Vincent et al., 2011). In these cases also gemcitabine is indicative for palliative care depending on the performance of the patients. In combination with gemcitabine, the only drug showing a small but significant effect in survival among advanced patients is the small-molecule inhibitor erlotinib acting against EGFR (Moore et al., 2007). Unfortunately, erlotinib therapy is possibly limited due to high frequencies of *Kras* mutations, which were shown to hamper the therapeutic benefit of EGFR inhibition for other tumors, like CRC for instance (Lievre et al., 2006). Obviously, there is space for improvement in therapy of pancreatic cancer and it became clear that mutations in *Tp53* and *Kras*, two of the candidates we chose for our targeted immune-therapeutic approach, are essential drivers in pancreatic carcinogenesis. One possible scenario arising from these facts is that immunological targeting of mutant *Kras* (*Tp53*) could complement erlotinib/gemcitabine treatment.

### 1.2.5. Colorectal cancer

According to WHO statistics colorectal cancer (CRC) is the third common tumor entity worldwide. It accounts for around 9 % of all malignancies and disease-specific mortality rate is ~ 33 % in the developed countries. The incidence of CRC increases with urbanization and industrialization and with advanced age accounting for the fact that 70 % of patients are over 65 years of age at diagnosis. An early onset under the age of 45 years is uncommon and points towards a genetic predisposition. As for pancreatic cancer CRC is more common in males and there are similar dietary risk factors: high-fat and red meat diet, inadequate intake of dietary fiber, and a high consumption of alcohol. Moreover, unhealthy lifestyle habits like smoking and a lack of physical exercise, with a causative link to the risk factors obesity and diabetes mellitus, account for an increased CRC risk. Patients with inflammatory bowel diseases (ulcerative colitis and Crohn's disease) have higher risk for CRC which is increasing with the duration of illness. Nearly 6 % of CRC cases underlie hereditary syndromes. The majority of hereditary cases are caused by the Lynch syndrome (also known as hereditary non-polyposis colorectal cancer (HNPCC)) and the familiar adenomatous polyposis (FAP) syndrome. Lynch-syndrome patients and FAP patients carry distinct genetic germline alterations. FAP patients show mutations in or loss of the tumor suppressor gene *APC* (adenomatous polyposis coli) and Lynch syndrome patients carry mutations in mismatch repair (*MMR*) genes (review in (Cunningham et al., 2010) and (Labianca et al., 2010)).

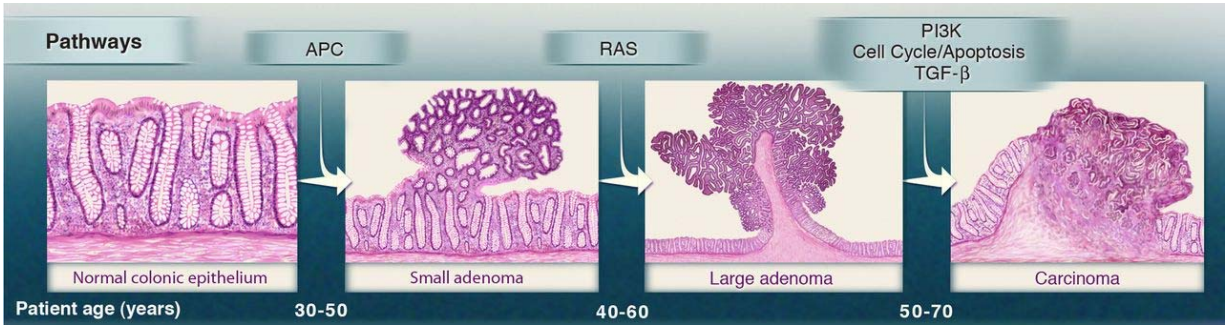


**Figure 1.12**: **Progression model of colorectal cancer**. Major signaling components driving colorectal carcinogenesis are indicated at the transitions between tumor stages. One of several genes encoding for signaling components in each pathway can be mutated. Depicted patient age stands for the time frames in which the driver genes are normally altered. (TGF-β: transforming growth factor-β). This figure is adapted from (Vogelstein et al., 2013).

Currently, there are two different models hypothesized how CRC could develop on a genetic basis reflecting two clinically distinct phenotypes of sporadic CRC (75 – 80 % of total CRC cases). The first model for colorectal carcinogenesis was introduced more than 20 years ago by Vogelstein and Fearon (Fearon & Vogelstein, 1990) and is comparable to the progression model of pancreatic cancer. It is also referred to as the adenoma-carcinoma sequence and describes the genetic alteration (mutations and chromosomal instabilities (CIN), like allelic imbalance (e.g. LOH) and aneuploidy) coinciding with histopathological progression from benign adenomas (polyps) to malignant carcinomas, as shown in figure 1.12. Early genetic events are the inactivation of *APC* trough mutations and LOH rendering the Wnt-signaling pathway (critically regulating the cell cycle) constitutively active. This is followed by activating mutations in *Kras*. The inactivation of tumor suppressors, like *Tp53* and *DCC* (deleted in colorectal

cancer) trough mutation and LOH during transition from large adenomas to carcinomas is promoting further genetic instability and deregulation of signaling cascades. The Vogelstein model applies to 85 % of sporadic CRCs, also called “CIN” or “suppressor” tumors. The remaining 15 % of cases are mechanistically correlated to the second model of colorectal carcinogenesis. These so called “mutator” tumors are characterized by huge accumulations of mutations in microsatellite sequences. Microsatellites are short tandem-repeat sequences which can be found all over the genome. Microsatellite instability (MSI) leads to frame-shift mutations and is attributed to defects in DNA mismatch repair genes (*MMR*s). Functional MMRs repair replicational errors made by the DNA polymerase in microsatellite sequences. Except MSI mutator tumors rarely show other genetic alterations. Colorectal cancer implicated genes which are affected by microsatellite instability are, for instance, *TGFβRII* or *APC* (reviewed in (Moran et al., 2010)).

The 5-year survival rate for colorectal cancers encouragingly increased throughout the last decades. Since the 1970 the 5-year survival rose by 9 % in both genders to ~ 60 %. This improvement is mainly attributed to early prevention efforts (colonoscopy screening starting at 50 years of age), a better understanding of the molecular mechanisms (see the paragraph above) and advances in postoperative follow-up treatment. The primary treatment for patient with potentially curable CRC is surgery. This is followed, depending on the staging, by chemotherapy. Adjuvant chemotherapy treatment is given to patients with a high risk for relapse (high-risk stage IIB and stage III TMN classification of colon cancer). Also for metastatic disease chemotherapy is standard of care to improve quality of life and survival, reduce tumor burden and lessen symptoms. Standard chemotherapy is a cocktail containing 5-floururcail (5-FU), leucovorin and oxiplatin (short FOLFOX) for 6 month. For metastatic disease additional targeted biological therapy with EGFR-inhibiting antibodies was established in the last decade. The EGFR-inhibiting monoclonal antibodies Cetuximab and Pantiumumab showed increase in progression-free survival even in patients with refractory disease to oxaliplatin. As indicated in the section about pancreatic cancer the response to anti-EGFR therapy is depending on the *Kras* mutation status of the patients treated. Kras is the major molecular switch downstream the EGF receptor (see figure 1.9). The effect of EGFR inhibition is invalid if the downstream signaling components (Kras, Braf) are rendered constitutively active through activating mutations. Consequently, the *Kras* mutation status is establishing as eligibility criteria for patients undergoing anti-VEGF therapy (review in(Labianca et al., 2010)). A similar connection is drawn to the mutations status of *Braf*, signaling downstream from Kras, as patients with V600E mutations showed a shorter progression free survival than patients with wt *Braf* (Di Nicolantonio et al., 2008). Actually, the patient cohort with *Kras* and *Braf* mutant tumors showing resistance to VEGF-therapy could constitute an optimal target group for the immune-therapeutic approach we are suggesting.

## 1.3. Interactions between cancer and the immune system

The interaction between cancer and the immune system is of an ambivalent nature. On the one hand (chronic) inflammation can be a driving force for the development of cancer and on the other hand immune effector functions are essential for tumor control. This ambivalence was recently integrated into the hallmarks of cancer by Weinberg and Hanahan. They state that inflammation fosters multiple hallmarks (enabling characteristic of cancer), whereas one emerging hallmark of caner is the avoidance of immune destruction (Hanahan & Weinberg, 2011). Indeed, research in the past two decades elucidated how cancer corrupts the main tasks of the immune system for its own benefit. Cancers display versatile features and mechanisms to circumvent immune recognition. Furthermore, cancer hijacks immune regulation to shut down anti-tumor immune effector functions (Cavallo, De Giovanni, Nanni, Forni, & Lollini, 2011). Again, underlining the ambivalence, the immune system could actively contribute in putting a Darwinian selection pressure on the emerging tumors, which favors the formation of immune-escape tumor variants. There are thick lines of evidence, that interaction with the immune system fundamentally influences the whole course of the disease cancer. Schreiber and colleagues tried to connect these conflicting interpretations in formulating the cancer immunoediting hypothesis (Dunn, Old, & Schreiber, 2004b).

### 1.3.1. The Cancer immunoediting hypothesis

The cancer immunoediting hypothesis is based on the older conceptual framework of immunosurveillance, which was first phrased by Burnet and Thomas already in the 1950s. According to observations they made in mice they postulated that a functional immune system is crucial to prevent the development of cancer (Burnet, 1957). Schreiber's group found that the immune system seems to be able to shape the immunogenicity of tumors, and therewith is not only controlling tumor quantity but also tumor quality in terms of immunogenicity (Shankaran et al., 2001). Hence, the immunoediting hypothesis is an extension of the immunosurveillance concept (R. D. Schreiber, Old, & Smyth, 2011). The cancer immunoediting process is divided into three distinct phases, termed the three "E"s: elimination, equilibrium and escape. During the elimination phase the innate and adoptive immunity successfully cooperate by detecting and eliminating transformed cells. Rare tumor cell variants possibly survive immune destruction and enter the equilibrium phase. Herein, basically the adoptive immune system is assumed to be responsible to prevent the outgrowth of the tumor by keeping transformed cells in a functional state of dormancy (Aguirre-Ghiso, 2007). In this phase, however, immunoediting of the tumor cells occurs, presumably because the immune system imposes a selection pressure in favor for tumor cells with immunoevasive features. New characteristics of tumor cells arise from additionally acquired mutations, which in turn accumulate due to increasing genomic instability (see also section 1.2). In the last phase tumor cells escape from immune control which leads to progressive tumor growth and clinical manifestation. The escape could be a consequence of immunoediting and/or increasing immune suppression by the developing tumor.

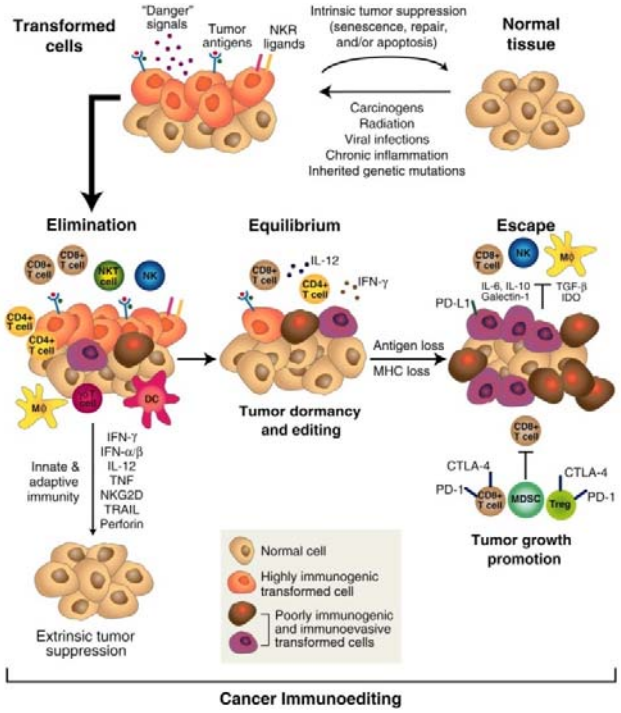


**Figure 1.13**: **The multi-step process of the cancer immunoediting concept**. Immunological constituents which interact with the developing tumor throughout the three phases of the immunoediting process are indicated. During the elimination and equilibrium phase the immune system can eliminate and control tumor outgrowth, respectively. Upon the escape phase the tumor has acquired traits to escape from immune control and actively suppress immune effector functions. This figure is taken form (R. D. Schreiber et al., 2011).

Figure 1.13 sketches the numerous mechanisms by which the immune system can eliminate tumor cells. Briefly, little is known about how the immune system can sense emerging transformed cells. For sure tumor cells can be recognized by T cells through the presentation of tumor antigens on MHC molecules. T cells, especially CTLs, can kill tumor cells with their whole arsenal of cytotoxic mechanisms (e.g. FasL expression, secretion of cytotoxic granules). Expression of NKG2D ligands by tumor cells can lead to NK and γδ-T cell activation. Moreover, T cells and NK cells can secrete IFN-γ, which can inhibit tumor cell proliferation and angiogenesis. Danger signals, like type I IFNs and damage-associated molecular pattern molecules (DAMPs) expressed by malignant cells could contribute to the recruitment of innate and adaptive immune cells. Dendritic cells can uptake dying tumor cells and cross-present tumor antigens to T cells. Innate immune cells, like macrophages (M1) and granulocytes, are also described to contribute substantially to the anti-tumor immune response by for instance secreting cytokines like TNF-α and IL-12 or reactive oxygen species (ROS) (reviewed in (Dunn, Old, & Schreiber, 2004a; Mittal, Gubin, Schreiber, & Smyth, 2014). During the equilibrium phase $CD4^+$ and $CD8^+$ T cells and the cytokines IFN-γ and IL-12 seem to counterbalance immunosuppressive mechanisms and keep tumor cells in dormancy (Koebel et al., 2007). The mechanisms tumors acquire to escape immune control are versatile and are discussed in the next chapter.

### 1.3.2. Cancer immune escape mechanisms

Cancers are shown to be resourceful in their abilities to circumvent immune recognition and destruction. Extensive research up to date resulted in an ever growing list of cancer immune escape mechanisms, which are too numerous to be discussed here. Therefore, the focus is set on phenomena which appeared to be crucial for the presented work.

Tumors display increased survival and resistance to hostile conditions. This can be attributed, besides the altered cellular survival programs, to the ability of tumors to remodel their environment in favor of their own benefit. Tumors themselves can exert direct immunosuppression, by up-regulation of the inhibitory molecule PD-L1. Furthermore, tumor cells can produce immunosuppressive cytokines, like TGF-β and VEGF (vascular endothelial growth factor), or molecules like IDO. This can lead to the recruitment of regulatory immune cells, which inhibit effector T cell responses. Next to myeloid-derived suppressor cells (MDSCs) and M2 polarized macrophages, regulatory T cells are attracted by tumors (reviewed in (Mittal et al., 2014; Vesely, Kershaw, Schreiber, & Smyth, 2011)). $T_{reg}$ cells are described to display their whole spectrum of suppressive mechanisms (described in chapter 1.1.7.) to inhibit effector T cells infiltrating the tumor or the tumor microenvironment.

Loss of tumor antigen presentation by tumor cells is a well characterized tumor escape mechanism, which can occur due to three different reasons. First, the expression of MHC class I molecules can be down-regulated or completely lost. Down-regulation of MHC class I molecules is often found in *Ras*-oncogene driven tumors and can be restored upon IFN-γ treatment (El-Jawhari et al., 2014). Aberrant processing through structural alterations (mutations, deletions, LOH) or deregulation of components of the antigen-processing and loading machinery (e.g. mutations in the TAP proteins) are the second reason for impaired presentation of tumor antigens (Seliger, 2012). The last cause is the appearance of tumor cell variants which lack the expression of strong rejection antigens.

The loss of strong rejection antigens by tumor cells might be a direct consequence of the cancer immunoediting progress. Mouse studies by Schreiber and colleagues provided evidence for this notion. In an elegant series of experiments tumors were chemically induced through administration of 3-methylcholanthrene (MCA) in immune-deficient (*Rag2*$^{-/-}$) and immune-competent mice. Thereby, tumors from immune-deficient hosts (unedited tumors) appeared to be more immunogenic than similar tumors from immune-competent mice (edited tumors). This was shown by spontaneous rejection of some subclones of unedited tumors when re-transplanted into immune-competent hosts (regressor tumors) (Shankaran et al., 2001). In follow-up experiments they could identify a rejection antigen of a regressor tumor by exome analysis, which was harboring an epitope recognized by T cells. CTL recognition of this antigen (mutated spectrin-β2) led to rejection of the regressor tumors in immune-competent hosts. However, in some mice the tumor did grow out and analysis of these “regressor-progressor” tumors showed that they no longer expressed the rejection antigen (Matsushita et al., 2012). Similar observations were made by DuPage in a *Kras*/*Tp53* oncogene driven sarcoma mouse model and artificially introduced

ovalbumin epitopes, which served as rejection antigens (DuPage, Mazumdar, Schmidt, Cheung, & Jacks, 2012). Moreover, Schreiber could show that all of his progressor and regressor clones, derived from a single parental cell line, were genomically related, which implies that they share common driver mutations. The strongly immunogenic mutated rejection antigen, however, maybe presents a passenger mutation as the loss of expression was tolerable or even beneficial for the respective tumor clones. This reinforces the before mentioned thought, that targeting driver mutations by cancer immunotherapy reduces the risk of selecting escape variants and circumventing at least partially the problem of tumor heterogeneity.

The presented work made use of MCA induced tumors. Injection of MCA subcutaneously into mice leads to the development of sarcomas within three to four month. These sarcomas can be identified as originating from fibroblasts by vimentin positive staining (Wakita et al., 2009). More importantly, MCA-induced tumors show high frequencies of *Kras* mutations at the codon G12 (Fritz, Dwyer-Nield, Russell, & Malkinson, 2010), which identified them as an attractive model system for our work.

### 1.3.3. Tumor antigens – cornerstones of cancer immunotherapy

The expression of antigens which discriminate tumor from non-transformed cells and the recognition of those by T cells forms the basis of cancer immunotherapeutic approaches (Coulie, Van den Eynde, van der Bruggen, & Boon, 2014). Tumor antigens were first discovered as rejection antigens in mouse tumor transplantation experiments. Today many tumor antigens are known for both humans and mice and due to the revolutionary progress in sequencing techniques their number is steadily increasing. Tumor antigens can be grouped according to their tumor specificity.

The first group of highly tumor specific antigens (TSAs) comprises three subgroups. Strictly tumor-specific antigens are mutated and oncoviral antigens. Mutated antigens, as already discussed in the previous chapter, can be derived from mutations in oncogenes and tumor suppressor genes and, as we just learned, can be targets of immunoediting due to their high immunogenicity. Also oncogenes derived from chromosomal translocations, like BCR-ABL, belong to this group of TSAs. Oncoviral proteins are exclusively expressed by respective oncovirus-driven tumors and are not shared with normal tissue, either. Extensively studied examples are the transforming proteins E6 and E7 from human papilloma virus type 16 (HPV type 16) one causative strain for cervical carcinoma (Ressing et al., 1995). The third group is not strictly tumor-specific. Cancer germline-antigens (also kwon as cancer-testis antigens) are not expressed in normal tissue with exception of male germline cells and trophoblastic cells. However, these cells do not express MHC molecules and therefore cannot present antigens, which makes them invisible for the immune system. Germline-antigens are re-expressed by many tumors. The members of the MAGE (melanoma antigen) gene family were the first antigens discovered in this group and are often expressed in melanomas and breast cancer (van der Bruggen et al., 1991). Another famous example is NY-ESO-1 (New York, Esophageal Squamous Cell Carcinoma-1), which is expressed in a variety of tumors including melanoma (Gnjatic et al., 2006).

Tumor associated antigens (TAAs) form the second big category of tumor antigens with a rather low tumor specificity. Herein again three subgroups can be distinguished. Differentiation antigens are expressed only in particular types of tissues, often the tissue from which the tumor originates. Again melanoma, a very immunogenic tumor, is the best studied example. Tyrosinase and Melan-A (melanoma antigen recognized by T cells 1, also known as MART-1) are also expressed in normal melanocytes and high frequencies against epitopes derived from these TAAs can be found in melanoma patients. The growth factor HER2/NEU is the best known for its role in breast cancer but is also overexpressed in many other epithelial tumors (e.g. ovarian carcinoma) and represents a prototypical overexpressed antigen (Fisk, Blevins, Wharton, & Ioannides, 1995). The last subgroup of TAAs might be the most tumor specific one as it comprises proteins which show abnormal posttranslational modifications. The underglycosylated mucin, MUC-1, is expressed on most adenocarcinomas, like breast and pancreatic cancer (Vlad, Kettel, Alajez, Carlos, & Finn, 2004).

The group of van der Bruggen established a database of T cell-defined human tumor antigens. Herein peptides derived from tumor antigens which are expressed by tumor cells and recognized by T cells are listed. Potential peptides and validated peptides are distinguished. Validated peptides have to fulfill six requirements, among these the identification of the presenting HLA molecule, prove of recognition by T cells and evidence for natural processing by tumor cells ((Vigneron, Stroobant, Van den Eynde, & van der Bruggen, 2013), http://www.cancerimmunity.org/peptide/). In table 1.3 validated epitopes for *Tp53*, *Kras* and *Braf* are listed. The fact that mutated epitopes within our target antigens could be identified in different HLA contexts shows immunological feasibility to elicit T cell responses against these mutated antigens.

**Table 1.3**: **List of validated mutated and non-mutated epitopes in *Tp53*, *Kras* and *Braf***. Information taken from (http://www.cancerimmunity.org/peptide/)

| Gene/ Protein | Tumor | HLA | Peptide | Position | Reference |
|---|---|---|---|---|---|
| ***Braf*** | melanoma | DR4 | EDLTVKIGDFGLATEKSRWSGSHQFEQLS | 586-614 | (Sharkey, Lizee, Gonzales, Patel, & Topalian, 2004) |
| ***Tp53*** | Head & neck squamous cell carcinoma | A2 | VVPCEPPEV | 217-255 | (Ito et al., 2007) |
| ***Kras*** | Pancreatic adeno-carcinoma | B35 | VVVGAVGVG | 7-15 | (Gjertsen, Bjorheim, Saeterdal, Myklebust, & Gaudernack, 1997) |
| ***Tp53*** | Ubiquitous (low level) | A2 | LLGRNSFEV | 264-272 | (Ropke et al., 1996) |
| | | A2 | RMPEAAPPV | 65-73 | (Barfoed et al., 2000) |
| | | B46 | SQKTYQGSY | 99-107 | (Azuma et al., 2003) |
| | | DP5 | PGTRVRAMAIYKQ | 153-165 | (Fujita et al., 1998) |
| | | DR14 | HLIRVEGNLRVE | 193-204 | (Fujita et al., 1998) |

An interesting aspect to discuss it this context is immune dominance. More precisely, whether cancer antigens often present subdominant epitopes and are therefore less frequently recognized which could in turn hamper vaccine efficacy. As we learned, the pool of naïve T cells is highly diverse and

comprises TCRs that differ in their affinity for the same antigen. In the context of virus infections it was observed that dominant and subdominant $CD8^+$ populations specific for the same pathogen elicit equal kinetics (Munitic et al., 2009). Furthermore, if the TCR epitope:MHC affinity of a T cell clone towards a certain antigen is beyond a critical threshold its expansion will be aborted and no memory is formed, excluding TCR affinity as the driving force of immune dominance (Zehn, Lee, & Bevan, 2009). What seems to be more important is the precursor frequency towards an antigen within the endogenous naïve repertoire. It was shown for $CD8^+$ as well as for $CD4^+$ T cells that the magnitude of responses correlated with the precursor frequency within the endogenous repertoire (Kotturi et al., 2008; Moon et al., 2007). This could mean for the design of a vaccine: as long as the TCR-epitope:MHC binding affinity is above the required threshold for successful expansion and memory formation of naïve antigen-specific T cell clones, it should be feasible to elicit T cell responses also for a subdominant epitopes. Following this thought the crux in fact seems to be the expansion of rare naïve precursors, which recognize this epitope.

## 1.4. Cancer Immunotherapy

At the end of last year the Science journal announced cancer immunotherapy as the breakthrough of the year 2013. After many decades of investigation and establishments of strategies how to train the patient's immune system to attack cancer these efforts yielded in convincing clinical responses. The success stories of the last years are only the tip of the iceberg of many immunological approaches to treat cancer (see figure 1.14).

Let us start with a brief overview. Antibody therapies belong to the most successful immunological cancer treatments. Already in the 1990s the Her2/Neu blocking antibody trastuzumab (Herceptin) was approved for Her2/Neu overexpressing breast-cancer in combination with standard chemotherapy and significantly increased the survival of Her2/Neu positive breast cancer patients (Piccart-Gebhart et al., 2005; Romond et al., 2005). Immunocheckpoint blockade is also attributed to antibody-based therapies. However, this approach conceptually differs from Her2/Neu antibody therapy as it un-specifically targets the hosts' T cells rather than the tumor. Blocking of the inhibitory receptors CTLA-4 and PD-1 (immunocheckpoints) on T cells by antibodies can activate the whole T cell pool of the patient to become more effective in tumor eradication. Impilimumab, a CTLA-4 blocking antibody, was approved by the FDA in 2011 for the treatment of late-stage metastatic melanoma after showing prolonged overall survival in these patients (Hodi et al., 2010). Another unspecific immunotherapy approach is the administration of cytokines like IL-2 or GM-CSF, which leads to the unspecific activation of T cells or enhances the maturation of DCs with the goal to increase antigen presentation, respectively. IL-2 administration can contribute to the regression of large established tumors and was also approved by the FDA for treatment of metastatic renal cell carcinoma and metastatic melanoma (Rosenberg et al., 1985; F. O. Smith et al., 2008).

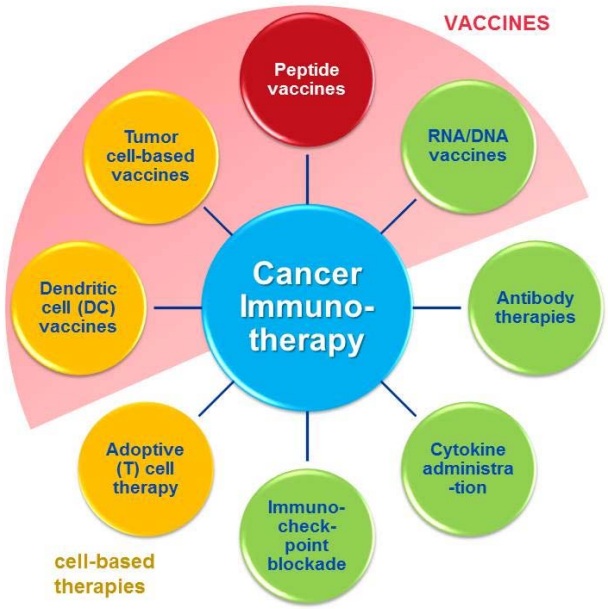


**Figure 1.14**: **Overview of different immunotherapeutic cancer treatment modalities**

A variety of adoptive cell transfer (ACT) approaches have been developed throughout the past 20 years and most of them employ (genetically engineered) T cells (Restifo, Dudley, & Rosenberg, 2012). Tumor infiltrating lymphocytes (TILs) can be isolated from resected patients' tumors, expanded *in vitro* to large numbers and are then re-infused into the patients. The Rosenberg group could record success employing this regimen for metastatic melanoma after non-myeloablative lymphodepletion prior TIL-ACT (Rosenberg et al., 2011). Another ACT method makes use of patients' T cells which are engineered to express tumor-antigen specific high-affinity TCRs (Rosenberg, 2011). Similarly, T cells derived from the peripheral blood of patients can be engineered with chimeric antigen receptors (CARs). CARs are not restricted to antigen presentation by MHC molecules, as they are chimeric molecules which combine the antigen-recognition domains of antibodies with intracellular signaling moieties of T cells. The group around C. June developed a CAR targeting the CD19 B cell antigen, which is expressed in the majority of patients with non-Hodgkin lymphomas and chronic lymphocytic leukemia (CLL). They could obtain complete remissions in patients with CLL (Porter, Levine, Kalos, Bagg, & June, 2011) and pediatric patients with ALL (acute lymphoid leukemia) (Grupp et al., 2013).

One major weak point of immunocheckpoint blockade and high-dose IL-2 regimens are immune-related adverse effects of differing grade occurring in most patients, which need clinical care (Weber, Kahler, & Hauschild, 2012). Also ACT regimens can lead to severe side effects. A major complication is off-target toxicity, which can occur when the targeted tumor-antigen is not exclusively expressed by the tumor but also on some normal tissues. For example treatment of cancer patients with anti-MAGE-A3 TCR lead to fatal neurologic toxicity in patients, which was most probably attributed to cross-reactivity of the TCR with MAGE-A12 obviously expressed in human brain tissue (Morgan et al., 2013).

In contrast vaccination approaches are generally considered as save, but unfortunately far less effective. There are myriads of different approaches employing recombinant viruses, bacteria and plasmid DNA to sensitize the host to recognize tumor antigens. Other methods use autologous heat-inactivated tumor cells or tumor cell lysates for vaccination (reviewed e.g. in (Kruger, Greten, & Korangy, 2007)). A different vaccination approach targets or employs DCs to deliver and present the tumor-antigen to the host's immune system. One promising example is the dendritic cell based vaccine Sipuleucel-T (Provenge®) for treatment of metastatic castration-resistant prostate cancer, which was approved by the FDA in 2010. The vaccine consists of autologous peripheral blood mononuclear cells (PBMCs) which are cultured with PAP-GM-CSF (the tumor antigen prostate acid phosphatase fused to GM-CSF) to have autologous APCs enriched and are then re-infused into the patient. In the double-blind, placebo-controlled IMPACT (Immunotherapy for prostate adenocarcinoma treatment) study Sipuleucel-T lead to a significant improvement in overall survival. Unfortunately, this did not correlate with progression free survival. Even more striking, from an immunological point of view, was the fact that there was no survival difference between patients the in the Sipuleucel-T group who showed an immune response to PAP and those who did not (Kantoff et al., 2010). The phenomenon that immune responses in patients after vaccination do not correlate with an improved outcome is observed for many vaccination trials. Other general issues and strategies how to improve cancer vaccination efficiency are discussed in the next chapter in the light of cancer peptide vaccination, the therapeutic approach taken as a basis for the presented work.

### 1.4.1. Critical aspects for the design of a peptide vaccine

For the design of a potentially successful anti-cancer peptide vaccine several critical parameter have been identified. Van der Burg and van Haal described seven 'hallmarks of peptide vaccination' in analogy to Hanahan and Weinberg's hallmarks of cancer (van Hall & van der Burg, 2012). Taking these aspects into consideration is thought to prevent unwanted outcomes like tolerance and hyperactivity and instead lead to immunity.

First to mention are the hallmarks which are connected to the nature of the administered peptide. Peptide length was shown to be a substantially critical parameter in a study which directly compared short synthetic peptides (SSPs) with long synthetic peptides (LSPs, generally 30 – 35-mer peptides) (Bijker et al., 2007). Pioneering work to unravel the mode of action of long peptide vaccination and its advantages was carried out C. Melief and other groups in Leiden, Netherlands (Melief & van der Burg, 2008). Minimal MHC-binding peptide-epitopes are less effective in creating a long-term memory response and can even lead to tolerance due to presentation by non-professional APCs. Elongation of the peptides can convert previously tolerizing short peptides in effective epitopes. Moreover, it can improve the immunogenicity of low-affinity CTL epitopes and enhance the strength of the immune response induced by the vaccine. This improved performance can be attributed to other hallmarks, namely the proper activation the professional antigen-presenting DCs. Dendritic cells can take up long peptides at the side of vaccination, migrate to the vaccinations-site draining LN and present it to T cells including all co-stimulatory signals needed for efficient priming of naïve T cells (Bijker et al., 2008).

The recruitment of DCs to the vaccination site, in turn, can be achieved by including 'danger signals' as adjuvants. One such danger signal, which was repeatedly proven to be effective in mice and humans, are unmethylated CpG motives which stimulate TLR9 expressed by DCs (Bode, Zhao, Steinhagen, Kinjo, & Klinman, 2011; Welters et al., 2007). Optimal adjuvant efficacy can thereby be achieved when CpG is maintained in close proximity to the administered antigens (Nierkens et al., 2008). TLR3 ligand poly-IC is another danger signal which proved to be successful in animal studies and is contemporary tested in clinical trials. Conjugates of peptide-TLR ligands or combinations of several TLR ligands (summed up in (Arens, van Hall, van der Burg, Ossendorp, & Melief, 2013)) are explored for synergistic effects. In most clinical and experimental settings peptide vaccine formulations are administered as water in oil emulsions (Incomplete Freund's Adjuvant - IFA). IFA forms depots from which the antigen is slowly released for reported time periods of more than 200 days. Moreover, IFA depots are thought to improve the antigen uptake by DCs (Bijker et al., 2007). However, in many clinical trials employing SSPs with for instance melanoma antigens CTL responses are detectable but the clinical outcome is not altered significantly. A recent study by Overwijk and colleagues provides an explanation for these unsatisfactory results. Instead of migrating to and infiltrating the tumor antigen-specific T cells accumulate at the vaccination site, which leads to dysfunction and deletion. In contrast, T cell dysfunction was not observed for long peptide/IFA formulations (Hailemichael et al., 2013).

As described above $CD4^+$ T cell help ($T_H1$) is important for the priming of naïve $CD8^+$ T cells by DCs (see section 1.1.2). $CD4^+$ T cells also seem to provide help to CTLs in the tumor microenvironment, thereby enhancing their recruitment and cytolytic function (Bos & Sherman, 2010). In peptide vaccine settings it was demonstrated that the addition of helper cell epitopes to the vaccine improves protective T-cell responses (Bijker et al., 2007; Zwaveling et al., 2002). Hence, the inclusion of T helper cell epitopes is crucial for the vaccine's success. This can be done by either adding common agonistic sequences to the vaccine (PRADE) or specific antigen-derived peptides (van Hall & van der Burg, 2012). Interestingly in this context is the phenomenon of antigen linkage. Proteins often contain immunogenic stretches that function as hotspots for immune recognition. Therein, nested $CD4^+$ and $CD8^+$ epitopes can be found. Hence elongation of minimal CTL epitopes with their natural adjacent sequences can result in the inclusion of $CD4^+$ T helper cell epitopes. Several TAAs harboring linked CTL and $T_H$ epitopes are described (e.g. NY-ESO-1 and Her2/Neu (Perez et al., 2010)). These have the advantage that they probably presented by the same DC, which potentially enhances the efficiency of cross-priming.

Another probable improvement is to combine several TAAs in one vaccine, which would have major advantages. For example several MHC class I and class II alleles can be covered. This would reduce the likeliness of tumor escape from immunosurveillance (equilibrium phase) trough down-regulation of one targeted immunodominant epitope or MCH allele. Moreover, coming back to immune dominance, multi-epitope long peptide vaccine might broaden the responses towards sub-dominant epitopes. As discussed before immune dominance depends on partially the avidity and the frequency of preexisting T cell clones against a given epitope. A strong epitope might increase the generation of natural

responses towards other (sub-dominant) epitopes of the same or other proteins (epitope-spreading, (Tian, Gregori, Adorini, & Kaufman, 2001)). As pointed out before, once elicited, also sub-dominant T cell clones with lower-affinity TCRs are efficient in mediating tumor protection (Lustgarten, Dominguez, & Cuadros, 2004). Conclusively, pluralism in anti-tumor response in which several different TAA-specific helper and cytolytic T cells contribute will be more efficient in tumor eradication.

So far five hallmarks of peptide vaccination were listed: APC targeting, peptide length, $CD4^+$ T cell help, epitope breadth and the supply with danger signals. The last two hallmarks, bio-distribution and peptide dosage go hand in hand. Quick systemic spread (administration in saline) and removal as well as continuous exposure of minimal CTL epitopes (e.g. via osmotic pumps) can lead to tolerance, as antigens are probably presented by non-professional APCs and in the absence of danger signals, which are required for maturation of DCs (van Hall & van der Burg, 2012). Furthermore, individual peptides show completely distinct pharmacokinetics, which might be crucial in terms of tolerance (Weijzen et al., 2001). Interestingly, long peptides administered in saline together with TLR agonist do not lead to induction of tolerance, because they are specifically drained to LNs instead of becoming distributed systemically and therewith presentation lasts longer (probably due to the need of processing). Moreover, the duration of antigen availability is also critical for memory formation (Blair et al., 2011). Summed up a slower and localized release to ensure antigen presentation on mature, professional APCs in draining LNs is crucial for T cell activation upon vaccination.

### 1.4.2. Anti-cancer T cell responses and their induction by vaccination

The pre-existence of anti-cancer T cell responses is reported for many different cancer entities. Immune infiltrates into the tumor and tumor microenvironment and the existence of tumor antigen-specific T cells in the peripheral blood and bone marrow of cancer patients are establishing as predictable markers for the clinical prognosis and outcome (Galon et al., 2006; Ogino, Galon, Fuchs, & Dranoff, 2011).

Our group and others proved the pre-existence of both $CD4^+$ and $CD8^+$ memory T cells in cancer patients prior any immunotherapeutic intervention (Feuerer, Rocha, et al., 2001; Muller-Berghaus et al., 2006; Schmitz-Winnenthal et al., 2006; Sommerfeldt, Beckhove, et al., 2006; Sommerfeldt, Schutz, et al., 2006). The tumor-antigen specific memory T cell pool seems to be polyvalent and consists phenotypically of effector as well as central memory T cells. Moreover, tumor antigen-specific memory T cells are proven to be functional in *ex vivo* studies. Upon antigen re-encounter they are producing IFN-γ, mediate tumor-antigen specific lysis of autologous tumor cells and can also lead to the rejection of autologous tumors in xenograft models (Beckhove et al., 2004; Feuerer, Beckhove, et al., 2001; Schmitz-Winnenthal et al., 2005). Hence, there is a huge potential to activate tumor antigen-specific T cells or reactive already existing memory T cells by preventive or therapeutic vaccination, respectively (Khazaie et al., 1994). Thereby, $T_H1$ responses are favorable over $T_H2$ responses because $T_H1$ T cells contribute substantially in eliciting cellular, cytotoxic immune responses.

Unfortunately there is also increasing evidence that tumor-induced immune suppression can be mediated in an antigen-specific manner. Our group showed in $T_{reg}$ cell specificity assays that tumor-antigen specific $T_{reg}$ cells can be found in the blood and BM of cancer patients (Bonertz et al., 2009; Schmidt et al., 2013). Moreover, these $T_{reg}$ cells can suppress the proliferation of poly-clonally activated conventional T cells *in vitro*. The origin of tumor-antigen specific $T_{reg}$ cells and to which extent natural thymic-derived $T_{reg}$ cells and $T_{reg}$ cells induced by the suppressive tumor-microenvironment are involved is not clarified yet. In addition, increased numbers of $T_{reg}$ cells detected in cancer patients do not seem to correlate *per se* with a detrimental outcome for the patient. Across a range of cancers (lung, ovarian, liver, pancreas) higher proportions of $T_{reg}$ cells seem to correlate with reduced patient survival (Curiel et al., 2004; Ghebeh et al., 2008; Hiraoka, Onozato, Kosuge, & Hirohashi, 2006; Kobayashi et al., 2007; Petersen et al., 2006). For melanoma and CRC, however, is picture is less clear (for melanoma see (Miracco et al., 2007; Schwartzentruber et al., 2011)). In case of CRC our group found that antigen-specific $T_{reg}$ cells can control conventional T cell responses *in vitro (Bonertz et al., 2009)*. Another study showed that higher levels of $T_{reg}$ cells were associated with better overall and progression-free survival of CRC patients undergoing chemotherapy or immunotherapy (Correale et al., 2010).

Summed up in cancer (vaccination) therapy the desired T cell responses are predominantly the activation of tumor-antigen specific, IFN-γ producing $T_H1$ helper cells and CTLs accompanied by a robust memory formation (Melero et al., 2014; Vesely et al., 2011). Furthermore, the reduction of immune suppressive influences (decreasing of $T_{reg}$ cell and MDSC numbers) is favorable and their induction by therapeutic intervention should be avoided. Interestingly, the right choice of adjuvant combinations in therapeutic vaccines seems to have a substantial influence on the ratio of induced antigen-specific effector T cells to $T_{reg}$ cells (Kalli et al., 2013; Perret et al., 2013).

### 1.4.3. Recent improvements in peptide vaccine therapy and clinical trials

Animal studies provided revealing insights in the mechanistic background of anti-cancer peptide vaccination and were often effective in eliciting tumor-protective immunity in the host. Unfortunately, translation into the clinics was considerably less successful throughout the first 20 years since initial anti-cancer peptide vaccine trials were launched. However, in recent years (as other cancer immunotherapies) also peptide vaccination seems to “come of age” and several approaches reached phase III clinical trials (Mellman, Coukos, & Dranoff, 2011; Perez et al., 2010).

And still, there is room for improvement. Water in oil emulsions (Incomplete Freund’s Adjuvant) do not seem to be an optimal delivery system for all peptide vaccine settings and therefore more suitable antigen-delivery strategies are needed. Technically speaking, mature antigen-loaded DCs are most probably the best possible vehicles but their generation is complex and laborious compared to non-biological systems. Biodegradable PLGA (poly-lactic-co-glycolic acid) microspheres are FDA-approved and could be alternatives for IFA, which can be loaded with antigen and other adjuvants (e.g. TLR

ligands). Loaded microsphere are taken up by DCs, which in turn can in efficiently induce T cell responses (Mueller, Schlosser, Gander, & Groettrup, 2011; Schliehe et al., 2011).

Furthermore, different strategies are tested how to improve the immunogenicity of the administered antigenic peptides. For example, based on the idea of co-delivery of antigen and adjuvant to the same APC, TLR-ligand-peptide conjugates have been tested successfully in animal models and are planned to be translated into the clinics (Zom et al., 2014). Another strategy is to modify the peptide amino acid sequences to improve the affinity of epitopes towards the MHC molecule and/or the TCR. A prominent example is the sequence-optimized gp100:209-217(210M) peptide. Herein a methionine replaces the natural threonine at position 210, which leads to higher affinity binding to HLA.A2 (Rosenberg et al., 1998). This peptide emulsified in the IFA Montanide® ISA 51 and in combination with high-dose systemic IL-2 administration showed an improved outcome in a randomized, multi-center phase III trial carried out in patients with metastatic melanoma (Schwartzentruber et al., 2011). Progression free as well as overall survival was significantly higher in patients who received the gp100 vaccine compared to the control group, which was treated with high-dose IL-2 only. Similar to the IMPACT study anti-peptide immune responses did not correlate with objective clinical response. Strikingly, post-treatment levels of $T_{reg}$ cells were higher in patients who had a clinical response than in those who did not show a response to treatment. The authors speculate that elevated $T_{reg}$ cell levels might represent a counter-regulatory response after a strong anti-tumor immune reaction. Moreover, the same gp100 peptide was tested in combinations with ipilimumab. But the combination of CTLA-4 blockage with the vaccine was not superior to ipilimumab alone (Hodi et al., 2010).

Clinical peptide vaccine trials have recently been reviewed by Melero et al. and Yamada et al. (Melero et al., 2014; Yamada, Sasada, Noguchi, & Itoh, 2013). Thereby, a clear trend towards combinatorial therapies becomes apparent, whereas immune-based mono-therapies were less successful in the past. Cancer employs various mechanisms in parallel which hamper immune effector functions and favor immune suppression. It appears logical that successful treatment of cancer, therefore, might be more successful by combining therapies which not only elicit anti-tumor effector functions but also counteract tumor-mediated immune suppression and tumor immune evasion. Researchers mounted strategies throughout the last decades which are able to target various facets of detrimental tumor biology. The future challenge will be to combine these strategies to act synergistically. Using TLR ligands and cytokines as adjuvants for peptide anti-cancer vaccination already displays a combinatorial therapy. Also the adjustment with conventional cancer-therapies is highly indicative. For instance, debulking of tumor mass by surgery can reduce tumor mediated immune-suppression (Napoletano et al., 2010), radiotherapy can modify the tumor-microenvironment (Shiao & Coussens, 2010) and enhance effector T cell infiltration (Klug et al., 2013), and some chemotherapeutic agents can induce immunological cell death (e.g. doxorubicin, (Green, Ferguson, Zitvogel, & Kroemer, 2009; Vacchelli et al., 2012)) or reduce the abundance of immune suppressive cells (e.g. the depletion of $T_{reg}$ cells by cyclophosphamide, (Ghiringhelli et al., 2007)). Table 1.4 tries to give an overview (not exhaustive) of combinatorial

possibilities between different treatment modalities. A successful combination of chemotherapy and peptide vaccination is a phase II clinical trial launched by Rammensee and colleagues (Walter et al., 2012). They succeeded in prolonging the survival of HLA.A2 positive renal cell cancer (RCC) patients by treatment with a therapeutic vaccine called IMA901 consisting of nine tumor-associated peptides (TUMAPs) overexpressed in RCC in combination with a single dose of cyclophosphamide (CXC). Thereby CXC reduced the number of $T_{reg}$ cells and responses against multiple TUMAPs were associated with longer overall survival. A consecutive randomized phase 3 study is ongoing.

**Table 1.4**: **Possibilities for combination of active immunotherapy with other treatment modalities**, HDAC: histone deacetylases, information is gathered form (Arens et al., 2013; Melero et al., 2014).

| **Conventional treatment modalities** | **Immunotherapeutic approaches** | | | | | | **Small drugs** |
|---|---|---|---|---|---|---|---|
| Debulking of tumor mass | **Antigenic stimulation (active immune-therapy)** | Co-stimulatory signals | Cytokines | APC stimulation ('danger signals') | Depletion of tumor-promoting immune cells | Immuno-checkpoint blockage | Small molecule inhibitors |
| -Chemo-therapy<br>-Radio-therapy<br>-Surgery | -Synthetic peptides<br>-Viral vectors<br>-DNA vectors<br>-Dendritic cells<br>Etc. | -Agonistic antibodies (OX40, 4-1BB, CD27) | -GM-CSF<br>-IL-2<br>-IL-7<br>-IL-12<br>-IL-15<br>-IL-21 | -TLR ligands<br>-CD40 antibodies | -$T_{reg}$ cell depletion<br>-Depletion of MDMCs | -CTLA-4 blockade<br>-PD-1 blockade | -HDAC inhibitor<br>-Signal transducer inhibitors (e.g. Braf V600E inhibitor vemura-fenib or sunitinib) |
| **Tumor antigen release** | **Induction and maintenance of tumor specific T cells** | | | | **Counteracting suppressive immunity** | | |

The latest innovation in the field of cancer vaccination moves along with the common trend in cancer medicine: personalization. This is especially challenging for the 'disease' cancer taken into account that not only each host is different but also each tumor has its own unique set of genomic (and epigenomic) alterations. Consequently, this would result (in the setting of cancer vaccination) in screening for somatic mutations in tumors of each single patient to identify individual tumor antigens (the tumor mutanome). Contemporary several groups are exploring approaches to make individualized tumor sequencing possible (Matsushita et al., 2012; Robbins et al., 2013; van Rooij et al., 2013). Sahin and colleagues, for example, are establishing an experimental platform based on next generation sequencing (NGS) to prioritize and select mutations suitable for active vaccination approaches (Castle et al., 2012; Lower et al., 2012). They are about to develop DC-targeting mRNA constructs coding for several mutated tumor antigens combined in a polytope, which they previously identified via NGS of the individual patient's tumor. Moreover, their ambitious goal is to narrow down the production time for each individual patient's vaccine formulation to less than two weeks (CIMT Meeting 2014, Mainz, Germany).

Future challenges will be to identify reliable biomarker to stratify patients for specific therapies, possibly on an individualized basis (Leary et al., 2010; Ogino et al., 2011). Probably, also the timing of immunotherapeutic interventions is crucial. So far mainly late stage patients with few remaining treatment options have been treated by vaccination and other immunological therapies. Especially for vaccination approaches it would make sense to treat patients in a preventive setting at an earlier time point of disease (Hale et al., 2012). And indeed, slowly this notion finds its way into clinical trials. The group of O. Finn, a pioneer in the field of cancer vaccine trials employing the TAA MUC1, carried out a 'cancer immunoprevention feasibility study' for a MUC1 targeting vaccine in patients with advanced adenoma of the colon (Kimura et al., 2013). They showed that they could elicit anti-tumor immunity and memory in these patients. Moreover, they found that the lack of immune responses in some patients correlated with a higher number of MDSCs prior vaccination indicating that immune suppression can already occur in a premalignant state and underlining the necessity for early therapeutic intervention.

### 1.4.4. Clinical studies employing mutated Kras and p53 peptides

Soon after their discovery mutated *Kras* and *Tp53* genes awakened researchers' interest in their therapeutic potential. As mutations in these genes are frequent in many different tumor entities it appears intuitive to target them in therapeutic approaches.

As indicated earlier in this chapter mutated *Kras* and *Tp53* genes can give rise to immunogenic epitopes. Gaudernack and colleagues showed that overlapping epitopes around the Kras G12R mutation can be recognized and responded to by T cell clones derived from healthy donors' PBMCs. The $Kras_{1-25}$-G12R peptides they tested was presented by HLA-DR2, -DP3 and -DQ7 alleles and recognized by respectively HLA-restricted T cells indicating a certain promiscuity of this epitope in regard to MHC restriction (Fossum et al., 1993). The core region of the $Kras_{1-25}$ G12R peptide was determined to span the residues 9-16 for all HLA alleles tested. Later the same group identified a HLA.A3 restricted epitope inside the 17-mer $Kras_{5-21}$ G12C peptide. The actual 9-mer epitope within the long peptide comprises the amino acid residues 8-16 and was recognized by T cell clones derived from pancreatic cancer patients carrying this mutation in their tumors and being vaccinated against with the long peptide. The fact that patient derived T cell responded to Kras G12C transfected tumor cells *in vitro* points towards natural processing and presentation of the peptide *in vivo (Gjertsen, Saeterdal, Saeboe-Larssen, & Gaudernack, 2003)*. Furthermore, they found a nested Kras epitope comprising the G12V mutation within a longer $Kras_{5-21}$ G12V peptide that was recognized by cytotoxic $CD4^+$ as well as $CD8^+$ T cells (HLA.B35 restricted) from previously vaccinated pancreatic cancer patients (Gjertsen et al., 1997). The group around Schlom provided evidence that the *Kras* G12V mutation can also be presented in BALB/c mice in a $H\text{-}2K^d$ restricted manner. The tested $Kras_{4-12}$ G12V peptide was able to elicit $CD8^+$ as well as $CD4^+$ T cell response and most probably it is overlapping with a $CD4^+$ epitope (Abrams, Stanziale, Lunin, Zaremba, & Schlom, 1996). Further they found that the peptide $Kras_{5-17}$ G12V to be HLA.DQ and the nested 10-mer peptide $Kas_{4-12}$ G12D to be HLA.A2 restricted (Abrams et al., 1997). Summed up these and other studies indicate that Kras G12 mutations are processed naturally and presented by a wide range of mouse and

human MHC class I and II alleles. These obviously quite promiscuous mutated Kras epitopes can be recognized by $CD4^+$ as well as $CD8^+$ T cells.

The potential of mutated and wild-type p53 sequences to give rise to T cell responses has also widely been studies. In this context again Melief and colleagues have to be mentioned. They explored the possibilities of p53 wt sequences for active vaccination employing long peptides. By mining the whole p53 protein for wt epitopes they could show that self-tolerance does not seem to restrict the $T_H$ cell responses against p53 sequences (Lauwen et al., 2008). Previous studies by other groups imply that the wild-type p53-specific CTL repertoire, however, is considerably restricted by self-tolerance (Hernandez, Lee, Davis, & Sherman, 2000; Theobald et al., 1997). In small phase I/II clinical trials launched by Melief and van der Burg they could show that vaccination with overlapping long wt p53 peptides is safe and capable to induce antigen-specific T cell responses in CRC and ovarian cancer patients (Leffers et al., 2009; Speetjens et al., 2009). The Khleif group tested the $p53_{264-272}$ wt peptide in a phase II trial for vaccination of ovarian cancer patients at high risk of recurrence. They directly compared two vaccination approaches: the peptide emulsified in Montanide and GM-CSF to peptide-pulsed dendritic cells. Both regimens appeared to be safe and were able to elicit comparable specific immune response (Rahma et al., 2012). Several potential mutated p53 epitopes are described, as well. The mutations C234W and C135Y are for example presented in a murine MHC context (Ciernik, Berzofsky, & Carbone, 1996; Mayordomo et al., 1996; Yanuck et al., 1993).

Mutated Kras and p53 sequences also found their way into the clinics (Gjertsen & Gaudernack, 1998; Rahma & Khleif, 2011). Three interesting trials in this context should be mentioned. The Gaudernack group carried out trials with mutated Kras peptides in advanced-stage pancreatic cancer patients. In a phase I/II trial they found that after vaccination with Kras G12 mutant peptides survival was longer in immune-responders compared to non-responding patients (Gjertsen et al., 2001). In a second study they vaccinated resected pancreatic cancer patient with a cocktail of $Kras_{5-21}$ peptides harboring mutations at position G12 and G13 (G12A/C/D/R/S/V, G13D) without analyzing their individual *Kras* mutation status. Immune responses against mutated peptides were detected in 85 % of the patients. A long-term follow-up reported that the 10-year survival of theses cohort was 20 % compared to 0 % in a non-vaccinated control group (Weden et al., 2011). Khleif and colleagues have been running several trials vaccinating patients with mainly late-stage gastrointestinal cancers with mutant Kras peptides. In one of their earlier trials they found the $Kras_{5-14}$ G12V mutation seems to be presented in HLA.A2 restricted manner (Khleif et al., 1999). Further they tested mutant Kras peptide vaccine as an adjuvant treatment for CRC and pancreatic cancer and found it to be well tolerated. Specific immune responses were elicited and seemed to have a positive effect on overall survival (Toubaji et al., 2008). In their latest trial comparing the influence of GM-CSF and IL-2 in combination with mutant Kras vaccine ($Kras_{5-17}$ G12C/D/V) they found that IL-2 might have a negative influence on mutant Kras specific immune responses induced by vaccination (Rahma et al., 2014). Last but not least, Carbone et al. immunized cancer patients (varying stages of disease and varying tumor entities) with their own PBMCs loaded with a

single peptide comprising either a p53 or Kras mutation (Carbone et al., 2005). More precisely, they determined the *Kras* and *Tp53* mutations found in the patients' tumors and treated the patients with individual long peptides (17-mers) carrying the mutation found in their tumors. They reported their vaccine formulation to be safe and could detect mutation-specific immune responses in 42 % of patients after vaccination. In patients showing immune responses prior vaccination, these could be enhances. Furthermore, survival seemed to be prolonged in immune responders.

### 1.4.5. T cells responses against mutations in *Tp53*, *Kras* and *Braf* in colorectal cancer patients

In a previous work (C. Schlude PhD thesis: 'Die Bedeutung patienten-individueller Antigene bei der T-Zell-Antwort gegen kolorektale Tumore') a small cohort of CRC patients was analyzed to investigate the relevance of mutation specific T cell responses. Therefore, the blood and bone marrow of 26 CRC patients was screened for memory T cell reactivity against the same panel of long peptide also employed in the presented work. The samples were screened for responses against the peptides harboring the chosen most frequent hot-spot mutations for CRC and pancreatic carcinoma in *Tp53*, *Kras* and *Braf* compared to their wt counterparts employing IFN-γ ELISpot analysis. Piling up the data from all analyzed patients, responses against every mutated peptide significantly higher than the controls and higher than the corresponding wt peptides could be detected in the peripheral blood and/or the bone marrow of certain percentages of patients. Furthermore, accumulated responses showed that the peptide representing the mutation p53 R175H was recognized by roughly 40 % of patients, whereas the corresponding wt peptide was recognized by only 10 % of patients' peripheral blood T cells. Peptide p53 R248Q was responded to by 15 % of patients' BM T cells and 13 % of patients' T cells derived from PBMCs. Moreover, 15 % of patient-derived BM T cells recognized p53 R248W and Kras G12D, respectively. Braf, Kras and p53 wild-type peptides were highly responsive (in 40-55 % of patients). Of relevance, the peptides p53 R175H and p53 R248Q/W were responded to in HLA.A2 restricted context.

Cumulative analysis further demonstrated that the frequencies of responsive T cells against wt and mutated peptides in the peripheral blood were higher than within the BM. Comparing the frequencies of T cell responses (BM and PBMC-derived pooled) against wt and mutated peptides, those against mutated peptides are generally higher than against wt peptides.

To gain further insight into the relevance of preexisting mutation-specific memory T cell responses in CRC patients, samples of patients' primary tumors and metastases (24 of 26 patients) were sequenced for the abundance of *Tp53*, *Kras*, and *Braf* mutations in the relevant hot-spot mutation sites. Sequencing analyzes showed that 20 of the 24 tested patients (83.3 %) carried *Kras* and/or *Tp53* mutations in their primary tumor and/or metastasis, whereas no *Braf* mutations could be detected. *Tp53* (75 %, 18 patients) mutations were more abundant than *Kras* mutations (29.2 %. 7 patients). Thereby 11 patients' tumors and/or metastasis harbored mutations included in the panel of long peptides (45.8 % of all patients

analyzed). Correlation of the ELISpot results with the abundance of *Tp53* and *Kras* mutations identified in the patients' primary tumors and metastases revealed that patients carrying mutations included in the panel of tested peptides were more likely to be responsive against mutated and wt or only mutated peptides than patients with different mutations in their tumors (54.5 % and 18.2 % respectively compared to 44.4 % and 11.1 %). Patients carrying mutations different from panel mutations showed a higher percentage of wt peptide responses (33.3 % compared to 18.2 % for patients carrying panel mutations). Therewith, the overall response rate against the mutated peptides is higher in patients carrying the tested mutations (72.2 %) than in patients with tumors harboring mutations different from those tested in the panel of long peptides.

Taken together memory T cell responses against the chosen mutations in *Tp53*, *Kras* and *Braf* and corresponding wt sequences seem to be of relevance in CRC patients. More precisely, the frequency of mutation-responding T cells is generally higher than of wt-responding T cells and anti-peptide responses are more frequent in patients carrying the tested mutations in their tumors. Interestingly, patients responding against certain mutated peptide often also respond against the corresponding wt counterparts, which could be a hint for epitope spreading.

## 1.5. Objectives of the thesis

Pancreatic and colorectal carcinomas are, like all cancers, genetic diseases. Their carcinogenesis is accompanied by a successive accumulation of mutations in specific genes. The oncogenes *Kras*, *Braf* and the tumor suppressor *Tp53* are among the essential genes driving colorectal and pancreatic tumorigenesis. Mutations in oncogenes and tumor suppressor genes display true tumor-specific antigens. As they are exclusively expressed in the tumor and not shared with normal tissue T cell responses against TSAs should neither be restricted by mechanisms of central tolerance nor elicit autoimmunity. Moreover, the targeting of driver mutations by therapeutic interventions are less likely to select for tumor escape variants as the tumor's survival critically depends on the physiological effects of these oncogenic gene products. All these characteristics identify mutations in *Kras*, *Braf* and *Tp53* as attractive targets for immunotherapeutic intervention.

Long peptide vaccination presents a miscellaneous and handy therapeutic platform for active vaccination. Several tumor antigens and thoroughly chosen adjuvants are readily combinable in one formulation. Furthermore, employing long peptides for vaccination has major advantages: they are effectively presented by professional APCs, possibly cover several MHC alleles and allow combination of both MHC class I and class II epitopes. Furthermore, HLA-transgenic mice present an optimal experimental system to identify new epitopes presented in a human MHC context.

Earlier studies indicate that mutations in *Kras*, *Braf* and *Tp53* are recognized by the immune system and can elicit mutation-specific effector T cell responses. Facilitating synthetic long peptides displaying mutations in these three target genes for active vaccination can elicit or boost preexisting

mutation-specific T cell responses in mice and humans. Initial clinical trials for the treatment on late-stage patients were shown to be save but little effective. Going one step back into a preclinical model allows us to test oncogene mutation-specific long-peptide vaccination in a preventive setting and for therapeutic intervention at earlier time points of disease.

Hence, the goals of the presented work are:

I. To combine the most frequent mutations in *Kras*, *Braf* and *Tp53* found in pancreatic and colorectal carcinoma and explore their cancer immune-therapeutic potential in a multiple epitope long peptide vaccination setting by utilizing HLA-transgenic mice.
II. Establishment of a suitable tumor model for the employed HLA-transgenic mouse strain.
III. Analysis of the T cell responses elicited by active vaccination with mutated oncogenic peptides by comparison to their wt counterparts.
IV. Identification of immunogenic mutated epitopes within *Kras*, *Braf* and *Tp53*.
V. Investigation of the tumor protective capacity of immunogenic mutated peptides in a preventive vaccination setting.

By working off the defined goals we hope to gain more insight into vaccination induced T cell responses towards mutated oncogene of tumor suppressor gene derived TAAs, their effects during tumor development and mechanisms to improve effectiveness in order to design more successful vaccines in the future.

# 2. Material and Methods

## 2.1. Materials

### 2.1.1. Antibodies

#### 2.1.1.1. Antibodies for Flow Cytometry

| Specificity | Reactivity | Species | Isotype | Clone | Conjugate | Supplier |
|---|---|---|---|---|---|---|
| **CD3e** | mouse | Syrian hamster | IgG2, κ | 500A2 | Pacific Blue™ | BD Biosciences; Heidelberg, Germany |
| **CD4** | mouse | rat | IgG2a, κ | RM4-5 | FITC | BD Biosciences |
| **CD4** | mouse | rat | IgG2a, κ | RM4-5 | V500 | BD Biosciences |
| **CD8a** | mouse | rat | IgG2a, κ | 53-6.7 | Pacific Blue™ | BD Biosciences |
| **CD11c** | mouse | Armenian hamster | IgG1, λ2 | HL3 | PE-Cy™7 | BD Biosciences |
| **CD25** | mouse | rat | IgM | 7D4 | PE | Miltenyi Biotec, Bergisch Gladbach, Germany |
| *KLH* | *KL* | *rat* | *IgM* | *eBRM* | *PE* | *STEMEGNT – Miltenyi Biotec* |
| **CD107a** | mouse | rat | IgG2a, κ | 1D4B | FITC | BD Biosciences |
| *None* | *none* | *rat* | *IgG2a, κ* | *R35-95* | *FITC* | *BD Biosciences* |
| **CD178 (FasL)** | mouse | Armenian hamster | IgG | MFL3 | PE | BioLegend |
| *TNP-Keyhole Limpet Hemocyanin* | *KL* | *Armenian hamster* | *IgG* | *HTK888* | *PE* | *BioLegend* |
| **NK-1.1** | mouse | mouse | IgG2a, κ | PK136 | PE-Cy™7 | BD Biosciences |
| **IL-2** | mouse | rat | IgG2b | JES6-5H4 | FITC | BD Biosciences |
| *TNP-Keyhole Limpet Hemocyanin* | *KL* | *rat* | *IgG2b, κ* | *A95-1* | *FITC* | *BD Biosciences* |
| **IFN-γ** | mouse | rat | IgG1, κ | XMG1.2 | Alexa Flour® 647 | BD Biosciences |
| *None* | *none* | *rat* | *IgG1, κ* | *R3-34* | *Alexa Flour® 647* | *BD Biosciences* |
| **TNF** | mouse | rat | IgG1 | MP6-XT22 | APC-Cy™7 | BD Biosciences |
| *None* | *none* | *rat* | *IgG1, κ* | *R3-34* | *APC-Cy™7* | *BD Biosciences* |
| *None* | *none* | *rat* | *IgG1, κ* | *R3-34* | *PE* | *BD Biosciences* |
| *TNP-Keyhole Limpet Hemocyanin* | *KL* | *rat* | *IgG2b, κ* | *A95-1* | *APC* | *BD Biosciences* |
| **HLA-A2** | human | mouse | IgG2b, κ | BB7.2 | FITC | BD Biosciences |
| *Dansyl* | *none* | *mouse* | *IgG2b, κ* | *27-35* | *FITC* | *BD Biosciences* |
| **HLA-A2** | human | mouse | IgG2b, κ | BB7.2 | APC | BD Biosciences |
| *Dansyl* | *none* | *mouse* | *IgG2b, κ* | *27-35* | *APC* | *BD Biosciences* |
| **HLA-DR** | human | mouse | IgG2a, κ | G46-6 | APC | BD Biosciences |
| *TNP-Keyhole Limpet Hemocyanin* | *KL* | *mouse* | *IgG2a, κ* | *G155-178* | *APC* | *BD Biosciences* |

| | | | | | | |
|---|---|---|---|---|---|---|
| **H-2Kb** | mouse | mouse | IgG2a, κ | AF6-88.5 | PE | BD Biosciences |
| *TNP-Keyhole Limpet Hemocyanin* | *KL* | *mouse* | *IgG2a, κ* | *G155-178* | *PE* | *BD Biosciences* |
| **H-2D[b]** | mouse | mouse | IgG2b, κ | KH95 | PE | BD Biosciences |
| *Unknown* | *none* | *mouse* | *IgG2b, κ* | *MPC-11* | *PE* | *BD Biosciences* |
| **I-Ad/I-Ed** | mouse | rat | IgG2a, κ | 2G9 | PE | BD Biosciences |
| *None* | *none* | *rat* | *IgG2a, κ* | *R35-95* | *PE* | *BD Biosciences* |
| **I-A[b]** | mouse | mouse | IgG2a, κ | AF6-120.1 | FITC | BD Biosciences |
| *TNP-Keyhole Limpet Hemocyanin* | *KL* | *mouse* | *IgG2a, κ* | *G155-178* | *FITC* | *BD Biosciences* |
| **Caspase-3** | human | rabbit | IgG | C92-605 | PE | BD Biosciences |
| *None* | *none* | *rabbit* | *IgG* | *polyclonal* | *PE* | *Abcam* |
| **Foxp3** | mouse | rat | IgG2b | MF23 | Alexa Flour® 647 | BD Biosciences |
| *TNP-Keyhole Limpet Hemocyanin* | *KL* | *rat* | *IgG2b, κ* | *A95-1* | *Alexa Flour® 647* | *BD Biosciences* |
| **Perforin** | mouse | rat | IgG2a, κ | eBioOMAK-D | APC | eBioscience, San Diego, USA |
| *none* | *none* | *rat* | *IgG2a, κ* | *eBR2a* | *APC* | *eBioscience* |
| **Perforin** | mouse | rat | IgG2a, κ | eBioOMAK-D | FITC | eBioscience |
| *none* | *none* | *rat* | *IgG2a, κ* | *eBR2a* | *FITC* | *eBioscience* |
| **Granzyme B** | mouse | rat | IgG2a, κ | NGZB | PE | eBioscience |
| *none* | *none* | rat | IgG2a, κ | *eBR2a* | PE | eBioscience |
| **CD62L** | mouse | rat | IgG2a, κ | MEL-14 | PE-Cy™7 | BD Biosciences |
| *None* | *none* | *rat* | *IgG2a, κ* | *R35-95* | *PE-Cy™7* | *BD Biosciences* |
| **CD62L** | mouse | rat | IgG2a, κ | MEL-14 | PerCP-Cy™5.5 | BD Biosciences |
| *None* | *none* | *rat* | *IgG2a, κ* | *R35-95* | PerCP-Cy™5.5 | *BD Biosciences* |
| **CD44** | mouse | rat | IgG2b, κ | IM7 | APC-Cy™7 | BD Biosciences |
| *TNP-Keyhole Limpet Hemocyanin* | *KL* | *rat* | *IgG2b, κ* | *A95-1* | *APC-Cy™7* | *BD Biosciences* |

2.1.1.2. Antibodies for Western Blot

| Specificity | Reactivity | Species | Isotype | Clone | Conjugate | Supplier |
|---|---|---|---|---|---|---|
| **HA-tag** | HA-tag | mouse | IgG1 | HA-7 | none | Sigma-Aldrich |
| **Actin** | mouse, human | mouse | IgG1 | C4 | none | MP Biomedicals, Santa Ana, CA, USA |
| **mouse IgG** | mouse | donkey | - | polyclonal | HRP | Santa Cruz Biotechnology, Dallas, TX, USA |

### 2.1.2. Kits, Columns and Beads

| Product | Reactivity | Supplier | Catalog number |
|---|---|---|---|
| **CD4** (L3T4) MicroBeads | mouse | Miltenyi Biotec | 130-049-201 |
| **CD8a** (Ly-2) MicroBeads | mouse | Miltenyi Biotec | 130-049-401 |
| **CD11c** (N418) MicroBeads | mouse | Miltenyi Biotec | 130-052-001 |
| **CD90.2** MicroBeads | mouse | Miltenyi Biotec | 130-049-001 |
| **Pan T Cell** Isolation Kit II | mouse | Miltenyi Biotec | 130-095-130 |
| Mouse **IL-2 Secretion Assay** Detection Kit (APC*) | mouse | Miltenyi Biotec | 130-090-987 |
| Mouse **IFN-γ Secretion Assay** Detection Kit (PE) | mouse | Miltenyi Biotec | 130-090-516 |
| **$CD4^+CD25^+$ Regulatory T Cell** Isolation Kit | mouse | Miltenyi Biotec | 130-091-041 |
| **MS Columns** | - | Miltenyi Biotec | 130-042-201 |

### 2.1.3. Media, Supplements and Cytokines

#### 2.1.3.1. Cytokines

| Product | Stock concentration | Working Concentration | Supplier | Catalog number |
|---|---|---|---|---|
| Mouse **GM-CSF** | 10 µg/ml | 100 ng/ml | Miltenyi Biotec | 130-094-043 |
| Recombinant Murine **IFN-γ** | 100 µg/ml | 50-100 ng/ml | PeproTech, Rocky Hill, USA | 315-06 |
| Mouse **IL-2** Recombinant Protein Carrier-Free | 5 x $10^6$ U/ml | 25-50 U/ml | eBioscience | 34-8021 |

#### 2.1.3.2. Stimuli and Inhibitors

| Product | Stock concentration | Working Concentration | Supplier | Catalog number |
|---|---|---|---|---|
| Mouse **GM-CSF** | 10 µg/ml | 100 ng/ml | Miltenyi Biotec | 130-094-043 |
| Recombinant Murine **IFN-γ** | 100 µg/ml | 50-100 ng/ml | PeproTech, Rocky Hill, USA | 315-06 |
| Mouse **IL-2** Recombinant Protein Carrier-Free | 5 x $10^6$ U/ml | 25-50 U/ml | eBioscience | 34-8021 |

#### 2.1.3.3. Cell Culture Media and Supplements

| Product | Supplier | Catalog number |
|---|---|---|
| **X-Vivo-20** | Lonza | BE04-448Q |
| **D**ulbecco's **M**odified **E**agle's **M**edium (**DMEM**) | SIGMA-Aldrich | D6429 |
| **RPMI**-1640 Medium | SIGMA-Aldrich | R8758 |
| **OPTI-MEM**® I (1x) | Gibco | 31985-062 100 ml |
| **D**ulbecco's Modified **P**hosphate **B**uffered **S**aline (**D-PBS**) | SIGMA-Aldrich | D8537 |
| **F**etal **c**alf **s**erum **(FCS)** | Biochrom AG | S0415 |
| **Trypsin**-EDTA Solution (1x) | SIGMA-Aldrich | T3924-100ML |
| **HEPES** Buffer | SIGMA-Aldrich | H0887 |
| **EDTA** (Versen) 1 % w/v in PBS w/o $Ca^{2+}$/$Mg^2$ | Biochrom AG | L2113 |
| **Sodium Pyruvate** | SIGMA-Aldrich | S8636 |
| **2-Mercaptoethanol** 20 ml 50 mM | Gibco | 31350-010 |
| **Gentamicin** Solution | SIGMA-Aldrich | G1397-100ML |
| **Pen Strep** Penicillin-Streptomycin (10,000 U/ml) | Gibco | 15140-122 100 ml |

### 2.1.3.4. Antibiotics

| Product | Supplier | Catalog number |
|---|---|---|
| **Ampicillin –** Ready Made Solution (100 mg/ml) | SIGMA-Aldrich | A5354 |
| **Chloramphenicol** – Ready Made Solution (100 mg/ml) | SIGMA-Aldrich | R4408 |
| **Ciprofloxacin - Ciprobay** (100 mg/50ml Infusionslösung) | Bayer, Leverkusen, Germany | - |
| **Doxycycline** Hydrochloride, Ready Made Solution (100 mg/ml in DMSO) | SIGMA-Aldrich | D3072 |
| **Hygromycin B** (solution 1 g in 20 ml) | Invitrogen | 10687-010 |
| **Kanamycin** solution (50 mg/ml) | SIGMA-Aldrich | K0254 |
| **Neomycin** solution (10 mg/ml) | SIGMA-Aldrich | N1142 |
| **Puromycin** dihydrochloride (10 mg/ml) | Life Technologies | A11138-03 |

### 2.1.3.5. Recipes Culture Media

| ***"Mouse" Medium*** | **Components** | **Volumes [ml]** |
|---|---|---|
| | DMEM | 450 |
| | FCS | 50 |
| | HEPES | 5 |
| | Gentamicin | 2,5 |
| | 2-Mercaptoethanol | 0,5 |

| ***SW480 Medium*** | **Components** | **Volumes [ml]** |
|---|---|---|
| | RPMI | 450 |
| | FCS | 50 |
| | HEPES | 5 |
| | Pen Strep | 5 |
| | Sodium Pyruvate | 5 |

| ***B16-F1 Medium*** | **Components** | **Volumes [ml]** |
|---|---|---|
| | DMEM | 450 |
| | FCS | 50 |
| | HEPES | 5 |
| | Pen Strep | 5 |
| | Sodium Pyruvate | 5 |
| | L-Glutamate | 5 |

| ***HEK-293T Medium*** | **Components** | **Volumes [ml]** |
|---|---|---|
| | DMEM | 450 |
| | FCS | 50 |
| | HEPES | 5 |
| | Pen Strep | 5 |

| ***LB Medium(1 l)/(*Agar for LB plates)*** | **Components** | **Weight [g/l]** |
|---|---|---|
| | Peptone | 10 |
| | Yeast extract | 5 |
| | NaCl | 10 |
| | ***(Bacto Agar**** | ***15 (1.5 %))*** |

### 2.1.4. Recipes for Buffers

| *FACS buffer* | Components | Volumes [ml] |
|---|---|---|
| | D-PBS | 500 |
| | FCS | 5 (1 %) |

| *MACS buffer (mouse)* | Components | Volumes [ml] |
|---|---|---|
| | D-PBS | 470 |
| | FCS | 5 (1 %) |
| | EDTA (1 % w/v) | 25 |

| *1 X ACK buffer (1l)* | Components | Amount [g] |
|---|---|---|
| | $NH_4Cl$ | 8.29 (= 150 mM) |
| | $KHCO_3$ | 1.0 (= 10 mM) |
| | $(Na_2)EDTA$ | 0.037 (= 100 µM) |

Salts were solubilized in 800 ml of $ddH_2O$ and pH was adjusted to 7,2 to 7,4 with 1 N HCl. Afterwards volume was added up to 1 ml with $ddH_2O$. Unsterile ACK buffer was stored at RT protected from light. After sterile filtration the buffer was stored at 4 °C in the fridge.

### 2.1.5. Peptides

Peptides were produced by the in house core facility for peptide synthesis. After solid phase synthesis peptides were HPLC purified and lyophilized. Lyophilized peptides were either stored at -20 °C or directly reconstituted in 100 % DMSO to stock concentrations of either 25 mM (short and long peptides) or 10 mM (long peptides). Stocks were aliquoted (25 µl, 50 µl) and stored at -20 °C.

**hu**: human protein sequence, **mu**: murine protein sequence, **LP**: long peptide, **SP**: short peptide, **S**: species, **L**: length

| **Long peptides with human protein backbone sequences** | | | | |
|---|---|---|---|---|
| **S, L** | **Protein** | **Position** | **Mutation** | **AS Sequence** |
| hu, LP | p53 | 160-180 | R175 wt | MAIYKQSQHMTEVVR **R** CPHHERCSDSDGLAP |
| hu, LP | p53 | 160-180 | R175H | MAIYKQSQHMTEVVR **H** CPHHERCSDSDGLAP |
| hu, LP | p53 | 201-231 | R216 wt | EGNLRVEYLDDRNTF **R** HSVVV PCEPPEVGSD |
| hu, LP | p53 | 201-231 | R216L | EGNLRVEYLDDRNTF **L** HSVVVPCEPPEVGSD |
| hu, LP | p53 | 205-235 | Y220 wt | YLDDRNTFRHSVVVP **Y** EPPEVGSDCTTIHYN |
| hu, LP | p53 | 205-235 | Y220C | YLDDRNTFRHSVVVP **C** EPPEVGSDCTTIHYN |
| hu, LP | p53 | 230-264 | G245 wt R248 wt | TTIHYNYMCNSSCMG **G** MN **R** RPILTIITLEDSSGNL |
| hu, LP | p53 | 230-264 | G245S | TTIHYNYMCNSSCMG **S** MNRRPILTIITLEDSSGNL |
| hu, LP | p53 | 230-264 | G245D | TTIHYNYMCNSSCMG **D** MNRRPILTIITLEDSSGNL |
| hu, LP | p53 | 230-264 | G248Q | TTIHYNYMCNSSCMGGMN **Q** RPILTIITLEDSSGNL |
| hu, LP | p53 | 230-264 | G248W | TTIHYNYMCNSSCMGGMN **W** RPILTIITLEDSSGNL |
| hu, LP | p53 | 258-292 | R273 wt R282 wt | EDSSGNLLGRNSFEV **R** VCACPGRD **R** RTEEENLRKK |
| hu, LP | p53 | 258-292 | R273C | EDSSGNLLGRNSFEV **C** VCACPGRDRRTEEENLRKK |
| hu, LP | p53 | 258-292 | R273H | EDSSGNLLGRNSFEV **H** VCACPGRDRRTEEENLRKK |
| hu, LP | p53 | 258-292 | R282W | EDSSGNLLGRNSFEVRVCACPGRD **W** RTEEENLRKK |
| hu, LP | Kras | 1-29 | G12 wt G13 wt | TEYKLVVVGA **G G** VGKSALTIQLIQNHFV |
| hu, LP | Kras | 1-29 | G12D | TEYKLVVVGA **D** GVGKSALTIQLIQNHFV |
| hu, LP | Kras | 1-29 | G12V | TEYKLVVVGA **V** GVGKSALTIQLIQNHFV |

| | | | | |
|---|---|---|---|---|
| hu, LP | Kras | 1-29 | G12C | TEYKLVVVGA **C** GVGKSALTIQLIQNHFV |
| hu, LP | Kras | 1-29 | G12A | TEYKLVVVGA **A** GVGKSALTIQLIQNHFV |
| hu, LP | Kras | 1-29 | G12S | TEYKLVVVGA **S** GVGKSALTIQLIQNHFV |
| hu, LP | Kras | 1-29 | G12R | TEYKLVVVGA **R** GVGKSALTIQLIQNHFV |
| hu, LP | Kras | 1-29 | G13D | TEYKLVVVGAG **D** VGKSALT IQLIQNHFV |
| hu, LP | Kras | 46-76 | Q61 wt | IDGETCLLDILDTAG **Q** EEYSAMRDQYMRTGE |
| hu, LP | Kras | 46-76 | Q61H | IDGETCLLDILDTAG **H** EEYSAMRDQYMRTGE |
| hu, LP | Braf | 584-614 | V600 wt | LHEDLTVKIGDFGALT **V** KSRWSGSHQFEQLS |
| hu, LP | Braf | 584-614 | V600E | LHEDLTVKIGDFGALT **E** KSRWSGSHQFEQLS |
| **Long peptides with murine protein backbone sequences** | | | | |
| **S, L** | **Protein** | **Position** | **Mutation** | **AS Sequence** |
| mu, LP | p53 | 160-180 | R175 wt | MAIYK**K**SQHMTEVVR **R** CPHHERCSD**G**DGLAP |
| mu, LP | p53 | 160-180 | R175H | MAIYK**K**SQHMTEVVR **H** CPHHERCSD**G**DGLAP |
| mu, LP | p53 | 230-264 | R248 wt | TTIHY**K**YMCNSSCMGGMN **R** RPILTI ITLEDSSGNL |
| mu, LP | p53 | 230-264 | R248W | TTIHY**K**YMCNSSCMGGMN **W** RPILTIITLEDSSGNL |
| mu, LP | p53 | 258-292 | R273 wt | EDSSGNLLGR**D**SFEV **R** VCACPGRDRRTEEE N**F**RKK |
| mu, LP | p53 | 258-292 | R273H | EDSSGNLLGR**D**SFEV **H** VCACPGRDRRTEEE N**F**RKK |
| **Long peptides with MCA sarcoma intrinsic mutations** | | | | |
| **S, L** | **Protein** | **Position** | **Mutation** | **AS Sequence** |
| mu, LP | p53 | 230-264 | R248H | TTIHY**K**YMCNSSCMGGMN **H** RPILTIITLEDSSGNL |
| mu, LP | p53 | 230-264 | G244R | TTIHY**K**YMCNSSCM **R** GMNRRPILTIITLEDSSGNL |
| mu, LP | p53 | 160-180 | R176F | MAIYK**K**SQHMTEVVRR **F** PHHERCSD**G**DGLAP |
| **SHORT PEPTIDES** | | | | |
| **Predicted HLA ligands (short peptides: 10-mers & 15-mers) for the long peptide Kras G12(V)** | | | | |
| **S, L** | **Protein** | **Position** | **Mutation** | **AS Sequence** |
| hu, SP | Kras | 4-13 | G12 wt | KLVVVGA **G** GV |
| hu, SP | Kras | 4-13 | G12V | KLVVVGA **V** GV |
| hu, SP | Kras | 2-16 | G12 wt | EYKLVVVGA **G** GVGKS |
| hu, SP | Kras | 2-16 | G12V | EYKLVVVGA **V** GVGKS |
| **9-mer peptides excised from long peptide p53 R248W around the mutation for epitope mapping** | | | | |
| **S, L** | **Protein** | **Position** | **Mutation** | **AS Sequence** |
| hu, SP | p53 | 239-247 | R248W | NSSCMGGMN |
| hu, SP | p53 | 240-248 | R248W | SSCMGGMN**W** |
| hu, SP | p53 | 241-249 | R248W | SCMGGMN**W**R |
| hu, SP | p53 | 242-250 | R248W | CMGGMN**W**RP |
| hu, SP | p53 | 243-251 | R248W | MGGMN**W**RPI |
| hu, SP | p53 | 244-252 | R248W | GGMN**W**RPIL |
| hu, SP | p53 | 245-253 | R248W | GMN**W**RPILT |
| hu, SP | p53 | 246-254 | R248W | MN**W**RPILTI |
| hu, SP | p53 | 247-255 | R248W | N**W**RPILTII |
| hu, SP | p53 | 248-256 | R248W | **W**RPILTIIT |
| hu, SP | p53 | 249-247 | R248W | RPILTIITL |
| **10-mer peptides excised from long peptide p53 R248W carrying the mutation for epitope mapping** | | | | |
| **S, L** | **Protein** | **Position** | **Mutation** | **AS Sequence** |
| hu, SP | p53 | 239-248 | R248W | NSSCMGGMN**W** |
| hu, SP | p53 | 240-249 | R248W | SSCMGGMN**W**R |
| hu, SP | p53 | 241-250 | R248W | SCMGGMN**W**RP |
| hu, SP | p53 | 242-251 | R248W | CMGGMN**W**RPI |
| hu, SP | p53 | 243-252 | R248W | MGGMN**W**RPIL |
| hu, SP | p53 | 244-253 | R248W | GGMN**W**RPILT |
| hu, SP | p53 | 245-254 | R248W | GMN**W**RPILTI |
| hu, SP | p53 | 246-255 | R248W | MN**W**RPILTII |

| | | | | |
|---|---|---|---|---|
| hu, SP | p53 | 257-256 | R248W | N**W**RPILTIIT |
| hu, SP | p53 | 258-257 | R248W | **W**RPILTIITL |
| **Corresponding 10-mer peptides excised from long peptide p53 R248 wt** | | | | |
| **S, L** | **Protein** | **Position** | **Mutation** | **AS Sequence** |
| hu, SP | p53 | 242-251 | R248 wt | CMGGMN**R**RPI |
| hu, SP | p53 | 245-254 | R248 wt | GMN**R**RPILTI |
| hu, SP | p53 | 257-256 | R248 wt | N**R**RPILTIIT |
| **15-mer peptides excised from long peptide p53 R248W carrying the mutation for epitope mapping** | | | | |
| **S, L** | **Protein** | **Position** | **Mutation** | **AS Sequence** |
| hu, SP | p53 | 234-248 | R248W | YNYMCNSSCMGGMN**W** |
| hu, SP | p53 | 235-249 | R248W | NYMCNSSCMGGMN**W**R |
| hu, SP | p53 | 236-250 | R248W | YMCNSSCMGGMN**W**RP |
| hu, SP | p53 | 237-251 | R248W | MCNSSCMGGMN**W**RPI |
| hu, SP | p53 | 238-252 | R248W | CNSSCMGGMN**W**RPIL |
| hu, SP | p53 | 239-253 | R248W | NSSCMGGMN**W**RPILT |
| hu, SP | p53 | 240-254 | R248W | SSCMGGMN**W**RPILTI |
| hu, SP | p53 | 241-255 | R248W | SCMGGMN**W**RPILTII |
| hu, SP | p53 | 242-256 | R248W | CMGGMN**W**RPILTIIT |
| hu, SP | p53 | 243-257 | R248W | MGGMN**W**RPILTIITL |
| hu, SP | p53 | 244-258 | R248W | GGMN**W**RPILTIITLE |
| hu, SP | p53 | 245-259 | R248W | GMN**W**RPILTIITLED |
| hu, SP | p53 | 246-260 | R248W | MN**W**RPILTIITLEDS |
| hu, SP | p53 | 247-261 | R248W | N**W**RPILTIITLEDSS |
| hu, SP | p53 | 248-262 | R248W | **W**RPILTIITLEDSSG |
| **Corresponding 15-mer peptides excised from long peptide p53 R248 wt** | | | | |
| **S, L** | **Protein** | **Position** | **Mutation** | **AS Sequence** |
| hu, SP | p53 | 234-248 | R248 wt | YNYMCNSSCMGGMN**R** |
| hu, SP | p53 | 235-249 | R248 wt | NYMCNSSCMGGMN**R**R |
| hu, SP | p53 | 240-254 | R248 wt | SSCMGGMN**R**RPILTI |
| hu, SP | p53 | 242-256 | R248 wt | CMGGMN**R**RPILTIIT |
| hu, SP | p53 | 245-259 | R248 wt | GMN**R**RPILTIITLED |
| **Short peptides with wt backbone sequences around the mutation p53 R248W** | | | | |
| **S, L** | **Protein** | **Position** | **Mutation** | **AS Sequence** |
| hu, SP | p53 | 230-244 | R248 wt | TTIHYNYMCNSSCMG |
| hu, SP | p53 | 231-245 | R248 wt | TIHYNYMCNSSCMGG |
| hu, SP | p53 | 232-246 | R248 wt | IHYNYMCNSSCMGGM |
| hu, SP | p53 | 233-247 | R248 wt | HYNYMCNSSCMGGMN |
| hu, SP | p53 | 230-247 | R248 wt | TTIHYNYMCNSSCMGGMN |
| hu, SP | p53 | 249-264 | R248 wt | RPILTIITLEDSSGNL |
| **OVA peptide used for regulatory T cell specificity assay** | | | | |
| **S, L** | **Protein** | **Position** | **Mutation** | **AS Sequence** |
| -, SP | OVA | 323-339 | - | ISQAVHAAHAEINEAGR |
| **IgG control peptides used as 'irrelevant', negative control peptides** | | | | |
| **S, L** | **Protein** | **Position** | **Mutation** | **AS Sequence** |
| mu, LP | IgG | 47-81 | - | SSGVHTFPAVLQSDLYTLSSSVTVPSSPRPSETVT |
| mu, LP | IgG | 273-304 | - | PIMNTNYFVYSKLNVQKSNWEAGNTFTCSV |

### 2.1.6. Chemicals

| Product | Supplier | Product | Supplier |
|---|---|---|---|
| Acetic Acid | Fulka, SIGMA-Aldrich | Milk powder | Carl Roth |
| Acetone | SIGMA-Aldrich | NaCl (sodium chloride) | SIGMA-Aldrich |
| Agarose | Invitrogen, Darmstadt, Germany | $Na_2{}^{51}CrO_4$ (5 mCi, 185 MBq) | Perkin-Elmer |
| Aqua ad iniectabilia | B. Braun, Melsungen, Germany | Paraformaldehyde | Merck |
| Bovine Serum Albumin (BSA) | SIGMA-Aldrich | Propidium Iodide (PI) | BD Biosciences |
| Dimethyl sulfoxide (DMSO) | SIGMA-Aldrich | Rompun 2 % | Bayer-Schering Pharma, Leverkusen, Germany |
| Ethanol absolute | SIGMA-Aldrich | SDS | Carl Roth |
| Ethidium Bromide | SIGMA-Aldrich | Spitacid | Ecolab, Duesseldorf, Germany |
| Isofluran | Baxter | Sodium Azide ($NaN_3$) | GBiosciences, St. Luois, MO, USA |
| Isopropanol | Fluka, SIGMA-Aldrich | Sodiumhydroxide pellets | SIGMA-Aldrich |
| Ketanest S | Pfizer, Karlsruhe, Germany | Triton X-100 | Fluka, SIGMA-Aldrich |
| Loading Dye solution (6 X) | Fermentas | Trypan blue solution (0,4 %) | Fluka, SIGMA-Aldrich |
| Methanol | Fluka, SIGMA-Aldrich | Tween-20 | SIGMA-Aldrich |
| [methyl-$^3$H]-Thymidine (5 mCi, 185 mBq) | Perkin-Elmer | β-Mercaptoethanol for molecular biology | SERVA Electrophoresis, Heidelberg, Germany |

### 2.1.7. Consumables

| Product | Supplier |
|---|---|
| Cell strainer (40 µm, 100 µm) | BD Falcon |
| Conical reaction tubes with screw cup (15 and 50 ml) – referred to as “Falcon tubes” | TPP, Trasadingen, Switzerland |
| Cyrovials with screw cup (2 ml) | Corning, VWR, Darmstadt, Germany |
| Cell-culture dishes, tissue-culture treated (100 x 20 mm, 150 x 20 mm) | TPP, Trasadingen, Switzerland |
| Cell-culture dishes, non-tissue culture treated (Optilux, 100 x 20 mm) | BD Falcon |
| Cell-culture flaks – tissue-culture treated with filter cap (25 $cm^2$ (T25), 75 $cm^2$ (T75), 150 $cm^2$ (T150)) | TPP |
| Disposable needles | BD Biosciences |
| Disposable needles – 27 G x ¾’’, 0.4 x 20 mm (Neolus 100) | Terumo Europe, Leuven, Belgium |
| Disposable scalpel, Feather | PfM, Cologne, Germany |
| Erlenmeyer glass flaks | Thermo Fisher Scientific |
| Luer Lock Connector double female | Didactic, Etainhus, France |
| MACS MS Columns | Miltenyi Biotec |
| Multi-well plates, non-tissue culture treated (6-well, 12-well, 24-well, 48-well, 96-well (round bottom)) | BD Falcon |
| Multi-well plates, tissue-culture treated (6-well, 12-well, 24-well, 48-well, 96-well (round and flat | TPP |

| | |
|---|---|
| bottom)) | |
| **Product** | **Supplier** |
| QIAshredder columns | Qiagen |
| Parafilm | Pechiney Plastic Packaging, Chicago, USA |
| Pipette tips (10 µl, 200 µl, 1000 µl) | Starlab, Ahrensberg, Germany |
| Pipette filter tips (10 µl, 20 µl, 100 µl, 200 µl, 1000 µl) | Starlab, Ahrensburg, Germany |
| Pipette tips (200 µl) for multi-channel pipettes | Ranin |
| Plastic serum pipettes (2 ml, 5 ml, 10 ml, 25ml, 50 ml) | Greiner Bio-One, Frickenhausen, Germany |
| Polystyrene round-bottom tube with cell-strainer cap (5 ml) | BD Flacon (REF 352235) |
| Polypropylene round bottom tubes (5 ml) | BD Falcon |
| Polystyrene round bottom tubes with cup (5 ml) | BD Falcon |
| Polyvinylidene difluoride (PVDF) membrane | Millipore |
| Printed Filtermate A for 1450 MicroBeta Counter (90 x 120 mm) | Perkin-Elmer, Ueberlingen, Germany |
| Reagent reservoir, sterile (50 ml) | Corning |
| Safe-lock tubes (0,5 ml, 1,5 ml and 2,0 ml) | Eppendort, Wesseling-Berzdorf, Germany |
| Sample Bag for 1450 MicroBeta Counter | Perkin Elmer |
| Serological pipetted (5 ml, 10 ml, 25 ml) | BD Falcon |
| Syringe, Norm-Ject tuberkulin (1 ml) | Henke Sass Wolf, Tuttlingen, Germany |
| Syringes (10 and 20 ml) | BD Falcon |
| Syringes (1, 5, 10, 30 and 50 ml) | Terumo, Eschborn, Germany |
| Sterile syringe driven filter (0,22 µm) | Milipore, Eschborn, Germany |
| Whatman 3MM gel blot paper | Sigma-Aldrich |

### 2.1.8. Technical Equipment

| **Product** | **Supplier** |
|---|---|
| Analytical balance (PB602-S/FACT) | Mettler Toledo, Gießen, Germany |
| Autoclip wound clip applier / remover | Becton Dickinson (BD), Heidelberg, Germany |
| Caliper | Carl Roth, Karlsruhe, Germany |
| Cell culture incubator | Sanyo, Bad Nenndorf, Germany |
| Cell culture incubator – Heracell 150 | Thermo Scientific, Heraeus, Karlsruhe, Germany |
| Centrifuge Biofuge frecso | Heraeus, Karlsruhe, Germany |
| Centrifuge Megafuge 2.0R | Heraeus, Karlsruhe, Germany |
| Centrifuge Multifuge X3 FR | Thermo Scientific Heraeus |
| Deep freezer (-20 °C) | Liebheer, Ochsenhausen, Deutschland |
| Deep freezer (-80 °C) | Thermo Fisher Scientific, Karlsruhe, Deutschland |
| Dissecting cutlery | Fine Science Tools, Heidelberg, Germany |
| Electrophoresis power supply | Biotec-Fischer, Reiskirchen, Germany |
| Flow Cytometer – FACS Canto II | BD, Franklin Lakes, USA |
| Fluorescence Microscope Axiovert 40 CFL | Zeiss, Göttingen, Germany |
| Gammacell1000 | Atomic Energy of Canada, Ottawa, Canada |
| Glassware | Schott, Mainz, Germany |
| GeneMate compact gel system | StarLab, Hamburg, Germany |
| Heatable magnetic stirrer | Heidolph Instruments, Schwabach, Germany |
| Heat block, thermo mixer | Grant Instrument, Cambridgeshire, UK |
| Heat Sealer | Perkin-Elmer, Ueberlingen, Germany |
| Heated magnetic stirrer | Heidolph Instruments, Schwabach, Germany |
| Ice machine | Hoshizaki, Willich-Münchheide, Germany |
| Innova 44 incubator / shaker | New Brunswick, Wesseling-Berzdorf, Germany |
| Liquid Scintillation Counter (1450 MicroBetac) | Perkin Elmer, Waltham, USA |
| Micro pipettes (2 µl, 10 µl, 20 µl, 100 µl, 200 µl, 100 µl) | Gilson, Middleton, WI, USA |

| | |
|---|---|
| Microscope AXIO Vert A1 | Zeiss |
| **Product** | **Supplier** |
| Microwave | Bosch, Heidelberg, Germany |
| Milli-Q® Integral Water Purification System | Millipore, Eschborn, Germany |
| Multi-channel pipettes (8 channels, 12 channels; 50 µl, 200 µl) | Rainin, Leiden, Netherlands |
| Nanodrop 2000 c Spectrophotometer | PEQLAB Biotechnology, Erlangen, Germany |
| Neubauer hemocytometer | Brand, Wertheim, Germany |
| Novex mini-cell gel chamber | Invitrogen |
| OctoMACS separator | Miltenyi Biotech, Bergisch Galdbach, Germany |
| Owl EasyCast gel electrophoresis system (B2-BP) | Nunc, Thermo Fisher Scientific |
| PCR machine – PTC-100 Programmable Thermal Controller | MJ Research™, Incorporated, Boston, MA, USA |
| pH meter | WTW, Weilheim, Germany |
| Pipetboy | Brand, Wertheim, Germany |
| PowerPac Basic Power Supply | Bio-Rad Laboratories |
| Refrigerator (4 °C) | Liebherr, Ochsenhausen, Germany |
| Roller-mixer RM5 | Karl Hecht, Sondheim, Germany |
| Shaver for mice (type 1556) | Moser, Berlin, Germany |
| Sterile laminar flow cabinet | SterilGRAD Hood Baker, Stanford, USA |
| Sterile laminar flow cabinet (Class II biological safety cabinet) | Integra Biosciences, Fernwald, Germany |
| Table Top Centrifuge | Haraeus |
| Tomtec Harvester Mach 3 | Tom Tec, Unterschleißheim, Germany |
| TopCount NXT™ | Packard, Perkin Elmer |
| Ultracentrifuge | Beckman Coulter, Krefeld, Germany |
| UV gel documentation system | PEQLAB Biotechnology, Erlangen, Germany |
| Vacuum pump | neoLab |
| Video graphic printer UP-890 CE | Sony, Berlin, Germany |
| Vortexer (Reax 2000) | Heidolph Instruments, Schwabach, Germany |
| Water bath (SW21) | Julabo, Seelbach, Schwabach, Germany |

### 2.1.9. Software

| **Product** | **Supplier** |
|---|---|
| Chromas Lite Software | Technelysium, Brisbane, Australia |
| EndNote (X) | Adept Scientific, Frankfurt |
| FACS Diva software (FCS 3.0) | BD Biosciences |
| FlowJo software (Version 6) | Miltenyi Biotec |
| GraphPad Prism (5) | GraphPad Software, La Jolla, USA |
| Microsoft Office 2010 | Microsoft, Redmond, WA, USA |
| Microsoft Windows 7 | Microsoft, Redmond, WA, USA |
| Quantum Capt | Vilber Lourmat, Marne-la-Vallée Cedex, France |
| Image Lab™ Software | Bio-Rad laboratories |
| Serial Cloner | SerialBasics |

## 2.2. Methods

### 2.2.1. Work with laboratory mice

#### 2.2.1.1. Mouse strains

Except the NOD/SCID mice all mouse strains were bred in house by the central animal core facility under specific pathogen free conditions. For experiments the animals were transferred to and maintained in IVC (individually ventilated cages) stations. Nutrition (food and water) was provided *ad libitum* and animals were kept at a day night rhythm of 12 h. All animal experiments were approved and authorized by the regulatory authorities (Karlsruhe, Germany). They were carried out according to German animal experimental ethics committee guidelines and protection of animals act.

##### *2.2.1.1.1. C57BL/6J mice*

C57BL/6 is the most commonly used inbred mouse strain. The final letter "J" is an acronym for the sub-strain from the Jackson Laboratory (Bar Harbor, USA).

##### *2.2.1.1.2. NOD/SCID mice*

NOD/SCID (NOD.Cb17-*Prkdc*$^{scid}$/NcrCrl) mice were purchased from Charles River Laboratories (Sulzfeld, Germany) and kept in IVC stations during experiments.

NOD/SCID stands for severe combined immunodeficiency (SCID) on a non-obese diabetic (NOD) background. A mutation in the *Prkdc* gene (*Prkdc*$^{scid}$), coding for the catalytic subunit of the DNA-dependent protein kinase (DNA-PKcs) accounts for the SCID phenotype. The DNA-PKcs enzyme is an important player in DNA repair mechanisms and is also required for V(D)J recombination during lymphocyte development. Homozygous mice suffer from lymphopenia as they have no functional T and B cells. Moreover, the NOD background exhibits additional defects of immune functions, among these defective NK cell function and cytokine production of macrophages. Due to the described aberrant immune phenotypes NOD/SCID mice accept allo- as well as xenografts without rejection.

##### *2.2.1.1.3. OT-II TCR-tg mice*

The OT-II mice (C57BL/6 genetic background) are transgenic for a murine MHC-class II-restricted, OVA-specific T cell receptor (Barnden, Allison, Heath, & Carbone, 1998; Szymczak-Workman, Workman, & Vignali, 2009). More precisely, the introduced TCR was derived from a C57BL/6 $CD4^+$ T cell hybridoma restricted to the peptide $OVA_{323-339}$ in the murine H-2 $I\text{-}A^b$ MHC context.

#### *2.2.1.1.4. A2.DR1 dtg mice*

The A2.DR1 dtg is a HLA class I/II humanized mouse strain on a C57BL/6 genetic background. The mice were generated through intercrossing of different MHC transgenic and knock-out mice, resulting in H2 class I-/class II-knockout (murine $\beta_2$ microglobulin deficient), HHD and HLA.DR1 double transgenic mice ((Pajot et al., 2004) for a detailed description see section 1.1.1.2). The ratio of $CD4^+$ and $CD8^+$ T cells is considerably altered in the A2.DR1 dtg mice. 13-14 % of splenocytes represent $CD4^+$ T cells and 2-3 % are $CD8^+$ T cells.

### 2.2.1.2. Genotyping of A2.DR1 dtg mice

For preparation of genomic DNA from mouse tails the DNeasy Blood and Tissue Kit (QIAGEN) was used precisely according to manufacturer's instruction described in the handbook's protocol "Purification of Total DNA from Animal Tissues (Spin-Column Protocol)". Thereby, the tail tissue was always digested overnight in Proteinase K/Buffer-ATL mix at 56 °C and DNA was finally eluted from the column by only pipetting a volume of 100 µl elution buffer AE onto the column to achieve higher concentrations of eluted DNA. The purified DNA was used without any further treatment as template for genotyping PCR reactions.

Genotyping of one animal required five different PCR reactions. PCR reactions 1 and 2 (Abeta° and Beta2M) served to verify the knockout of the murine MHC (*H-2*) and the murine $\beta_2$ microglobulin (*B2m*) genes. The PCR reactions 3 to 5 (HLA.A2, HLA.DRA1 and HLA.DRB1) were detecting the inserted transgenes for the chimeric molecule *HHD* and *HLA.DRA1*/*HLA.DRB*0101* genes respectively. In the following tables the primers' sequences and the individual PCR reactions are listed. Four template controls were performed along with: water (DNA contamination control), C57BL/6 mouse genomic DNA (wild-type negative control), HHD stg mouse genomic DNA (positive control for the MHC class I transgene), genomic DNA of an already typed A2.DR1 dtg mouse (positive control).

**Table 2.1**: PCR Primers for A2.DR1 dtg Genotyping, **WT**: wild-type, **KO**: knock out, **Tg**: transgene

| Reaction | Primer | Sequence | Band Size [bp] |
|---|---|---|---|
| **Abeta°** | Abeta3 | 5' - TTC GTG TAC CAG TTC ATC GG - 3' | WT allele: **230**<br>KO allele: **730** |
| | Abeta2 | 5' - TAG TTG TGT CTG CAC ACC GT - 3' | |
| **Beta2M** | Beta2M0 | 5' - CTG AGC TCT GTT TTC GTC TC - 3' | WT allele: **270**<br>KO allele: **600** |
| | Beta2M4 | 5' - CTT ACC TCT GCA GGC GTA TG - 3' | |
| | Neo 55 a | 5' - CCT GCC GAG AAA GTA TCC A - 3' | |
| **HLA.A2** | HLAA2 F | 5' - CAT TGA GAC AGA GCG CTT GGC ACA GAA GCA G - 3' | Tg allele: **400** |
| | HLAA2 R | 5' - GGA TGA CGT GAG TAA ACC TGA ATC TTT GGA GTA CGC - 3' | |
| **HLA.DRA1** | HLADRA1 F | 5' - CTC CAA GCC CTC TCC CAG AG - 3' | Tg allele: **153** |
| | HLADRA1 R | 5' - ATG TGC CTT ACA GAG GCC CC - 3' | |
| **HLA.DRB1** | HLADRB1 F | 5' - TTC TTC AAC GGG ACG GAG CGG GTG - 3' | Tg allele: **228** |
| | HLADRB1 R | 5' - CTG CAC TGT GAA GCT CTC ACC AAC - 3' | |

**Table 2.2:** PCR reactions for A2.DR1 dtg genotyping

| **PCR 1: Abeta°** | **Components** | **Volume [µl]** |
|---|---|---|
| | 5 x colored reaction buffer (Bioline, Luckenwalde, Germany) | 10.0 |
| | MgCl2 (50 mM, Bioline) | 2.5 |
| | dNTP-Mix (je 2,5 mM, Bioline) | 4.0 |
| | **Primer Abeta 3 (10 nM)** | **3.8** |
| | **Primer Abeta 2 (10 nM)** | **3.3** |
| | **Primer Neo55 a (10 nM)** | **1.1** |
| | Mango Taq Polymerase (5 units/µl, Bioline) | 0.5 |
| | Template DNA | 3.0 |
| | $ddH_2O$ | 21.5 |
| | **Final volume** | **50,0** |

| **PCR 2: Beta2M** | **Components** | **Volume [µl]** |
|---|---|---|
| | 5 x colored reaction buffer (Bioline) | 10.0 |
| | MgCl2 (50 mM, Bioline) | 2.5 |
| | dNTP-Mix (je 2,5 mM, Bioline) | 4.0 |
| | **Primer beta2M0 (10 nM)** | **4.6** |
| | **Primer beta2M4 (10 nM)** | **3.3** |
| | **Primer Neo55 a (10 nM)** | **1.4** |
| | Mango Taq Polymerase (5 units/µl, Bioline) | 0.5 |
| | Template DNA | 3.0 |
| | $ddH_2O$ | 20.7 |
| | **Final volume** | **50.0** |

| **PCR 3: HLAA2** | **Components** | **Volume [µl]** |
|---|---|---|
| | 5 x colored reaction buffer (Bioline) | 10.0 |
| | MgCl2 (50 mM, Bioline) | 2.5 |
| | dNTP-Mix (je 2,5 mM, Bioline) | 4.0 |
| | **Primer HLAA2 F (10 nM)** | **0.8** |
| | **Primer HLAA2 R (10 nM)** | **6.8** |
| | Mango Taq Polymerase (5 units/µl, Bioline) | 0.5 |
| | Template DNA | 3.0 |
| | $ddH_2O$ | 22.4 |
| | **Final volume** | **50.0** |

| **PCR 4: HLADRA1** | **Components** | **Volume [µl]** |
|---|---|---|
| | 5 x colored reaction buffer (Bioline) | 10.0 |
| | MgCl2 (50 mM, Bioline) | 2.5 |
| | dNTP-Mix (je 2,5 mM, Bioline) | 4.0 |
| | **Primer HLADRA1 F (10 nM)** | **1.3** |
| | **Primer HLADRA1 R (10 nM)** | **1.3** |
| | Mango Taq Polymerase (5 units/µl, Bioline) | 0.5 |
| | Template DNA | 3.0 |
| | $ddH_2O$ | 27.4 |
| | **Final volume** | **50.0** |

| **PCR 5: HLADRB1** | **Components** | **Volume [µl]** |
|---|---|---|
| | 5 x colored reaction buffer (Bioline) | 10.0 |
| | MgCl2 (50 mM, Bioline) | 2.5 |
| | dNTP-Mix (je 2,5 mM, Bioline) | 4.0 |
| | **Primer HLADRB1 F (10 nM)** | **1.1** |
| | **Primer HLADRB1 R (10 nM)** | **1.1** |
| | Mango Taq Polymerase (5 units/µl, Bioline) | 0.5 |
| | Template DNA | 3.0 |
| | $ddH_2O$ | 27.8 |
| | **Final volume** | **50.0** |

PCR reaction mixes were pipetted on ice in 0,5 ml Eppendorf tubes. A PTC-100 Programmable Thermal Controller (MJ Research) PCR machine was used to run the following PCR program:

**Table 2.3:** A2.DR1 dtg genotyping PCR reactions

| PCR Cycle | Time [min] | Temperature [°C] | Cycles |
|---|---|---|---|
| Initial denaturation | 5 | 94 | - |
| Denaturation | 1 | 94 | |
| Annealing | 1 | 57 | **X 35** |
| Elongation | 2 | 72 | |
| Final elongation | 5 | 72 | - |
| Storage | forever | 4 | - |

To separate the amplified PCR product according to size agarose gel electrophoresis was performed. For preparation of a 1,5 % gel 1,5 g of agarose (Agarose NEEO Ultra-Qualität, Roti®grose, Carl Roth) was resuspended in 100 ml of 1 X TAE-Buffer (TAE buffer 50 x pH 8,3, (MERCK, Darmstadt , Germany) diluted with dd$H_2O$ to 1 X or ) in an Erlenmeyer flask. The suspension was boiled at 900 W in a microwave until the agarose was dissolved completely. Under occasional shaking the solution was cooled down to 50 to 60 °C before 0,004 % ethidium bromide (SIGMA-Aldrich) was added. Immediately after addition of ethidium bromide the gel was casted in a gel carrier with combs. After curing, combs were removed and the gel (plus carrier) was inserted into the gel chamber (GeneMate, StarLab) filled with 1 X TAE as running buffer. Hence, the gel was ready to be loaded with the samples and a ladder (Hyper Ladder™ 50 bp, Bioline, Luckenwalde, Germany). Electrophoresis was performed for 1 to 1,5 h at constant voltage of 120 V until the bands were sufficiently separated. For imaging the gels were exposed to UV light facilitating a UV documentation system (PEQLAB, Erlangen, Germany). Analysis was done employing Quantum-Capt software. An exemplary gel picture is shown in figure 2.1.

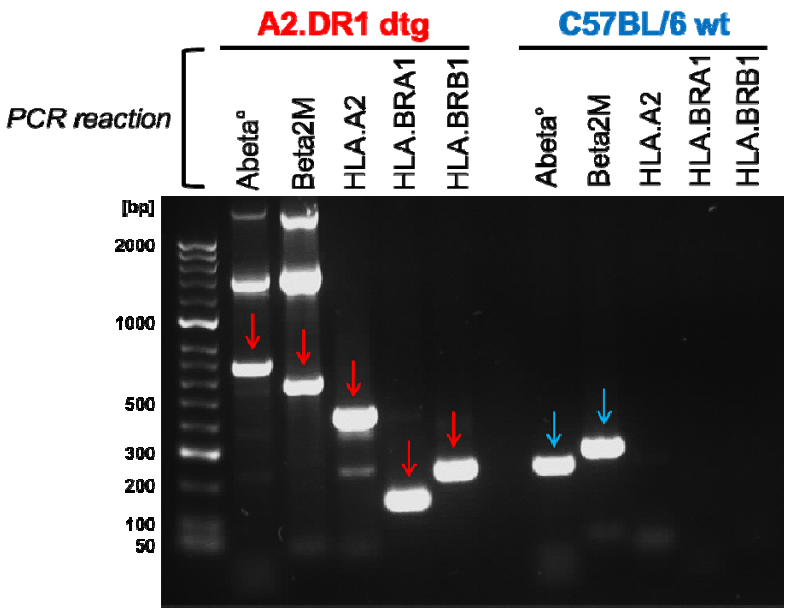


**Figure 2.1**: **PCR products resulting from A2.DR1 genotyping**
A2.DR1 dtg genomic template DNA (red) is opposed to C57BL/6 wt (blue) template DNA.

#### 2.2.1.3. Sterile preparation of organs from mice

Animals were anesthetized and killed with carbon dioxide. Via cervical dislocation it was made sure that the animals were dead. The mice's bodies were bathed in 70 % ethanol for disinfection and dissected sterile under the laminar flow. Animals were pinned to a dissection rubber board and to dislocate the joints of the hint limbs the legs were stretched. Using forceps and scissors the skin was carefully cut without opening the peritoneum along the median line and along the hint limbs to the feet.

##### *2.2.1.3.1. Preparation of peripheral lymph nodes and spleen*

Lymph nodes were exposed by pulling the skin outwards from the body and pinning it down. Inguinal, axillary and cervical lymph nodes were collected in an ice-cooled 50 ml Falcon tube filled with 40 ml sterile PBS. Afterwards the peritoneum was carefully opened near the rib cage on the left half of the mouse's body to take out the spleen. Spleens were collected in a PBS filled Falcon tube on ice.

##### *2.2.1.3.2. Preparation of T cells from peripheral lymphoid organs*

Dissected organs were washed twice in ice-cooled PBS. Spleens were minced through 100 µm cell strainers and lymph nodes through 40 µm cell strainers by employing a plunger form a 1 ml disposable syringe. During that process continuously fresh PBS was added into the strainer by pipetting. The resulting cell suspensions were centrifuged at 1700 rpm for 5 min at 4 °C and supernatants were discarded. The lymph node cell pellet was washed again in 10 ml of cooled PBS. Erythrocytes in spleen samples were lysed by resuspending the cell pellets in 2.5 ml ACK buffer per spleen and incubation for 60 s at room temperature. Lysis was stopped by adding 10 ml PBS per spleen. Samples were centrifuged and supernatants discarded. The cell pellets were resuspended in 20 ml MACS buffer each and cell numbers were determined after Trypan blue staining. After centrifugation the cells were resuspended in cooled MACS buffer and cell numbers were adjusted to 1 x $10^8$ cells/ml. T cells were purified from lymph node and spleen samples with either CD90.2 MicroBeads (Miltenyi Biotec) or Pan T Cell Isolation Kit II (Miltenyi Biotec) according to manufacturer's instructions. For purification of single $CD8^+$ or $CD4^+$ T cells populations CD8a (Ly-2) MicroBeads or CD4 (L3T4) MicroBeads were used. Cell numbers of purified cells were determined after Trypan blue staining, cells were spun down and the supernatant was removed completely. Purified T cells were adjusted to respective cell numbers in X-Vivo-20 medium for subsequent experiments.

##### *2.2.1.3.3. Preparation of bone marrow*

For preparation of bone marrow femur and tibia were resected from mice. Therefore, all muscles and tendons had to be removed using forceps and scissors as good as possible. The bones were cut out after dislocation and braking of the joints. Extra care had to be taken to prevent damage of the bones. Remaining tissue was removed from the bones by rubbing them with paper towels. The cleaned bones were collected in a 50 ml ice cooled Falcon tube filled with PBS. Bones were sterilized in 70 % ethanol by

incubation for two to five minutes at room temperature. Ethanol was discarded and bones were washed twice by rinsing them with PBS. Afterwards the bones were transferred to a mortar and cracked open by using a pistil which sets free the red bone marrow. During grinding the mortar had to be constantly rinsed with ice-cold PBS and the gained bone marrow was removed by pipetting. The bone marrow suspension was collected in a 50 ml Falcon tube. All bone marrow was removed when bone splinters turned white. Bone marrow suspension was centrifuged for 5 min at 1700 rpm for 5 min and the supernatant was discarded. The pellet was resuspended in 10 ml mouse medium and filtered through a 100 µm cell strainer to remove the remaining bone splinters. Filtered suspension was spun down again for 5 min at 1700 rpm and RT.

*2.2.1.3.4. Generation of dendritic cells from bone marrow derived monocyte progenitors*

The cell pellet gained from bone marrow preparation was resuspended in mouse medium supplemented with recombinant murine GM-CSF (working concentration 10 ng/ml). For maturation cells were incubated for six days at 37 °C and 5 % $CO_2$. Cells were fed after 3 days with additional 10 to 15 ml fresh medium supplemented with GM-CSF.

*2.2.1.3.5. Purification of dendritic cells from bone marrow cultures*

After six days of maturation dendritic cells were attached to the ground of the dish. Cells were resuspended by pipetting and cell suspension was collected in 50 ml Falcon tubes. Petri dishes were rinsed several times with fresh mouse medium to remove all remaining dendritic cells. Cells were centrifuged at 1700 rpm for 5 min at 4 °C. The supernatant was discarded, cells were resuspended in ice-cooled MACS buffer and pooled in one Falcon. Afterwards the sample was spun down again, supernatant was discarded and the cell pellet was resuspended in 20 ml of fresh ice-cold MACS buffer. Cell number was determined after Trypan blue staining. Cells were adjusted to 2 X $10^8$ cells/ml and dendritic cells were purified with the CD11c MicroBeads according to manufacturer's instructions. Following purification the cell number of $CD11c^+$ DCs was determined after Trypan blue staining. Cells were adjusted to 7,5 X $10^5$ cells/ml in X-Vivo-20 medium and then pulsed with peptides for *in vitro* re-stimulation of T cells.

2.2.1.4. Vaccination of mice

*2.2.1.4.1. Adjuvants*

2.2.1.4.1.1. Toll-like receptor 9 ligand CpG ODN 1668

Toll-like receptor 9 ligand CpG ODN 1668 is a synthetic 20-mer oligonucleotide with the following sequence: 5'- TCC ATG ACG TTC CTG ATG CT – 3'. It was purchased as a HPLC-purified, lyophilized primer (Eurofins MWG Operon, Germany, Ebersberg). Under sterile conditions CpG oligonucleotides were reconstituted in PBS to a concentration of 10 µg/µl. The samples were incubated for 20 min at room

temperature and occasional vortexed. Reconstituted CpG stock solution was stored at -20 °C and thawed before use at room temperature.

2.2.1.4.1.2. Toll-like receptor 3 ligand poly(I:C)

Toll-like receptor 3 ligand poly(I:C) is a polyinosinic-polycytidylic acid analog of double stranded RNA. We used Poly(I:C) HMW VacciGrade™ (InvivoGen, San Diego, CA, USA). It was reconstituted according to manufacturer's instructions to a stock concentration of 5 mg/ml, aliquoted and stored at -20 °C.

2.2.1.4.1.3. Incomplete Freund's Adjuvants (IFA) Montanide ISA 720 and ISA 51

Incomplete Freund's Adjuvant is an very slowly biodegradable water in oil emulsion. The aqueous phase can contain additional soluble adjuvants (like CpG or poly(I:C)) and the antigens, in our case the peptides used for vaccination. The emulsion is injected subcutaneously and forms depots under the skin of the animals, which are thought to slowly but continuously release antigen and moreover protect the stored antigens from degradation. We tested two different oils for vaccination purchased from the company SEPPIC (Cologne, Germany). Montanide ISA 51 VG (ISA stands for Incomplete SEPPIC adjuvant and VG for vaccination grade) is based on mineral oil and Montanide ISA 720 VG on non-mineral oil. Both adjuvants are approved for clinical trials.

Montanide ISA 51 VG had to be mixed with the aqueous phase in a 50 % / 50 % (W/W) ratio and for Montanide ISA 720 VG the ratio was 30 % / 70 % (W(aqueous phase) / W(oily phase)). Emulsifying was performed by premixing the aqueous and oily phase in 2 ml Eppendorf tubes using a vortex. The mixture was drawn up into a 1 ml luer lock syringe (Norm-Ject tuberculin, Henke Sass Wolf). The syringe was connected to an I-connector (Luer Lock Connector double female, Didactic). The plunger was pushed very slowly to drain air from the system. A second empty syringe was adapted to the opposite opening of the I-connector closing the emulsification system and resulting in a syringe-connector-syringe apparatus. Now the formulation was moved from one syringe to the other and back by pressing the plungers, thereby passing twice through the diminution of the I-connector. Moving the liquid once back and force through the connector is referred two was one cycle. The first 20 cycles were carried out in a very slow rhythm (one cycle lasting in average 8 s) for pre-emulsification. The next 40 cycles were carried out at the highest speed possible when using Montanide ISA 51. This was when the emulsion was formed. During the process the mixture got its typical creamy viscous appearance which made it harder to press the syringe plungers. When working with Montanide ISA 720 the number of fast cycles had to be increased to 60. After complete emulsification the whole liquid was pushed into one syringe and the syringe was disconnected from the apparatus ready to be used for injections.

*2.2.1.4.2. Vaccination schedules*

Animals were vaccinated with altering vaccination schedule according to the experimental application.

To determine the immunogenicity of mutated peptides compared to corresponding wild type sequences C57BL/6 and A2.DR1 dtg mice were vaccinated. The testing was performed in a multi-peptide vaccination setting using TLR9 ligand CpG ODN 1668 as an adjuvant. The following peptides mixes were used for vaccination:

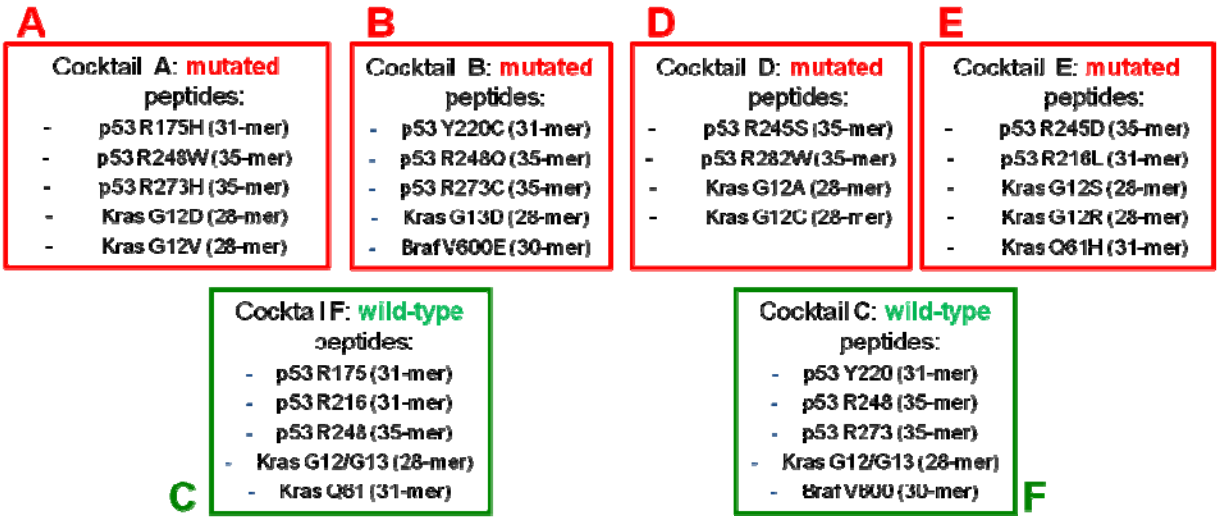


The peptides (with stock concentrations of 10 mM) were mixed in sterile PBS together with CpG ODN 1668. An example for vaccination mixes with peptide cocktail A for 3 mice is displayed in table 2.4.

**Table 2.4**: Example for an immunization cocktails used for peptide screening

| Neck Cocktail | | | Tail Cocktail | |
|---|---|---|---|---|
| **Components** | **Volume [µl]** | | **Components** | **Volume [µl]** |
| 1 x D-PBS | 400.0 | | 1 x D-PBS | 200.0 |
| CpG ODN 1668 [10 µg/µl] | 2.0 | | CpG ODN 1668 [10 µg/µl] | 2.0 |
| p53 R175H (hu, LP) | 2.0 | | p53 R175H (hu, LP) | 2.0 |
| p53 R248W (hu, LP) | 2.0 | | p53 R248W (hu, LP) | 2.0 |
| p53 R273H (hu, LP) | 2.0 | | p53 R273H (hu, LP) | 2.0 |
| Kras G12D (hu, LP) | 2.0 | | Kras G12D (hu, LP) | 2.0 |
| Kras G12V (hu, LP) | 2.0 | | Kras G12V (hu, LP) | 2.0 |

Immunization cocktails were either drawn up in 1 ml syringes (Norm-Ject tuberculin, Henke Sass Wolf) each and used right away for vaccination or stored at -20 °C. For subcutaneous injections 27-gauge needles (27G x ¾'', 0,4 x 20 mm, Neolus, TERUMO Europe, Leuven, Belgium) were used. For each immunization shot 100 µl "neck cocktail" were injected subcutaneously into the neck and 50 µl of the higher concentrated "tail cocktail" were injected subcutaneously into the tail base of one animal. Each

vaccination group comprised three gender- and age matched animals, preferentially siblings. The animals were vaccinated on a biweekly basis and analyzed four weeks after the first vaccination (the scheme below).

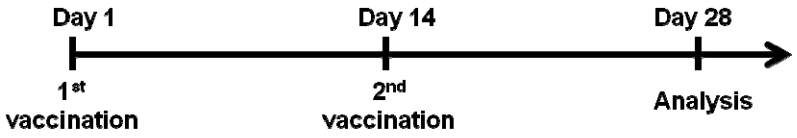


After the peptide screening was completed the animals were vaccinated in consecutive experiments (tumor challenge experiments, *in vitro* kill assays, epitope mapping, etc.) with IFA formulations. A preparation for a prototypical IFA immunization is listed in table 2.5. As the DMSO concentration in the aqueous phase is critical for emulsification higher concentrated long peptides stocks (25 mM) were used. Moreover, Montanide ISA 720 VG approved to be more effective for immunization than ISA 51 VG. This is why all following experiments after initial testing were carried out using ISA Montanide 720 VG. Emulsions were always freshly prepared as described above and never stored for longer than 3 h.

Immunization emulsions were drawn up in 1 ml syringes and injected subcutaneously employing 27-gauge needles. 100 µl were injected in the neck and 50 µl in each flank of a respective animal.

**Table 2.5**: Example for the components of an IFA immunization cocktail with peptides from group A

| Aqueous Phase | | | Oily Phase | |
|---|---|---|---|---|
| **Components** | **Volume [µl]** | | **Components** | **Volume [µl]** |
| 1 x D-PBS | 220.0 | | Montanide ISA 720 VG | 560 |
| CpG ODN 1668 [10 µg/µl] | 20.0 | | | |
| p53 R175H (hu, LP) | 1.6 | | | |
| p53 R248W (hu, LP) | 1.6 | | | |
| p53 R273H (hu, LP) | 1.6 | | | |
| Kras G12D (hu, LP) | 1.6 | | | |
| Kras G12V (hu, LP) | 1.6 | | | |

The vaccination interval between two vaccination shots had to be increased to three weeks. For some experiments (e.g. *in vitro* kill experiments) an additional boost vaccination was performed one week before the experiment (see scheme below). The immunization cocktail for the boost vaccination was not done as an IFA formulation, but as a PBS, CpG and peptide mixture exactly like the “neck cocktail” as described above. For the boost immunization 100 µl “neck cocktail” were injected subcutaneously into the neck of each animal.

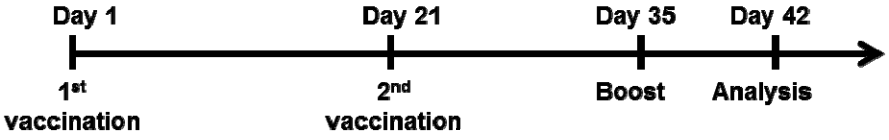

### 2.2.1.5. Tumor Challenges

Before initiation of tumor challenges the mice were vaccinated in a preventive setting. For this purpose, combinations of only two peptides were injected. Therefore, the concentration of the injected peptides was increased to the total peptide concentration used for mixes containing five peptides (meaning 2,5 mM of each peptide resulting in a total concentration of 5 mM of peptides per shot and mouse). Moreover, only one depot immunization with an IFA formulation was made followed by several non-IFA boost immunizations before tumor inoculation and during the challenge. An exemplary vaccination scheme is displayed in the following.

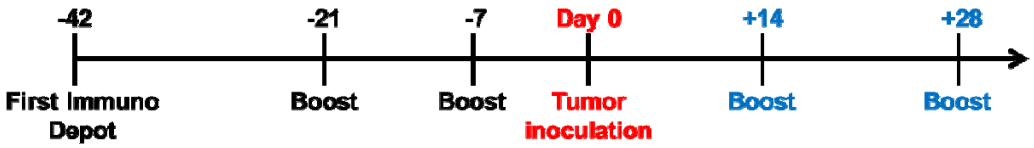


The injected cells were cultured in extra flaks. It was taken care that the cells were between passages 3 to 10 on the day of tumor inoculation and cell densities reached between 75 % to 100 % confluence. Cells were harvested by trypsinization and washed again in fresh culture medium. Cell numbers were determined twice after trypan blue staining. Then cell suspensions were filtered through 40 µm cell strainers and spun down at 4 °C. The supernatant was taken off completely and the cell pellets were kept and resuspended on ice.

Tumor cells were injected in BD Matrigel™ Basement Membrane Matrix (BD Biosciences). BD Matrigel™ was stored in 2 ml aliquots at -20 °C where it is solid. Extra caution had to be taken that matrigel and materials are kept cool during preparation because it starts to gel above 10 °C. Thawing of matrigel on ice was lasting two to three hours. The cell pellets, prone to be injected, were resuspended in liquid matrigel on ice with pre-chilled pipettes. Cells were always injected in a volume of 100 µl of matrigel per animal. In table 2.6 injected cell numbers for the different cell lines used are listed.

**Table 2.6**: Injected tumor cell numbers in tumor challenge experiments

| Tumor cell line | Cell numbers in 100 µl of BD Matrigel™ (per mouse) |
|---|---|
| **2277-NS** | $2.5 \times 10^5$ |
| **2277-NS clones** | $5.0 \times 10^5$ |
| **Line 39** | $2.5 \times 10^5$/$5.0 \times 10^5$ |
| **Line 10** | $2.5 \times 10^5$/$5.0 \times 10^5$ |

Tumor cell/matrigel suspensions were drawn up into 1 ml disposable syringes and injected with 27-gauche needles (27G x ¾'', 0,4 x 20 mm, Neolus 100, TERUMO Europe) subcutaneously into the right flank of the animals. Syringes and needles were stored on ice (in between the injections) to keep the cell suspension in a liquid state. Animals were shaved and the skin was disinfected prior injection. The cell suspensions had to be injected slowly due to high viscosity of the matrigel formulation. Cell suspensions

directly gelled after injection and formed palpable knobs under the skin of the animals. Tumors sizes were measured and documented every three to four days employing a digital caliper (Carl Roth).

To induce transgene expression in the engineered 2277-NS tumor cell line clones *in vivo* the animals had to be fed doxycycline (DOX) upon day 7 after tumor inoculation until the end of the challenge experiment. DOX was administered in the drinking water of the animals at a concentration of 2 g/l. As DOX is photosensitive black bottles had to be used. Furthermore, the antibiotic is bitter in taste and for better compliance 5 pieces of sugar were added per liter of drinking water.

#### 2.2.1.6. Generation of carcinogen-induced syngeneic A2.DR1 dtg sarcoma cell lines

##### *2.2.1.6.1. Carcinogen-induced tumorigenesis with MCA (3-Methylcholanthrene)*

The carcinogen 3-Methylcholanthere (MCA) is often used in mouse models to induce tumorigenesis (Matsushita et al., 2012). Depending on the site of application it can cause formation of carcinomas or sarcomas. Sarcomas are formed upon subcutaneous injection. Intradermal application of MCA can lead to the development of carcinomas and sarcomas. (Wakita et al., 2009).

Treatment of animals with the carcinogen MCA was performed with the kind help of Dr. K. Müller-Decker and D. Kucher from the in house core facility for tumor models. For injection 5 µg of the highly hydrophobic MCA (3-Methylcholanthrene, 98 %, SIGMA-Aldrich, 213942-100MG) were solubilized as good as possible in 1 ml of peanut oil (SIGMA-Aldrich, P2144-250ML) resulting in a concentration of 5 mg/ml. Although using a hydrophobic solvent, like peanut oil, MCA appeared to be hardy soluble at high concentrations. Five female A2.DR1 dtg mice at the age of 8 to 12 weeks were subcutaneously (using 27-gauge needles) injected with 100 µl of MCA solution (counting for 500 µg of MCA per mouse) at the back. Mice were monitored for several months and not until month 3.5 after MCA-injection tumors started growing. After 4.5 month, however, all five animals had developed subcutaneous, fast growing tumors.

##### *2.2.1.6.2. In vitro an in vivo passaging of MCA-induced sarcomas for tumor cell line generation*

When tumors of the MCA-treated mice reached a critical size the animals were killed and tumors were resected under sterile conditions. A small piece of each tumor was transferred into paraformaldehyde solution and send to the NCT tissue bank, where the samples were imbedded into paraffin by Dr. med. E. Herpel and colleagues. They kindly performed H&E stainings with paraffin-imbedded tissue sections from our tumors following an established, routine, clinical protocol. Pictures from H&E stainings were processed using ImageScope software.

The remaining tumor tissue was cut into small pieces with a diameter of one or two mm using sterile, disposable forceps and scalpels. One part of the tumor pieces was used for *in vitro* propagation and the other half was used for direct *in vivo* passaging though immune-competent and immune-sufficient hosts.

#### *2.2.1.6.3. Establishment of MCA-induced sarcoma lines in vitro*

For *in vitro* propagation tumor pieces were transferred into 10 cm tissue-culture treated petri dishes or into tissue-culture treated T75 flasks. Small volumes of mouse medium were added to the tissue pieces in such way that the pieces were not floating. Culture dishes were then incubated at 37 °C and 5 % $CO_2$. Preparations were checked for cells growing out from the tumor pieces under the microscope every second day. The medium was exchanged partially once or twice a week (depending on the color) by pipetting off the old medium very carefully without moving the tumor pieces. The removed medium was replaced with fresh mouse medium again pipetted with extra care to keep tumor pieces in original positions. Tumor pieces tended to attach to the dishes' bottoms after 5 to 7 days. Adherent, spindle-shaped cells started to grow out from tumor pieces after 10 to 21 days of culture. Tumor pieces were carefully removed from the culture flaks when the grown-out cells were half confluent. When the flaks were 90 – 100 % confluent the cells were split for the first time via trypsinization. In case the cells survived the first passage they were expanded strongly and cryopreserved upon passage 3. Some cells of each cell line, established as described, were kept in culture for further analysis (MHC expression staining, screening for mutations, etc.).

#### *2.2.1.6.4. In vivo passaging of MCA-induced sarcomas*

One part of the tumor pieces gained from MCA-treated mice were directly transplanted back to host mice without *in vitro* culturing in between. Tumor pieces were either transplanted into immune-competent 8 to 10 week old A2.DR dtg mice or into immune-deficient NOD/SCID mice of the same age.

The tumor pieces were suspended in 4°C cooled, liquid matrigel. The suspension was drawn up into a 1 ml disposable syringe and the syringe was kept on ice until transplantation of tumor pieces.

Host mice were generally anesthetized by intra-peritoneal injection of a mixture composed of Rompun (active pharmaceutical ingredient: xylazin) and Ketanest C (active pharmaceutical ingredient: ketamin). The two drugs were premixed in PBS: 2.0 ml of Rompun 2% (20 mg/ml stock solution) and 4.0 ml Ketanest S (25 mg/ml stock solution) plus 4.0 ml sterile PBS. Up to a body weight of 30 g a volume of 100 µl of the mixture was injected per animal (accounting for 0,4 mg xylazin and 1,0 mg of ketamin per mouse). To test whether general anesthesia was successful plantar reflexes were tested by pinching the foot pad. Fully anesthetized mice showed no reflexes. Then the mice's flanks were shaved and the skin was sterilized. Shaved mice were placed on a 37 °C pre-warmed thermal mat for surgery and droplets of sterile PBS were put on their ice to avoid dehydration-induced blindness of the animals. Using extra fine scissors a 5 – 10 mm hole was cut into the skin of the mice at the shaved flank. Forceps were carefully inserted into the hole and by spreading them very slowly and carefully a pocket was formed under the skin. Roughly 200 µl of the suspension of matrigel and tumor pieces was filled into the whole with a syringe. After the matrigel turned jellied the margins of the cut in the skin were pressed together using forceps and the skin wound was closed using surgical clips. Animals were monitored until they were fully

awake from anesthesia. One week after surgery the wounds were closed and the surgical clips could be removed.

Tumors in transplanted mice started growing two to three weeks after transplantation. When tumors reached critical sizes (6 to 8 week post transplantation) the mice were killed and tumor cell lines were established *in vitro* as described in the passage before.

Also *in vitro* established MCA-induced sarcoma cells lines were passaged *in vivo* through A2.DR1 dtg and/or NOD/SCID mice. Therefore 1 x $10^6$ cells in 100 µl of matrigel were injected subcutaneously into the flanks of host animals in the same way as it was done for tumor challenge experiments (see passage 2.2.1.5).

### 2.2.2. Cell culture techniques

2.2.2.1. Cell lines

*2.2.2.1.1. Murine cell lines*

2.2.2.1.1.1. B16-F1

The B16 melanoma is a widely used, tumorigenic, C57BL/6 derived, aggressively growing tumor model. There are several lines of the B16 melanoma available (F1 to F10) with differences in their metastatic potential (Fidler, 1973; Fidler & Kripke, 1977). B16-F1 is described to have low potential for lung colonization. The MHC expression of these cells is low but can be enhanced upon IFN-γ treatment. Therefore, B16-F1 was used as positive control for IFN-γ-induced MHC up-regulation experiments. Moreover, B16-F1 cells served as controls in *in vitro* kill experiments.

2.2.2.1.1.2. TC1

TC1 is a tumorigenic cell line derived from C57BL/6 lung epithelial cells (Lin et al., 1996). The cells were *in vitro* immortalized with the HPV-16 viral oncogenes E6 and E7 and transformed with the oncogene c-Has-*ras*. The cells are expressing high levels of murine MHC class I molecules H-2 $D^b$ and $K^b$ and served as controls in FACS stainings and *in vitro* kill assays.

*2.2.2.1.2. Human cell lines*

2.2.2.1.2.1. SW480

SW480 is an adherent, male, human colorectal adenocarcinoma cell line carrying mutations in *Tp53* and in several *ras* oncogenes at the position G12. It expresses high levels of HLA.A*0201 (and B8, B17) and therefore served as positive control for HLA.A2 FACS staining.

#### 2.2.2.1.2.2. HEK 293T cells

HEK 293 is an acronym for human embryonic kidney 293 cells. The cells have a high transfectability. The T in the cell line's name stands for expression of simian virus 40 (SV40) large T antigen which makes them especially suitable for viral transduction.

### 2.2.2.2. Thawing and freezing of cell lines

Frozen cells were stored in liquid nitrogen tanks. During thawing and freezing it was necessary to work fast to reduce the time the cells are exposed to the toxic concentration of DMSO which is required for freezing. When thawing cells, respective cryo vials were taken out of the nitrogen tank and transported on dry ice to the cell culture laboratory. Cryotubes were thawed at 37 °C in the water bath. In the meantime 50 ml Falcon tubes were filled with 25 ml of cool culture medium. Directly after complete thawing cells were transferred into the prepared tubes and mixed properly. Cells were then centrifuged for 8 min at 1400 rpm and 4 °C. The supernatant was completely taken off and the pellet was washed again in 20 ml of culture medium to remove all remaining DMSO. Washed cells were resuspended in 15 ml of culture medium and seeded in a T75 tissue culture flask. The next day (roughly 24 h after thawing) the medium was exchanged again to remove dead cells.

For freezing adherent cells were harvested by trypsinization. Cells were washed twice in 15 ml of culture medium each and cell numbers were estimated. Washed cells were quickly resuspended in cool (4 °C) freezing medium (90 % sterile filtered FCS + 10 % DMSO) and aliquoted into cryo vials, resulting in 1,5 ml of cell suspension containing roughly 2 x $10^6$ cells per vial. Vials were inserted into CoolCells (BioCision, LLC, Mill Valley, CA, USA) which allowed a consistent cool down of 1 °C/min after placing them in the -80 °C freezer. The next day the cryo tubes were transferred from the -80 °C freezer to the liquid nitrogen tank for permanent storage.

### 2.2.2.3. Culturing and passaging of cells

All cell lines were cultured at 37 °C and 5 % $CO_2$ under sterile conditions. Cells were grown in 75 $cm^2$ (T75) or 150 $cm^2$ (T150) tissue-culture treated flasks. Every second week the culture flaks were exchanged and none of the cell lines was culture longer than 20 passages. After passage 20 they were discarded and fresh cells were thawed.

Cells were split twice a week and whenever flaks reached 100 % confluence. To passage adherent cells they were treated with trypsin. Therefore, cells in T75 tissue culture flaks were washed once with sterile PBS. Then 2.5 ml Trypsin-EDTA solution (for T75, 4 ml for T150 flaks and 1 ml for 6 well plates or T25 flasks) was added and flaks were incubated for 4-5 min in the incubator (37 °C, 5 % $CO_2$) until cells detached. Detached cells were resuspended thoroughly by pipetting up and down with additional 10 ml of fresh culture medium. Cells were then split 1 to 10 by pipetting 1 part of the cell suspension back to be flaks and discard the other 10 parts (if not used elsewise for an assay). 15 ml of

fresh culture medium was added to the flaks and cells were further cultivated until they reached 100 % confluence again

#### 2.2.2.4. Harvest of cultured cells

To harvest adherent cells they were trypsinized as described above. The whole cell suspension was transferred into a 15 ml Falcon tube and centrifuged (10 min, 1400 rpm, RT). The supernatant was removed completely and cells were washed by resuspending them in 10 ml PBS. After a second centrifugation (10 min, 1400 rpm, RT), supernatant was removed, cells were resuspended in 1 ml of PBS and passed over to a 1,5 ml Eppendorf tube.

#### 2.2.2.5. Determination of cell number and cell viability

For the quantification of living cells within a sample cell were stained with trypan blue dye. Trypan blue can only penetrate through damaged plasma membranes of dead cells and therewith distinguish dead from living cells. 10 µl of sample cells suspension was diluted 1:10 in ready to use trypan blue dye. Living cells were counted by utilizing a Neubauer hemocytometer. All four large squares of the counting chamber and in total at least 100 living cells were counted. Cell number in the respective sample was calculated as follows:

$$total\ cell\ numer = \frac{\text{counted cell number}}{\text{number of large squares (4)}}\ \text{X dilution factor (10) X sample volume X chamber factor } (10^4)$$

#### 2.2.2.6. IFN-γ treatment of cells for up-regulation of MHC expression

Before tumor challenges and *in vitro* kill experiments tumor cell lines were pretreated with IFN-γ (PeproTech, Rocky Hill, USA). Therefore, the tumor cells were seeded in extra flaks and grown to a density of 75 % (to 100 %) confluence. Then culture medium was exchanged with medium containing 50, 75 or 100 ng/ml of IFN-γ and flaks were incubated for further 48 h. One day before the actual experiments the IFN-γ supplemented medium was taken off, cells were carefully washed with fresh pre-warmed culture medium and cultured overnight in IFN-γ-free medium. The next day cells were harvested for challenge or kill experiments.

#### 2.2.2.7. Transient transfection of HEK 293T cells – Calcium phosphate precipitation method

HEK 293T cells were transiently transfected with the Gateway-pDest-N-eGFP constructs to prepare positive controls for western blot from transfected cells.

Before seeding HEK 293T cells for transfection tissue-culture treated petri dishes (diameter of 10 cm) had to be pretreated with Poly-L-Lysine (0,01 %, sterile-filtered, SIGMA, Aldrich) to increase the stickiness of the cells to the culture dish. This was necessary to reduce cell detachment and loss in the numerous washing steps which are required during the transfection process. 5 ml Poly-L-Lysine solution

was pipetted onto each dish and dishes were tilted to coat the whole surface. Then all solution was taken off and the dishes were air-dried under sterile conditions in the laminar flow.

When the dishes were completely dried 5.0 x $10^6$ HEK 293T cells were seeded in 10 ml of culture medium per plate and incubated over night at 37 °C and 5 % $CO_2$ in the incubator. The next day in the morning the medium was removed entirely and replaced with 10 ml of fresh 37 °C pre-warmed medium per dish.

In the evening cells were transfected employing the calcium phosphate precipitation method. 10 µg of respective plasmid DNA were pre-mixed with 100 µl of $CaCl_2$ (2.5 M, cell culture grade, SIGMA-Aldrich) solution added up to volume of 1 ml with ultra pure water (Biochrom). In a 5 ml tube 1 ml 2 X HBS buffer was put. The tube was permanently vortexed to create a swirl. Droplet-wise the DNA pre-mix was pipetted into swirl. The solution turns faintly milky indicating that DNA-$Ca_3(PO_4)_2$ crystals formed. After the complete DNA pre-mix was added to the HBS buffer the transfection formulation was incubated for 5 min at RT. Then the formulation was carefully applied onto the previously prepared HEK 293T cells by slowly dropping under occasional tilting of the dishes to completely cover all cells.

The cells were incubated over night at 37 °C and 5 % $CO_2$. Transfection efficiency was checked the next day visually for expression of GFP by regarding the cells under the fluorescent microscope. 16 to 24 h after transfection the medium was exchanged again by completely taking off the old medium and adding 10 ml of pre-warmed fresh medium. The cells were further incubated overnight and harvested the latest 48 h after transfection by trypsinization. Sometimes (depending on transfection efficiency) cells were already harvested 24 h post transfection. Transfection efficiency was quantified via FACS prior processing the cells to protein lysates for western blot.

*2.2.2.7.1. Preparation of 2 X HBS buffer for calcium phosphate transfection*

The HBS buffer is a critical parameter for the success of the transfection. 2 X HBS buffer contained 280 mM NaCl, 1.5 mM $Na_2HPO_4$ and 10 mM HEPES. To prepare a 500 ml of stock solution 28 ml of 5 M NaCl, 1.5 ml 0.5 M $Na_2HPO_4$ and 50 ml 1 X HEPES were added up with water to 450 ml total volume. Then the pH was set precisely to 7.12. The success of the transfection critically depends on a precise pH. Afterwards the volume was added up with water to exactly 500 ml. Then the buffer was sterilized through a 0.2 µm filter. The sterile buffer was dispensed in 10 ml aliquots and aliquots were stored at -20 °C. Before use HBS buffer was thawed at room temperature.

2.2.2.8. Transient transfection of A2.DR1 dtg fibrosarcoma line 2277-NS

2277-NS fibrosarcoma cells were transiently transfected with the Gateway-pDest-N-eGFP constructs for *in vitro* kill experiments and to estimate possible toxicity of the introduced transgenes for stable transfection.

In 6-well tissue culture-treated plates 1.5 x $10^5$ 2277-NS cells were seeded per well in 5 ml mouse medium. Plates were incubated over night at 37 °C and 5 % $CO_2$. The next day in the evening medium was changed. The old medium was taken off completely and pre-warmed 2 ml OptiMEM medium was pipetted per well. Plates were incubated for another hour before transfection.

In the meantime the transfection formulations were prepared. Transient transfections were carried out using X-tremeGENE HP DNA Transfection Reagent (Roche Applied Science, Mannheim, Germany). X-tremeGENE HP DNA transfection reagent, plasmid DNA and OptiMEM medium was equilibrated to RT. The transfection reagent was briefly vortexed prior use. For transfection of cells in one well of a 6-well plate 2 µg of plasmid DNA was mixed with OptiMEM medium to a total volume of 200 µl. The transfection reagent was used in a 1:3 ratio (DNA:transfection reagent) – accounting for 6 µl per transfection reagent. When adding the transfection reagent extra care had to be taken that it was pipetted directly into the diluted DNA without coming into contact with the walls on the reaction tube, which would decrease transfection efficiency. The transfection:DNA complex was mixed gently by tapping the test tube and incubated for 30 min at RT. After incubation the transfection complex was added droplet-wise to the cells. Plates were gently rocked to distribute the formulation all-over the cells.

The plates were incubated overnight for 18 h at 37 °C and 5 % $CO_2$. 18 h post transfection the efficiency was checked visually for expression of GFP by regarding the cells under the fluorescent microscope. Cells were then harvested by trypsinization. Transfection efficiency was quantified via FACS and afterwards transfected cells were used as target cells for *in vitro* kill assays.

#### 2.2.2.9. Generation of stable mutant *Tp53*/*Kras* transgene expressing 2277-NS clones

##### *2.2.2.9.1. Generation of the 2277-NS acceptor cell lines*

The generation of stable 2277-NS clones was performed by Dr. R. Will and R. Schatten from the core facility for proteomics and genomics as an in house service. Therefore, it will be only briefly sketched. To generate stable 2277-NS acceptor cell lines, a vector containing a Flp recombinase target site, an antibiotic selection marker (neomycin), an eGFP fluorescence marker as wells as homologous recombination sites for mRosa26 was stably integrated into the Rosa26 locus of the 2277-NS cell line by ZNF targeting (CompoZr® Targeted Integration Kit - mRosa26 Sigma). Targeting of the mRosa26 locus was confirmed by junction PCR according to the manufacturer's recommendations. The 2277-NS/Flp isogenic acceptor lines were further validated for single-copy integration of the FRT site by Southern blotting.

##### *2.2.2.9.2. Generation of 2277-NS transgenic clones expressing chimeric mutant Tp53/Kras transgenes*

For the generation of 2277-NS mutant *Tp53*/*Kras* transgene expressing sub-lines, FRT expression vectors containing a hygromycin resistance gene, tet repressor gene (tetR) as well as a

tetracycline-responsive CMV promoter were cloned upstream of the wt and mutant chimeric mutant Tp53/Kras transgenes' ORFs, respectively, for inducible transgene expression. After sequence verification, the wt and mutated constructs were individually co-transfected together with a Flp recombinase expression vector (pOG44 / Invitrogen) to integrate the respective expressions constructs into the mouse Rosa26 locus of the 2277-NS acceptor cell line by site specific recombination. After selection (hygromycin positive / eGFP negative), single colonies were picked and analyzed.

### 2.2.3. Flow cytometric experiments

#### 2.2.3.1. Two color cytokine secretion assays

To determine the immunogenicity of long and short peptides cytokine secretion assays were performed. A modified protocol was established in a 96 well plate format. A schematic overview of the method is shown in figure 2.2.

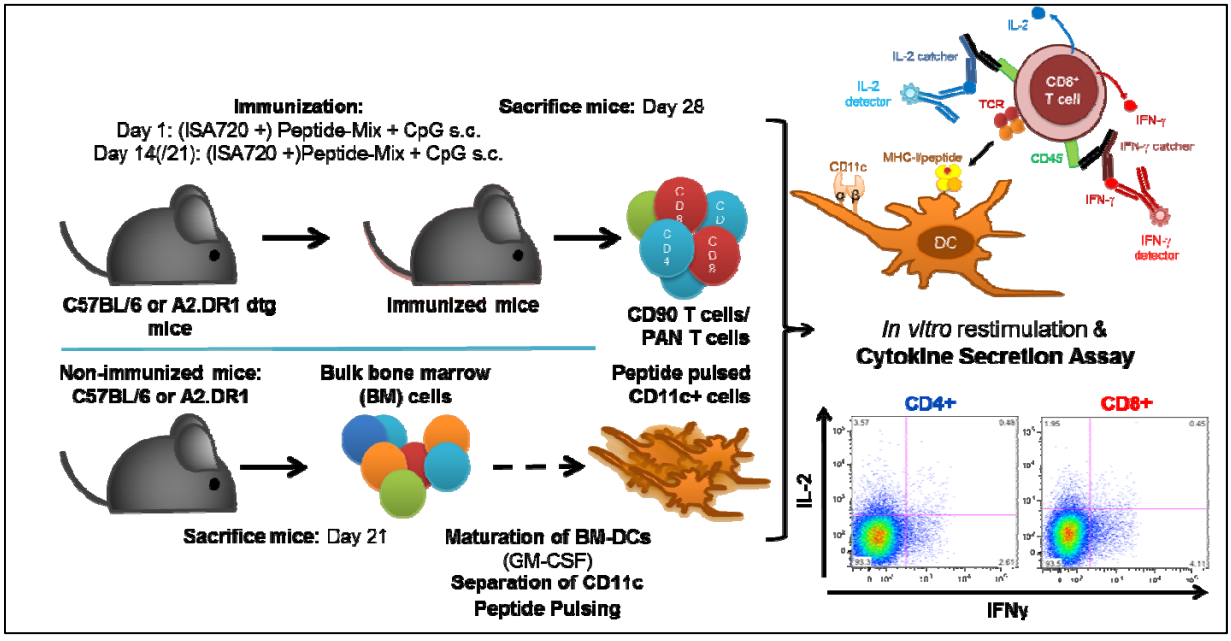


**Figure 2.2**: **Schematic overview sketching the assay procedure of a two color cytokine secretion assay**

##### *2.2.3.1.1. In vitro re-stimulation of T cells on peptide pulsed dendritic cells*

Purified $CD11c^+$ dendritic cells served as antigen presenting cells for *in vitro* re-stimulation. 7.5 x $10^4$ dendritic cells were seeded in 100 µl per well in a round bottom, tissue-culture treated 96-Well plate (TPP). Cells were pulsed with 1 µl of 10 mM long peptides or 1 µl of 25 mM short peptides, resulting 1 µl of DMSO per well (1:100 dilution). Following controls were performed: un-pulsed DCs, DCs pulsed with the solvent DMSO only and DCs pulsed with irrelevant IgG peptides. Triplicates were carried out for each peptide tested and each control. Plates were incubated overnight to allow processing of long peptides by dendritic cells.

The following day splenic and lymph node derived T cells from untreated, immunized and/or tumor bearing mice were added to the peptide pulsed dendritic cells. 100 µl T cell suspension comprising 3.75 x $10^5$ cells in X-Vivo-20 medium were pipetted per well, resulting in a total volume of 200 µl medium per well and a DC to T cell ratio of 1 : 5. The co-culture served as short *in vitro* re-stimulation of antigen-specific T cells and was carried out for exactly 16 h per assay to insure comparability between different assays. Additional wells comprising only T cells were seeded as negative controls to get an impression of basal T cell activity and for staining/gating controls.

*2.2.3.1.2. Cytokine secretion period*

After 16 h of *in vitro* re-stimulation cytokine secretion assays were initiated. Plates were centrifuged for 3 min at 2000 rpm (4 °C) and supernatants were discarded. Cells were washed once in 200 µl FACS buffer per well by resuspending via pipetting, centrifugation and discarding the supernatants. Afterwards an Fc receptor blocking was performed. Therefore 10 µl of a culture supernatant from hybridoma cell line 2.4G2 producing an antibody against the murine Fc gamma receptor (FcRII, CD32) was mixed with 90 µl of FACS buffer (1:10 dilution) per sample. Cells in each well were resuspended in 100 µl of the diluted hybridoma supernatant and plates were incubated on ice. After 20 min of incubation 100 µl FACS buffer were added per well and plates were spun down. The supernatant was discarded and cells were washed again in 200 µl of FACS buffer.

Next the cells were labeled with cytokine catching bidirectional antibodies, referred to as “Catch reagents”. Catch reagents were pre-mixed with X-Vivo-20 medium for a single sample as follows:

**Table 2.7**: Pre-mix of IL-2 and IFN-γ cytokine catch reagents

| Components | Volumes [µl] |
|---|---|
| X-Vivo-20 | 90.0 |
| IL-2 catch reagent | 5.0 |
| IFN-γ catch reagent | 5.0 |
| *Total volume* | *100.0* |

Pellets in each well were resuspended in 100 µl of pre-mixed catch reagent dilution and incubated for 20 min on ice. In the meantime a PMA/Ionomycin dilution was prepared in X-Vivo-20 according to the working concentrations listed in passage 2.1.3.2. PMA/Ionomycin unspecific activated T cells (producing high levels of cytokines) served as staining controls. After 20 min cells were spun down and resuspended in 200 µl fresh, 37 °C pre-warmed X-Vivo-20 per well. Staining controls were resuspended in 200 µl PMA/Ionomycin dilution. During the cytokine secretion period plates were incubated for 3 h at 37 °C and 5 % $CO_2$.

*2.2.3.1.3. Cytokine Secretion Assay – FACS staining*

After 3h of incubation plates were first pun down, the supernatant was discarded and cells were washed again in 200 µl FACS buffer each well to remove all medium.

Before surface marker staining viability staining was performed for subsequent dead cell discrimination. This was done employing the LIVE/DEAD® Fixable Yellow Dead Cell Stain Kit (Life Technologies - Molecular Probes, Eugene, Oregon, USA). The lyophilized dye was reconstituted in DMSO under sterile conditions in the laminar flow according to manufacturer's instructions. The resulting stock solution was further diluted 1:500 (sometimes 1:750) in FACS buffer to achieve working concentration. Cells were resuspended thoroughly by pipetting in 200 µl working solution per well and incubated in the dark on ice for 20 min. Then plates were spun down, supernatant was discarded and cells were washed twice to remove all unbound viability dye completely.

Besides the actual surface staining several controls were performed. For all markers being not clearly and strongly expressed like lineage markers (CD3, CD4, etc.) isotype controls (ISO) were performed to estimate the unspecific biding of respective antibodies, in this case for the makers IFN-γ and IL-2. As afore mentioned markers do not result in distinct populations in FACS blots, FMO (fluorescence minus one) controls were conducted to allow proper and accurate gating. All together the following antibody mixes were prepared:

**Table 2.8**: Antibody mixes for cytokine secretion assay surface staining and corresponding FMO controls (100 µl for a maximum of 1 x $10^6$ cells/sample)

| Components | Full Stain | IL-2-FMO | IFN-γ-FMO | CD11c-FMO |
|---|---|---|---|---|
| **IFN-γ-Detector-PE** | **5.0 µl** | 5.0 µl | - | 5.0 µl |
| **IL-2-Detector-PE** | **5.0 µl** | - | 5.0 µl | 5.0 µl |
| **CD11c-PE-Cy7** | **0.5 µl** | 0.5 µl | 0.5 µl | - |
| **CD4-FITC** | **0.75 µl** | 0.75 µl | 0.75 µl | 0.75 µl |
| **CD8-Pacific Blue** | **1.0 µl** | 1.0 µl | 1.0 µl | 1.0 µl |
| **FACS-Buffer** | **87.75 µl** | 92.75 µl | 92.75 µl | 88.25 µl |
| ***Total volume*** | ***100.0 µl*** | *100.0 µl* | *100.0 µl* | *100.0 µl* |

**Table 2.9**: Antibody mixes for isotype controls of the two color cytokine secretion assay (100 µl for a maximum of 1 x $10^6$ cells/sample)

| Components | IL-2-ISO | | Components | IFN-γ-ISO |
|---|---|---|---|---|
| **IFN-γ-Detector-PE** | 5.0 µl | | **Rat *IgG1,κ*-PE** | 1.0 µl |
| **Rat *IgG2b,κ*-APC** | 1.0 µl | | **IL-2-Detector-PE** | 5.0 µl |
| **CD11c-PE-Cy7** | 0.5 µl | | **CD11c-PE-Cy7** | 0.5 µl |
| **CD4-FITC** | 0.75 µl | | **CD4-FITC** | 0.75 µl |
| **CD8-Pacific Blue** | 1.0 µl | | **CD8-Pacific Blue** | 1.0 µl |
| **FACS-Buffer** | 91.75 µl | | **FACS-Buffer** | 91.75 µl |
| ***Total volume*** | *100.0 µl* | | ***Total volume*** | *100.0 µl* |

Cells were resuspended in 100 µl of respective antibody mixes per sample and incubated on ice in the dark. After 20 min of incubation 100 µl FACS buffer was added per well and plates were spun down. Supernatant was discarded and cells were washed once more in 200 µl FACS buffer each well. For the acquisition of the samples with FACS Canto II the cells were resuspended in 120 µl FACS buffer per well. In table 2.10 an exemplary plate scheme including all control is shown.

**Table 2.10**: Exemplary plate scheme for a two color cytokine secretion assay (DC: dendritic cells, TC: T cells, Pep: peptide, wt: wild type, mut: mutated, unp.: un-pulsed, Irr.: irrelevant, PMA/I: PMA/Ionomycin full stain control, Auto: auto fluorescence (unstained) control)

| | 1 | 2 | 3 | 4 | 5 | (…) | 8 | 9 | 10 | 11 | 12 |
|---|---|---|---|---|---|---|---|---|---|---|---|
| **A** | | **Tested peptides** | | | | | **Assay Controls** | | | | |
| **B** | | Pep1-wt | Pep2-mut | Pep2-wt | Pep2-mut | (…) | DC-DMSO | DC unp. | TC only | Irr. pep | |
| **C** | | Pep1-wt | Pep2-mut | Pep2-wt | Pep2-mut | (…) | DC-DMSO | DC unp. | TC only | Irr. pep | |
| **D** | | Pep1-wt | Pep2-mut | Pep2-wt | Pep2-mut | (…) | DC-DMSO | DC unp. | TC only | Irr. pep | |
| **E** | | **Staining controls** | | | | | | | | | |
| **F** | | PMA/I | IL-2-FMO | IFN-γ-FMO | CD11c-FMO | | | | | | |
| **G** | | IL-2-ISO | IFN-γ-ISO | Viability dye only | Auto (un-stained) | | | | | | |
| **H** | | | | | | | | | | | |

*2.2.3.1.4. Staining of beads for compensation*

The process of determination, calculation and subsequent subtraction of spectral overlaps from one fluorescent detector channel in FACS Canto II to the other is called compensation. The compensation was calculated and applied to all acquired samples of one experiment using the BD FACS Diva software auto-compensation tool. To determine the spectral overlap from one channel to the other additional single color samples from each color used in the staining panel had to be conducted and acquired. This was done by coding beads with the same antibodies used for staining. Two different sets of compensation beads were used: for antibodies derived from murine origin CompBead anti-Mouse Ig, κ/negative Controls (FBS) Compensation Particles (BD Biosciences) and for antibodies originating from rats or hamsters Anti-Rat and Anti-Hamster Ig κ/Negative Control Compensation Particles (BD Biosciences).

For each antibody a 1,5 ml test tube was prepared and 100 µl FACS buffer were pipetted each. Bead stock tubes were resuspended thoroughly by shaking and one droplet of respective CompBeads and negative controls were added in each tube according to the species the antibodies are originating from (resulting in a volume of roughly 200 µl per test tube). Bead suspensions were vortexed. Single antibodies were added in respective tubes in the same concentrations used for staining of cells in the actual assay. Samples were tapped for resuspending the antibodies and afterwards incubated in the dark for 5 to 20 min on ice. After labeling 1 ml FACS buffer was added per test tube for washing and beads were spun down in a 4 °C cooled table centrifuge for 20 s at 13'000 rpm. The supernatants were taken off completely and beads were resuspended in 500 µl FACS buffer per sample. The beads were then ready to be acquired with FACS Canto II for compensation.

As a reference the autofluorescence of the cells had to be determined as well by acquiring completely unstained cells. Moreover additional cells had to be stained with only the viability dye as a single color staining because viability cannot be accessed via bead staining.

#### 2.2.3.2. Combined IFN-γ secretion assay and intracellular cytokine staining

For further functional analysis of mutation specific T cells induced by vaccination the IFN-γ secretion assay was combined with intracellular staining for cytokines (ICCS). These assays were also carried out in a 96 well plate format. In a first step an IFN-γ secretion assay was performed. *In vitro* re-stimulation of T cells from immunized mice on peptides pulsed dendritic cells was performed in exactly the same way as described in the passage 2.2.3.1.1. "*In vitro* re-stimulation of T cells on peptide pulsed dendritic cells". The labeling with the bidirectional IFN-γ catch antibody was carried out as for the two color cytokine secretion assay leaving out the IL-2 Catch reagent (see table below).

**Table 2.11**: Pre-mix of IFN-γ cytokine catch reagent

| Components | Volumes [µl] |
|---|---|
| X-Vivo-20 | 95.0 |
| IFN-γ catch reagent | 5.0 |
| *Total volume* | *100.0* |

##### *2.2.3.2.1. Stopping secretion of cytokines by inhibitors of the Golgi apparatus*

To facilitate the accumulation of intracellular cytokines for staining and detection via FACS analysis the secretion had to be stopped. Blocking of cytokine secretion was achieved by treating the cells with the protein transport inhibitor monensin. An alternative reagent which is also frequently used to inhibit the cytokine secretion in T cells would be brefeldin A. It was tested in pilot experiments and turned out to be less suitable for the detection of cytokines in this experimental set-up.

After the secretion period of 3 h at 37 °C and 5 % $CO_2$ plates were spun down & the medium was discarded. The cells were resuspended in 200 µl of X-Vivo-20 supplemented with BD GolgiStop™ (BD Biosciences) containing monensin in a 1:1500 dilution. Assay plates were incubated for further 8 h at 37 °C and 5 % $CO_2$ for the intracellular accumulation of cytokines. Additional controls had to be added for intracellular staining. To estimate the efficiency of the protein transport inhibition one sample was not treated with monensin. As for the secretion assay a staining control was required. In this case the cells were un-specifically activated by treatment with a cell stimulation cocktail containing PMA, ionomycin, monensin and brefeldin A. The Cell Stimulation Cocktail (plus protein inhibitors, 500X, eBioscience) was diluted 1:500 in X-Vivo-20 and control cells were resuspended in 200 µl of the diluted cocktail instead of being incubated in the X-Vivo-20 containing only monensin.

##### *2.2.3.2.2. Combined IFN-γ-Cytokine Secretion Assay/ICCS – FACS staining*

For FACS staining plates were spun down and medium was discarded. Cells were washed again in 200 µl FCAS buffer per well. As first step a viability staining employing the dye Ethidium bromide monoazide (EMA) was performed. EMA is penetrating dead cells' membranes and cross-links to DNA by UV-light exposure, therewith staining dead cells specifically. Cells were thoroughly resuspended by pipetting in FACS buffer containing 150 µg/ml EMA (Sigma Aldrich). The EMA stock solution was

prepared by reconstituting the solid dye in PBS to a concentration of 1 mg/ml. Aliquots were stored at -20 °C in the dark and a freshly thawed aliquot was used for each experiment. The plates were incubated on ice exposed to bright light for 10 min and then washed twice in FACS buffer to remove all unbound EMA dye. Cells were resuspended in 100 µl of respective antibody mixes for surface staining and plates were incubated for 20 min on ice in the dark. Antibody mixes for the complete staining and respective controls are listed in tables 2.12 and 2.13.

**Table 2.12**: Antibody mixes for surface staining of the combined IFN-γ secretion assay/ICCS and corresponding FMO controls (100 µl for a maximum of 1 x $10^6$ cells/sample)

| Components | Full Stain | IFN-γ-FMO | NK-1.1-FMO | CD11c-FMO | CD11c/NK-1.1-FMO |
|---|---|---|---|---|---|
| **IFN-γ-Detector-PE** | **5.0 µl** | - | 5.0 µl | 5.0 µl | 5.0 µl |
| **NK-1.1-PE-Cy7** | **0.5 µl** | 0.5 µl | - | 0.5 µl | - |
| **CD11c-PE-Cy7** | **0.5 µl** | 0.5 µl | 0.5 µl | - | - |
| **CD4-V500** | **1.0 µl** | 1.0 µl | 1.0 µl | 1.0 µl | 1.0 µl |
| **CD8-Pacific Blue** | **1.0 µl** | 1.0 µl | 1.0 µl | 1.0 µl | 1.0 µl |
| **FACS-Buffer** | **92.0 µl** | 97.0 µl | 92.5 µl | 92.5 µl | 93.0 µl |
| ***Total volume*** | ***100.0 µl*** | *100.0 µl* | *100.0 µl* | *100.0 µl* | *100.0 µl* |

**Table 2.13**: Antibody mix for the combined IFN-γ secretion assay /ICCS IFN-γ isotype control (100 µl for a maximum of 1 x $10^6$ cells/sample)

| Components | IFN-γ-ISO |
|---|---|
| **Rat *IgG1,κ*-PE** | 5.0 µl |
| **NK-1.1-PE-Cy7** | 0.5 µl |
| **CD11c-PE-Cy7** | 0.5 µl |
| **CD4-V500** | 1.0 µl |
| **CD8-Pacific Blue** | 1.0 µl |
| **FACS-Buffer** | 92.0 µl |
| ***Total volume*** | *100.0 µl* |

After 20 min of incubation 100 µl FACS buffer were added per well and plates were spun down. Supernatant was discarded and cells were washed once more in 200 µl FACS buffer each well. In the next step the samples had to be fixed for intracellular cytokine staining employing the BD Cytofix/Cytoperm™ Fixation/Permeabilization Solution Kit (BD Biosciences). Cell were resuspended thoroughly by pipetting in 200 µl of Fixation/Permeabilization solution and incubated for 1 h 30 min one ice in the dark. 10 X Perm/Wash™ buffer was diluted in sterile dd$H_2O$ to 1 X working concentration and cooled down on ice. After fixation cells were washed twice in 200 µl 1 X Perm/Wash™ buffer. Sometimes the assay was interrupted at this point. Therefore, cells were resuspended in 200 µl Perm/Wash buffer and plates were stored overnight in the refrigerator wrapped in aluminum foil to protect the samples from light exposure.

Antibody mixes for intracellular staining were diluted in 1 X Perm/Wash buffer instead of FACS buffer to keep the cell membranes of the fixed cells permeable and therewith allow the entry of the staining antibodies. The following full stain mix and control mixes were prepared as shown in tables 2.14 and 2.15. Cells were resuspended in 100 µl of the respective mixes. Plates were incubated for 30 min on ice in the dark. (In a variation of the assay the IL-2-FITC antibody was excluded from the panel and

instead of the CD4-Pacific Orange antibody a CD4-FITC conjugated antibody was used instead for surface staining.)

**Table 2.14**: Antibody mixes for intracellular staining of the combined IFN-γ secretion assay/ICCS and corresponding FMO controls (100 µl for a maximum of 1 x $10^6$ cells/sample)

| Components | Full Stain | IL-2-FMO | IFN-γ-FMO | TNFα-FMO |
|---|---|---|---|---|
| **IL-2-FITC** | **0.25 µl** | - | 0.25 µl | 0.25 µl |
| **IFN-γ-A647** | **0.25 µl** | 0.25 µl | - | 0.25 µl |
| **TNFα-APC-Cy7** | **0.25 µl** | 0.25 µl | 0.25 µl | - |
| **1 X Perm/Wash buffer** | **99.25 µl** | 99.5 µl | 99.5 µl | 99.5 µl |
| ***Total volume*** | ***100.0 µl*** | *100.0 µl* | *100.0 µl* | *100.0 µl* |

**Table 2.15**: Antibody mixes for the combined IFN-γ secretion assay /ICCS: Isotype controls for intracellular staining (100 µl for a maximum of 1 x $10^6$ cells/sample)

| Components | IL-2-ISO | Components | IFN-γ-ISO | Components | TNFα-ISO |
|---|---|---|---|---|---|
| **Rat *IgG2b,κ*-FITC** | 0.25 µl | IL-2-FITC | 0.25 µl | IL-2-FITC | 0.25 µl |
| IFNγ-A647 | 0.25 µl | **Rat *IgG1,κ*-A647** | 0.25 µl | IFNγ-A647 | 0.25 µl |
| TNFα-APC-Cy7 | 0.25 µl | TNFα-APC-Cy7 | 0.25 µl | **Rat *IgG1,κ*-APC-Cy7** | 0.25 µl |
| Perm/Wash buffer | 99.25 µl | Perm/Wash buffer | 99.25 µl | Perm/Wash buffer | 99.25 µl |
| *Total volume* | *100.0 µl* | *Total volume* | *100.0 µl* | *Total volume* | *100.0 µl* |

After intracellular staining 100 µl FACS buffer was added per well and plates were spun down. Supernatant was discarded and cells were washed once more in 200 µl FACS buffer each well. For the acquisition of the samples with FACS Canto II the cells were resuspended in 120 µl FACS buffer per well. In table 2.16 an exemplary plate scheme including all controls is shown. For compensation beads and cells were prepared as described in passage 2.2.3.1.4.

**Table 2.16**: Exemplary plate scheme for a combined IFN-γ secretion assay/ICCS (DC: dendritic cells, TC: T cells, Pep: peptide, wt: wild type, mut: mutated, unp.: un-pulsed, Irr.: irrelevant, PMA/I: PMA/Ionomycin full stain control, Auto: auto fluorescence (unstained) control, Stim. Cock.: stimulation cocktail treated, w/o GolgiS.: without GolgiStop inhibitor)

| | 1 | 2 | 3 | 4 | 5 | (…) | 8 | 9 | 10 | 11 | 12 |
|---|---|---|---|---|---|---|---|---|---|---|---|
| **A** | | **Tested peptides** | | | | | **Assay Controls** | | | | |
| **B** | | Pep1-wt | Pep2-mut | Pep2-wt | Pep2-mut | (…) | DC-DMSO | DC unp. | TC only | Irr. pep | |
| **C** | | Pep1-wt | Pep2-mut | Pep2-wt | Pep2-mut | (…) | DC-DMSO | DC unp. | TC only | Irr. pep | |
| **D** | | Pep1-wt | Pep2-mut | Pep2-wt | Pep2-mut | (…) | DC-DMSO | DC unp. | TC only | Irr. pep | |
| **E** | | **Surface Staining Controls** | | | | | **Intracellular (Staining) Controls** | | | | |
| **F** | | PMA/I | IFN-γ-FMO | IFN-γ-ISO | CD11c-FMO | | w/o GolgiS. | Stim. Cock. | IL-2-ISO | IL-2-FMO | |
| **G** | | NK-1.1-FMO | CD11c /NK-1.1-FMO | Viability (EMA) dye only | Auto (un-stained) | | IFN-γ-ISO | IFN-γ-FMO | TNFα-ISO | TNFα-FMO | |
| **H** | | | | | | | | | | | |

### 2.2.3.3. CD107a Degranulation Assay

CD107a is a marker for degranulation of cytotoxic granules on T cells and NK cells which can indicate a cytolytic activity of these cells. We performed CD107a degranulation assays in combination with intracellular IFN-γ staining to estimate the cytolytic potential of vaccination induced mutated antigen specific T cells.

Similar to the assays mentioned before an antigen-specific re-stimulation of T cells purified from immunized mice was performed on peptide pulsed dendritic cells. 2 x $10^5$ dendritic cells in 100 µl of X-Vivo-20 medium were seeded in a tissue culture treated 96 plates and pulsed with peptides. The following day T cells were added in 1:5 ratio, meaning 1 x $10^6$ T cells in 50 µl of X-Vivo-20 and resulting in a volume of 150 µl per well. Before co-culture a Fc-block with the T cells was performed as described above. Afterwards cells were carefully washed to remove Fc-blocking antibodies and cells were then resuspended in X-Vivo-20 to be seeded on the dendritic cells.

Then 2 µl of CD107a-FITC antibodies were directly added into the medium of each re-stimulation sample. One well was supplemented with the corresponding isotype antibody Rat *IgG2a, κ*-FITC instead of the actual specific antibody. The samples were incubated for 2 h at 37 °C and 5 % $CO_2$. Then secretion was stopped by adding 50 µl of GolgiStop pre-dilution in X-Vivo-20 (1:375) to a final working concentration of 1:1500 per well. As for the combined secretion assay/ICCS a staining control was performed. Cells were again un-specifically activated by treatment with cell stimulation cocktail (plus protein inhibitors, 500X) (eBioscience). It was diluted to a working concentration of 1:500 in X-Vivo-20 per well by adding 50 µl pre-dilution (1:125) in X-Vivo-20 instead of the GolgiStop pre-dilution. All samples were then incubated for 12 h at 37 °C and 5 % $CO_2$.

After incubation period was over, cells were spun down and washed once in FACS buffer. Then a viability staining employing EMA was performed as described before. Cells were washed twice in FACS buffer followed by surface staining. For surface staining cell pellets were resuspended in 100 µl antibody surface mix or controls mixes (see table below) and incubated for 20 min on ice in the dark.

**Table 2.17**: Antibody mixes for surface staining of CD107a degranulation assay and corresponding FMO control (100 µl for a maximum of 1 x $10^6$ cells/sample)

| Components | Full Stain | CD11c-FMO |
|---|---|---|
| **CD11c-PE-Cy7** | **0.5 µl** | - |
| **CD4-V500** | **1.0 µl** | 1.0 µl |
| **CD8-Pacific Blue** | **1.0 µl** | 1.0 µl |
| **FACS-Buffer** | **97.5 µl** | 98.0 µl |
| ***Total volume*** | ***100.0 µl*** | *100.0 µl* |

After 20 min of incubation 100 µl FACS buffer were added per well and plates were spun down. Supernatant was discarded and cells were washed once more in 200 µl FACS buffer each well. In the next step the samples were fixed for intracellular cytokine staining employing the BD Cytofix/Cytoperm™

Fixation/Permeabilization Solution Kit (BD Biosciences). Cell were resuspended thoroughly by pipetting in 200 µl of Fixation/Permeabilization solution and incubated for 1 h 30 min one ice in the dark. After fixation cells were washed twice in 200 µl 1 X Perm/Wash™ buffer. The following full stain mix and control mix were prepared as shown in table 2.18. Cells were resuspended in 100 µl of the respective mixes and plates were incubated for 30 min on ice in the dark.

**Table 2.18**: Antibody mix for intracellular cytokine staining in context of a CD107a degranulation assay and corresponding isotype control (100 µl for a maximum of 1 x $10^6$ cells/sample)

| **Components** | **IL-2-ISO** | | **Components** | **IFN-γ-ISO** |
|---|---|---|---|---|
| **IFN-γ-A647** | **0.5 µl** | | **Rat *IgG1,κ*-A647** | **0.5 µl** |
| 1 X Perm/Wash buffer | 99.5 µl | | 1 X Perm/Wash buffer | 99.5 µl |
| *Total volume* | *100.0 µl* | | *Total volume* | *100.0 µl* |

After intracellular staining 100 µl FACS buffer was added per well and plates were spun down. Supernatant was discarded and cells were washed once more in 200 µl FACS buffer each well. For the acquisition of the samples with FACS Canto II the cells were resuspended in 200 µl FACS buffer per well. For compensation beads and cells were prepared as described in passage 2.2.3.1.4.

A variation of this assay was carried out by replacing IFN-γ staining with staining for granzyme B and perforin, two makers of cytotoxicity. This is why this assay is also referred to as the cytotoxicity staining. After viability staining with EMA the cells were directly fixed in the way described earlier in the passage. Antibody mixes for the full stain and controls were prepared in Perm/Wash buffer (see tables 2.19 & 2.20). Cells were resuspended in 100 µl of the respective mixes and incubated on ice in the dark. After 40 min of incubation 100 µl FACS buffer was added per well and plates were spun down. Supernatant was discarded and cells were washed once more in 200 µl FACS buffer each well. For the acquisition of the samples with FACS Canto II the cells were resuspended in 200 µl FACS buffer per well.

**Table 2.19**: Antibody mix for cytotoxicity staining and corresponding FMO controls (100 µl for a maximum of 1 x $10^6$ cells/sample)

| **Components** | **Full Stain** | **GranzymeB-FMO** | **Perforin-FMO** |
|---|---|---|---|
| **GranzymeB-PE** | 0.7 µl | - | 0.7 µl |
| **Perforin-APC** | 5.0 µl | 5.0 µl | - |
| **CD11c-PE-Cy7** | 0.5 µl | 0.5 µl | 0.5 µl |
| **CD4-V500** | 1.0 µl | 1.0 µl | 1.0 µl |
| **CD8-Pacific Blue** | 1.0 µl | 1.0 µl | 1.0 µl |
| **Perm/Wash buffer** | 91.8 µl | 91.8 µl | 91.8 µl |
| ***Total volume*** | *100.0 µl* | *100.0 µl* | *100.0 µl* |

**Table 2.20**: Mixes for isotype controls for cytotoxicity staining (100 µl for a maximum of 1 x $10^6$ cells/sample)

| **Components** | **GranzymeB-ISO** | | **Components** | **Perforin-ISO** |
|---|---|---|---|---|
| **Rat *IgG2a,κ*-PE** | **5.0 µl** | | GranzymeB-PE | 0.7 µl |
| Perforin-APC | 5.0 µl | | **Rat *IgG2a,κ*-APC** | **5.0 µl** |
| CD11c-PE-Cy7 | 0.5 µl | | CD11c-PE-Cy7 | 0.5 µl |
| CD4-V500 | 1.0 µl | | CD4-V500 | 1.0 µl |
| CD8-Pacific Blue | 1.0 µl | | CD8-Pacific Blue | 1.0 µl |
| Perm/Wash buffer | 87.5 µl | | Perm/Wash buffer | 91.8 µl |
| *Total volume* | *100.0 µl* | | *Total volume* | *100.0 µl* |

### 2.2.3.4. Staining of regulatory T cells

#### *2.2.3.4.1. Preparation of samples for $T_{reg}$ cell staining*

Regulatory T cells were stained for in the spleen and in tumor tissue of mice. Spleens and tumor tissue were resected from tumor bearing mice. Single cell suspension from spleens were generated by mashing the organs through 100 µl cell strainers and erythrocyte lysis was performed as described in passage 2.2.1.3.2. The lysed samples were resuspended after centrifugation in 10 µl of FACS buffer and filtered through a 40 µl cell strainer to remove the cell debris. Spleen samples were then used right away without further purification for FACS staining. Tumor tissue was cut into small pieces (diameter of 1 to 2 mm) using sterile disposable scalpels and forceps. Tissue pieces were transferred into a PBS pre-wet 100 µl cell strainer and the tissue was minced through the strainer employing a plunger form a 1 ml syringe. During that process continuously fresh PBS was added by pipetting. Gained cell suspension was centrifuged at 1700 rpm for 5 min at 4 °C and supernatant was discarded. The cell pellet was resuspended in 20 ml of ice-cooled FACS buffer and filtered through a 40 µm cell strainer. The resulting cell suspension was used for $T_{reg}$ staining.

#### *2.2.3.4.2. FACS staining of regulatory T cells*

The cells were plated and stained in non-tissue-culture treated 96 well plates (round-bottom, BD Falcon). Per sample at least 1 x $10^6$ cells were used for staining. First an Fc receptor blocking was performed as described before. This was followed by a viability staining using the LIVE/DEAD® Fixable Yellow Dead Cell Stain Kit (Life Technologies - Molecular Probes).

After viability staining and consecutive washing a surface staining was conducted. Each animal was analyzed individually, meaning two full stained samples and all controls were carried out for each mouse. Cell pellets were therefore resuspended in 100 µl full stain master mixes or individual control antibody mixes. Antibody combinations of the mixes are listed in the following table. The plates were incubated for 20 min on ice in the dark. Then 100 µl FACS buffer was added to each sample and plates were spun down. Cells were washed again in 200 µl FACS buffer.

**Table 2.21**: Antibody mixes for $T_{reg}$ cell surface staining and corresponding controls (100 µl for a maximum of 2 x $10^6$ cells/sample)

| **Components** | **Full Stain** | **CD25-FMO** | | **Components** | **CD25-ISO** |
|---|---|---|---|---|---|
| **CD4-FITC** | **1.0 µl** | 1.0 µl | | CD4-FITC | 1.0 µl |
| **CD3-PB** | **2.0 µl** | 2.0 µl | | CD3-PB | 2.0 µl |
| **CD25-PE** | **2.0 µl** | - | | **Rat *IgM* -PE** | **2.0 µl** |
| **FACS-Buffer** | **95.0 µl** | 97.0 µl | | FACS-Buffer | 95.0 µl |
| ***Total volume*** | ***100.0 µl*** | *100.0 µl* | | *Total volume* | *100.0 µl* |

Following surface staining the cells were fixed for intra-nuclear staining of the master transcription factor for regulatory T cells Foxp3. To facilitate the staining a special buffer system optimized for detection of nuclear proteins had to be used for fixation, the Foxp3/Transcription Factor Staining Buffer Set

(eBioscience). Concentrated buffers were diluted to working concentrations according to manufacturers' instructions. Cell pellets were resuspended thoroughly by pipetting up and down in 200 µl 1 X Fixation/Permeabilization Buffer and incubated for 60 min on ice in the dark. In between, after 30 min of incubation, cells were resuspended again via pipetting to increase fixation efficiency. Cells were washed twice in 200 µl 1 X Permeabilization buffer per sample after the total incubation time of 60 min was over. Again cells were resuspended thoroughly in 200 µl 1 X Permeabilization buffer and plates were incubated on ice for 15 min in the dark. Then plates were spun down and washed again in 1 X Permeabilization buffer.

For the intra-nuclear staining the antibody had to be diluted in Permeabilization buffer to keep the membranes open and therewith allowing the entry of the antibody into the cell/nucleus. The cells were resuspended again very thoroughly by pipetting up and down in 100 µl of the diluted antibody mixes (see table 2.22). For the Foxp3 FMO control only buffer was added to the cells. Cells were incubated for 30 min on ice in the dark. Afterwards 100 µl FACS buffer were added per sample and plates were spun down. Cells were washed again in 200 µl FACS buffer. For acquisition with FACS Canto II cells were resuspended in 200 µl FACS buffer. Compensation beads were prepared accordingly to passage 2.2.3.1.4.

**Table 2.22**: Antibody mixes for $T_{reg}$ cell intracellular staining and corresponding controls (100 µl for a maximum of 2 x $10^6$ cells/sample)

| **Components** | **Full Stain** | **Foxp3-FMO** | | **Components** | **Foxp3-ISO** |
|---|---|---|---|---|---|
| **Foxp3-A647** | **2.0 µl** | - | | Rat *IgG2b,κ*-A647 | 2.0 µl |
| **Permeabilization buffer** | **98.0 µl** | 100.0 µl | | Permeabilization buffer | 98.0 µl |
| ***Total volume*** | ***100.0 µl*** | *100.0 µl* | | *Total volume* | *100.0 µl* |

### 2.2.3.5. Combined Memory and regulatory T cell staining

To further assess the phenotype of effector and regulatory T cells two more markers were included into the antibody panel of the regulatory T cell staining, namely CD62L and CD44. The assay was performed exactly as described before. The only change was made for the surface staining by adding the two additional antibodies to the mixes and conducting respective isotype and FMO controls as shown in tables 2.23 and 2.24. An exemplary plate scheme is displayed in table 2.25.

**Table 2.23**: Antibody mixes for combined memory and $T_{reg}$ cell surface staining and corresponding FMO controls (100 µl for a maximum of 2 x $10^6$ cells/sample)

| **Components** | **Full Stain** | **CD25-FMO** | **CD44-FMO** | **CD62L-FMO** |
|---|---|---|---|---|
| **CD4-FITC** | **1.0 µl** | 1.0 µl | 1.0 µl | 1.0 µl |
| **CD3-PB** | **2.0 µl** | 2.0 µl | 2.0 µl | 2.0 µl |
| **CD25-PE** | **2.0 µl** | - | 2.0 µl | 2.0 µl |
| **CD44-APC-Cy7** | **0.5 µl** | 0.5 µl | - | 0.5 µl |
| **CD62L-PerCP-Cy5.5** | **0.5 µl** | 0.5 µl | 0.5 µl | - |
| **FACS-Buffer** | **94.0 µl** | 96.0 µl | 94.5 µl | 94.5 µl |
| ***Total volume*** | ***100.0 µl*** | *100.0 µl* | *100.0 µl* | *100.0 µl* |

**Table 2.24**: Antibody mixes for combined memory and $T_{reg}$ cell surface staining isotype controls (100 µl for a maximum of 2 x $10^6$ cells/sample)

| **Components** | **CD25-ISO** | **Components** | **CD44-ISO** | **Components** | **CD62L-ISO** |
|---|---|---|---|---|---|
| CD4-FITC | 1.0 µl | CD4-FITC | 1.0 µl | CD4-FITC | 1.0 µl |
| CD3-PB | 2.0 µl | CD3-PB | 2.0 µl | CD3-PB | 2.0 µl |
| **Rat *IgM* -PE** | **2.0 µl** | CD25-PE | 2.0 µl | CD25-PE | 2.0 µl |
| CD44-APC-Cy7 | 0.5 µl | **Rat *IgG2b,κ*-APC-Cy7** | **0.5 µl** | CD44-APC-Cy7 | 0.5 µl |
| CD62L-PerCP-Cy5.5 | 0.5 µl | CD62L-PerCP-Cy5.5 | 0.5 µl | **Rat *IgG2a,κ*-PerCP-Cy5.5** | **0.5 µl** |
| FACS-Buffer | 94.0 µl | FACS-Buffer | 94.0 µl | FACS-Buffer | 94.0 µl |
| *Total volume* | *100.0 µl* | *Total volume* | *100.0 µl* | *Total volume* | *100.0 µl* |

**Table 2.25**: Exemplary plate scheme for a combined memory and $T_{reg}$ cell staining (FS: full staining, M(n): analyzed mouse number (n), SC: staining/compensation controls, Auto: auto fluorescence (unstained) control, PO: cells stained with the yellow viability dye only)

| | **1** | **2** | **3** | **4** | **5** | **6** | **7** | **8** | **9** | **10** | **11** | |
|---|---|---|---|---|---|---|---|---|---|---|---|---|
| **A** | **M1** | FS | FS | CD25-ISO | CD25-FMO | CD44-ISO | CD44-FMO | CD62L-ISO | CD62L-FMO | Foxp3-ISO | Foxp3-FMO | |
| **B** | **M2** | FS | FS | CD25-ISO | CD25-FMO | CD44-ISO | CD44-FMO | CD62L-ISO | CD62L-FMO | Foxp3-ISO | Foxp3-FMO | |
| **C** | **M3** | FS | FS | CD25-ISO | CD25-FMO | CD44-ISO | CD44-FMO | CD62L-ISO | CD62L-FMO | Foxp3-ISO | Foxp3-FMO | |
| **(…)** | **(…)** | | | | | | | | | | | |
| **H** | **SC** | PO | PO | Auto | Auto | | | | | | | |

### 2.2.3.6. Staining for MHC molecules

To investigate the MHC expression of primary murine cells and MCA-induced tumor cell lines cell suspensions were stained for murine and human MHC molecules in FACS analysis. Cultured cells were harvested by trypsinization and washed twice. Tumor tissue and spleen samples were prepared in the same way as described for the staining of $T_{reg}$ cells. The cells were plated and stained in non-tissue-culture treated 96 well plates (round-bottom, BD Falcon). Per sample at least 1 x $10^6$ cells were used for staining. First an Fc receptor blocking was performed as described before. This was followed by a viability staining using the LIVE/DEAD® Fixable Yellow Dead Cell Stain Kit (Life Technologies - Molecular Probes).

For the surface staining the cells of the each sample were resuspended in 100 µl of a certain combination of MHC detecting antibodies or respective isotype controls. As the combinations of antibodies were altering frequently depending on the carried out experiment only the titrated concentrations of the antibodies used in 100 µl of FACS buffer per sample are listed in table 2.26. Samples were incubated for 20 min on ice in dark. Afterwards 100 µl FACS buffer were added per sample and plates were spun down. Cells were washed again in 200 µl FACS buffer. For acquisition with FACS Canto II cells were resuspended in 200 µl FACS buffer. Prior acquisition tumor and cultured cell line samples were transferred into 40 µl cell strainer cupped tubes (BD Falcon) to avoid clogging of the FACS machine by cell aggregates.

**Table 2.26**: Antibody dilutions for staining of murine and human MHC molecules

| MHC specific antibody | Volume per 100 µl [µl] | Corresponding isotype antibody | Volume per 100 µl [µl] |
|---|---|---|---|
| **HLA-A2-FITC** | 0,5 µl | Mouse IgG2b,κ-FITC | 20,0 µl |
| **HLA-A2-APC** | 5,0 µl | Mouse IgG2b,κ-APC | 20,0 µl |
| **HLA-DR1-APC** | 20,0 µl | Mouse IgG2a,κ-APC | 20,0 µl |
| **H-2Kb-PE** | 1,25 µl | Mouse IgG2a,κ-PE | 1,25 µl |
| **H-2D[b]-PE** | 1,25 µl | Mouse IgG2b,κ-PE | 1,25 µl |
| **I-Ad/I-Ed-PE** | 1,25 µl | Rat IgG2a,κ-PE | 20,0 µl |
| **I-A[b]-FITC** | 1,0 µl | Mouse IgG2a,κ-FITC | 1,0 µl |

### 2.2.4. Analysis of T cell effector functions

#### 2.2.4.1. *In vitro* cytotoxicity assay – Chromium Release Method

*In vitro* cytotoxicity assays were carried out to investigate the cytotoxic capacity of T cells from oncogene mutation carrying long peptides vaccinated mice (effector cells). Moreover, this assay can provide evidence of natural processing of antigens (in our case mutated putative epitopes) by tumor cells (target cells).

##### *2.2.4.1.1. Target cells*

*In vitro* kill assays were either performed with transient transfectants or stable transfectants of the cell line 2277-NS. As negative controls B16-F1 melanoma cells with a murine (not the human) MHC background were used, which should not be recognized by T cells from immunized A2.DR1 dtg mice. Transfected target cells were prepared as described in the passage “transient transfection of A2.DR1 dtg fibrosarcoma line 2277-NS” (passage 2.2.2.8.). Stable transfected 2277-NS clones were seeded in 10 ml tissue culture-treated dishes. 1 x $10^6$ cells were seeded in 10 ml of mouse medium supplemented with selection antibiotics (Puromycin 1 mg/ml, Hygromycin 200 µg/ml). The next day transgene expression was induced in the seeded cells by replacing the medium with medium containing selection antibiotics and 1 µg/ml Doxycycline. To induce transgene expression cells were incubated with Doxycycline for 72 h before using the cells as target cells for *in vitro* kill assays.

##### *2.2.4.1.2. Effector cells*

Effector cells were prepared from mice immunized with respective two long peptides as described before. T cells from spleen and peripheral LN were purified and *in vitro* re-stimulated in two different ways. Besides, also T cells from non-immunized mice were *in vitro* re-stimulated on peptide-pulsed DCs and used for kill assays as negative controls.

When *in vitro* kill assays with transient transfected target cells were performed the effector cells were only short-term re-stimulated for 16 h overnight on peptide-pulsed dendritic cells. Therefore, DCs were pulsed and seeded in tissue-culture treated 24-well plates. 2 x $10^6$ dendritic cells were seeded in 400

µl of X-Vivo-20 per well and pulsed with 20 nmol of peptide p53 R248W and 20 nmol (= 2 µl of 10 mM stock solution) of peptide Kras G12V. Plates were incubated overnight. The next day PAN T cells from spleen and LNs of immunized and untreated mice were purified. 1 x $10^7$ purified PAN T cells in 2 ml of X-Vivo-20 were added to the peptide-pulsed DCs and co-cultured for 16 h. The next day T cells were resuspended, spun down and washed in MACS buffer. $CD8^+$ T cells were positively purified via MACS separation. The non-$CD8^+$ fraction was considered as $CD4^+$ T cells and also used as effector cells for *in vitro* kill. Purified effector cells were washed once in 10 ml of X-Vivo-20 and adjusted in fresh X-Vivo-20 for seeding.

For *in vitro* kills employing stable transfectants as target cells the effector T cells were re-stimulated differently for a longer time frame to increase their killing capacity. Purified CD11c positive dendritic cells were pulsed with long peptides p53 R248W and Kras G12V (25 nmol final concentration of each peptide) and seeded in tissue-culture treated 24-Well plates. 2 x $10^5$ DCs were plated in 0.4 ml X-Vivo-20 per well and incubated overnight. The next day PAN T cells from spleen and lymph nodes from immunized and untreated animals were purified. The T cell negative fractions from MACS purification were used as feeder cells. Feeder cells were γ-irradiated with a lethal dose of 33 Gy employing a Cesium-source (Gamma cell 1000 irradiation device). Irradiated feeder cells and PAN T cells were washed and afterwards resuspended in X-Vivo-20. 4 x $10^6$ purified PAN T cells together with 5 x $10^6$ Feeder cells were added to the peptide-pulsed DCs resulting in a volume of 3 ml X-vivo-20 per well. PAN T cells were re-stimulated for 6 days. On day 3 of culture 1.5 ml of medium per well were replaced with 1.5 ml of fresh X-Vivo-20.

One the day of the *in vitro* kill assay (day 6 of *in vitro* re-stimulation) cells in the 24-well plates were resuspended, wells of respective pre-treated mice were pooled, spun down and washed in MACS buffer. $CD8^+$ T cells were positively purified via MACS beads. $CD8^+$ negative fractions were also used as $CD4^+$ T cells for *in vitro* kill preparations. Cells were washed and resuspended in X-Vivo-20 for seeding. The activity of T cells from vaccinated and untreated mice used as effector cells was monitored via 2-Colour-cytokine secretion assay and CD107a degranulation assay in parallel to the kill assays.

Purified effector cells were adjusted to 3.0 x $10^6$ or 1.5 x $10^6$ cells/ml (depending on the yield after MACS purification) in X-Vivo-20 and plated in 96 round-bottom tissue-culture treated 96-well plates (TPP). Effector cells were seeded in triplicates and titrated by serial dilution as shown in the scheme below. The dilutions of effector cells were done in 6 steps as follows: In the first well of each row (A) 200 µl of each stock concentration were pipetted. The following wells were filled with 100 µl X-Vivo-20 each. 100 µl of cell suspension from well A were transferred to well B and mixed. Then 100 µl of cell suspension from well B were transferred to Row C and mixed with the medium. The dilution was continued until Row F. From well F 100 µl cell suspension were taken off and discarded. In the wells of Row G only 100 µl of pure X-Vivo-20 were pipetted. In these wells the spontaneous lysis of target cells was measured. Row H wells were

filled with 100 µl of 10 % Triton-X (v/v) in X-Vivo-20 to induce maximum lysis of target cells. Plates were kept until effector cells were added at 37 °C and 5 % $CO_2$ in the incubator.

**Table 2.27**: Serial dilutions of effector T cells for *in vitro* kill assays

| | | | Serial Dilution starting with 3.0 x $10^6$ cells/well | | | Serial Dilution starting with 1.5 x $10^6$ cells/well | |
|---|---|---|---|---|---|---|---|
| **Row** | **# Target cells** | | **# Effector cells** | **E:T Ratio** | | **# Effector cells** | **E:T Ratio** |
| **A** | 3'000 | | 300'000 | 1:100 | | 150'000 | 1:50 |
| **B** | 3'000 | | 150'000 | 1:50 | | 75'000 | 1:25 |
| **C** | 3'000 | | 75'000 | 1:25 | | 37'500 | 1:12.5 |
| **D** | 3'000 | | 37'500 | 1:12.5 | | 18'750 | 1:6.25 |
| **E** | 3'000 | | 18'750 | 1:6.25 | | 9'375 | 1:3.13 |
| **F** | 3'000 | | 9'375 | 1:3.13 | | 4'688 | 1:1.57 |
| **G** | 3'000 | | X-Vivo-20 only | - | | X-Vivo-20 only | - |
| **H** | 3'000 | | 10 % Triton-X | - | | 10 % Triton-X | - |

#### *2.2.4.1.3. Loading of target cells with chromium ($^{51}Cr$)*

Harvested target cells were adjusted to a concentration of 1.0 x $10^7$ cells/ml in X-Vivo-20- 200 µl (2 x $10^6$ cells) of each target cells suspension were transferred into 5 ml tubes. $Na_2{}^{51}CrO_4$-solution (5 mCi, 185 MBq, Perkin-Elmer) was added to the target cells in each tube and samples were mixed by tapping the tube. Cells were incubated for 60 to 90 min at 37 °C and 5 % $CO_2$. The amount of chromium added was depending on the age of the Chromium-stock-solution after delivery from the manufacturer (see table below).

**Table 2.28**: Amount of chromium to be added to target cells

| Age of Chromium solution | Volume [µl] |
|---|---|
| 1 week | 100 |
| 2 weeks | 125 |
| 3 weeks | 150 |
| 4 weeks | 175 |

After labeling target cells were washed thoroughly. 2.5 ml of X-Vivo-20 were added to the cells in each tube. Cells were spun down and the radioactive supernatant was discarded in special waste cans. Cells were washed again in 2.5 ml of X-Vivo-20, spun down and the SN was discarded. The cell pellets were then resuspended in 1.0 ml X-Vivo-20 each. Cell numbers were determined again after trypan blue staining. Cell suspensions were adjusted to 30'000 cells/ml.

#### *2.2.4.1.4. Co-culture of target cells with effector cells*

100 µl of target cell suspensions were pipetted per well to the T cells of the respective dilutions. The samples for maximum lysis were resuspended very thoroughly by pipetting to lyse the cells completely. Plates were centrifuged for 3 min at 500 rpm and RT. This step is important to bring target cells and effector cells into close proximity. The plates were incubated for 6 h at 37 °C and 5 % $CO_2$. 6 h after incubation plates were spun down for 3 min at 1'500 rpm and RT. 100 µl supernatant were taken off

from each well and transferred to LumaPlates (Perkin Elmer). LumaPlates were air-dried under the extractor hood overnight. Wells of culture plates were filled-up with 100 µl fresh X-Vivo-20 each and plates were spun down again for 3 min at 500 rpm and RT. They were incubated for further 12 h to 14 h at 37 °C and 5 % $CO_2$. The next day plates were spun down for 3 min at 1500 rpm and RT. Again 100 µl of supernatant were transferred to LumaPlates. The plates were dried until the next day under the hood. Culture plates were discarded. LumaPlates were read employing a γ-counter (TopCount NXT$^{TM}$; Packard, Perkin Elmer). Specific cytotoxicity (lysis) was calculated according to following formula:

$$\% \text{ specific lysis } = \left[\frac{\text{cpm(sample)} - \text{cpm(spontaneous lysis)}}{\text{cpm (maximum lysis)} - \text{cpm (spontaneous lysis)}}\right] \text{X } 100$$

### 2.2.4.2. Regulatory T cell specificity assay

The development of a $T_{reg}$ cell specificity assay in the murine system was a part of this project which was carried out together with Michael Bartoschek. The method was already published as part of M. Bartoschek's master thesis. $T_{reg}$ cell specificity assays were performed to investigate the possibility of a vaccine mediated induction of $T_{reg}$ cells. Briefly, $T_{reg}$ cells purified from vaccinated mice were *in vitro* Ag-specifically re-stimulated and their capacity to suppress proliferation of pre-activated Ovalbumin-specific $CD4^+$ T conventional cells (OT-II $T_{con}$s) was measured by Tritium uptake (see scheme below).

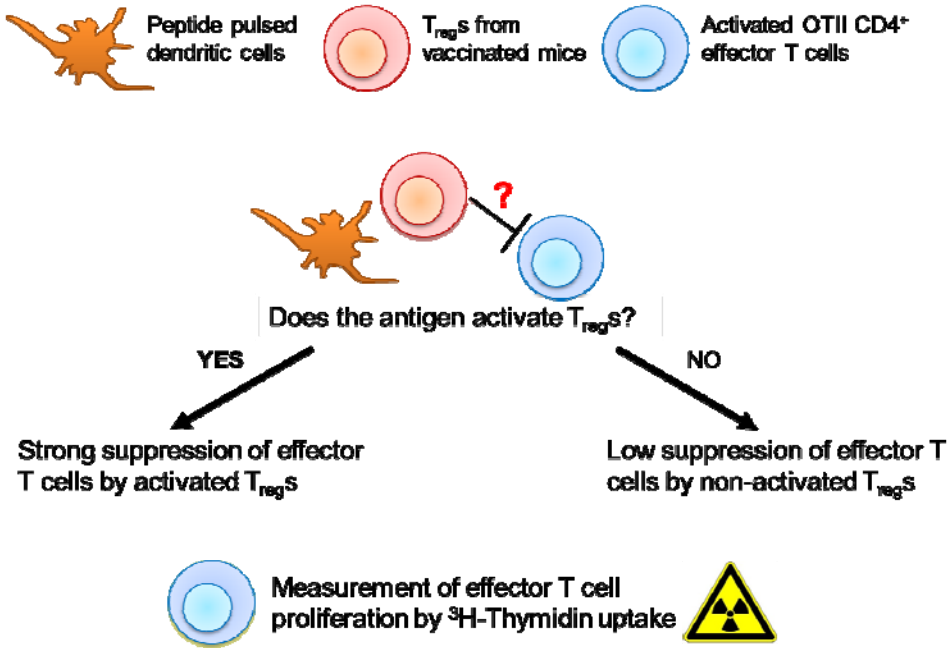


**Figure 2.3**: **Schematic overview of a $T_{reg}$ cell specificity assay in the murine system**

#### 2.2.4.2.1. *Immunization of C57BL/6 mice for the $T_{reg}$ cell specificity assay*

Mice were immunized with a combination of long peptides which showed to be unresponsive in the cytokine-secretion assay staining: p53 R216L, p53 Y220C, Kras Q61H. Above this the two strongly immunogenic peptides p53 R248W and Kras G12V were added. Groups of 3 gender matched 8 to 10 week old mice were vaccinated with a Montanide ISA 720 VG IFA formulation together with CpG as an additional adjuvant in the same manner as described in the vaccination passage (2.2.1.4.). Mice received two IFA shots in 3 week intervals without a further boost vaccination. Six weeks after the first vaccination mice were sacrificed to purify regulatory T cells. Beside vaccination with mutated peptides several groups of mice were vaccinated with corresponding wild type peptides (see lists below). Regulatory T cells from differently vaccinated mice were compared to $T_{reg}$ cells purified from completely untreated mice.

| $T_{reg}$ cocktail with **mutated** peptides: | $T_{reg}$ cocktail with **wild-type** peptides: |
|---|---|
| - p53 R216L (31-mer) | - p53 R216 (31-mer) |
| - p53 Y220C (31-mer) | - p53 Y220 (31-mer) |
| - p53 R248W (35-mer) | - p53 R248 (35-mer) |
| - Kras G12V (28-mer) | - Kras G12 (28-mer) |
| - Kras Q61H (31-mer) | - Kras Q61 (31-mer) |

#### 2.2.4.2.2. *Preparation and pulsing of dendritic cells*

Dendritic cells from C57BL/6 mice were matured from bone marrow cultures and CD11c positive dendritic cells were purified after 6 days of culture (see passages 2.2.1.3.3 to 2.2.1.3.5). One part of $CD11c^+$ BM-DCs was pulsed with peptide $OVA_{323-339}$ to activate $CD4^+$ T effector cells from OT-II mice. $1.25 \times 10^5$ DCs in a volume 200 µl X-Vivo-20 medium were seeded per well into a tissue-cultured treated 12-well plate and pulsed with 50 nmol (2 µl) of 25 mM $OVA_{323-339}$ peptide stock. The other part of $CD11c^+$ DCs was seeded in tissue-culture treated, round-bottom 96-well plates for the $T_{reg}$ cell specificity assay itself. Two identical plates were made. One plate served as a control plate, in which no $T_{reg}$ cells were added but only OT-II effector T cells and peptide pulsed DCs were co-cultured. This was done to be able to calculate the specific suppression for each individual peptide later. DCs and individual peptides were premixed and then seeded in triplicates on both plates. $1 \times 10^4$ DCs in 50 µl of X-Vivo-20 were pipetted per well pulsed with 5 nmol (accounting for 0.5 µl of 10 mM stock solution) of tested peptide. Plates with peptide pulsed DCs were incubated over night at 37 °C and 5 % $CO_2$.

#### 2.2.4.2.3. *Purification and activation of OT-II $CD4^+$ effector T cells*

$CD4^+$ effector T cells were isolated from the spleen and lymph nodes of OT-II mice one day after DC purification and pulsing. Single cell suspensions from the organs were generated via straining as described before and erythrocytes in spleen samples were lysed with ACK buffer. Samples were washed in ice-cooled MACS buffer and pooled (LN and spleen cells were purified together). Cells were counted

after trypan blue staining and PAN T cells were purified employing the PAN T cell isolation kit II (Miltenyi Biotec) according to manufacturer's instructions. After purification T cells were once washed in X-Vivo-20 medium and cell numbers were determined. 6.25 x $10^5$ OT-II effector T cells in 800 µl X-Vivo-20 were added per well to the peptides pulsed DCs in the 12-well plate prepared the previous day, resulting in a 1 : 5 ratio of DCs to T cells. OT-II specific effector T cells were antigen-specifically *in vitro* re-stimulated on $OVA_{323-399}$ pulsed dendritic cells overnight.

#### *2.2.4.2.4. Purification of $T_{reg}$ cells from vaccinated mice*

Regulatory T cells from differently vaccinated and untreated mice were purified from spleens and peripheral lymph nodes of these animals one day after DC pulsing. Single cell suspensions from the organs were generated via straining as described before and erythrocytes in spleen samples were lysed with ACK buffer. Samples were washed in ice-cooled MACS buffer and pooled (LN and spleen cells were purified together). Cells numbers were determined after trypan blue staining. Regulatory T cells were purified from organ suspensions with the $CD4^+CD25^+$ Regulatory T Cell Isolation Kit (Miltenyi Biotec) following a modified protocol. To achieve a higher purity of $T_{reg}$ cells the first purification step – the depletion of non-$CD4^+$ T cells – was performed in parallel with a PAN T cell purification using the PAN T cell isolation Kit II (Miltenyi Biotec). Extra care was taken to keep MACS buffer and MS columns cooled, because $T_{reg}$ cell yield critically depends on low temperature.

Washed cells were spun down (1700 rpm, 5 min, 4 °C) and the supernatant was pipetted off completely. The cell pellet was resuspended in 40 µl of ice-cooled MACS buffer per 1 x$10^7$ cells for the additional PAN T cell purification in 15 ml Falcon tube. Another 40 µl of MACS buffer per 1 x $10^7$ cells were added to the suspension, which accounts for the non-$CD4^+$ T cell depletion. 10 µl of PAN T cell biotin-antibody cocktail (form the PAN T cell isolation kit) and 10 µl of biotin-antibody cocktail from the $T_{reg}$ cell purification kit per 1 x $10^7$ cells were added to the sample. The samples were incubated on a roll mixer at low speed for 10 min at 4 °C. An addition of 60 µl MACS buffer and 40 µl of anti-biotin MircoBeads (the same beads were used in both kits) per 1 x $10^7$ cells followed and samples were incubated for another 15 min at 4 °C on the roll mixer. In the meantime 4 cooled MS Columns were prepared by placing them in the MACS separator magnet and equilibrating them with 500 µl ice-cooled MACS buffer each. After 15 min the cells were washed by filling up the test tube with cooled MACS buffer and spinning them down. The supernatant was removed completely and cells were resuspended in 2 ml of fresh MACS buffer. 500 µl of cell suspension was loaded onto each of the prepared columns. The flow through, representing the untouched $CD4^+$ T cell fraction, was collected. The columns were washed three times with 500 µl of MACS buffer in each washing step.

Samples were spun down and murine Fc blocking was performed as described for FACS staining with the difference that MACS buffer was used instead of FACS buffer. Cells were washed in MACS buffer after Fc blocking and cell numbers were determined after trypan blue staining for the second purification step. For the positive selection of $CD4^+CD25^+$ regulatory T cells the pellet was resuspended in 90 µl of MACS buffer

and 10 µl of CD25-PE antibody per 1 x $10^7$ $CD4^+$ T cells. The sample was incubated for 10 min at 4 °C on the roll mixer. Then 10 ml MACS buffer were added for washing and cells were spun down. The cells were resuspended in 90 µl of MACS buffer and 10 µl anti-PE MicroBeads per 1 x $10^7$ cells. After incubation of the sample for 15 min at 4 °C on the roll mixer, the test tube was filled up with MACS buffer to wash off the unbound beads. The tube was spun down and the supernatant was removed completely by pipetting. The pellet was resuspended in 1 ml of MACS buffer and 500 µl cell suspension each was loaded onto 2 equilibrated MACS columns. The columns were washed 3 times with 500 µl MACS buffer. The flow through was collected as effector T cell fraction used later for FACS analysis. After washing the columns were removed from the magnetic field of the MACS separator and placed in a 15 ml Faclon tube. 1 ml of buffer was pipetted onto the columns each and the magnetically labeled $CD4^+CD25^+$ T cells were immediately flushed out by firmly pushing the supplied plunger into the column. The plunger was removed and the flushing step was repeated once more after adding another 1 ml of MACS buffer onto the column. Then columns were discarded and cells were spun down. The pellet was resuspended in 1 ml of MACS buffer and the whole positive purification process was repeated with two fresh MS columns to increase the purity of the $T_{reg}$ fraction. After the second elution step the cells were spun down. The pellet was resuspended in 500 µl of 37 °C pre-warmed X-Vivo-20 medium and cells numbers were determined after trypan blue staining. Cell numbers were adjusted to 1 x $10^6$ $T_{reg}$ cells per ml and 50 µl of cell suspension per well (accounting for 50'000 $T_{reg}$ cells) was added to one plate with peptide pulsed DCs prepared the day before. This was accounting for a 1:5 ratio of peptides pulsed DCs to $T_{reg}$ cells. 50 µl of X-Vivo-20 was added per well to the control plate instead of $T_{reg}$ cell suspension. Plates were incubated overnight at 37 °C and 5 % $CO_2$. The purity of $T_{reg}$ cells and effector $CD4^+$ cells after MACS purification was determined via $T_{reg}$ cell FACS staining (see passage 2.2.3.4.).

#### *2.2.4.2.5. Co-culture of regulatory T cells and effector T cells*

After activation of OT-II effector T cells overnight on peptide-pulsed DCs, T cells were harvested the next day. OT-II cells were resuspended and transferred into 15 ml Falcon tubes. Wells were washed again with 2 ml of X-vivo-20 to remove all T cells. Cell number was determined after trypan blue staining and cells were spun down. The supernatant was discarded and cells were adjusted to 1 x $10^6$ cells/ml in fresh X-Vivo-20 medium. 50 µl (50'000 cells) of OT-II effector T cell suspension was pipetted per well into the 96-well $T_{reg}$ cell specificity assay plates, resulting in a $T_{reg}$ cell to effector T cell ratio of 1:1. OT-II T cells were also pipetted into the wells of the control plates. The plates were incubated for 2 days at 37 °C and 5 % of $CO_2$.

**Table 2.29**: Exemplary plate scheme for $T_{reg}$ specificity assay (DC: dendritic cells, TC: effector T cells, Pep: peptide, wt: wild type, mut: mutated, unp.: un-pulsed)

| | 1 | 2 | 3 | 4 | 5 | (…) | 9 | 10 | 11 | 12 |
|---|---|---|---|---|---|---|---|---|---|---|
| **A** | | **Tested peptides** | | | | | | | | |
| **B** | | Pep1-wt | Pep2-mut | Pep2-wt | Pep2-mut | (…) | | | | |
| **C** | | Pep1-wt | Pep2-mut | Pep2-wt | Pep2-mut | (…) | | | | |
| **D** | | Pep1-wt | Pep2-mut | Pep2-wt | Pep2-mut | (…) | | | | |
| **E** | | | | | | (…) | DC-DMSO | DC unp. | TC only | |
| **F** | | | | | | (…) | DC-DMSO | DC unp. | TC only | |
| **G** | | | | | | (…) | DC-DMSO | DC unp. | TC only | |
| **H** | | | | | | | **Assay Controls** | | | |

To quantify the proliferation of OT-II effector T cells and therewith the suppressive activity of $T_{reg}$ cells from vaccinated mice, 20 µl X-Vivo-20 supplemented with $^{3}$H-thymidine (1:20 dilution of [methyl-$^{3}$H]-Thymidine stock concentration (5 mCi, 185 mBq), resulting in 1 µCi/well) was added to each well of the co-cultures 48 h after adding of effector T cells. The plates were incubated for another 24 h at 37 °C to have proliferating cells incorporating radio-active labeled $^{3}$H-thymidine into their DNA. A scheme summarizing the whole assay procedure is shown in the following figure.

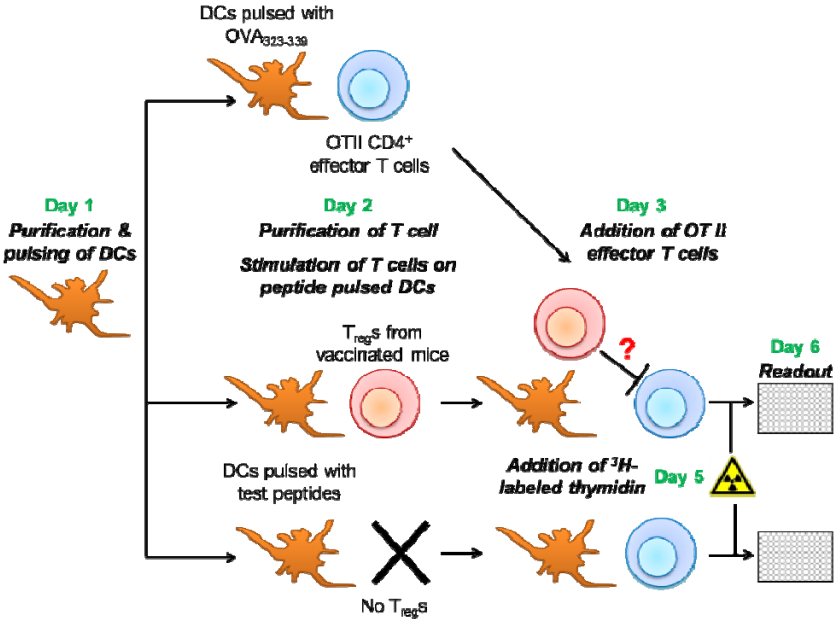


**Figure 2.4**: **Scheme of the $T_{reg}$ cell specificity assay procedure**

Then the cells were lysed by two consecutive freeze-thawing cycles. The samples were harvested by lysing remaining intact cells with distilled water and the DNA (situated in the supernatant of the samples) was transferred onto filter-mats employing a Tomtec Harvester. The filter-mats had the pattern of the 96-well plate imprinted. Membranes were dried for 2 min at 150 °C in a microwave (600 W). Dried

filter-mats were placed in plastic bags and soaked completely with 5 to 7 ml of scintillation liquid (Scintillation medium Beta Scint, Perkin Elmer). The samples transferred on the filter-mats were assessed employing a liquid scintillation counter (1450 MicroBeta, Perkin Elmer) and the counts per minute were measured for each field on the mat. Each field of the pattern on the filter-mat had the radio-active labeled DNA of one sample imprinted. The amount of radioactivity is proportional to the proliferation of effector T cells inside the respective samples. The percentage of specific suppression for each sample was calculated with the following formula:

$$\%\ \text{specific supression} = \left[\frac{\text{cpm(sample w/o Tregs)} - \text{cpm(sample} + \text{Tregs)}}{\text{cpm (sample w/o Tregs)}}\right] \text{X } 100$$

### 2.2.5. Molecular Biology

#### 2.2.5.1. Screening for mutations in A2.DR1 dtg fibrosarcoma cell lines

##### *2.2.5.1.1. Preparation of genomic DNA from culture cells*

Syngenic A2.DR1 dtg fibrosarcoma cell lines were genotyped like A2.DR1 dtg mice for genotype verification. Therefore genomic DNA had to be prepared from cultured cells as template DNA for PCR reactions. Cells to be analyzed, were cultured in T75 flaks and harvested by trypsinization. They were washed twice in PBS and cell number was determined after trypan blue staining. The cells were spun down and adjusted to 5 x $10^6$ cells/ml and 1 ml (5 x $10^6$ cells) of cell suspensions were transferred to 1.5 Eppendorf tubes. Tubes were spun down in a table centrifuge for 5 min at 2000 rpm and RT. Supernatants were aspirated completely. It was possible to freeze down the samples at -20 °C and process them at a later time point. Frozen cells were thawed on ice before proceeding with DNA extraction. Genomic DNA was extracted from cell pellets using the DNeasy Blood and Tissue Kit (QIAGEN) according to the protocol “Purification of total DNA from animal blood or cells (spin-column protocol) for cultured cells” in the manufacturer’s handbook. Purified genomic DNA samples were stored at 4 °C in the refrigerator.

##### *2.2.5.1.2. Extraction of RNA from cultured cells*

RNA was extracted from A2.DR1 dtg fibrosarcoma cell lines to have cDNA synthesized for gene specific amplification and consecutive sequencing to detect expressed mutations in *Tp53* and *Kras* genes. When working with RNA pipettes and all required equipment was cleaned with RNaseZap (Ambion, Life technology) to remove nucleases. Test tubes were autoclaved with a prolonged regimen to eliminate all nucleases. Moreover, nuclease free filter tips were used for pipetting.

Cells to be analyzed cultured in T75 flaks were harvested by trypsinization. They were washed twice in PBS and cell number was determined after trypan blue staining. Then cells were centrifuged and

adjusted to 2 x $10^6$ cells/ml and 1 ml (2 x $10^6$ cells) of cell suspensions were transferred to 1.5 Eppendorf tubes. Samples were spun down in a table centrifuge for 5 min at 2000 rpm and RT. Supernatants were aspirated completely.

RNA was purified from cell pellets using the RNeasy® Mini Kit (QIAGEN) according the protocol "Purification of total RNA from animal cells - spin technology" according to manufacturer's instructions. Cells were homogenized using QIAshredder spin columns. On-column DNAse digestion to eliminate genomic DNA contamination was not performed. In the last step RNA was eluted from the columns twice with 30 µl of RNase-free water into two separate RNase-free 1.5 ml Eppendorf tubes. RNA concentrations of the samples were assessed by measuring absorption at λ = 260 nm ($A_{260}$) utilizing NanoDrop 2000 c spectrophotometer. Samples were either stored at -80 °C or directly processed further.

*2.2.5.1.3. Elimination of DNA contaminations from RNA samples*

To eliminate possible genomic DNA contaminations the RNA samples were treated with DNase. DNase digestion was performed employing the DNA-free™ Kit (Ambion, Life technology, Carlsbad, CA, USA) with an altered protocol. 50 µl of each RNA sample containing 10 µg of RNA were mixed gently with 5 µl 10 X DNase I buffer and 1 µl rDNase I. The sample was incubated at 37 °C. After 20 min 1 more µl of rDNase I was added per sample and samples were incubated for another 20 min at 37 °C. Then 5 µl of DNase inactivation reagent was added to each sample. Under occasional vortexing the samples were incubated for 2 min at RT. Afterwards the samples were centrifuged for 90 s at full speed in a table centrifuge. 50 µl of supernatants (containing the purified RNA) were transferred into fresh RNA-free tubes. RNA concentrations of the samples were assessed again at $A_{260}$ utilizing NanoDrop.

*2.2.5.1.4. Complementary DNA synthesis from total RNA samples*

Complementary DNA (cDNA) was synthesized from RNA templates using the RETROscript® Kit (Ambion, Life technology). 1 µg sample RNA was transcribed into cDNA according to the protocol "Two step RT-PCR procedure – RT without heat denaturation of the RNA" using Oligo(dT) primers according to manufacturer's instructions. The RT reaction mix as used directly as template for gene specific amplification.

*2.2.5.1.5. Amplification of Tp53 and Kras sequences from cDNA and genomic DNA samples*

To amplify *Tp53* and *Kras* sequences form cDNA and genomic DNA for sequencing gene specific primers were designed. They were purchased from Eurofins (MWG Operon). Primer sequences are listed in table 2.30. Lyophilized primers were reconstituted in DNase-free water after short centrifugation and adjusted to stock concentrations of 100 µM. 1:10 pre-dilutions were made for PCR reactions and all stock solutions were stored at -20 °C.

**Table 2.30**: PCR primers for the amplification of *Tp53* and *Kras* sequences form cDNA and genomic DNA, **blue** marked primers were used for sequencing

| Reaction | Primer | Sequence | Band Size [bp] | Template |
|---|---|---|---|---|
| **Kras orf** | **Kras_orf_fwd** | 5' – GGA GAG AGG CCT GCT GAA A - 3' | **359** | cDNA |
| | Kras_ord_rev | 5' – CCA GGA CCA TAG GCA CAT CT - 3' | | |
| **Tp53 DBD orf** | **p53_dbd_fwd** | 5' – TTT TGA AGG CCC AAG TGA AG - 3' | **832** | cDNA |
| | p53_dbd_rev | 5' – GCG GAT CTT GAG GGT GAA AT - 3' | | |
| **Kras Exon1** | Kras_genom Exon1_fwd | 5' – CCC TGC CTA AAA GAC ACC AA - 3' | **616** | genomic DNA |
| | **Kras_genom Exon1_rev** | 5' – TCA CTG AAT TCG GAA TAT CTT AGA G - 3' | | |
| **Kras Exon2** | Kras_genom Exon2_fwd | 5' – TGC AGG CAT AAC AAT TAG CAA - 3' | **488** | genomic DNA |
| | **Kras_genom Exon2_rev** | 5' – GGT GCT TGC CAA TCC CCA TC - 3' | | |

PCRs were carried out using Platinum Taq High Fidelity DNA polymerase (Invitrogen) and 10 mM dNTP Mix (PCR Grade, Invitrogen, Life technologies). Reaction mixes were pipetted on ice in 0.5 ml tubes according to table 2.31 and PCRs were run in a PCR machine (PTC-100 Programmable Thermal Cycler, MJ Research) following the program shown in table 2.32.

**Table 2.31:** Exemplary PCR reaction mix for *Tp53* and *Kras* gene specific amplification of genomic DNA/cDNA

| PCR reaction mix | Components | Volume [µl] |
|---|---|---|
| | 10 X High Fidelity Buffer | 2.5 |
| | 10 mM dNTP mixture | 0.5 |
| | 50 mM $MgSO_4$ | 1.0 |
| | 10 nM forward primer | 0.5 |
| | 10 nM reverse primer | 0.5 |
| | Template genomic DNA/cDNA | 2.0 |
| | Platinum Taq Polymerase | 0.1 |
| | $ddH_2O$ | 17.9 |
| | *Final volume* | *25.0* |

**Table 2.32:** PCR program for *Tp53* and *Kras* gene specific amplification

| PCR Cycle | Time [min] | Temperature [°C] | Cycles |
|---|---|---|---|
| Initial denaturation | 3 | 94 | - |
| Denaturation | 0.5 | 94 | |
| Annealing | 0.5 | 55 | **X 35** |
| Elongation | 1 | 68 | |
| Final elongation | 7 | 68 | - |
| Storage | forever | 4 | - |

After amplification 10.0 µl of PCR product of each sample was mixed with 2.0 µl 5 X sample loading dye (5XDNA Loading buffer, Bioline) and analyzed on a 1.5 % TAE-agarose gel. Exemplary gel pictures for the four different gen specific amplifications are shown in figure 2.5.

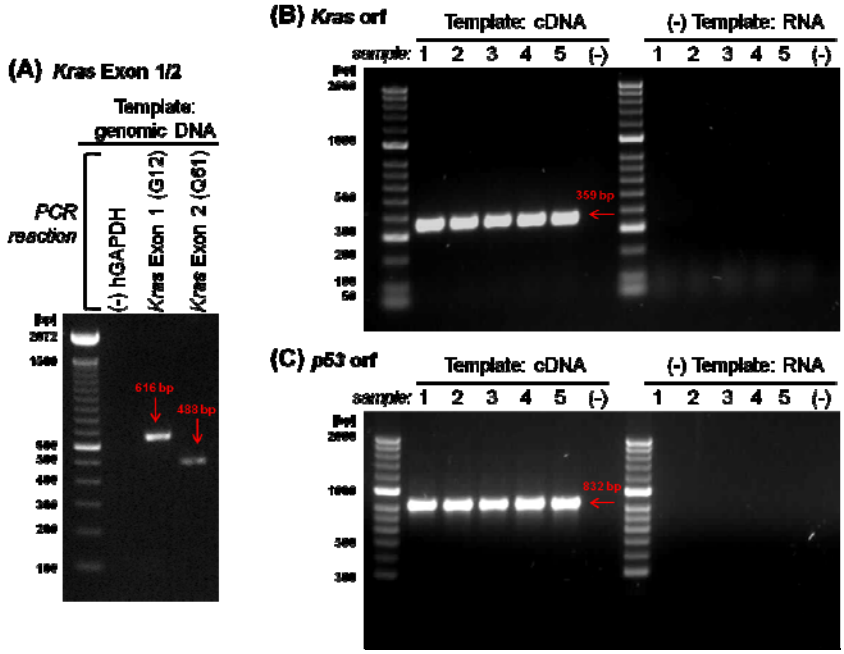


**Figure 2.5**: **PCR products resulting from gene specific amplification of *Kras* and *Tp53* sequences. (A)** Amplification of *Kras* exons 1 and 2 from genomic template DNA, Amplification of the *Kras* **(B)** and *Tp53* **(C)** open reading frames form cDNA as template, hGAPDH: negative control, orf: open reading frame

#### *2.2.5.1.6. Sequencing of amplified of Tp53 and Kras sequences*

*Tp53* and *Kras* PCR products were sent for Sanger sequencing to external companies (GATC Biotech, Konstanz, Germany and LGC Genomics, Berlin, Germany). Samples were sent without further purification together with the respective primers (indicated in blue in table 2.30) in concentrations requested by the companies. Received sequences were screened for mutations by alignment with corresponding wild type sequences (Serial Cloner, SerialBasics and BLAST, NCBI) and analysis of sequencing histograms employing Chromas Lite software (Technelysium, Brisbane, Australia).

### 2.2.5.2. Design and Cloning of chimeric (mutated) *Tp53*/*Kras* transgenes

The A2.DR1 dtg fibrosarcoma cell line 2277-NS was chosen to be engineered to express the most immunogenic mutations found in the panel of long peptides tested. Therefore, transgenes carrying the two mutations p53 R248W and Kras G12V within their natural adjacent protein backbones were designed. The wild-type sequences for the murine and human *Kras* and *Tp53* open reading frames were taken from the NCBI database. The DNA-binding domain (DBD) from *Tp53* (positions 108-288) was joint with a short peptide linker (AS sequence: GSGSGS) to the first 3 exons of *Kras* (positions 1-150). The truncated pieces of *Tp53* and *Kras* should not be functional, because most of the functional domains of these two proteins are missing. On the C terminus after the truncated part of *Kras* the sequence of an HA-tag (AS sequence: YPYDVPDYA) followed by a stop codon (nucleotide sequence: TGA) was fused in frame. The

HA-tag served for the detection of the transgene. In front of the transgene at the N-terminus a consensus mammalian Kosak sequence with a start codon (nucleotide sequence: ACC ATG) was placed. Transgenes with wild-type and mutated, human and murine sequences and with or without HA-tag were designed this way. Complete nucleotide sequences of all transgenes are listed in the appendix and schematic pictures are displayed in figure 2.6.

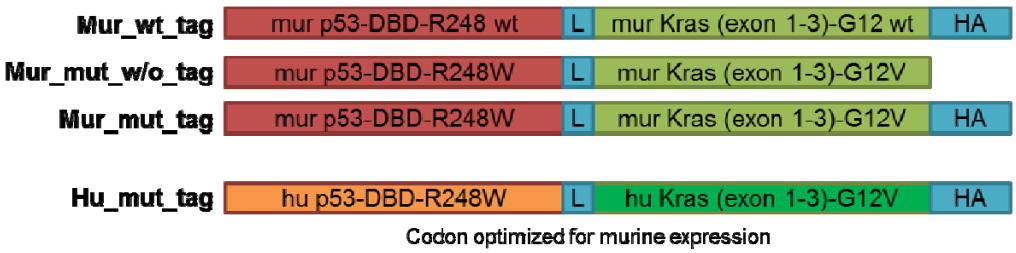


**Figure 2.6**: **Scheme of chimeric *Tp53*/*Kras* transgenes** (hu = human, mur = murine, mut = mutated, wt = wild-type, DBD = DNA binding domain, HA = HA-tag, L = short peptide linker)

Transgene sequences were further processed by the company Geneart (Life technologies, Darmstadt, Germany). The human construct "hu_mut_tag" was codon optimized by Geneart for optimal expression in a murine system. Moreover *att*-sequences were added to the constructs which are acceptor sites for sub-cloning with the Gateway™ technology (Invitrogen). The genes were synthesized by Geneart and delivered already inserted into pDonor221 gateway vectors.

#### 2.2.5.3. Gateway Cloning of chimeric *Tp53*/*Kras* transgenes into an expression vector for functional analysis

The transgenes were shuttled from the pDonor221 vector ("entry clone") to the pDest26-N-eGFP vector ("destination vector") for expression of the transgenes in mammals (for vector maps see appendix). Gateway clonase reactions were performed exactly according to the manufacturer's instructions in the datasheet for the Gateway® LR Clonase™ II Enzyme Mix (Invitrogen, Karlsruhe, Germany). A part of the respective clonase reaction mixes were directly used to transform Library Efficiency ® DH5α™ Competent Cells (Invitrogen).

The competent bacteria strain DH5α *E.coli* was transformed via the heat shock transfection method. Competent bacteria were thawed on ice and 1 µl of respective clonase reaction mix was added to 100 µl of cell suspension. Samples were mixed by tapping the tube and incubated for 30 min on ice. Afterwards the heat-shock was performed by incubating the bacteria for 45 s at 42 °C in a pre-warmed water batch. The cells were cooled down again for 2 min on ice. Then 900 µl 37 °C pre-warmed SOC medium was added per sample and bacteria were incubated shaking for 60 min at 37 °C. 200 µl of each cell suspension were plated on LB agar plates supplemented with 100 µg/ml Ampicillin (SIGMA Aldrich, Stock concentration 100 mg/ml) as selecting agent. Plates were incubated over night at 37 °C.

The next day colonies were picked and 5 ml LB medium (supplemented with Ampicillin) miniprep cultures were inoculated. Miniprep samples were incubated overnight at 37 °C on the bacterial shaker. The following day plasmid DNA was isolated from miniprep cultures using the QIAprep® Spin Miniperp Kit (QIAGEN) according to manufacturer's instructions.

Plasmid DNA was digested with the restriction enzymes *XhoI* (NEB (New England BioLAbs), Ipswich, MA, USA) and *Nhe I* (NEB) for 1 h at 37 °C to verify the insertion of transgenes (for restriction digest mix see table 2.33). Digested samples were loaded onto 1.5 % agarose gels. In case the transgene was successfully shuttled into the destination vector a band running at a size of 1272 bp could be detected beside the bigger plasmid band (see figure 2.7).

**Table 2.33**: Restriction digest mix for verification of pDEST-N-eGFP constructs

| Components | Volume [µl] |
|---|---|
| **XhoI** | 0.5 µl |
| **NheI** | 0.5 µl |
| **10 X NEBuffer 4 (NEB)** | 2.0 µl |
| **BSA 1:10** | 2.0 µl |
| **plasmid DNA** | 4.0 µl |
| **nuclease-free water** | 11.0 µl |
| ***Total volume*** | *20.0 µl* |

One plasmid DNA sample from a positive clone was sent to GATC Biotech for Sanger sequencing for each construct employing a common eGFP primer (eGFP_fwd primer: 5' - GAT CGC ATG GTC CTG CTG – 3').

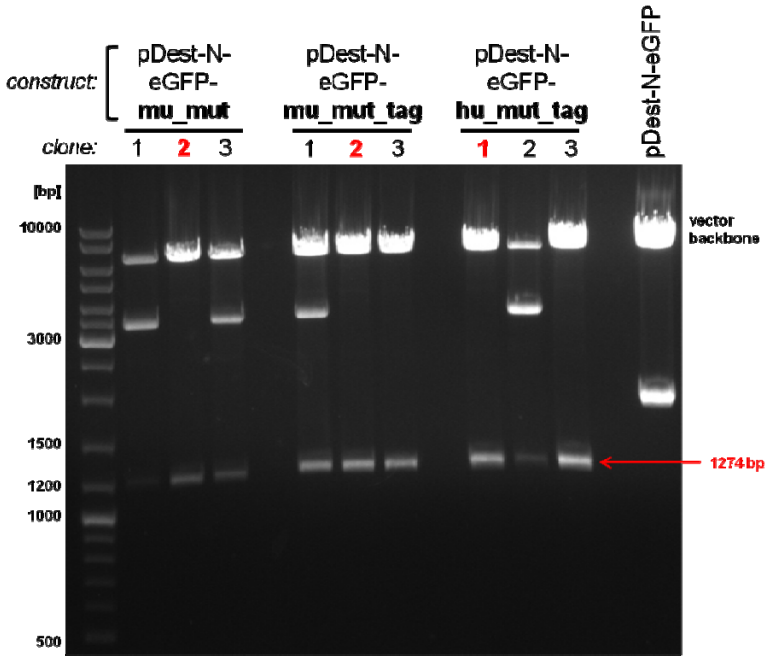


**Figure 2.7**: **Restriction digests from different clones of the pDest-N-eGFP constructs,** indicated in red are the clones which were sent for sequencing

When the transgene sequences were verified by the results from Sanger sequencing Maxiprep cultures were inoculated with respective clones. Cultures with a volume of 250 ml LB medium supplemented with 100 µg/ml Ampicillin were shaken overnight at 37 °C. The next day a maxi plasmid preparation was performed using the EndoFree® Plasmid Maxi Kit (QIAGEN) according to manufacturer's instructions. It was very important to use a kit which removed endotoxins, because plasmids were used for transient transfection of mammalian cells, namely HEK 293T cells and the A2.DR1 dtg fibrosarcoma cell line 2277-NS.

### 2.2.6. Work with Proteins: Western Blot

#### 2.2.6.1. Preparation of whole protein lysates form cultured cells

Cells cultured in T75 tissue culture flaks were harvested by trypsinization. The resulting cell suspension was transferred into a 15 ml Falcon tube and centrifuged (10 min, 1400 rpm, RT). The supernatant was discarded and cells were washed by resuspending in 10 ml PBS. After centrifugation (10 min, 1400 rpm, RT) the supernatant was removed, the pellet resuspended in 1 ml of PBS and passed over to a 1.5 ml Eppendorf tube. Then cells were centrifuged in a table centrifuge for 5 min at 2000 rpm and 4 °C. After centrifugation the supernatant was removed completely and cells were resuspended thoroughly in protein extraction buffer by pipetting up and down. Depending on the cell density the extraction was performed in 250 µl (half-confluent flask) to 500 µl (confluent flask) of extraction buffer. Tubes were rocked for 10 min at RT on a shaker and then centrifuged at maximum speed for 15 min at 4 °C. Afterwards the supernatant (protein extract) was transferred on ice to a new 1.5 ml Eppendorf tube and the pellet (cell debris) was discarded. The protein concentration was determined by measuring the absorption at A 280 nm wavelength utilizing NanoDrop 2000c Spectrophotometer (peQLab Biotechnology GmbH, Erlangen, Germany). Resulting protein extracts were either used directly for PAGE or stored at -80 °C after snap freezing in liquid nitrogen.

##### *2.2.6.1.1. Preparation of Protein Extraction Buffer*

To prepare protein extraction buffer 10 ml of M-PER® Mammalian Protein Extraction Reagent (Thermo Scientific) was supplemented with one tablet of proteinase inhibitors (cOmplete ULTRA Tablets, Mini, ETDA-free; Roche (Applied Science), Mannheim, Germany) by vortexing and incubation at RT until the tablet was dissolved completely.

#### 2.2.6.2. Preparation of whole protein lysates from mouse tumor tissue

To prepare protein lysates fresh tumor tissue or - 80 °C frozen tissue was used. In case of frozen samples, the tissue had to be thawed on ice. A tissue piece of approximately 30-50 mg was placed into a round bottom 5 ml tube (5 ml PP Tube sterile, 115 261, Greiner bio-one, Frickenhausen, Germany, diameter app. 1 cm). The use of a round bottom tube was mandatory to achieve a complete disruption of

the tissue by the disperser's knives (Ultra-Turrax® T25 basic, IKA-Werke, Staufen, Germany). Depending on the size of the tissue piece 0.5 to 1.0 ml of complete protein extraction buffer was added to the tissue. Prior use and after each sample the disperser's knives had to cleaned by washing three times with 0.3 M NaOH. To remove remaining NaOH the knives were washed again three times with sterile water and gently dried with a tissue. Homogenization of tumor tissue was done by carefully moving the tube up and down the running knives. To avoid heating up of the samples, a homogenization run never extended one minute. After the run the samples were immediately put back on ice, transferred into 1.5 ml Eppendorf tubes and centrifuged at maximum speed for 20 min at 4 °C. The supernatant (protein extract) was transferred on ice to a new 1.5 ml Eppendorf tube and the pellet (cell debris) was discarded. Determination of the protein concentration and storage of the samples was done as described above.

#### 2.2.6.3. SDS-PAGE and Western Blotting

##### *2.2.6.3.1. Sample preparation for PAGE*

Each well of the gel had to be loaded with the same amount and volume of protein. Therefore, the differing volumes resulting from individual sample protein concentrations were adjusted by adding deionized water (Nuclease free water, Ambion) to samples with lower volumes. Finally 4 X denaturing loading buffer (NuPAGE® LDS Sample Buffer (4X), Novex® by Life technologies™, Carlsbad, CA, USA) supplemented with DTT (100 mM) was added to each sample.

Example for denaturation mix:

5 µl denaturing loading buffer
x µl protein extract (volume for 20 – 150 µg of protein)
20 - x µl deionized water
_____
25 µl total volume

For denaturation and loading of the proteins with SDS molecules the samples were boiled for 10 min at 95 °C and afterwards spun down.

##### *2.2.6.3.2. SDS-PAGE*

NuPAGE® 4-12 % Bis-Tris Precast Gels (1,0 mm, 10 or 15 wells; Novex® by Life technologies™) were used for SDS-PAGE. The gels were adjusted to RT by bathing in lukewarm water prior use. Gels were fixed in the electrophoresis chambers (X Cell Sure lock™ Electrophoresis Cell, Invitrogen, Novex™) according to manufacturer's instructions. After filling up the chamber with 1 X Running Buffer (NuPAGE® MES SDS Running Buffer (20 X), Novex® by Life technologies™) the samples and 5 µl protein ladder (PageRuler Prestained Protein Ladder 10 to 170 kDa, Thermo Scientific) were loaded in respective wells. The PAGE was run for roughly 1 h at constant voltage of 120 V until the bromphenol blue color marker from the loading buffer reached the lower gel border.

*2.2.6.3.3. Western Blot*

After the SDS-PAGE run was complete the resulting gels were equilibrated for several minutes in transfer buffer. In the meantime 6 layers of Whatman filter paper (SIGMA-Aldrich) and the transfer membrane (Hybond-P PVDF Transfer Membrane 0.45 µm, Amersham – GE Healthcare Life Science, Chalfont St Giles, Buckinghamshire, UK) were prepared. The transfer membrane was activated by dipping it for 10 sec in absolute methanol and filter papers were soaked with transfer buffer. All components were then placed in transfer buffer and the transfer sandwich was assembled according to the following scheme into the blotting cassette.

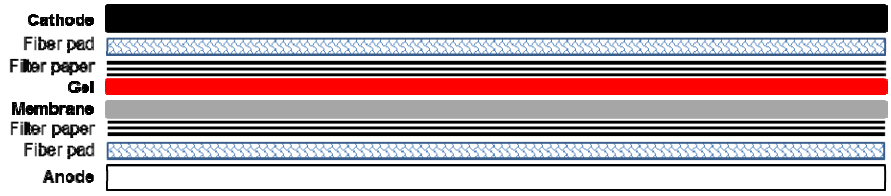


**Figure 2.8**: **Scheme of a western blot sandwich**

Extra care had to be taken to avoid the enclosure of air bubbles between the layers of the sandwich. This was done by thoroughly sweeping the surface with a glass pipette after addition of every consecutive layer.

**Table 2.34**: Recipe for 10 X Western Blot transfer buffer

| **10 x Transfer Buffer** (for PVDF membranes) | **Amount [g]** | **Components** |
|---|---|---|
| | 30.3 | Tris base |
| | 144.0 | Glycine |

Dissolve the salts completely and adjust total volume with $ddH_2O$ to 1000 ml (resulting pH = 8.3, stored at 4 °C)

**Table 2:35**: Recipe for 1 ml of 1 X Western Blot transfer buffer

| **1 x Transfer Buffer** (for PVDF membranes) | **Volume [ml]** | **Components** |
|---|---|---|
| | 100.0 | 10 x Transfer Buffer |
| | 200.0 | Methanol |
| | 700.0 | $ddH_2O$ |

The completely assembled sandwiches were inserted between the anode and cathode advice of a Mini Trans-Blot® Cell (Bio-Rad laboratories, Munich, Germany). After adding a frozen-ice cooling unit the tank was filled with blotting buffer. The transfer was run at constant amperage of 400 mA for 45 min in the 4 °C cold room under permanent magnetic agitation.

2.2.6.4. Immunoblotting

Prior actual immunoblotting freshly blotted western membranes had to be blocked in respective blocking reagents, preferentially by tilting over night at 4 °C in the cold room. For the detection of the HA-tag the membrane had to be blocked in 2.5 % BSA dissolved in PBS-T (PBS plus 0.1 % Tween-20).

- Step 1 - Incubation with the primary antibody: An anti-HA-tag antibody was used to detect transgene expression in tumor tissue and cultured cells. It was diluted 1:1500 in 2.5 % BSA/PBS-T and incubated tilting for 1 h at RT.
- Step 2 - Washing: After one hour the primary antibody was removed and the membrane was washed 3 times by tilting for 10 min in PBS-T at RT each.
- Step 3 - Incubation with the secondary antibody: The secondary HRP-conjugated goat-anti mouse antibody was diluted 1:3000 in 2.5 % BSA/PBS-T (similar to the primary antibody) and incubated tilting for 1 h at RT
- Step 4 - Washing: After 1 h the secondary antibody was discarded and the membrane was washed again three times as mentioned in Step 2. Before detection the membranes were tilted for 5 min in PBS only.
- Step 5 - Detection: For detection the washing buffer was removed completely. 1.5 ml of the luminol detection solution was mixed in a 1:1 ratio with 1.5 ml peroxide detection solution (Amersham™ ECL™ Prime, GE Healthcare) for each membrane. Then the detection-mixture was dropped carefully onto the membrane to make sure that it was completely covered. After incubation for 5 min at room temperature in the dark the blot was ready for detection facilitating a CCR camera unit (Molecular Imager ® ChemiDoc™ XRS+ with Image Lab™ Software, Bio-Rad).
- Step 6 - Washing: To remove the detection reagents the membranes were washed three times as described in step 2
- Step 7- Stripping: For stripping the membrane was tilted for 10 min in about 10 ml of stripping buffer (Restore PLUS Western Blot Stripping Buffer, Thermo Fisher Scientific, Waltham, MA , USA) at RT.
- Step 8 - Washing: To clear remaining stripping reagent completely the membranes were washed three times for 10 min in PBS-T at RT.
- Step 9 - Blocking: After stripping it was necessary to block the membrane again in 5 % blocking milk (5 % w/v powdered milk (blotting grade, Carl Roth, Karlsruhe, Germany) in PBS-T) for 1h at RT or overnight at 4 °C.
- Step 10 - Incubation with the primary antibody for loading control: An anti-β-actin antibody was used to verify equal loading of protein. It was diluted 1:10000 in 5 % blocking milk and incubated tilting for 1 h at RT.
- Step 11 - Washing: Washing was performed according to step 2
- Step 12 - Incubation with the secondary antibody: The secondary HRP-conjugated goat-anti mouse antibody was diluted 1:3000 in 5 % blocking milk (similar to the primary antibody) and incubated tilting for 1 h at RT.
- Step 13 - washing & detection was done as described in steps 4 to 6
- Step 14 - Storage of membranes: After immunoblotting was completed the membrane was dried by placing it between to filter papers and wrapped in plastic film for long term storage at 4 °C.

# 3. Results

## 3.1. T cells responses against mutations in p53 and Kras after multi-peptide vaccination

Observations made in the blood and bone marrow of CRC patients revealed the existence of memory T cell responses against wild-type and mutated sequences derived from hot-spot mutation sites of *Kras*, *Braf* and *Tp53* (see section 1.4.5). This encouraged us to investigate the potential of mixes of four to five mutated peptides or mixes of corresponding wild-type peptides (see section 2.2.1.4.2) for active vaccination. Therefore, C57BL/6 as well as A2.DR1 dtg mice were utilized. Animals were immunized for initial screenings through the whole panel of long peptides with PBS-based formulations of peptide mixes and the adjuvant CpG twice (on a biweekly base, see section 2.2.1.4.2). Groups of three mice (either male or female) were vaccinated with one out of six groups of peptides and analyzed on day 28 after the first vaccination via combined IFN-γ secretion assay and intracellular cytokine staining.

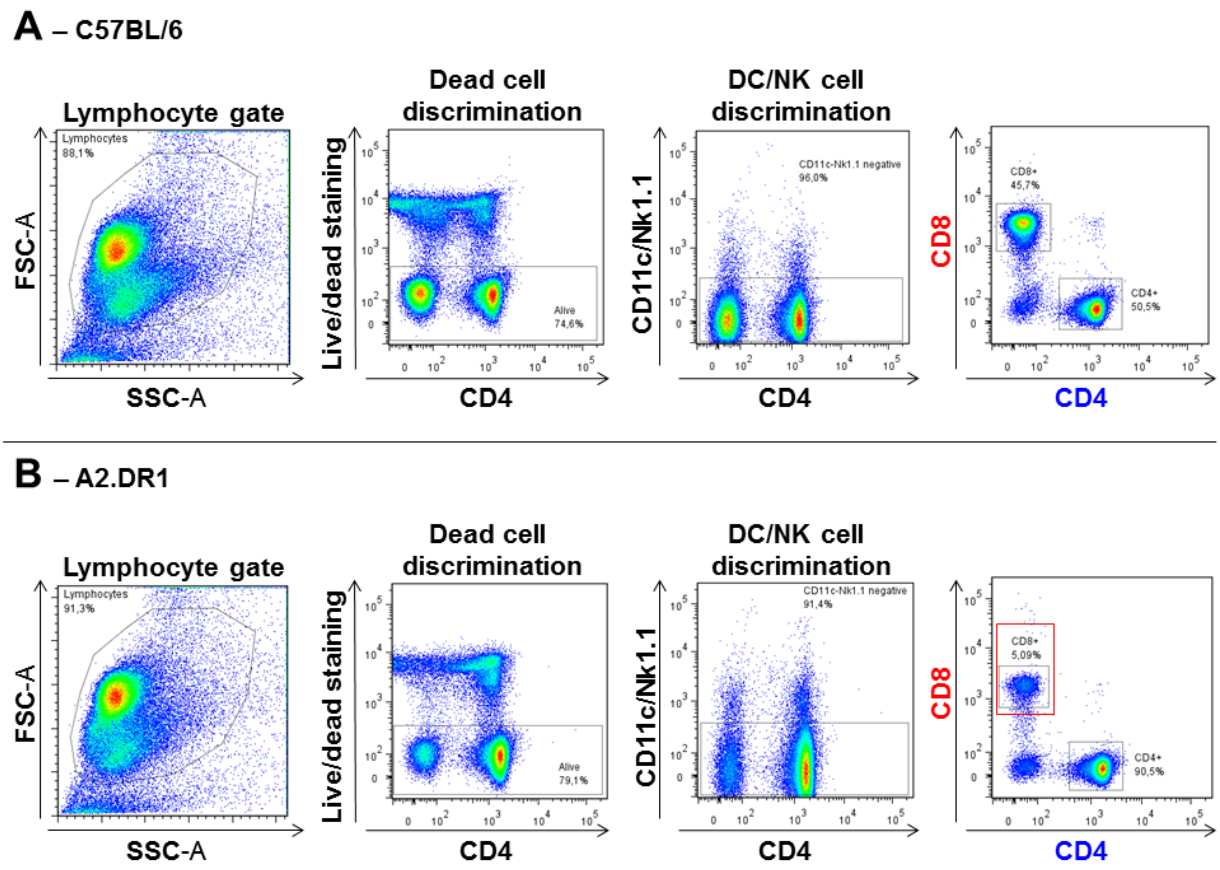


**Figure 3.1**: **Gating strategy for combined IFN-γ secretion assay and intracellular cytokine staining**. Splenic T cells were purified from best peptides immunized CD57BL/6 (**A**, sample p53 R248 wt) and A2.DR1 dtg (**B**, sample p53 R248 wt) mice. Cell surface was stained with fluorescent-labeled monoclonal antibodies against IFN-γ, CD4, CD8, CD11c and Nk1.1.

Optimal conditions for the combination of both assays were tested in a row of set-up experiments, which lead to the incubation periods described in section 2.2.3.2.2 (16 h of T cell re-stimulation on

peptide-pulsed DCs, 3 h of IFN-γ secretion period, followed by 8 h protein transport inhibition). Samples were stained with cytokine secretion kit detection anti-IFN-γ antibody and lineage markers CD4, CD8, CD11c and Nk1.1 following live/dead staining (with EMA). Afterwards samples were fixed and permeabilized to allow staining for intracellular cytokines with anti-IFN-γ and anti-TNF mAbs.

The gating was performed as shown in figure 3.1 A and B. Lymphocytes were gated on as a sub-population within forwards (FSC) and site (SSC) scatter. From the lymphocyte population dead cells were excluded by gating on dead cell stain negative cells. DCs and NK cells were stained with anti-CD11c and anti-NK1.1 monoclonal antibodies, respectively, conjugated with the same dye ('dump channel'). DCs and NK cells were excluded by gating on dye negative events. T helper cells were stained with anti-CD4 and cytotoxic T cells with anti-CD8 antibodies. Comparing the CD8 positive populations of C57BL/6 (roughly 45 % of the total T cells population) to that of A2.DR1 dtg mice (usually between 5-8 % of total T cells, highlighted by the red rectangle in figure 3.1 B) confirmed that the CTL population was strongly decreased in A2.DR1 dtg mice, as described in the original publication (Pajot et al., 2004).

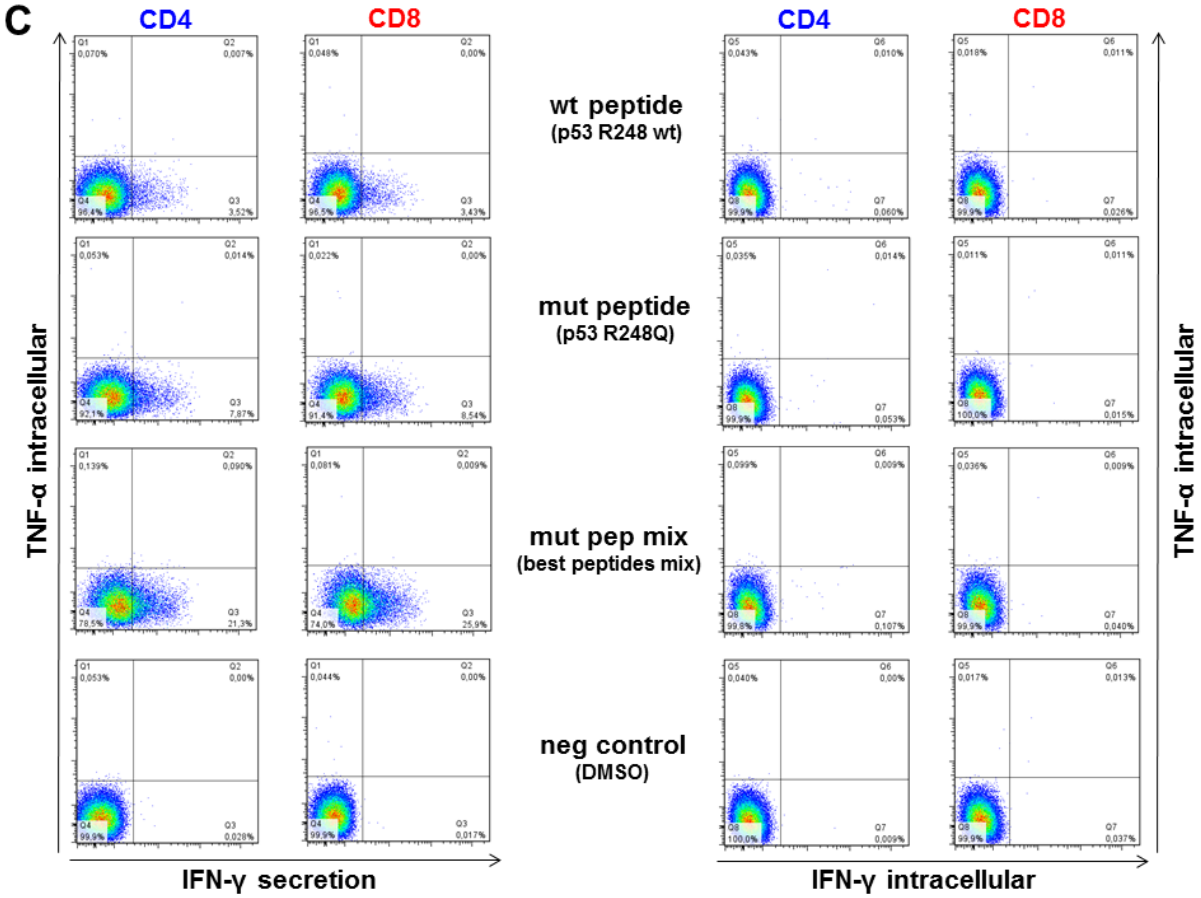


**Figure 3.1 C**: **Gating strategy for combined IFN-γ secretion assay and intracellular cytokine staining**. Splenic T cells were purified from best peptides immunized C57BL/6 mice (samples shown: T cells re-stimulated on DCs pulsed with wt peptide p53 R248 wt, mutated peptide p53 R248W, most immunogenic mutated peptides mixed; negative control: dendritic cells pulsed with peptide solvent only (DMSO)). Cells were stained for intracellular expression of cytokines IFN-γ and TNF with mAbs after surface-staining and consecutive fixation/permeabilization.

T cell subsets were further analyzed for their cytokine profiles by plotting either IFN-γ secretion against intracellular TNF-α or intracellular IFN-γ against intracellular TNF-α (shown in figure 3.1 C). Quadrant gates were set according to FMO and isotype controls. This revealed that percentages of IFN-γ secreting cells were generally clearly higher than those positive for intracellular cytokines. The exemplary samples displayed in figure 3.1 C indicate several general observations. $CD8^+$ as well as $CD4^+$ T cells secrete IFN-γ after re-stimulation on peptide-pulsed $CD11c^+$ dendritic cells. Some mutated peptides, like the peptide harboring the mutation p53 R248W (fig 3.1 C), elicited higher *in vitro* recall responses than its corresponding wt (p53 R248 wt) counterpart (after vaccination with mutated peptides). Moreover, re-stimulation of T cells from immunized mice on DCs pulsed with mixes of all peptides used for vaccination generally elicited the highest cytokines responses. DCs pulsed with the peptide solvent DMSO only, as well as the other negative controls (T cells cultured with completely un-pulsed DCs and T cells cultured alone) showed only minor or no cytokine responses.

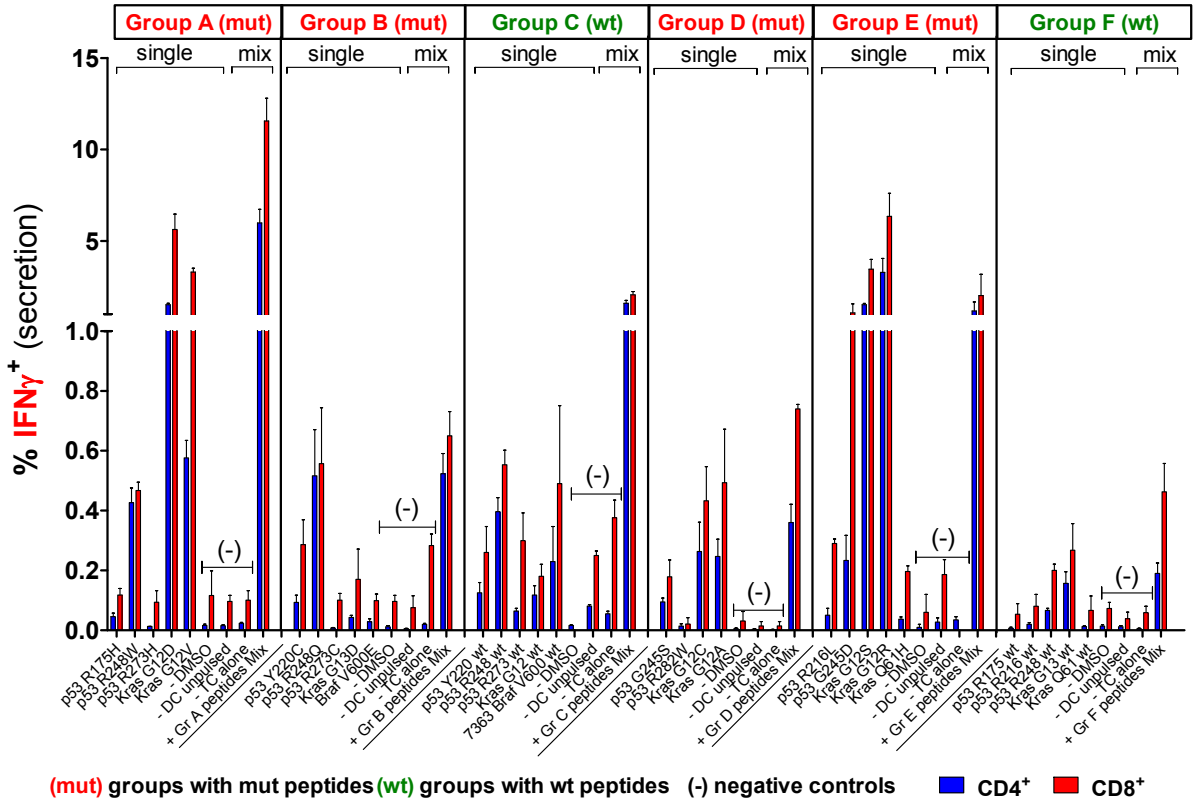


**Figure 3.2**: **Polyvalent T cell responses after vaccination with mutated and wt Braf, Kras and p53-derived long peptides in a human MHC context.** An overview of recall responses against all peptides tested in A2.DR1 dtg mice immunized with different long peptide cocktails is shown. Six cohorts of mice were immunized with one group of mutated (mut) or wild-type (wt) peptides (A to F), each, in PBS-based formulations including CpG ODN 1668 as an adjuvant. *In vitro* recall responses were obtained from combined IFN-γ secretion assay and intracellular cytokine staining performed with $CD90^+$ purified T cells from immunized mice. IFN-γ secretion of $CD8^+$ and $CD4^+$ T cells upon *in vitro* recall against single peptides of each respective mix (single) and against whole peptide mixes (mix) presented by $CD11c^+$ DCs are displayed. Each peptide, peptide mix and control sample was tested in triplicate instances. Results are plotted as means of triplicate assays ± SEM. Data obtained from one of two identical lines of experiments are shown.

Vaccination-induced *in vitro* splenic memory T cell recall responses against all wt and mutated p53, Kras, and Braf-derived peptides and mixes of those, were tested and analyzed towards IFN-γ

secretion and plotted as bar charts in figures 3.2 and 3.3 for A2.DR1 dtg and C57BL/6 mice, respectively. Six cohorts of three mice had to be immunized with one out of the six different mutated or corresponding wt peptide mixes, each, to test all panel peptides. For every group of peptides and both mouse strains each immunization experiment was performed at least twice and the resulting, representative data from one row of experiments are shown in figures 3.2 and 3.3. Herein, it became clear that it was possible to detect *in vitro* recall responses against several peptides in one respective mix, indicating the induction of multi-epitope or polyvalent T cell responses by the employed multi-peptide vaccination setting. These observations proofed to be true for both mutated and wild-type peptides mixes as well as for both mouse strains, meaning for a human and murine MHC context. Furthermore, some of the long peptides were highly immunogenic in C57BL/6 as well as in A2.DR1 dtg mice, thereby inducing $CD8^+$ as well as $CD4^+$ T cell cytokine responses, respectively. Interestingly, the peptides eliciting the strongest responses seem to be similar in both, the human and the murine MHC context. Within the C57BL/6 mice the mutated peptides p53 R248W/Q, p53 G245S, and Kras G12V/D were repeatedly highly responsive. Similarly, the peptides p53 R248W/Q and Kras G12V/D/R excelled in the human MHC context within A2.DR1 dtg mice.

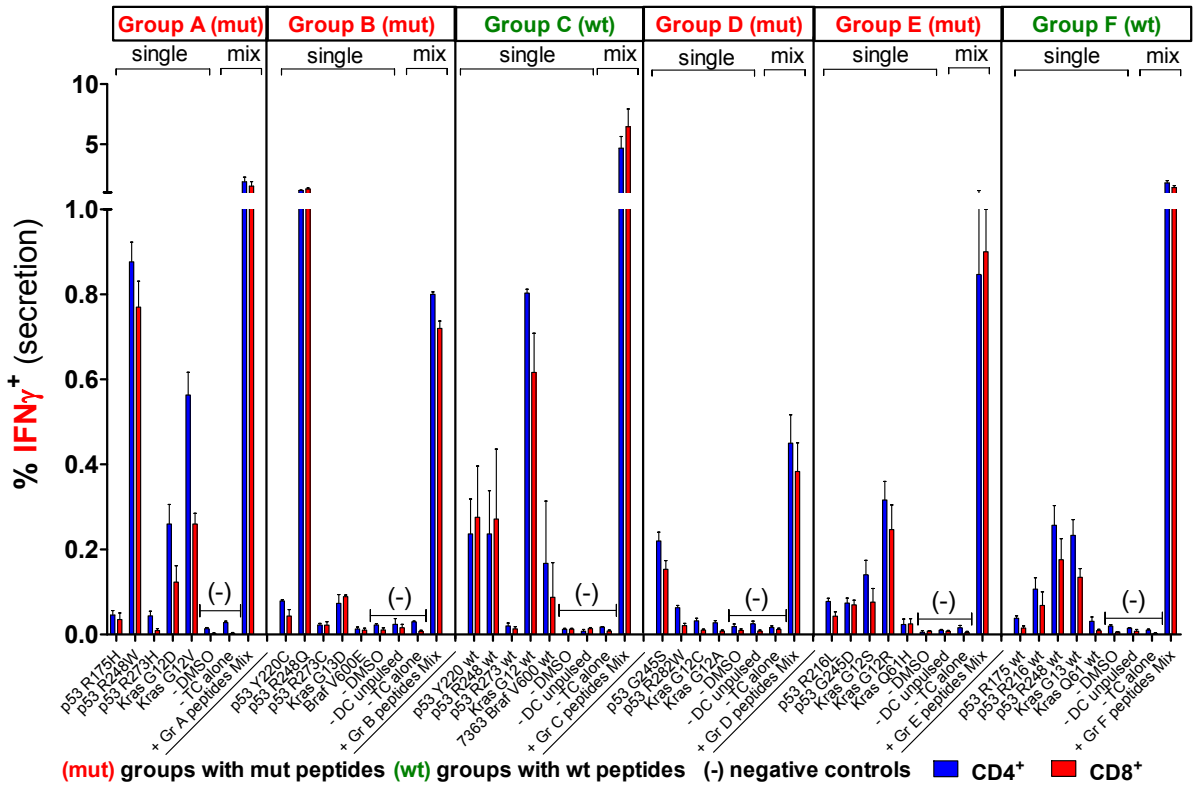


**Figure 3.3**: **Polyvalent T cell responses after vaccination with mutated and wt Braf, Kras and p53-derived long peptides in a murine MHC context.** Overview of recall responses against all peptides tested in C57BL/6 mice immunized with different long peptide cocktails are shown. Six cohorts of mice were immunized with one group of mutated (mut) or wild-type (wt) peptides (A to F), each, in PBS-based formulations including CpG ODN 1668 as an adjuvant. *In vitro* recall responses were obtained from combined IFN-γ secretion assay and intracellular cytokine staining performed with $CD90^+$ purified T cells from immunized mice. IFN-γ secretion of $CD8^+$ and $CD4^+$ T cells upon *in vitro* recall against single peptides of each respective mix (single) and against whole peptide mixes (mix) presented by $CD11c^+$ DCs are displayed. Each peptide, peptide mix and control sample was tested in triplicate instances. Results are plotted as means of triplicate assays ± SEM. Data obtained from one of two identical lines of experiments are shown.

In figure 3.4 A and B the T cell responses analyzed for IFN-γ secretion after vaccination with mutated group A peptides and corresponding wt peptides (group C, shown also in the previous figures) are zoomed in. The direct comparison of strongly immunogenic mutated peptides like p53 R248W or Kras G12V to their wt counterparts in group C (p53 R248 wt, Kras G12 wt) indicated that also the underlying wt peptides seemed to display (depending on the MHC context) a higher immunogenicity than other wt sequences (e.g. p53 R273 wt).

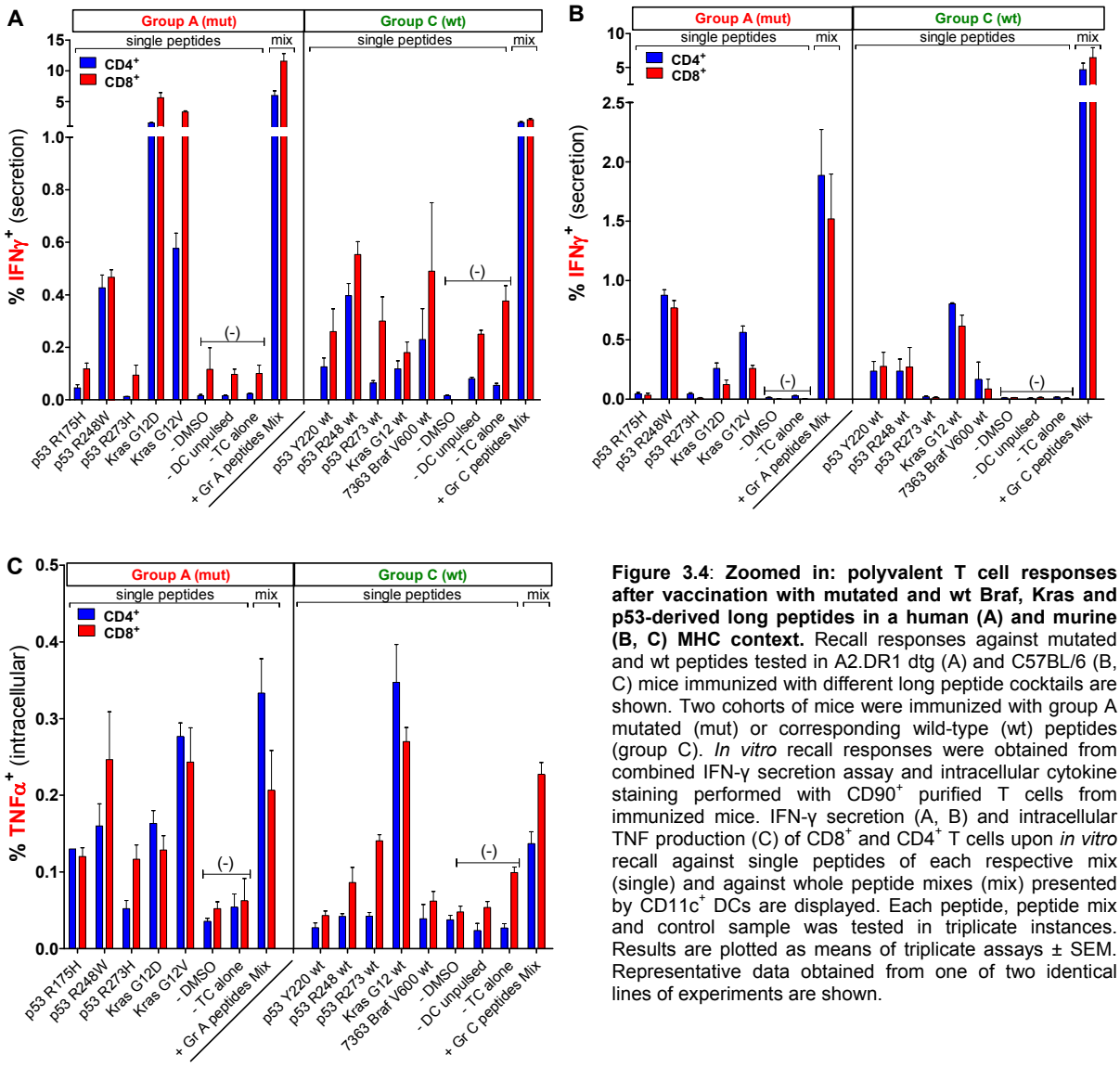


**Figure 3.4**: **Zoomed in: polyvalent T cell responses after vaccination with mutated and wt Braf, Kras and p53-derived long peptides in a human (A) and murine (B, C) MHC context.** Recall responses against mutated and wt peptides tested in A2.DR1 dtg (A) and C57BL/6 (B, C) mice immunized with different long peptide cocktails are shown. Two cohorts of mice were immunized with group A mutated (mut) or corresponding wild-type (wt) peptides (group C). *In vitro* recall responses were obtained from combined IFN-γ secretion assay and intracellular cytokine staining performed with $CD90^+$ purified T cells from immunized mice. IFN-γ secretion (A, B) and intracellular TNF production (C) of $CD8^+$ and $CD4^+$ T cells upon *in vitro* recall against single peptides of each respective mix (single) and against whole peptide mixes (mix) presented by $CD11c^+$ DCs are displayed. Each peptide, peptide mix and control sample was tested in triplicate instances. Results are plotted as means of triplicate assays ± SEM. Representative data obtained from one of two identical lines of experiments are shown.

Next to the IFN-γ secretion also the intracellular accumulation of the cytokines IFN-γ and TNF-α was analyzed. Unfortunately, the intracellular signals for these two cytokines were of a very low percentage and negative controls were considerably high, resulting in low signal to noise ratio and complicating the identification of responses towards the tested peptides. The TNF staining performed

slightly better than the staining for intracellular IFN-γ. In figure 3.4 TNF production of splenic T cells from group A and group C vaccinated C57BL/6 mice after *in vitro* re-stimulation is shown. In the depicted experiments the negative controls were comparatively low allowing for the speculation that also TNF responses towards the mutated Kras G12V and p53 R248W peptides are higher compared to other peptides. Hence, TNF production seemed to reinforce the same trends found for IFN-γ secretion after *in vitro* re-stimulation and could point towards a multi-functionality of vaccination-induced T cells. To investigate the issue further secretion assays and intracellular cytokines stainings were carried out independently additionally including the detection of the cytokine IL-2. Results obtained will be shown in the context of the next chapter dealing with the detailed analysis of the T cell responses elicited by vaccination.

Next to the IFN-γ secretion also the intracellular accumulation of the cytokines IFN-γ and TNF-α was analyzed. Unfortunately, the intracellular signals for these two cytokines were of a very low percentage and negative controls were considerably high, resulting in low signal to noise ratio and complicating the identification of responses towards the tested peptides. The TNF staining performed slightly better than the staining for intracellular IFN-γ. In figure 3.4 TNF production of splenic T cells from group A and group C vaccinated C57BL/6 mice after *in vitro* re-stimulation is shown. In the depicted experiments the negative controls were comparatively low allowing for the speculation that also TNF responses towards the mutated Kras G12V and p53 R248W peptides are higher compared to other peptides. Hence, TNF production seemed to reinforce the same trends found for IFN-γ secretion after *in vitro* re-stimulation and could point towards a multi-functionality of vaccination-induced T cells. To investigate the issue further, secretion assays and intracellular cytokines stainings were carried out independently additionally including the detection of the cytokine IL-2. Results obtained will be shown in the context of the next chapter dealing with the detailed analysis of the T cell responses elicited by vaccination.

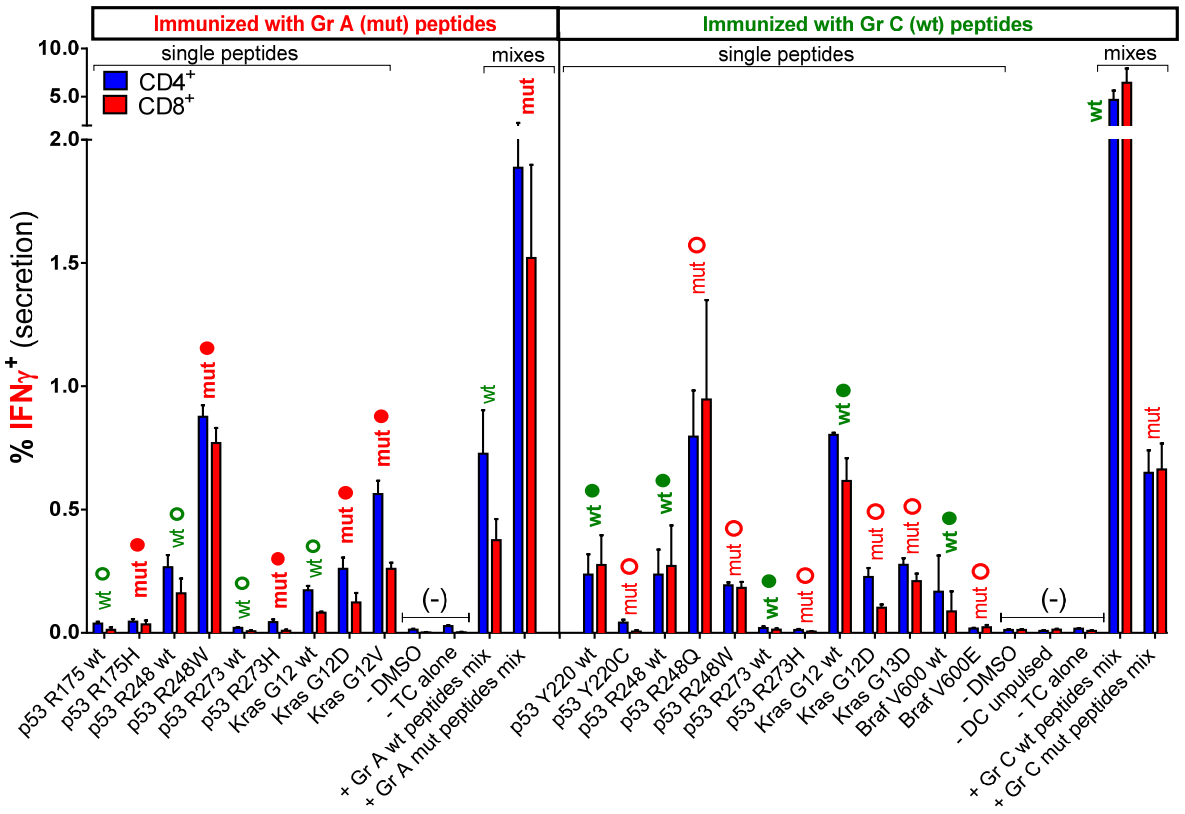


**Figure 3.5**: **Polyvalent *in vitro* T cell responses towards wt and mutated peptides after vaccination with wt or mutated peptides.** Recall responses against mutated and wt peptides tested in C57BL/6 mice immunized with different long peptide cocktails are shown. Two cohorts of mice were immunized with group A mutated (mut) or corresponding wild-type (wt) peptides (group C). *In vitro* recall responses were obtained from combined IFN-γ secretion assay and intracellular cytokine staining performed with $CD90^+$ purified T cells from immunized mice. IFN-γ secretion of $CD8^+$ and $CD4^+$ T cells upon *in vitro* recall against single peptides of each respective mix (single), corresponding wt and mutated peptides, and against whole peptide mixes (mix) presented by $CD11c^+$ DCs are displayed. Each peptide, peptide mix and control sample was tested in triplicate instances. Results are plotted as means of triplicate assays ± SEM. Representative data obtained from one of two identical lines of experiments are shown. Filled dots: peptides used for vaccination and *in vitro* recall response testing, open dots: peptides used for *in vitro* recall response testing only, wt: wild-type peptides, mut: mutated peptides

Further we addressed the question whether there was a general difference between the immunogenicity of mutated and wt peptides when employed for active vaccination. Therefore, cumulative analysis of *in vitro* recall responses towards wt and mutated peptides after vaccination with mutated or wt peptides cocktails was carried out. As indicated in figure 3.5, the readout of *in vitro* recall responses after vaccination did not only include the peptides used for vaccination, but T cell activity was also screened for responsiveness towards their corresponding wt or mutated peptide counterparts. In the concrete example, T cells from mice vaccinated with peptides of group A were not only tested against responses towards single and mixed group A peptides, but also for their *in vitro* responsiveness against single and mixed corresponding wt peptide sequences. The same testing was conducted *vice versa* with T cells from wt peptides vaccinated mice.

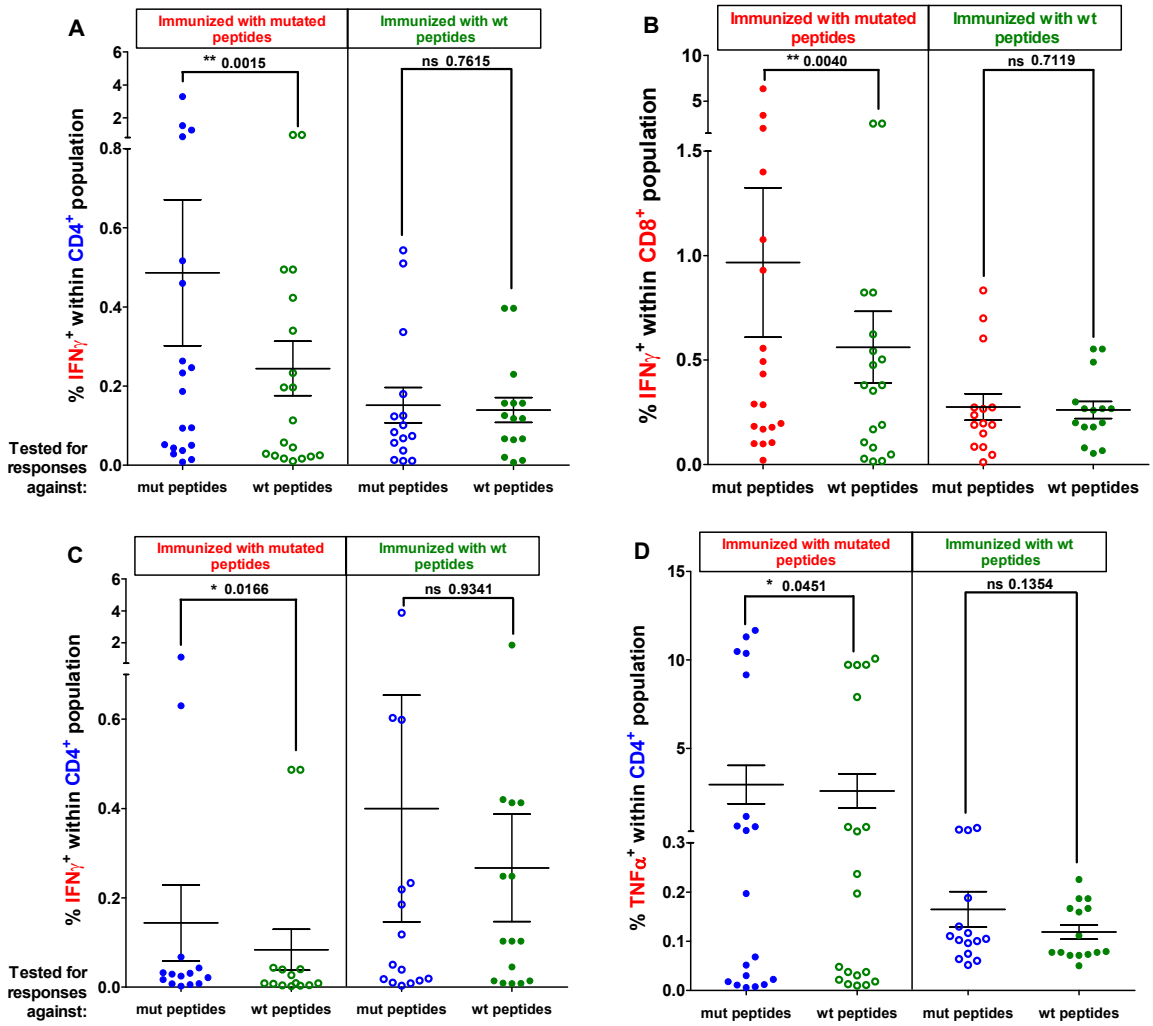


**Figure 3.6**: **Accumulated responses of CD8$^+$ and CD4$^+$ T cells point towards mutation specificity after vaccination of HLA-humanized A2.DR1 dtg mice with mutated peptides.** Results were accumulated from six cohorts of mice immunized with one group of mutated (mut) or wild-type (wt) peptides (A to F), each, in PBS-based formulations including CpG ODN 1668 as an adjuvant. *In vitro* recall responses were obtained from combined IFN-γ secretion assay and intracellular cytokine staining performed with CD90$^+$ purified T cells from immunized mice. Percentages of IFN-γ secreting splenic CD4$^+$ (**A**) and CD8$^+$ (**B**) T cells upon *in vitro* recall against mutated (mut) and wild-type (wt) peptides represented on CD11c$^+$ DCs are shown. The same analysis was made for the IFN-γ secretion of CD4$^+$ T cells from vaccination site draining lymph nodes (**C**) and with the percentages of intracellular TNF positive, splenic CD4$^+$ T cells (**D**). Each peptide was tested in triplicate instances. Means of mutated and wt peptide triplicates are plotted and tested against one another by two-tailed Wilcoxon signed rank test. Representative data obtained from one of two identical lines of experiments are shown. Filled dots: peptides used for vaccination and *in vitro* recall response testing, open dots: peptides used for *in vitro* recall response testing only.

Hereupon, all T cells responses from mutated and wt peptide vaccinated mice were accumulated in two groups, respectively, namely cytokine production induced by mutated (group 1 – mut peptides) peptides and corresponding wt (group 2 – wt peptides) peptides. Differences between accumulated mutated and wt peptides couples were tested for by two-tailed Wilcoxon signed rank test, as shown in figures 3.6 for A2.DR1 dtg mice and in figure 3.7 for C57BL/6 mice, respectively. The analysis was done for the IFN-γ secretion of splenic CD4$^+$ (figures 3.6 A and 3.7 A) and CD8$^+$ (figures 3.6 B and 3.7 B) T cells, which was leading to the same tendencies in both MHC contexts. Accumulated responses of CD8$^+$ and CD4$^+$ T cells point towards a mutation specificity after vaccination with mutated peptides, whereas

there were no significant differences between the percentages of IFN-γ positive T cells towards wt and mutated peptides after vaccination with wt peptides. Indeed, upon vaccination with mutated peptides the cumulative $CD4^+$ and $CD8^+$ T cell responses against those were significantly higher in A2.DR1 dtg mice ($CD4^+$ p = 0.0015, and $CD8^+$ p = 0,0040) as well as in C57BL/6 mice ($CD4^+$ p = 0,0002, and $CD8^+$ p < 0,0001). Next to splenic T cells also T cells purified from vaccination site draining lymph nodes were analyzed, as exemplarily shown for $CD4^+$ T cells in figure 3.6 C. Pooled IFN-γ secretion responses of lymph node T cells of A2.DR1 dtg mice again indicate a mutation specificity after vaccination with mutated peptides (p = 0.0166). The same trend was found when analyzing for the intracellular TNF-α accumulation after vaccination with mutated peptides, as displayed in figure 3.6 D for splenic $CD4^+$ T cells (p = 0.0451). Likewise, these tendencies towards mutation specificity (although not resulting in statistically significant results) could be observed for $CD8^+$ T cell responses, intracellular IFN-γ production and in identical analysis of C57BL/6 intracellular cytokine responses (data not shown).

Conclusively, cumulative analysis of wt and mutated peptides immunized mice suggest that it was possible to generally generate mutation specific $CD4^+$ and $CD8^+$ T cell responses after active vaccination with oncogene-mutation harboring long peptides in both a murine and human MHC context.

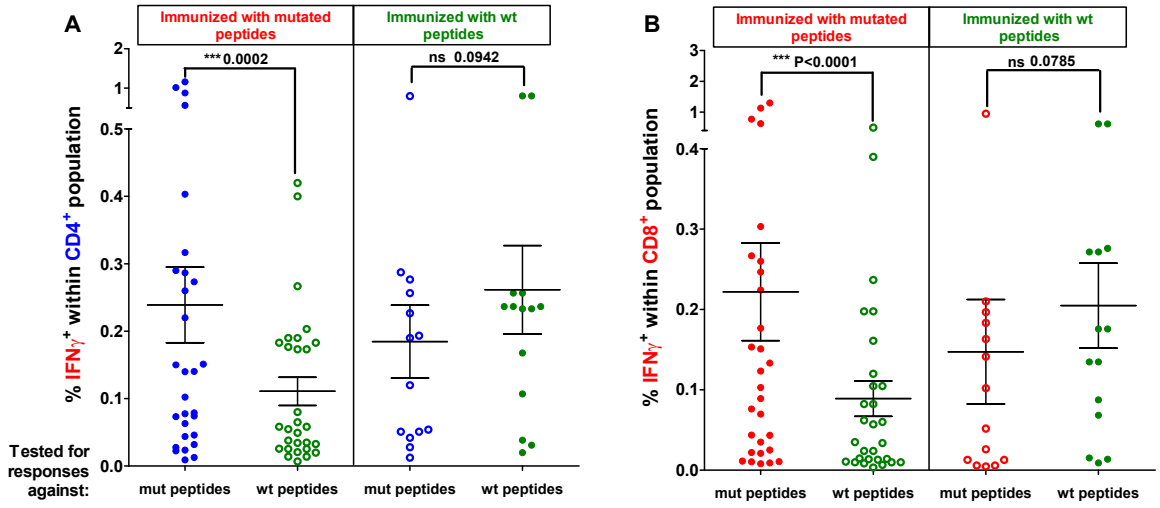


**Figure 3.7**: **Accumulated responses of $CD8^+$ and $CD4^+$ T cells point towards mutation specificity after vaccination of C57BL/6 mice with mutated peptides.** Results were accumulated from six cohorts of mice immunized with one group of mutated (mut) or wild-type (wt) peptides (A to F), each, in PBS-based formulations including CpG ODN 1668 as an adjuvant. *In vitro* recall responses were obtained from combined IFN-γ secretion assay and intracellular cytokine staining performed with $CD90^+$ purified T cells from immunized mice. Percentages of IFN-γ secreting splenic $CD4^+$ (**A**) and $CD8^+$ (**B**) T cells upon *in vitro* recall against mutated (mut) and wild-type (wt) peptides represented on $CD11c^+$ DCs are shown. Each peptide was tested in triplicate instances. Means of mutated and wt peptide triplicates are plotted and tested against one another by two-tailed Wilcoxon signed rank test. Representative data obtained from one of two identical lines of experiments are shown. Filled dots: peptides used for vaccination and *in vitro* recall response testing, open dots: peptides used for *in vitro* recall response testing only.

## 3.2. Detailed analysis of vaccination-induced T cell responses towards oncogene-derived long peptides

### 3.2.1. No spontaneous responses towards oncogene-derived wt and mutated peptides in untreated animals

After testing the immunogenicity of wt and mutated oncogene-derived peptides for active vaccination, the pre-existence of spontaneous T cell reactivity towards the peptides was investigated. To do so, combined IFN-γ secretion assays and intracellular cytokine stainings were carried out, for which either purified T cells from vaccinated or untreated mice were re-stimulated on peptide pulsed $CD11c^+$ BM-derived DCs. In figure 3.8 the results obtained from group A (mutated peptides) and C (wt peptides) vaccinated mice are opposed to spontaneous T cell activity against these peptides detected in untreated A2.DR1 dtg animals (panel 'untreated mice'). Compared to peptide directed T cell responses in vaccinated mice, the IFN-γ responses of T cells derived from untreated animals were insignificant. T cell responsiveness against none of the peptides tested (neither wt nor mutated sequences) was above those of negative controls and generally background T cell activity was lower in non-vaccinated mice. Similar observations were made for the C57BL/6 strain (data not shown). This leads to the conclusion that there are no pre-existing or spontaneous T cell responses towards the chosen oncogene-derived wt and mutated sequences in untreated animals (after short-term *in vitro* re-stimulation).

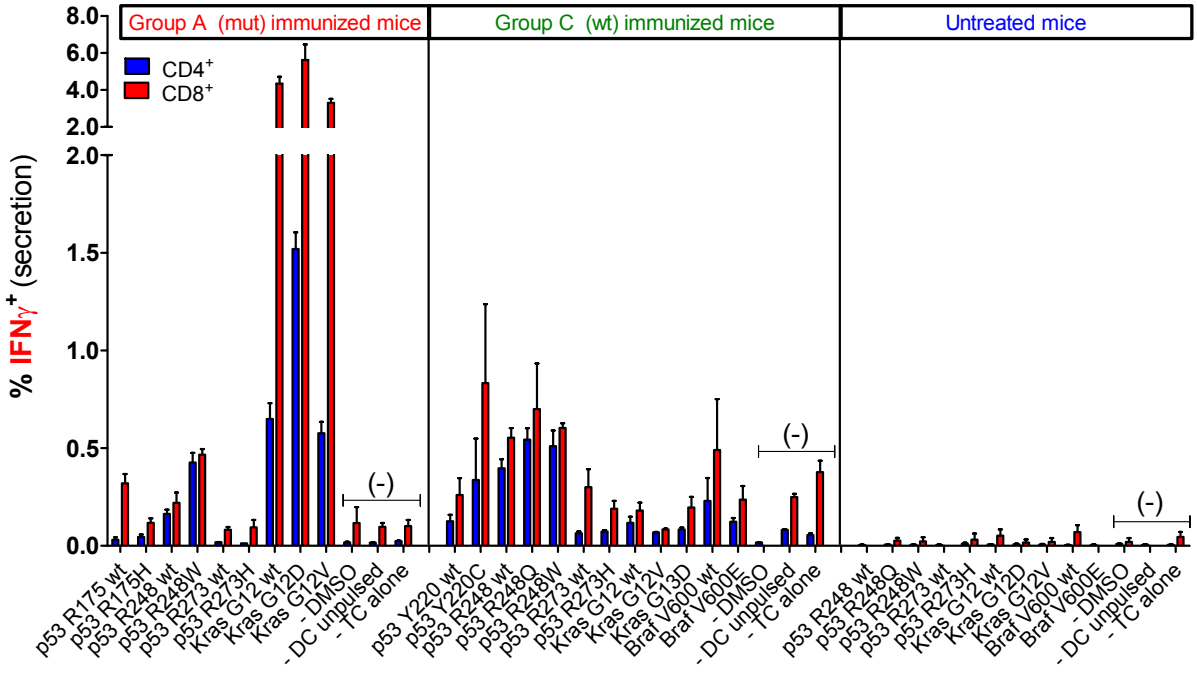


**Figure 3.8**: **No spontaneous responses towards mutated and wild-type oncogene-derived peptides in untreated mice.** Recall responses against mutated and wt peptides tested in A2.DR1 dtg mice immunized with group A and C long peptide cocktails or untreated mice are shown. *In vitro* recall responses were obtained from combined IFN-γ secretion assay and intracellular cytokine staining performed with splenic $CD90^+$ purified T cells from immunized mice. IFN-γ secretion of $CD8^+$ and $CD4^+$ T cells upon *in vitro* recall against single peptides of each respective mix (corresponding wt and mutated peptides) presented by $CD11c^+$ DCs are displayed. Each peptide and control sample was tested in triplicate instances. Results are plotted as means of triplicate assays ± SEM. Representative data obtained from one of two identical lines of experiments are shown.

### 3.2.2. Sequence alterations in peptide backbones between mouse and human do not influence the mutation-specificity induced by vaccination

Three couples of p53-derived wt and mutated peptides within the tested panel harbored sequence differences in the peptide backbone surrounding the targeted oncogene mutation between human and mouse. The p53 R175 peptides display two amino acid substitutions, namely at position 165 K (lysine, mouse) to Q (glutamine, human) and at position 185 G (glycine, mouse) to S (serine, human). Second, the p53 R248 peptides carried a substitution K (lysine, mouse) to N (asparagine, human) at position 235. Within in the p53 R273 peptides the positions 268 and 289 were altered from D (aspartic acid, mouse) to N (asparagine, human) and F (phenylalanine, mouse) to L (leucine, human), respectively. These sequence differences could be recognized as “foreign”, possibly giving rise to immunogenic epitopes, when mice are vaccinated with human backbone sequence peptides. To prove that the responsiveness towards the human backbone peptides, of special relevance towards mutated peptides, is not attributed to the species-intrinsic amino acid sequence differences, mice were vaccinated with murine backbone sequence long peptides. Groups of three mice were either immunized with a cocktail containing the three murine backbone wt peptides (p53 R175 wt (mur), p53 R248 wt (mur), p53 R273 wt (mur)), a second cocktail containing three mutated murine backbone peptides (p53 R175H (mur), p53 R248W (mur), p53 R273H (mur)) or group A human peptide cocktail (containing the mutated peptides p53 R175H, p53 R248W, p53 R273H). Purified splenic T cells from differentially vaccinated mice were tested in combined IFN-γ secretion assays and intracellular cytokine stainings for responses against murine and human backbone wt and mutated peptides.

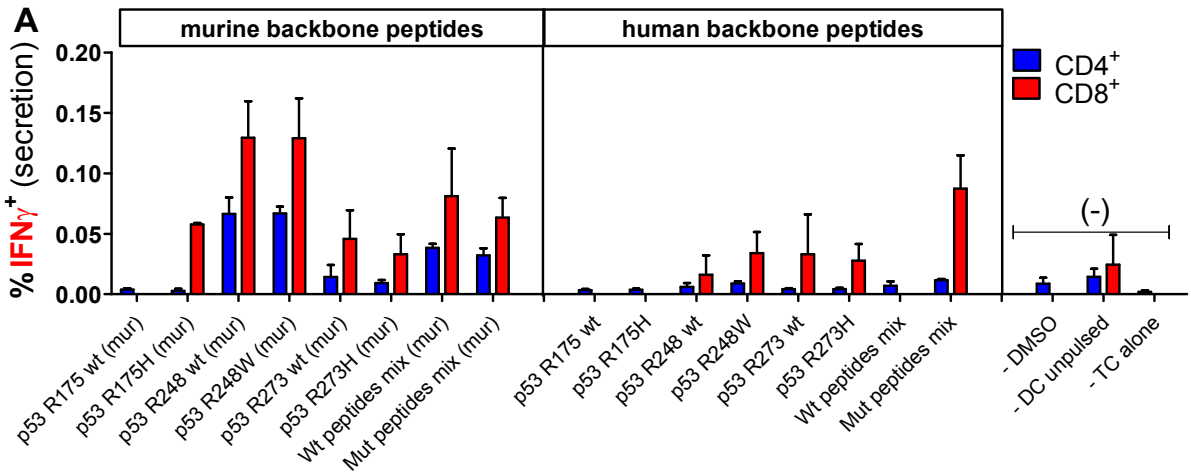


**Figure 3.9 A**: **Polyvalent *in vitro* T cell responses towards wt and mutated peptides with murine backbone sequences presented in a human HLA class I and II context.** For the complete figure legend see the consecutive page.

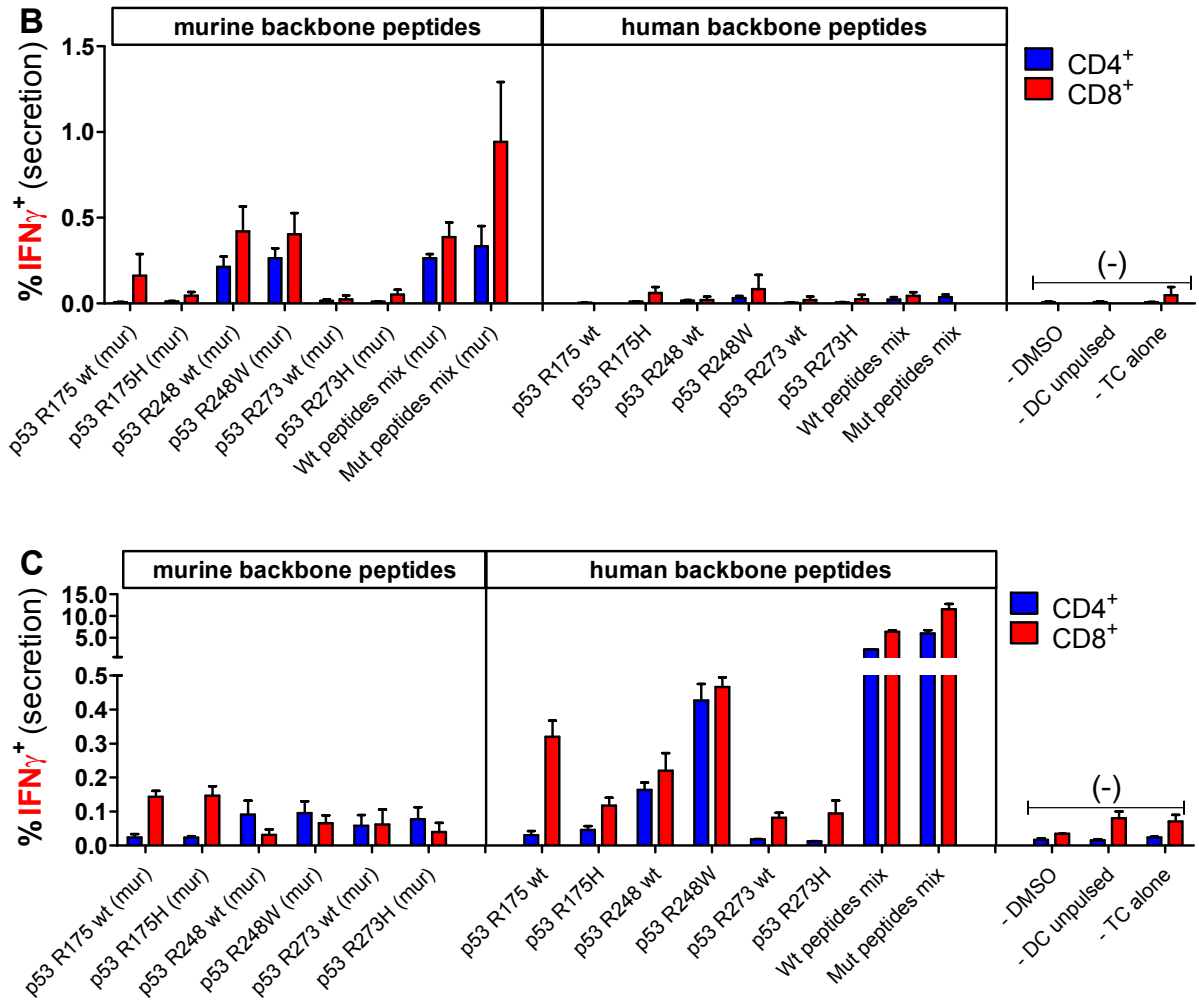


**Figure 3.9**: **Polyvalent *in vitro* T cell responses towards wt and mutated peptides with murine backbone sequences presented in a human HLA class I and II context.** Recall responses against mutated and wt peptides with human and murine backbone sequences tested in A2.DR1 dtg mice immunized with either murine (mur) or human backbone long peptide cocktails are shown. Three cohorts of mice were vaccinated with either a (**A**) wt murine backbone peptide cocktail (p53 R175 wt (mur), p53 R248 wt (mur), p53 273 wt (mur), a (**B**) mutated murine backbone cocktail (p53 R175H (mur), p53 R248W (mur), p53 R273H (mur)), or with the (**C**) group A mutated human backbone peptides (including p53 R175H, p53 R248W, p53 R273H). *In vitro* recall responses were obtained from combined IFN-γ secretion assay and intracellular cytokine staining performed with splenic CD90$^+$ purified T cells from immunized mice. IFN-γ secretion of CD8$^+$ and CD4$^+$ T cells upon *in vitro* recall against single peptides of each respective mix, corresponding wt and mutated peptides with either human or murine (mur) backbone sequences, and against whole peptide mixes (mix) presented by CD11c$^+$ DCs are displayed. Each peptide, peptide mix and control sample was tested in triplicate instances. Results are plotted as means of triplicate assays ± SEM.

Figures 3.9 and 3.10 comprise the results gathered for A2.DR1 dtg mice and C57BL/6 mice, respectively. Thereby, vaccination with murine wt (subfigures A) and mutated (subfigures B) backbone peptides gave rise to polyvalent T cell responses against murine wt as well as mutated peptides. When tested against human backbone peptides, however, the IFN-γ secretion of T cells purified from murine backbone peptide vaccinated mice, was lower than those towards murine backbone peptides. When the experiment was performed *vice versa* with T cells from human backbone peptides vaccinated mice (as exemplary shown in figure 3.9 C for vaccination of A2.DR1 dtg mice with group A mutated human peptides) the reverse trend was observed. The IFN-γ secretion of T cells from these mice was higher

upon re-stimulation with human backbone peptides compared to re-stimulation with murine backbone peptides. Although the quantity of *in vitro* recall responses towards murine and human peptide backbone sequences seemed to depend on the peptides used for vaccination the, quality in terms of response pattern is rather unaltered. Hence, mutation-specificity, especially in case of the highly immunogenic peptide p53 R248W, seemed to be retained after vaccination with mutated peptides. Irrespective of the peptide backbones used for *in vitro* re-stimulation responses towards the mutated peptides p53 R248W or p53 R248W (mur) are higher than towards the corresponding wt counterparts. This observation was clearly shown for the murine MHC context (fig 3.10 B), whereas the respective responses in the human HLA context remained rather ambiguous (fig 3.9 B).

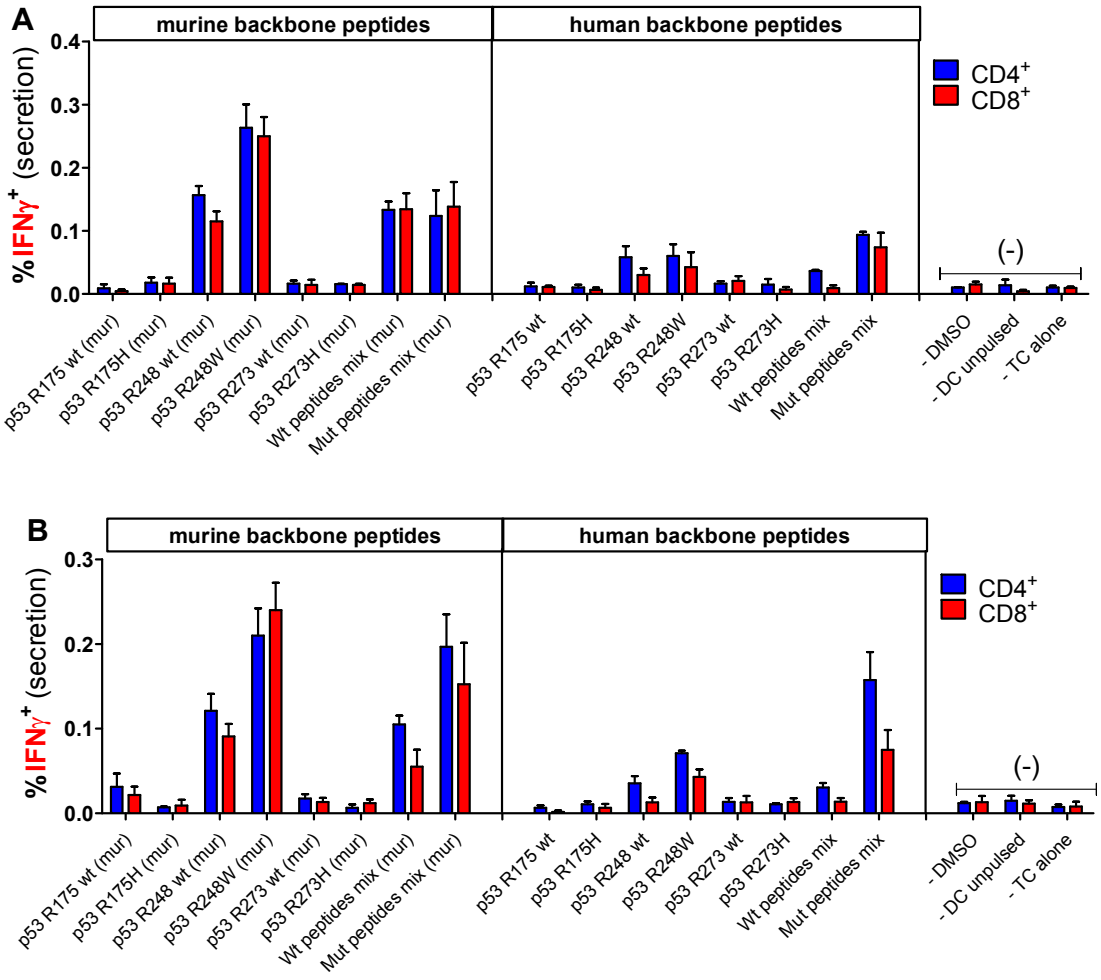


**Figure 3.9**: **Polyvalent *in vitro* T cell responses towards wt and mutated peptides with murine backbone sequences presented in a murine MHC context.** Recall responses against mutated and wt peptides with human and murine backbone sequences tested in C57BL/6 mice immunized with either murine (mur) or human backbone long peptide cocktails are shown. Two cohorts of mice were vaccinated with either a (**A**) wt murine backbone peptide cocktail (p53 R175 wt (mur), p53 R248 wt (mur), p53 273 wt (mur) or a (**B**) mutated murine backbone cocktail (p53 R175H (mur), p53 R248W (mur), p53 R273H (mur). *In vitro* recall responses were obtained from combined IFN-γ secretion assay and intracellular cytokine staining performed with splenic $CD90^+$ purified T cells from immunized mice. IFN-γ secretion of $CD8^+$ and $CD4^+$ T cells upon *in vitro* recall against single peptides of each respective mix, corresponding wt and mutated peptides with either human or murine (mur) backbone sequences, and against whole peptide mixes (mix) presented by $CD11c^+$ DCs are displayed. Each peptide, peptide mix and control sample was tested in triplicate instances. Results are plotted as means of triplicate assays ± SEM.

### 3.2.3. The presence of CD4$^+$ T cells influences CD8$^+$ T cell *in vitro* responsiveness

As described in the introduction, it is desirable to elicit CD8$^+$ as well as CD4$^+$ T cell responses by multi-epitope long peptide vaccination. Alongside with several direct tumor-eradicating functions, CD4$^+$ T cells are prone to interact and provide help to CD8$^+$ T cells. In the previously described section it already became obvious that multi-peptide vaccination in the applied setting gave rise to both peptide-specific CD4$^+$ and CD8$^+$ cytokine responses when tested *in vitro*. To gain an impression under which conditions T cell subsets are most responsive and about possible interactions between the two major subsets of CD4$^+$ and CD8$^+$ T cells, differentially purified T cell subsets from immunized mice were tested in IFN-γ secretion assays. Data was obtained from vaccination of six cohorts of either A2.DR1 dtg and C57BL/6 mice with the wild-type and mutated peptide cocktails (A to F) in PBS-based formulations employing CpG ODN 1668 as an adjuvant. T cells from splenic and vaccination-site draining lymph nodes were either purified for CD8$^+$ T cells or CD90$^+$ T cells (comprising CD4$^+$ and CD8$^+$ subsets) and T cells were tested against respective wt and mutated peptides in IFN-γ secretion assays without staining for intracellular cytokines.

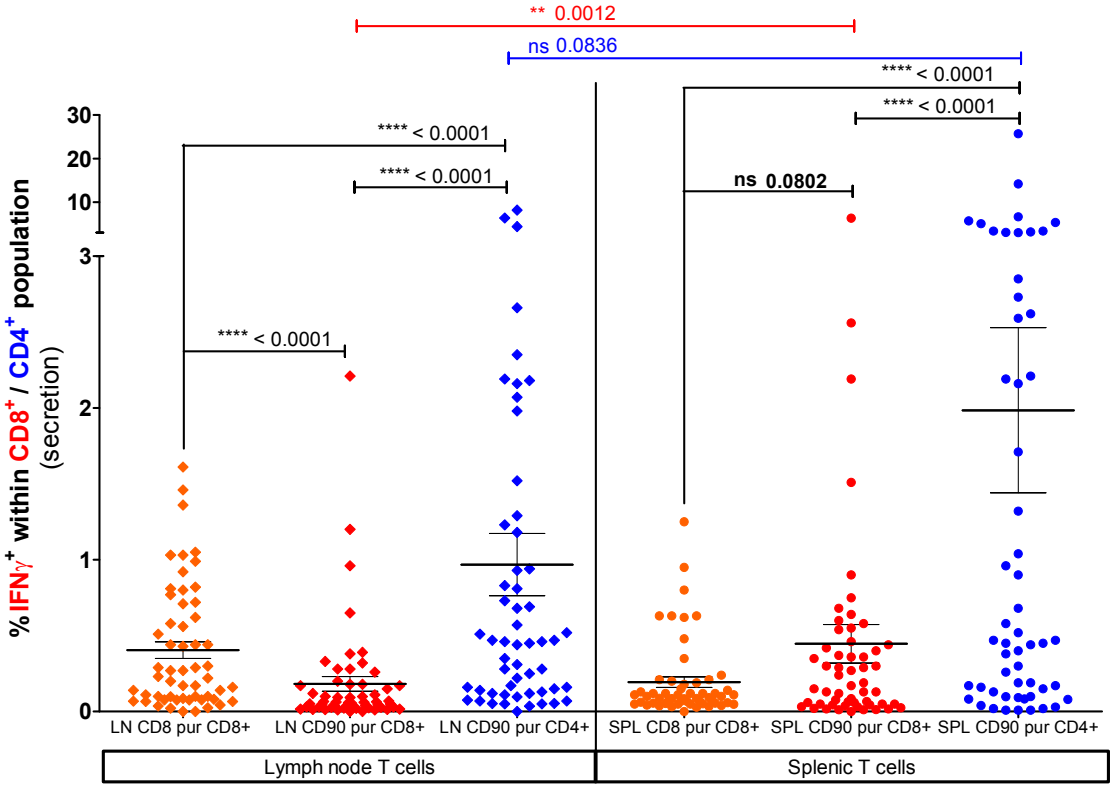


**Figure 3.11**: **The presence of CD4$^+$ T cells influences CD8$^+$ cell *in vitro* responsiveness.** Results were accumulated from six cohorts of A2.DR1 dtg mice immunized with one group of mutated (mut) or wild-type (wt) peptides (A to F), each, in PBS-based formulations including CpG ODN 1668 as an adjuvant. *In vitro* recall responses were obtained from IFN-γ secretion assays performed with either CD90$^+$ (CD90 pur) or CD8$^+$ (CD8 pur) purified T cells from immunized mice. Percentages of IFN-γ secreting splenic (SPL) and vaccination site draining lymph nodes derived (LN) CD4$^+$ and CD8$^+$ T cell subsets upon *in vitro* recall against mutated (mut) and wild-type (wt) peptides represented on CD11c$^+$ DCs are shown. CD8$^+$ T cells were either tested alone or in combination with CD4$^+$ T cells in CD90$^+$ purified samples. Each peptide was tested as a single instance. Values of mutated and wt peptides are plotted and tested cumulative against one another by Wilcoxon matched pairs signed rank test. Dots: splenic T cells, squares: LN-derived T cells, orange: percentage of IFN-γ positive CD8$^+$ purified T cells in the absence of CD4$^+$ T cells, red: IFN-γ responses of CD8$^+$ T cells within CD90$^+$ cultures (meaning in the presence of CD4$^+$ T cells), blue: percentages of IFN-γ positive CD4$^+$ T cells within CD90$^+$ co-cultures. SPL: spleen, LN: lymph nodes, pur: purified, ns: not significant.

Percentages of distinct IFN-γ positive T cell subsets responsive against wild-type and mutated peptides presented on $CD11c^+$ BM-derived DCs were cumulated in groups and groups were tested against one another by Wilcoxon matched pairs signed rank tests. Analysis of data from A2.DR1 dtg mice and C57BL/6 mice are shown in figures 3.11 and 3.12, respectively. Therein, it becomes obvious that the percentages of IFN-γ secreting splenic $CD4^+$ and $CD8^+$ T cells in $CD90^+$ co-cultures were (significantly) higher than those of vaccination-site draining lymph nodes. This observation was made for both A2.DR1 dtg ($CD4^+$, not significant, p = 0.0836, $CD8^+$ p = 0.0012) and C57BL/6 ($CD4^+$ p < 0.0001 and $CD8^+$ p = 0.0002) mice. In case $CD8^+$ T cells were cultured alone, this difference between splenic and lymph node subsets was not present.

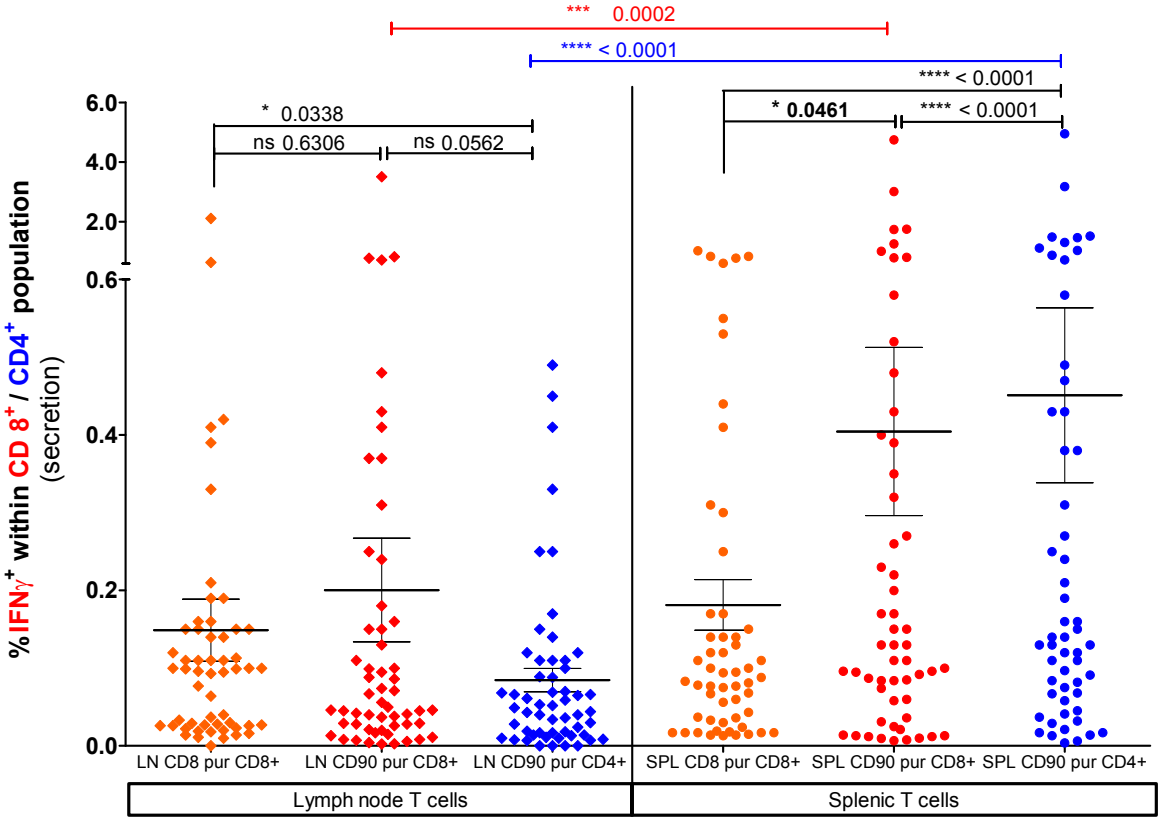


**Figure 3.12**: **The presence of $CD4^+$ T cells influences $CD8^+$ T cell *in vitro* responsiveness.** Results were accumulated from six cohorts of C57BL/6 mice immunized with one group of mutated (mut) or wild-type (wt) peptides (A to F), each, in PBS-based formulations including CpG ODN 1668 as an adjuvant. *In vitro* recall responses were obtained from IFN-γ secretion assays performed with either $CD90^+$ (CD90 pur) or $CD8^+$ (CD8 pur) purified T cells from immunized mice. Percentages of IFN-γ secreting splenic (SPL) and vaccination site draining lymph nodes derived (LN) $CD4^+$ and $CD8^+$ T cell subsets upon *in vitro* recall against mutated (mut) and wild-type (wt) peptides represented on $CD11c^+$ DCs are shown. $CD8^+$ T cells were either tested alone or in combination with $CD4^+$ T cells in $CD90^+$ purified samples. Each peptide was tested as a single instance. Values of mutated and wt peptides are plotted and tested cumulative against one another by Wilcoxon matched pairs signed rank test. Dots: splenic T cells, squares: LN-derived T cells, orange: percentage of IFN-γ positive $CD8^+$ purified T cells in the absence of $CD4^+$ T cells, red: IFN-γ responses of $CD8^+$ T cells within $CD90^+$ cultures (meaning in the presence of $CD4^+$ T cells), blue: percentages of IFN-γ positive $CD4^+$ T cells within $CD90^+$ co-cultures. SPL: spleen, LN: lymph nodes, pur: purified, ns: not significant.

Moreover, spleen-derived $CD4^+$ T cells were the most responsive T cell subsets tested, showing the highest percentages of IFN-γ secretion. Secretion was, in fact, highly significantly elevated when compared to those of co-cultured splenic $CD8^+$ T cells and $CD8^+$ T cells re-stimulated alone. Therewith, representing yet another observation which proved to be true in both mouse strains tested. Staying with

splenic T cell subsets, the presence of $CD4^+$ T cells seemed to enhance the *in vitro* responsiveness of co-cultured $CD8^+$ T cell compared to $CD8^+$ T cells re-stimulated on DCs in the absence of $CD4^+$ T cells. This was indicated by a significantly higher IFN-γ secretion of the $CD90^+$ co-culture derived $CD8^+$ T cells compared to $CD8^+$ T cells re-stimulated alone in CD57BL/6 mice ($p = 0,0461$) and a trend towards a higher responsiveness of splenic, co-cultured $CD8^+$ cells in A2.DR1 dtg mice ($p = 0,082$). Importantly, directly compared $CD90^+$ and $CD8^+$ T cell subsets were purified from the very same groups of mice excluding the possibility that the differences in responsiveness of T cell subsets might be attributed to an artifact of intra-experimental variability. Interestingly, regarding the subset responses of vaccination-site draining lymph node derived T cells differences between the two investigated mouse strains became obvious. LN-derived $CD4^+$ T cells are in case of A2.DR1 dtg mice the most responsive subset of LN T cells whereas in C57BL/6 mice they are the subset showing the lowest percentage of IFN-γ secreting cells. Moreover, whereas in A2.DR1 dtg mice LN-derived $CD8^+$ T cell cultured alone are more responsive than those co-cultured with $CD4^+$ T cells, in C57BL/6 mice an opposite trend, similar to the observations made for splenic T cells was found. Conclusively, the presence of $CD4^+$ T cells in *in vitro* cultures seemed to influence $CD8^+$ T cell *in vitro* IFN-γ responsiveness.

### 3.2.4. No evidence of epitope competition between different mutated oncogene-derived peptides

In the following row of experiments the question of epitope competition was investigated. In the initial screening throughout the panel of long peptides in became evident that there are stronger and weaker immunogenic sequences. We wanted to know whether the responses towards weaker immunogenic peptides or peptides which did not elicit cytokine secretion at all were outcompeted by stronger immunogenic peptides in the same mix or peptide-specific responses were superimposed by those of strongly immunogenic peptides. In order to solve this issue, low immunogenic mutated peptides from the mixes A, B, D and E were depicted in one mix leaving out strongly immunogenic peptides. Moreover, we explored whether the combination of all strongly immunogenic peptides combined in a single mix and used for vaccination might lead to suppression of responses towards one of the strongly immunogenic peptides.

Before conducting these experiments, however, improvements in the *in vitro* read-out system were explored. As it was not possible to detect the T cell survival factor cytokine IL-2 in the setting of a combined IFN-γ secretion assay and intracellular cytokine staining, a combination of cytokine secretion assays was established. We decided for a combination of secretion assays because secretion of cytokines represents a better marker for the functionality of T cells than the staining for intracellular cytokines. ICCS does not provide direct evidence, whether or not, the viable T cells actively secret the produced cytokines. Furthermore, we expected to be able to detect higher frequencies of multi-functional, cytokine double-positive T cells via the cytokine secretion assay method. Therefore, IFN-γ secretion and IL-2 secretion assays were combined in a two color cytokine secretion assay. We intended to also asses

the cytokine TNF-α in a secretion assay format, but for the murine system a suitable assay is presently not available on the market.

IL-2/IFN-γ two color cytokine secretion assays were down-scaled to a 96-well plate format and were carried out as described in the material and method section (see chapter 2.2.3.1). Again a three hours cytokine secretion period proved to be optimal for detection of cytokine positive cells employing reduced cell numbers in the 96 well plate format and was allowing for testing singe peptides in consistent triplicate instances. Figures 3.13 and 3.14 show exemplary FACS plots and the gating strategy applied for C57BL/6 and A2.DR1 dtg mice, respectively. Similarly to the combined ICCS and secretion assay, lymphocytes were gated on as a sub-population within the FSC and SSC. Consecutively, dead cells and $CD11c^+$ DCs and $Nk1.1^+$ natural killer cells were discriminated. Within the DC and NK cell negative population $CD8^+$ and $CD4^+$ T cells were gated on respectively. The two T cell subsets were further analyzed by plotting IFN-γ against IL-2 secretion and setting quadrant gates according to FMO and isotype controls.

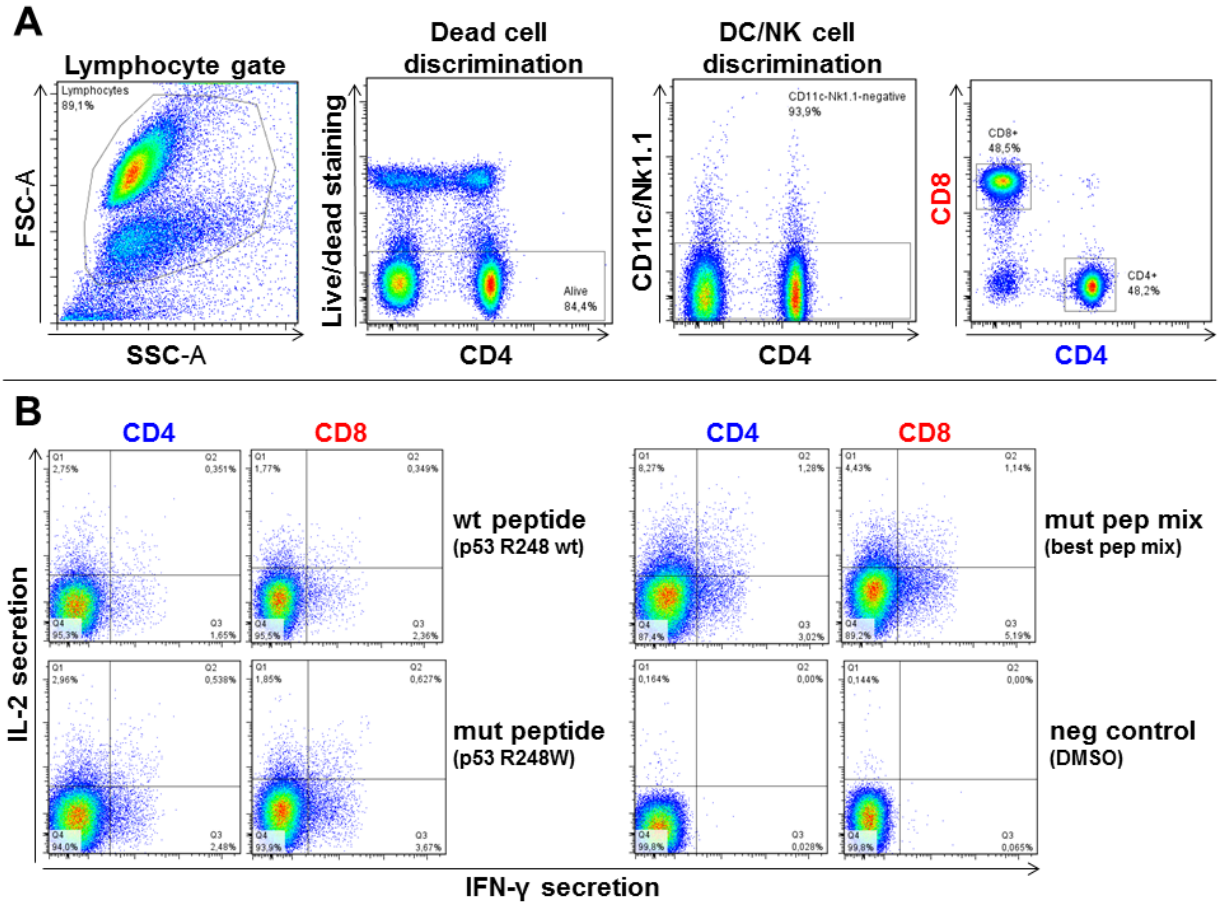


**Figure 3.13**: **Gating strategy for the IFN-γ/IL-2 two color cytokine secretion assay in C57BL/6 mice.** Splenic T cells were purified from most immunogenic peptides immunized C57BL/6 mice. Cell surface was stained with fluorescently labeled monoclonal antibodies against IFN-γ (detection Ab), IL-2 (detection Ab), CD4, CD8, CD11c and Nk1.1. (samples shown: T cells re-stimulated on DCs pulsed with wt peptide p53 R248 wt, mutated peptide p53 R248W, most immunogenic mutated peptides mixed; negative control: dendritic cells pulsed with peptide solvent only (DMSO)).

In the respective B subfigures cytokine secretion of $CD4^+$ and $CD8^+$ T cells upon *in vitro* re-stimulation on $CD11c^+$ BM-derived DCs are shown for the p53 R248W mutated peptide, its corresponding wild-type p53 R248 wt peptide, the whole mix of most immunogenic mutated peptides used for vaccination and the negative control of DCs pulsed with the peptide solvent DMSO. The detection of the secreted cytokine IL-2 was possible in the setting of the two-color cytokine secretion assay and the percentages of IL-2 secreting $CD4^+$ as well as $CD8^+$ T cell exceed those of IFN-γ secretion. Moreover, considerable numbers of cytokine double positive T cells were recorded (figures 3.13 B and 3.14 B, upper right quadrants Q2). Negative controls show a clear background for IFN-γ signals and low percentages of IL-2 secretion, which did not influence the signal to noise ratio substantially, due to the high peptide-specific signals.

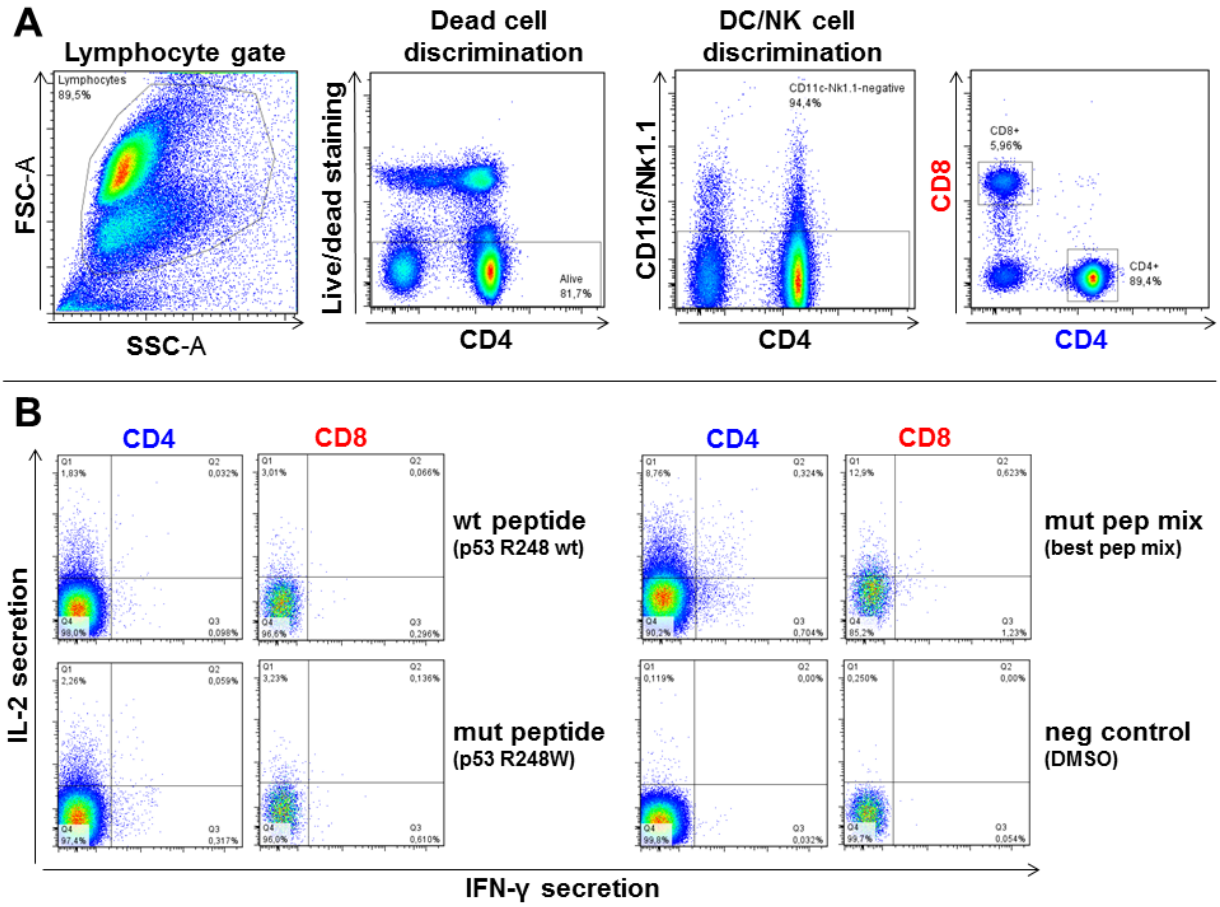


**Figure 3.14**: **Gating strategy for the IFN-γ/IL-2 two color cytokine secretion assay in A2.DR1 dtg mice**. Splenic T cells were purified from most-immunogenic peptides immunized A2.DR1 dtg mice. Cell surface was stained with fluorescently labeled monoclonal antibodies against IFN-γ (detection Ab), IL-2 (detection Ab), CD4, CD8, CD11c and Nk1.1. (samples shown: T cells re-stimulated on DCs pulsed with wt peptide p53 R248 wt, mutated peptide p53 R248W, most immunogenic mutated peptides mixed; negative control: dendritic cells pulsed with peptide solvent only (DMSO)).

In the following figures the results obtained from vaccination of A2.DR1 dtg and C57BL/6 mice with the most immunogenic peptide mixes and peptide mixes comprising only low immunogenic peptides are displayed. In the murine MHC context the previously identified highly immunogenic peptides p53 R245S, p53 R248W/Q, and Kras G12G/V constituted the peptide mix of most immunogenic peptides. In

case of A2.DR1 dtg mice the peptides p53 R248W/Q and Kras G12V/D/R were combined in the mix of most immunogenic peptides. The mix of low immunogenic peptides was the same for both mouse strains tested, including the mutated peptides p53 R175H, p53 R216L, p53 Y220C, p53 R282W, Kras Q61H, and Braf V600E. Peptide mixes were administered as ISA Montanide 720 formulations in combination with the adjuvant CpG ODN 1668 (for details see section 2.2.1.4.2). Figures 3.15 and 3.16 indicated that the response patterns in terms of IFN-γ single positive (respective subfigures A), IL-2 single positive (respective subfigures B) and IFN-γ/IL-2 double positive (respective subfigures C) T cells towards certain tested peptides are similar for the different cytokines tested. Hence, in case a certain peptide elicited high percentage IL-2 secretion relative to other peptides this relation can also be found in the percentages of IFN-γ secreting or cytokine double positive T cells. Moreover, $CD4^+$ as well as $CD8^+$ T cells responded by secretion of both cytokines in the two tested MHC contexts and percentages of IL-2 secreting T cells were found to be the highest compared to those of double positive or IFN-γ single positive T cells.

The results obtained from testing of T cells purified from most immunogenic peptide vaccinated mice revealed that each of the peptides included in the mix was able to elicit high cytokine responses *in vitro* when compared to background controls (and also when compared towards low immunogenic peptides). This was true for both of the MHC contexts investigated. As also observed previously in *in vitro* re-stimulations, corresponding wt peptides tested were able to elicit cytokine secretion, although to a lower percentage than respective mutated peptides. In the human MHC context the responses towards the Kras peptides appeared stronger compared to the p53 peptides, whereas in the murine MCH context the peptides harboring a p53 mutation at the position R248 lead to higher percentages of cytokine secretion than Kras peptides with a mutation at the position G12.

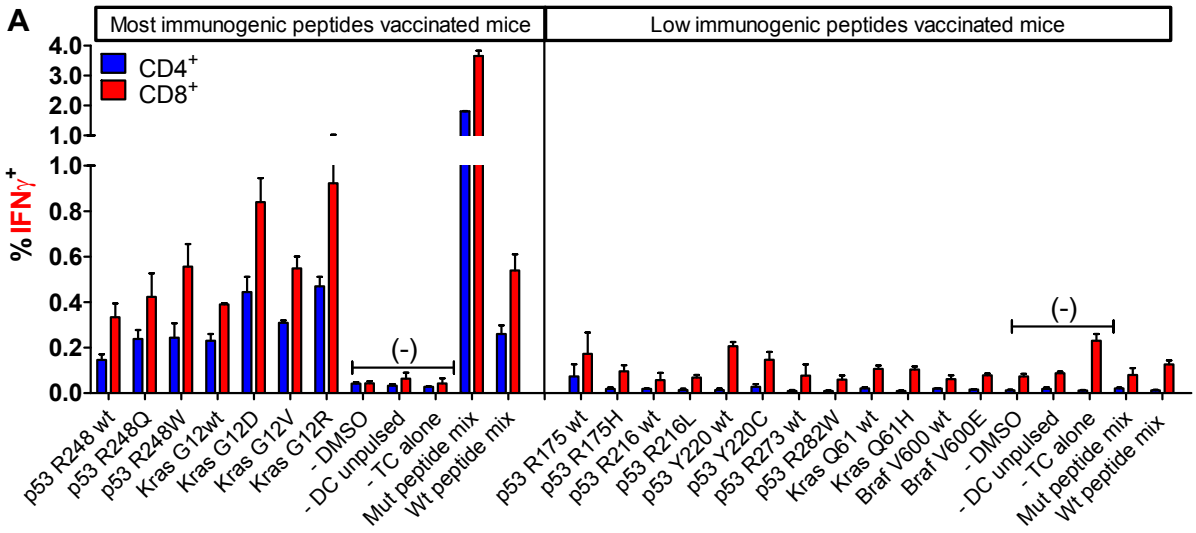


**Figure 3.15 A**: **No evidence of epitope competition within T cell responses towards most immunogenic peptides and low immunogenic peptides after vaccination in A2.DR1 dtg mice.** For the complete figure legend see the consecutive page.

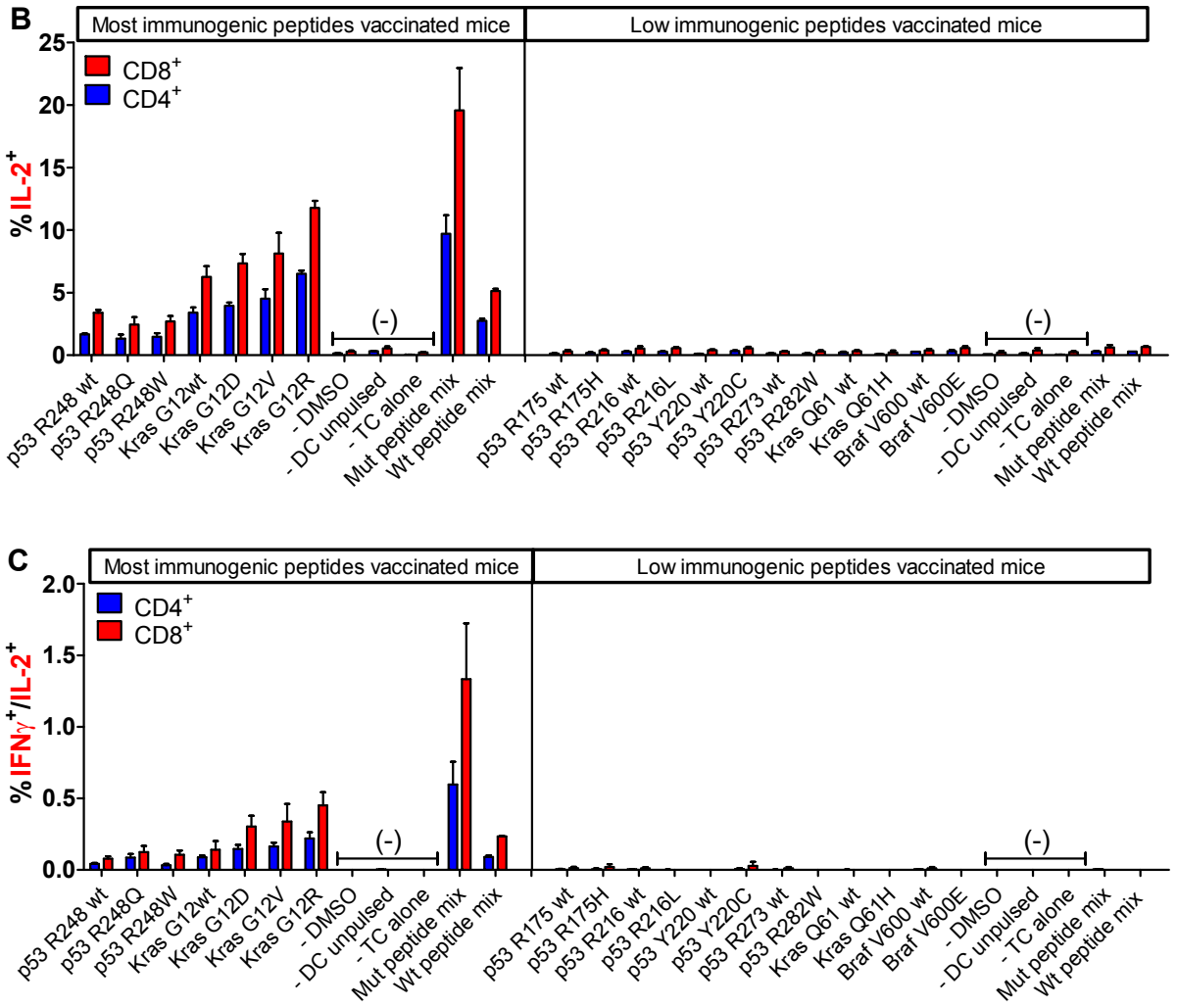


**Figure 3.15**: **No evidence of epitope competition within T cell responses towards most immunogenic peptides and low immunogenic peptides after vaccination in A2.DR1 dtg mice.** Recall responses against mutated and wt peptides sequences tested for A2.DR1 dtg mice immunized with either a mix of most immunogenic mutated peptides (p53 R24Q/W, Kras G12V/D/R) or low immunogenic mutated peptides (p53 R175H, p53 R216L, p53 Y220C, p53 R282W, Kras, Q61H, Braf V600E) are shown. *In vitro* recall responses were obtained from two-color cytokine secretion assays (IL-2, IFN-γ) with pan T cells purified from immunized mice. Percentages of IFN-γ (**A**), IL-2 (**B**) and IFN-γ/IL-2 (**C**) double positive of $CD8^+$ and $CD4^+$ T cells upon *in vitro* recall against single peptides of each respective mix, corresponding wt peptides and against whole peptide mixes (mix) presented by $CD11c^+$ DCs are displayed. Each peptide, peptide mix and control sample was tested in triplicate instances. Results are plotted as means of triplicate assays ± SEM. Representative data obtained from one of two identical lines of experiments are shown.

Compared to the most immunogenic peptides, the responses towards the low immunogenic peptides after vaccination with the low immunogenic peptide mixes were barely detectable and ranged within the percentages of background controls for the murine as well as for the human MHC systems. None of the low immunogenic mutated peptides used for vaccination elicited stronger T cell responses than in previous experiments with other peptide combinations used for vaccination. These findings indicate that at least in *in vitro* recall experiments there was no evidence for competition between low and high immunogenic peptides and between different highly immunogenic peptides.

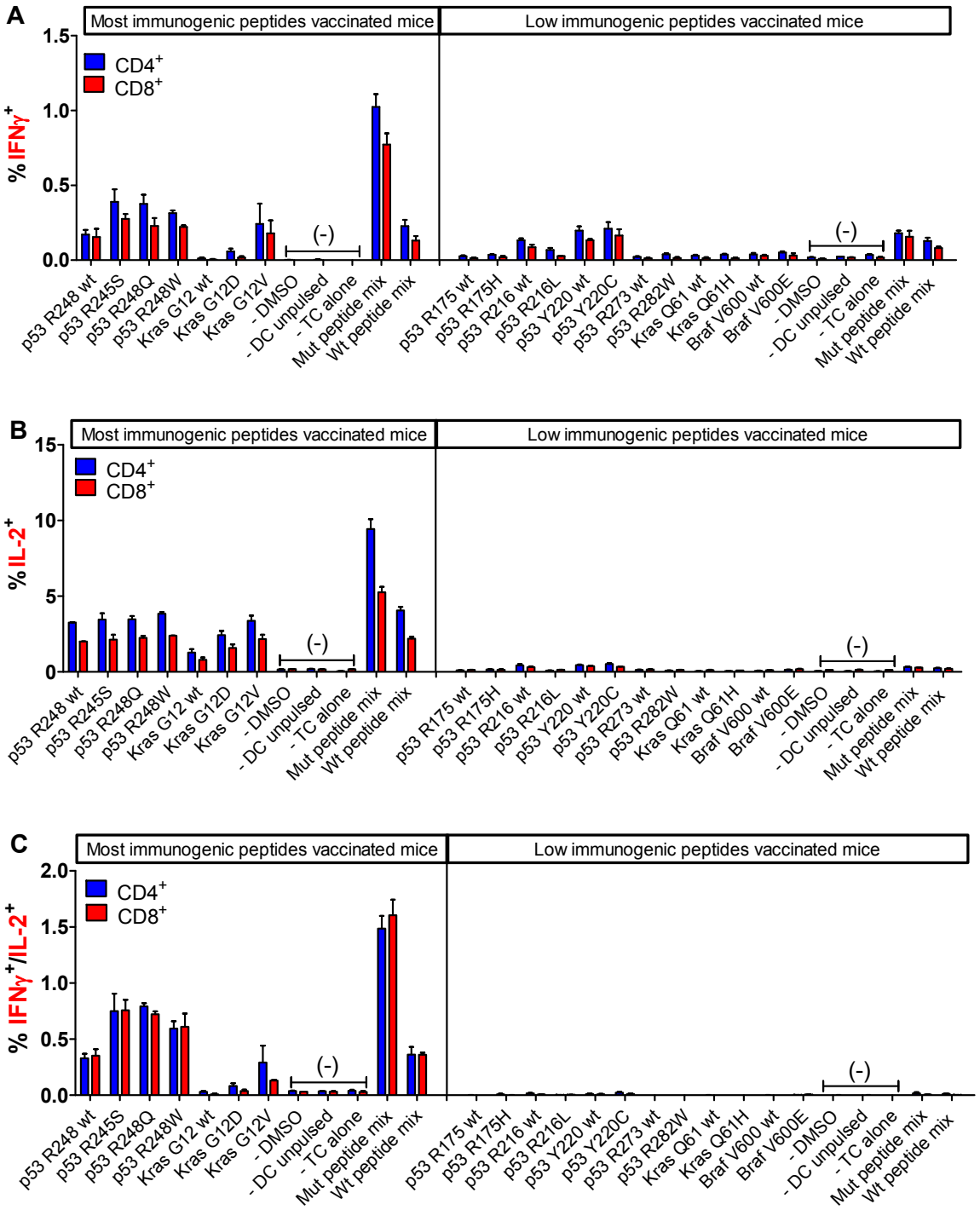


**Figure 3.16**: **No evidence of epitope competition within T cell responses towards most immunogenic peptides and low immunogenic peptides after vaccination in C57BL/6 mice.** Recall responses against mutated and wt peptides sequences tested for C57BL/6 mice immunized with either a mix of most immunogenic mutated peptides (p53 R245S, p53 R24Q/W, Kras G12V/D) or low immunogenic mutated peptides (p53 R175H, p53 R216L, p53 Y220C, p53 R282W, Kras, Q61H, Braf V600E) are shown. *In vitro* recall responses were obtained from two-color cytokine secretion assays (IL-2, IFN-γ) with pan T cells purified from immunized mice. Percentages of IFN-γ (**A**), IL-2 (**B**) and IFN-γ/IL-2 (**C**) double positive of $CD8^+$ and $CD4^+$ T cells upon *in vitro* recall against single peptides of each respective mix, corresponding wt peptides and against whole peptide mixes (mix) presented by $CD11c^+$ DCs are displayed. Each peptide, peptide mix and control sample was tested in triplicate instances. Results are plotted as means of triplicate assays ± SEM. Representative data obtained from one of three identical lines of experiments are shown.

### 3.2.5. $T_{reg}$ cell specificity assays indicate the induction of antigen-specific regulatory T cells against distinct oncogene-derived sequences after long peptide vaccination

In addition to effector $CD4^+$ and $CD8^+$ T cells, regulatory T cells display another T cell subset which seems to be of relevance for the success of anti-cancer peptide vaccination. As indicated in the introduction, a reduction of $T_{reg}$ cell levels by cyclophosphamide treatment, for instance, was correlated with increased patients' survival after peptide vaccination for late stage renal cancer (Walter et al., 2012). Moreover and as also discussed before, there is an increasing line of evidence that intra-tumoral $T_{reg}$ cell levels are critically determining the course of the disease and the outcome while simultaneously influencing treatment options (see section 1.3.2. and 1.4.2.). Due to their crucial role in cancer prognosis and especially for the outcome of anti-cancer peptide vaccination, regulatory T cells were also investigated in this work. More precisely, we asked the question whether vaccination with the mutated (and wt) oncogene and tumor suppressor gene derived peptide sequences we used, leads to the activation of antigen-specific regulatory T cells. We found this issue to be investigated important because in case we increase the number of tumor-antigen specific $T_{reg}$ cells via vaccination, this could possibly lead to higher infiltration of $T_{reg}$ cells into the tumor. Increased intra-tumoral $T_{reg}$ cell numbers, in term, could severely hamper the tumor-protective capacity by suppressing and therewith outcompeting effector T cell activity. Furthermore, we were interested whether some of the non-responding mutated oncogene-derived peptide sequences (see low immunogenic peptides in the previous section) were found to be only low immunogenic, because of the presence of $T_{reg}$ cells suppressing conventional T cell function or the capacity of these peptides to specifically activate $T_{reg}$ cells.

To investigate whether there was an antigen-specific induction of regulatory T cells upon vaccination prevalent in our experimental system a suitable assay had to be established. Our laboratory developed a proliferation-based regulatory T cell specificity assay to screen the peripheral blood of cancer patients for the existence of tumor-antigen specific $T_{reg}$ cells, the regulatory T cell specificity assay (Bonertz et al., 2009). We decided to transfer this method to the murine system for the detection of possible vaccination activated increased numbers of tumor-antigen specific $T_{reg}$ cells. The establishment of a regulatory T cell specificity assay protocol in the C57BL/6 system was part of the work M. Bartoschek conducted in his master thesis and was already published therein. In course of his master thesis M. Bartoschek collected parts of the data presented in this section, which was the data obtained from mutated peptides vaccinated groups of mice and initial data gained from the analysis from wt peptide vaccinated and untreated mice. Thereto, additional data sets from wt peptides immunized and untreated animals were added in the presented thesis. The added data made a grouped and cumulative analysis possible and was not presented like shown in the following here before.

To investigate the connection of vaccination and possible tumor antigen-specific regulatory T cells a new combination of peptides displaying differing immunogenicities in previous assays was arranged. The two highly immunogenic peptides Kras G12V and p53 R248W were tested along the with the

peptides p53 R216L, p53 Y220C and Kras Q61H, which were found to elicit only low percentages of cytokine positive cells when used for vaccination. Next to this '$T_{reg}$ mix' of mutated peptides, also the effect of vaccination with corresponding wt peptides (wt mix: p53 R216 wt, p53 Y220 wt, p53 R248 wt, Kras G12 wt, and Kras Q61 wt) was investigated. Cohorts of three C57BL/6 mice each were immunized with respective peptide mixes administered in Montanide ISA 720 together with CpG ODN 1668 (50 µg per vaccination shot and animal). $T_{reg}$ cells purified from differentially vaccinated mice or untreated animals were *in vitro* antigen specifically re-stimulated (on peptide-pulsed $CD11c^+$ BM-DCs) and their capacity to suppress proliferation of pre-activated Ovalbumin-specific $CD4^+$ T conventional cells (OT-II $CD4^+$ T cells) was measured by Tritium uptake (for further details see section 2.2.4.2.). Reference values for each peptide tested were obtained from cultures of respective peptide-pulsed DCs and activated OT-II $CD4^+$ T cells in the absence of regulatory T cells.

Figure 3.17 shows representative proliferation data from two independently performed experiments (fig. 3.17 A and B) using $T_{reg}$ cells purified from mutated peptides vaccinated mice (data was generated by M. Bartoschek). The performed controls (indicated as (-) controls in the figure) revealed that regulatory T cells do not contribute to the proliferative response measured, as in the control without conventional OT-II $CD4^+$ T cells (- w/o Tcon) scintillation counts were hardly detectable. Furthermore, the other two employed controls, namely DCs pulsed with the peptide solvent DMSO only or sample without DCs at all, were inconsistent between the identically performed assays. We expected to detect the highest proliferation measured in the assay, because there are no antigens added which could activate the suppressive activity of antigen-specific regulatory T cells. Therefore, also the proliferation should be equally high for both controls in the presence and absence of $T_{reg}$ cells. Whereas scintillation counts in the experiment shown in sub-figure 3.17 A were the highest, as expected, control values were the lowest for the experiment shown in 3.17 B. Moreover, scintillation counts for samples with or without $T_{reg}$ cells are strongly different for the without DC control.

Comparing the with or without $T_{reg}$ cells data couples for the tested antigens showed that nearly all tested wt and mutated peptides showed a reduced proliferation in the presence of $T_{reg}$ cells. This would mean *argumentum e contrario* that nearly all of the tested peptides were able to re-stimulate $T_{reg}$ cells to suppress the proliferation of activated conventional T cells. Only the peptides Kras Q61 wt and Kras Q61H lead to inconsistent results in between the two assays causing suppression in one (Fig. 3.17 A) but not in the other exemplary shown experiment (Fig. 3.17 B).

To be able to seek general trends from the performed experiments percentages of suppression were calculated according to the following formula.

$$\%\ \text{specific supression} = \left[\frac{\text{cpm(sample w/o Tregs)} - \text{cpm(sample + Tregs)}}{\text{cpm (sample w/o Tregs)}}\right] \text{X } 100$$

Thereby, the means of the obtained scintillation counts from triplicates of certain test antigen samples containing $T_{reg}$ cells were not normalized towards the negative control samples but towards the corresponding sample without regulatory T cells. In this way it became possible to circumvent the problem of the inconsistent negative controls between experiments and achieving specific suppression values for each individual peptide tested.

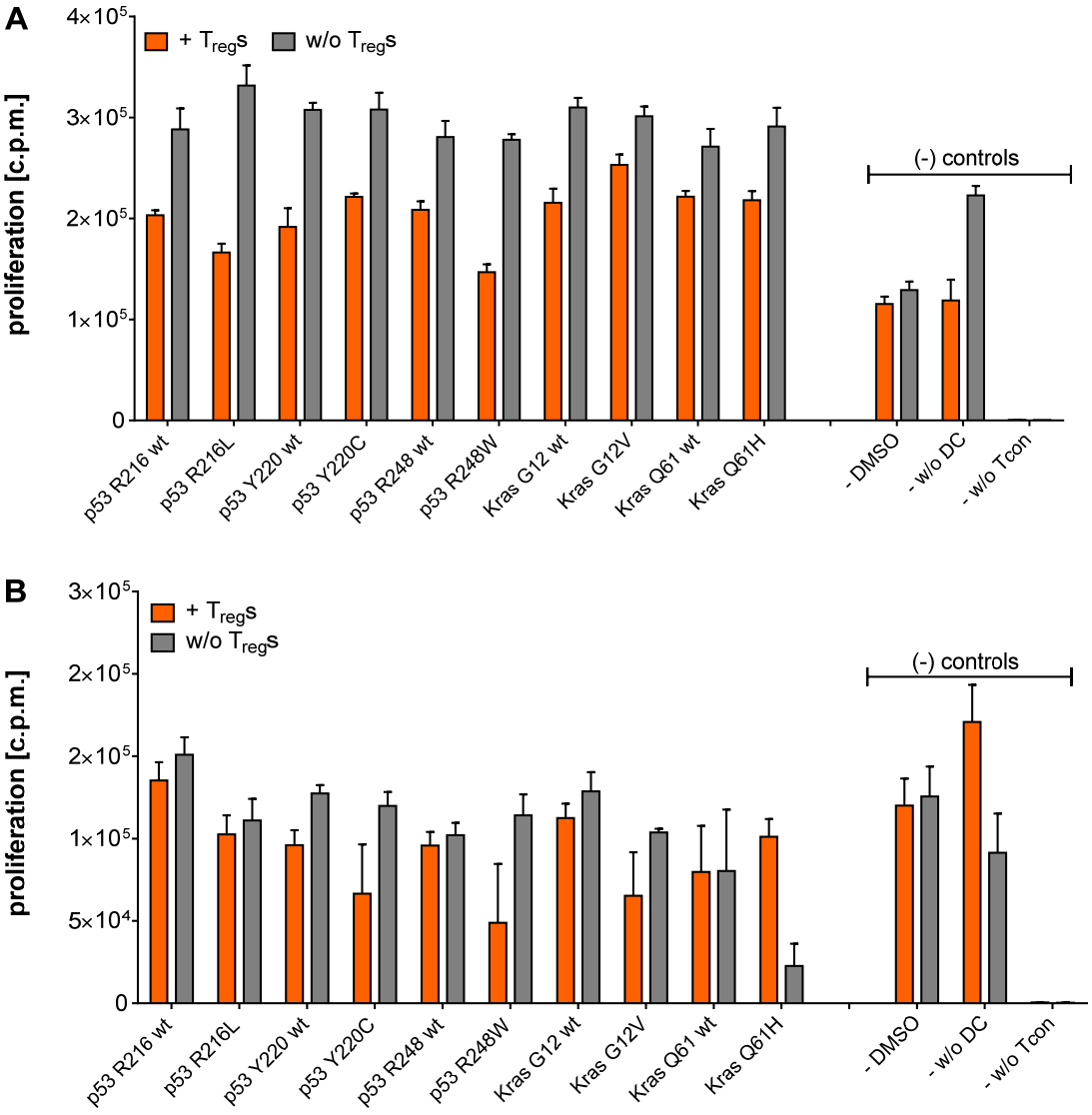


**Figure 3.17**: **Reduced proliferation of conventional T cells in the presence of $T_{reg}$ cells purified from mutated peptides vaccinated mice suggested the activation of antigen-specific $T_{reg}$ cells after vaccination with mutated long peptides**. The antigen-specific activity of $T_{reg}$ cells purified from the spleen and lymph nodes of mutated peptides vaccinated C57BL/6 mice were analyzed in $T_{reg}$ specificity assays. Purified $T_{reg}$ cells were re-stimulated on $CD11c^+$ BM-DCs pulsed with single peptides of the mix used for vaccination and corresponding wt peptides. The next day $OVA_{323-339}$ antigen-specifically activated OT-II $CD4^+$ conventional T cells were added to the culture and proliferation was measured additional 2 days later via the uptake of radioactive labeled $^3H$-thymidine employing a scintillation counter. Respective control samples containing only peptide pulsed DCs and activated conventional OT-II T cells but no purified regulatory T cells were proceeded with identically. This leads to two sets of triplicate data per tested peptide: one with $T_{reg}$ cells added (+ $T_{reg}$s) and one without $T_{reg}$ cells (w/o $T_{reg}$s). Each peptide and control sample was tested in triplicate instances. Results are plotted as means of triplicate assays ± SEM. Data from two representative (**A** and **B**) out of in total four identically performed experiments are shown. c.p.m.: counts per minute. Experiments were performed by M. Bartoschek.

Cumulative analysis of percentages of specific suppression with peptide-specific results grouped into wt and mutated for each of the differentially treated groups of mice is shown in figure 3.18. Data collected from three identically performed experiments for each of the three different treatment groups were accumulated. Compared to the cytokine responses of conventional $CD4^+$ and $CD8^+$ T cells (see section 3.1. figures 3.6 and 3.7) there were no statistically significant differences found between suppressive responses induced by wt or mutated peptides. This finding was made for regulatory T cells purified from mutated peptides vaccinated mice, as well as for wt peptide vaccinated mice and untreated mice implying that vaccination with neither wt nor mutated peptides leads to an increased activity of $T_{reg}$ cells when compared to untreated mice in general. Also in between the differentially treated groups suppression levels of wt and mutated peptides were not significantly alternating.

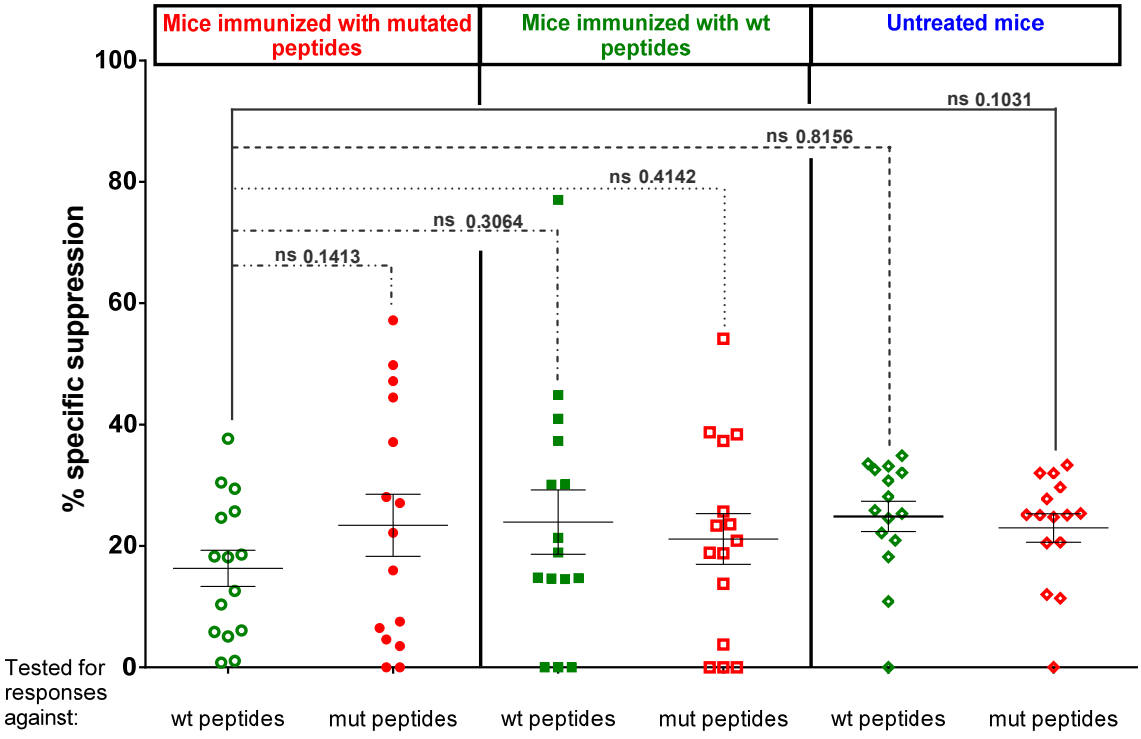


**Figure 3.18**: **Cumulative data did not imply a general activation of antigen-specific regulatory T cells after vaccination with mutated or wt oncogene-derived peptides compared to results obtained from untreated animals**. The antigen-specific activity of $T_{reg}$ cells purified from the spleen and lymph nodes of mutated or wt peptides vaccinated and untreated C57BL/6 mice was analyzed in $T_{reg}$ specificity assays. Groups of n = 3 mice were vaccinated with either wt or mutated peptide '$T_{reg}$ mixes'. Each experiment (mut vaccinated, wt vaccinated and untreated) was performed three times and data of all three experiments of respective groups were accumulated. Purified $T_{reg}$ cells were re-stimulated on $CD11c^+$ BM-DCs pulsed with single peptides of the same mix used for vaccination and corresponding wt or mutated peptides. The next day $OVA_{323-339}$ antigen-specifically activated OT-II $CD4^+$ conventional T cells were added to the culture and proliferation was measured additional 2 days later via the uptake of radioactive labeled $^3$H-thymidine employing a scintillation counter. Respective control samples containing only peptide pulsed DCs and activated conventional OT-II T cells but no purified regulatory T cells were proceeded with identically. This leads to two sets of triplicate data per tested peptide: one with $T_{reg}$ cells added (+ $T_{reg}$s) and one without $T_{reg}$ cells (w/o $T_{reg}$s). Each peptide and control sample was tested in triplicate instances. Percentages of specific suppression were calculated according to the indicated formula by using means of triplicate c.p.m. values. Values for specific suppression of mutated and wt peptides are plotted and tested against one another by paired two-tailed t test. Filled symbols: peptides used for vaccination and *in vitro* recall response testing, open symbols: peptides used for *in vitro* recall response testing only. Experiments were performed by M. Bartoschek and J. Quandt.

As cumulative data did not imply a general activation of antigen-specific $T_{reg}$ cells after vaccination with either mutated nor wt, peptide responses against individual peptides were investigated. Therefore, the same data as shown in the previous figure was plotted in figure 3.19 for each individual peptide tested according to the different treatment groups. For none of the tested wt and mutated peptide couples statistically significant differences in suppression are recordable between the differentially treated groups expect for the p53 Y220 wt peptide. For this peptide vaccination with wt peptides lead to a significantly lower specific suppression compared to vaccination with mutated peptides (p = 0,0067 (**, paired two-tailed t test) not charted in the figure). However, for the previously shown to be highly immunogenic peptide p53 R248W and its wt counterpart an interesting observation could be made.

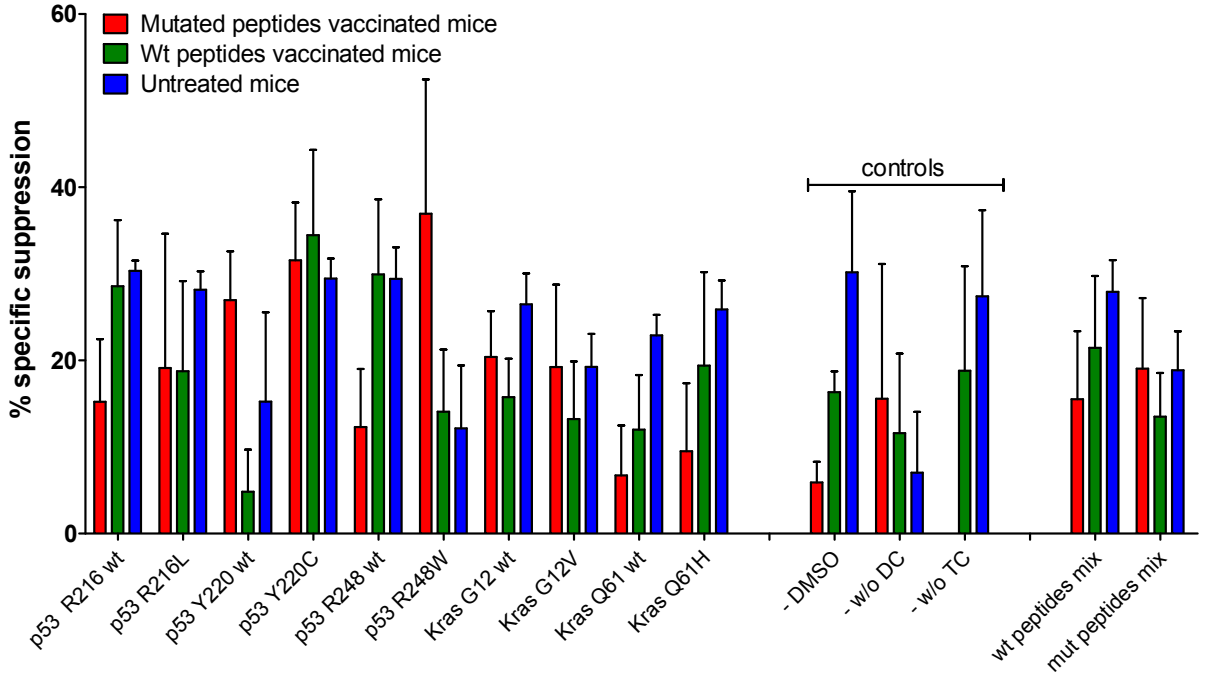


**Figure 3.19**: **Analysis of cumulative result deconvoluted towards responses against single peptides points towards an activation of antigen-specific regulatory T cells after vaccination with mutated or wt oncogene-derived sequences for some peptide candidates included in the respective vaccination mixes.** The antigen-specific activity of $T_{reg}$ cells purified from the spleen and lymph nodes of mutated or wt peptides vaccinated and untreated C57BL/6 mice was analyzed in $T_{reg}$ specificity assays. Groups of n = 3 mice were vaccinated with either wt or mutated peptide '$T_{reg}$ mixes'. Each experiment (mut vaccinated, wt vaccinated and untreated) was performed three times and data of all three experiments of respective groups are accumulated. Purified $T_{reg}$ cells were re-stimulated on $CD11c^+$ BM-DCs pulsed with single peptides of the same mix used for vaccination and corresponding wt or mutated peptides. The next day $OVA_{323-339}$ antigen-specifically activated OT-II $CD4^+$ conventional T cells were added to the culture and proliferation was measured additional 2 days later via the uptake of radioactive labeled $^3$H-thymidine employing a scintillation counter. Respective control samples containing only peptide pulsed DCs and activated conventional OT-II T cells but no purified regulatory T cells were proceeded with identically. This leads to two sets of triplicate data per tested peptide: one with $T_{reg}$ cells added (+ $T_{reg}$s) and one without $T_{reg}$ cells (w/o $T_{reg}$s). Percentages of specific suppression were calculated according to the indicated formula by using means of triplicate c.p.m. values. Results are plotted as means of specific suppression obtained from three assays per treatment group ± SEM. Experiments were performed by M. Bartoschek and J. Quandt.

Figure 3.20 zooms in some of the peptide specific suppressive $T_{reg}$ cell responses obtained from specificity assays with cells purified from wt and mutated peptides vaccinated mice leaving out the untreated group (shown also in figures 3.18 and 3.19). Herein, it becomes apparent that there was a clear trend towards a higher suppression of $T_{reg}$ cells gained from mutated peptide vaccinated mice upon re-

stimulation with the mutated peptide p53 R248W (bright red bar, left hand side panel) compared to the corresponding wt peptide and also compared to the couples of wt and mutated Kras sequences. Within the results derived from assays using $T_{reg}$ cells purified from wt peptides vaccinated mice the highest suppression was detected after re-stimulation with the p53 R248 wt peptide (bright green bar, right hand side panel).

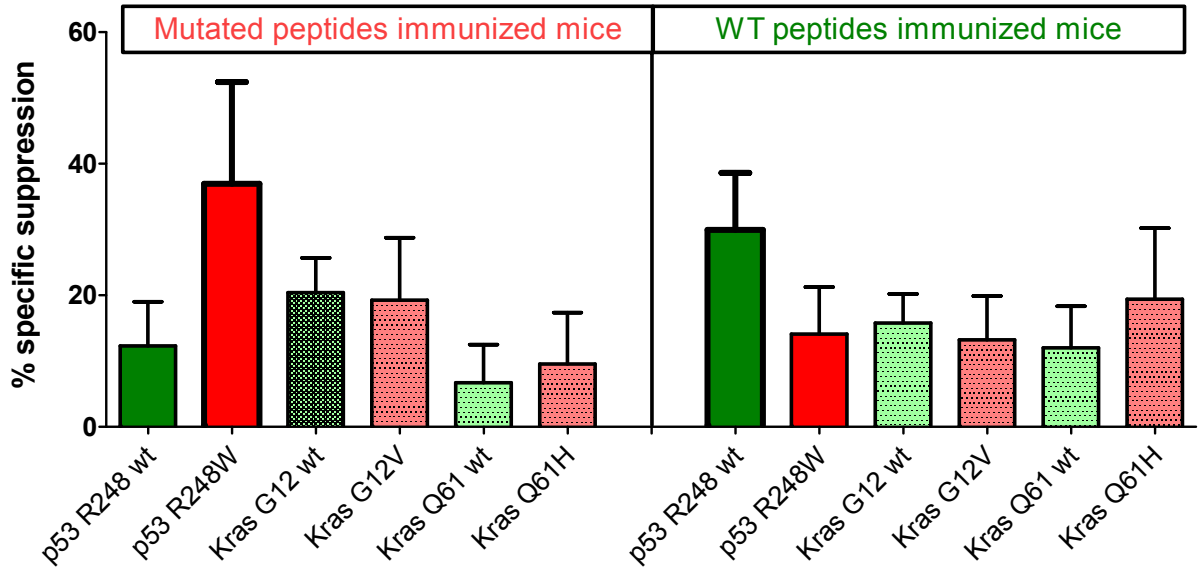


**Figure 3.20: Mutated peptide p53 R248W and the corresponding wt peptide p53 R248 wt seemed to enhance antigen-specific $T_{reg}$ cell activity when used for vaccination.** The antigen-specific activity of $T_{reg}$ cells purified from the spleen and lymph nodes of mutated or wt peptides vaccinated C57BL/6 mice was analyzed in $T_{reg}$ specificity assays. Groups of n = 3 mice were vaccinated with either wt or mutated peptide $T_{reg}$ mixes. Each experiment (mut vaccinated or wt vaccinated) was performed three times and data of all three experiments of respective groups are accumulated. Purified $T_{reg}$ cells were re-stimulated on $CD11c^+$ BM-DCs pulsed with single peptides of the same mix used for vaccination and corresponding wt or mutated peptides. The next day $OVA_{323-339}$ antigen-specifically activated OT-II $CD4^+$ conventional T cells were added to the culture and proliferation was measured additional 2 days later via the uptake of radioactive labeled $^3$H-thymidine employing a scintillation counter. Respective control samples containing only peptide pulsed DCs and activated conventional OT-II T cells but no purified regulatory T cells were proceeded with identically. This leads to two sets of triplicate data per tested peptide: one with $T_{reg}$ cells added (+ $T_{reg}$s) and one without $T_{reg}$ cells (w/o $T_{reg}$s). Percentages of specific suppression were calculated according to the indicated formula by using means of triplicate c.p.m. values. Results are plotted as means of specific suppression obtained from three assays per treatment group ± SEM. Experiments were performed by M. Bartoschek and J. Quandt.

In conclusion, regulatory T cell specificity assays showed no overall evidence of a general induction of mutation or wt peptides specific $T_{reg}$ cells in cumulative results from differentially treated groups. Regarding the individual peptides tested neither the strongly immunogenic Kras G12 peptide couple nor the weakly immunogenic Kras Q61 wt and mutated peptide couple led to a specific activation of $T_{reg}$ cells. The same was true for the weakly immunogenic p53 R216 peptide couple. In contrast, vaccination seems to influence regulatory T cell suppressive responses against the weakly immunogenic p53 Y220 wt and p53 Y220C peptides. Interestingly, there was also a trend towards an elevated suppressive activity of $T_{reg}$ cells purified from mutated and wt peptides vaccinated mice, after re-stimulation with the strongly immunogenic p53 R248W and its corresponding wt p53 R248 peptide, respectively.

## 3.3. Identification of epitopes within most immunogenic peptides

### 3.3.1. Identification and validation of the two mutated peptides with the strongest immunogenicity

In order to identify and validate the most immunogenic mutated oncogene-derived sequences within the panel of long peptides the responses towards mutated peptides were directly compared to those of corresponding wt counterparts, in both the murine and human MHC contexts. Figure 3.21 displays the comparison for the A2.DR1 dtg system identifying the peptides p53 R248W and Kras G12V to be more immunogenic than their wt counterparts when used for vaccination as the percentages of IFN-γ secreting $CD8^+$ T cells upon *in vitro* re-stimulation was significantly increased. In the middle panel of figure 3.17 IFN-γ secretion of T cells purified from untreated animals detected upon re-stimulation with the aforementioned peptides are depicted to underline that spontaneous responses are negligible.

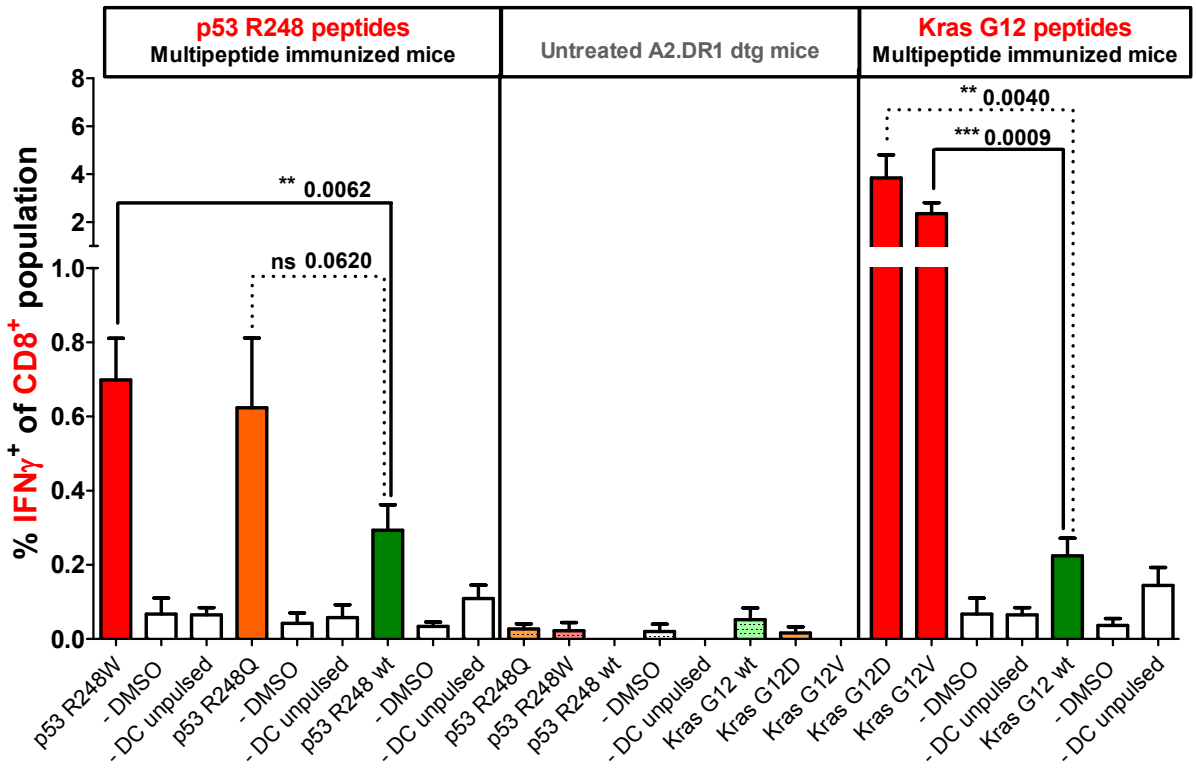


**Figure 3.21**: **Mutated p53 R248W and Kras G12D/V peptides are more immunogenic than corresponding wt peptides when used for vaccination of A2.DR1 dtg mice.** Recall responses against mutated and wt peptides tested in A2.DR1 dtg mice immunized with group A, B and C long peptide cocktails or untreated mice are shown. *In vitro* recall responses were obtained from combined IFN-γ secretion assay and intracellular cytokine staining performed with splenic $CD90^+$ purified T cells from immunized mice. IFN-γ secretion of $CD8^+$ T cells upon *in vitro* recall against certain single peptides presented by $CD11c^+$ DCs is displayed. Each peptide and control sample was tested in triplicate instances. Results are plotted as means of triplicate assays ± SEM. Significant differences were tested for by unpaired, two-tailed t test.

Figure 3.22 shows the same analysis with respective data obtained from C57BL/6 mice. Both mutations at the position p53 R248 included in our panel of long peptides, namely Q and W, were able to elicit a significantly higher IFN-γ secretion of $CD8^+$ T cells from mutated peptides vaccinated mice than the

corresponding wt counterpart did when tested with $CD8^+$ T cell from respective wt peptides vaccinated mice. Spontaneous responses, again shown in the middle panel, were also insignificant in the C57BL/6 mouse system. Of the Kras peptides, just as within the human MHC context, the mutation G12V was most immunogenic (see figure 3.22 right panel).

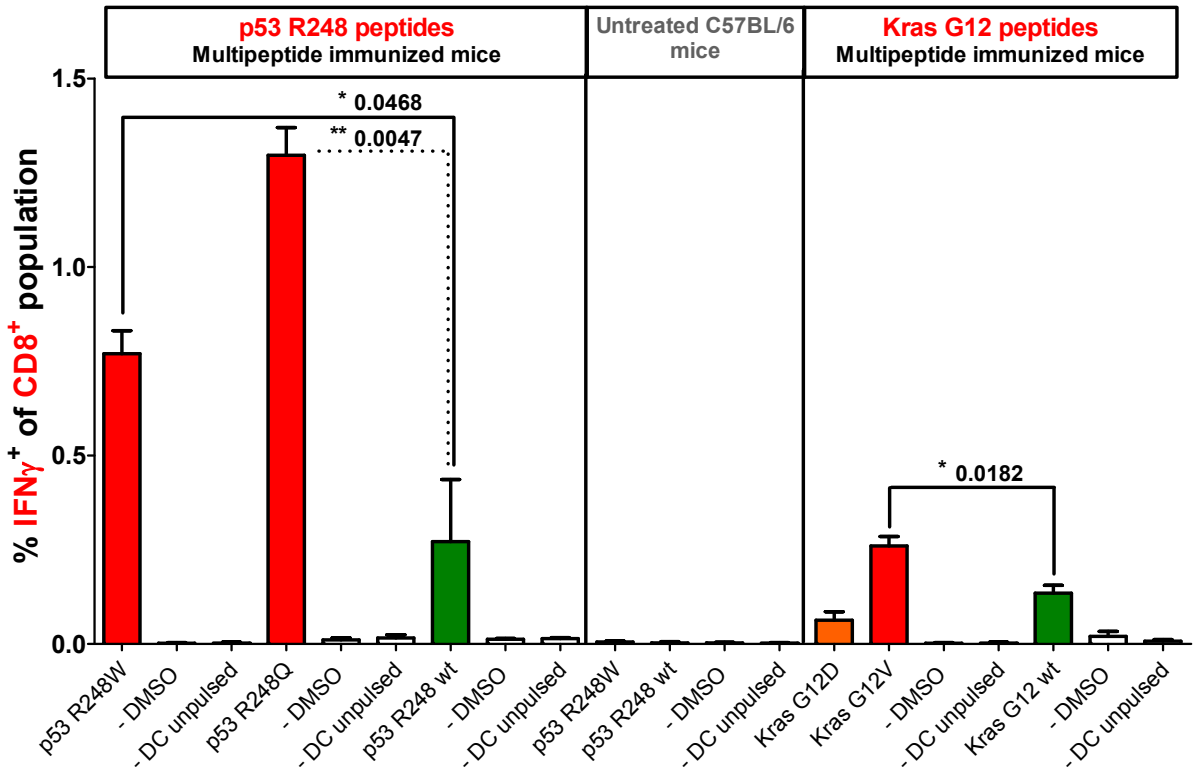


**Figure 3.22**: **Mutated p53 R248W/Q and Kras G12V peptides are more immunogenic than corresponding wt peptides when used for vaccination of C57BL/6 mice.** Recall responses against mutated and wt peptides tested in C57BL/6 mice immunized with group A, B and C long peptide cocktails or untreated mice are shown. *In vitro* recall responses were obtained from combined IFN-γ secretion assay and intracellular cytokine staining performed with splenic $CD90^+$ purified T cells from immunized mice. IFN-γ secretion of $CD8^+$ T cells upon *in vitro* recall against certain single peptides presented by $CD11c^+$ DCs is displayed. Each peptide and control sample was tested in triplicate instances. Results are plotted as means of triplicate assays ± SEM. Significant differences were tested for by unpaired, two-tailed t test.

The Braf mutation only elicited minor T cell cytokine responses as it became clear in previous sections and moreover failed the criteria to elicit significantly higher response than its corresponding wt sequence. This was the reason why further investigations employing mutated peptide Braf V600E were discontinued.

After identification of the two most immunogenic mutated Kras and p53 derived peptide sequences, the next step was to determine possible epitopes which might be processed from the long peptides and presented in the employed HLA context. The content of the following chapter will depict respective results.

### 3.3.2. Identification of potential epitopes within the most immunogenic peptides Kras G12V and p53 R248W in the human MHC context

In the previous section, the mutated peptides Kras G12V and p53 R248W were identified as the most immunogenic peptides in the A2.DR1 dtg system, which were eliciting mutation specific responses significantly higher than those against wt peptides when used for active vaccination. This leads to the conclusion that it was likely that these peptides harbor HLA.A2 and HLA.DRB1 restricted mutated epitopes. In order to identify possible HLA binding shorter peptide sequences within the two long peptides, long peptide sequences were fed into *in silico* prediction algorithms of the NetMHC and the SYFPEITHI databases. This was done as a first step to have the affinity scores for all possible overlapping 9-mer, 10-mer and 15-mer small peptides possibly binding to HLA.A2 and HLA.DRB1 predicted. Always affinity scores for wt and mutated sequences were opposed. Thereupon, high affinity, predicted short peptide candidates were tested in *in vitro* re-stimulation assays with T cells derived from respective long peptide vaccinated mice.

*In silico* analysis revealed for the Kras G12 peptides that in case of possible MHC class I HLA.A*0201 (HLA.A2) binders 10-mer peptides attained higher affinity scores than 9-mer peptides. Of note, a high SYFPEITI score stands for a high peptide-MHC affinity whereas a low affinity value indicates a strong binding in the NetMHC prediction. The 10-mer peptides with the highest affinities within the wt and the mutated Kras G12V long peptide comprising the mutation site are displayed in figure 3.19. Thereby, the mutated 10-mer peptide was predicted to have a higher affinity for the MHC molecule than the corresponding wt 10-mer (NetMHC scores: 781 nM versus 543 nM, SYFPEITHI scores: 22 versus 24), although both wt and mutated 10-mers were not suggested to be strong binders. In case of potential MHC class II binders there were a strong binding wt and a strong binding mutated 15-mer peptide predicted for the HLA.DRB*0101 (HLA.DRB1) allele (see figure 3.23). Whereas the SYFPEITHI scores are identical, the NetMHC algorithm suggest a slightly higher affinity of the mutated peptide (7,9 nM versus 7,8 nM).

| | 2 | 3 | 4 | 5 | 6 | 7 | 8 | 9 | 10 | 11 | 12 | 13 | 14 | 15 | 16 | 17 | 18 | 19 | 20 | 21 | 22 | 23 | 24 | 25 | 26 | 27 | 28 | 29 |
|---|---|---|---|---|---|---|---|---|---|---|---|---|---|---|---|---|---|---|---|---|---|---|---|---|---|---|---|---|
| **Kras G12 wt** | T | E | Y | K | L | V | V | V | G | A | G | G | V | G | K | S | A | L | T | I | Q | L | I | Q | N | H | F | V |
| **Kras G12V** | T | E | Y | K | L | V | V | V | G | A | V | G | V | G | K | S | A | L | T | I | Q | L | I | Q | N | H | F | V |

**10-mer**

| sequence | position | NetMHC (affinity [nM]) | SYFPEITHI Score |
|---|---|---|---|
| KLVVVGAGGV | 5-14 | 781 | 22 |

**15-mer**

| sequence | position | NetMHC (affinity [nM]) | SYFPEITHI Score |
|---|---|---|---|
| EYKLVVVGAGGVGKS | 3-17 | 7,9 (SB) | 34 |

**10-mer**

| sequence | position | NetMHC (affinity [nM]) | SYFPEITHI Score |
|---|---|---|---|
| KLVVVGAVGV | 5-14 | 543 | 24 |

**15-mer**

| sequence | position | NetMHC (affinity [nM]) | SYFPEITHI Score |
|---|---|---|---|
| EYKLVVVGAVGVGKS | 3-17 | 7,8 (SB) | 34 |

**Figure 3.23**: ***In silico* prediction of putative HLA.A2 and HLA.DRB1 epitopes within the sequence of the long mutated peptide Kras G12V.** *In silico* prediction was carried out employing NetMHC and SYFPEITHI prediction algorithms. Putative HLA.A2 and HLA.DRB1 binding 10-mer and 15-mer peptides within in the long Kras G12V or G12 wt peptides surrounding the mutation site and achieving the highest affinity scores are depicted. Green tables display sequences and affinity scores for short peptides with wt sequences and red tables those of corresponding mutated short peptides. WB: weak binder, SB, strong binder

After *in silico* analysis the four peptides, which were predicted to have the highest MHC affinities, were synthesized and tested in *in vitro* re-stimulation assays. T cells purified from mice immunized with

the two strongly immunogenic mutated peptides p53 R248W and Kras G12V were re-stimulated on CD11c$^+$ DCs pulsed with putative wt and mutated MHC binders or respective long peptides. T cell responses after *in vitro* re-stimulation were assessed employing IL-2/IFN-γ secretion assays. Results from a representative assays are compiled in figure 3.24.

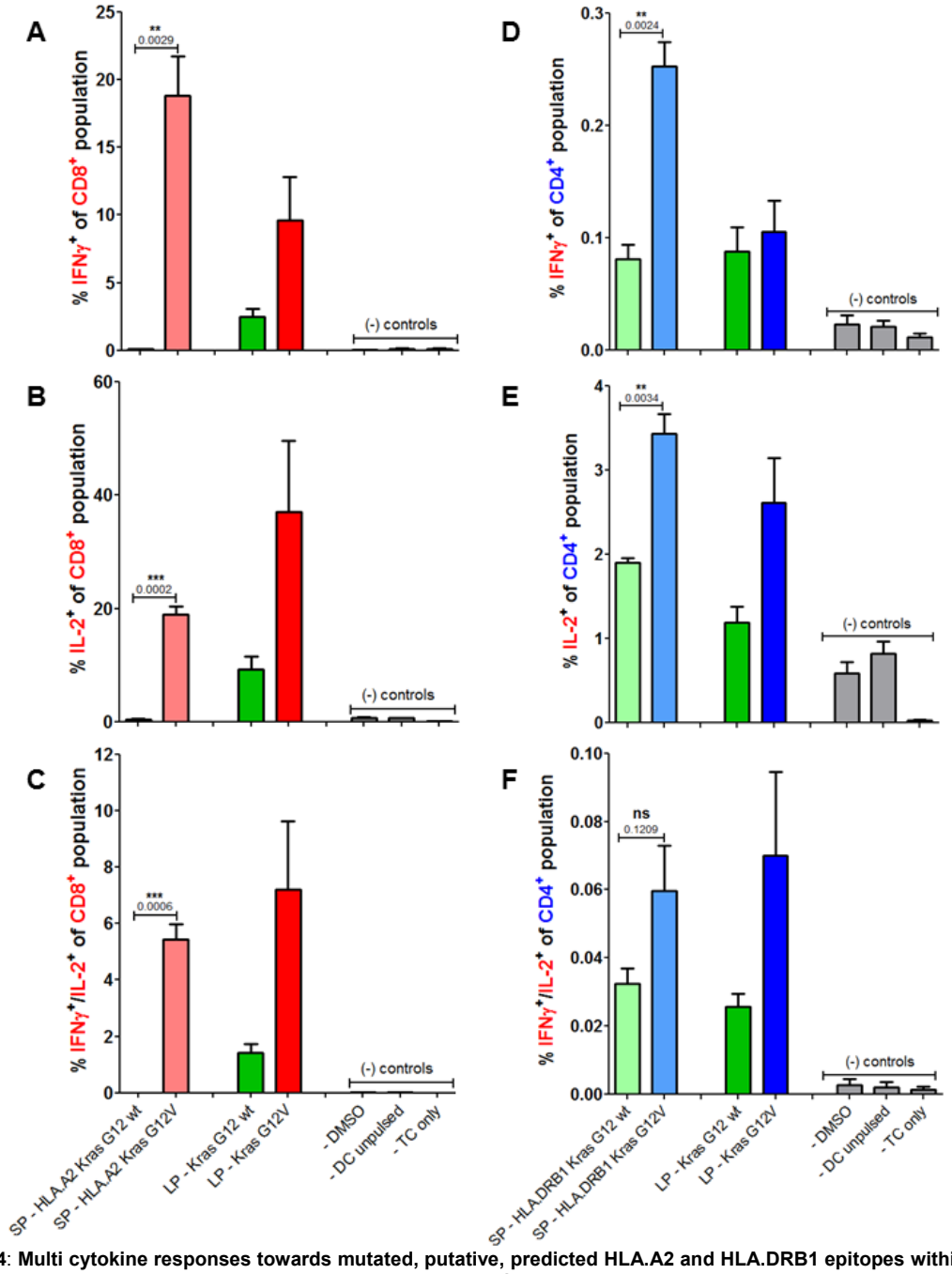


**Figure 3.24**: **Multi cytokine responses towards mutated, putative, predicted HLA.A2 and HLA.DRB1 epitopes within the long Kras G12V peptide.** Recall responses against mutated and wt Kras G12(V) peptides tested in A2.DR1 dtg mice immunized with the long peptides Kras G12V and p53 R248W. *In vitro* recall responses were obtained from two color cytokine secretion assays performed with splenic pan T cells from immunized mice. Percentages of IFN-γ (**A**, **D**), IL-2 (**B**, **E**) and IFN-γ/IL-2 (**C**, **F**) double positive of CD8$^+$ (**A**, **B**, **C**) and CD4$^+$ (**D**, **E**, **F**) T cells upon *in vitro* recall against short and long Kras peptides presented by CD11c$^+$ DCs are displayed. Each peptide and control sample was tested in triplicate instances. Results are plotted as means of triplicate assays ± SEM. Representative data obtained from one of two identical lines of experiments are shown. Significant differences were tested for by unpaired, two-tailed t test. ns: not significant.

The predicted mutated 10-mer peptide showed a significantly higher percentage of IFN-γ secreting (Fig 3.24 A, light red bar), IL-2 secreting (Fig. 3.24 B) and IFN-γ/IL-2 double positive (Fig. 3.24 C) $CD8^+$ T cells than the corresponding wt 10-mer peptide. In fact, the wt 10-mer peptide barely elicited any $CD8^+$ T cell cytokine response. Moreover, the strength of the cytokine response towards the short mutated peptide was comparable to that of the mutated long peptide. Also the mutated potential MHC class II 15-mer peptide elicited significantly higher levels of IFN-γ secretion (Fig. 3.24 D, light blue), IL-2 secretion (Fig 3.24 E) and a trend towards a higher percentage of IFN-γ/IL-2 double positive (Fig. 3.24 F) $CD4^+$ T cells than the respective 15-mer wt peptide (light green bars). Additionally, the 15-mer wt peptide, although weaker than the mutated peptide, was able to elicit cytokine responses similar as those against the long Kras G12 wt peptide. Conclusively, contributed to the fact that the predicted 10-mer and 15-mer peptides seem to be as responsive as the long peptides they originate from when used for *in vitro* re-stimulation of vaccination induced peptide-specific T cells, suggested them as putative minimal HLA-binding epitopes.

| | 230 | 231 | 232 | 233 | 234 | 235 | 236 | 237 | 238 | 239 | 240 | 241 | 242 | 243 | 244 | 245 | 246 | 247 | 248 | 249 | 250 | 251 | 252 | 253 | 254 | 255 | 256 | 257 | 258 | 259 | 260 | 261 | 262 | 263 | 264 |
|---|---|---|---|---|---|---|---|---|---|---|---|---|---|---|---|---|---|---|---|---|---|---|---|---|---|---|---|---|---|---|---|---|---|---|---|
| **p53 R248 wt** | T | T | I | H | Y | N | Y | M | C | N | S | S | C | M | G | G | M | N | R | R | P | I | L | T | I | I | T | L | E | D | S | S | G | N | L |
| **p53 R248W** | T | T | I | H | Y | N | Y | M | C | N | S | S | C | M | G | G | M | N | W | R | P | I | L | T | I | I | T | L | E | D | S | S | G | N | L |

**9-mers**

| sequence | position | NetMHC (affinity [nM]) | SYFPEITHI Score |
|---|---|---|---|
| SSCMGGMNR | 240-248 | 27258 | 4 |
| SCMGGMNRR | 241-249 | 25888 | 8 |
| CMGGMNRRP | 242-250 | 29008 | 10 |
| MGGMNRRPI | 243-251 | 23902 | 8 |
| GGMNRRPIL | 244-252 | 23406 | 13 |
| GMNRRPILT | 245-253 | 7298 | 14 |
| MNRRPILTI | 246-254 | 26654 | 16 |
| NRRPILTII | 247-255 | 26223 | 14 |
| RRPILTIIT | 248-256 | 24166 | 7 |

**10-mers**

| sequence | position | NetMHC (affinity [nM]) | SYFPEITHI Score |
|---|---|---|---|
| NSSCMGGMNR (1) | 239-248 | 31170 | 0 |
| SSCMGGMNRR (2) | 240-249 | 32985 | 3 |
| SCMGGMNRRP (3) | 241-250 | 30349 | 5 |
| CMGGMNRRPI (4) | 242-251 | 7745 | 18 |
| MGGMNRRPIL (5) | 243-252 | 25799 | 11 |
| GGMNRRPILT (6) | 244-253 | 22425 | 6 |
| GMNRRPILTI (7) | 245-254 | 722 | 25 |
| MNRRPILTII (8) | 246-255 | 21744 | 12 |
| NRRPILTIIT (9) | 247-256 | 29199 | 6 |
| RRPILTIITL (10) | 248-257 | 11492 | 16 |

**15-mers**

| sequence | position | NetMHC (affinity [nM]) | SYFPEITHI Score |
|---|---|---|---|
| TTIHYNYMCNSSCMG | 230-244 | 34,82 (SB) | 8 |
| TIHYNYMCNSSCMGG | 231-245 | 27,48 (SB) | 17 |
| IHYNYMCNSSCMGGM | 232-246 | 26,67 (SB) | 15 |
| HYNYMCNSSCMGGMN | 233-247 | 36,53 (SB) | 16 |
| YNYMCNSSCMGGMNR (1) | 234-248 | 68,95 (WB) | 10 |
| NYMCNSSCMGGMNRR (2) | 235-249 | 211,77 (WB) | 11 |
| YMCNSSCMGGMNRRP (3) | 236-250 | 528,72 | 8 |
| MCNSSCMGGMNRRPI (4) | 237-251 | 1304,73 | 15 |
| CNSSCMGGMNRRPIL (5) | 238-252 | 686,02 | 2 |
| NSSCMGGMNRRPILT (6) | 239-253 | 639,04 | 9 |
| SSCMGGMNRRPILTI (7) | 240-254 | 528,20 | 23 |
| SCMGGMNRRPILTII (8) | 241-255 | 533,08 | 9 |
| CMGGMNRRPILTIIT (9) | 242-256 | 441,06 (WB) | 6 |
| MGGMNRRPILTIITL (10) | 243-257 | 309,31 (WB) | 17 |
| GGMNRRPILTIITLE (11) | 244-258 | 319,07 (WB) | 11 |
| GMNRRPILTIITLE D (12) | 245-259 | 348,38 (WB) | 14 |
| MNRRPILTIITLEDS (13) | 246-260 | 357,00 (WB) | 19 |
| NRRPILTIITLE DSS (14) | 247-261 | 329,05 (WB) | 2 |
| RRPILTIITLE DSSG (15) | 248-262 | 264,40 (WB) | 20 |
| RPILTIITLEDSSGN | 249-263 | 279,16 (WB) | 26 |
| PILTIITLEDSSGNL | 250-264 | 167,12 (WB) | 11 |

**9-mers**

| sequence | position | NetMHC (affinity [nM]) | SYFPEITHI Score |
|---|---|---|---|
| SSCMGGMNW | 240-248 | 25768 | 4 |
| SCMGGMNWR | 241-249 | 23604 | 8 |
| CMGGMNWRP | 242-250 | 20273 | 10 |
| MGGMNWRPI | 243-251 | 16478 | 8 |
| GGMNWRPIL | 244-252 | 14779 | 13 |
| GMNWRPILT | 245-253 | 1897 | 14 |
| MNWRPILTI | 246-254 | 7756 | 17 |
| NWRPILTII | 247-255 | 21986 | 14 |
| WRPILTIIT | 248-256 | 23297 | 7 |

**10-mers**

| sequence | position | NetMHC (affinity [nM]) | SYFPEITHI Score |
|---|---|---|---|
| NSSCMGGMNW (1) | 239-248 | 30220 | 0 |
| SSCMGGMNWR (2) | 240-249 | 31884 | 3 |
| SCMGGMNWRP (3) | 241-250 | 21174 | 5 |
| CMGGMNWRPI (4) | 242-251 | 2169 | 18 |
| MGGMNWRPIL (5) | 243-252 | 19424 | 11 |
| GGMNWRPILT (6) | 244-253 | 12886 | 6 |
| GMNWRPILTI (7) | 245-254 | 163 (WB) | 25 |
| MNWRPILTII (8) | 246-255 | 6534 | 13 |
| NWRPILTIIT (9) | 247-256 | 27196 | 6 |
| WRPILTIITL (10) | 248-257 | 12614 | 16 |

**15-mers**

| sequence | position | NetMHC (affinity [nM]) | SYFPEITHI Score |
|---|---|---|---|
| TTIHYNYMCNSSCMG | 230-244 | 34,82 (SB) | 8 |
| TIHYNYMCNSSCMGG | 231-245 | 27,48 (SB) | 17 |
| IHYNYMCNSSCMGGM | 232-246 | 26,67 (SB) | 15 |
| HYNYMCNSSCMGGMN | 233-247 | 36,53 (SB) | 16 |
| YNYMCNSSCMGGMNW (1) | 234-248 | 68,95 (WB) | 10 |
| NYMCNSSCMGGMNWR (2) | 235-249 | 217,76 (WB) | 11 |
| YMCNSSCMGGMNWRP (3) | 236-250 | 548,31 | 8 |
| MCNSSCMGGMNWRPI (4) | 237-251 | 1259,82 | 15 |
| CNSSCMGGMNWRPIL (5) | 238-252 | 714,72 | 2 |
| NSSCMGGMNWRPILT (6) | 239-253 | 503,55 | 8 |
| SSCMGGMNWRPILTI (7) | 240-254 | 364,10 (WB) | 23 |
| SCMGGMNWRPILTII (8) | 241-255 | 247,28 (WB) | 9 |
| CMGGMNWRPILTIIT (9) | 242-256 | 52,59 (WB) | 6 |
| MGGMNWRPILTIITL (10) | 243-257 | 28,68 (SB) | 17 |
| GGMNWRPILTIITLE (11) | 244-258 | 23,44 (SB) | 9 |
| GMNWRPILTIITLE D (12) | 245-259 | 24,16 (SB) | 24 |
| MNWRPILTIITLE DS (13) | 246-260 | 36,27 (SB) | 19 |
| NWRPILTIITLE DSS (14) | 247-261 | 60,00 (WB) | 2 |
| WRPILTIITLEDSSG (15) | 248-262 | 121,37 (WB) | 20 |
| RPILTIITLEDSSGN | 249-263 | 279,16 (WB) | 26 |
| PILTIITLEDSSGNL | 250-264 | 167,12 (WB) | 11 |

**Figure 3.25**: ***In silico* affinity prediction of all possible short HLA.A2 and HLA.DRB1 binding peptides within the sequence of the long p53 R248W and R248 wt peptides used for epitope mapping.** All possible HLA.A2 and HLA.DRB1 binding 9-mer, 10-mer, and 15-mer peptides within in the long p53 R248W or R248 wt peptides are depicted. *In silico* affinity prediction for short peptides was carried out employing NetMHC and SYFPEITHI prediction algorithms. Green tables display sequences and affinity scores for short peptides with wt sequences, red tables those of corresponding mutated short peptides and indicated in blue are wt sequences within the long wt and mutated p53 R248 peptides which do not cover the site of mutation. WB: weak binder, SB, strong binder.

As for the Kras G12V peptide *in silico* prediction was performed with the p53 R248W peptide. Initial testing with the predicted strongest binding short peptides possible processed from the long peptides, however, failed to provide clear evidence in similar *in vitro* re-stimulation experiments. As an alternative the approach of epitope mapping with overlapping short peptides was performed. To identify a potential mutated HLA.A2 CTL epitope within the long p53 R248W peptide all possible 10-mer and 9-mer peptides harboring the mutation site were synthesized and tested in *in vitro* analysis. The *in silico* analysis, which is shown in figure 3.25, indicated that affinity scores of all possible peptides are low. Only the mutated 10-mer #7 was predicted to be a week binder and the second highest score showed the corresponding wt peptide (highlighted in red and green, respectively). The HLA.DRB*0101 affinity scores of all possible overlapping, MHC class II binding wt and mutated peptides are listed in the tables in the lower part of the figure 3.25. In blue script 15-mer peptides which are located before and after the mutation site and therewith comprising wt sequences found in both the wt and mutated long p53 R248(W) peptides are shown. These 'common' non-mutated 15-mers lying in front of the mutation site were predicted to be strong binders according to NetMHC prediction and also the two 'common' 15-mers following after the mutation site are suggested to be weak binders. As these sequences might contribute to the immunogenicity of both the wt and mutated long p53 R248(W) peptides they were tested along with overlapping peptides harboring the mutation site. Concerning the overlapping peptides comprising the mutation site the mutation R248W was predicted to render the weak binding wt peptides #10 (indicated in bold green letters) to #13 into strong binders (bold, red letters).

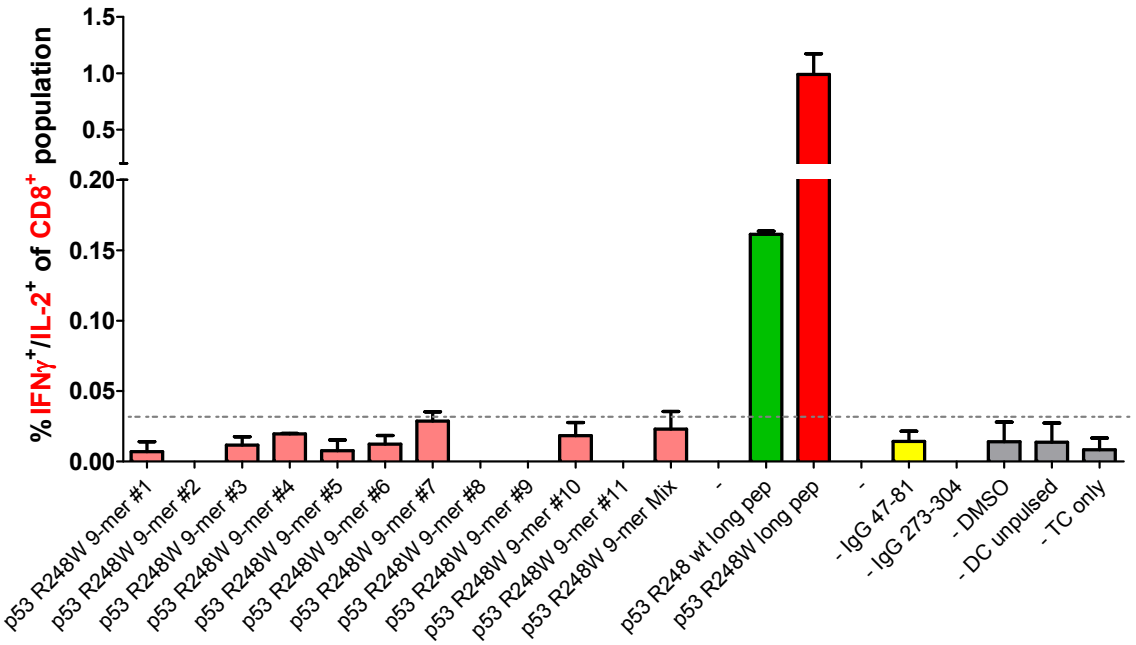


**Figure 3.26**: **Epitope mapping experiment with overlapping 9-mer peptides provide no evidence for a 9-mer HLA.A2 restricted epitope within the long p53 R248W peptide.** Recall responses against mutated and wt p53 R248W peptides tested in A2.DR1 dtg mice immunized with the long p53 R248W peptide. *In vitro* recall responses were obtained from two color cytokine secretion assays performed with splenic pan T cells from immunized mice. Percentages of IFN-γ/IL-2 double positive $CD8^+$ T cells upon *in vitro* recall against short and long p53 R248 peptides presented by $CD11c^+$ DCs are displayed. Each peptide and control sample was tested in triplicate instances. Results are plotted as means of triplicate assays ± SEM. Representative data obtained from one of two identical lines of experiments are shown.

Overlapping 9-mer, 10-mer and 15-mer p53 R248(W) wt and mutated peptides were tested *in vitro* for their potential to re-stimulate T cells purified from p53 R248W mutated long peptide immunized A2.DR1 dtg mice and were compared to recall responses against long peptides. Data obtained from IFN-γ/IL-2 two color cytokine secretion assays revealed that none of the overlapping 9-mer peptides tested elicited a cytokine response higher than background controls as exemplary shown in figure 3.26 for the percentages of IFN-γ/IL-2 double positive $CD8^+$ T cells. Figure 3.27 shows the cytokine responses of $CD8^+$ T cells detected after testing 10-mer peptides for their *in vitro* stimulating capacity. 10-mer peptide #9 elicited significantly higher percentages of IL-2 secreting (Fig. 3.27, B) and IFN-γ/IL-2 double positive (Fig. 3.27 C) $CD8^+$ T cells when compared to background controls. Also IFN-γ secretion seemed to be enhanced after re-stimulation with 10-mer peptide #9 (Fig. 3.27, A, not significant). Although cytokine responses were significantly higher than background controls the strength of responses towards 10-mer #9 was considerably lower than cytokine responses obtained from re-stimulation with the long wt and mutated p53 R248(W) peptides. Responses towards the 10-mer #7, which was predicted to have the highest affinity towards the HLA.A2 molecule, were not significantly higher than those towards background controls.

Testing of overlapping mutated 15-mer peptides comprising the mutation site p53 R248W did not yield in a clear candidate peptide in two consecutive, identically performed experiments. Percentages of cytokine responses towards the mutated 15-mer peptides, as shown for IFN-γ/IL-2 double positive $CD4^+$ T cells in figure 3.28, were only insignificantly higher than those towards background controls and far lower than those towards long mutated and wt p53 R248(W) peptides (shown in bright colors). The mutated 15-mer peptides #1, 2, 7, 9, and 12 were, therefore, chosen to become revalidated in a third cytokine secretion experiment in which they were tested against their corresponding wt 15-mer counterpart peptides. Furthermore, the 'common' non-mutated 15-mer sequences surrounding the mutation site within the long peptides were tested along with. Indeed, some of these non-mutated 'common' peptides (highlighted as 'potential non-mutated HLA class II ligands') were able to elicit cytokine responses which were clearly higher than control samples and also higher than 15-mer peptides comprising the mutation site (see figure 3.28). There within especially the peptides $p53_{231-245}$ and a longer 18-mer peptide ($p53_{230-247}$, spanning the whole long peptide backbone sequence before the mutation site) elicited the highest percentages of $CD4^+$ T cells responding with secreting of IFN-γ (Fig. 3.29 A), IL-2 (Fig. 3.29 B) or both (Fig. 3.29 C). Out of the mutated 15-mer peptides the most promising candidate peptide turned out to be peptide #7 when tested against its corresponding short wt counterpart. As found in the two previous assays cytokine responses towards none of the shorter peptides exceeded those against the long wt and mutated p53 R248(W) peptides. Taken together the identification of possible HLA.A2 and HLA.DRB1 ligands within the strongly immunogenic p53 R248W peptide was not resulting in affirmation of the short peptides predicted to have the highest affinity towards the HLA alleles tested but was suggesting the 10-mer #9 and the 15-mer #7 with lower affinity scores after *in vitro* testing of overlapping short peptides.

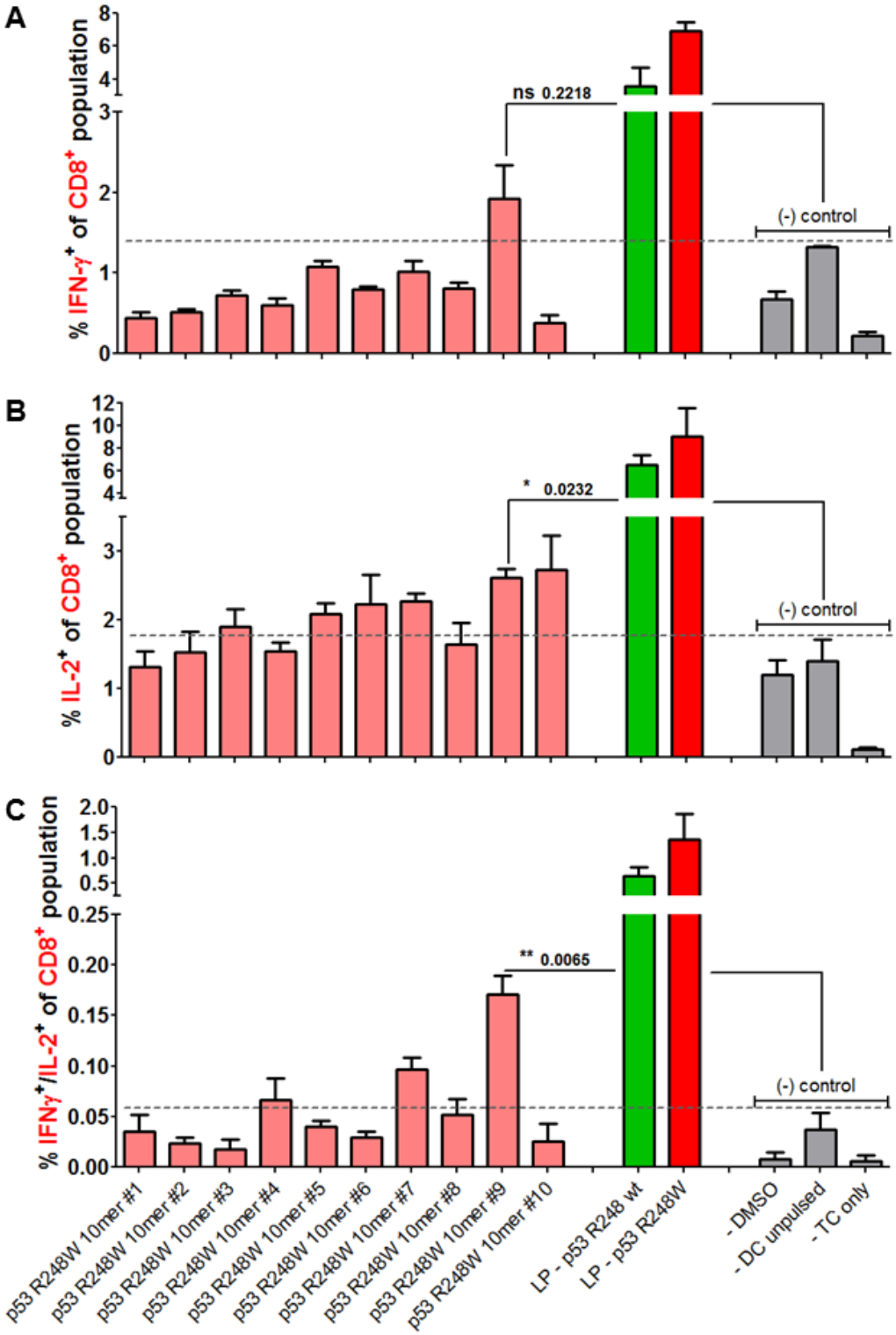


**Figure 3.27**: **Multi-cytokine responses in an epitope mapping experiment with overlapping 10-mer peptides suggest 10-mer #9 as putative mutated HLA.A2 ligands within the long p53 R248W peptide.** Recall responses against mutated 10-mer p53 R248W peptides of $CD8^+$ T cells purified A2.DR1 dtg mice immunized with the long p53 R248W peptide, assessed by two color cytokine secretion assays. Percentages of IFN-γ (**A**), IL-2 (**B**) and IFN-γ/IL-2 (**C**) double positive $CD8^+$ T cells upon *in vitro* recall against short and long p53 R248(W) peptides presented by $CD11c^+$ DCs are displayed. Each peptide and control sample was tested in triplicate instances. Results are plotted as means of triplicate assays ± SEM. Representative data obtained from one of two identical lines of experiments are shown. Significant differences were tested for by unpaired, two-tailed t test. ns: not significant.

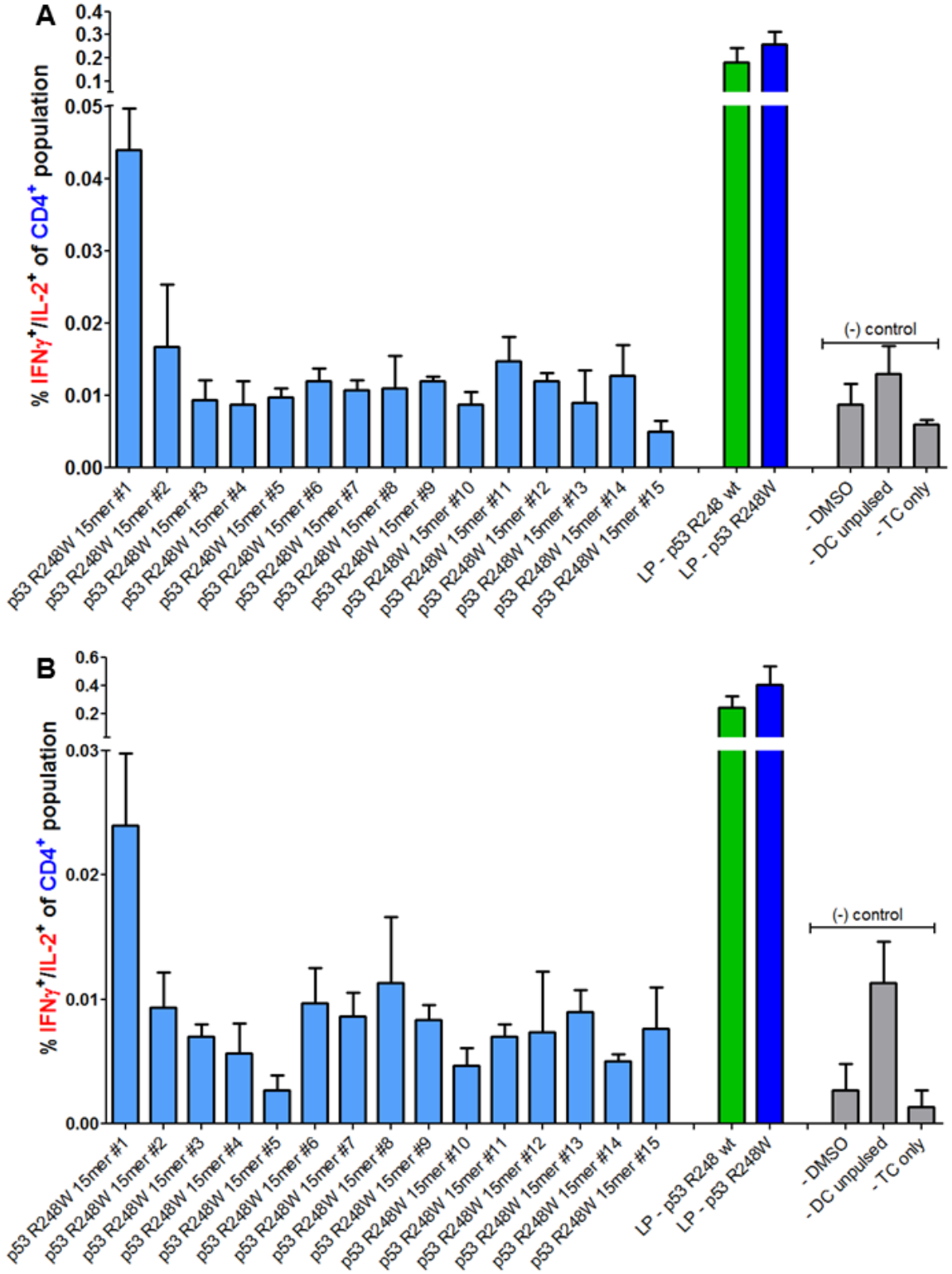


**Figure 3.28**: **Initial epitope mapping experiment with overlapping 15-mer peptides revealed no clear-cut 15-mer HLA.DRB1 epitope candidate within the long p53 R248W peptide.** Recall responses against mutated 15-mer p53 R248W peptides of $CD4^+$ T cells purified from A2.DR1 dtg mice immunized with the long p53 R248W peptide assessed by two color cytokine secretion assays. Percentages of IFN-γ/IL-2 double positive $CD4^+$ T cells upon *in vitro* recall against short and long p53 R248(W) peptides presented by $CD11c^+$ DCs are displayed. Each peptide and control sample was tested in triplicate instances. Results are plotted as means of triplicate assays ± SEM. Data obtained from two identical experiments (**A**, **B**) are shown.

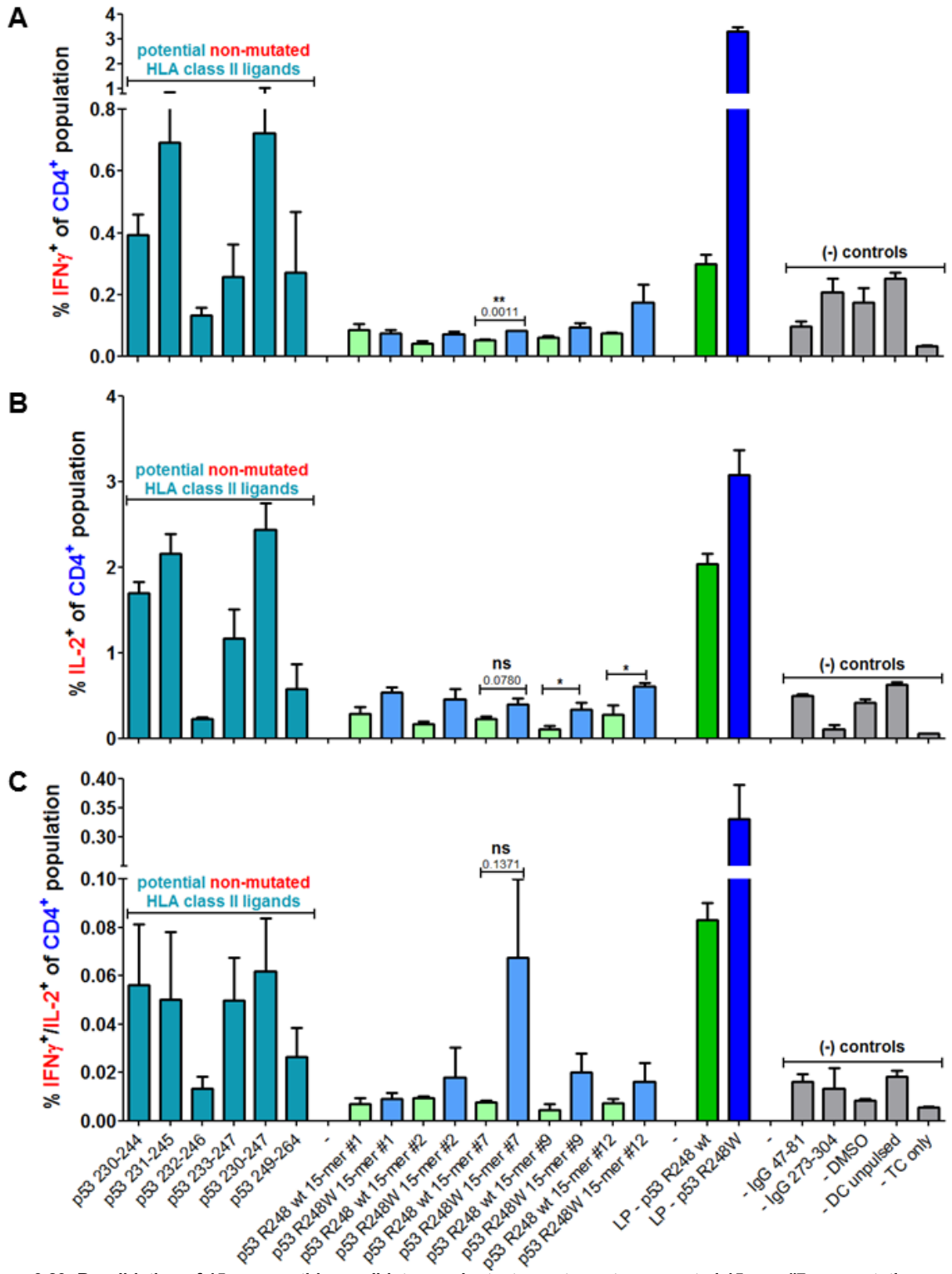


**Figure 3.29**: **Revalidation of 15-mer peptide candidates against wt counterparts suggested 15-mer #7 as a putative mutated HLA.DRB1 epitope within the long p53 R248W peptide.** Recall responses against mutated and wt p53 R248W 15-mer peptides of $CD4^+$ T cells purified from A2.DR1 dtg mice immunized with the long p53 R248W peptide assessed by two color cytokine secretion assays. Percentages of IFN-γ (**A**), IL-2 (**B**) and IFN-γ/IL-2 (**C**) double positive $CD4^+$ T cells upon *in vitro* recall against short and long p53 R248(W) peptides presented by $CD11c^+$ DCs are displayed. Each peptide and control sample was tested in triplicate instances. Results are plotted as means of triplicate assays ± SEM. Significant differences were tested for by unpaired, two-tailed t test. ns: not significant.

Figure 3.30 summarizes the findings of the presented chapter. Potential minimal HLA.A2 and HLA.DRB1 ligands identified within the sequences of the long, strongly immunogenic peptides p53 R248W (Fig. 3.26 A) and Kras G12V (Fig. 3.26 B) are highlighted in yellow. It becomes apparent, that HLA class I and II potential minimal epitopes sequences are overlapping for the p53 peptide, whereas the HLA class I restricted Kras G12V 10-mer is nested within the putative longer 15-mer HLA class II epitope.

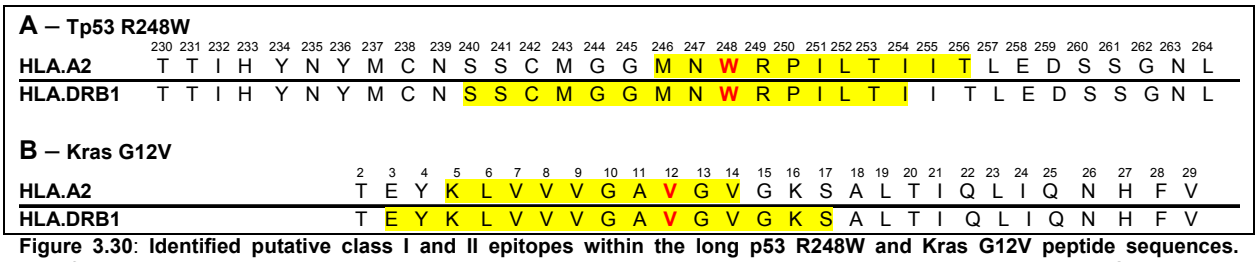


**Figure 3.30**: **Identified putative class I and II epitopes within the long p53 R248W and Kras G12V peptide sequences.** Identified, putative HLA.A2 and HLA.DRB1 epitopes within in the long mutated peptides p53 R248W (**A**) and Kras G12V (**B**) are highlighted in yellow.

## 3.4. Improvement of the vaccination formulation

After analysis of the T cell responses elicited by long peptide vaccination with mutated and wt peptides the question was addressed whether changes in the vaccination strategy might increase the number and/or function of vaccination-induced T cells. Increased numbers and an improved functionality of induced T cells after vaccination are favorable regarding the tumor protective capacity of a vaccine. As discussed in the introduction the choice of adjuvant and the formulation are sensitive parameters for the success of long peptide vaccination (see section 1.4.1). Especially crucial in this context are toll like receptor ligands, which are necessary for proper activation of DCs by providing danger signals. Activated DCs are, in term, the key APCs for the chosen vaccination approach, because long peptides need to be processed for presentation to T cells. Moreover, as professional APCs, DCs are most potent for the proper activation of both $CD4^+$ and $CD8^+$ T cells. In fact, next to CpG also other TLR ligands can act as suitable adjuvants. TLR 3 ligand poly(I:C) is frequently used in peptide vaccination studies and is able to enhance the induction of poly-functional effector T cell responses upon vaccination. This is why we decided to directly compare these two TLR ligands in our experimental vaccination system. Moreover, peptide vaccinations are classically administered as water in oil emulsions known as incomplete Freund's adjuvant (IFA). IFA does not only protect the peptide antigens from degradation and facilitates a slow and lasting release but also mediates immune-activating effects. The use of two oils, produced by the company SEPPIC, are established for peptide vaccinations and approved for clinical studies. The mineral oil based Montanide ISA 51 and the non-mineral oil Montanide ISA 720 are also generally used in animal peptide vaccination studies. In order to investigate the question whether immunogenic depot formulations might have a positive effect on the induction of peptide-specific T cell responses or are even superior to the employed water-based (more precisely, PBS-based) approach they were included in the testing.

For setting up the adjuvant testing experiment, we formulated three issues to be addressed. First, are the tested adjuvants, alone or in combination, changing the general activation status of the immune system (in our case focused on T cells) in the absence of the peptide antigen? To answer this question several groups of animals were vaccinated only with single adjuvants or combinations of those in the absence the antigenic peptide mix chosen for testing. In the literature there are differing concentrations of the TLR ligands suggested (for example (Qiu et al., 2008)). After comparing several sources we decided to test two concentrations of CpG (50 and 100 µg), whereas poly(I:C) was used in a concentration of 50 µg per injection. Second, TLR ligands are often used in combination with IFA formulations yielding in the highest T cells responses in published adjuvant testing experiments (Jin et al., 2007) and having us tested combinations in three component mixes. In other words we asked the central question, which adjuvant or combination of adjuvants does lead to the highest T cell induction when used along with an antigenic peptide mix? Third, strong adjuvant induced antigen-specific immune responses might be accompanied by high unspecific immune activity, possibly leading to undesired site effects and rising the question of safety. Summed up, we sought to investigate which adjuvant combination would induce high T cell responses in terms of cytokine secretion and antigen-specific T cell numbers, is save, and concurrently shows the highest signal to noise ratio.

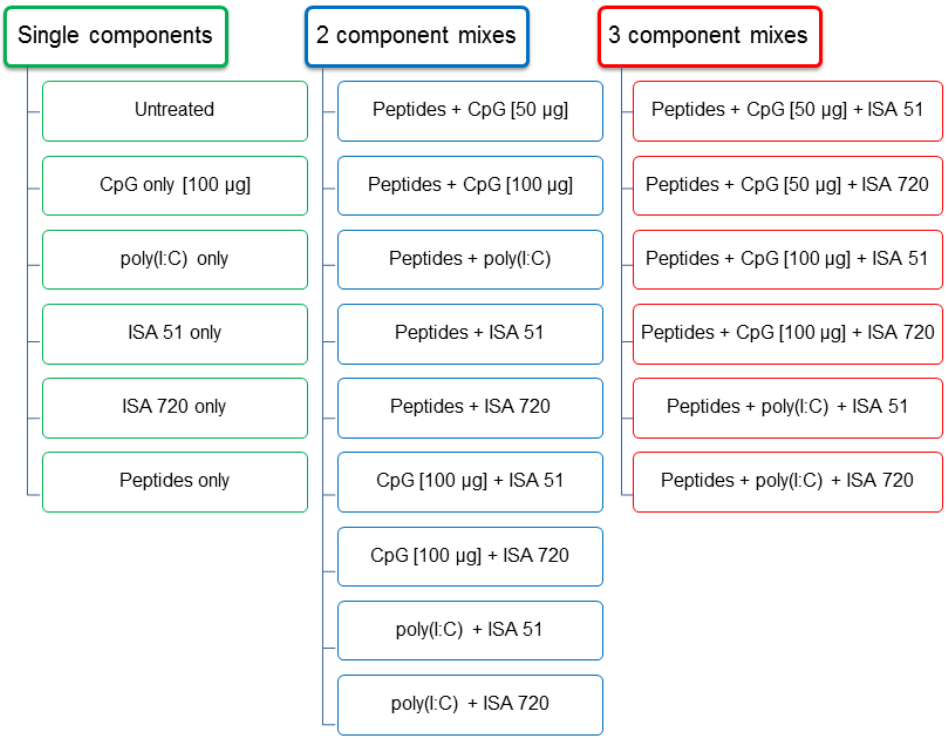


**Figure 3.31**: **Different peptide/adjuvant combinations tested for the improvement of the vaccination success.**

Experimentally, 20 groups of two C57BL/6 mice each were treated with different adjuvant formulations and were compared to results obtained from completely untreated animals. Figure 3.31 gives an overview of all peptide and/or adjuvant combinations tested. To start with, single components,

(indicated in green) meaning that either the peptides or the respective adjuvants were tested alone, are accounting for in total 6 different groups. In the second arm, two component mixes (blue frames) consisting of either two adjuvants without antigenic peptides (4 groups) or antigenic peptides and a single adjuvant (5 groups) were investigated. Three component mixes (framed in red) comprised the antigenic peptide mix, one TLR ligand and one of two the IFAs, respectively (6 groups). The group A mutated peptides were chosen as the antigenic peptide mix for testing. The animals were vaccinated twice with respective adjuvant/peptide mixes. However, due to the use of IFA it was necessary to increase the interval between the two consecutive vaccinations from two to three weeks. Hence, mice were vaccinated first on day 0, again three weeks later at day 21, and T cell responses were analyzed six weeks after the first vaccination on day 42. No animal of any group did show symptoms of immune related adverse effects, like weight or hair loss, but animals were completely healthy during the vaccination experiment. This argued for the safety of all vaccine formulations tested. In more than half of the animals treated with depot formulations, however, Montanide encapsulations were found under the skin at the vaccination site (neck) on the day of sacrifice. These encapsulations were also palpable as regidifications under the skin in the living animals. On day of analysis, pan purified T cells were re-stimulated for 16 h before combined IFN-γ secretion assay and intracellular cytokine staining on peptide pulsed $CD11c^+$ DCs. T cells were tested for responses against the single p53 R248W peptide, the whole group A mutated peptide mix, a mix of long peptides which was not used for vaccination (irrelevant peptide mix) and DCs treated with the peptide solvent only.

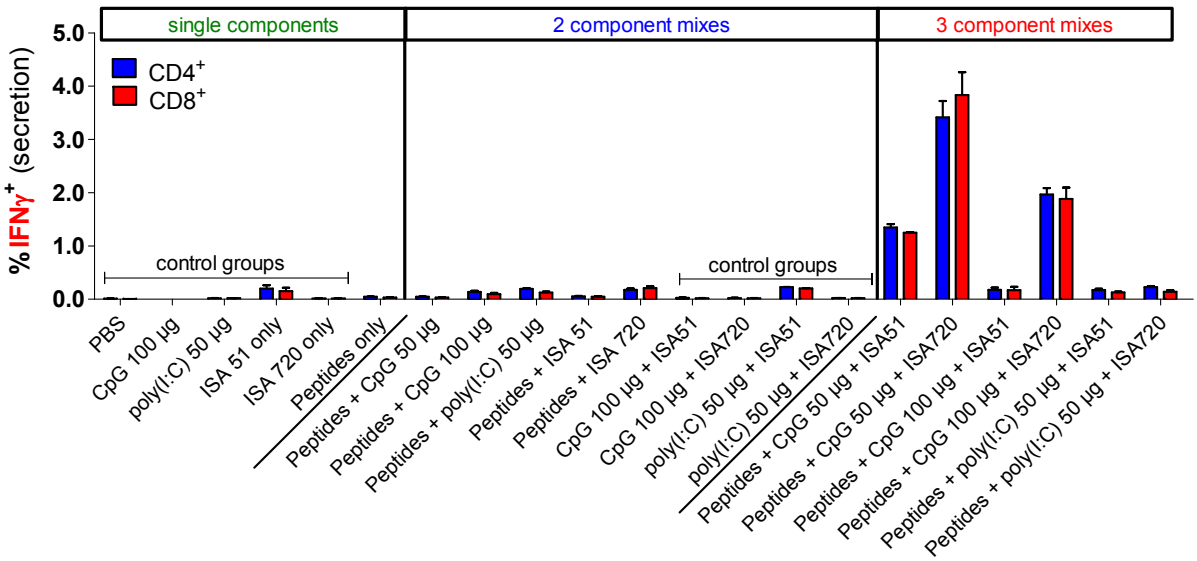


**Figure 3.32**: **Screening for the optimal vaccine formulation favors water in oil emulsion in combination with TLR agonists.** *In vitro* recall responses of $CD90^+$ purified T cells derived from differentially vaccinated C57BL/6 mice. For immunization group A peptide cocktails were administered in the different vaccine formulations or different vaccine formulations were applied without peptides (all tested combinations are listed in the previous figure) resulting in a total of 21 groups of two mice each. *In vitro* recall responses were obtained from combined IFN-γ secretion assay and intracellular cytokine staining performed with splenic $CD90^+$ purified T cells from immunized mice. IFN-γ secretion of $CD8^+$ and $CD4^+$ T cells upon *in vitro* recall against group A peptide mix presented by $CD11c^+$ DCs are displayed. Each test was performed in triplicate instances. Results are plotted as means of triplicate assays ± SEM.

In figure 3.32 all responses against the group A mutated peptide mix of $CD4^+$ and $CD8^+$ T cells derived from each respectively vaccinated adjuvant test group are opposed. Single adjuvants and mixes containing only adjuvant combinations are indicated as 'control groups'. Compared to the other control groups, vaccination with Montanide ISA 51 alone and ISA 51 in combination with 50 µg poly(I:C) seemed to increase $CD4^+$ and $CD8^+$ T cell responsiveness in terms of IFN-γ secretion towards the mutated peptide mix tested, although there were no antigens included in the vaccination formulations. For the tested vaccination formulations containing the antigenic mutated peptide mix the T cell, responses after vaccination with 3 component mixes (indicated in red script in the right hand side panel) clearly exceeded those of 2 component mixes.

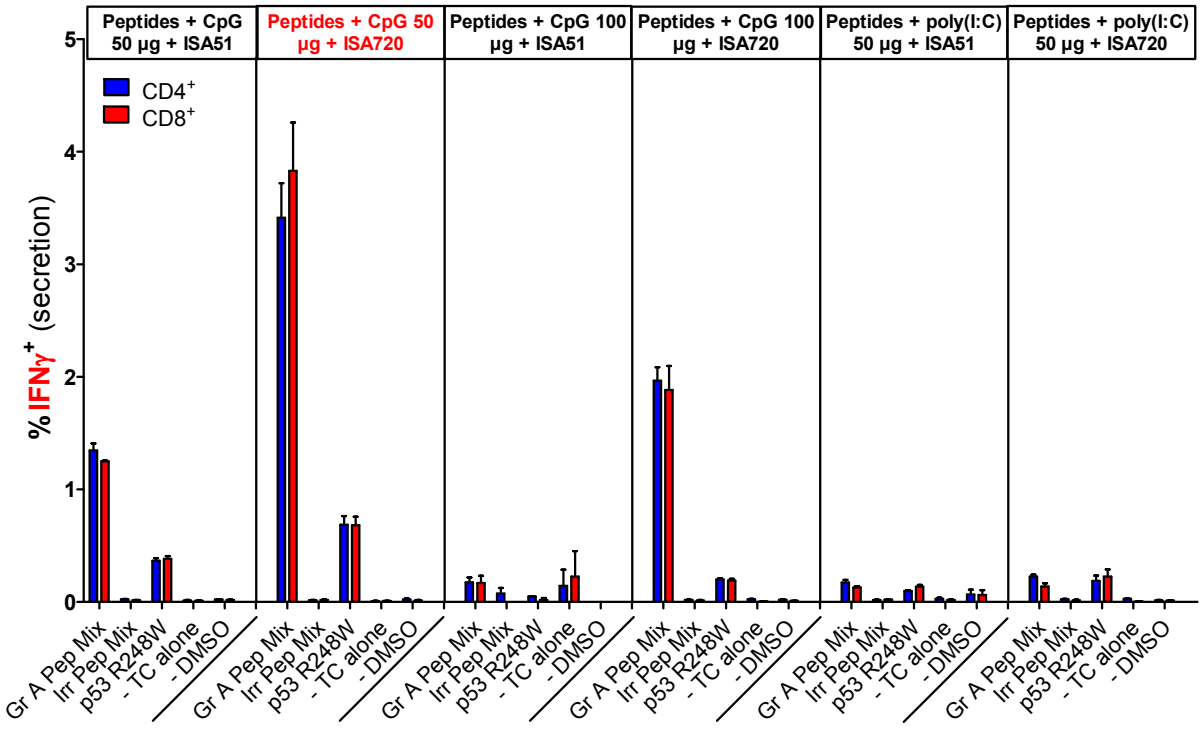


**Figure 3.33**: **Combination of ISA Montanide 720 and CpG ODN 1668 (50 µg per shot) was the best performing vaccine formulation in the applied multiple long peptide setting.** *In vitro* recall responses of $CD90^+$ purified T cell subsets derived from differentially vaccinated C57BL/6 mice. For immunization group A peptide cocktails were administered in the different vaccine formulations. *In vitro* recall responses were obtained from combined IFN-γ secretion assay and intracellular cytokine staining performed with splenic $CD90^+$ purified T cells from immunized mice. IFN-γ secretion of $CD8^+$ and $CD4^+$ T cells upon *in vitro* recall against single peptide p53 R248W, group A peptide mix presented by $CD11c^+$ DCs and respective controls are displayed. Each test was performed in triplicate instances. Results are plotted as means of triplicate assays ± SEM.

Figure 3.33 shows the $CD4^+$ and $CD8^+$ T cell responses obtained after vaccination with three component mixes in more detail. Again Montanide ISA 51 seemed to occasionally increase the background T cell activity as samples containing only T cells already secrete IFN-γ in case the mice were vaccinated with peptides, 100 µg CpG and ISA 51 (the third panel starting from the left hand side). Interestingly, vaccination mixes containing TLR 3 ligand poly(I:C) induced far less cytokine responsive T cells than formulations containing CpG. Moreover, the concentration of CpG administered per vaccination shot had an impact on the percentage of IFN-γ secreting T cells after *in vitro* re-stimulations. In fact, the

lower concentration of 50 µg per shot lead to higher induction of IFN-γ secretion of $CD4^+$ and $CD8^+$ T cells than respective mixes containing 100 µg of CpG per vaccination. Comparing both Montanide oils tested, ISA 720 was superior to ISA 51 in combination with CpG.

Compared to all other groups tested, the Montanide ISA 720 formulation containing next to the peptide mix 50 µg of CpG ODN 1668 resulted in the highest percentages of IFN-γ secreting $CD4^+$ and $CD8^+$ T cells after re-stimulation with the whole peptide mix and the single peptide p53 R248W. Furthermore, this adjuvant peptide combination (column header highlighted in red letters in figure 3.33) did not lead to an increase of any unspecific T cell response, neither for the irrelevant peptide sample ('Irr pep mix') nor for the two other controls which did not contain peptides. Therewith, the formulation of peptides in Montanide ISA 720 together with 50 µg of CpG ODN 1668 per shot fulfilled the initially formulated criteria of safety, a high signal to noise ratio and was clearly more potent in induction of antigen-specific T cells than the previously used water-based approach. Following vaccination experiments (e.g. for the investigation of the vaccine's tumor protective capacity) were therefore in most instances conducted employing the identified IFA-based formulation.

## 3.5. Establishment of a tumor model for the A2.DR1 dtg mouse system

### 3.5.1. Generation of A2.DR1 dtg syngenic tumor cell lines by carcinogen-induced tumorigenesis

After detailed analysis of vaccination induced T cell responses and the improvement of the vaccination formulation, we headed towards the investigation of the tumor protective capacity of the mutated oncogene-derived long peptide vaccine. Thereby, we decided to focus on the HLA humanized A2.DR1 dtg system as it mimics closer the situation within the human immune system than a murine MHC context would do. For continuing with the A2.DR1 dtg system, however, it was necessary to establish a suitable tumor model, because there were no syngenic tumor models (commercially) available and engineered non-syngenic tumor cell lines did not grow in these animals.

Tumors can be induced in mice by exposure of the animals to carcinogens. Treatment of mice with the potent carcinogen 3-Methylcholanthere (MCA) is an established method to study carcinogen-induced tumorigenesis (Matsushita et al., 2012). Therefore, we decided to make use of MCA to induce tumors in a small cohort of A2.DR1 dtg mice. Moreover, MCA-induced tumors are described to frequently carry *Kras* and *Tp53* mutations (Fritz et al., 2010) which made this method particularly suitable for our purpose.

Five female A2.DR1 dtg mice were injected with 500 µg of MCA subcutaneously in the back (see figure 3.34 A). We decided for female mice to be treated with MCA because females do not express y-chromosomal genes, whose gene products could act as rejection antigens when tumors from male mice are transplanted into female individuals. The first three month after MCA-injection no macroscopic tumor

development was observed and the mice were completely healthy. In month four after MCA treatment all five animals started to develop subcutaneously growing tumors. When tumors reached a critical size, mice were sacrificed and tumors were resected. Figure 3.34 B shows one of the female A2.DR1 dtg mice treated with MCA, which developed a subcutaneously growing tumor, at the day of sacrifice. What is more, none of the animals showed macroscopically visible metastasis.

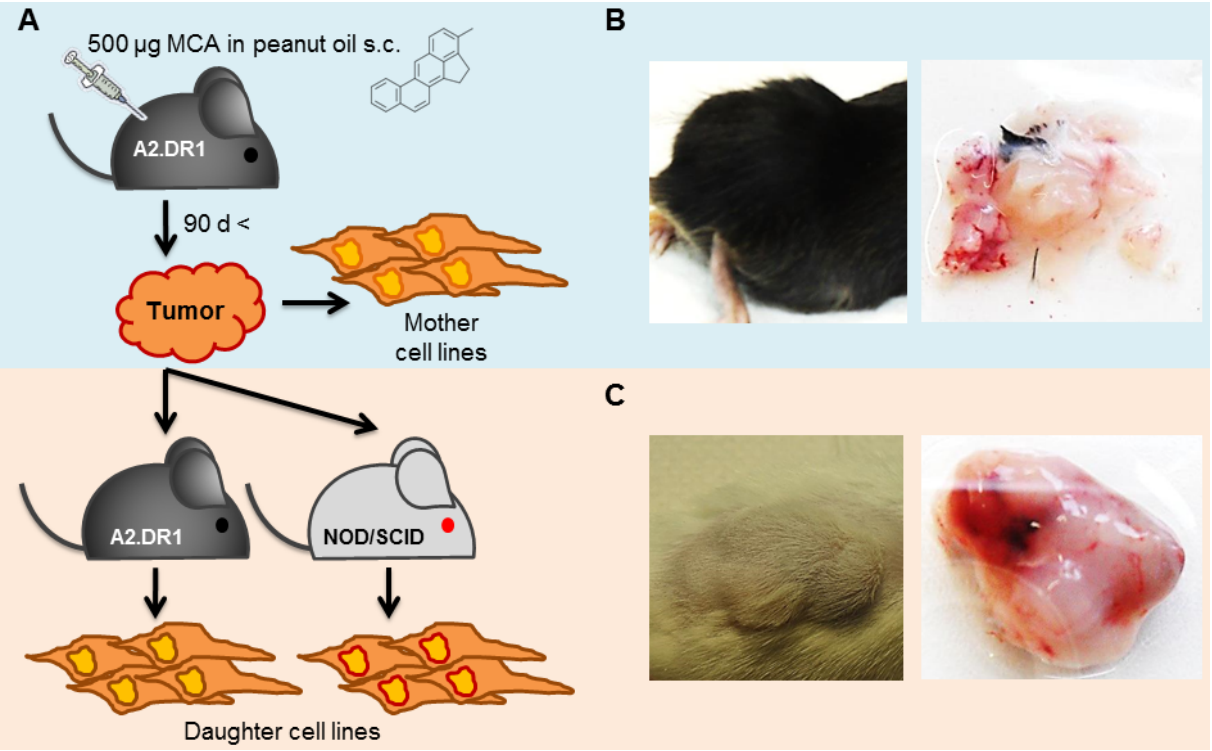


**Figure 3.34**: **Generation of A2.DR1 dtg syngenic tumor cell lines by carcinogen tumorigenesis using 3-Methylcholanthrene (MCA). (A)** Scheme of carcinogen-induced tumorigenesis and *in vivo* and *in vitro* passaging of MCA-induced tumors to generate stable *in vitro* growing cell lines. **(B)** A2.DR1 dtg mouse (#2280) treated with MCA on day of sacrifice (left hand side picture of the mouse's back) and parts of the excised tumor (right hand side picture). **(C)** Female NOD/SCID recipient mouse bearing a tumor which arose after transplantation of tissue pieces of a primary MCA-induced tumor derived from A2.DR1 dtg mice (left hand side picture shows the mouse's flank on the day of sacrifice). The left hand site picture shows the excised 'daughter' tumor.

The first resected tumor was processed to a single cell suspension by enzymatic digestion and dissimilation using cells strainers. This attempt to generate *in vitro* growing tumor cells, however, failed and all cells died during *in vitro* culture within two weeks. The second tumor was consequently processed using different methods for *in vitro* and *in vivo* propagation of tumor tissue. After resection the tumor was cut into small pieces of one to two mm of size. For *in vitro* propagation tumor pieces were transferred into tissue-culture treated petri dishes or into tissue-culture treated flasks. Small volumes of medium were added to the tissue pieces in such way that the pieces were not floating. Tumor pieces began attaching to the dishes' bottoms after 5 to 7 days. Adherent, spindle-shaped cells started to grow out from tumor pieces after 10 to 21 days of culture. Tumor pieces were carefully removed from the culture flaks when the grown-out cells were half confluent. When the flaks were completely confluent the cells were split via trypsinization. Generally cells survived the first passage and gave rise to *in vitro* growing cells lines. The

other part of tumor pieces were either transplanted into immune-competent A2.DR dtg mice or into immune-deficient NOD/SCID mice for *in vivo* propagation. Transplanted tumor pieces were able to give rise to tumors in both immune-competent as well as in immune-deficient hosts (see figure 3.34 C) within one month after transplantation. Tumors from recipient mice were again either *in vitro* or *in vivo* propagated. In total we were able to generate more than 40 different cell lines originating from four initial tumors, which were successfully passaged through different hosts, *in vitro* or both. The next step was to characterize the generated syngenic cell lines, which will be shown in the following section.

### 3.5.2. Characterization of syngenic A2.DR1 dtg tumor cell lines generated by carcinogen-induced tumorigenesis

This chapter will deal with the characterization of the A2.DR1 syngenic cell lines generated by carcinogen-induced tumorigenesis. The cell lines were analyzed for the *Kras* and *Tp53* mutations they carried, their MHC expression properties, the tissue origin they were originating from and their *in vivo* growth capacities. M. Bartoschek greatly contributed to the experiments performed to characterize the generated MCA cell lines in the course of his master thesis. Some of the data shown in the following was therefore already published before, though in a different version, in M. Bartoschek's master thesis (indicated in relevant figure legends). It was included into the presented thesis to provide a full picture of the cell lines profiles.

First, the *Tp53* and *Kras* mutational status of the MCA induced cell lines was assessed. For this purpose, gene specific primer couples for the *Kras* exons 1 and 2, the *Kras* open reading frame (orf) spanning exon 1 to 3, and the orf of the DNA binding domain (DBD) of *Tp53* spliced cDNA were designed. Due to the complexity of the *Tp53* gene locus (Bienz, Zakut-Houri, Givol, & Oren, 1984; Bourdon et al., 2005) only cDNA but not genomic DNA was analyzed for *Tp53* mutations, whereas *Kras* mutations were analyzed on genomic (sequencing of exon 1 and 2) and cDNA level (primer couple spanning *Kras* cDNA sequence from exons 1 to 3). Genomic DNA and total RNA was purified from cultured cells. RNA was then transcribed to cDNA. Resulting cDNA and genomic DNA served as templates for gene specific PCR amplification using the previously designed primer couples. Resulting PCR product were send for Sanger sequencing with gene specific primers. Sequencing data was screened for mutations by alignment of fasta sequences and analysis of sequencing histograms, which provided information whether a mutation was homozygous (single peak in the histogram) or heterozygous (double peak in the histogram, see e.g. figure 3.38 D).

Sequencing results revealed that mutations in the *Kras* and/or *Tp53* genes or transcripts (into cDNA transcribed and amplified mRNA) were found in nearly the entire cell lines analyzed. Figure 3.35 gives a schematic overview of the generated cell lines and the mutations detected therein. Mother cell line 2277 was extensively passaged through NOD/SCID and A2.DR1 dtg hosts which gave rise to the generation of several daughter cell lines. Whereas there was no *Kras* and *Tp53* mutation found in the mother cell line several mutations could be detected in its progenies. Thereby, some daughter cell lines

accumulated mutations in their *Kras* and *Tp53* genes (e.g. line #2277 ♀ A2.DR1). In general three different kinds of mutations were found: silent mutations (e.g. p53 R175R$^{+/-}$), mutations in only one allele (indicated as '+/-' in fig. 3.35) and mutations of both alleles (indicated as '+/+', e.g. Kras G12C$^{+/+}$). Moreover, the majority of mutations was found at the hot spot mutation sides we investigated in our panel of long peptides or in codons directly adjacent to those (e.g. p53 R244R$^{+/-}$). Indeed, only for the hot spot mutation sites Tp53 Y220, Tp53 R216 and Kras Q61 included in our peptide panel there were no mutations found in the MCA-induced A2.DR1 dtg cell lines. Analysis of the *Braf* gene was not performed for two reasons. One the one hand the V600E mutation was not found to be immunogenic in our experimental system and on the other hand MCA-induced sarcomas were not described to frequently carry Braf mutations. For following experiments we selected cell lines bearing two or more mutations and the cell lines we thought to be suitable candidates are highlighted in figure 3.35 with red framed boxes.

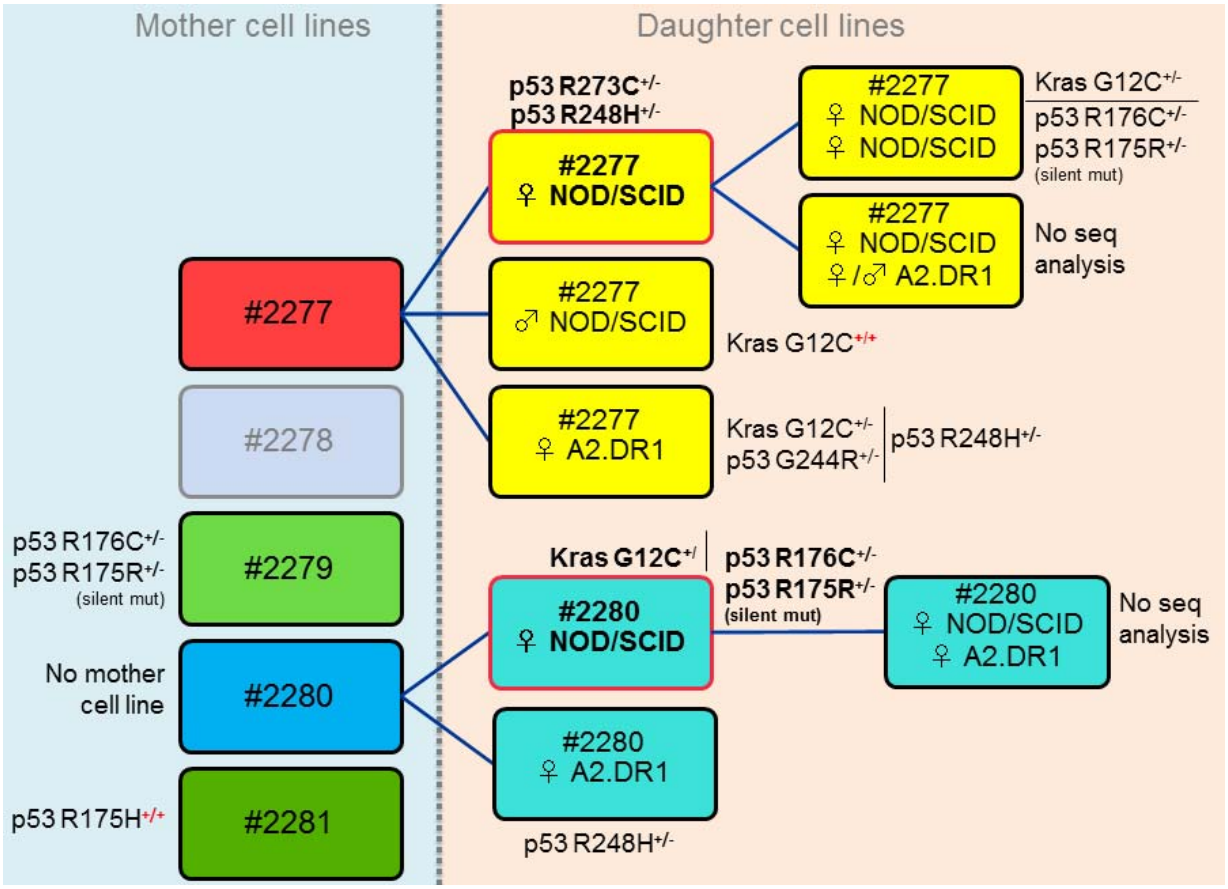


**Figure 3.35**: **Schematic overview of MCA-induced tumor cell lines and mutations in *Kras* and *Tp53* detected by Sanger sequencing.** Daughter cell lines were derived from mother cell lines by *in vivo* passaging through NOD/SCID and/or A2.DR1 dtg hosts. Chromosomal DNA as well as cDNA from mother and daughter cell lines was used as templates for amplification with gene specific primers (*Kras* and *Tp53*). Amplified PCR products were analyzed by Sanger sequencing to detect mutations in *Kras* and *Tp53* genes and mRNAs. Detected mutations are shown: +/- heterozygous mutation (one allele mutated), +/+ homozygous mutations (both alleles mutated), silent mut: silent mutation, no seq analysis: no sequencing analysis was performed with these cell lines. From the primary tumor of mouse #2280 no mother cell line could be established *in vitro* but daughter cell lines after *in vivo* passaging. It was not possible to generate any cell lines from MCA-treated mouse #2278. Red framed boxes highlight the cell lines which were chosen for further analysis and experiments. Sequencing data was obtained in teamwork with M. Bartoschek, who also designed the primers, and a similar scheme is shown in M. Bartoschek's thesis.

For optimal antigen presentation it would be favorable to work with cell lines which display high levels of MHC expression. To investigate this issue FACS-based MHC stainings were performed with the entire cell lines generated. Cells were stained for human MHC class I HLA.A2 and human MHC class II HLA.DR monoclonal fluorescent-labeled antibodies. For revalidation of the MHC phenotype of our A2.DR1 dtg mice and the generated syngenic cell lines we additionally stained for murine MHC class I (H2-$K^b$ and H2-$D^b$) and class II molecules (Pan I-$A^b$/I-$E^b$ specific antibody) of the C57BL/6 haplotype. As the A2.DR1 dtg strain has a C57BL/6 background we wanted to make sure that the knockout of murine MHC molecules was complete resulting in no detectable murine MHC surface expression. Primary splenocytes (indicated as 1° cells in figure 3.36) of A2.DR1 dtg and C57BL/6 mice, the C57BL/6 cell lines TC1 and the human CRC cell line SW480 served as controls. MCA-induced cell lines and controls were stained with mixes of human and murine MHC-specific antibodies and respective isotype controls for MHC phenotype analysis.

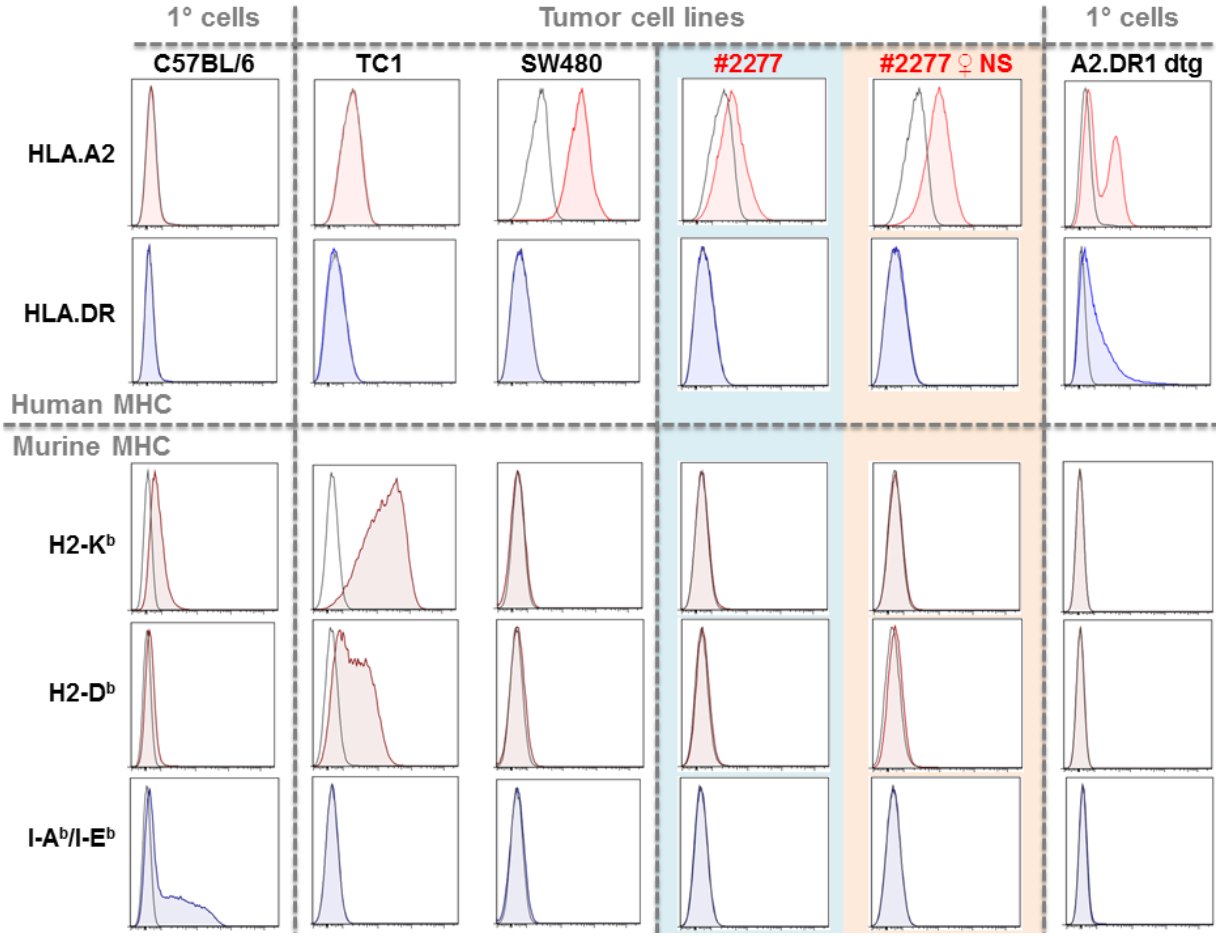


**Figure 3.36**: **MHC expression analysis reveals that MCA-induced tumors express HLA.A2 but no HLA class II.** Primary murine splenocytes (1° cells) derived from A2.DR1 dtg and C57BL/6 mice and cultured cells were stained for with murine (H2-$K^b$, H2-$D^b$ (MHC class I), and I-$A^b$/I-$E^b$ (MHC class II)) and human (HLA.A2 (HLA class I) and HLA.DR (HLA class II)) fluorescent-labeled MHC-specific antibodies and analyzed with FACS Canto II. TC1 cells served as positive control for murine MHC molecules and SW480 as HLA.A2 positive control. Red lines, tinted filling: MHC class I stainings, blue lines, tinted filling: MHC class II stainings, grey lines: isotype controls.

Figure 3.36 displays FACS histogram analysis of a representative murine and human MHC staining experiment. Two MCA-induced cell lines are exemplarily shown, namely the mother cell line 2277 and its daughter cell line 2277 ♀ NS (referred to from here onwards as 2277-NS). As expected C57BL/6 splenocytes express no human MHC molecules but the murine H2-$K^b$, low levels of H2-$D^b$ and murine MHC class II I-$A^b$/I-$E^b$ molecules. In contrast, the C57BL/6 tumor cell line TC1 does not express MHC class II molecules but high levels of class I H2-$K^b$ and H2-$D^b$. The human CRC tumor cell line SW480 served as positive control for HLA.A2 expression and was conclusively negative for all other MHC molecules tested. A2.DR1 dtg splenocytes express HLA.A2 and HLA.DR1 on their cell surface and were not stained positive for any of the murine MHC molecules of the C57BL/6 haplotype (very right hand side row). As the A2.DR1 dtg splenocytes also the two MCA-induced tumor cell lines (highlighted in tinted background and in bold red script in fig. 3.36) shown, were negative for murine MHC molecules. Moreover, they did not express HLA class II but HLA class I. Thereby, the mother cell line 2277 expressed lower levels of HLA.A2 than its progeny 2277-NS. Generally, all of the MCA-induced tumor lines analyzed showed differing HLA.A2 expression levels and none of them expressed HLA.DR (data not shown). Interestingly, there seemed to be a trend of a higher HLA.A2 expression of cell lines which were derived from *in vivo* passaging through NOD/SCID mice. As for the two MCA-lines displayed in figure 3.36, all other A2.DR1 dtg syngenic cell lines generated and analyzed did not show expression of murine MHC molecules which confirmed a clear background.

In the introduction the phenomenon about the ability of certain IFNs to induce the transcriptional up-regulation of MHC molecules and components of the antigen-processing machinery was described (see chapter 1.1.1.). IFN-γ is one of these interferons and can cause the up-regulation of MHC expression resulting in increased cell surface levels of MHC class I and II molecules. We speculated that IFN-γ treatment of our MCA-induced cell lines, especially of those which show low HLA.A2 levels, could lead to an increase of surface HLA class I and to an induction of HLA class II expression. Hence, MCA-induced A2.DR1 dtg cell lines were cultured for 48 h with IFN-γ supplemented medium. Two different concentrations of murine, recombinant IFN-γ were tested (50 ng/ml and 100 ng/ml). Afterwards, cells were harvested and stained for MHC class I and II molecules as described before. As a positive control served the C57BL/6 glioblastoma cell line 261 (kindly provided by Dr. T. Schumacher), which strongly up-regulates murine MHC class I and II molecules upon IFN-γ treatment.

In figure 3.37 FACS analysis of a representative IFN-γ treatment experiment is displayed. The left hand side panel shows that treatment with both tested concentration of IFN-γ (50 ng/ml shown as blue and 100 ng/ml as red lines in FACS histograms) were sufficient to achieve maximal up-regulation of basal levels of H2-$K^b$ (shown as green lines). Furthermore, 50 ng/ml of IFN-γ lead to the induction of H2-$D^b$ and the induction of MHC call II I-$A^b$/I-$E^b$ molecules (, which could not be enhanced further through increasing the IFN-γ concentration to 100 ng/ml). Again, of the MCA-induced A2.DR1 dtg derived cell lines the mother cell line 2277 was tested along with two of its progeny cell lines (2277-NS and 2277-A2.DR1) for

the IFN-γ treatment experiment shown in figure 3.37 (right hand side of the figure). As shown for the glioblastoma cell line an IFN-γ concentration of 50 ng/ml was sufficient to increase basal HLA.A2 expression levels. Even two weeks after IFN-γ withdrawal pre-treated cell lines still showed an increased HLA.A2 expression compared to completely untreated cells (data not shown). However, HLA class II expression was not inducible upon IFN-γ treatment in any of the MCA-induced cell lines tested (see staining for HLA.DR in figure 3.37). Taken together, IFN-γ was able to up-regulate HLA class I expression in our MCA-induced A2.DR1 dtg syngenic cell lines but failed to induce the expression HLA class II.

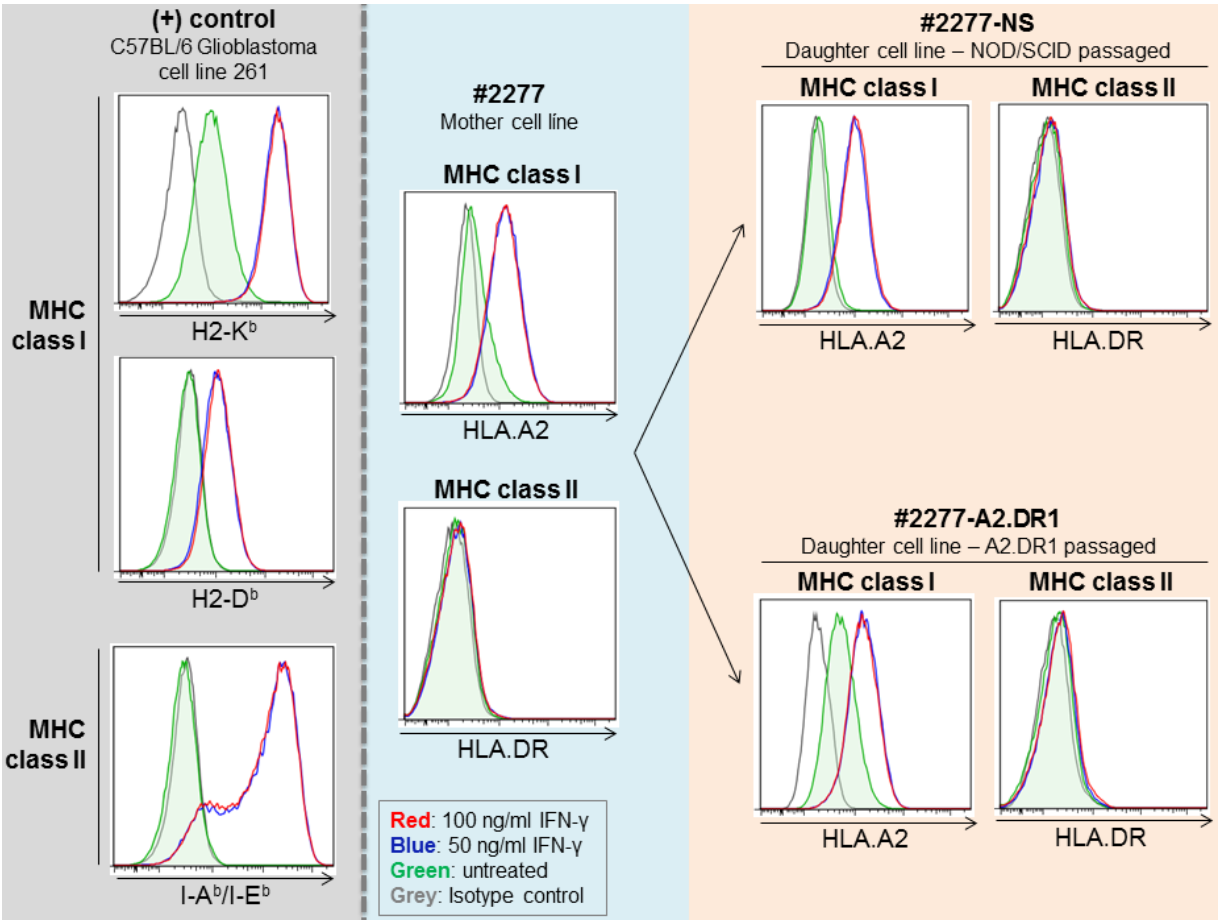


**Figure 3.37**: **IFN-γ treatment led to up-regulation of HLA.A2 but not HLA.DR expression of MCA-induced tumor cell lines.** Cultured tumor cell lines (80 % confluence) were treated for 48 h with indicated concentrations of murine, recombinant IFN-γ before FACS analysis. Cells were stained for with murine (H2-K$^b$, H2-D$^b$ (MHC class I), and I-A$^b$/I-E$^b$ (MHC class II)) and human (HLA.A2 (HLA class I) and HLA.DR (HLA class II)) fluorescent-labeled MHC-specific antibodies and analyzed with FACS Canto II. C57BL/6 glioblastoma cell line served as positive control for IFN-γ induced MHC up-regulation. Red lines: cells treated with 100 ng/ml IFN-γ, blue lines: cells treated with 50 ng/ml IFN-γ, green lines: untreated cells, grey lines: isotype controls.

Next, we sought to correlate the MCA-induced tumor cell lines to their tissue of origin. Therefore, several histological stainings were performed and results are summarized in figure 3.38. A2.DR1 dtg mice were challenged with tumor cell line 2277-NS to have subcutaneous tumors grown out, anticipating at this point that line 2277-NS is tumorigenic (shown in figure 3.39). Parts of the tumor tissue were embedded in paraffin. The pathologist Dr. E. Herpel and colleagues kindly performed tissue sectioning and H&E

stainings of paraffin-embedded tumor tissue. Figure 3.38 A shows an exemplary snapshot of an H&E stained 2277-NS tumor section revealing spindle shaped cells. Dr. Herpel speculated due to the morphology of the cells that the tumor is most probably of mesenchymal origin, pointing towards a sarcoma. Moreover, she reported that in some sections of rare tumors (not shown) she saw how the tumor invaded adjacent muscle tissue which was a sing of an invasive and aggressive phenotype. Also, she was able to observe poly-nucleated giant cells throughout the sections.

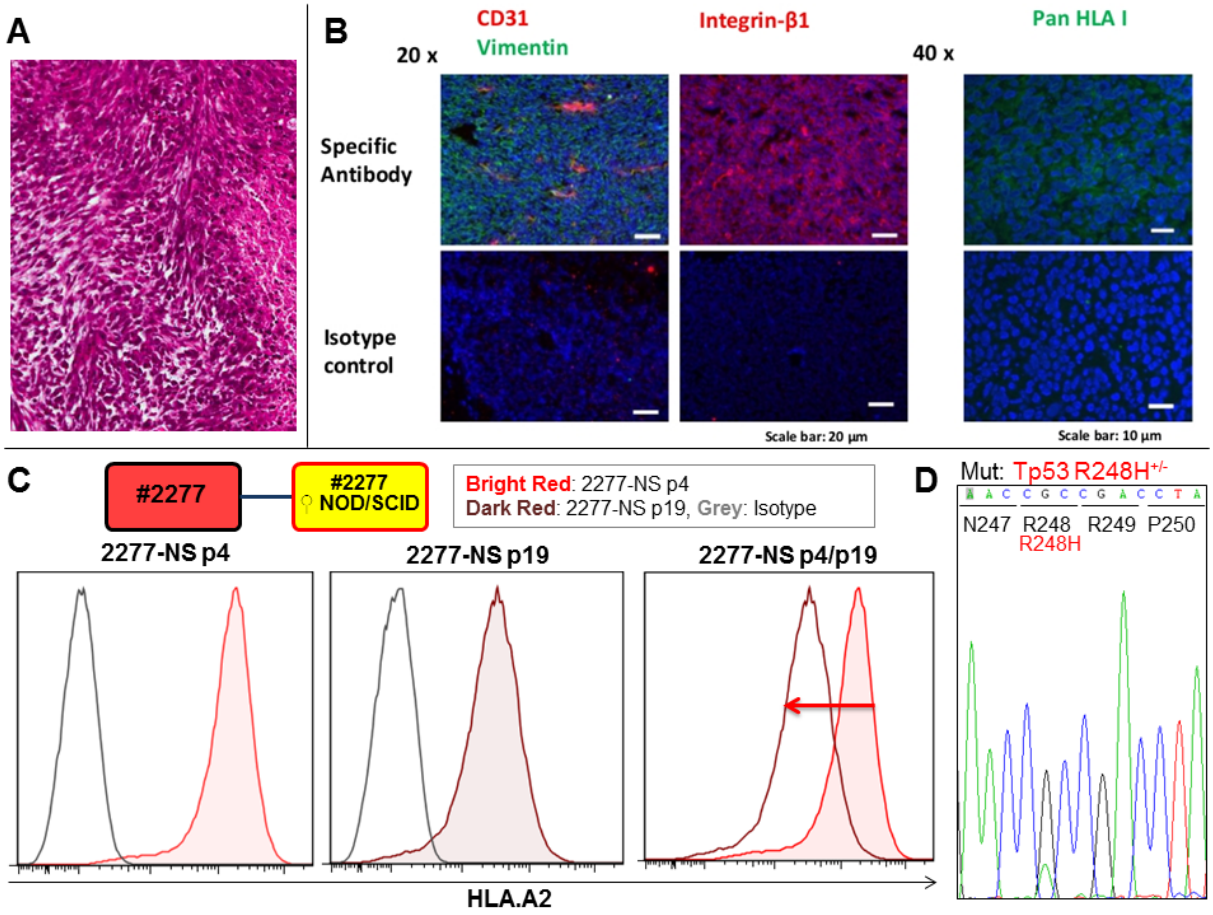


**Figure 3.38**: **Immunohistochemistry analysis identifies MCA-induced tumor cell lines as (fibro) sarcomas. (A)** H&E-staining of MCA-induce tumor cell line 2277-NS. Tumor pieces were excised from MCA-treated A2.DR1 dtg mice and passaged through NOD/SCID mice. Afterwards cells were *in vitro* cultured (Line 2277-NS) and re-transplanted into A2.DR1 dtg mice. **(B)** Cryosections and immunohistology of tumors excised from tumor cell line 2277-NS challenged mice. Cryosections (4 µm thickness) were stained with CD31 (left hand side pictures, red), Vimentin (left hand side pictures, green), Integrin-β1 (pictured middle panel, red) and PAN HLA I (right hand side pictures, 40 fold magnification, green) antibodies. Isotype stained control sections are shown in the respective lower pictures. Nuclei were stained blue with dapi. These pictures were generated by M. Bartoschek and are also shown in his master thesis. **(C) HLA.A2 down-regulation of 2277-NS sarcoma cell line after long-term *in vitro* culturing**. Cultured cells were stained for human HLA.A2 (HLA class I) with fluorescent-labeled MHC-specific antibodies and analyzed with FACS Canto II. Bright red, tinted: 2277-NS *in vitro* passage p4, dark red, tinted: 2277-NS *in vitro* passage p19, grey lines: isotype controls. **(D)** Sequencing histogram analysis of tumor cell line 2277-NS. Chromosomal DNA as well as cDNA of cell line 2277-NS were used as templates for amplification with gene specific primers (*Kras* and *Tp53*). Amplified PCR products were analyzed by Sanger sequencing to detect mutations in *Kras* and *Tp53* genes and mRNAs.

In addition, we analyzed cryo-sections of 2277-NS tumors for markers which could provide further evidence for the mesenchymal origin of our MCA-induced tumors. MCA-induce tumors were described to be fibro-sarcomas when stained positive for the mesenchymal marker Vimentin (Wakita et al., 2009) and

the endothelial marker Integrin β-1. It was part of M. Bartoschek's master thesis work to establish and perform corresponding stainings. The immunohistochemical pictures of cryosections displayed in figure 3.38 B reveal that 2277-NS tumors obviously expressed both markers Vimentin (shown in green color) and Integrin β-1 (shown in red color). What is more, tumors were stained for CD31, a maker for endothelial cells and vascularization. In a co-staining with Vimentin (upper left picture) islets of cells expressed CD31 (red color), which suggested a micro-vascularization of the tumors. Also HLA class I expression could be confirmed in immunohistochemistry (upper right picture). Conclusively, immuno-histological analysis reinforced the assumption that the MCA-induced A2.DR1 dtg syngenic cell lines were able to give rise to (fibro-)sarcomas *in vivo*, which showed signs of vascularization and expressed HLA class I.

Concerning the MHC expression of the A2.DR1 dtg sarcoma lines another observation was made for several lines during *in vitro* culturing. HLA.A2 expression was gradually decreasing while passaging. As shown in figure 3.38 C the peak of HLA.A2 expression displayed in FACS histograms was shifted towards lower intensity when comparing 2277-NS cells at passage 4 ('2277-NS p4', bright red lines, tinted) to 2277-NS cells at passage 19 of culture ('2277-NS p19', dark red lines in the FACS histograms). The down-regulation of HLA.A2 was also noticed for other sarcoma lines generated and extensively cultured, like line 39 and line 10 (data not shown), which will be characterized in more detail in the following. Obviously, HLA class I down-regulation during *in vitro* culturing seemed to be a common trait of the MCA-induced sarcoma lines derived from the A2.DR1 dtg mouse strain. Moreover, it was possible to restore HLA.A2 expression in excessively cultured cell lines by IFN-γ treatment (data not shown).

For *in vitro* kill and tumor challenge experiments we decided to continue with three cell lines, which will be introduced in further detail in the following section. The cell lines we chose to investigate the tumor protective capacity of mutated long peptide vaccination with oncogene and tumor suppressor gene derived sequences had to fulfill the criteria listed in the beginning of the section: robust HLA expression, a suitable *Kras* and *Tp53* mutation status, and *in vivo* tumorigenicity.

Sarcoma cell line 2277-NS was already partially introduced. It expresses high levels of HLA.A2 (see figure 3.38) and carries the intrinsic heterozygote mutation *Tp53 R248H* as shown in the sequencing histogram in figure 3.38 D. We already know that A2.DR1 dtg sarcoma cell line 2277-NS was tumorigenic. Figure 39.9 A shows a picture of a A2.DR1 dtg mouse which was initially challenge with 5.0 x $10^5$ 2277-NS cells on the right flank and 1.0 x $10^6$ tumor cells on the left flank. 2277-NS cells were injected in Matrigel mimicking the extracellular matrix for better engraftment of the tumors. The animal shown in figure 3.39 A belonged to the mice used for the tumorigenicity testing challenge experiment shown in figure 3.39 C. The picture shows the dissected mouse shortly after sacrifice. Both tumors were able to attract blood vessels from the armpit and the loins as indicated with the left pointing red arrow. The macroscopic visible singes of angiogenesis coincided with the CD31 positive staining in microscopic

cryosections of 2277-NS tumors (see again figure 3.38 B). Also when excised tumors were cut open blood vessels were lancing the whole tumor tissue. Further examination of the animals revealed that most of the tumor bearing mice had splenomegaly (to the right pointing red arrow). According to observations made during several tumor challenge experiments it seemed that splenomegaly was more frequently found in animals bearing large tumors at the day of sacrifice (not quantified). Probably splenomegaly was a phenomenon of late stage disease in our experimental system.

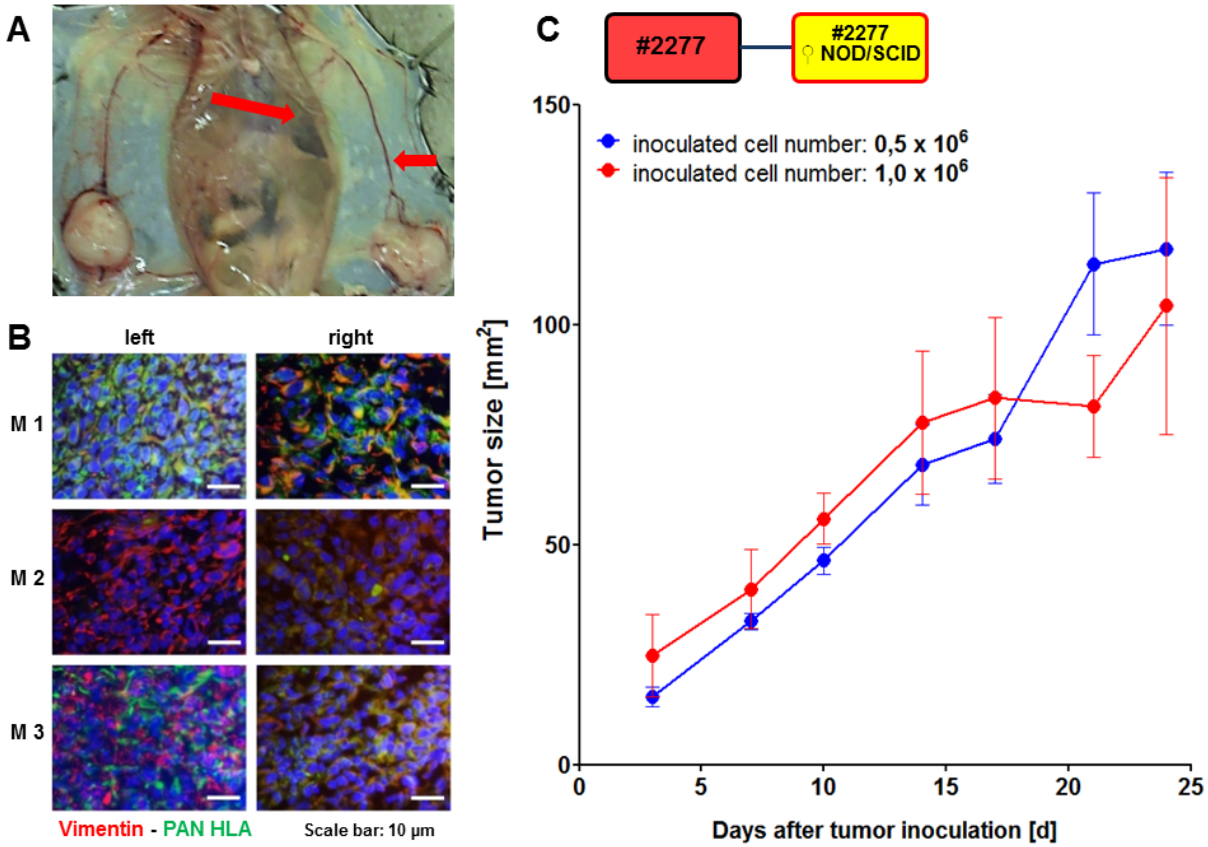


**Figure 3.39**: **Characterization of A2.DR1 dtg sarcoma cell line 2277-NS. (A)** Picture of a dissected tumor bearing A2.DR1 dtg mouse challenged with two tumors, one on each side of the body. Red arrows point at blood vessels attracted by the tumor and an enlarged spleen. **(B)** Cryosections and immunohistology of tumors excised from sarcoma cell line 2277-NS challenged mice used for the *in vivo* growth testing experiment shown in (C). Cryosections (4 µm thickness) were stained with, Vimentin (green) and PAN HLA I B9 (green) antibodies. Nuclei were stained blue with dapi. Tumors from the left and the right flank of the three mice (M1, M2, and M3) were analyzed. **(C)** Test *in vivo* tumor growth experiment with tumor cell line 2277-NS. Cells were resuspended in Matrigel for inoculation. Three A2.DR1 dtg mice were inoculated subcutaneously with 0.5 x $10^6$ 2277-NS tumor cells on one flank and 1.0 x $10^6$ cells on the other flank of the body. n: number of biological replicates; error bars, mean ± SEM. Immunohistochemistry data was generated by M. Bartoschek and tumor challenge experiments were performed by J. Quandt. Figures were already published in the context of M. Bartoschek's master thesis.

To assess the HLA.A2 expression status of 2277-NS tumor tissue derived from challenged mice for the tumorigenicity testing experiment, tumors were frozen for cryo-sectioning and immuno-histochemistry. Figure 39.9 B shows HLA/Vimentin co-stainings of resulting cryosections (conducted by M. Bartoschek). Whereas all tumors analyzed expressed Vimentin (shown in red color) the expression of HLA.A2 was not homogenous. For example the tumor on the left half of mouse 2 (M 2 left)'s body barely stained positive for Pan HLA antibody. Finally, regarding the tumor growth curve shown in figure 3.39 C

indicated that initial inoculation of 5 x $10^5$ 2277-NS sarcoma cells (blue line) was sufficient for stable *in vivo* tumor outgrowth. Tumor growth over time was almost linear when using this initial cell number for tumor inoculation.

None of the tumor cell lines generated carried *Kras* and *Tp53* mutations which were both included in our panel of mutated oncogene-derived peptides. Therefore, we decided first to engineer a suitable cell line to express the most immunogenic mutations included in the panel of long peptides. Second we proceeded with cell lines carrying two intrinsic mutations in *Tp53* and/or *Kras* by having long peptides synthesized carrying tumor intrinsic mutations and used for vaccination. Conclusively, we sought to work with two systems one engineered and focusing on the most immunogenic mutations and the other exploring tumor intrinsic *Kras* and *Tp53* mutations for tumor protective effect when used for long peptide vaccination. Initially we thought to select a cell line for engineering which did not carry an intrinsic *Kras* or *Tp53* mutation. Only mother cell line 2277 was free of detectable *Kras* and *Tp53* mutations. But we decided against it because it HLA.A2 expression was low and rapidly decreasing to zero during culturing. Hence, the daughter sarcoma line 2277-NS was chosen to be engineered to express a transgene expressing the two most immunogenic *Kras* and *Tp53* mutations included in our panel of long peptides. Although 2277-NS carried the mutation *Tp53 R248H* on one allele, we selected this sarcoma line because it showed a high HLA.A2 expression and a stable *in vivo* growth capacity. The engineering of cell line 2277-NS to express the most immunogenic mutations will be the content of the following chapter.

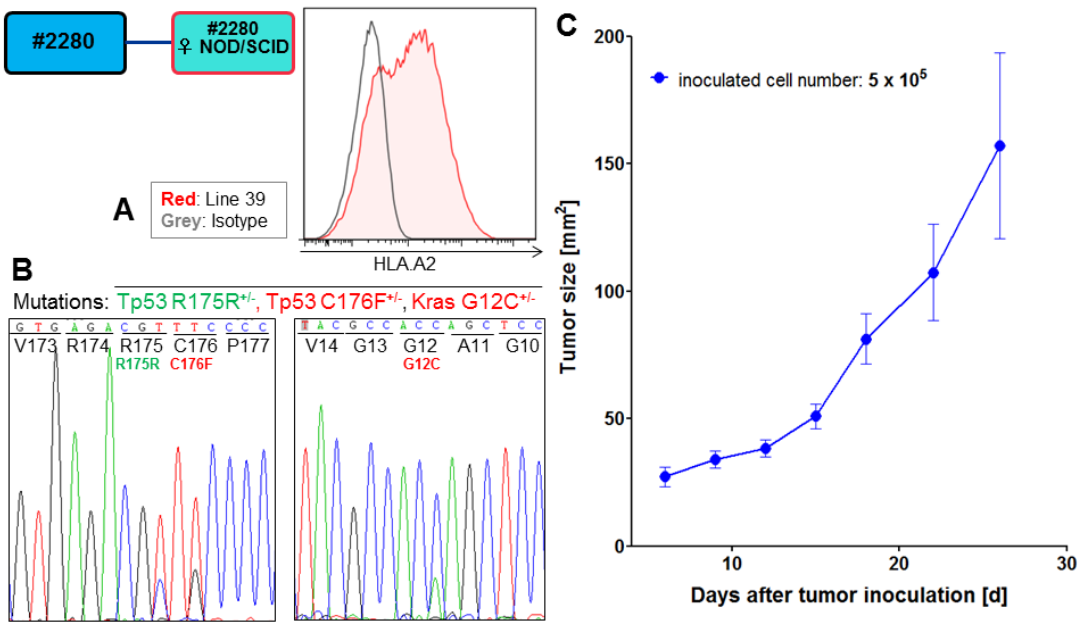


**Figure 3.40**: **Characterization of MCA-induced A2.DR1 dtg sarcoma cell line 39. (A)** HLA.A2 expression of sarcoma line 39. Cultured cells were stained for human HLA.A2 (HLA class I) by fluorescent-labeled MHC-specific antibody and analyzed with FACS Canto II. Bright red, tinted: line 39 cells stained with specific antibody, grey lines: isotype control. **(B)** Sequencing histogram analysis of sarcoma cell line 39. Chromosomal DNA as well as cDNA of line 39 were used as templates for amplification with gene specific primers (*Kras* and *Tp53*). Amplified PCR products were analyzed by Sanger sequencing to detect mutations in *Kras* and *Tp53* genes and mRNAs. **(C)** Test *in vivo* tumor growth experiment with sarcoma cell line 39. Tumor cells were resuspended in Matrigel for inoculation. Five male A2.DR1 dtg were inoculated subcutaneously with 5 x $10^5$ line 39 tumor cells on the right flank of the body. n: number of biological replicates; error bars, mean ± SEM

Two MCA-induced A2.DR1 dtg syngenic sarcoma lines qualified for the second approach exploring long peptides comprising tumor intrinsic *Tp53* and *Kras* mutations for tumor protective vaccination. Line 39, originating from the initially MCA-treated mouse #2280 and passaged through a NOD/SCID host, is introduced in figure 3.40. It had an intermediate HLA.A2 expression (fig. 3.40 A) which could be boosted with IFN-γ treatment (data not shown). The sequencing histograms displayed in sub-figure 3.40 B revealed that this cell line had a suitable mutation profile. Next to a silent mutation in codon *Tp53* R175 it harbored a mutation on one allele of *Tp53* in the neighboring codon C176F. Also one allele of the *Kras* gene was mutated carrying the point mutation G12C. Challenge of A2.DR1 dtg mice (n = 5) with 5 x $10^5$ line 39 cells inoculated into the right flank of each animal assigned for the testing proved that line 39 was tumorigenic and showed a nearly linear tumor growth curve. Similar to line 2277-NS splenomegaly was observed in some cases at late time points of challenge experiments.

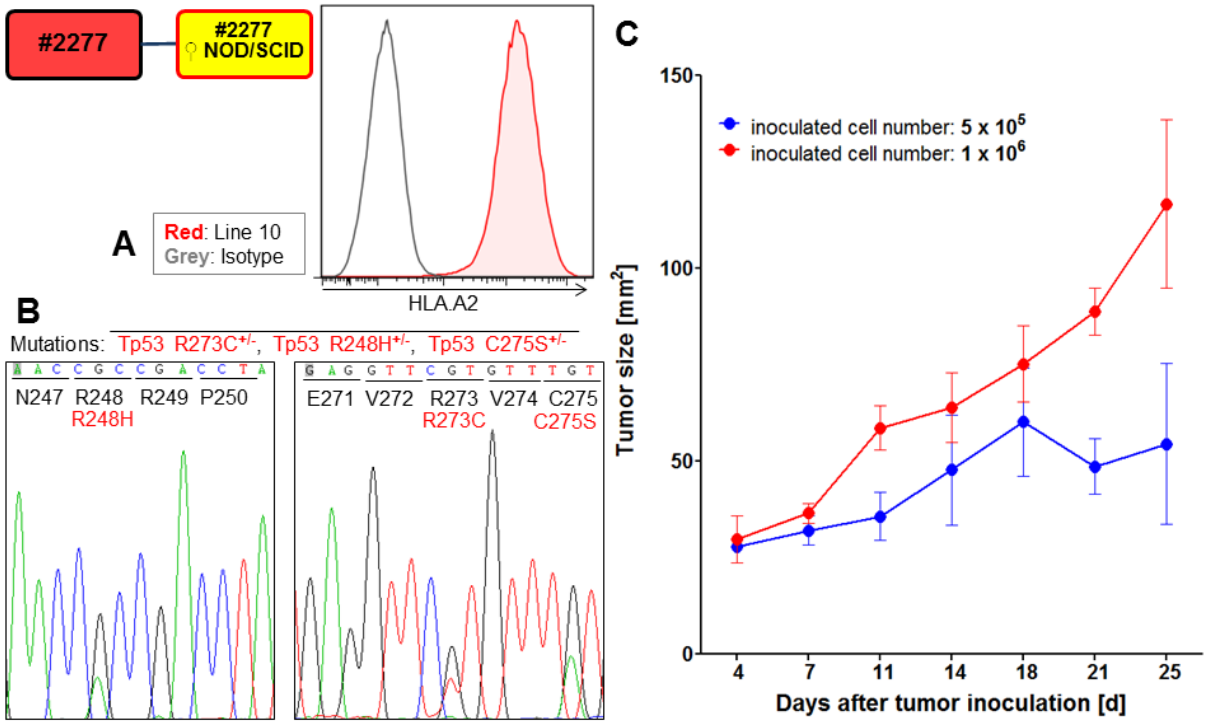


**Figure 3.41**: **Characterization of MCA-induced A2.DR1 dtg sarcoma cell line 10. (A)** HLA.A2 expression of sarcoma line 10. Cultured cells were stained for human HLA.A2 (HLA class I) by fluorescent-labeled MHC-specific antibody and analyzed with FACS Canto II. Bright red, tinted: line 10 cells stained with specific antibody, grey lines: isotype control. **(B)** Sequencing histogram analysis of sarcoma cell line 10. Chromosomal DNA as well as cDNA of line 10 cells were used as templates for amplification with gene specific primers (*Kras* and *Tp53*). Amplified PCR products were analyzed by Sanger sequencing to detect mutations in *Kras* and *Tp53* genes and mRNAs. **(C)** Test *in vivo* tumor growth experiment with sarcoma cell line 10. Tumor cells were resuspended in Matrigel for inoculation. Three A2.DR1 dtg mice were inoculated subcutaneously with 0.5 x $10^6$ line 39 tumor cells on one flank and 1.0 x $10^6$ cells on the other flank of the body. n: number of biological replicates; error bars, mean ± SEM

The second candidate sarcoma selected was line 10. Line 10 was another progeny of mother cell line 2277 which was derived from a different NOD/SCID host than cell line 2277-NS. As figure 3.41 A indicates line 10 showed an high HLA.A2 expression, which was also very stable during culturing. Although Line 10 carried no mutation in the *Kras* gene three heterozygote mutations in *Tp53* were

detected (see fig. 3.41 B), which could imply that both *Tp53* alleles might have been mutated. Challenge of A2.DR1 dtg mice with two different cell numbers (resuspended in Matrigel) used for tumor inoculation evidenced that also line 10 was tumorigenic. Compared to line 2277-NS, however, a higher cell number of 1 x $10^6$ inoculated cells was necessary for a stable, linear tumor growth (red line in figure 3.41 C).

### 3.5.3. Engineering of the A2.DR1 dtg sarcoma cell line 2277-NS for the expression of the most immunogenic *Tp53* and *Kras* mutations

Peptides comprising the mutations Kras G12V and p53 R248W were previously identified to be the most immunogenic in the HLA.A2 and HLA.DRB1 context. They were more immunogenic than corresponding wt counterparts when used for active vaccination and possibly comprise mutated $CD4^+$ as well as $CD8^+$ T cell epitopes. Hence, we were wondering whether these two peptides were most potent to envisage the effects of long peptide vaccine targeting oncogene-derived mutations on the course of tumor outgrowth. As none of the generated, tumorigenic, A2.DR1 dtg syngenic sarcoma lines carried these two mutations we decided to genetically engineer a suitable candidate cell line for their expression. In the previous chapter A2.DR1 dtg sarcoma line 2277-NS was pointed out to be suitable for this purpose. It expressed high levels HLA.A2, showed stable *in vivo* tumor growth kinetics and carried only one intrinsic heterozygote mutation within the *Tp53* and *Kras* genes (namely *Tp53* R248H).

To mimic the natural conditions best possible by concurrently inserting only one transgene into cell line 2277-NS we designed the following chimeric gene construct. For enabling antigen processing similar to those of the natural p53 and Kras proteins we thought that it would be favorable to design transgenes comprising the p53 R248W and Kras G12V mutations within long sequences of their natural adjacent protein backbones. Therefore, the wild-type sequences for the murine and human *Kras* and *Tp53* open reading frames (orf) were gathered from the NCBI database. The DNA-binding domain (DBD) from *Tp53* (aa positions 108-288) was joint via a short peptide linker (aa sequence: GSGSGS) to the first 3 exons of *Kras* (aa positions 1-150). The included truncated *Tp53* and *Kras* sequences should not give rise to functional proteins, because they were chosen to have the majority of their functional domains missing. On the C terminus the sequence of an HA-tag (aa sequence: YPYDVPDYA) was linked in frame to the truncated *Kras* orf followed by a stop codon (nucleotide sequence: TGA). The HA-tag was added to monitor transgene expression. In front of the whole transgene construct an N-terminal consensus mammalian Kosak sequence containing a start codon (nucleotide sequence: ACC ATG) was fused. Transgenes coding for mutated human or murine protein backbone sequences with or without HA-tag were designed accordingly. In figure 3.42 A schemes of respective chimeric transgenes are shown. We decided to test both human and murine backbone sequences. On the one hand because the peptides used for vaccination displayed the human backbone sequence, too. On the other hand introduction of a transgene with a foreign, human protein sequence into a murine system might increase the immunogenicity of the murine tumor, which might prevent *in vivo* tumor growth of engineered cell lines *per*

*se*. In this context, also the HA-tag, although it was not described in the literature, might increase the immunogenicity of the tumor.

Before using the designed transgenes for stable integration into the genome of cell line 2277-NS they were tested in transient transfections for cytotoxicity. For this purpose, the constructs were cloned into the mammalian expression vector pDEST-N-eGFP using the gateway technology. This vector added an N-terminal eGFP to the transgene sequence for detection of transgene expression in living cells. First, easily transfectable HEK 293T cells were transfected with the pDEST-N-eGFP constructs using the calcium phosphate precipitation method. Transfected cells were analyzed by fluorescent microscopy and FACS analysis as shown in figure 3.42 B.

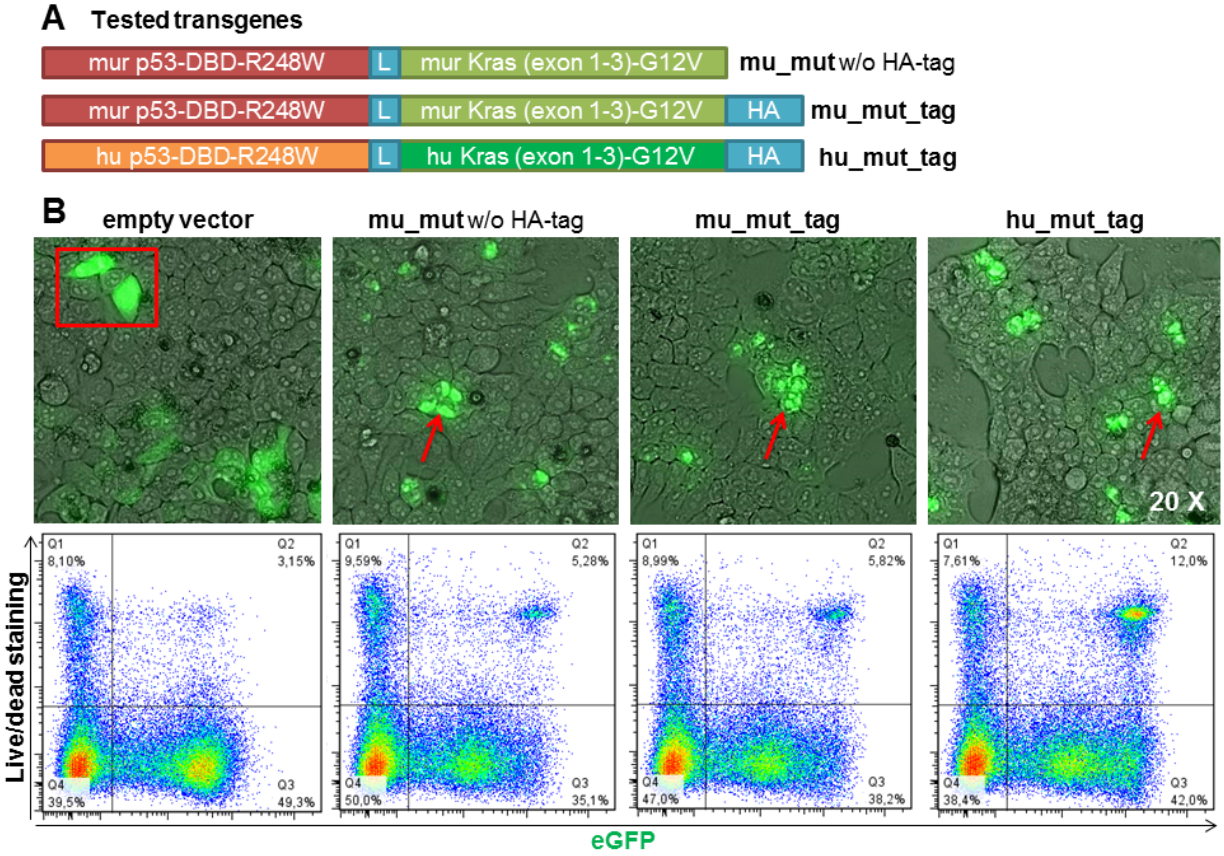


**Figure 3.42**: **Transient expression of mutated *Kras* and *Tp53* chimeric transgenes in HEK 293T cell was feasible and did not result in cytotoxicity. (A)** Schemes of chimeric mutated transgenes prone to be used for stable cell line generation. DBD: *Tp53* DNA binding domain. L: peptide linker, HA: HA-tag, mur: murine cDNA sequence, hu: human cDNA sequence, w/o: without. Human cDNA sequences were codon-optimized for expression in the murine system. **(B)** Transient transfection of HEK 293T cells with mutated *Tp53-Kras*-transgene pDEST-N-eGFP constructs. HEK 293T cells were transfected with pDEST-N-eGFP constructs using the calcium phosphate precipitation method. Fluorescent microscopy pictures were taken and FACS analysis was performed 24 h post transfection. PI was used for live/dead staining in FACS samples.

Fluorescent microscopy pictures implied (upper row) that the eGFP signal in cells transfected with the empty vector was equally distributed over the entire cell body (see the red box in the very left picture). Compared to cells transfected with the empty vector the eGFP signal in cells transfected with transgene

carrying plasmids was restricted to very bright granule-like aggregates within the cells (pointed at with red arrows). The aggregates were found for all transgenes tested (mu_mut without HA-tag and mu_mut and hu_mut with HA-tag). The transfection efficiency for all three transgene constructs was similar (according to figure 3.42 B: mu_mut 35,1 %, mu_mut_tag 38.2 % and hu_mut_tag 42.0 %) and slightly lower than for the empty vector (49.3 %). The viability of HEK 293T cells was not severely decreased after transfection. However, the number of eGFP positive dead cells (quadrant Q2 in displayed FACS dot blots) transfected with one of the three transgene constructs (mu_mut 5.28 %, mu_mut_tag 5.82 % and hu_mut_tag 12.0 %) was slightly higher compared to cells transfected with the empty vector (3.15 %).

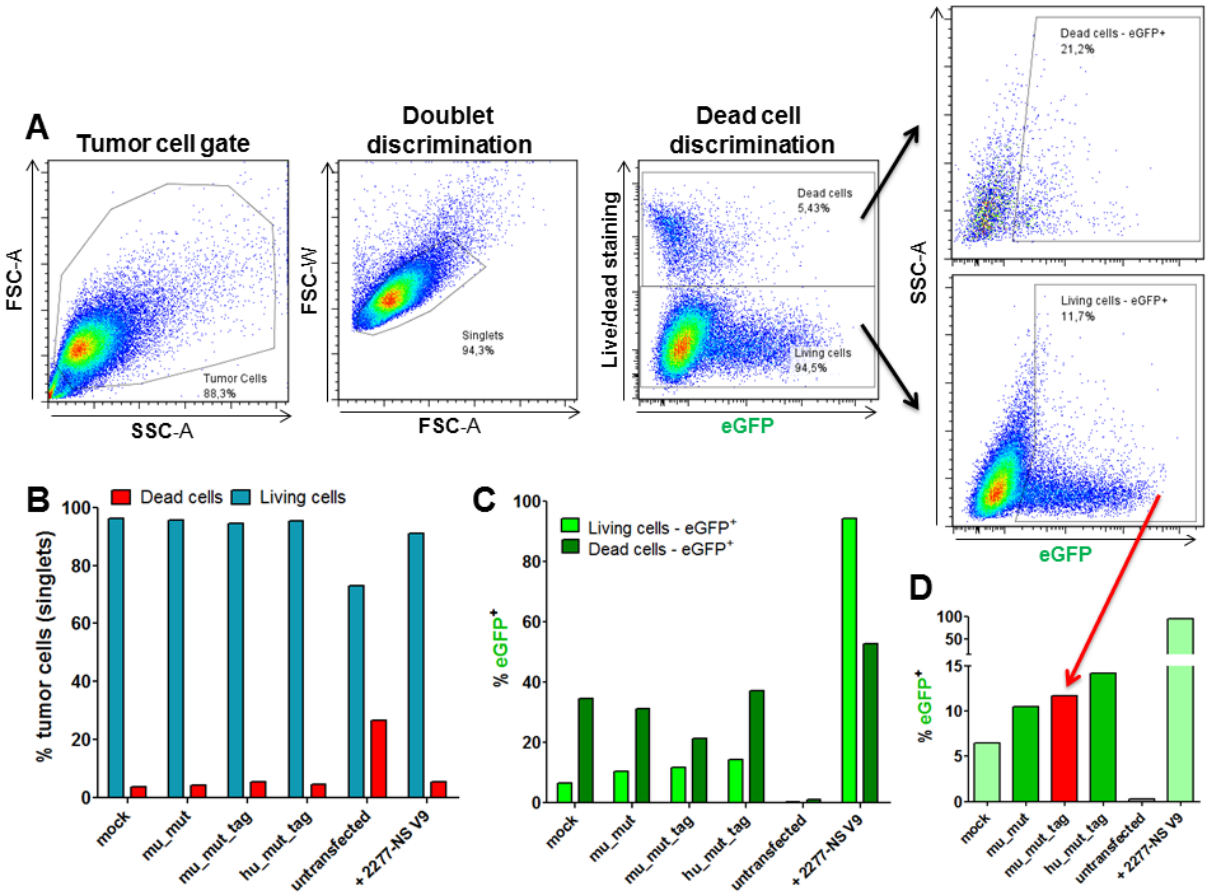


**Figure 3.43**: **Transient expression of mutated *Kras* and *Tp53* chimeric transgenes in 2277-NS A2.DR1 dtg sarcoma cells was feasible and did not result in cytotoxicity. (A)** FACS transgene expression analysis of a transient transfection of 2277-NS A2.DR1 dtg sarcoma cells with mutated *Tp53*-*Kras*-transgene pDEST-N-eGFP constructs. 2277-NS cells were transiently transfected with pDEST-N-eGFP constructs using the X-tremeGENE HP DNA transfection reagent (Roche). FACS analysis was performed 24 h post transfection. PI was used for live/dead staining of FACS samples and gating strategy is exemplary shown for the mu_mut_tag construct transfected sample. **(B)** Percentages of dead and living cells assed by FACS analysis 24 h post transfection with mutated transgene constructs. Mock: cells transfected with the empty pDEST-eGFP vector, + 2277-NS V9: 2277-NS cells infected with retrovirus V9 expressing eGFP and serving as a positive control (viral transduction was kindly performed by Dr. M. Pincha, who also provided the virus). **(C)** Percentages of eGFP positive cells (which stands for transgene expression positive cells) within total living and dead cell populations. **(D)** Zoomed in graph of (C) showing only the percentages of living eGFP (transgene) positive cells 24 h post transfection assessed by FACS analysis.

After finding that expression of the transgene constructs was feasible in HEK 293T cells and did not cause severe cytotoxicity we also tested the constructs in transient transfections of 2277-NS cells

using the X-tremeGENE HP DNA transfection reagent (Roche). Similarly to the finding in HEK 293T cells, eGFP signals after transfection with the chimeric *Kras*/*Tp53* transgenes were restricted to bright granule-like aggregates within the cells (pictures not shown). eGFP expression of transfected cells was quantified by FACS analysis, as well, and results are summarized in figure 3.43. As shown in sub-figure A tumor cells were gated on in forward and side scatter and consequently doublets were discriminated. The live/dead stain signal of singlet cells was plotted against the eGFP signal and dead and living cells were gated on with two separate gates. Then eGFP positive cells were gated on in dead and living cell populations. Figure 3.43 B displays the percentages of dead and living cells after transfection with different plasmids in a bar chart. As a positive control for eGFP expression served 2277-NS infected with retrovirus V9 expressing eGFP. Compared to cells transfected with the empty vector (in the following referred to as 'mock' control) the percentages of dead cells were not increased after transfection with either of the *Kras*/*Tp53* transgene constructs, neither was the percentage of eGFP positive cells within the dead cell populations (see sub-figure 3.43 C). The transfection efficiency, when taking the percentage of eGFP positive living cells into account, was slightly higher for the transgene constructs compared to the empty vector (see sub-figure 3.43 D).

Conclusively, none of the three designed mutated *Kras*/*Tp53* chimeric transgenes (severely) decreased cell viability when transiently expressed in HEK 293T and 2277-NS cells. Also the inclusion of the HA-tag did not have an influence. To estimate the immunogenicity of the three different transgene constructs, they were tested in transiently transfected 2277-NS cells which served as target cells *in vitro* cytotoxicity assays (data will be shown in the following chapter) using T cells from most immunogenic peptides vaccinated mice. Also herein, the HA-tag did not seem to contribute to the immunogenicity of the transgene construct. The findings *in vitro* do not provide a full picture of what might happen in the *in vivo* situation. As we found no sign that the HA-tag might contribute to the immunogenicity of the constructs or impair cell viability after transfection, neither in our experiments nor in the literature, we concluded that the addition of an HA-tag to the transgene construct was uncritical. Concerning the origin of the protein backbone we were not able to estimate the contribution to the immunogenicity *in vivo*. This is why we had stable cell lines generated for each of the respective backbone sequences. Additionally, we wanted to compare cell lines expressing the mutated transgenes to a cell line which expressed a non-mutated version of the murine backbone transgene construct. In conclusion our goal was to construct three different 2277-NS cell lines stably expressing either the mu_mut_tag, hu_mut_tag or the mu_wt_tag construct (see figure 3.44 C).

The in house core facility for proteomics and genomics developed an elegant system to generate stable isogenic recombinant cell lines and offered this as a service, which we made use of. Figure 3.44 A gives an overview of the method's work flow. In a first step recombination sites (FRT) were stably integrated into the genome of the engineered tumor cell line, in our case sarcoma line 2277-NS, using a so called acceptor plasmid. This plasmid carried, next to a neomycin selection marker, an eGFP reporter

gene. Therefore, acceptor cell lines which have stably integrated the acceptor plasmid into *Rosa26* locus became eGFP positive. The core facility performed this first step as an in house service for us and sent us five different acceptor cell lines (also referred to as 'parental cell lines'), which we tested for their HLA.A2 expression status in FACS. This was necessary because the generation of the acceptor cell lines was associated with vigorous passaging during which some of the generated parental lines might have down-regulated HLA.A2 expression which was indeed the case. Figure 3.44 B shows the results of the HLA.A2 FACS staining for the two acceptor cell lines we chose to be continued with. Thereby, parental line #5 showed an intermediate, whereas parental line #4 showed a high HLA.A2 expression.

After selection of the most suitable acceptor cell lines the core facility continued with the integration of the three *Kras*/*Tp53* chimeric transgenes. Transgenes were cloned via the Gateway technology into expression shuttle vectors resulting in 'expression plasmids', which carried a doxycycline (DOX) inducible expression system and sequences for site-specific recombination. Acceptor cell lines were then transfected with transgene carrying expression clones facilitating site-specific recombination between recombination sites integrated in the first step into the genomes of the acceptor cell lines and recombination sites in the expression clone. Recombination yielded in eGFP negative cells. These cells were selected for by a simultaneously integrated hygromycin selection gene. Single cell clones were picked during selection and consecutively expanded. The core facility provided us with two clones for the hu_mut_tag construct (clone 4.1.2.1 and clone 5.1.2.1), two clones for the mu_mut_tag construct (clone 5.2.2.1 and 5.2.2.2) and one clone for the mu_wt_tag construct (clone 5.3.2.2). In a first step we tested the received clones for HLA.A2 expression status via FACS analysis as shown in figure 3.44 D. The two clones carrying the hu_mut_tag transgenes (first two histogram form the left) displayed a high HLA.A2 expression whereas the HLA.A2 expression of the other three clones was intermediate. The *in vitro* doubling time was decreased compared to the sarcoma line 2277-NS for all of the clones, but especially the mu_wt_tag clone grew particularly slow. The best growing clones *in vitro* were those carrying the mu_mut_tag transgene. What is more, Dr. R. Will from the core facility recommended us to keep the clones under hygromycin and puromycin selection pressure during *in vitro* culture. Thereby, hygromycin selected for the *Kras*/*Tp53* chimeric transgenes and puromycin contributed to sustained HLA.A2 expression, because the HLA.A2 transgene was introduced into the mice using a puromycin resistance gene for selection. Nonetheless, the core facility assured us that *in vivo* transgene expression would be sustained over the course of tumor challenge experiments in the absence of hygromycin. Additionally important is the fact that the transgene expression was inducible by treating the cells with the antibiotic doxycycline (DOX). We initially tested the induction of transgene expression by *in vitro* treating cells with DOX for 72 h, harvesting the cells and performing western blots to detect transgene expression via a HA-tag specific antibody in order to determine the best expressing clones. The results (data not shown) were ambiguous and pointing towards a strong leakiness of the DOX-inducible system, because also cells which were not treated with DOX partially expressed the transgene.

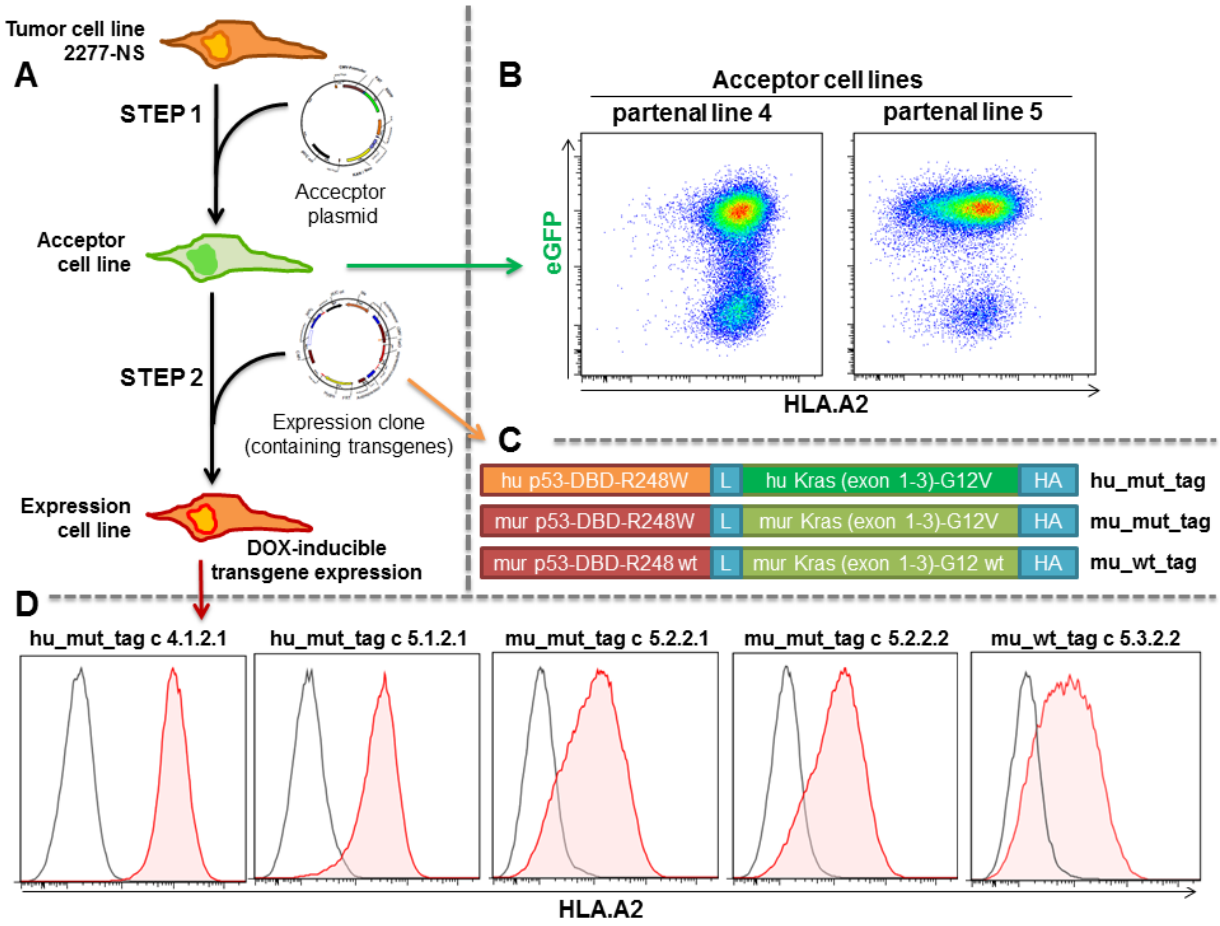


**Figure 3.44**: **Generation of stable 2277-NS A2.DR1 dtg sarcoma cell line clones expressing mutated *Kras* and *Tp53* chimeric transgenes. (A)** Scheme of the procedure for the generation of stable mutated and wt *Kras* and *Tp53* chimeric transgene expression clones. The method was developed by Dr. R. Will and colleagues from in the house core facility of proteomics and genomics. Generation of stable expression clones was done as an in house service. In step 1 recombination sites (FRT) are stably integrated into the genome of the tumor cell line using the so called acceptor plasmid. This plasmid carries, next to a neomycin selection marker, an eGFP reporter gene. Therefore, acceptor cell lines which have stably integrated the acceptor site into their genomes are eGFP positive. Transgenes are cloned via the Gateway technology into the expression clones, which also carry a doxycycline (DOX) inducible expression system. Acceptor cell lines are then transfected with transgene carrying expression clones facilitating site-specific recombination between recombination sites integrated in step 1 into the genomes of the acceptor cell lines and recombination sites in the expression clone. Recombination yields in eGFP negative cells. These cells were selected for by a simultaneously integrated hygromycin selection gene. Single cell clones are picked during selection. **(B)** Two out of five acceptor cell lines analyzed for HLA.A2 and eGFP expression by FACS. Parental line 4 and 5 were chosen to be continued with because of high HLA.A2 expression. Cultured cells were stained for human HLA.A2 (HLA class I) with fluorescent-labeled MHC-specific antibody and dead cells were excluded by PI positive staining. **(C)** Schemes of chimeric mutate and wt transgenes shuttled into expression clones for genomic integration by site-directed recombination. DBD: *Tp53* DNA binding domain. L: peptide linker, HA: HA-tag, mur: murine cDNA sequence, hu: human cDNA sequence. Human cDNA sequences were codon-optimized for expression in the murine system. **(D)** Surface HLA.A2 expression of stable DOX-inducible transgene expression clones. Cultured cells were stained for human HLA.A2 (HLA class I) with fluorescent-labeled MHC-specific antibody and analyzed with FACS Canto II. Bright red, tinted: expression clone cells stained with specific anti-HLA.A2 antibody, grey lines: isotype control. c: clone with respective number.

After finishing *in vitro* analysis the next step was to analyze the tumorigenicity and transgene induction of the 2277-NS *Kras*/*Tp53* chimeric transgene expressing clones *in vivo*. Therefore, two A2.DR1 dtg mice were inoculated subcutaneously with 5 x $10^5$ cells of a respective 2277-NS clone resuspended in Matrigel each, resulting in in total 5 groups of mice. One week later (day 7 after tumor inoculation) one mouse per group was fed with 2 g/l DOX in the drinking water *ad libitum* until the end of the challenge experiment to induce and sustain transgene expression, whereas the second mouse of each respective

group received normal drinking water. During the first week for DOX administration some of the mice lost weight but soon recovered in the second week of DOX treatment and kept this state until the end of the experiment. Figure 3.45 A shows the tumor growth curves of each individual, differentially treated mouse. The clone expressing the wt *Kras*/*Tp53* HA-tagged construct with the murine backbone sequence (bright green line) did not give rise to tumors *in vivo* neither in the mouse treated with DOX nor in the untreated mouse. Due to its additionally hampered *in vitro* growth capacities we concluded that the clone's fitness was not sufficient for *in vivo* experiments. The mu_mut_tag clone 5.2.2.2 as well as the hu_mut_tag clone 5.1.2.1 grew out with similar kinetics in both animals tested per group regardless of DOX treatment. (Unfortunately the animal challenged with clone 5.1.2.1 and not receiving DOX died on day 30 of the challenge experiment.) Interestingly, the second mu_mut_tag clone 5.2.2.1 and the second hu_mut_tag clone 4.1.2.1 showed altered growth kinetics between the respective DOX-treated (filled symbols, squares) and untreated animals (filled symbols, dots). Upon DOX-treatment in both cases tumors did not grow out whereas they did in the corresponding untreated animals.

We were wondering whether this observation might be attributed to the immunogenicity of the introduced transgenes. To answer this question all accessible tumors were excised from the tumor bearing animals at the end of the challenge experiment after mice were sacrificed. Whole protein extracts were performed from tumor lysates and used for western blot analysis. Transgene expression was detected using an anti-HA-tag specific antibody and equal loading was validated by the detection of the house keeping gene β-actin. Figure 3.45 B zooms in the tumor growth curves for the two different mu_mut_tag clones leaving out all the growth curves of all the other clones tested. This highlights that tumors of three animals were accessible for western blot analysis at the end of the challenge experiment, which are 5.2.2.1 untreated, 5.2.2.2 untreated and 5.2.2.2 + DOX. In the mouse challenged with clone 5.2.2.1 and fed with DOX no tumor tissue was found at the side of tumor inoculation, but only a small encapsulation which did not provide enough material for western blot analysis. Figure 3.45 C shows the corresponding western blot picture. Whole protein lysates from mu_mut_tag transfected HEK 293T cells served as positive controls for transgene detection. The specific band, though, is bigger than those of the transgene detected in the tumors because of the additional N-terminal eGFP protein (originating from the use of the pDEST-N-eGFP constructs for transient transfection). Protein lysates from the original cell line 2277-NS, the C57BL/6 melanoma line B16-F1 and the CRC cell line SW480 served as negative controls. The HA-tagged transgene bands are highlighted with a red square. Having a look at the transgene signals detected, tumor lysates of animals which did not receive DOX for the induction of transgene expression, showed thick bands, which reinforced the *in vitro* evidence that the DOX-inducible system seemed to be very leaky. Hence, one could conclude that the rejection of the clones 5.2.2.1 and 4.1.2.1 tumors after DOX treatment could not be exclusively attributed to the potentially immunogenic introduced transgenes, as they were also highly expressed in animals which did not receive DOX due to the leakiness of the inducible system. On the other, one could argue that an extremely high transgene expression after DOX treatment could lead to rejection. For the clone 5.2.2.2 transgene expression could not be further

enhanced upon DOX treatment (at least according to the western blot results of fig. 3.45 D). However, it might have been of relevance for clone 5.2.2.1.

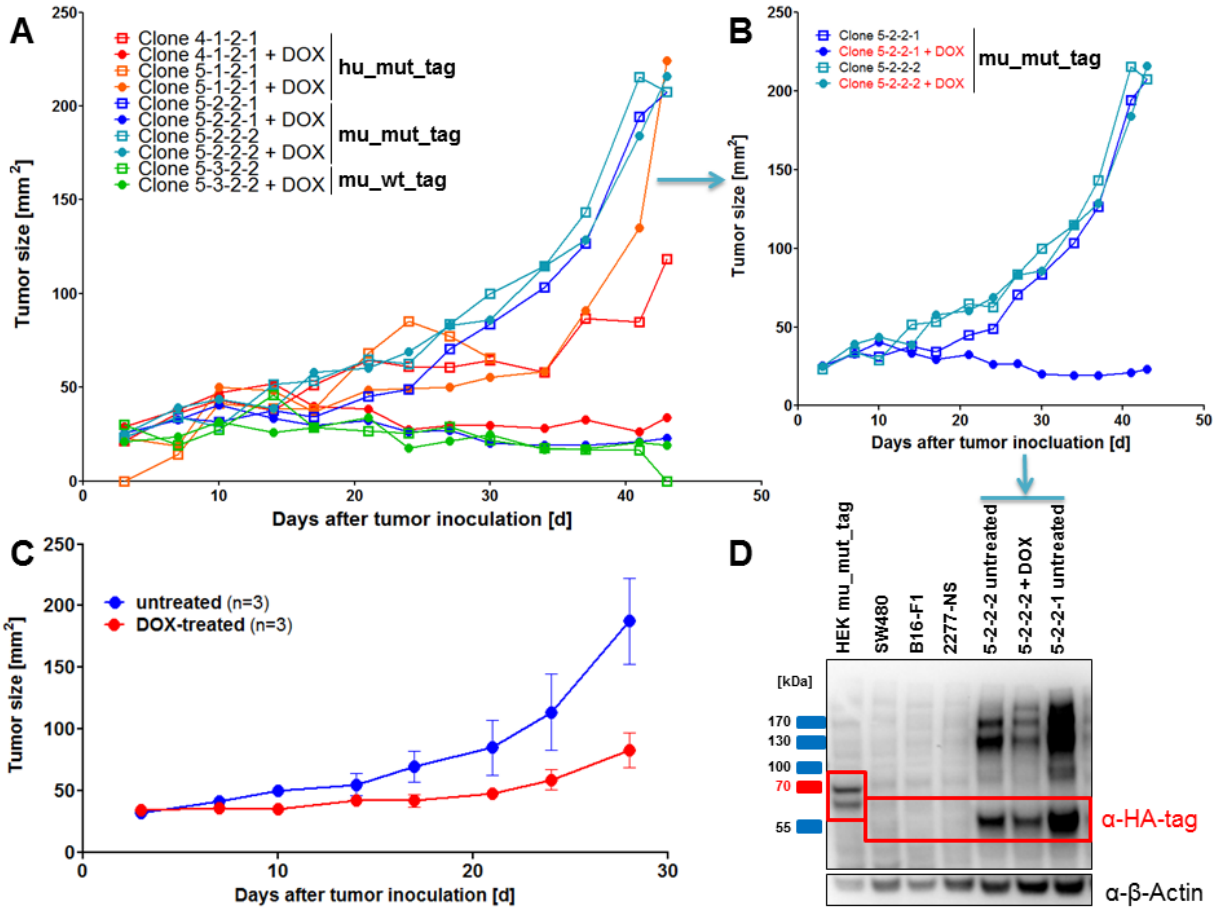


**Figure 3.45**: ***In vivo*** **tumor growth characteristics and transgene expression of chimeric mutated and wt *Tp53* and *Kras* transgenes in DOX-inducible expression cell lines. (A)** Test tumor challenge with the 5 different 2277-NS transgene expression clones. Two female A2.DR1 dtg mice were inoculated with one out of the five different expression clones tested, resulting in five groups of two mice each. 5 x $10^5$ tumor cells resuspended in matrigel were injected subcutaneously into the right flank of each animal. One week (7 d) after tumor inoculation one mouse per group was fed 2 g/l DOX in the drinking water *ad libitum* until the end of the tumor challenge experiment to induce and sustain transgene expression. The second mouse of each group was fed with normal drinking water. One day 43 of the challenge mice were sacrificed and tumors were excised for western blot analysis. **(B)** Zoomed in figure of the test tumor challenge shown in (A) displaying only the tumor growth curves for the expression clones 5.2.2.1 and 5.2.2.2 which are expressing the mu_mut_tag transgene. **(C)** Influence of DOX treatment on 2277-NS mother cell line *in vivo* tumor growth. Six male A2.DR1 dtg mice were inoculated with 2,5 x $10^5$ tumor cells resuspended in matrigel by subcutaneous injection into the right flank of each animal. One week (7 d) after tumor inoculation three mice were fed 2 g/l DOX in the drinking water *ad libitum* until the end of the tumor challenge experiment. The remaining three mice were fed with normal drinking water. n: number of biological replicates; error bars, mean ± SEM **(D)** Western blot analysis of protein extracts from tumor lysates of tumor tissue taken from mice of the test tumor challenge shown in (A) and (B) and protein extracts of cultured cells serving as controls. Whole protein extract from mu_mut_tag-pDEST-N-eGFP transfected HEK 293T cells served as positive control for transgene expression. SW480, B16-F1 and mother cell line 2277-NS extracts served as negative controls. The HA-tag was stained for by anti-HA-specific monoclonal antibody (α-HA-tag) and as a loading control served a staining for β-actin (α-β-Actin specific monoclonal antibody). Detection of primary antibodies was performed with secondary HRP-conjugated goat-anti mouse antibody and ECL reagent.

Compared to the original cell line 2277-NS all clones tested showed a delayed tumor outgrowth. We were wondering whether DOX treatment might account for this observation or was even responsible for the rejections of tumors in the cases described before. In order to solve this issue, mice were

challenged with the original sarcoma cell line 2277-NS. One week after the beginning of the challenge one group of mice was fed DOX in the drinking water. As it becomes apparent in figure 3.45 C that DOX administration indeed delayed also the outgrowth of the original cell line 2277-NS (red growth curve) compared to untreated mice (blue tumor growth). Rejection of the tumor, however, was not the case in any of the DOX treated mice which argues against the hypothesis that DOX treatment might be responsible for the rejection of some tumors in the clone testing experiment.

At the end of the experiment, immune responses of T cells purified from the mice challenged with the different clones were monitored by two-color cytokine secretion assays after short term *in vitro* re-stimulation on DCs pulsed with the mutated peptide Kras G12V and p53 R248W and corresponding wt counterparts (data not shown). Interestingly, in some of the animals we found evidence for mutation specific responses although background controls were high and the experiment was not representative due to the limited number of tested animals. Nonetheless, as we will see in the last chapter, the detection of mutation specific T cell responses in non-vaccinated tumor-bearing animals proved true.

## 3.6. *In vitro* cytotoxicity assays and tumor challenge experiments provide evidence for the natural processing of epitopes comprising the mutations p53 R248W and Kras G12V

In chapter 3.3. we identified potential epitopes within the most immunogenic long peptides Kras G12V and p53 R248W by *in silico* and *in vitro* analysis. For the *in vitro* analysis we used DCs pulsed with peptides as antigen presenting cells. The question which remained unsolved is whether also tumor cells are able to naturally process and present the mutated antigens to T cells. Evidence was found when the influence of *in vivo* growing tumors on effector T cell responses in tumor bearing mice was explored. Moreover, the next step in our work flow of the analysis of mutated tumor antigen-specific T cells induced by long peptides vaccination was to analyze their potential to actively kill tumor cells expressing the respective mutated antigens. Therefore, the *in vitro* cytotoxicity of mutated long peptide induced effector T cells subsets towards mutated antigen-expressing tumor cells was investigated.

To investigate the cytolytic potential of long peptide vaccination-induced, mutated tumor-antigen specific T cells, we employed those as effector cells in *in vitro* cytotoxicity assays. Therefore, A2.DR1 dtg mice were vaccinated with the two most immunogenic peptides p53 R248W and Kras G12V in IFA-based formulations together with CpG as an adjuvant. Pan T cells were then purified from these animals and re-stimulated in two different ways. In pilot experiments (to adjust the assay parameters) T cells were short term re-stimulated for 16 h on mutated peptide pulsed DCs. Later experiments made use of T cells which were fully re-stimulated on mutated peptides pulsed DCs and in presence of irradiated splenic feeder cells for 6 d. In both cases $CD8^+$ T cells were separated from $CD4^+$ T cells on the day of the cytotoxicity assay and used right away as effector cells. Furthermore, effector T cells purified from untreated, non-immunized mice were used as controls.

For the pilot assays 2277-NS cells transiently transfected with the pDEST-N-eGFP constructs carrying the mutated *Kras*/*Tp53* transgenes (see previous chapter) served as target cells. In the second row of experiment the stably transgene expressing 2277-NS clones were used as effector cells. Thereby, the transgene expression of the clones had to be induced by DOX-treatment for 72 h prior the assay. We employed the classical chromium release method as it is still the gold standard for cytotoxicity assays and very sensitive. Consequently, target cells were labeled with radioactive $Na_2{}^{51}CrO_4$-solution. Labeled target cells were co-cultured with either re-stimulated, purified $CD8^+$ or $CD4^+$ effector T cells. Supernatants from co-cultures were harvested for analysis after 6 and 20 h. Generally the 20 h samples did not result in reliable data but provided the information whether cytotoxicity increased upon longer co-incubation, which was indeed rarely the case. We tested both $CD8^+$ and $CD4^+$ T cells as cytolytic effectors because also $CD4^+$ T cells are described to be able to display a cytotoxic phenotype. Due to the strongly reduced $CD8^+$ population in the A2.DR1 dtg mice we were speculating that it might be very likely to find cytotoxic $CD4^+$ T cell in our system to compensate for the partial lack of $CD8^+$ T cells. Next to the direct *in vitro* cytolytic activity we stained the effector T cells for the cytotoxicity markers CD107a, granzyme B and perforin in FACS and assessed the cytokine response pattern by IL-2/IFN-γ two color cytokine secretion assays.

Figures 3.46 and 3.47 summarize the results of cytotoxicity assays and cytokine response patterns obtained with $CD8^+$ and $CD4^+$ effector T cells, respectively. Because of the limited number of $CD8^+$ T cells only few target cells could be tested compared to $CD4^+$ T cells. Starting with the $CD8^+$ effector T cells, the cytotoxicity measured as percentage of specific lysis is low and ranging between 5 to 25 per cent. The experiment shown in subfigure 3.46 A employed short term re-stimulated effectors and transient transfectants as target cells, whereas the experiments of figure 3.47 C was conducted with fully re-stimulated effector cells and stable 2277-NS clones. In both experiments target cells expressing the mutated *Tp53 R248W*/*Kras G12V* transgene with the human backbone sequence were killed most efficiently (hu_mut_tag, blue curves). Target cells expressing the murine backbone sequence mutated transgene were ranging second place (mu_mut_tag, red curves). No cytotoxicity was detected for target cells expressing the wt, murine transgene (green curve, in the second experiment, mu_wt_tag) and unmodified 2277-NS cells (experiment shown in (C), grey curve) or empty vector transfected 2277-NS cells (experiment shown in (A), grey curve). Effector T cells obtained from untreated mice (curves indicated with UN, in light colors) did not show any cytolytic activity neither against the mu_mut_tag transgene expressing target cells (light red curves) nor against empty vector transfected 2277-NS cells (light grey curve, experiment (A)).

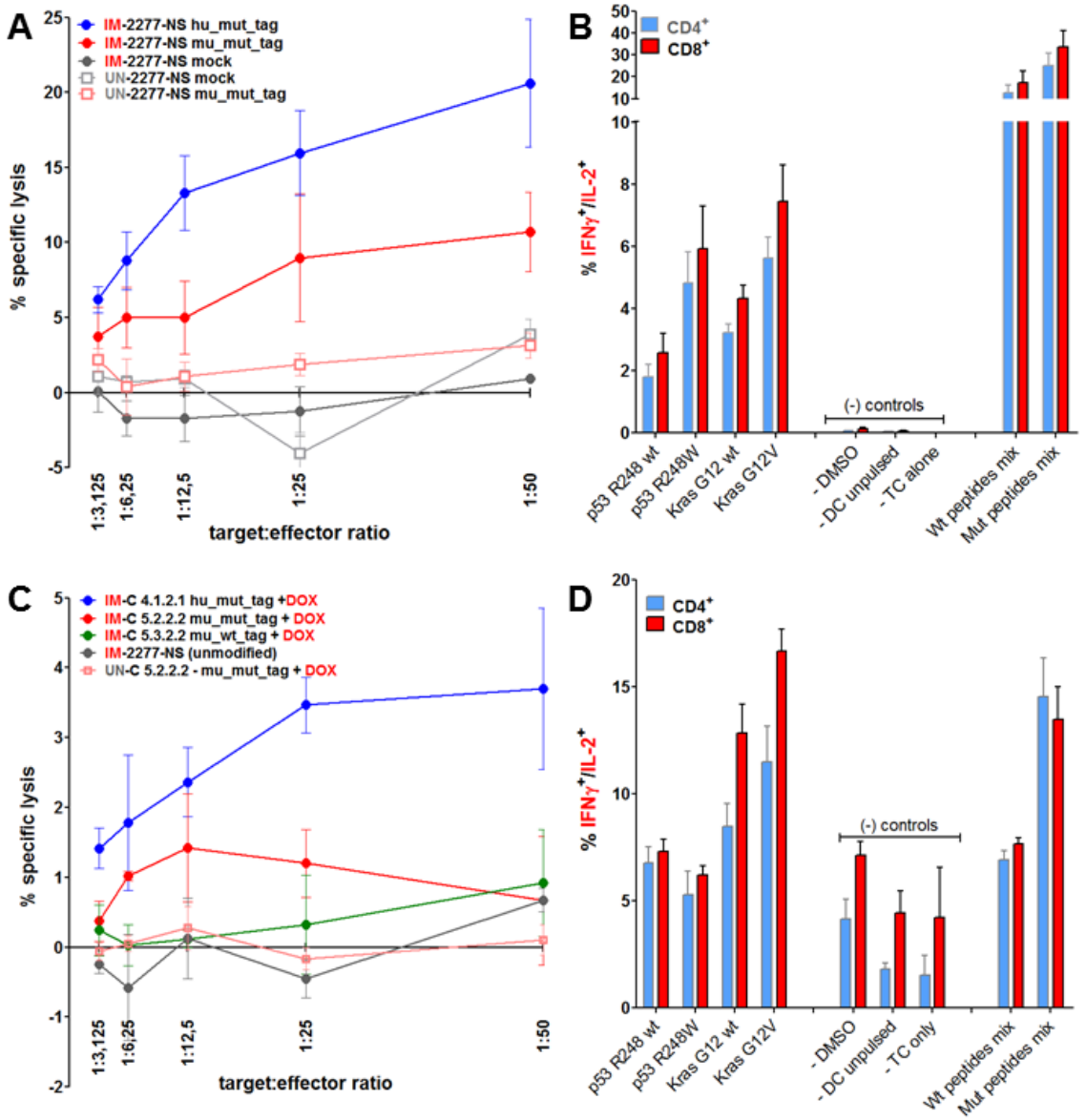


**Figure 3.46**: **CD8$^+$ T cells from mutated Kras G12V and p53 R248W peptides vaccinated A2.DR1 dtg mice kill mutations expressing target cells *in vitro* (A)** $^{51}$Cr release *in vitro* cytotoxicity assay with CD8$^+$ effector T cells from mutated peptides vaccinated mice and transiently transfected 2277-NS cells as targets. Target 2277-NS cells were transfected with mutated *Tp53*/*Kras*-transgene carrying pDEST-N-eGFP constructs 20 h before the beginning of the cytotoxicity assay. Transfected target cells were harvested and labeled with radioactive $Na_2{}^{51}CrO_4$-solution. Effector pan T cell derived from Kras G12V/p53 R248W mutated peptides vaccinated A2.DR1 dtg mice were short term re-stimulated for 16 h on mutated peptides pulsed CD11c$^+$ BM-DCs. Thereafter, CD8$^+$ T cells were purified by positive MCAS separation. Effector and $^{51}$Cr-labeled target cells were co-incubated for 6 h. mock: 2277-NS transfected with the empty pDEST-N-eGFP vector, IM: effector cells derived from mutated peptides vaccinated mice, UN: effector T cells derived from naïve mice. error bars, mean ± SEM **(B)** Cytokine responsiveness of effector T cells used for the cytotoxicity assay shown in (A) after 16 h *in vitro* re-stimulation on mutated peptides pulsed DCs assed by two color-cytokine secretion assay. CD8$^+$ T cell responses are highlighted in bright colors. **(C)** $^{51}$Cr release *in vitro* cytotoxicity assay with CD8$^+$ effector T cells from mutated peptides vaccinated mice and mutated and wt *Kras*/*Tp53* transgene expressing stable 2277-NS clones. Transgene expression in 2277-NS clones (target cells) was induced by DOX treatment for 72 h before the cytotoxicity assay (indicated as '+DOX'). Induced target cells were harvested and labeled with radioactive $Na_2{}^{51}CrO_4$-solution. Effector pan T cell derived from Kras G12V/p53 R248W mutated peptides vaccinated A2.DR1 dtg mice were *in vitro* re-stimulated for 6 d on mutated peptides pulsed CD11c$^+$ BM-DCs and irradiated splenocytes as feeder cells. Thereafter, CD8$^+$ T cells were purified by positive MCAS separation. Effector and $^{51}$Cr-labeled target cells were co-incubated for 6 h. IM: effector cells derived from mutated peptides vaccinated mice, UN: effector T cells derived from naïve mice, C: 2277-NS clone with respective number. error bars, mean ± SEM **(D)** Cytokine responsiveness of effector T cells used for the cytotoxicity assay shown in (C) after 6 d *in vitro* re-stimulation assed by two color-cytokine secretion assay. CD8$^+$ T cell responses are highlighted in bright colors. Each test was performed in triplicate instances. Results are plotted as means of triplicate assays ± SEM.

The cytokine responses of effector T cells for both experiments are shown in subfigures 3.46 B and D as percentages of IFN-γ/IL-2 double positive cells. The short term re-stimulated $CD8^+$ T cells (bright red bars, fig. 3.46 B) were found, as expected, to display Kras G12V and p53 R248W mutation specific cytokine responses higher than corresponding wt counterparts upon *in vitro* re-stimulation with respective peptides pulsed DCs. In contrast, mutation specificity of effector T cells which were re-stimulated for 6 d *in vitro* seemed to be partially washed out as the response against the mutated p53 R248W peptide did not exceed the wt response. Moreover, a generally higher *in vitro* cytokine responsiveness observed in the 6 d cultures was accompanied by a rise of unspecific signals towards background controls (indicated as (-) controls), which was especially striking for $CD8^+$ T cells.

Also A2.DR1 dtg $CD4^+$ T cells displayed, as speculated, a cytotoxic activity in chromium release assays. Figure 4.47 (A) shows an experiment with short term re-stimulated effector $CD4^+$ T cells and transiently transfected 2277-NS target cells, which were co-cultured for 20 h. As mentioned before, 20 h samples normally did not yield in reliable data and the displayed experiment was definitely an exception. Nonetheless it is presented here, because it suggests that $CD4^+$ T cells could be potent killers. All three target cell groups expressing the mutated transgene with either the human (again shown as a blue curve) or the murine (red (HA-tagged transgene) and orange (no HA-tag) curves) backbone were killed with efficiencies between 80 and 100 per cent specific lysis at highest target to effector ratios. The killing of the two control targets, untreated (light gray curve) and empty vector transfected (dark gray curve) 2277-NS cells, was comparably low and did not exceed 20 % specific lysis.

The second experiment displayed in subfigures 3.47 C and D was carried out with stable transgene-expressing 2277-NS clones serving as target cells and 6 d *in vitro* re-stimulated effector T cells. As for the $CD8^+$ T cells the mutation specificity for mutated p53 R248W could not be detected in the cytokine profile of the $CD4^+$ effector cells (figure 3.47 B) and IFN-γ/IL-2 responses towards the background controls were increased. The highest killing efficiency in this experiment was detected for the hu_mut_tag expressing target cells (bright blue curves) and was ranging around 20 % specific lysis at highest effector to target ratios. With lower efficiency target cells expressing the mutated murine backbone transgene (mu_mut_tag, bright red curve), the wt murine transgene (mu_wt_tag, bright green curve) and unmodified 2277-NS (dark gray curve) cells were killed. The additional negative control B16-F1, expressing murine MHC molecules of the C57BL/6 haplotype, was barely recognized (light gray curve dot symbols). In contrast, effector T cell derived from untreated A2.DR1 dtg mice did not kill any of the five target cell lines tested (curves in light colors and with open square symbols). Conclusively, as for the $CD8^+$ effector T cells the target cells expressing the human backbone mutated transgene were killed most efficiently by $CD4^+$ T cells. However, the killing of murine backbone wt and mutated transgene expressing cells lay in the same range of detected specific lysis. And also unmodified 2277-NS cells were killed equally well.

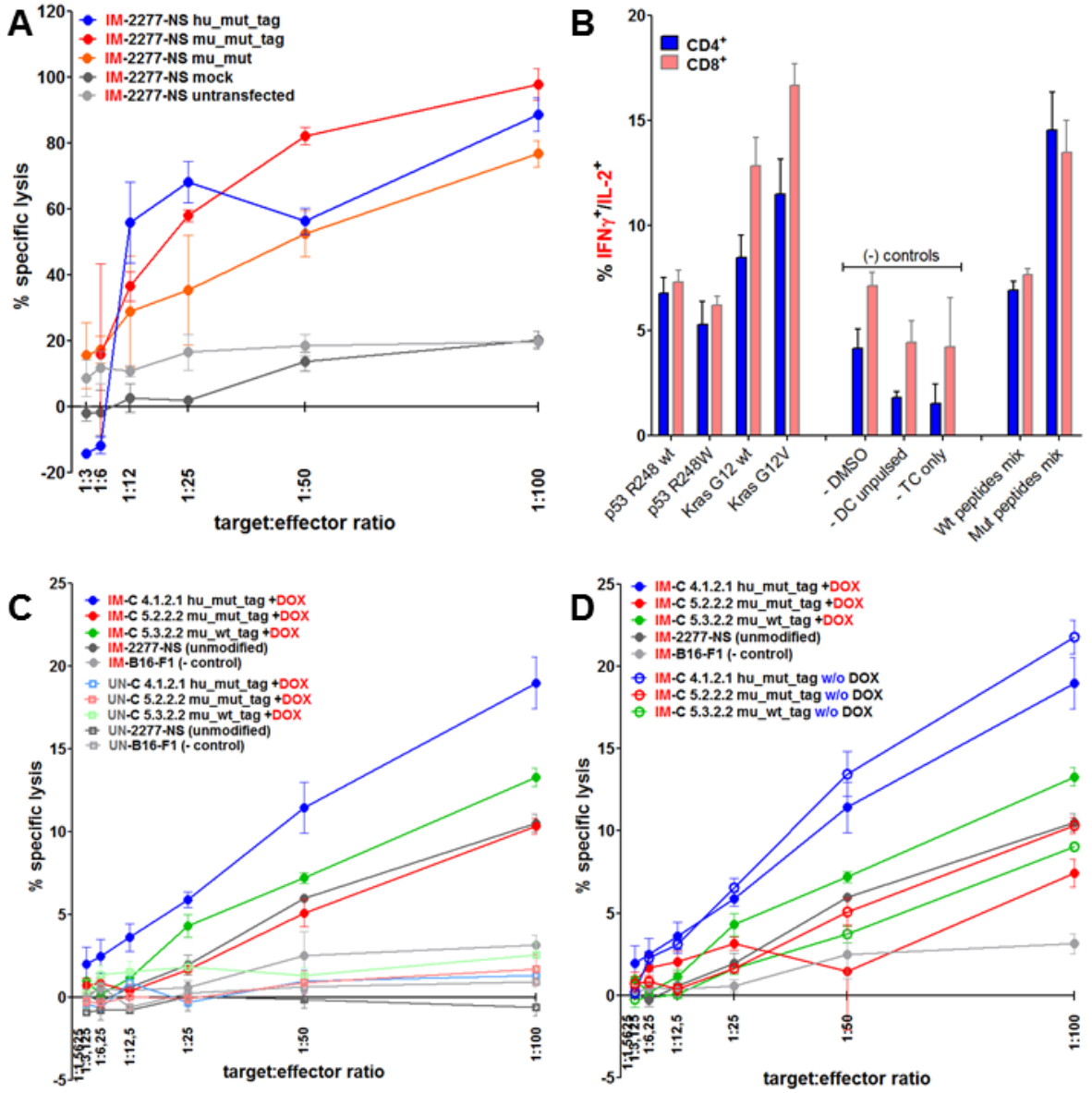


**Figure 3.47**: **CD4$^+$ T cells from mutated Kras G12V and p53 R248W peptides vaccinated A2.DR1 dtg mice kill mutations expressing target cells *in vitro* (A)** $^{51}$Cr release *in vitro* cytotoxicity assay with CD8$^+$ effector T cells from mutated peptides vaccinated mice and transiently transfected 2277-NS cells as targets. Target 2277-NS cells were transfected with mutated *Tp53*/*Kras*-transgene carrying pDEST-N-eGFP constructs 20 h before begin of the cytotoxicity assay. Transfected target cells were harvested and labeled with radioactive $Na_2{}^{51}CrO_4$-solution. Effector pan T cell derived from Kras G12V/p53 R248W mutated peptides vaccinated A2.DR1 dtg mice were short term re-stimulated for 16 h on mutated peptides pulsed CD11c$^+$ BM-DCs. Thereafter, CD8$^+$ T cells were purified by positive MCAS separation and the resulting CD8 negative CD4$^+$ fraction was used as effector cells. Effector T cells and $^{51}$Cr-labeled target cells were co-incubated for 20 h. mock: 2277-NS cells transfected with the empty pDEST-N-eGFP vector, IM: effector cells derived from mutated peptides vaccinated mice, UN: effector T cells derived from naïve mice. **(B)** Cytokine responsiveness of effector T cells used for the cytotoxicity assay shown in (C) and (D) after 6 d of *in vitro* re-stimulation on mutated peptides pulsed DCs assed by two color-cytokine secretion assay. CD4$^+$ T cell responses are highlighted in bright colors. **(C) & (D)** $^{51}$Cr release *in vitro* cytotoxicity assay with CD4$^+$ effector T cells from mutated peptides vaccinated mice and mutated and wt *Kras/Tp53* transgene expressing stable 2277-NS clones. Transgene expression in 2277-NS clones (target cells) was induced by DOX treatment for 72 h before the cytotoxicity assay (indicated as '+DOX'). Induced and non-induced (indicated as 'w/o DOX') 2277-NS clones, unmodified 2277-NS and B16-F1 (negative control) target cells were harvested and labeled with radioactive $Na_2{}^{51}CrO_4$-solution. Effector pan T cells derived from Kras G12V/p53 R248W mutated peptides vaccinated A2.DR1 dtg mice were *in vitro* re-stimulated for 6 d on mutated peptides pulsed CD11c$^+$ BM-DCs and irradiated splenocytes as feeder cells. Thereafter, CD8$^+$ T cells were purified by positive MCAS separation and the resulting CD8 negative CD4$^+$ fraction was used as effector cells. Effector and $^{51}$Cr-labeled target cells were co-incubated for 6 h. IM: effector cells derived from mutated peptides vaccinated mice, UN: effector T cells derived from naïve mice, C: 2277-NS clone with respective number. Each test was performed in triplicate instances. Results are plotted as means of triplicate assays ± SEM.

Moreover, sub-figure 3.47 D is comparing target cells in which transgene expression was induced ('+ DOX') to targets which were not treated with DOX ('w/o DOX', curves with open dot symbols) prior the chromium release assay. For couples of respective DOX treated (closed dot symbols) and untreated (open dot symbols) targets the two respective killing curves progress side by side, which means they are killed with the same efficiency. In the previous chapter it became obvious from western blot analysis that the transgene expression of the DOX-inducible expression system of the stable 2277-NS clones was extremely leaky. The finding that also non-induced 2277-NS clone target cells were efficiently killed reinforces the previous finding.

Before, we found that wt transgene expressing and unmodified 2277-NS cells were killed with the same efficiency by $CD4^+$ T cells as those targets expressing the mutated murine transgene. One reason for this observation might be attributed to the intrinsic p53 R248H mutation 2277-NS cells and all its progenies were carrying and which might contribute to the recognition by T cells. We tested the immunogenicity of the p53 R248H mutation by vaccinating of A2.DR1 dtg mice with a long peptide carrying the mutation and displaying the murine backbone sequence. The *in vitro* recall responsiveness of T cells purified from vaccinated mice was tested for the murine and human long wt peptides and the murine mutated peptide in two-color cytokine secretion assays. As shown in figure 3.48 it was possible to detect IFN-γ (subfigure A), IL-2 (subfigure B) and IFN-γ/IL-2 double (subfigure B) positive T cells after stimulation with the p53 R248H mutated peptide. Also the murine and human wt sequences were responded to by both $CD4^+$ and $CD8^+$ T cells, although, to a lesser extent than the mutated peptide (except the murine wt sequence in case of IL-2 secretion). Hence, it might well be that the mutation p53 R248H expressed by 2277-NS cells contributed to the cell line's immunogenicity as wt or even p53 R248W specific T cells might cross-react with a p53 R248H carrying peptide sequences possibly presented by 2277-NS.

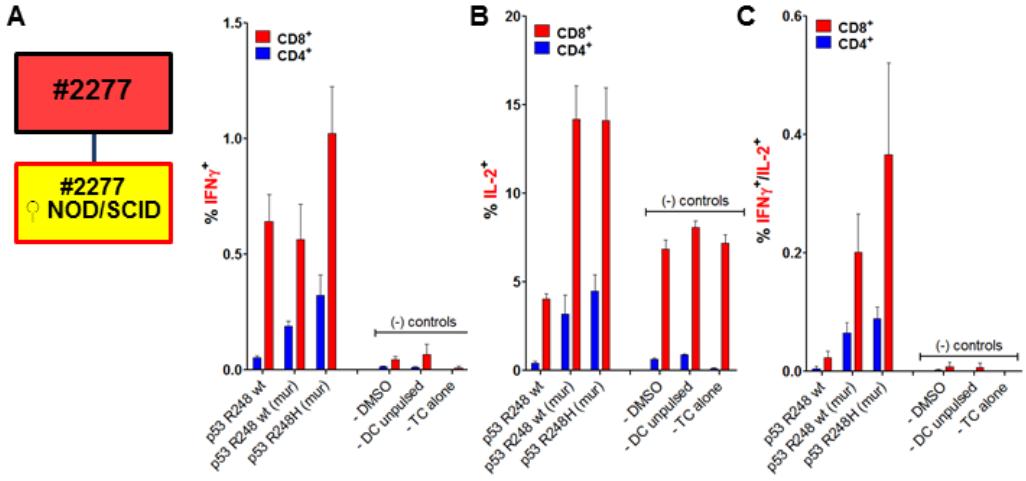


**Figure 3.48**: **2277-NS intrinsic mutation *Tp53* R248H was immunogenic when used for active vaccination.** Recall responses against mutated and wt peptides sequences tested in A2.DR1 dtg mice immunized with p53 R248H (mur) and p53 R273C mutated peptides. *In vitro* recall responses were obtained from two-color cytokine secretion assays (IL-2, IFN-γ) with pan T cells purified from immunized mice. Percentages of IFN-γ (**A**), IL-2 (**B**) and IFN-γ/IL-2 (**C**) double positive $CD8^+$ and $CD4^+$ T cells upon *in vitro* recall against single wt and mutated peptides presented by $CD11c^+$ DCs are displayed. Each peptide and control sample was tested in triplicate instances. Results are plotted as means of triplicate assays ± SEM.

Next to the direct killing efficiency in *in vitro* cytotoxicity assays we also analyzed the effector T cells for the expression of cytotoxicity and degranulation markers by FACS. More precisely, we stained for the cytolytic proteins Granzyme B and Perforin and the degranulation marker CD107a. In figure 3.49 part I resulting FACS dot blots for $CD4^+$ (light blue background) and $CD8^+$ (light red background) positive T cells are sown. $CD8^+$ as well as $CD4^+$ T cells expressed the degranulation marker CD107a and granzyme B upon re-stimulation on DCs pulsed with either mutated mixed (Kras G12V, p53 R248W) or wt mixed (Kras G12 wt, p53 R248 wt) peptides. Whereas for the $CD8^+$ T cell population roughly 15 % of cells were CD107a/granzyme B double positive, hardly any double positive cells were detected for the $CD4^+$ T cell population. A similar finding was made when analyzing the perforin and granzyme B expression together (subfigure 3.49 B). $CD8^+$ and $CD4^+$ T cells were found to be single positive for each respective marker but only $CD8^+$ T cells were positive for both. It seems that fewer cells were analyzed for the negative DMSO controls. This was, however, not the case as the same cell number was initially used for *in vitro* re-stimulation samples. Cells of negative controls probably died during re-stimulation which became obvious by high percentages of dead-stained cells in FACS and resulting in less living cells in the comparison to peptide test samples. (In case of short term re-stimulations the T cells of the controls samples did not die, see figure 3.49 C).

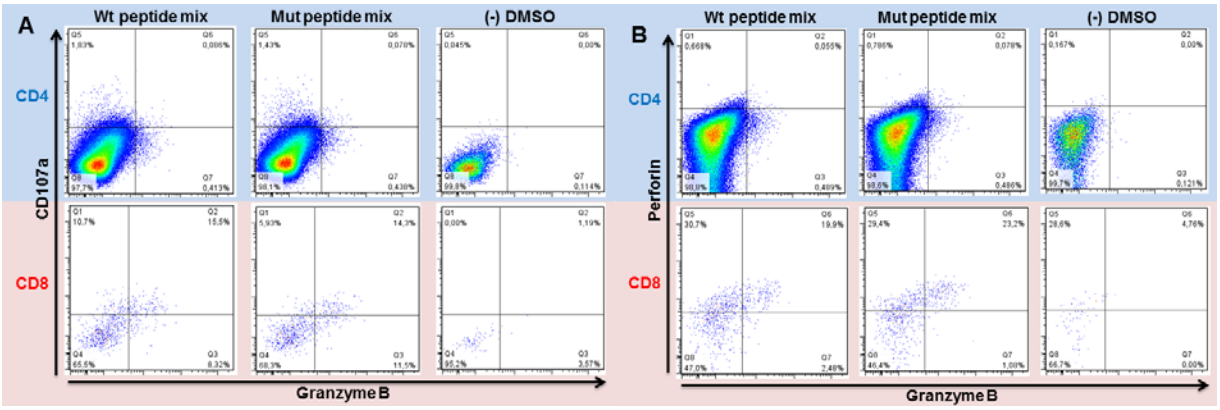


**Figure 3.49 part I**: **$CD8^+$ and $CD4^+$ effector T cells derived from Kras G12V and p53 R248W mutated peptides vaccinated A2.DR1 dtg mice express markers of cytotoxicity upon *in vitro* antigen-specific re-stimulation**. Effector pan T cells derived from Kras G12V/p53 R248W mutated peptides vaccinated A2.DR1 dtg mice were *in vitro* re-stimulated for 6 d on mutated peptides pulsed $CD11c^+$ BM-DCs and irradiated splenocytes as feeder cells (see same T cells used for the *in vitro* cytotoxicity assays described before). This was followed by a second short term re-stimulated for 12 h on different peptides pulsed $CD11c^+$ BM-DCs. Fluorescent-labeled anit-CD107a mAb and GolgiStop reagent were added to the co-culture. Thereafter, live dead staining was performed and samples were fixed. Fixed cells were stained for the markers granzymeB, perforin, CD11c, CD4, and CD8 with fluorescent-labeled mAbs. Within the living, CD11c negative population cells were gated on $CD4^+$ and $CD8^+$ T cell populations. CD107a blotted against Granzyme B **(A)** or Perforin blotted against Granzyme B **(B)** for both the $CD8^+$ and $CD4^+$ T cell populations are shown. Samples displayed: T cells re-stimulated on DCs pulsed with mixed mutated peptides (p53 R248W and Kras G12V) or wt peptides mixed (p53 R248 wt and Kras G12wt), negative control: dendritic cells pulsed with peptide solvent only (DMSO). Gates were set according to FMO and isotype controls.

Also short term re-stimulated T cells expressed markers for cytotoxic activity. When effector T cells were re-stimulated for 12 h on peptide pulsed DCs mainly the degranulation marker CD107a and (to a far lesser percentage) also granzyme B were expressed whereas perforin was hardly detectable (data not shown). CD107a/granzyme B double positive cells were not found neither for $CD8^+$ nor for $CD4^+$ T cells (see subfigure 3.49 C). In particular, the re-stimulation with Kras G12 peptides (wt and mutated) led

to relatively high percentage of CD107a positive events (subfigures C and E) for both $CD4^+$ and $CD8^+$ T cell populations. The p53 R248W peptide elicited the highest percentage of granzyme B signals in $CD8^+$ T cells (subfigure D). Moreover, numbers of CD107a and granzyme B positive T cells pointed towards a mutation specificity. Percentage of granzyme B and CD107a positive $CD4^+$ and $CD8^+$ T cells were higher when they were re-stimulated with mutated mixed peptides and single mutated p53 R248W peptide pulsed DCs than those of corresponding wt samples. Concerning the Kras peptides there was no clear evidence for mutation specificity.

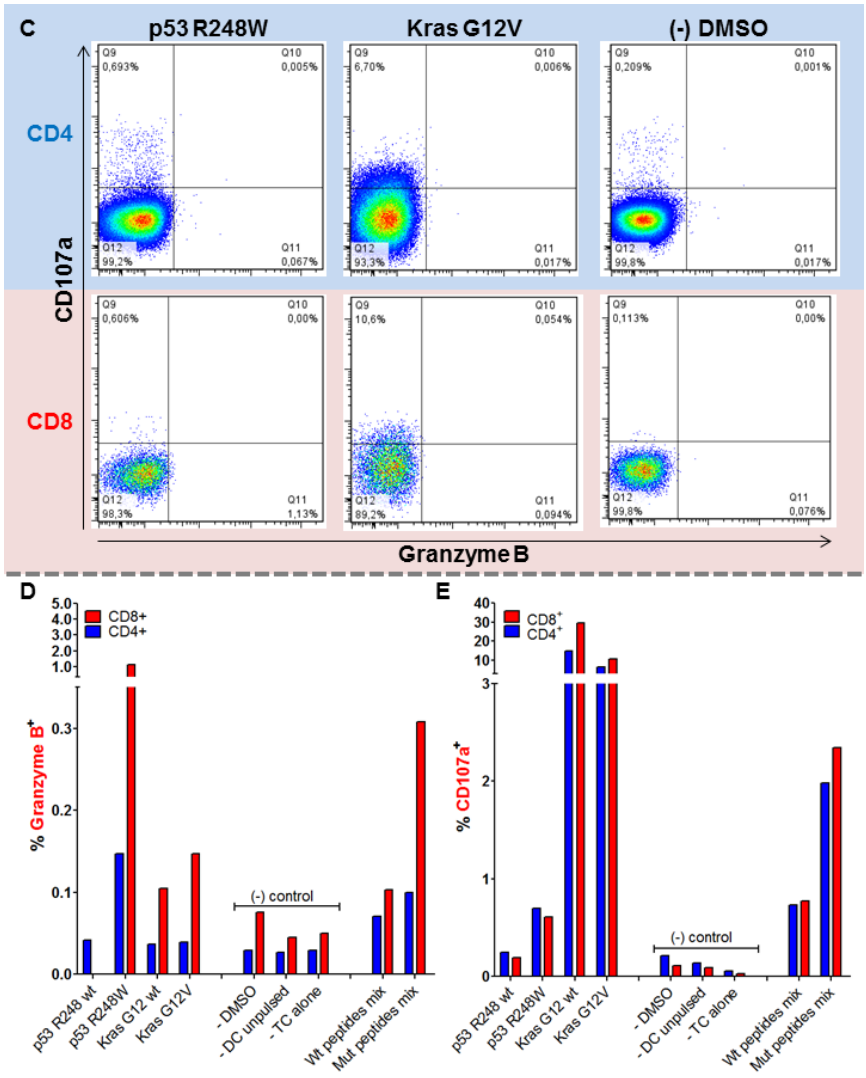


**Figure 3.49 part II**: **$CD8^+$ and $CD4^+$ effector T cells derived from Kras G12V and p53 R248W mutated peptides vaccinated mice express markers of cytotoxicity upon *in vitro* antigen-specific re-stimulation**. **(C)** Effector pan T cell derived from Kras G12V/p53 R248W mutated peptides vaccinated A2.DR1 dtg mice were *in vitro* re-stimulated for 12 h on different peptides pulsed DCs. Fluorescent-labeled anit-CD107a mAb and GolgiStop reagent were added to the co-culture. Thereafter, live dead staining was performed and samples were fixed. Fixed cells were stained for the markers granzymeB, IFN-γ, CD11c, CD4, and CD8 with fluorescent-labeled mAbs. Within the living, CD11c negative population cells were gated on $CD4^+$ and $CD8^+$ populations. CD107a plotted against granzymeB for both the $CD8^+$ and $CD4^+$ T cell populations are shown. Samples displayed: T cell re-stimulated on DCs pulsed with mutated peptide p53 R248W and mutated peptide Kras G12V, negative control: dendritic cells pulsed with peptide solvent only (DMSO). Percentages of granzyme B **(D)** and CD107a **(E)** positive of $CD8^+$ and $CD4^+$ T cells from all samples tested are shown.

Taken together, *in vitro* cytotoxicity assays and staining for cytolytic markers provided evidence that $CD8^+$ and $CD4^+$ T cell elicited by mutated long peptide vaccination with Kras G12V and p53 R248W peptides displayed cytotoxic features. Although killing efficiency and the expression of cytotoxic makers were rather low they showed certain mutation specificity. Moreover, the fact that mutated antigen transfected target cells were preferentially killed gave a first hint that mutated tumor antigens might be naturally processed. Another evidence was found when we analyzed the *in vitro* cytokine recall responses of T cells from tumor bearing mice. More precisely, we compared the T cell responses of mutated Kras G12V and p53 R248W peptides vaccinated mice which were challenged with 2277-NS clone 5.2.2.2 expressing the mutated murine *Kras/Tp53* transgene with non-challenges vaccinated A2.DR1 dtg mice. The same was done for mice which were not vaccinated.

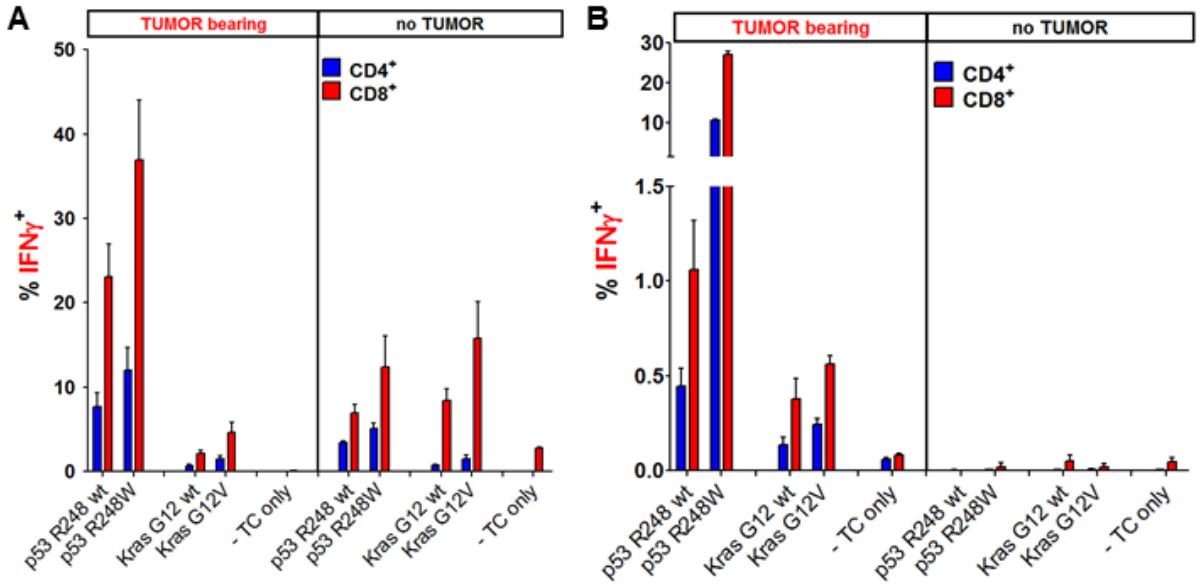


**Figure 3.50**: **Kras G12V and p53 R248W vaccinated and untreated A2.DR1 dtg mice show altered T cell response patterns in the presence of mutated tumor-antigen expressing tumors.** T cell responses against mutated and wt peptide sequences tested for A2.DR1 dtg mice immunized with p53 R248W and Kras G12V mutated peptides **(A)** or non-vaccinated mice **(B)** either challenged with 2277-NS clone 5.2.2.2 mu_mut_tag (indicated as 'TUMOR bearing' groups) or not ('no TUMOR' groups) are shown. *In vitro* recall responses were obtained from two-color cytokine secretion assays (IL-2, IFN-γ) with pan T cells purified from immunized or non-vaccinated. Percentages of IFN-γ positive $CD8^+$ and $CD4^+$ T cells upon *in vitro* recall against single wt and mutated peptides presented by $CD11c^+$ DCs are displayed. Each peptide and control sample was tested in triplicate instances. Results are plotted as means of triplicate assays ± SEM.

Figure 3.50 shows the IFN-γ secretion of T cells upon *in vitro* re-stimulation on respective peptide pulsed DCs assessed by FACS-based cytokine secretion assays. Thereby, the presence of mutated tumor-antigen expressing tumors ('TUMOR bearing' panel) seemed to boost the IFN-γ response of $CD4^+$ and $CD8^+$ T cells towards the p53 R248W mutated and wt peptides (subfigure 3.50 A), when compared to the T cell responses of mice which were vaccinated but tumor free ('no TUMOR' panel). More strikingly, we detected mutation specific IFN-γ responses of T cells in tumor bearing mice for both the mutated Kras G12V and p53 R248W peptides which were higher than those towards corresponding wt peptides ('TUMOR bearing' panel subfigure 3.50 B), when the animals had not previously been vaccinated. In

completely naïve mice, however, spontaneous responses towards any of the peptides were not detected ('no TUMOR' panel, subfigure B). This could mean that tumors expressing mutated p53 R248W and mutated Kras G12V were able to naturally process and present epitopes comprising the mutations, which in turn possibly induced mutated tumor antigen-specific T cells *in vivo*.

## 3.7. The influence of mutated p53 and Kras long peptide vaccination on *in vivo* growth of tumors expressing targeted mutations

So far we studied the ability of active long peptide vaccination targeting mutations in *Kras* and *Tp53* to elicit tumor antigen-specific T cell responses. What we found was that our vaccine reproducibly induced polyvalent, multi-functional T cell responses. Especially the two mutated Kras G12V and p53 R248W peptides were very potent in eliciting multi-cytokine secreting $CD4^+$ and $CD8^+$ effector T cells in A2.DR1 dtg mice. We discovered that this property of the two long peptides was most probably attributed to the fact that they carried potential nested mutated $CD4^+$ and $CD8^+$ T cell epitopes within their sequences. In the previous chapter we found evidence that mutated epitopes might be naturally processed and presented by tumor cells. In this context we also discovered that effector $CD4^+$ and $CD8^+$ Kras G12V and p53 R248W specific T cells derived from vaccinated mice displayed signs of (*in vitro*) cytotoxicity. Next to effector T cell responses also regulatory T cells might be induced along with conventional effector T cells upon vaccination. $T_{reg}$ cell specificity assays suggested that there is not a general induction of mutated antigen-specific $T_{reg}$ cells after vaccination when taking the mean over all tested peptides. However, there was a trend towards increased antigen-specific suppression of $T_{reg}$ cells in response to the mutated p53 R248W peptide and its wt counterpart. Alongside with analyzing vaccination induced T cells, we established two syngenic, tumorigenic sarcoma models for the A2.DR1 dtg mouse strain. The first one was engineered to express the most immunogenic mutations found in the tested panel of long peptides (p53 R248W and Kras G12V). In a second approach we sought to investigate tumors carrying intrinsic *Tp53* and *Kras* mutations. Having these tools in our hands, we proceeded to investigate the influence of mutated p53 and Kras derived long peptide vaccination on *in vivo* growing tumors expressing the targeted mutations.

### 3.7.1. Influence of long peptides vaccination on *in vivo* growth of tumors expressing the most immunogenic mutations

To investigate the influence of vaccination with strongly immunogenic Kras/p53 mutations harboring long peptides the A2.DR1 dtg syngenic sarcoma line 2277-NS was engineered to stably express mutated chimeric *Kras/Tp53* transgenes in a DOX-inducible transgene system. For tumor challenge experiments groups of age and gender-matched A2.DR1 dtg mice were vaccinated with either mutated (Kras G12V, p53 R248W), wt (Kras G12 wt, p53 R248 wt), or irrelevant (murine IgG sequences comprising peptides $IgG_{47\text{-}81}$, $IgG_{273\text{-}304}$, see figure 3.51 A) peptides in a preventive setting three times prior tumor inoculation. Thereby, the first immunization six weeks before tumor inoculation was either

formulated in Montanide ISA 720 (resulting in slow-release depot containing peptides and 50 µg CpG ODN 1668 per mouse) or water based (only 50 µg of CpG ODN 1668 plus peptides). Either formulation did not change the outcome of the experiment. Animals were boosted twice with water-based formulations three and one week before tumor inoculation. Boost immunization cocktails contained the same amount of peptides (5 mM total) and adjuvant CpG (50 µg per mouse and shot) as used in the initial immunization shot. During the challenge experiments mice were boosted twice, two weeks and four weeks after tumor inoculation, with water based-formulations (see figure 3.51 A).

Preventively vaccinated mice were inoculated with 5 x $10^5$ tumor cells on day 0 of the challenge experiment. 2277-NS sarcoma clones 5.2.2.1 and 5.2.2.2 expressing the mutated *Kras/Tp53* chimeric, HA-tagged transgene were pre-treated for 48 h with 50 ng/ml murine recombinant IFN-γ to up-regulate HLA.A2 expression. The evening before the challenge experiment IFN-γ was washed of and cells were cultured overnight in IFN-γ free medium. On the day of the tumor inoculation tumor cells were harvested and HLA.A2 expression was assessed by FACS staining (see figure 3.51 B). Clone 5.2.2.1 and clone 5.2.2.2 cells were mixed in one to one ratio and of this mixture 5 x $10^5$ tumor cells were resuspended in 100 µl Matrigel on ice. 100 µl cell-Matrigel suspensions were injected subcutaneously into the right flank of each animal. One week after tumor inoculation all mice were fed with 2 g/l DOX in the drinking water *ad libitum* until the end of the challenge experiment to induce and sustain transgene expression.

In figure 3.51 one representative experiment of in total three similar tumor challenge experiments is displayed. Subfigure C showes the tumor growth curves recorded for the differentially vaccinated groups of mice. In some few mice, generally one or two animals per group and randomly distributed over all differentially vaccinated groups tested, tumors stopped growing during the challenge experiment and/or shrank again. This caused the very high standard deviation of time points measured in the tumor growth curves. When comparing the differentially pre-treated groups, vaccination with mutated (red curve) and wt (green curve) peptides rather accelerated tumor outgrowth compared to the irrelevant peptides vaccinated group (purple curve) than leading to protection by delaying tumor growth. To find an explanation for this puzzling results we stained for regulatory T cells in periphery of challenged animals on the day of sacrifice (see figure 3.51 C). In fact, the number of splenic $T_{reg}$ cells was significantly increased in tumor-bearing animals vaccinated with mutated (red group) and wt (green group) peptides compared to tumor bearing mice vaccinated with irrelevant peptides (purple group) or to completely naïve mice (gray group). Next to the $T_{reg}$ cell staining, we also assessed the functionality of conventional effector $CD4^+$ and $CD8^+$ T cells in late-stage tumor bearing mice on the day of sacrifice by two color IFN-γ/IL-2 cytokine secretion assays. Therefore, pan purified T cells were *in vitro* re-stimulated on peptide pulsed DCs for 16 h. In figure 3.51 D the percentages of IFN-γ/IL-2 double positive $CD4^+$ and $CD8^+$ T cells from differentially vaccinated tumor bearing mice are shown. Very high percentages of cytokine responsive cells were detected in mutated vaccinated and wt vaccinated mice. Also, the mutation specificity was preserved for responses towards the Kras G12V peptide and the mutated peptide mix of T cell derived from mutated peptides vaccinated

mice. Interestingly, also in irrelevant peptides vaccinated mice $CD8^+$ responses against the mutated peptide mix were detected. This is reinforcing the former finding in untreated mice (shown in the very right panel in blue) in which the presence of a mutated Kras G12V and p53 R248W expressing tumors induced mutation-specific T cell responses.

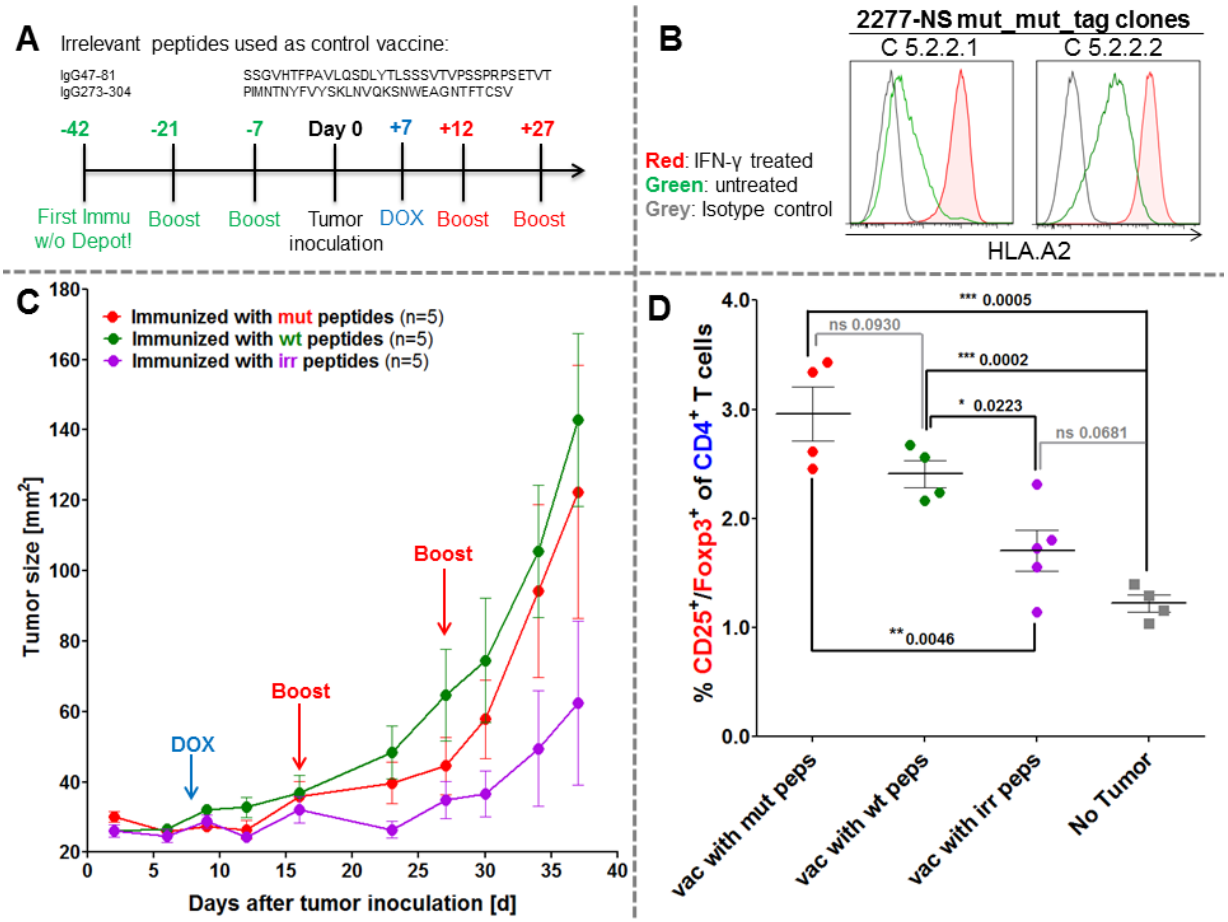


**Figure 3.51 part I**: **Influence of long peptide vaccination on *in vivo* growth of engineered tumors expressing the most immunogenic mutations Kras G12V and p53 R248W. (A)** IgG derived peptide sequences used as 'irrelevant peptides' for vaccination of control group mice and the vaccination's time schedule are shown. Depot: IFA-based formulation, Boost: boost vaccination containing CpG ODN 1668 and peptides in PBS (water-based formulation). **(B)** HLA.A2 expression of inoculated tumor cells assessed by FACS. The two mu_mut_tag transgene expressing 2277-NS clones 5.2.2.1 and 5.2.2.2 were pre-treated with IFN-γ for 48 h. The night before tumor inoculation IFN-γ was removed. Staining of the two clones with fluorescent-labeled HLA.A2 mAb was performed on the day of tumor inoculation. **(C)** Tumor growth curves of differently vaccinated A2.DR1 dtg mice inoculated with a 1:1 mixture of 2277-NS clones 5.2.2.1 and 5.2.2.2. In total 5 x $10^5$ tumor cells were subcutaneously administered in 100 µl of Matrigel on the right flank of each animal at day 0. Three groups of 5 A2.DR1 dtg mice each (n = 5), have been vaccinated prior to the challenge according to the vaccination schedule shown in (A) with either mutated ('mut' group: p53 R248W, Kras G12V), wt ('wt' group: p53 R248 wt, Kras G12 wt), or irrelevant ('irr' group: $IgG_{47\text{-}81}$, $IgG_{273\text{-}304}$) peptides. Beginning on day 7 after tumor inoculation all groups of mice were fed 2 g/l DOX in the drinking water *ad libitum* until the end of the challenge experiment. Mice were boosted twice with respective water-based peptide/CpG formulations during the challenge. n: number of biological replicates; error bars, mean ± SEM **(D)** Number of splenic $T_{reg}$ cells of differentially vaccinated tumor bearing mice compared to non-tumor bearing mice on the day of sacrifice (day 38 of the tumor challenge experiment). $T_{reg}$ cells were stained for in whole splenocyte suspensions with fluorescent-labeled mAbs as $CD4^+CD3^+CD25^+Foxp3^+$ living cells in FACS. P values as per unpaired, two-tailed t test are shown. vac: vaccinated, peps: peptides, irr: irrelevant, mut: mutated.

Finally, the *in vivo* transgene expressing of tumor tissue excised from challenged mice was monitored by western blot analysis. Whole protein lysates from mu_mut_tag transfected HEK 293T cells

served as positive controls for transgene detection as well as a positive tumor protein extract from a previous experiment. Protein lysates from the original cell line 2277-NS and the C57BL/6 melanoma line B16-F1 represent negative controls. The HA-tagged transgene bands were highlighted with a red square. By comparing the transgene bands of tumor protein lysates of challenged mice it becomes obvious that transgene expression is not homogenous between all mice tested. Some mice carried tumors showing a strong transgene expression, whereas for other mice the transgene band was barely detectable. Again, as for the spontaneous stop of tumor growth in some animals, strong and weak transgene expression was randomly distributed over all differentially vaccinated groups tested.

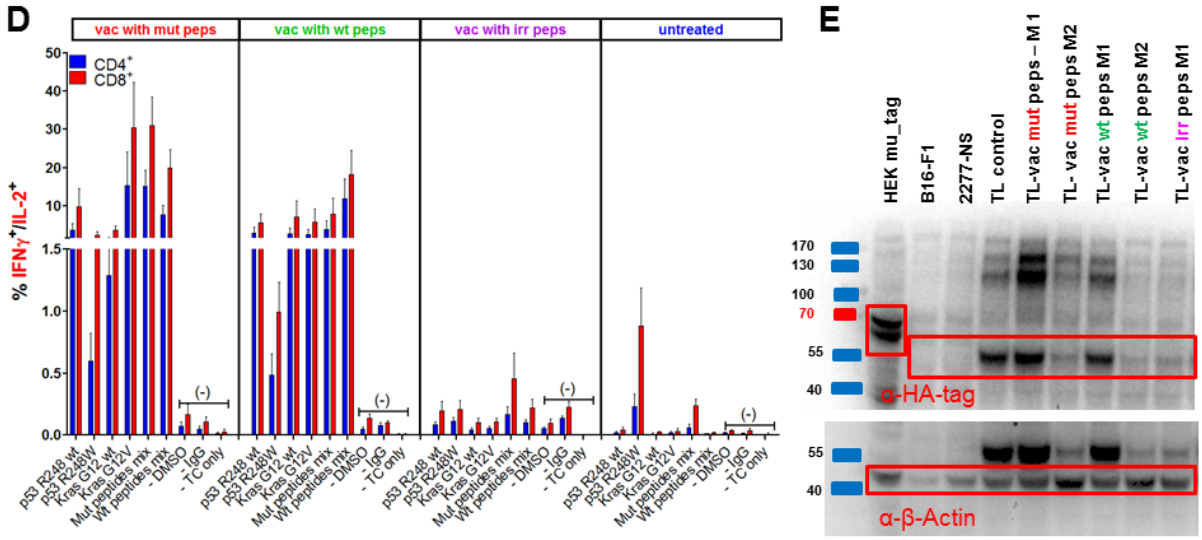


**Figure 3.51 part II**: **Differentially vaccinated mice challenged with tumors expressing the most immunogenic mutations Kras G12V and p53 R248W showed high peripheral T cell cytokine responsiveness. (D)** T cell responses against mutated and wt peptide sequences tested for mice of the tumor challenge experiment shown in (C). *In vitro* recall responses were obtained from two-color cytokine secretion assays (IL-2, IFN-γ) with pan T cells purified from differentially vaccinated or untreated, tumor bearing mice. Percentages of IFN-γ positive $CD8^+$ and $CD4^+$ T cells upon *in vitro* recall against single wt and mutated peptides and peptide mixes presented by $CD11c^+$ DCs are displayed. Each peptide, peptide mix and control sample was tested in triplicate instances. Results are plotted as means of triplicate assays ± SEM. **(E)** Validation of transgene expression of tumors in differentially vaccinated and tumor challenged mice on the day of sacrifice. Western blot analysis of protein extracts from lysates of tumor tissue obtained from mice of the tumor challenge experiment shown in sub-figure (C) and protein extracts of cultured cells serving as controls. Whole protein extract from mu_mut_tag-pDEST-N-eGFP transfected HEK 293T cells served as positive control for transgene expression. B16-F1 and mother cell line 2277-NS extracts served as negative controls. The HA-tag was stained for by anti-HA-specific monoclonal antibody (α-HA-tag) and as a loading control β-actin was stained for (α-β-Actin specific monoclonal antibody). Detection of primary antibodies was performed with secondary HRP-conjugated goat-anti mouse antibody and ECL reagent. vac: vaccinated, peps: peptides, irr: irrelevant, mut: mutated.

Taken together, vaccination with wt and mutated peptides in the system exploring the effects of the strongly immunogenic peptides Kras G12V and p53 R248W on tumor growth rather accelerated tumor outgrowth than delaying it. Although effector T cell responses of vaccinated mice were not hampered but boosted in tumor bearing mice they did not result in protection. Next to increased numbers cytokine responsive effector T cells, however, also significantly increased numbers of peripheral $T_{reg}$ cells were found in mutated and wt peptides vaccinated animals.

### 3.7.2. Influence of long peptide vaccination on *in vivo* growth of tumors expressing intrinsic *Tp53* and *Kras* mutations

Initially, two sarcoma cell lines, 10 and 39, were chosen to be tested for the intrinsic mutation long peptide vaccination system. As experiments with line 10 did not yield in convincing results in preliminary test experiments (data not shown) work on line 10 was discontinued and only data obtained from experiments with line 39 will be shown in this chapter.

Similar to the engineered system mice were vaccinated in a preventive setting following the same vaccination schedule (see figure 3.52 A). Groups of age and gender-matched A2.DR1 dtg mice were vaccinated with either mutated (Kras G12C, p53 C176F), wt (Kras G12 wt, p53 C176 wt), or irrelevant ($IgG_{47\text{-}81}$, $IgG_{273\text{-}304}$) peptides. The first immunization, six weeks before tumor inoculation, was always formulated in Montanide ISA 720. Animals were boosted twice with water-based formulations three and one week before tumor inoculation. During the challenge experiments mice were boosted twice, two weeks and four weeks after tumor inoculation, with water based-formulations (see figure 3.52 A). Preventive vaccinated mice were inoculated with $2.5 \times 10^5$ line 39 cells each on day 0 of the challenge experiment. 100 µl cell-Matrigel suspensions were injected subcutaneously into the right flank of each animal.

Prior tumor challenge experiments the immunogenicity of the two peptides comprising the line 39 intrinsic mutations Kras G12C and p53 C176F (sequence see figure 3.52 A) were used for active vaccination of A2.DR1 dtg mice. T cells purified from vaccinated mice were re-stimulated by respective peptides pulsed DCs for 16 h and cytokine secretion was monitored by IFN-γ/IL-2 two-color cytokine secretion assays. In figure 3.52 B the percentages of IL-2/IFN-γ double positive $CD4^+$ and $CD8^+$ T cells are shown. Both T cell subsets show a clear mutation specific cytokine response for both mutated peptides higher than towards corresponding wt peptides. The responses towards the p53 C176F peptides were thereby lower than those towards the Kras G12C peptide.

In total four challenge experiments were conducted of which two are shown in figure 3.52 C and F. The first experiment shown in C is representative for three of four experiments. Two groups of A2.DR1 dtg mice were vaccinated with either wt or mutated peptides and challenged with sarcoma line 39. Vaccination with mutated peptides (red growth curve) delayed tumor outgrowth compared to mice being vaccinated with wt peptides (green curve). Mutated peptide vaccination also delayed the tumor outgrowth compared to non-vaccinated groups of tumor challenged mice (tested in the other two challenge experiments, data not shown). When we stained for the number of splenic peripheral $T_{reg}$ cells in tumor bearing mice at the day of sacrifice we found that their number was not elevated in mutated peptides vaccinated mice compared to those of completely naïve mice (see figure 3.52 D). The number of peripheral $T_{reg}$ cells in wt peptides (green group) vaccinated tumor-bearing mice, however, was significantly higher than mutated peptides vaccinated and naïve mice.

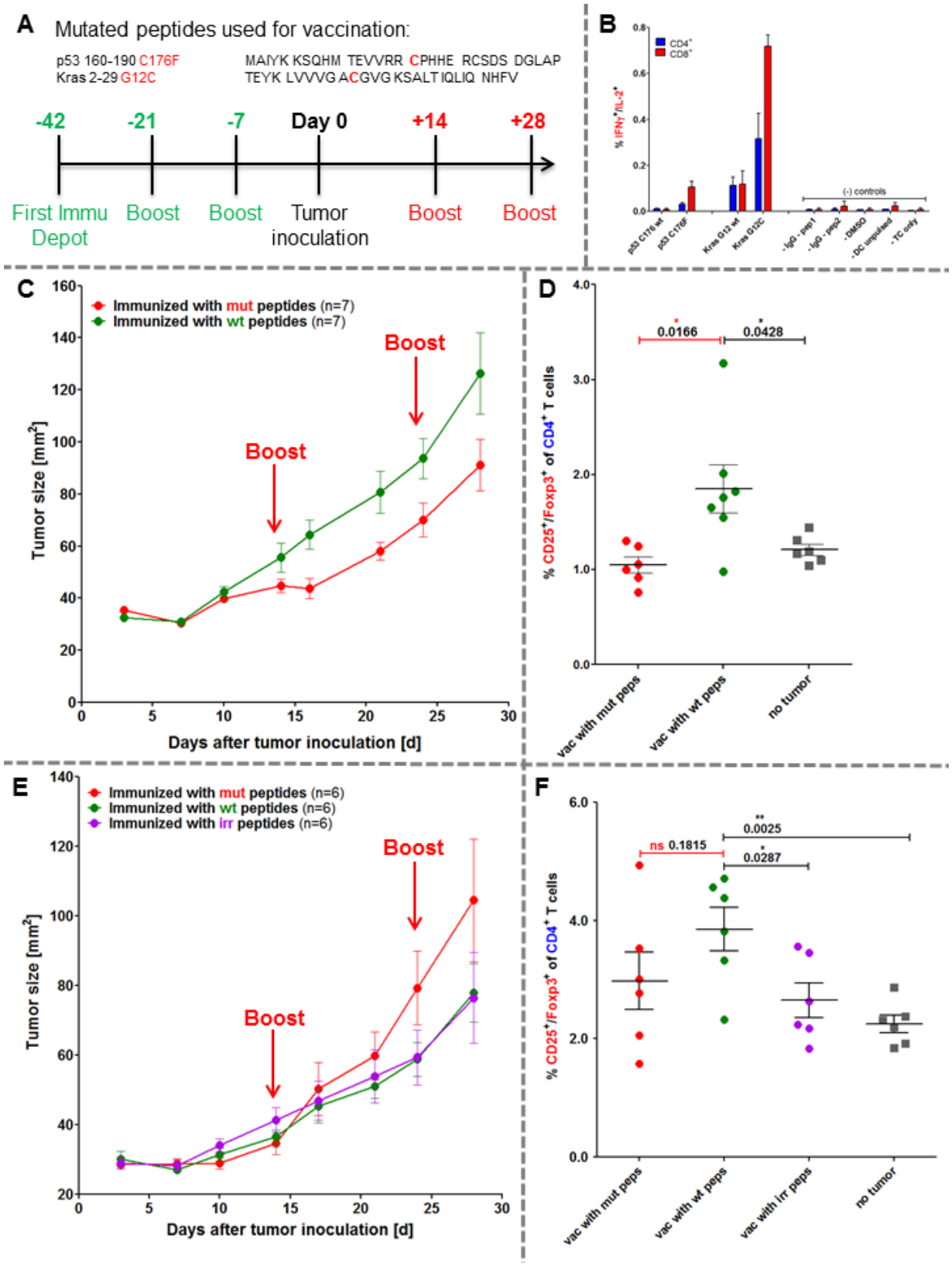


**Figure 3.52**: **Influence of long peptide vaccination on *in vivo* growth of tumors expressing the intrinsic mutations Kras G12C and p53 R176C.** *(for the complete figure legend see the next page →)*

**→Figure 3.52**: **Influence of long peptide vaccination on *in vivo* growth of tumors expressing the intrinsic mutations Kras G12C and p53 R176C. (A)** Sequences of mutated long peptides carrying the intrinsic mutations of sarcoma line 39 and the vaccination's time schedule are shown. Depot: IFA-based formulation, Boost: boost vaccination containing CpG ODN 1668 and peptides in PBS (water-based formulation). **(B)** Recall responses against mutated and wt peptides sequences tested in A2.DR1 dtg mice immunized with p53 R176H (mur) and Kras G12C mutated peptides. *In vitro* recall responses were obtained from two-color cytokine secretion assays (IL-2, IFN-γ) with pan T cells purified from immunized mice. Percentages of IFN-γ/IL-2 double positive $CD8^+$ and $CD4^+$ T cells upon *in vitro* recall against single wt and mutated peptides presented by $CD11c^+$ DCs are displayed. Each peptide and control sample was tested in triplicate instances. Results are plotted as means of triplicate assays ± SEM. **(C)** Tumor growth curves of differently vaccinated A2.DR1 dtg mice inoculated with sarcoma line 39. 2.5 x $10^5$ tumor cells were subcutaneously administered in 100 µl of Matrigel on the right flank of each animal at day 0. Two groups of 7 A2.DR1 dtg mice each (n = 7), have been vaccinated prior to the challenge according to the vaccination schedule shown in (A) with either mutated ('mut' group: p53 C176F, Kras G12V) or wt ('wt' group: p53 C176 wt, Kras G12 wt) peptides. Mice were boosted twice with respective water-based peptide/CpG formulations during the challenge. n: number of biological replicates; error bars, mean ± SEM **(D)** Number of splenic $T_{reg}$ cells of differentially tumor bearing mice of the experiment shown in (C) compared to no tumor bearing mice on the day of sacrifice. $T_{reg}$ cells were stained for in whole splenocyte suspensions with fluorescent-labeled mAbs as $CD4^+CD3^+CD25^+Foxp3^+$ living cells in FACS. P values as per unpaired two-tailed t test are shown. vac: vaccinated, peps: peptides, mut: mutated. **(E)** Tumor growth curves of differently vaccinated A2.DR1 dtg mice inoculated with sarcoma line 39. In total 2.5 x $10^5$ tumor cells were subcutaneously administered in 100 µl of Matrigel on the right flank of each animal at day 0. Three groups of 6 A2.DR1 dtg mice each (n = 6), have been vaccinated prior to the challenge according to the vaccination schedule shown in (A) with either mutated ('mut' group: p53 C176F, Kras G12C), wt ('wt' group: p53 C176 wt, Kras G12 wt), or irrelevant ('irr' group: $IgG_{47-81}$, $IgG_{273-304}$) peptides. Mice were boosted twice with respective water-based peptide/CpG formulations during the challenge. n: number of biological replicates; error bars, mean ± SEM **(F)** Number of splenic $T_{reg}$ cells of differentially tumor bearing mice of the experiment shown in (E) compared to no tumor bearing mice on the day of sacrifice. $T_{reg}$ cells were stained for in whole splenocyte suspensions with fluorescent-labeled mAbs as $CD4^+CD3^+CD25^+Foxp3^+$ living cells in FACS. P values as per unpaired two-tailed t test are shown. vac: vaccinated, peps: peptides, irr: irrelevant, mut: mutated.

In the fourth experiment of this row, three groups of mice were vaccinated with either mutated, wt or irrelevant IgG peptides before and during the challenge with line 39 sarcoma cells. Until two weeks after tumor inoculation tumor growth curves started separating as expected with mice being vaccinated with mutated peptides carried the smallest tumors (see figure 3.52 E). But from the beginning of the third experimental week onwards tumors of mutated vaccinated mice (red curve) started growing out faster than those of wt vaccinated (green curve) and irrelevant peptides vaccinated (purple curve) A2.DR1 dtg mice. When we stained again for the number of peripheral $T_{reg}$ cells of challenged mice on the day of sacrifice we could not find a significant difference between mutated vaccinated and wt peptides vaccinated mice (figure 3.52 F). Although wt peptide vaccinated mice still showed a significantly higher number of peripheral $T_{reg}$ cells than irrelevant peptide vaccinated/naïve mice and mutated vaccinated mice did not, the relative number $T_{reg}$ cells from mutated peptides vaccinated mice was elevated compared to the previous experiment.

To obtain more information about the regulatory T cells we investigated their phenotype with respect to their differentiation status and also stained for regulatory T cells in tumor cell suspensions. Therefore, we added antibodies against the markers CD62L for naïve T cell and the maker CD44 for effector-memory T cells to our $T_{reg}$ cell FACS staining panel.

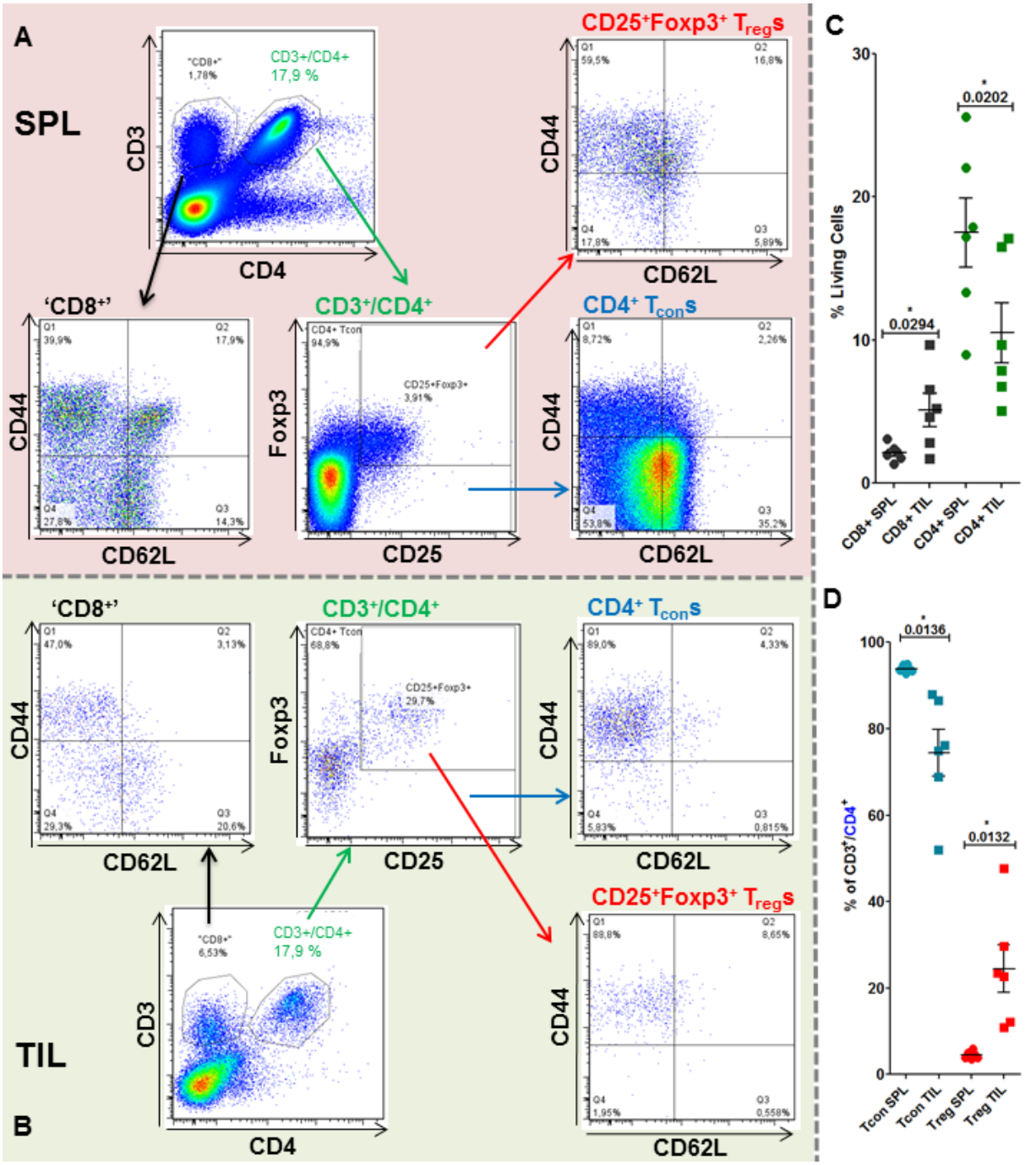


**Figure 3.53**: **Tumor infiltrating regulatory T cells showed an activated phenotype**. $T_{reg}$ cells were stained for in whole splenocyte (**A**) and whole tumor cell (**B**) suspensions with fluorescent-labeled mAbs as $CD4^+CD3^+CD25^+Foxp3^+$ living cells in FACS. CD3 single positive (putative '$CD8^+$'), $CD3^+CD4^+CD25^+Foxp3^-$ (blue script, $CD4^+T_{con}s$) and $CD4^+CD3^+CD25^+Foxp3^+$ (red script, $CD25^+Foxp3^+$ $T_{reg}s$) were analyzed for their CD44 and CD62L expression. Samples displayed: tumor cell suspension and splenocyte suspension derived from mutated peptides vaccinated tumor bearing mouse. **(C)** Percentages of $CD8^+$ and $CD3^+CD4^+$ T cell subsets in total living cells of splenocytes (SPL) and tumor cell suspensions (TIL for tumor infiltrating lymphocytes) assessed by the FACS analysis displayed in (A) and (B). Exemplary shown for the mutated peptides vaccinated group of mice. P values as per paired, two-tailed t test are shown. **(D)** Percentages of $CD3^+CD4^+CD25^+Foxp3^-$ conventional T cell (Tcon) and $CD3^+CD4^+CD25^+Foxp3^+$ regulatory T cell (Treg) subsets in total $CD3^+CD4^+$ T cells of splenocytes (SPL) and tumor cell suspensions (TIL for tumor infiltrating lymphocytes) assessed by the FACS analysis displayed in (A) and (B). Exemplary shown for the mutated peptides vaccinated group of mice. P values as per paired, two-tailed t test are shown.

Figure 3.53 A and B show the gating performed according to isotype and FMO controls for splenic (SPL) and tumor (TIL for tumor infiltrating lymphocytes) samples, respectively. Within the living cell population gates were set on CD3 single positive cells (which were considered to be mainly CD8 T cells) and $CD4^+CD3^+$ events. The $CD4^+CD3^+$ population (green script) was further subdivided into $CD4^+CD3^+CD25^+Foxp3^-$ conventional T cells ($T_{con}$s, blue script) and $CD4^+CD3^+CD25^+Foxp3^+$ regulatory T cells ($T_{reg}$s, red script). For each T cell subpopulation the markers CD62L and CD44 were plotted against each other. Compared to splenic T cells nearly the whole TIL $T_{con}$ cell population as well as the whole TIL $T_{reg}$ cell population was single positive for CD44, whereas the majority of splenic $T_{con}$ cells expressed CD62L and only roughly 60 % of peripheral $T_{reg}$ cells were CD44 positive. These findings were made for all groups of differentially vaccinated mice.

To better assess differences, if any, between the differentially vaccinated groups we validated the percentages of individual cell populations of individual mice in grouped graphs. In figure 3.53 C the percentages of TIL total $CD4^+CD3^+$ and putative $CD8^+$ T cells opposed to the respective peripheral populations, are exemplarily shown for the group of mutated peptides vaccinated mice. The percentages of TIL $CD8^+$ T cells were increased compared to the periphery, whereas the population of TIL total $CD4^+$ T cells was significantly decreased. The same observations were made for the other two groups of wt and irrelevant peptides vaccinated mice. Figure 3.53 D displays the percentages of the two $CD4^+$ T cell population comparing the tumor to the periphery. Whereas the number of conventional T cells ('Tcons') was lower in the tumor than in the periphery, the percentage of regulatory T cells was significantly elevated. Again the graph exemplarily shows the group of mutated vaccinated mice, but the trends were the same for wt and irrelevant peptide vaccinated groups of mice.

Furthermore, the percentages of TIL and splenic $T_{reg}$ cells were directly compared for the three differentially vaccinated groups of mice as shown in figure 3.54 A. In all three groups the population of TIL regulatory T cells was significantly increased. The numbers of TIL $T_{reg}$ cells in the tumor vaccinated group scattered the most, though. Next, the percentages of effector CD44 positive TIL $T_{reg}$ and $T_{con}$ cells were opposed to their peripheral (SPL) counterparts (subfigure 3.54 B). Both TIL populations ($CD44^+$ $T_{reg}$s and $T_{con}$s) were significantly increased in all groups tested and especially for the $T_{reg}$ cells the differences were highly significant. As mentioned above, nearly all TIL $T_{reg}$ cells were CD44 positive. Moreover, the percentages $CD44^+$ $T_{reg}$ cells in both the tumor and the spleen were considerably higher than the percentages of $CD44^+$ splenic and TIL $T_{con}$ cells. One difference in between the groups was found for the TIL $T_{con}$ populations of mutated vaccinated and irrelevant peptide vaccinated mice (indicated in dark red). In fact, the percentage of TIL $CD44^+$ $T_{con}$ cells in mutated peptides vaccinated mice was significantly decreased compared to the irrelevant peptides vaccinated group.

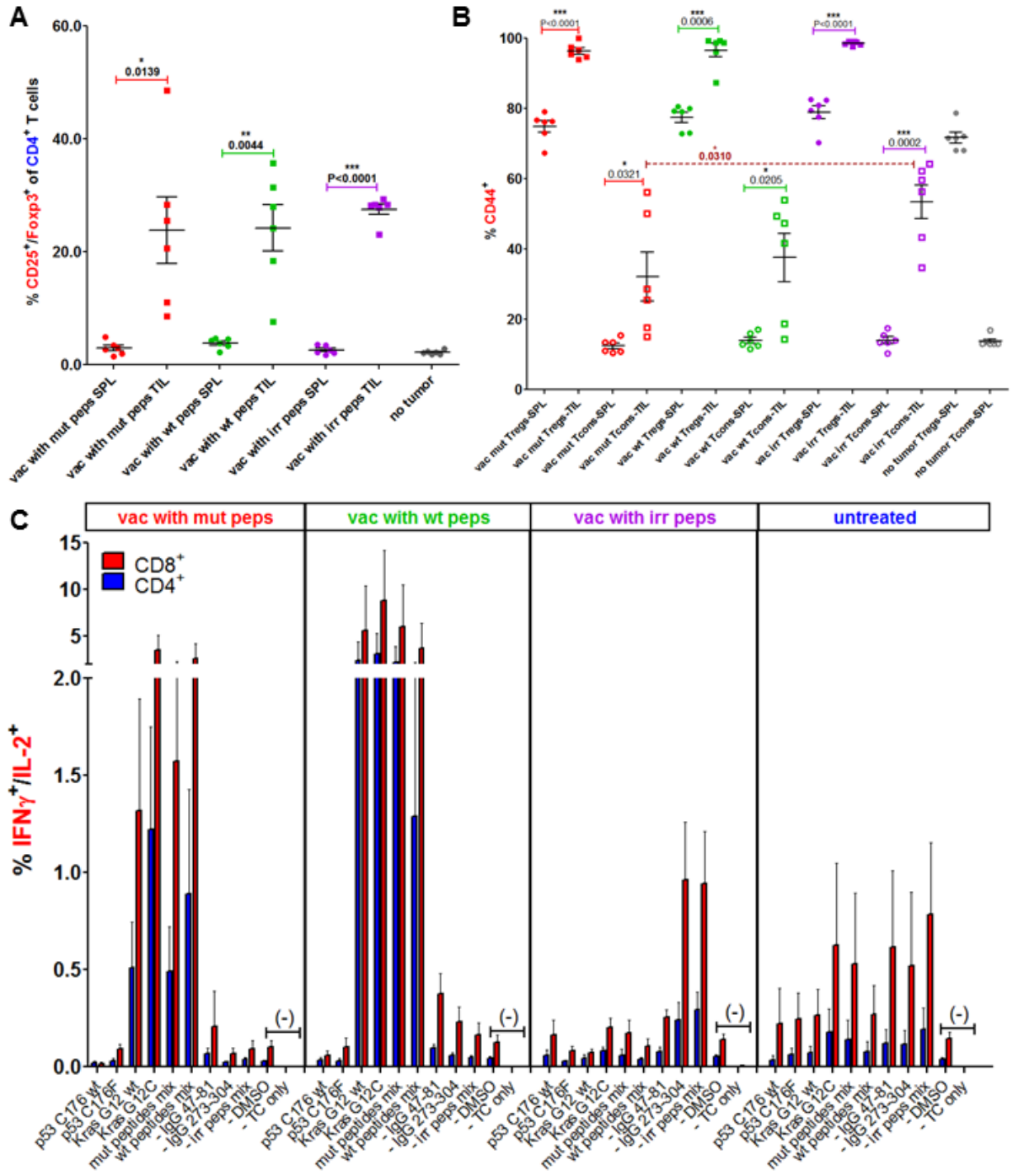


**Figure 3.54**: **Analysis of tumor infiltrating lymphocytes and peripheral T cell responses derived from differentially vaccinated tumor bearing mice**. **(A)** Number of splenic and tumor-infiltrating $T_{reg}$ cells of differentially vaccinated, tumor bearing mice of the experiment shown in fig. 3.52 (E) compared to no tumor bearing mice on the day of sacrifice. $T_{reg}$ cells were stained for in whole splenocyte and whole tumor cell suspensions with fluorescent-labeled mAbs as $CD4^+CD3^+CD25^+Foxp3^+$ living cells in FACS. P values as per paired, two-tailed t test are shown. (B) Percentages of CD44 expressing cells of $CD3^+CD4^+CD25^+Foxp3^-$ conventional T cell (Tcon) and $CD3^+CD4^+CD25^+Foxp3^+$ regulatory T cell (Treg) subsets of splenocytes (SPL) and tumor cell suspensions (TIL for tumor infiltrating lymphocytes) assessed by the FACS analysis. P values as per paired two-tailed t test are shown. vac: vaccinated, peps: peptides, irr: irrelevant, mut: mutated. **(C)** Effector T cell cytokine *in vitro* recall responses were obtained from two-color cytokine secretion assays (IL-2, IFN-γ) with pan T cells purified from differentially vaccinated or untreated, tumor bearing mice. Percentages of IFN-γ/IL-2 double positive $CD8^+$ and $CD4^+$ T cells upon *in vitro* recall against single wt and mutated peptides and peptide mixes presented by $CD11c^+$ DCs are displayed. Each peptide, peptide mix and control sample was tested in triplicate instances. Results are plotted as means of triplicate assays ± SEM.

Finally, we analyzed, as for the most immunogenic mutated peptides system, the cytokine responsiveness of peripheral effector T cells purified as pan T cells from the spleens of differentially vaccinated tumor bearing mice on the day of sacrifice. T cells were antigen-specifically *in vitro* re-stimulated on mutated, wt and irrelevant peptides pulsed DCs for 16 h and their cytokine responses were assessed by IFN-γ/IL-2 two color cytokine secretion assay. Percentages of IFN-γ/IL-2 double positive T cells are shown in figure 3.54 C. Within in the mutated peptides vaccinated group the mutated peptides elicited higher numbers of cytokine responsive $CD4^+$ and $CD8^+$ T cells. As shown before in non-tumor bearing mice the responses against the Kras peptides were considerably higher (first panel from the left hand side) than those against p53 peptides. Interestingly, also in the wt peptide vaccinated group the mutated peptides seemed to perform slightly better than corresponding wt peptides (second panel from the left hand side). Vaccination with irrelevant peptides seemed to induce specific T cells, too. $CD8^+$ T cells derived from respective vaccinated mice responded to the $IgG_{273-304}$ peptide and the IgG mix. In the first panel from the right hand side and indicated in blue script data from untreated line 39 tumor bearing mice was added. Compared to the system with the most immunogenic sequences, line 39 tumors did not seem to be able to elicit mutated antigen-specific T cell response in untreated animals as there was no difference in the percentages of cytokine responsive $CD4^+$ and $CD8^+$ T cells between mutated, wt and irrelevant peptides.

Conclusively, vaccination with mutated peptides comprising tumor intrinsic mutations led to a delayed tumor outgrowth compared to untreated or wt peptides vaccinated mice in three of four experiments. In these experiments the number of peripheral $T_{reg}$ cells was comparable to those of naïve mice and therewith significantly lower than in wt peptides vaccinated mice. In a fourth experiment this difference between mutated and wt peptide vaccinated groups was not found. Herein, the tumors of mutated peptides vaccinated mice grew out faster than in wt and irrelevant peptides vaccinated groups (starting at the end of week two after tumor inoculation). Peripheral T cell responses were not hampered, as high percentages of cytokine secreting peripheral $CD8^+$ and $CD4^+$ T cells were detected in two color cytokine secretion assays. Numbers of tumor infiltrating $T_{reg}$ cells in all differentially vaccinated mice were significantly higher than in the periphery and TIL $T_{reg}$ cells were nearly completely positive for the effector marker CD44. However, striking differences between the differentially vaccinated groups of mice were not found.

# 4. Discussion

Immunotherapy has developed into a versatile, rapidly advancing tool box for the treatment of malignant diseases throughout the last decades. However, it was not until recently that blockbusters, like the anit-CTLA-4 antibody ipilimumab (Hodi et al., 2010) or C. June's CD19-targeting CARs (Grupp et al., 2013), raised the awareness of its clinical potential. As other immunotherapeutic anti-cancer approaches monoclonal antibodies and engineered T cells are not novel inventions from the scratch but were developed and improved over time. Peptide vaccination is yet another crafty tool having a long history, with the first small clinical trials being launched already in the 1980ies not long after their first targets, the tumor antigens, had been discovered. Today we know that cancer is a genetic disease, which accumulates somatic mutations to initiate, sustain and equip a malignant phenotype. The gene products of mutated cancer genes are a potent source of tumor-specific antigens (TSAs). TSAs are in turn optimal targets for anti-cancer peptide vaccination. They are not shared with normal tissue, which provides major advantages over non-mutated targets. Specific immune responses against TSAs should neither be restricted by mechanisms of central tolerance nor elicit autoimmunity. Moreover, cancer is a disease as individual as its hosts, meaning that every tumor has its own set of mutations, which can become even more complex through phenomena like tumor heterogeneity (Gerlinger et al., 2012). This leads to a common trend in cancer therapy, namely individualized approaches. In fact, individualized therapies targeting tumor-specific mutated antigens have become an increasingly active field of research lately. Due to groundbreaking progress in sequencing technologies it has become feasible to identify the patient's individual 'mutanome' (Castle et al., 2012; Overwijk, Wang, Marincola, Rammensee, & Restifo, 2013). The central question in this context is which mutations can give rise to immunogenic epitopes and are therewith able to elicit effective T cell responses. Interesting candidates are driver mutations in oncogenes and tumor suppressor genes which are essential for the survival of the tumor and are common in patients of a given cancer entity (Vogelstein et al., 2013). Furthermore, the targeting of driver mutations by therapeutic interventions is less likely to select for tumor escape variants as the tumor's survival critically depends on the physiological effects of these oncogenic gene products. The afore mentioned criteria have identified hotspot mutation sites in the oncogenes *Kras*, *Braf* and the tumor suppressor *Tp53* as attractive targets for immunotherapeutic intervention in case of colorectal and pancreatic carcinoma. The targeting of common oncogene mutations in a novel immunotherapeutic approach is indeed indicative as therapeutic options for late stage CRC and pancreatic cancer (which is generally diagnosed late at an already metastasized stage) are limited and leave room for improvement.

Our group has investigated in a small cohort of CRC patients the relevance of pre-existing memory T cell responses towards mutations in the oncogenes *Kras* and *Braf* and the tumor suppressor *Tp53* (PhD thesis C. Schlude). Therefore, a panel of long peptides was screened, which comprised Kras, Braf and p53 sequences harboring hotspot mutation sites identified for CRC and pancreatic cancer, as well as corresponding wt sequences. In the majority of patients, memory T cell responses were detected

against both wt and mutated oncogenic peptides by ELISpot analysis. Moreover, mutation-responding T cells showed a generally higher frequency than wt-responding T cells, while mutation-specific responses were more abundant in patients carrying the tested mutations in their tumors. Within the scope of the presented work the potential of the chosen panel of long peptides comprising hotspot mutations in *Kras*, *Braf* and *Tp53* for active vaccination was investigated. In a multi-peptide vaccination setting HLA-humanized A2.DR1 dtg and C57BL/6 mice were utilized and the induction of T cell responses towards the oncogenic peptides was analyzed. In this context, immunogenic epitopes within responding long peptides were to be identified. To investigate the tumor protective capacity of mutated oncogenic sequences comprising long peptide vaccination a tumor model for the A2.DR1 dtg mouse strain was established and tested.

## 4.1. Induction of polyvalent T cell responses against mutations in *Tp53* and *Kras* by long peptide vaccination

Anti-cancer vaccination with tumor-antigen comprising peptides exists in various modes of action. Thereby, the inclusion of multiple peptides derived from different tumor antigens displays several advantages (Pilla et al., 2009) over vaccination with a single, specific HLA restricted antigenic epitope. Epitope-restricted single-peptide vaccination can cause the selection of tumor-escape variants, which specifically down-regulate the targeted antigen (Maeurer et al., 1996; R. D. Schreiber et al., 2011). A vaccine targeting several tumor antigens can, in contrast, compensate the effect of tumor heterogeneity, which displays a source of tumor-escape variants. What is more, minimal MHC-binding peptide-epitopes are less effective in creating a long-term memory response and can even lead to tolerance due to presentation by non-professional APCs (Bijker et al., 2007). Moreover, HLA-restriction implicates that only patients carrying matching HLA alleles can benefit from the vaccine. Including multiple peptides, which cover several different HLA alleles, a broader cohort of patients can be treated. Furthermore, $CD4^+$ T cells can efficiently contribute to tumor eradication in various ways: indirectly by providing help to CTLs or through the secretion of soluble factors and directly by displaying cytolytic activity (van Hall & van der Burg, 2012). Hence, including MCH class II alleles (next to CTL epitopes) into a multi-peptide vaccine allows for the induction and/or activation of tumor antigen specific effector $CD4^+$ T cells, which in combined action with anti-tumor reactive $CD8^+$ T cells could exert more fulminant anti-tumor immune responses (Bijker et al., 2007).

Two different multi-peptide vaccine strategies have been established taking into account the aforementioned considerations. The first one employs mixes of HLA restricted class I and II epitopes derived from multiple tumor antigens. A second approach makes use of synthetic long peptides (SLPs), which are longer than the minimal $CD4^+$ and $CD8^+$ T cell restricted epitopes (peptides with usually 13 to 30 aa length) (Melief & van der Burg, 2008). Long peptides have additional advantages over short peptides. The major gain of long peptides is that in combination with a properly chosen adjuvant antigen-presentation by professional APCs (DCs) can be assured (Welters et al., 2007). Dendritic cells were

shown to take up long peptides at the side of vaccination, migrate to the vaccination site draining LN and present the processed antigenic cargo including all co-stimulatory signals needed for efficient priming of naïve T cells (Bijker et al., 2008). In addition, elongation of the peptides can convert previously tolerizing short peptides in effective epitopes by restricting presentation to professional APCs (Bijker et al., 2007; Bijker et al., 2008). Furthermore, it was shown for several proteins that they harbor immunogenic stretches within their aa sequence, where numerous (nested) MHC class I and II epitopes can be located in close proximity (Disis et al., 2002; Zeng et al., 2002). One example displays the nested, mutated Kras G12 epitopes described by the Gauderack group (Gjertsen et al., 1997). Using long peptides comprising those immunogenic protein stretches it becomes possible to simultaneously target $CD8^+$ and $CD4^+$ T cells specific for the same antigen and to supersede the addition of $CD4^+$ targeting peptides. Moreover, long peptides can possibly target several HLA alleles at the same time.

In the presented study we sought to explore the potential of mutations in driver genes of pancreatic and colorectal cancer to serve as tumor-specific antigens for active vaccination. The oncogenes *Kras* and *Braf* as well as the tumor suppressor *Tp53* were chosen as targets, because they were described to be essential components in the multi-step carcinogenesis progress of CRC and pancreatic cancer (Bardeesy & DePinho, 2002; Cunningham et al., 2010). By screening published data, the hotspot mutations site and the most prevalent amino acid substitutions found for CRC and pancreatic cancer were determined (Bamford et al., 2004; Petitjean et al., 2007). To test their immunogenic capacity it appeared most convenient to us to work with long peptides. As most of the mutated *Tp53* sequences have not been tested for active vaccination hitherto, there was only little information available about possible MHC restriction and immunogenicity. By employing long peptides we could circumvent these uncertainties and were able to screen the mutations sites for both immunogenic MHC class I and class II epitopes. Consequently, we decided to work with peptides comprising the respective mutation site flanked by roughly 15 aa of the natural adjacent human protein backbone on each site. In addition to the mutated sequences corresponding wt long peptides were also tested for active vaccination in order to investigate whether the mutation is more immunogenic than the wt sequence.

HLA-humanized A2.DR1 dtg and C57BL/6 mice were utilized for vaccination with multi-peptide mixes. Each peptide mix consisted of four to five peptides and contained a combination of Kras, (Braf,) and p53 sequences, resulting in four mixes of mutated and two mixes of wt peptides. Animals were immunized for initial screenings through the whole peptide panel with PBS-based formulations containing peptide mixes and the adjuvant CpG ODN 1668. We chose TLR9 ligand CpG as an adjuvant, because it was suitable for mouse vaccination studies by providing danger signals to DCs which hereupon become fully activated to take up, process and present the up-taken antigens to naïve T cells (Welters et al., 2007). After vaccination splenic and LN-derived T cell responses were tested by monitoring cytokine production upon *in vitro* re-stimulation using DCs pulsed with the peptides employed for vaccination and their corresponding wt or mutated counterparts. In FACS-based IFN-γ secretion assays we found that it was possible to detect *in vitro* recall responses against several peptides (Kras and p53) in one respective

mix, which indicated that the induction of polyvalent T cell responses after vaccination with multiple mutated and wt long peptide mixes was feasible. Moreover, $CD8^+$ as well as $CD4^+$ T cells secreted IFN-γ after re-stimulation with peptide-pulsed $CD11c^+$ dendritic cells. Vaccination studies in patients indicated that the induction of polyvalent effector T cell response by vaccination seems to be crucial for the therapeutic benefit. For example multi-peptide immune responses were associated with improved clinical outcome after multi-peptide vaccination with minimal-restricted epitopes. Rammensee and colleagues were able to correlate a longer overall survival with T cell responses against multiple peptides in renal cell cancer patients after vaccination with IMA901. IMA901 is a vaccine comprising several different tumor-associated peptides (TUMAPs) which were confirmed to be naturally processed (Walter et al., 2012). Moreover, tumor-antigen specific $CD4^+$ and $CD8^+$ T cell secreting IFN-γ were found to be of relevance in a study by Melief's group employing more than ten HPV-16 E6 and E7-derived synthetic long peptides for treatment of women suffering from vulvar intraepithelial neoplasia. They observed that IFN-γ secretion of Ag-specific T cells was the highest in complete responding patients and the number of $CD8^+$ epitopes which elicited a response was increased in this group compared to patients without a clinical response after vaccination (Kenter et al., 2009).

Polyvalent $CD4^+$ and $CD8^+$ T cell responses after vaccination were detected in a human (A2.DR1 dtg mice) and a murine (C57BL/6) MHC-restricted context. This argues in favor of the ability of long peptides to reduce the problem of MHC restriction. This finding was in agreement with those of the above mentioned HPV study. Herein, although not HLA typed, all the patients (100 %) were positive for anti-peptide $CD4^+$ T cells responses and the majority (83 %) showed as well a $CD8^+$ response (Kenter et al., 2009).

Interestingly, the peptides eliciting the strongest responses seem to be similar in both, the human and the murine MHC context. Within the C57BL/6 mice the mutated peptides p53 R248W/Q, p53 G245S, and Kras G12V/D were repeatedly highly responsive. Similarly, the peptides p53 R248W/Q and Kras G12V/D/R excelled in the human MHC context within A2.DR1 dtg mice. Moreover, memory T cell responses against the very same mutations seemed to be also of relevance in human CRC patients. As pointed out in the introduction, earlier studies in our laboratory screened the blood and bone marrow of CRC patients for pre-existing memory T cell responses against the same panel of wt and mutated oncogene-derived peptides by ELISpot analysis. This revealed that the mutated peptide p53 R175H was most often mutation specifically recognized by patients, whereas it was of minor relevance in the active immunization of the two mouse strains. Roughly 40 % of the analyzed CRC patients responded to peptide p53 R175H, whereas the corresponding wt peptide was recognized by only 10 % of patients' peripheral blood T cells. However, responses against the peptides p53 R248Q/W and Kras G12D were ranked second in patients. More precisely, peptide p53 R248Q was recognized by 15 % of patients' BM T cells and 13 % of patients' T cells derived from PBMCs. 15 % of patient-derived BM T cells recognized p53 R248W and Kras G12D, respectively. Of relevance, one part of the tested patients were HLA typed and in some patients carrying the HLA.A2 allele, responses against the peptides p53 R175H and p53 R248Q/W

were detected. The fact, that the mutations p53 R248Q and W were recognized in CRC patients in a apparently HLA.A2 restricted manner, underlines the findings in A2.DR1 dtg mice that these mutations are immunogenic. One reason for the differing immunogenicity between HLA.A2 positive mice and humans concerning the p53 R175H peptide might be attributed to differences in the antigen processing machinery between mouse and man.

One major question was whether there was a general difference between the immunogenicity of mutated and wt peptides. Cumulative analysis comparing the frequencies of memory T cell responses of CRC patients (BM and PBMC-derived pooled) against wt and mutated peptides showed that responses against mutated peptides were significantly higher than wt peptides. When using the panel of long peptides for active vaccination of mice a similar incident was found. Cumulative analysis of *in vitro* recall responses towards wt and mutated peptides after vaccination with respective cocktails was carried out. T cells responses from mutated and wt peptide vaccinated mice were accumulated in two groups respectively: cytokine production induced by mutated peptides and by corresponding wt peptides. Cumulative responses of $CD8^+$ and $CD4^+$ T cells pointed towards a mutation specificity after vaccination with mutated peptides. In contrast, there was no significant difference between the percentages of IFN-γ positive T cells responding towards wt or mutated peptides after vaccination with wt peptides. Again, this observation was made for C57BL/6 as well as for A2.DR1 dtg mice. In conclusion, the analyzed mutation within *Tp53*, *Kras* and *Braf* seemed to give rise to sequences, which were more immunogenic than corresponding wt counterparts. This finding was made for both memory T cell responses in CRC patients and active vaccination induced T cell responses.

## 4.2. Mutated Kras and p53 targeting long peptide vaccination induced $CD4^+$ and $CD8^+$ T cells displaying multifunctional phenotypes

Previous studies of our laboratory and others have proven the pre-existence of both $CD4^+$ and $CD8^+$ memory T cells in cancer patients prior to any immunotherapeutic intervention in many different tumor entities (Feuerer, Rocha, et al., 2001; Muller-Berghaus et al., 2006; Schmitz-Winnenthal et al., 2006; Sommerfeldt, Beckhove, et al., 2006; Sommerfeldt, Schutz, et al., 2006). The tumor-antigen specific memory T cell pool seems to be polyvalent and memory T cells were shown to be functional in *ex vivo* studies. Upon antigen re-encounter they are producing IFN-γ, mediate tumor-antigen specific lysis of autologous tumor cells and can also lead to the rejection of autologous tumors in xenograft models (Beckhove et al., 2004; Feuerer, Beckhove, et al., 2001; Schmitz-Winnenthal et al., 2005). Hence, there is a huge potential to activate tumor antigen-specific T cells or reactivate already existing memory T cells by preventive or therapeutic vaccination in patients (Khazaie et al., 1994). Thereby, $T_H1$ responses are superior to $T_H2$ responses, as they contribute substantially in eliciting cellular, cytotoxic immune responses.

In the presented work we performed cytokine secretion assays, intracellular cytokine stainings, stainings for cytotoxic and degranulation markers, and *in vitro* cytotoxicity assays to assess the functionality of T cells induced by mutated oncogene-derived long peptide vaccination. Therefore, T cells purified from the spleen and lymph nodes of vaccinated mice were short term (16 h) *in vitro* re-stimulated with antigenic peptide-pulsed BM-derived $CD11c^+$ DCs. Cytokine secretion assays and intracellular cytokine stainings revealed that $CD4^+$ as well as $CD8^+$ T cells responded to antigen stimulation by production of cytokines. Secretion assays provided the additional information that the T cells were not only producing but also functionally secreting the cytokines. Moreover, results obtained from cytokine secretion assays provided us in general with more meaningful results than intracellular cytokine stainings, which often showed weak signals and a high background noise. We were interested to explore TNF-α production of vaccination-induces T cells by a cytokine secretion assay, but unfortunately none such assay is presently available for the murine system.

Upon peptide-specific *in vitro* re-stimulation we found that $CD4^+$ as well as $CD8^+$ T cells secreted IFN-γ, IL-2 or both cytokines. Thereby, percentages of IL-2 secreting T cells were generally higher in $CD4^+$ than in $CD8^+$ T cells. We expected this finding as one typical trait of $CD4^+$ T cells is to provide the T cell survival factor IL-2 to stimulate proliferation of antigen-specific T cells and sustain survival. However, it was striking we could also obtain high percentages of IL-2 positive $CD8^+$ T cells (in case of strongly immunogenic peptides double-digit values), which were not substantially lower than those of $CD4^+$ T cells and provided evidence for a strong activation. Compared to IFN-γ responses or percentages of IL-2/IFN-γ double positive T cells, IL-2 responses were more 'bleary'. This meant that the negative background controls sometimes showed relatively high percentages of IL-2 positive T cells and differences between responses towards single peptides were less distinct than for IFN-γ staining in the very same samples, especially after vaccination with IFA formulations. Possibly vaccination with highly immunogenic peptides in combination with a strong vaccine formulation containing Montanide ISA 720 increases the general activation status of the T cells, which could be accompanied by high basal levels of IL-2 secretion. Concerning IFN-γ, again both $CD8^+$ as well as $CD4^+$ T cells showed secretion upon antigen-specific re-stimulation. Interestingly, IFN-γ levels were thereby generally higher for (splenic) $CD4^+$ T cells than for $CD8^+$ T cells (see figures 3.11 and 3.12). In addition, IFN-γ responses of $CD4^+$ and $CD8^+$ T cells towards a certain peptide correlated well. The same observations were made for IFN-γ/IL-2 double positive T cells. In the case that a mutated peptide was clearly stronger immunogenic than its corresponding wt counterpart (e.g. p53 R248W or Kras G12V) we detected significantly higher percentages of IL-2, IFN-γ and IL-2/IFN-γ double positive T cells. This means that mutation-specificity could be read out in the induction of highly responsive, multi-cytokine secreting T cells. Furthermore, intracellular cytokine stainings provided evidence that both $CD8^+$ as well as $CD4^+$ T cells were able to produce TNF-α (which was at least clearly seen for the T cells specific against strongly immunogenic peptides).

The induction of IFN-γ (IL-2 and TNF-α) producing $CD8^+$ T cells by vaccination is typical and was shown to be a favorable trait in numerous (peptide) vaccine studies and for TIL CTLs (for example (Attig

et al., 2009; Buhrman & Slansky, 2012; Kenter et al., 2009)). Simultaneous production of the effector cytokines IL-2 and IFN-γ (and possibly also TNF-α) by vaccination-induced $CD4^+$ T cells strongly argues for a $T_H1$ phenotype. What is more, a study analyzing the potential of different TLR ligands as DC-activating agonistic adjuvants showed that CpG (a strong agonist) was prone to give rise to high numbers of antigen-specific IFN-γ secreting $CD4^+$ and $CD8^+$ T cells when included into the vaccine (Welters et al., 2007). Two recent studies underline the potential of mutation-specific (poly-functional) T cells for tumor eradication. S.A. Rosenberg and colleagues showed that mutation-specific $CD4^+$ TILs displaying exactly the same $T_H1$ phenotype as our vaccination induced $CD4^+$ T cells (showing production of the effector cytokines IFN-γ, IL-2 and TNF-α) used for adoptive TIL therapy in a patient with metastatic epithelial cancer lead to tumor regression (Tran et al., 2014). In the second study, to which we also contributed, a peptide vaccine employing a mutated IDH-1 epitope comprising long peptide for vaccination elicited $T_H1$ effector $CD4^+$ T cell responses. These $T_H1$ T cells were responsible for the delay in outgrowth of IDH-1 mutant sarcomas upon vaccination in A2.DR1 dtg mice (Schumacher et al., 2014). According to the cytokine profile it is merely impossible to judge which type of memory subsets were preferentially induced by our vaccine as both central memory and effector memory T cells basically display the same cytokine profile (IFN-γ, IL-2, TNF-α) upon antigen-reencounter (Farber et al., 2014). Therefore, a staining with specific memory markers, like the expression of homing receptors (e.g. CD62L), would have been necessary.

The presence of tumor antigen-specific $CD4^+$ T helper cells during the course of a vaccination induced immune response is of major importance for proper CTL induction and function. Long peptides most probably have to be processed and cross-presented by DCs to naïve $CD8^+$ T cells (Melief & van der Burg, 2008). Thereby, $T_H1$ T cells are described to be involved in the cross-priming process through licensing of DCs via the CD40-CD40L axis (C. M. Smith et al., 2004). Moreover, $CD4^+$ T cells are important for the secondary expansion of CTLs and memory formation (Janssen et al., 2003). Synthetic long peptides comprising additional $CD4^+$ T cell epitopes next to CTL epitopes seem to be especially suitable for the successful recruitment of antigen-specific $CD4^+$ T helper cells and DC licensing. As DCs are able to present these antigenic peptides simultaneously to both $CD8^+$ and $CD4^+$ T cells, as it is so to say on the same cell, they are predestined to assure proper naïve $CD8^+$ T cell priming (van Hall & van der Burg, 2012). We found an indirect evidence for $CD4^+$ T cell help in our short term *in vitro* antigen-specific re-stimulation cultures used for T cell response readout after vaccination. When we compared the $CD8^+$ IFN-γ responses after re-stimulation with peptide-pulsed DCs between cultures of $CD8^+$ cells stimulated alone and cultures of $CD8^+$ T cells containing also $CD4^+$ T cells, the presence of $CD4^+$ T cells seemed to influence $CD8^+$ T cell *in vitro* responsiveness. In case of splenic T cell subsets a cumulative analysis of peptide-specific responses revealed that the presence of $CD4^+$ T cells seemed to enhance the *in vitro* responsiveness of co-cultured $CD8^+$ T cell (compared to $CD8^+$ T cells re-stimulated with DCs in the absence of $CD4^+$ T cells). This was indicated by a significantly higher IFN-γ secretion of the $CD90^+$ co-culture derived $CD8^+$ T cells compared to $CD8^+$ T cells re-stimulated alone in CD57BL/6 mice ($p = 0{,}0461$)

and a trend towards a higher responsiveness of splenic, co-cultured $CD8^+$ cells in A2.DR1 dtg mice (p = 0,082).

Next to the cytokine profile of mutated oncogene-derived long peptide vaccine induced T cells we also analyzed their cytotoxic activity. Therefore, we first stained for markers of cytotoxicity by FACS. Fully activated effector CTLs store effector molecules in cytotoxic granules (modified lysosomes). CD107a is located in the membranes of lysosomes and can therefore serve as a marker for degranulation of cytotoxic granules (Aktas et al., 2009). The pore-forming protein perforin and the protease granzyme B, stored within in the cytotoxic granules, induce apoptosis of the target cells upon degranulation (Chowdhury & Lieberman, 2008). Also cytotoxic $CD4^+$ T cells ('ThCTLs') can kill MHC class II antigen-presenting targets in a CTL cytolytic manner by secreting cytotoxic granules carrying granzymes and perforin. Moreover, degranulation can also be detected by CD107a (Marshall & Swain, 2011). Hence, we stained for these three markers, after *in vitro* antigen-specific re-stimulation of vaccination induced $CD4^+$ and $CD8^+$ T cells on peptide pulsed DCs and secretion blocking. We were able to detect all three markers on $CD4^+$ as well as $CD8^+$ T cells, which were derived from p53 R248W and Kras G12V vaccinated A2.DR1 dtg mice and *in vitro* re-stimulated with respective peptides. Whereas we detected GranzymeB/perforin and granzymeB/CD107a double positive $CD8^+$ T cells, $CD4^+$ T cells were rather single positive for each marker. Moreover, CD107a and granzymeB expression seemed to be higher after re-stimulation with the mutated peptides used for vaccination than after re-stimulation with the corresponding wt peptides, which indicated a mutation-specificity. In conclusion, according to the FACS data some of the vaccination induced $CD8^+$ but also $CD4^+$ T cells expressed cytotoxic proteins and degranulation markers. Interestingly, cytotoxic T cells were described to display a $T_H1$ like cytokine secretion pattern, as they are able to secret combinations of IFN-γ, TNF-α and IL-2 (Casazza et al., 2006), which fits to the cytokine profile we found for our vaccination induced $CD4^+$ T cells.

To find a direct evidence for the cytotoxic activity of mutated tumor antigen-specific T cells induced by long peptide vaccination we analyzed their potential to actively kill tumor cells expressing the respective mutated antigens. For this purpose we performed *in vitro* cytotoxicity assays with T cells purified from A2.DR1 dtg mice vaccinated with the two most immunogenic peptides p53 R248W and Kras G12V as effector cells and A2.DR1 dtg sarcoma line 2277-NS expressing respective mutated *Kras*/*Tp53* transgenes as target cells. Effector pan T cells purified from immunized mice were *in vitro* re-stimulated and separated into $CD4^+$ and $CD8^+$ T cell populations directly prior to their use. $CD4^+$ as well as $CD8^+$ T cells served as effector cells, which secreted IFN-γ and IL-2 in an antigen-specific manner at high percentages and were partially stained positive for the cytotoxicity markers CD107a, granzyme B and perforin in FACS. Killing efficiency ranged between 20 % and 25 % specific lysis at most. Taking into consideration that roughly 10-20 % of effector T cells were cytokine positive in the secretion assays and assuming that these cytokine positive T cells were Ag-specific, the employed effector T cell pool consisted of 10-20 % of mutated tumor antigen-specific T cells and 80-90 % of T cells showing other unknown specificities. Hence, one could argue that the relatively low killing efficiency could be to some extent

attributed to the fact that only a maximum of one fifth of the effector T cells used for the kill assay were antigen-specific. We considered to purify the cytokine secretion assay positive T cells by magnetic cell sorting but the resulting T cell numbers wouldn't have been sufficient to compare several targets. Another option would have been to work with T cell clones. Initial attempts to generate clones *in vitro*, however, failed for the A2.DR1 dtg system. Nonetheless, we were able to clearly detect specific kills of target cells which expressed the chimeric *Kras*/*Tp53* transgene carrying the mutations p53 R248 and Kras G12V and displaying a human backbone when using effector $CD8^+$ as well as $CD4^+$ T cells. Target cells expressing a murine backbone transgene were also killed but less efficiently. Moreover, $CD4^+$ but not $CD8^+$ effector T cells killed wt-transgene expressing targets as well as the unmodified mother cell line 2277-NS, whereas a control cell line with different MHC background (murine, B16-F1) was not recognized at all. A possible reason which might account for this finding could be that transgene-expressing target cells originated from the sarcoma line 2277-NS, which harbors the intrinsic, most likely also immunogenic mutation p53 R248H. Vaccination induced p53 R248W specific $CD4^+$ T cells might have cross-reacted with targets expressing the mutation p53 R248H.

Conclusively, multi-peptide vaccination employing mutated Kras and p53 sequences led to the induction of multifunctional $CD4^+$ and $CD8^+$ T cells. Both subsets secreted IFN-γ and/or IL-2 after antigen-specific *in vitro* re-stimulation and the presence of $CD4^+$ T cells in co-cultures seemed to enhance $CD8^+$ *in vitro* responsiveness. Moreover, $CD8^+$ as well as $CD4^+$ T cells expressed cytolytic markers and were able to kill mutated antigen-expressing sarcoma cell targets *in vitro*.

However, the question remained how the $CD4^+$ T cells killed their targets when these targets did not express MHC class II. We showed that the generated A2.DR1 dtg sarcoma cell lines neither expressed HAL.DR nor was HLA class II expression inducible by IFN-γ treatment. One possibility could be that some of the vaccination induced $CD4^+$ T cells in A2.DR1 dtg mice are MHC class I restricted, which would contradict the paradigm of MHC restriction. Actually, a limited number of studies has reported MHC class I restricted $CD4^+$ T cells. In one study MHC class I restricted $CD4^+$ T cell lines were generated *in vitro* from human PBMCs by re-stimulation with MCH-class II deficient T2 cells. Moreover, some of the $CD4^+$ T cell lines were HLA.A2 restricted (Boyle, Goodall, & Gaston, 2004). Other studies used engineered $CD4^+$ T cells that expressed MHC class I restricted TCRs to address the question how $CD4^+$ help could be provided to $CD8^+$ T cells in case tumors are MHC class II negative. Antigen-specific help was induced by these TCR engineered $CD4^+$ T cells, but seemed to depend on expression of the CD8β co-receptor chain (Kessels, Schepers, van den Boom, Topham, & Schumacher, 2006). Another study showed that the affinity of the introduced TCR was critical for the *in vivo* tumor eradicable function of MHC class I-restricted $CD4^+$ T cells in a mouse melanoma model (Soto et al., 2013). In a small row of experiments we tried to block MHC class I and II molecules by specific antibodies, in order to investigate the MHC restriction of $CD4^+$ T cells in *in vitro* cytotoxicity and cytokine secretion assays but unfortunately did not succeed.

## 4.3. Detailed analysis of mutation specific responses revalidated a Kras G12V mutant epitope and suggested novel mutated p53 R248W epitopes

In the initial screening throughout the panel of long peptides we found stronger and weaker immunogenic sequences. There are several lines of evidence for competition between T cells, which are specific for different or the same MHC/antigen (Kedl, Kappler, & Marrack, 2003). These phenomena were, moreover, observed to be crucial in some vaccine studies targeting viruses (Kastenmuller et al., 2007). Hence, we were wondering whether the responses towards weaker immunogenic peptides or peptides which did not elicit cytokine secretion at all were outcompeted by stronger immunogenic peptides in the same mix or whether weak peptide-specific responses were superimposed by those of strongly immunogenic peptides. In order to solve this issue about epitope competition and immunodominance, low immunogenic mutated peptides (p53 R175H, p53 R216L, p53 Y220C, p53 R282W, Kras Q61H, and Braf V600E) were depicted in one mix leaving out strongly immunogenic peptides. Additionally, we tested all strongly immunogenic peptides combined in a single mix used for vaccination, in order to investigate whether this might lead to suppression of responses towards one or more of the strongly immunogenic peptides. What we found was that each of the strongly immunogenic peptides included in the mix was able to induce high cytokine responses *in vitro*, whereas none of the low immunogenic mutated peptides applied in one mix for vaccination elicited stronger T cell responses than in previous experiments with other peptide combinations. These findings indicate that at least in *in vitro* recall experiments there was no evidence for competition between low and high immunogenic peptides and between different highly immunogenic peptides in eliciting $CD4^+$ as well as $CD8^+$ T cell responses.

In our hands the tested Braf V600E mutation elicited only minor T cell cytokine responses and failed to elicit significantly higher response than its corresponding wt sequence in both the murine and the human MHC context. However, this mutation was shown to be immunogenic in patients as a mutated HLA.DR4 and HLA.A2 restricted Braf V600E epitopes have been described before (Sharkey et al., 2004; Somasundaram et al., 2006). Maybe due to differences in the antigen processing machinery between mice and humans this mutation did not give rise to immunogenic epitopes in our model system.

Another reason responsible for low responses towards certain mutated peptides after vaccination may be the function of regulatory T cells. Our group found that TAA-specific regulatory T cells in the peripheral blood of cancer patients were able to antigen specifically suppress poly-clonally activated T cells in $T_{reg}$ cell specificity assays. Moreover, after depleting the PBMC T cell pool from $T_{reg}$ cells effector T cell responses towards some of the tested TAAs increased (Bonertz et al., 2009). Hence we speculated, that maybe non-responding mutated oncogene-derived peptide sequences were found to be only low immunogenic in the presented study, because of the presence of vaccination induced peptide-specific $T_{reg}$ cells suppressing conventional T cell function in *in vitro* co-cultures. To solve this question we established and performed regulatory T cell specificity assays with $T_{reg}$ cells derived from C57BL/6 mice vaccinated with mixes of peptides showing different immunogenicities. These showed no overall evidence of a

general induction of mutation or wt peptides specific $T_{reg}$ cells in cumulative results from differentially treated groups (mutated or wt peptides vaccinated mice compared to untreated mice). Regarding the individual peptides tested neither the weakly immunogenic Kras Q61 wt/mutated peptide couple nor the p53 R216 peptide couple led to a specific activation of $T_{reg}$ cells. In contrast, vaccination with the mutated peptide seemed to enhance regulatory T cell suppressive responses against the weakly immunogenic p53 Y220 wt peptide. Specific suppression against the mutated peptide p53 Y220C was in all three differentially treated or untreated groups relatively high compared to other peptides tested. Therefore, $T_{reg}$ cells might suppress effector T cell responses towards the mutated peptide and therewith render it non-responsive. Along this line, Ito *et al* described an HLA.A2 restricted mutated $p53_{217-255}$ Y200C epitope which is actually comprised in our long peptide sequence as well (Ito et al., 2007). The second peptide couple showing suppressive reactivity in $T_{reg}$ specificity assays was the strongly immunogenic peptide p53 R248W and its wt counterpart. A clear trend towards an elevated suppressive activity of $T_{reg}$ cells purified from mutated and wt peptides vaccinated mice, after re-stimulation with the strongly immunogenic p53 R248W and its corresponding wt p53 R248 peptide, respectively, was discovered.

Taken together, most of the low immunogenic peptides seemed to be neither affected by immune competition nor by induction of regulatory T cells (excepted the peptide p53 Y220 (C) couple), which leads to the conclusion that these peptide sequences did not give rise to immunogenic epitopes *per se*. This in turn can have several reasons. First, the respective peptide sequence is simply not processed or processing does not produce suitable peptide ligands to be loaded on specific MHC molecules. Second, the TCR epitope:MHC affinity of T cell clones towards the antigen is beyond a critical threshold. Consequently, expansion of naïve T cell clones will be aborted and no memory is formed (Zehn et al., 2009).

Studies exploring the immunogenicity of the whole p53 protein imply that the wt p53-specific CTL repertoire is considerably restricted by self-tolerance (Hernandez et al., 2000; Theobald et al., 1997). Mutations could render self-restricted sequences into immunogenic epitopes. However, this does not necessarily have to be the case and as our data suggested that mutated epitopes might still underlie mechanisms of peripheral tolerance, like suppression by $T_{reg}$ cells. Melief's group, furthermore, showed that self-tolerance does not seem to restrict $CD4^+$ T cell responses against p53 sequences (Lauwen et al., 2008). They located murine MHC class II b-haplotype (C57BL/6 haplotype) restricted immunodominant epitopes between aa positions 77-91, 205-219, and 344-358. Furthermore, in a small clinical trial they vaccinated HLA.DRB1 positive ovarian cancer patients with overlapping long wt p53 peptides (spanning aa 70-248) and found that the peptides covering the sequence 190-248 were recognized most often (Leffers et al., 2009). Furthermore, in previous work we found memory T cell responses in IFN-γ ELISpot analysis against three of the five p53 wt peptide sequences included in our panel of long peptides (p53 160-180, 230-264, 258-292) with percentages ranging between 20 % to 50 % of CRC patients. Within our vaccination experiments we found the peptide $p53_{230-264}$ R248 wt to be most immunogenic in both A2.DR1 dtg and C57BL/6 mice, which was recognized by roughly 30 % of the CRC patients tested. Moreover, this

sequence partially overlaps with the immunogenic wt sequences found in the ovarian cancer study (Leffers et al., 2009).

As some of the wt sequences (p53 R248 wt, Kras G12 wt) analyzed in the context of active vaccination were also shown to be immunogenic, we sought to identify those mutated peptides which are more immunogenic than the corresponding wt peptides. In order to clearly validate the most immunogenic mutated oncogene-derived sequences within the panel of long peptides the responses towards mutated peptides were directly compared to those of corresponding wt counterparts, in both the murine and human MHC contexts. The mutated peptides Kras G12V and p53 R248W were identified as the most immunogenic peptides in the A2.DR1 dtg system (and also in the C57BL/6 system) because they elicited mutation-specific responses significantly higher than those against wt peptides when used for active vaccination. This led us to the conclusion that these peptides most probably harbor HLA.A2 and HLA.DRB1 restricted mutated epitopes. In order to identify possible HLA binding shorter peptide sequences within the two long peptides, long peptide sequences were fed into *in silico* prediction algorithms of the NetMHC and the SYFPEITHI databases. This was done to have the affinity scores for all overlapping 9-mer, 10-mer and 15-mer small peptides possibly binding to HLA.A2 and HLA.DRB1 predicted. Always affinity scores for wt and mutated sequences were opposed. Thereupon, high affinity, predicted short peptide candidates were tested in *in vitro* re-stimulation assays with T cells derived from the respective long peptide vaccinated mice. The prediction worked out for the Kras peptide but failed for the mutated p53 peptide. This is why we performed an epitope mapping with overlapping short peptides for the p53 R248W long peptide. The predicted 10-mer $Kras_{5\text{-}14}$ G12V and 15-mer $Kras_{3\text{-}17}$ G12V peptides were as responsive as the long peptide when used for *in vitro* re-stimulation of vaccination induced peptide-specific T cells, which suggested them as putative minimal HLA-binding epitopes. Identification of possible HLA.A2 and HLA.DRB1 ligands within the strongly immunogenic p53 R248W peptide was not resulting in affirmation of the short peptides predicted to have the highest affinity towards the HLA alleles tested. Instead, according to the *in vitro* testing of overlapping short peptides we suggested 10-mer $p53_{246\text{-}256}$ R248W and 15-mer $p53_{240\text{-}254}$ R248W (with lower affinity scores) as potential HLA class I and II binders. What is more, epitope mapping experiments indicate that the long peptide p53 R248W might comprise next to mutated epitopes also wt $CD4^+$ epitopes (lying in front and after the mutation site and are shared with the p53 R248 wt peptide), which could have given rise to wt-specific $CD4^+$ T cells.

HLA class I and II potential minimal epitope sequences were overlapping for the p53 peptide, whereas the HLA class I restricted Kras G12V 10-mer was nested within the putative longer 15-mer HLA class II epitope (figure 3.30). The nested Kras G12V epitopes have been previously described by other groups. Gaudernack and colleagues found a nested Kras epitope comprising the G12V mutation within a longer $Kras_{5\text{-}21}$G12V peptide that was recognized by cytotoxic $CD4^+$ as well as $CD8^+$ T cells (HLA.B35 restricted) from previously vaccinated pancreatic cancer patients (Gjertsen et al., 1997). Others provided evidence that the Kras G12V mutations can also be presented in BALB/c mice in an H-$2K^d$ restricted manner (Abrams et al., 1997). Khleif *et al* found the $Kras_{5\text{-}14}$ G12V mutation to be HLA.A2 restricted (Khleif

et al., 1999). Conclusively, the Kras G12V mutation is processed naturally and presented by a wide range of mouse and human MHC class I and II alleles. Hence, these obviously quite promiscuous mutated Kras epitopes can be recognized by $CD4^+$ as well as $CD8^+$ T cells. We therewith validated Khleif's finding that the 10-mer $Kras_{5-14}$ G12V is HLA.A2 restricted and added the HLA.DRB1 restricted 15-mer $Kras_{3-17}$ G12V to the list of class II alleles being able to present the Kras G12V mutation. To our best knowledge the potential HLA.A2 restricted 10-mer $p53_{246-256}$ R248W epitope and the overlapping HLA.DRB1-restricted 15-mer $p53_{240-254}$ R248W epitope have not been described before. Together with Melief's findings our results suggest that the region spanning the amino acids 190 to roughly 260 within the p53 protein seems to be an immunogenic stretch.

*In vitro* cytotoxicity assays provided first evidence that mutated tumor antigens might be naturally processed as mutated antigen transfected target cells got preferentially killed. Additional evidence we could find when we analyzed the *in vitro* cytokine recall responses of T cells from tumor bearing mice. The presence of mutated tumor-antigen expressing tumors seemed to boost the IFN-γ response of $CD4^+$ and $CD8^+$ T cells towards the p53 R248W mutated and wt peptides, when compared to the T cell responses of mice which were vaccinated but remained tumor free. More strikingly, we detected mutation-specific IFN-γ responses of T cells in tumor bearing mice for both the mutated Kras G12V and p53 R248W peptides which were higher than those towards the corresponding wt peptides, when the animals were not previously vaccinated. This could mean that tumors expressing mutated p53 R248W and mutated Kras G12V were able to naturally process and present epitopes comprising the mutations, which in turn possibly induced mutated tumor antigen-specific T cells *in vivo*.

The last finding again suggests that mutation-specific $CD4^+$ T cells can obviously recognize mutation-expressing sarcomas although they do not express MHC class II. As discussed before, *in vitro* studies showed that $CD4^+$ T cells can only very rarely and/or through manipulation (e.g. introducing MHC class I restricted TCRs) be restricted to MHC class I molecules. *In vivo*, however, recent mouse studies provided a more plausible explanation. *In vivo* tumor antigens can be taken up by host antigen presenting cells, which migrate to the tumor draining lymph nodes, where they can present their antigens to naïve $CD4^+$ T cells. Naïve $CD4^+$ T cells are then differentiating into $T_H1$ cells, which in turn migrate to the tumor (reviewed in (Haabeth et al., 2014)). In case the tumor is MHC class II positive, cytotoxic $CD4^+$ T cells were shown to be able to directly kill their targets by secreting granzyme B and perforin (Quezada et al., 2010). If the tumors are MHC class II negative, $CD4^+$ T cells act indirect through secreting IFN-γ which stimulates M1-like macrophages to eliminate MHC class II negative, antigen-expressing tumor cells (Tveita et al., 2014). Our long peptide vaccination / mutated antigen-expressing tumors induced $CD4^+$ T cells also display a $T_H1$ cytokine profile, which could be a hint for a similar mechanism underlying $CD4^+$ T cell recognition of the MHC class II negative sarcomas in our model system.

## 4.4. Vaccination with mutated p53 and Kras long peptides has an impact on *in vivo* tumor growth of tumors expressing the targeted mutations

After detailed analysis of vaccination induced T cell responses we sought to investigate the tumor protective capacity of the mutated oncogene-derived long peptide vaccine in the HLA humanized A2.DR1 dtg system. Therefore, it was necessary to establish a suitable tumor model. Via carcinogen induced tumorigenesis with MCA we induced (fibro) sarcomas in A2.DR1 dtg mice. Through *in vitro* and *in vivo* passaging of resulting tumors we generated numerous *in vitro* growing, A2.DR1 dtg syngenic sarcoma lines. These cell lines were analyzed for the *Kras* and *Tp53* mutations they carried, their MHC expression properties and their *in vivo* growth capacities. As expected we detected numerous *Kras* and *Tp53* mutations through gene-specific Sanger sequencing analysis. The analysis of MHC expression revealed that MCA-induced sarcoma lines expressed HLA.A2 but no HLA.DRB1. Treatment of the cell lines with IFN-γ increased HLA class I expression but did not result in any up-regulation of HLA class II. Moreover, HLA.A2 expression was not stable over the course of *in vitro* culturing. Fortunately, the MHC class I down-regulation was reversible after treatment with IFN-γ, concluding that there are no general defects in the Antigen presenting machinery of the tumor cell lines generated. This in turn did not necessarily mean that MHC class I down-regulation cannot occur in tumor challenge experiments. But once achieving an infiltration of effector T cells into the tumor they could contribute to maintain MHC class I expression and therewith the presentation of antigens by secreting inflammatory cytokines like IFN-γ.

Two tumorigenic sarcoma lines were chosen to carry out tumor challenge experiments. Sarcoma line 39 expressed an intermediate level of HLA.A2 and carried a silent mutation in codon *Tp53* R175, harbored a mutation on one allele of *Tp53* in the neighboring codon C176F and also one allele of the *Kras* gene was mutated (Kras G12C). Line 39 served as model with 'intrinsic mutations'. We had long peptides synthesized harboring the tumor intrinsic mutations and tested these for their tumor protective capacity in a preventive long peptide vaccination setting. In cytokine secretion assays with T cells derived from mice vaccinated respective peptides, we proved that both mutated peptides were immunogenic (although to a lesser extent than strong immunogenic peptides) and elicited higher *in vitro* recall responses than corresponding wt counterparts.

Second, we identified the peptides comprising the mutations Kras G12V and p53 R248W as the most immunogenic peptides in the HLA.A2 and HLA.DRB1 context. They were more immunogenic than corresponding wt counterparts when used for active vaccination and possibly comprise mutated $CD4^+$ as well as $CD8^+$ epitopes. Hence, we speculated that these two peptides were most potent to envisage the effects of long peptide vaccine targeting oncogene-derived mutations on the course of tumor outgrowth. A second A2.DR1 dtg sarcoma line, 2277-NS, was selected (Schumacher et al., 2014) to be engineered to express the two most immunogenic mutations. The unaltered 2277-NS sarcoma line expressed a high level of HLA.A2, showed stable *in vivo* tumor growth kinetics and carried only one intrinsic heterozygote mutation within the *Tp53* and *Kras* genes (namely Tp53 R248H). In cooperation with the in house core

facility for proteomics and genomics Doxycycline-inducible transgenes were stably introduced into the genome. The introduced transgenes were truncated, non-functional cDNA versions of *Kras* and *Tp53* mutated mRNA sequences joint by a linker and fused to an HA-tag for detection. To mimic antigen processing similar to those of the natural p53 and Kras proteins we thought that it would be favorable to design transgenes comprising the p53 R248W and Kras G12V mutations within long sequences of their natural adjacent protein backbones. We tested two transgenic 2277-NS clones with a murine and human protein backbone sequence, respectively. Tumor challenge experiments were conducted with the murine backbone sequence clones as their *in vivo* tumor growth was more stable and their transgenes should not give rise to rejection antigens which could result from a human protein backbone sequence.

In both tumor model system mice were vaccinated with mixes of either mutated, wt or irrelevant long peptides prior to tumor inoculation followed by two boost vaccinations during the challenge experiment. (In the engineered system transgene expression was induced at day seven of challenge by feeding mice with DOX in the drinking water until the end of the experiment.) We expected that vaccination with the mutated long peptide mix would have the strongest impact on tumor growth. Further, we speculated that it would delay tumor outgrowth or in the best case even prevent it. As we and others saw (Lauwen et al., 2008; Leffers et al., 2009), wt p53 derived long peptides are immunogenic and elicit specific T cell responses. Therefore, one could anticipate that vaccination with the wt peptide mix might also show a certain extent of protection compared to the control groups (non-vaccinated and irrelevant peptide mix vaccinated mice). However, as we knew that the mutated peptides elicited higher numbers of responsive T cells than wt peptides, we hypothesized that mutated peptide vaccination should have a bigger impact on the delay of tumor outgrowth than vaccination with wt peptides.

In the engineered system, vaccination with wt and mutated peptides rather accelerated tumor outgrowth than delaying it compared to mice vaccinated with irrelevant peptides. These findings completely contradicted our speculations. Even though effector T cell responses of vaccinated mice were not hampered but boosted in tumor bearing mice, they did not result in protection. What is more, next to increased numbers of cytokine responsive effector T cells, however, we could also detect significantly increased numbers of peripheral $T_{reg}$ cells in animals vaccinated with wt and mutated peptides. This led us to the speculation that regulatory T cells may co-decide about the success and failure of the presented vaccination experiments.

Using the intrinsic mutation system we conducted in total four challenge experiments. In three out of four experiments vaccination with mutated peptides delayed tumor outgrowth compared to mice being vaccinated with wt peptides or groups of non-vaccinated tumor challenged mice. When we stained for the number of splenic peripheral $T_{reg}$ cells in tumor bearing mice at the day of sacrifice we found that their number was not elevated in mutated-peptide vaccinated mice compared to those of completely naïve mice. The number of peripheral $T_{reg}$ cells in wt-peptide vaccinated tumor-bearing mice, in contrast, was significantly higher than in mutated-peptide vaccinated and naïve mice. In the fourth experiment of this

row, however, tumors of mutated-peptide vaccinated mice started growing out faster than those of wt and irrelevant-peptide vaccinated A2.DR1 dtg mice, starting from the beginning of the third experimental week. When we stained again for the number of peripheral $T_{reg}$ cells in challenged mice we could not find a significant difference between mutated-peptide vaccinated and wt or irrelevant-peptide vaccinated mice. Similar to the engineered system, T cell responses were not hampered, as high percentages of cytokine-secreting peripheral $CD8^+$ and $CD4^+$ T cells were detected. In contrast, line 39 tumors did not seem to be able to elicit mutated antigen-specific T cell responses in untreated animals. In order to find more differences between the differentially vaccinated groups we also analyzed TIL populations and compared them to peripheral T cell populations. (The results obtained are very preliminary as we only did this analysis once for the fourth intrinsic model challenge experiment.) We found that the percentages of TIL $CD8^+$ T cells were increased compared to the periphery, whereas the population of total TIL $CD4^+$ T cells was significantly decreased. When we directly compared the percentages of TIL and splenic $T_{reg}$ cells the population of regulatory T cells was significantly increased. Furthermore, the percentages of effector CD44 positive TIL $T_{reg}$ and $T_{con}$ cells were contrasted to their peripheral (SPL) counterparts. Both TIL populations ($CD44^+$ $T_{reg}$s and $T_{con}$s) were significantly increased in all groups tested and especially for the $CD44^+$ $T_{reg}$ cells the differences were highly significant. Nearly all TIL $T_{reg}$ cells were CD44 positive. These observations were made for all of the differentially treated groups analyzed, meaning that no further differences between the groups could be found expect one. In fact, the percentage of TIL $CD44^+$ $T_{con}$ cells in mutated-peptide vaccinated mice was significantly decreased compared to the irrelevant-peptide vaccinated group. In other words, it could be that in the mutated-peptide vaccination group the number of effector $CD4^+$ T cells in tumor was reduced.

Conclusively, the system employing the strongest immunogenic mutations completely missed our expectation, as vaccination with mutated and wt peptides accelerated tumor growth. Repeatedly we found that peripheral $T_{reg}$ numbers in mutated-peptide and wt-peptide vaccinated tumor-bearing mice were elevated. The system with the intrinsic, weaker immunogenic mutations partially met them. But there is evidence for the notion that vaccination with mutated long peptides only resulted in protection when the number of peripheral $T_{reg}$ levels was not elevated (fourth experiment). How can these finding be explained? Rammensee's group and others showed that the success of their vaccine critically depended on pre-treatment $T_{reg}$ levels and that depletion of $T_{reg}$ cells by cyclophosphamide treatment can restore T cell function and contribute to vaccination success (Ghiringhelli et al., 2007; Walter et al., 2012).

Apart from that another question arises: Are we inducing antigen-specific $T_{reg}$ cells through vaccination and therewith fatally increase the $T_{reg}$ levels prior to the challenge experiment? In the engineered system we worked with the strongly immunogenic peptides Kras G12V and p53 R248W. For the latter we found a trend towards a higher suppression in $T_{reg}$ cell specificity assays, when $T_{reg}$ cells from the respective mutated-peptide immunized mice were re-stimulated with the long peptide p53 R248W. The same observation was made for the corresponding wt peptide. This could provide evidence that our vaccine induced antigen-specific regulatory T cells against certain peptides. Indeed, induction of antigen-

specific $T_{reg}$ cells by vaccination has been previously observed. In the field of autoimmunity research, for example, the induction of antigen-specific $T_{reg}$ cells is discussed as a therapeutic option (von Herrath & Harrison, 2003). Coming back to cancer, Romero and colleagues investigated this issue in the murine system using OVA peptides as foreign antigens and melanoma-antigens as self-antigens. After adoptive transfer of TCR transgenic T cells, recognizing the antigens, they carried out peptide vaccinations and found that in both cases the number of regulatory T cells increased. Interestingly, by adding either CpG or poly(I:C) as adjuvants to the vaccine they were able to reverse the effect. $T_{eff}/T_{reg}$ ratios increased, which lead to the production of $T_H1$ cytokines, higher $CD8^+$ T cell infiltration at the tumor site and durable tumor rejection (Perret et al., 2013). In the preliminary TIL analysis we also found elevated levels of TIL $CD8^+$ T cells compared to the percentage in the periphery, whereas conventional $CD4^+$ T cell levels were reduced. This observation has also been made in another study investigating the influence of tumor-antigen specific induced $T_{reg}$ cells in the tumor microenvironment and how these in turn can suppress therapeutic vaccination (T. H. Schreiber, Wolf, Bodero, & Podack, 2012). They showed that TSA-specific induced $T_{reg}$ cells were able to suppress conventional $CD4^+$ T cells, specific for the same antigen, locally in the tumor microenvironment. Moreover, they stated that induced $T_{reg}$ cells preferentially resided in the tumor (a carcinogen-induced sarcoma!), when the tumor expressed the cognate non-self antigen (in their case ovalbumin). Possibly this mechanism is also of relevance in our experiments and could explain the difference between the engineered and the intrinsic mutation system. In the engineered system the mutated antigens are overexpressed, which could lead to both a higher infiltration of effector but also of antigen-specific regulatory T cells, which could lead to a more pronounced suppression of effector T cells. To prove that antigen-specific $T_{reg}$ cells are present in the tumor and elevated in the periphery $T_{reg}$ specificity assay employing splenic and TIL $T_{reg}$ cells could be conducted as future experiments. Another explanation of the stronger effect of this phenomenon in the engineered system could be connected to the high immunogenicity of the mutated antigens. Maybe the induction of higher regulatory T cell levels is even of physiological relevance to counterbalance the very strong effector T cell responses elicited through vaccination. However, this beneficial effect in non-tumor bearing animals converts into a disadvantage in the tumor situation, as the tumor preferentially attracts $T_{reg}$ cells through a suppressive environment and obviously also in an antigen-specific manner (as we learned above).

## 4.5. Conclusions and future perspectives

In the presented study the cancer immune-therapeutic potential of oncogene-derived mutated long peptides for active vaccination was investigated. The most frequent mutations at hot-spot sites in the oncogenes *Kras*, *Braf* and the tumor suppressor *Tp53* found in pancreatic and colorectal carcinoma were employed in a multiple epitope long peptide vaccination setting by utilizing HLA-transgenic A2.DR1 dtg mice (as well as C57BL/6 mice). Vaccination with mixes of up to five different mutated peptides resulted in polyvalent $CD4^+$ and $CD8^+$ T cell responses against mutated Kras and Tp53 peptides. To our best knowledge no other has study previously successfully tested both mutated Kras and p53 sequences (in

one formulation) for long peptide vaccination. Cumulative analysis of all peptides tested suggested that mutated peptides generally elicited higher $CD8^+$ as well as $CD4^+$ T cell cytokine responses compared to the corresponding wt peptides and were therewith more immunogenic. Vaccination induced peptide-specific T cells displayed a poly-functional profile, as they secreted (simultaneously) IFN-γ and IL-2 and exhibited signs of cytotoxic activity *in vitro*. Interestingly, $CD4^+$ T cells also possessed cytolytic traits and allocated to a $T_H1$-like phenotype according to their cytokine profile. Next, we identified the two long peptides Kras G12V and p53 R248W to be the most immunogenic peptides in a human HLA.A2/HLA.DRB1 restricted HLA context. Within the long Kras peptide we validated the previously described 10-mer $Kras_{5-14}$ G12V to be HLA.A2 restricted and added the HLA.DRB1 restricted 15-mer $Kras_{3-17}$ G12V to the list of class II alleles being able to present the Kras G12V mutation. After *in vitro* epitope mapping we further suggest the short peptides 10-mer $p53_{246-256}$ R248W and 15-mer $p53_{240-254}$ R248W as novel HLA.A2 and HLA.DRB1 restricted mutated epitopes situated within the long p53 R248W peptide. Further, we developed an A2.DR1 dtg syngenic sarcoma model to investigate the influence of long peptide vaccination on *in vivo* tumor growth. Tumor challenge experiments were performed with cell lines carrying intrinsic *Kras*/*Tp53* (p53 C176H, Kras G12C) mutations and cell lines which were engineered to express the most immunogenic mutations found in our vaccination studies (p53 R248W, Kras G12V). Tumor challenge experiments in preventive vaccinated A2.DR1 dtg mice indicated that vaccination with mutated oncogene derived peptides had an impact on tumor growth. Vaccination with mutated peptides resulted in delayed tumor outgrowth compared to vaccination with wt peptide counterparts for tumors with lower immunogenic *Kras* and *Tp53* intrinsic mutations. Surprisingly, animals vaccinated with mutated peptides performed worse in case of highly immunogenic introduced mutations. As an explanation for these contradicting results we suggest that the success of mutated long peptide vaccination seemed to critically depend on the immunogenicity of the employed mutations/peptides and their ability to induce (probably) tumor antigen-specific regulatory T cells.

The role of regulatory T cells in our model system has to be further elucidated in future investigations. To prove that the $T_{reg}$ cells are involved they should be depleted for example by cyclophosphamide treatment or administration of anti-CD25 antibodies prior to tumor challenge experiments. Depletion of $T_{reg}$ cells should reverse the detrimental outcome after vaccination with highly immunogenic (p53 R248W) mutated peptides in our engineered tumor system and ensure reproducible results after vaccination with tumor intrinsic, lower immunogenic mutated peptides. If we increase the levels of $T_{reg}$ cells through vaccination in a preventive setting before the tumor challenge experiments, it would be worth testing a therapeutic vaccination during the challenge experiment but without preventive vaccination to keep pre-treatment $T_{reg}$ levels low. In the previously mentioned IDH-1 peptide vaccination study, the effect of therapeutic vaccination on pre-established tumors was also superior over preventive vaccination prior to the challenge experiment (Schumacher et al., 2014). Furthermore, it would be interesting to learn more about the traits of tumor infiltrating, vaccination-inducted $T_{reg}$ cells. For example we saw that basically all TIL $T_{reg}$ cells strongly express the activation marker $CD44^+$. A recent study showed that Galectin-9 enhances the function and stability of induced $T_{reg}$ cells but not of natural $T_{reg}$ cells

through binding to CD44 (C. Wu et al., 2014). Hence, a strong CD44 expression also could argue in favor that our $T_{reg}$ cells are induced as they depend on CD44-Galectin-9 interactions. Antigen-specificity could be investigated in $T_{reg}$ specificity assays. It would be important to clarify, whether the (tumor-infiltrating) induced $T_{reg}$ cells are really mutation-specific or rather recognize wt sequences within the long peptides. In epitope mapping experiments for the p53 R248W peptides for instance, we saw that possible wt epitopes in proximity to the mutated epitopes could be comprised within the long peptide. What is more, $T_{reg}$ cell conversion and T cells plasticity are vividly discussed topics. Therefore, another interesting aspect would be to investigate the T cell receptor repertoire of effector $CD4^+$ T cells and induced $T_{reg}$ cells and figure out whether they are overlapping or distinct. An overlapping repertoire would for example evidence that $T_{reg}$ cells converted from conventional $CD4^+$ T cells. Next to $T_{reg}$ cells also other immune-suppressive cells like myeloid-derived suppressor cells and M2 polarized macrophages are attracted to the tumor and can contribute to suppression of effector immune responses (Mittal et al., 2014; Vesely et al., 2011). Maybe, we should also take these immune suppressive cells into consideration in future investigations. MDSCs for example were suggested as prognostic marker for the clinical outcome in the renal cell cancer peptide vaccine IMA901 trial (Walter et al., 2012) and as we learned above vaccination induced $T_H1$ cells interact with macrophages to mediate tumor eradication (Tveita et al., 2014).

As introduced, several small clinical trials employing mutated Kras and p53 peptides for vaccination of CRC and pancreatic cancer patients carrying respective mutations in their tumors have been conducted (Carbone et al., 2005; Gjertsen & Gaudernack, 1998; Khleif et al., 1999; Rahma et al., 2014; Toubaji et al., 2008; Weden et al., 2011). Therein, it became clear that this approach is safe and has a positive impact on clinical outcome. To our knowledge so far no study combined both mutated p53 and Kras peptides. Moreover, the targeting of several mutated oncogenes/tumor suppressor genes, especially if they are drivers of oncogenesis, might be advantageous. It was shown in several studies that targeting of a single mutated antigen can lead to the development of tumor escape variants, which specifically down-regulate or silence the targeted antigen expression (DuPage et al., 2012; Matsushita et al., 2012; Schumacher et al., 2014).

A common trend in cancer immunotherapy is heading towards combination of therapies. For this purpose peptide vaccination seems to be an optimal candidate (Arens et al., 2013; Melero et al., 2014). $T_{reg}$ cell depletion by cyclophosphamide to enhance the benefits of peptide vaccination already combines chemotherapy with immunotherapy. Generally conventional therapies, like chemotherapy, surgery and radiotherapy, for tumor mass debulking is indicative and easily combinable with immune therapies in a neoadjuvant or adjuvant setting. Immunotherapy can herein contribute to prevent recurrence or eliminate minimal residual disease. Also combinations of different immunotherapies are on the way. For example the gp100 peptide vaccination study in combination with high-dose systemic IL-2 administration showed an improved outcome in a randomized, multi-center phase III trial carried out in metastatic melanoma patients. Progression-free as well as overall survival was significantly higher in patients who received the gp100 vaccine compared to the control group, which was treated with high-dose IL-2 only

(Schwartzentruber et al., 2011). As in many other clinical studies, anti-peptide immune responses did not correlate with objective clinical response. Moreover, post-treatment levels of $T_{reg}$ cells were higher in patients who had a clinical response than in those who did not show a response to treatment. Obviously the combination of a targeted and a systemic treatment is feasible and superior to respective stand-alone therapies. The gp100 peptide used, was a sequence-optimized self-antigen. Possibly by targeting several, mutated (non-self) antigens the synergistic effect of this combined approach could be even further enhanced. In their latest report Kheilf and colleagues were actually comparing the influence of GM-CSF and IL-2 in combination with a mutant Kras vaccine ($Kras_{5-17}$G12C/D/V). They found that IL-2 might have a negative influence on mutant Kras specific immune responses induced by vaccination. Our data underlines the notion that depletion or reduction of $T_{reg}$ numbers is crucial for the success of long peptide anti-cancer vaccination also when mutations, meaning non-self antigens, are targeted. Possibly an additional depletion of $T_{reg}$ cells, which more than other T cell subsets depend on IL-2, would enhance the effects of combined cytokine and peptide vaccine therapy. Ipilimumab is suggested to counterbalance immune suppressive actions of $T_{reg}$ cells but is probably not depleting them (Kavanagh et al., 2008). The previously mentioned gp100 peptide was tested in combination with ipilimumab in a melanoma trial. But the combination of immune checkpoint CTLA-4 blockage with the vaccine was not superior to ipilimumab treatment alone (Hodi et al., 2010). Maybe also immune checkpoint blockade is combinable with other (more efficient) $T_{reg}$ depleting regimens to enhance the effects of peptide vaccination.

Finally we would conclude, that anti-cancer long peptide vaccination targeting oncogene mutations has a huge potential especially in combination with other (immune) therapies. However, attention has to be paid also when tumor-specific non-self antigens are targeted. They may not underlie immune control in the classical sense of central tolerance but through vaccination it seems possible to elicit a kind of ‘peripheral tolerance’ through induction of antigen-specific regulatory T cells. However, this might not be true for every mutated antigenic sequence. To provide more insight into this interesting topic, phenomena like T cell plasticity, differential TCR repertoires of distinct T cell subsets and the peptide’s antigenic properties have to be taken into account.

## 5. Literature


Abrams, S. I., Khleif, S. N., Bergmann-Leitner, E. S., Kantor, J. A., Chung, Y., Hamilton, J. M., & Schlom, J. (1997). Generation of stable CD4+ and CD8+ T cell lines from patients immunized with ras oncogene-derived peptides reflecting codon 12 mutations. *Cell Immunol, 182*(2), 137-151. doi: 10.1006/cimm.1997.1224

Abrams, S. I., Stanziale, S. F., Lunin, S. D., Zaremba, S., & Schlom, J. (1996). Identification of overlapping epitopes in mutant ras oncogene peptides that activate CD4+ and CD8+ T cell responses. *Eur J Immunol, 26*(2), 435-443. doi: 10.1002/eji.1830260225

Accapezzato, D., Visco, V., Francavilla, V., Molette, C., Donato, T., Paroli, M., . . . Barnaba, V. (2005). Chloroquine enhances human CD8+ T cell responses against soluble antigens in vivo. *J Exp Med, 202*(6), 817-828. doi: 10.1084/jem.20051106

Aguirre-Ghiso, J. A. (2007). Models, mechanisms and clinical evidence for cancer dormancy. *Nat Rev Cancer, 7*(11), 834-846. doi: 10.1038/nrc2256

Aktas, E., Kucuksezer, U. C., Bilgic, S., Erten, G., & Deniz, G. (2009). Relationship between CD107a expression and cytotoxic activity. *Cell Immunol, 254*(2), 149-154. doi: 10.1016/j.cellimm.2008.08.007

Alexandrov, L. B., Nik-Zainal, S., Wedge, D. C., Aparicio, S. A., Behjati, S., Biankin, A. V., . . . Stratton, M. R. (2013). Signatures of mutational processes in human cancer. *Nature, 500*(7463), 415-421. doi: 10.1038/nature12477

Allan, R. S., Waithman, J., Bedoui, S., Jones, C. M., Villadangos, J. A., Zhan, Y., . . . Carbone, F. R. (2006). Migratory dendritic cells transfer antigen to a lymph node-resident dendritic cell population for efficient CTL priming. *Immunity, 25*(1), 153-162. doi: 10.1016/j.immuni.2006.04.017

Altmann, D. M., Douek, D. C., Frater, A. J., Hetherington, C. M., Inoko, H., & Elliott, J. I. (1995). The T cell response of HLA-DR transgenic mice to human myelin basic protein and other antigens in the presence and absence of human CD4. *J Exp Med, 181*(3), 867-875.

Arens, R., & Schoenberger, S. P. (2010). Plasticity in programming of effector and memory CD8 T-cell formation. *Immunol Rev, 235*(1), 190-205. doi: 10.1111/j.0105-2896.2010.00899.x

Arens, R., van Hall, T., van der Burg, S. H., Ossendorp, F., & Melief, C. J. (2013). Prospects of combinatorial synthetic peptide vaccine-based immunotherapy against cancer. *Semin Immunol, 25*(2), 182-190. doi: 10.1016/j.smim.2013.04.008

Attig, S., Hennenlotter, J., Pawelec, G., Klein, G., Koch, S. D., Pircher, H., . . . Gouttefangeas, C. (2009). Simultaneous infiltration of polyfunctional effector and suppressor T cells into renal cell carcinomas. *Cancer Res, 69*(21), 8412-8419. doi: 10.1158/0008-5472.CAN-09-0852

Azuma, K., Shichijo, S., Maeda, Y., Nakatsura, T., Nonaka, Y., Fujii, T., . . . Itoh, K. (2003). Mutated p53 gene encodes a nonmutated epitope recognized by HLA-B*4601-restricted and tumor cell-reactive CTLs at tumor site. *Cancer Res, 63*(4), 854-858.

Bamford, S., Dawson, E., Forbes, S., Clements, J., Pettett, R., Dogan, A., . . . Wooster, R. (2004). The COSMIC (Catalogue of Somatic Mutations in Cancer) database and website. *Br J Cancer, 91*(2), 355-358. doi: 10.1038/sj.bjc.6601894

Bardeesy, N., & DePinho, R. A. (2002). Pancreatic cancer biology and genetics. *Nat Rev Cancer, 2*(12), 897-909. doi: 10.1038/nrc949

Barfoed, A. M., Petersen, T. R., Kirkin, A. F., Thor Straten, P., Claesson, M. H., & Zeuthen, J. (2000). Cytotoxic T-lymphocyte clones, established by stimulation with the HLA-A2 binding p5365-73 wild type peptide loaded on dendritic cells In vitro, specifically recognize and lyse HLA-A2 tumour cells overexpressing the p53 protein. *Scand J Immunol, 51*(2), 128-133.

Barnden, M. J., Allison, J., Heath, W. R., & Carbone, F. R. (1998). Defective TCR expression in transgenic mice constructed using cDNA-based alpha- and beta-chain genes under the control of heterologous regulatory elements. *Immunol Cell Biol, 76*(1), 34-40. doi: 10.1046/j.1440-1711.1998.00709.x

Beckhove, P., Feuerer, M., Dolenc, M., Schuetz, F., Choi, C., Sommerfeldt, N., . . . Umansky, V. (2004). Specifically activated memory T cell subsets from cancer patients recognize and reject xenotransplanted autologous tumors. *Journal of Clinical Investigation, 114*(1), 67-76. doi: 10.1172/jci200420278

Bedoui, S., Whitney, P. G., Waithman, J., Eidsmo, L., Wakim, L., Caminschi, I., . . . Heath, W. R. (2009). Cross-presentation of viral and self antigens by skin-derived CD103+ dendritic cells. *Nat Immunol, 10*(5), 488-495. doi: 10.1038/ni.1724

Bieging, K. T., Mello, S. S., & Attardi, L. D. (2014). Unravelling mechanisms of p53-mediated tumour suppression. *Nat Rev Cancer, 14*(5), 359-370. doi: 10.1038/nrc3711

Bienz, B., Zakut-Houri, R., Givol, D., & Oren, M. (1984). Analysis of the gene coding for the murine cellular tumour antigen p53. *EMBO J, 3*(9), 2179-2183.

Bijker, M. S., van den Eeden, S. J., Franken, K. L., Melief, C. J., Offringa, R., & van der Burg, S. H. (2007). CD8+ CTL priming by exact peptide epitopes in incomplete Freund's adjuvant induces a vanishing CTL response, whereas long peptides induce sustained CTL reactivity. *J Immunol, 179*(8), 5033-5040.

Bijker, M. S., van den Eeden, S. J., Franken, K. L., Melief, C. J., van der Burg, S. H., & Offringa, R. (2008). Superior induction of anti-tumor CTL immunity by extended peptide vaccines involves prolonged, DC-focused antigen presentation. *Eur J Immunol, 38*(4), 1033-1042. doi: 10.1002/eji.200737995

Blair, D. A., Turner, D. L., Bose, T. O., Pham, Q. M., Bouchard, K. R., Williams, K. J., . . . Lefrancois, L. (2011). Duration of antigen availability influences the expansion and memory differentiation of T cells. *J Immunol, 187*(5), 2310-2321. doi: 10.4049/jimmunol.1100363

Bode, C., Zhao, G., Steinhagen, F., Kinjo, T., & Klinman, D. M. (2011). CpG DNA as a vaccine adjuvant. *Expert Rev Vaccines, 10*(4), 499-511. doi: 10.1586/erv.10.174

Bollag, G., Tsai, J., Zhang, J., Zhang, C., Ibrahim, P., Nolop, K., & Hirth, P. (2012). Vemurafenib: the first drug approved for BRAF-mutant cancer. *Nat Rev Drug Discov, 11*(11), 873-886. doi: 10.1038/nrd3847

Bonertz, A., Weitz, J., Pietsch, D. H., Rahbari, N. N., Schlude, C., Ge, Y., . . . Beckhove, P. (2009). Antigen-specific Tregs control T cell responses against a limited repertoire of tumor antigens in patients with colorectal carcinoma. *J Clin Invest, 119*(11), 3311-3321. doi: 10.1172/JCI39608

Bopp, T., Becker, C., Klein, M., Klein-Hessling, S., Palmetshofer, A., Serfling, E., . . . Schmitt, E. (2007). Cyclic adenosine monophosphate is a key component of regulatory T cell-mediated suppression. *J Exp Med, 204*(6), 1303-1310. doi: 10.1084/jem.20062129

Bos, R., & Sherman, L. A. (2010). CD4+ T-cell help in the tumor milieu is required for recruitment and cytolytic function of CD8+ T lymphocytes. *Cancer Res, 70*(21), 8368-8377. doi: 10.1158/0008-5472.CAN-10-1322

Bossi, G., Trambas, C., Booth, S., Clark, R., Stinchcombe, J., & Griffiths, G. M. (2002). The secretory synapse: the secrets of a serial killer. *Immunol Rev, 189*, 152-160.

Bourdon, J. C., Fernandes, K., Murray-Zmijewski, F., Liu, G., Diot, A., Xirodimas, D. P., . . . Lane, D. P. (2005). p53 isoforms can regulate p53 transcriptional activity. *Genes Dev, 19*(18), 2122-2137. doi: 10.1101/gad.1339905

Boyle, L. H., Goodall, J. C., & Gaston, J. S. (2004). Major histocompatibility complex class I-restricted alloreactive CD4+ T cells. *Immunology, 112*(1), 54-63. doi: 10.1111/j.1365-2567.2004.01857.x

Buhrman, J. D., & Slansky, J. E. (2012). Improving T cell responses to modified peptides in tumor vaccines. *Immunologic Research, 55*(1-3), 34-47. doi: 10.1007/s12026-012-8348-9

Burmer, G. C., & Loeb, L. A. (1989). Mutations in the KRAS2 oncogene during progressive stages of human colon carcinoma. *Proc Natl Acad Sci U S A, 86*(7), 2403-2407.

Burnet, M. (1957). Cancer; a biological approach. I. The processes of control. *Br Med J, 1*(5022), 779-786.

Cao, X., Cai, S. F., Fehniger, T. A., Song, J., Collins, L. I., Piwnica-Worms, D. R., & Ley, T. J. (2007). Granzyme B and perforin are important for regulatory T cell-mediated suppression of tumor clearance. *Immunity, 27*(4), 635-646. doi: 10.1016/j.immuni.2007.08.014

Carbone, D. P., Ciernik, I. F., Kelley, M. J., Smith, M. C., Nadaf, S., Kavanaugh, D., . . . Berzofsky, J. A. (2005). Immunization with mutant p53- and K-ras-derived peptides in cancer patients: immune response and clinical outcome. *J Clin Oncol, 23*(22), 5099-5107. doi: 10.1200/JCO.2005.03.158

Casazza, J. P., Betts, M. R., Price, D. A., Precopio, M. L., Ruff, L. E., Brenchley, J. M., . . . Koup, R. A. (2006). Acquisition of direct antiviral effector functions by CMV-specific CD4+ T lymphocytes with cellular maturation. *J Exp Med, 203*(13), 2865-2877. doi: 10.1084/jem.20052246

Castle, J. C., Kreiter, S., Diekmann, J., Lower, M., van de Roemer, N., de Graaf, J., . . . Sahin, U. (2012). Exploiting the mutanome for tumor vaccination. *Cancer Res, 72*(5), 1081-1091. doi: 10.1158/0008-5472.CAN-11-3722

Cavallo, F., De Giovanni, C., Nanni, P., Forni, G., & Lollini, P. L. (2011). 2011: the immune hallmarks of cancer. *Cancer Immunol Immunother, 60*(3), 319-326. doi: 10.1007/s00262-010-0968-0

Challier, J., Bruniquel, D., Sewell, A. K., & Laugel, B. (2013). Adenosine and cAMP signalling skew human dendritic cell differentiation towards a tolerogenic phenotype with defective CD8(+) T-cell priming capacity. *Immunology, 138*(4), 402-410. doi: 10.1111/imm.12053

Cho, Y., Gorina, S., Jeffrey, P. D., & Pavletich, N. P. (1994). Crystal structure of a p53 tumor suppressor-DNA complex: understanding tumorigenic mutations. *Science, 265*(5170), 346-355.

Chowdhury, D., & Lieberman, J. (2008). Death by a thousand cuts: granzyme pathways of programmed cell death. *Annu Rev Immunol, 26*, 389-420. doi: 10.1146/annurev.immunol.26.021607.090404

Ciernik, I. F., Berzofsky, J. A., & Carbone, D. P. (1996). Human lung cancer cells endogenously expressing mutant p53 process and present the mutant epitope and are lysed by mutant-specific cytotoxic T lymphocytes. *Clin Cancer Res, 2*(5), 877-882.

Clark, R. A., Watanabe, R., Teague, J. E., Schlapbach, C., Tawa, M. C., Adams, N., . . . Kupper, T. S. (2012). Skin effector memory T cells do not recirculate and provide immune protection in alemtuzumab-treated CTCL patients. *Sci Transl Med, 4*(117), 117ra117. doi: 10.1126/scitranslmed.3003008

Correale, P., Rotundo, M. S., Del Vecchio, M. T., Remondo, C., Migali, C., Ginanneschi, C., . . . Tagliaferri, P. (2010). Regulatory (FoxP3+) T-cell tumor infiltration is a favorable prognostic factor in advanced colon cancer patients undergoing chemo or chemoimmunotherapy. *J Immunother, 33*(4), 435-441. doi: 10.1097/CJI.0b013e3181d32f01

Cosgrove, D., Gray, D., Dierich, A., Kaufman, J., Lemeur, M., Benoist, C., & Mathis, D. (1991). Mice lacking MHC class II molecules. *Cell, 66*(5), 1051-1066.

Coulie, P. G., Van den Eynde, B. J., van der Bruggen, P., & Boon, T. (2014). Tumour antigens recognized by T lymphocytes: at the core of cancer immunotherapy. *Nat Rev Cancer, 14*(2), 135-146. doi: 10.1038/nrc3670

Croce, C. M. (2008). Oncogenes and cancer. *N Engl J Med, 358*(5), 502-511. doi: 10.1056/NEJMra072367

Croft, M. (2003). Co-stimulatory members of the TNFR family: keys to effective T-cell immunity? *Nat Rev Immunol, 3*(8), 609-620. doi: 10.1038/nri1148

Crotzer, V. L., & Blum, J. S. (2010). Autophagy and adaptive immunity. *Immunology, 131*(1), 9-17. doi: 10.1111/j.1365-2567.2010.03321.x

Cunningham, D., Atkin, W., Lenz, H. J., Lynch, H. T., Minsky, B., Nordlinger, B., & Starling, N. (2010). Colorectal cancer. *Lancet, 375*(9719), 1030-1047. doi: 10.1016/S0140-6736(10)60353-4

Curiel, T. J., Coukos, G., Zou, L., Alvarez, X., Cheng, P., Mottram, P., . . . Zou, W. (2004). Specific recruitment of regulatory T cells in ovarian carcinoma fosters immune privilege and predicts reduced survival. *Nat Med, 10*(9), 942-949. doi: 10.1038/nm1093

Davies, H., Bignell, G. R., Cox, C., Stephens, P., Edkins, S., Clegg, S., . . . Futreal, P. A. (2002). Mutations of the BRAF gene in human cancer. *Nature, 417*(6892), 949-954. doi: 10.1038/nature00766

Deaglio, S., Dwyer, K. M., Gao, W., Friedman, D., Usheva, A., Erat, A., . . . Robson, S. C. (2007). Adenosine generation catalyzed by CD39 and CD73 expressed on regulatory T cells mediates immune suppression. *J Exp Med, 204*(6), 1257-1265. doi: 10.1084/jem.20062512

Delamarre, L., Pack, M., Chang, H., Mellman, I., & Trombetta, E. S. (2005). Differential lysosomal proteolysis in antigen-presenting cells determines antigen fate. *Science, 307*(5715), 1630-1634. doi: 10.1126/science.1108003

Di Nicolantonio, F., Martini, M., Molinari, F., Sartore-Bianchi, A., Arena, S., Saletti, P., . . . Bardelli, A. (2008). Wild-Type BRAF Is Required for Response to Panitumumab or Cetuximab in Metastatic Colorectal Cancer. *Journal of Clinical Oncology, 26*(35), 5705-5712. doi: 10.1200/jco.2008.18.0786

Disis, M. L., Gooley, T. A., Rinn, K., Davis, D., Piepkorn, M., Cheever, M. A., . . . Schiffman, K. (2002). Generation of T-cell immunity to the HER-2/neu protein after active immunization with HER-2/neu peptide-based vaccines. *J Clin Oncol, 20*(11), 2624-2632.

Dong, C., Juedes, A. E., Temann, U. A., Shresta, S., Allison, J. P., Ruddle, N. H., & Flavell, R. A. (2001). ICOS co-stimulatory receptor is essential for T-cell activation and function. *Nature, 409*(6816), 97-101. doi: 10.1038/35051100

Dunn, G. P., Old, L. J., & Schreiber, R. D. (2004a). The immunobiology of cancer immunosurveillance and immunoediting. *Immunity, 21*(2), 137-148. doi: 10.1016/j.immuni.2004.07.017

Dunn, G. P., Old, L. J., & Schreiber, R. D. (2004b). The three Es of cancer immunoediting. *Annu Rev Immunol, 22*, 329-360. doi: 10.1146/annurev.immunol.22.012703.104803

DuPage, M., Mazumdar, C., Schmidt, L. M., Cheung, A. F., & Jacks, T. (2012). Expression of tumour-specific antigens underlies cancer immunoediting. *Nature, 482*(7385), 405-409. doi: 10.1038/nature10803

El-Jawhari, J. J., El-Sherbiny, Y. M., Scott, G. B., Morgan, R. S., Prestwich, R., Bowles, P. A., . . . Cook, G. P. (2014). Blocking oncogenic RAS enhances tumour cell surface MHC class I expression but does not alter susceptibility to cytotoxic lymphocytes. *Mol Immunol, 58*(2), 160-168. doi: 10.1016/j.molimm.2013.11.020

Ellis, R. W., Defeo, D., Shih, T. Y., Gonda, M. A., Young, H. A., Tsuchida, N., . . . Scolnick, E. M. (1981). The p21 src genes of Harvey and Kirsten sarcoma viruses originate from divergent members of a family of normal vertebrate genes. *Nature, 292*(5823), 506-511.

Falk, K., Rotzschke, O., Stevanovic, S., Jung, G., & Rammensee, H. G. (1991). Allele-specific motifs revealed by sequencing of self-peptides eluted from MHC molecules. *Nature, 351*(6324), 290-296. doi: 10.1038/351290a0

Farber, D. L., Yudanin, N. A., & Restifo, N. P. (2014). Human memory T cells: generation, compartmentalization and homeostasis. *Nat Rev Immunol, 14*(1), 24-35. doi: 10.1038/nri3567

Fearon, E. R., & Vogelstein, B. (1990). A genetic model for colorectal tumorigenesis. *Cell, 61*(5), 759-767.

Fehres, C. M., Unger, W. W., Garcia-Vallejo, J. J., & van Kooyk, Y. (2014). Understanding the biology of antigen cross-presentation for the design of vaccines against cancer. *Front Immunol, 5*, 149. doi: 10.3389/fimmu.2014.00149

Feuerer, M., Beckhove, P., Bai, L., Solomayer, E. F., Bastert, G., Diel, I. J., . . . Umansky, V. (2001). Therapy of human tumors in NOD/SCID mice with patient-derived reactivated memory T cells from bone marrow. *Nat Med, 7*(4), 452-458. doi: 10.1038/86523

Feuerer, M., Rocha, M., Bai, L., Umansky, V., Solomayer, E. F., Bastert, G., . . . Schirrmacher, V. (2001). Enrichment of memory T cells and other profound immunological changes in the bone marrow from untreated breast cancer patients. *Int J Cancer, 92*(1), 96-105.

Fidler, I. J. (1973). Selection of successive tumour lines for metastasis. *Nat New Biol, 242*(118), 148-149.

Fidler, I. J., & Kripke, M. L. (1977). Metastasis results from preexisting variant cells within a malignant tumor. *Science, 197*(4306), 893-895.

Fisk, B., Blevins, T. L., Wharton, J. T., & Ioannides, C. G. (1995). Identification of an immunodominant peptide of HER-2/neu protooncogene recognized by ovarian tumor-specific cytotoxic T lymphocyte lines. *J Exp Med, 181*(6), 2109-2117.

Fossum, B., Gedde-Dahl, T., 3rd, Hansen, T., Eriksen, J. A., Thorsby, E., & Gaudernack, G. (1993). Overlapping epitopes encompassing a point mutation (12 Gly-->Arg) in p21 ras can be recognized by HLA-DR, -DP and -DQ restricted T cells. *Eur J Immunol, 23*(10), 2687-2691. doi: 10.1002/eji.1830231045

Fritz, J. M., Dwyer-Nield, L. D., Russell, B. M., & Malkinson, A. M. (2010). The Kras mutational spectra of chemically induced lung tumors in different inbred mice mimics the spectra of KRAS mutations in adenocarcinomas in smokers versus nonsmokers. *J Thorac Oncol, 5*(2), 254-257. doi: 10.1097/JTO.0b013e3181c8ce04

Frommer, F., & Waisman, A. (2010). B cells participate in thymic negative selection of murine auto-reactive CD4+ T cells. *PLoS One, 5*(10), e15372. doi: 10.1371/journal.pone.0015372

Fujita, H., Senju, S., Yokomizo, H., Saya, H., Ogawa, M., Matsushita, S., & Nishimura, Y. (1998). Evidence that HLA class II-restricted human CD4+ T cells specific to p53 self peptides respond to p53 proteins of both wild and mutant forms. *Eur J Immunol, 28*(1), 305-316. doi: 10.1002/(SICI)1521-4141(199801)28:01<305::AID-IMMU305>3.0.CO;2-3

Galon, J., Costes, A., Sanchez-Cabo, F., Kirilovsky, A., Mlecnik, B., Lagorce-Pages, C., . . . Pages, F. (2006). Type, density, and location of immune cells within human colorectal tumors predict clinical outcome. *Science, 313*(5795), 1960-1964. doi: 10.1126/science.1129139

Gattinoni, L., Klebanoff, C. A., & Restifo, N. P. (2012). Paths to stemness: building the ultimate antitumour T cell. *Nat Rev Cancer, 12*(10), 671-684. doi: 10.1038/nrc3322

Gattinoni, L., Lugli, E., Ji, Y., Pos, Z., Paulos, C. M., Quigley, M. F., . . . Restifo, N. P. (2011). A human memory T cell subset with stem cell-like properties. *Nat Med, 17*(10), 1290-1297. doi: 10.1038/nm.2446

Gerlinger, M., Rowan, A. J., Horswell, S., Larkin, J., Endesfelder, D., Gronroos, E., . . . Swanton, C. (2012). Intratumor heterogeneity and branched evolution revealed by multiregion sequencing. *N Engl J Med, 366*(10), 883-892. doi: 10.1056/NEJMoa1113205

Ghebeh, H., Barhoush, E., Tulbah, A., Elkum, N., Al-Tweigeri, T., & Dermime, S. (2008). FOXP3+ Tregs and B7-H1+/PD-1+ T lymphocytes co-infiltrate the tumor tissues of high-risk breast cancer patients: Implication for immunotherapy. *BMC Cancer, 8*, 57. doi: 10.1186/1471-2407-8-57

Ghiringhelli, F., Menard, C., Puig, P. E., Ladoire, S., Roux, S., Martin, F., . . . Chauffert, B. (2007). Metronomic cyclophosphamide regimen selectively depletes CD4+CD25+ regulatory T cells and restores T and NK effector functions in end stage cancer patients. *Cancer Immunol Immunother, 56*(5), 641-648. doi: 10.1007/s00262-006-0225-8

Gjertsen, M. K., Bjorheim, J., Saeterdal, I., Myklebust, J., & Gaudernack, G. (1997). Cytotoxic CD4+ and CD8+ T lymphocytes, generated by mutant p21-ras (12Val) peptide vaccination of a patient, recognize 12Val-dependent nested epitopes present within the vaccine peptide and kill autologous tumour cells carrying this mutation. *Int J Cancer, 72*(5), 784-790.

Gjertsen, M. K., Buanes, T., Rosseland, A. R., Bakka, A., Gladhaug, I., Soreide, O., . . . Gaudernack, G. (2001). Intradermal ras peptide vaccination with granulocyte-macrophage colony-stimulating factor as adjuvant: Clinical and immunological responses in patients with pancreatic adenocarcinoma. *Int J Cancer, 92*(3), 441-450.

Gjertsen, M. K., & Gaudernack, G. (1998). Mutated Ras peptides as vaccines in immunotherapy of cancer. *Vox Sang, 74 Suppl 2*, 489-495.

Gjertsen, M. K., Saeterdal, I., Saeboe-Larssen, S., & Gaudernack, G. (2003). HLA-A3 restricted mutant ras specific cytotoxic T-lymphocytes induced by vaccination with T-helper epitopes. *J Mol Med (Berl), 81*(1), 43-50. doi: 10.1007/s00109-002-0390-y

Gnjatic, S., Nishikawa, H., Jungbluth, A. A., Gure, A. O., Ritter, G., Jager, E., . . . Old, L. J. (2006). NY-ESO-1: review of an immunogenic tumor antigen. *Adv Cancer Res, 95*, 1-30. doi: 10.1016/S0065-230X(06)95001-5

Grakoui, A., Bromley, S. K., Sumen, C., Davis, M. M., Shaw, A. S., Allen, P. M., & Dustin, M. L. (1999). The immunological synapse: a molecular machine controlling T cell activation. *Science, 285*(5425), 221-227.

Green, D. R., Ferguson, T., Zitvogel, L., & Kroemer, G. (2009). Immunogenic and tolerogenic cell death. *Nat Rev Immunol, 9*(5), 353-363. doi: 10.1038/nri2545

Greenwald, R. J., Freeman, G. J., & Sharpe, A. H. (2005). The B7 family revisited. *Annu Rev Immunol, 23*, 515-548. doi: 10.1146/annurev.immunol.23.021704.115611

Grupp, S. A., Kalos, M., Barrett, D., Aplenc, R., Porter, D. L., Rheingold, S. R., . . . June, C. H. (2013). Chimeric antigen receptor-modified T cells for acute lymphoid leukemia. *N Engl J Med, 368*(16), 1509-1518. doi: 10.1056/NEJMoa1215134

Haabeth, O. A., Tveita, A. A., Fauskanger, M., Schjesvold, F., Lorvik, K. B., Hofgaard, P. O., . . . Bogen, B. (2014). How Do CD4(+) T Cells Detect and Eliminate Tumor Cells That Either Lack or Express MHC Class II Molecules? *Front Immunol, 5*, 174. doi: 10.3389/fimmu.2014.00174

Hailemichael, Y., Dai, Z., Jaffarzad, N., Ye, Y., Medina, M. A., Huang, X. F., . . . Overwijk, W. W. (2013). Persistent antigen at vaccination sites induces tumor-specific CD8(+) T cell sequestration, dysfunction and deletion. *Nat Med, 19*(4), 465-472. doi: 10.1038/nm.3105

Hale, D. F., Clifton, G. T., Sears, A. K., Vreeland, T. J., Shumway, N., Peoples, G. E., & Mittendorf, E. A. (2012). Cancer vaccines: should we be targeting patients with less aggressive disease? *Expert Rev Vaccines, 11*(6), 721-731. doi: 10.1586/erv.12.39

Hanahan, D., & Weinberg, R. A. (2000). The hallmarks of cancer. *Cell, 100*(1), 57-70.

Hanahan, D., & Weinberg, R. A. (2011). Hallmarks of cancer: the next generation. *Cell, 144*(5), 646-674. doi: 10.1016/j.cell.2011.02.013

Haniffa, M., Shin, A., Bigley, V., McGovern, N., Teo, P., See, P., . . . Ginhoux, F. (2012). Human tissues contain CD141hi cross-presenting dendritic cells with functional homology to mouse CD103+ nonlymphoid dendritic cells. *Immunity, 37*(1), 60-73. doi: 10.1016/j.immuni.2012.04.012

Heath, W. R., & Carbone, F. R. (2009). Dendritic cell subsets in primary and secondary T cell responses at body surfaces. *Nat Immunol, 10*(12), 1237-1244. doi: 10.1038/ni.1822

Hernandez, J., Lee, P. P., Davis, M. M., & Sherman, L. A. (2000). The Use of HLA A2.1/p53 Peptide Tetramers to Visualize the Impact of Self Tolerance on the TCR Repertoire. *The Journal of Immunology, 164*(2), 596-602. doi: 10.4049/jimmunol.164.2.596

Hidalgo, M. (2010). Pancreatic cancer. *N Engl J Med, 362*(17), 1605-1617. doi: 10.1056/NEJMra0901557

Hiraoka, N., Onozato, K., Kosuge, T., & Hirohashi, S. (2006). Prevalence of FOXP3+ regulatory T cells increases during the progression of pancreatic ductal adenocarcinoma and its premalignant lesions. *Clin Cancer Res, 12*(18), 5423-5434. doi: 10.1158/1078-0432.CCR-06-0369

Hodi, F. S., O'Day, S. J., McDermott, D. F., Weber, R. W., Sosman, J. A., Haanen, J. B., . . . Urba, W. J. (2010). Improved survival with ipilimumab in patients with metastatic melanoma. *N Engl J Med, 363*(8), 711-723. doi: 10.1056/NEJMoa1003466

Hollingsworth, R. E., Jr., Hensey, C. E., & Lee, W. H. (1993). Retinoblastoma protein and the cell cycle. *Curr Opin Genet Dev, 3*(1), 55-62.

Hruban, R. H., Adsay, N. V., Albores-Saavedra, J., Compton, C., Garrett, E. S., Goodman, S. N., . . . Offerhaus, G. J. (2001). Pancreatic intraepithelial neoplasia: a new nomenclature and classification system for pancreatic duct lesions. *Am J Surg Pathol, 25*(5), 579-586.

Ito, D., Visus, C., Hoffmann, T. K., Balz, V., Bier, H., Appella, E., . . . DeLeo, A. B. (2007). Immunological characterization of missense mutations occurring within cytotoxic T cell-defined p53 epitopes in HLA-A*0201+ squamous cell carcinomas of the head and neck. *Int J Cancer, 120*(12), 2618-2624. doi: 10.1002/ijc.22584

Janssen, E. M., Lemmens, E. E., Wolfe, T., Christen, U., von Herrath, M. G., & Schoenberger, S. P. (2003). CD4+ T cells are required for secondary expansion and memory in CD8+ T lymphocytes. *Nature, 421*(6925), 852-856. doi: 10.1038/nature01441

Jellison, E. R., Kim, S. K., & Welsh, R. M. (2005). Cutting Edge: MHC Class II-Restricted Killing In Vivo during Viral Infection. *The Journal of Immunology, 174*(2), 614-618. doi: 10.4049/jimmunol.174.2.614

Jemal, A., Bray, F., Center, M. M., Ferlay, J., Ward, E., & Forman, D. (2011). Global cancer statistics. *CA Cancer J Clin, 61*(2), 69-90. doi: 10.3322/caac.20107

Jin, B., Wang, R. Y., Qiu, Q., Sugauchi, F., Grandinetti, T., Alter, H. J., & Shih, J. W. (2007). Induction of potent cellular immune response in mice by hepatitis C virus NS3 protein with double-stranded RNA. *Immunology, 122*(1), 15-27. doi: 10.1111/j.1365-2567.2007.02607.x

Kalli, F., Machiorlatti, R., Battaglia, F., Parodi, A., Conteduca, G., Ferrera, F., . . . Filaci, G. (2013). Comparative analysis of cancer vaccine settings for the selection of an effective protocol in mice. *J Transl Med, 11*, 120. doi: 10.1186/1479-5876-11-120

Kanda, M., Matthaei, H., Wu, J., Hong, S. M., Yu, J., Borges, M., . . . Goggins, M. (2012). Presence of somatic mutations in most early-stage pancreatic intraepithelial neoplasia. *Gastroenterology, 142*(4), 730-733 e739. doi: 10.1053/j.gastro.2011.12.042

Kantoff, P. W., Higano, C. S., Shore, N. D., Berger, E. R., Small, E. J., Penson, D. F., . . . Investigators, I. S. (2010). Sipuleucel-T immunotherapy for castration-resistant prostate cancer. *N Engl J Med, 363*(5), 411-422. doi: 10.1056/NEJMoa1001294

Karosiene, E., Rasmussen, M., Blicher, T., Lund, O., Buus, S., & Nielsen, M. (2013). NetMHCIIpan-3.0, a common pan-specific MHC class II prediction method including all three human MHC class II isotypes, HLA-DR, HLA-DP and HLA-DQ. *Immunogenetics, 65*(10), 711-724. doi: 10.1007/s00251-013-0720-y

Kastenmuller, W., Gasteiger, G., Gronau, J. H., Baier, R., Ljapoci, R., Busch, D. H., & Drexler, I. (2007). Cross-competition of CD8+ T cells shapes the immunodominance hierarchy during boost vaccination. *J Exp Med, 204*(9), 2187-2198. doi: 10.1084/jem.20070489

Kavanagh, B., O'Brien, S., Lee, D., Hou, Y., Weinberg, V., Rini, B., . . . Fong, L. (2008). CTLA4 blockade expands FoxP3+ regulatory and activated effector CD4+ T cells in a dose-dependent fashion. *Blood, 112*(4), 1175-1183. doi: 10.1182/blood-2007-11-125435

Kedl, R. M., Kappler, J. W., & Marrack, P. (2003). Epitope dominance, competition and T cell affinity maturation. *Curr Opin Immunol, 15*(1), 120-127.

Keir, M. E., Freeman, G. J., & Sharpe, A. H. (2007). PD-1 Regulates Self-Reactive CD8+ T Cell Responses to Antigen in Lymph Nodes and Tissues. *The Journal of Immunology, 179*(8), 5064-5070. doi: 10.4049/jimmunol.179.8.5064

Keller, A. M., Xiao, Y., Peperzak, V., Naik, S. H., & Borst, J. (2009). Costimulatory ligand CD70 allows induction of CD8+ T-cell immunity by immature dendritic cells in a vaccination setting. *Blood, 113*(21), 5167-5175. doi: 10.1182/blood-2008-03-148007

Kenter, G. G., Welters, M. J., Valentijn, A. R., Lowik, M. J., Berends-van der Meer, D. M., Vloon, A. P., . . . Melief, C. J. (2009). Vaccination against HPV-16 oncoproteins for vulvar intraepithelial neoplasia. *N Engl J Med, 361*(19), 1838-1847. doi: 10.1056/NEJMoa0810097

Kessels, H. W., Schepers, K., van den Boom, M. D., Topham, D. J., & Schumacher, T. N. (2006). Generation of T cell help through a MHC class I-restricted TCR. *J Immunol, 177*(2), 976-982.

Khazaie, K., Prifti, S., Beckhove, P., Griesbach, A., Russell, S., Collins, M., & Schirrmacher, V. (1994). Persistence of dormant tumor cells in the bone marrow of tumor cell-vaccinated mice correlates with long-term immunological protection. *Proc Natl Acad Sci U S A, 91*(16), 7430-7434.

Khleif, S. N., Abrams, S. I., Hamilton, J. M., Bergmann-Leitner, E., Chen, A., Bastian, A., . . . Schlom, J. (1999). A phase I vaccine trial with peptides reflecting ras oncogene mutations of solid tumors. *J Immunother, 22*(2), 155-165.

Kimura, T., McKolanis, J. R., Dzubinski, L. A., Islam, K., Potter, D. M., Salazar, A. M., . . . Finn, O. J. (2013). MUC1 vaccine for individuals with advanced adenoma of the colon: a cancer immunoprevention feasibility study. *Cancer Prev Res (Phila), 6*(1), 18-26. doi: 10.1158/1940-6207.CAPR-12-0275

Klein, L., & Jovanovic, K. (2011). Regulatory T cell lineage commitment in the thymus. *Semin Immunol, 23*(6), 401-409. doi: 10.1016/j.smim.2011.06.003

Klein, L., Kyewski, B., Allen, P. M., & Hogquist, K. A. (2014). Positive and negative selection of the T cell repertoire: what thymocytes see (and don't see). *Nat Rev Immunol, 14*(6), 377-391. doi: 10.1038/nri3667

Klug, F., Prakash, H., Huber, P. E., Seibel, T., Bender, N., Halama, N., . . . Beckhove, P. (2013). Low-dose irradiation programs macrophage differentiation to an iNOS(+)/M1 phenotype that orchestrates effective T cell immunotherapy. *Cancer Cell, 24*(5), 589-602. doi: 10.1016/j.ccr.2013.09.014

Kobayashi, N., Hiraoka, N., Yamagami, W., Ojima, H., Kanai, Y., Kosuge, T., . . . Hirohashi, S. (2007). FOXP3+ regulatory T cells affect the development and progression of hepatocarcinogenesis. *Clin Cancer Res, 13*(3), 902-911. doi: 10.1158/1078-0432.CCR-06-2363

Koch, U., & Radtke, F. (2011). Mechanisms of T cell development and transformation. *Annu Rev Cell Dev Biol, 27*, 539-562. doi: 10.1146/annurev-cellbio-092910-154008

Koebel, C. M., Vermi, W., Swann, J. B., Zerafa, N., Rodig, S. J., Old, L. J., . . . Schreiber, R. D. (2007). Adaptive immunity maintains occult cancer in an equilibrium state. *Nature, 450*(7171), 903-907. doi: 10.1038/nature06309

Koller, B. H., Marrack, P., Kappler, J. W., & Smithies, O. (1990). Normal development of mice deficient in beta 2M, MHC class I proteins, and CD8+ T cells. *Science, 248*(4960), 1227-1230.

Kondo, M., Weissman, I. L., & Akashi, K. (1997). Identification of clonogenic common lymphoid progenitors in mouse bone marrow. *Cell, 91*(5), 661-672.

Kotturi, M. F., Scott, I., Wolfe, T., Peters, B., Sidney, J., Cheroutre, H., . . . Sette, A. (2008). Naive Precursor Frequencies and MHC Binding Rather Than the Degree of Epitope Diversity Shape CD8+ T Cell Immunodominance. *The Journal of Immunology, 181*(3), 2124-2133. doi: 10.4049/jimmunol.181.3.2124

Kovacsovics-Bankowski, M., & Rock, K. L. (1995). A phagosome-to-cytosol pathway for exogenous antigens presented on MHC class I molecules. *Science, 267*(5195), 243-246.

Kruger, C., Greten, T. F., & Korangy, F. (2007). Immune based therapies in cancer. *Histol Histopathol, 22*(6), 687-696.

Kurts, C., Robinson, B. W., & Knolle, P. A. (2010). Cross-priming in health and disease. *Nat Rev Immunol, 10*(6), 403-414. doi: 10.1038/nri2780

Labianca, R., Beretta, G. D., Kildani, B., Milesi, L., Merlin, F., Mosconi, S., . . . Wils, J. (2010). Colon cancer. *Crit Rev Oncol Hematol, 74*(2), 106-133. doi: 10.1016/j.critrevonc.2010.01.010

Lane, D. P. (1992). Cancer. p53, guardian of the genome. *Nature, 358*(6381), 15-16. doi: 10.1038/358015a0

Lauwen, M. M., Zwaveling, S., de Quartel, L., Ferreira Mota, S. C., Grashorn, J. A., Melief, C. J., . . . Offringa, R. (2008). Self-tolerance does not restrict the CD4+ T-helper response against the p53 tumor antigen. *Cancer Res, 68*(3), 893-900. doi: 10.1158/0008-5472.CAN-07-3166

Leary, R. J., Kinde, I., Diehl, F., Schmidt, K., Clouser, C., Duncan, C., . . . Velculescu, V. E. (2010). Development of personalized tumor biomarkers using massively parallel sequencing. *Sci Transl Med, 2*(20), 20ra14. doi: 10.1126/scitranslmed.3000702

Leffers, N., Lambeck, A. J., Gooden, M. J., Hoogeboom, B. N., Wolf, R., Hamming, I. E., . . . Nijman, H. W. (2009). Immunization with a P53 synthetic long peptide vaccine induces P53-specific immune responses in ovarian cancer patients, a phase II trial. *Int J Cancer, 125*(9), 2104-2113. doi: 10.1002/ijc.24597

Lefranc, M. P., Giudicelli, V., Ginestoux, C., Jabado-Michaloud, J., Folch, G., Bellahcene, F., . . . Duroux, P. (2009). IMGT, the international ImMunoGeneTics information system. *Nucleic Acids Res, 37*(Database issue), D1006-1012. doi: 10.1093/nar/gkn838

Lengauer, C., Kinzler, K. W., & Vogelstein, B. (1998). Genetic instabilities in human cancers. *Nature, 396*(6712), 643-649. doi: 10.1038/25292

Lennon, A. M., Wolfgang, C. L., Canto, M. I., Klein, A. P., Herman, J. M., Goggins, M., . . . Hruban, R. H. (2014). The Early Detection of Pancreatic Cancer: What Will It Take to Diagnose and Treat Curable Pancreatic Neoplasia? *Cancer Res*. doi: 10.1158/0008-5472.CAN-14-0734

Li, J., Park, J., Foss, D., & Goldschneider, I. (2009). Thymus-homing peripheral dendritic cells constitute two of the three major subsets of dendritic cells in the steady-state thymus. *J Exp Med, 206*(3), 607-622. doi: 10.1084/jem.20082232

Liang, B., Workman, C., Lee, J., Chew, C., Dale, B. M., Colonna, L., . . . Clynes, R. (2008). Regulatory T Cells Inhibit Dendritic Cells by Lymphocyte Activation Gene-3 Engagement of MHC Class II. *The Journal of Immunology, 180*(9), 5916-5926. doi: 10.4049/jimmunol.180.9.5916

Lievre, A., Bachet, J. B., Le Corre, D., Boige, V., Landi, B., Emile, J. F., . . . Laurent-Puig, P. (2006). KRAS mutation status is predictive of response to cetuximab therapy in colorectal cancer. *Cancer Res, 66*(8), 3992-3995. doi: 10.1158/0008-5472.CAN-06-0191

Lin, K. Y., Guarnieri, F. G., Staveley-O'Carroll, K. F., Levitsky, H. I., August, J. T., Pardoll, D. M., & Wu, T. C. (1996). Treatment of established tumors with a novel vaccine that enhances major histocompatibility class II presentation of tumor antigen. *Cancer Res, 56*(1), 21-26.

Liston, A., & Gray, D. H. (2014). Homeostatic control of regulatory T cell diversity. *Nat Rev Immunol, 14*(3), 154-165. doi: 10.1038/nri3605

Love, P. E., & Bhandoola, A. (2011). Signal integration and crosstalk during thymocyte migration and emigration. *Nat Rev Immunol, 11*(7), 469-477. doi: 10.1038/nri2989

Lower, M., Renard, B. Y., de Graaf, J., Wagner, M., Paret, C., Kneip, C., . . . Sahin, U. (2012). Confidence-based somatic mutation evaluation and prioritization. *PLoS Comput Biol, 8*(9), e1002714. doi: 10.1371/journal.pcbi.1002714

Lundegaard, C., Lund, O., & Nielsen, M. (2008). Accurate approximation method for prediction of class I MHC affinities for peptides of length 8, 10 and 11 using prediction tools trained on 9mers. *Bioinformatics, 24*(11), 1397-1398. doi: 10.1093/bioinformatics/btn128

Lustgarten, J., Dominguez, A. L., & Cuadros, C. (2004). The CD8+ T cell repertoire against Her-2/neu antigens in neu transgenic mice is of low avidity with antitumor activity. *Eur J Immunol, 34*(3), 752-761. doi: 10.1002/eji.200324427

Maeurer, M. J., Gollin, S. M., Martin, D., Swaney, W., Bryant, J., Castelli, C., . . . Lotze, M. T. (1996). Tumor escape from immune recognition: lethal recurrent melanoma in a patient associated with downregulation of the peptide transporter protein TAP-1 and loss of expression of the immunodominant MART-1/Melan-A antigen. *J Clin Invest, 98*(7), 1633-1641. doi: 10.1172/JCI118958

Marshall, N. B., & Swain, S. L. (2011). Cytotoxic CD4 T cells in antiviral immunity. *J Biomed Biotechnol, 2011*, 954602. doi: 10.1155/2011/954602

Mathis, D., & Benoist, C. (2009). Aire. *Annu Rev Immunol, 27*, 287-312. doi: 10.1146/annurev.immunol.25.022106.141532

Matsushita, H., Vesely, M. D., Koboldt, D. C., Rickert, C. G., Uppaluri, R., Magrini, V. J., . . . Schreiber, R. D. (2012). Cancer exome analysis reveals a T-cell-dependent mechanism of cancer immunoediting. *Nature, 482*(7385), 400-404. doi: 10.1038/nature10755

Maurer, T., Heit, A., Hochrein, H., Ampenberger, F., O'Keeffe, M., Bauer, S., . . . Wagner, H. (2002). CpG-DNA aided cross-presentation of soluble antigens by dendritic cells. *Eur J Immunol, 32*(8), 2356-2364. doi: 10.1002/1521-4141(200208)32:8<2356::AID-IMMU2356>3.0.CO;2-Z

Mayordomo, J. I., Loftus, D. J., Sakamoto, H., De Cesare, C. M., Appasamy, P. M., Lotze, M. T., . . . DeLeo, A. B. (1996). Therapy of murine tumors with p53 wild-type and mutant sequence peptide-based vaccines. *J Exp Med, 183*(4), 1357-1365.

McCaughtry, T. M., Baldwin, T. A., Wilken, M. S., & Hogquist, K. A. (2008). Clonal deletion of thymocytes can occur in the cortex with no involvement of the medulla. *J Exp Med, 205*(11), 2575-2584. doi: 10.1084/jem.20080866

McGrath, J. P., Capon, D. J., Smith, D. H., Chen, E. Y., Seeburg, P. H., Goeddel, D. V., & Levinson, A. D. (1983). Structure and organization of the human Ki-ras proto-oncogene and a related processed pseudogene. *Nature, 304*(5926), 501-506.

Melero, I., Gaudernack, G., Gerritsen, W., Huber, C., Parmiani, G., Scholl, S., . . . Mellstedt, H. (2014). Therapeutic vaccines for cancer: an overview of clinical trials. *Nat Rev Clin Oncol*. doi: 10.1038/nrclinonc.2014.111

Melief, C. J. (2008). Cancer immunotherapy by dendritic cells. *Immunity, 29*(3), 372-383. doi: 10.1016/j.immuni.2008.08.004

Melief, C. J., & van der Burg, S. H. (2008). Immunotherapy of established (pre)malignant disease by synthetic long peptide vaccines. *Nat Rev Cancer, 8*(5), 351-360. doi: 10.1038/nrc2373

Mellman, I., Coukos, G., & Dranoff, G. (2011). Cancer immunotherapy comes of age. *Nature, 480*(7378), 480-489. doi: 10.1038/nature10673

Mellor, A. L., & Munn, D. H. (2004). IDO expression by dendritic cells: tolerance and tryptophan catabolism. *Nat Rev Immunol, 4*(10), 762-774. doi: 10.1038/nri1457

Merzougui, N., Kratzer, R., Saveanu, L., & van Endert, P. (2011). A proteasome-dependent, TAP-independent pathway for cross-presentation of phagocytosed antigen. *EMBO Rep, 12*(12), 1257-1264. doi: 10.1038/embor.2011.203

Miracco, C., Mourmouras, V., Biagioli, M., Rubegni, P., Mannucci, S., Monciatti, I., . . . Luzi, P. (2007). Utility of tumour-infiltrating CD25+FOXP3+ regulatory T cell evaluation in predicting local recurrence in vertical growth phase cutaneous melanoma. *Oncol Rep, 18*(5), 1115-1122.

Mittal, D., Gubin, M. M., Schreiber, R. D., & Smyth, M. J. (2014). New insights into cancer immunoediting and its three component phases--elimination, equilibrium and escape. *Curr Opin Immunol, 27*, 16-25. doi: 10.1016/j.coi.2014.01.004

Miyara, M., Yoshioka, Y., Kitoh, A., Shima, T., Wing, K., Niwa, A., . . . Sakaguchi, S. (2009). Functional delineation and differentiation dynamics of human CD4+ T cells expressing the FoxP3 transcription factor. *Immunity, 30*(6), 899-911. doi: 10.1016/j.immuni.2009.03.019

Moon, J. J., Chu, H. H., Pepper, M., McSorley, S. J., Jameson, S. C., Kedl, R. M., & Jenkins, M. K. (2007). Naive CD4(+) T cell frequency varies for different epitopes and predicts repertoire diversity and response magnitude. *Immunity, 27*(2), 203-213. doi: 10.1016/j.immuni.2007.07.007

Moore, M. J., Goldstein, D., Hamm, J., Figer, A., Hecht, J. R., Gallinger, S., . . . National Cancer Institute of Canada Clinical Trials, G. (2007). Erlotinib plus gemcitabine compared with gemcitabine alone in patients with advanced pancreatic cancer: a phase III trial of the National Cancer Institute of Canada Clinical Trials Group. *J Clin Oncol, 25*(15), 1960-1966. doi: 10.1200/JCO.2006.07.9525

Moran, A., Ortega, P., de Juan, C., Fernandez-Marcelo, T., Frias, C., Sanchez-Pernaute, A., . . . Benito, M. (2010). Differential colorectal carcinogenesis: Molecular basis and clinical relevance. *World J Gastrointest Oncol, 2*(3), 151-158. doi: 10.4251/wjgo.v2.i3.151

Morgan, R. A., Chinnasamy, N., Abate-Daga, D., Gros, A., Robbins, P. F., Zheng, Z., . . . Rosenberg, S. A. (2013). Cancer regression and neurological toxicity following anti-MAGE-A3 TCR gene therapy. *J Immunother, 36*(2), 133-151. doi: 10.1097/CJI.0b013e3182829903

Mueller, M., Schlosser, E., Gander, B., & Groettrup, M. (2011). Tumor eradication by immunotherapy with biodegradable PLGA microspheres--an alternative to incomplete Freund's adjuvant. *Int J Cancer, 129*(2), 407-416. doi: 10.1002/ijc.25914

Muller-Berghaus, J., Ehlert, K., Ugurel, S., Umansky, V., Bucur, M., Schirrmacher, V., . . . Schadendorf, D. (2006). Melanoma-reactive T cells in the bone marrow of melanoma patients: association with disease stage and disease duration. *Cancer Res, 66*(12), 5997-6001. doi: 10.1158/0008-5472.CAN-04-0484

Muller, D., Koller, B. H., Whitton, J. L., LaPan, K. E., Brigman, K. K., & Frelinger, J. A. (1992). LCMV-specific, class II-restricted cytotoxic T cells in beta 2-microglobulin-deficient mice. *Science, 255*(5051), 1576-1578.

Munitic, I., Decaluwe, H., Evaristo, C., Lemos, S., Wlodarczyk, M., Worth, A., . . . Rocha, B. (2009). Epitope specificity and relative clonal abundance do not affect CD8 differentiation patterns during lymphocytic choriomeningitis virus inf

ection. *J Virol, 83*(22), 11795-11807. doi: 10.1128/JVI.01402-09

Murata, S., Sasaki, K., Kishimoto, T., Niwa, S., Hayashi, H., Takahama, Y., & Tanaka, K. (2007). Regulation of CD8+ T cell development by thymus-specific proteasomes. *Science, 316*(5829), 1349-1353. doi: 10.1126/science.1141915

Murphy, K. P. (2012). *Janeway's Immunobiology* (8th Edition ed.). New York, NY, USA: Garland Science.

Nakagawa, T., Roth, W., Wong, P., Nelson, A., Farr, A., Deussing, J., . . . Rudensky, A. Y. (1998). Cathepsin L: critical role in Ii degradation and CD4 T cell selection in the thymus. *Science, 280*(5362), 450-453.

Napoletano, C., Bellati, F., Landi, R., Pauselli, S., Marchetti, C., Visconti, V., . . . Nuti, M. (2010). Ovarian cancer cytoreduction induces changes in T cell population subsets reducing immunosuppression. *J Cell Mol Med, 14*(12), 2748-2759. doi: 10.1111/j.1582-4934.2009.00911.x

Neefjes, J., Jongsma, M. L., Paul, P., & Bakke, O. (2011). Towards a systems understanding of MHC class I and MHC class II antigen presentation. *Nat Rev Immunol, 11*(12), 823-836. doi: 10.1038/nri3084

Nierkens, S., den Brok, M. H., Sutmuller, R. P., Grauer, O. M., Bennink, E., Morgan, M. E., . . . Adema, G. J. (2008). In vivo colocalization of antigen and CpG [corrected] within dendritic cells is associated with the efficacy of cancer immunotherapy. *Cancer Res, 68*(13), 5390-5396. doi: 10.1158/0008-5472.CAN-07-6023

O'Shea, J. J., & Paul, W. E. (2010). Mechanisms underlying lineage commitment and plasticity of helper CD4+ T cells. *Science, 327*(5969), 1098-1102. doi: 10.1126/science.1178334

Ogino, S., Galon, J., Fuchs, C. S., & Dranoff, G. (2011). Cancer immunology--analysis of host and tumor factors for personalized medicine. *Nat Rev Clin Oncol, 8*(12), 711-719. doi: 10.1038/nrclinonc.2011.122

Oppermann, H., Levinson, A. D., Varmus, H. E., Levintow, L., & Bishop, J. M. (1979). Uninfected vertebrate cells contain a protein that is closely related to the product of the avian sarcoma virus transforming gene (src). *Proc Natl Acad Sci U S A, 76*(4), 1804-1808.

Overwijk, W. W., Wang, E., Marincola, F. M., Rammensee, H. G., & Restifo, N. P. (2013). Mining the mutanome: developing highly personalized Immunotherapies based on mutational analysis of tumors. *J Immunother Cancer, 1*, 11. doi: 10.1186/2051-1426-1-11

Pacholczyk, R., & Kern, J. (2008). The T-cell receptor repertoire of regulatory T cells. *Immunology, 125*(4), 450-458. doi: 10.1111/j.1365-2567.2008.02992.x

Pages, F., Berger, A., Camus, M., Sanchez-Cabo, F., Costes, A., Molidor, R., . . . Galon, J. (2005). Effector memory T cells, early metastasis, and survival in colorectal cancer. *N Engl J Med, 353*(25), 2654-2666. doi: 10.1056/NEJMoa051424

Pajot, A., Michel, M. L., Fazilleau, N., Pancre, V., Auriault, C., Ojcius, D. M., . . . Lone, Y. C. (2004). A mouse model of human adaptive immune functions: HLA-A2.1-/HLA-DR1-transgenic H-2 class I-/class II-knockout mice. *Eur J Immunol, 34*(11), 3060-3069. doi: 10.1002/eji.200425463

Paludan, C., Bickham, K., Nikiforow, S., Tsang, M. L., Goodman, K., Hanekom, W. A., . . . Munz, C. (2002). Epstein-Barr Nuclear Antigen 1-Specific CD4+ Th1 Cells Kill Burkitt's Lymphoma Cells. *The Journal of Immunology, 169*(3), 1593-1603. doi: 10.4049/jimmunol.169.3.1593

Pandiyan, P., Zheng, L., Ishihara, S., Reed, J., & Lenardo, M. J. (2007). CD4+CD25+Foxp3+ regulatory T cells induce cytokine deprivation-mediated apoptosis of effector CD4+ T cells. *Nat Immunol, 8*(12), 1353-1362. doi: 10.1038/ni1536

Pascolo, S., Bervas, N., Ure, J. M., Smith, A. G., Lemonnier, F. A., & Perarnau, B. (1997). HLA-A2.1-restricted education and cytolytic activity of CD8(+) T lymphocytes from beta2 microglobulin (beta2m) HLA-A2.1 monochain transgenic H-2Db beta2m double knockout mice. *J Exp Med, 185*(12), 2043-2051.

Pena-Diaz, J., Bregenhorn, S., Ghodgaonkar, M., Follonier, C., Artola-Boran, M., Castor, D., . . . Jiricny, J. (2012). Noncanonical mismatch repair as a source of genomic instability in human cells. *Mol Cell, 47*(5), 669-680. doi: 10.1016/j.molcel.2012.07.006

Perez, S. A., von Hofe, E., Kallinteris, N. L., Gritzapis, A. D., Peoples, G. E., Papamichail, M., & Baxevanis, C. N. (2010). A new era in anticancer peptide vaccines. *Cancer, 116*(9), 2071-2080. doi: 10.1002/cncr.24988

Perret, R., Sierro, S. R., Botelho, N. K., Corgnac, S., Donda, A., & Romero, P. (2013). Adjuvants that improve the ratio of antigen-specific effector to regulatory T cells enhance tumor immunity. *Cancer Res, 73*(22), 6597-6608. doi: 10.1158/0008-5472.CAN-13-0875

Petersen, R. P., Campa, M. J., Sperlazza, J., Conlon, D., Joshi, M. B., Harpole, D. H., Jr., & Patz, E. F., Jr. (2006). Tumor infiltrating Foxp3+ regulatory T-cells are associated with recurrence in pathologic stage I NSCLC patients. *Cancer, 107*(12), 2866-2872. doi: 10.1002/cncr.22282

Petitjean, A., Mathe, E., Kato, S., Ishioka, C., Tavtigian, S. V., Hainaut, P., & Olivier, M. (2007). Impact of mutant p53 functional properties on TP53 mutation patterns and tumor phenotype: lessons from recent developments in the IARC TP53 database. *Hum Mutat, 28*(6), 622-629. doi: 10.1002/humu.20495

Pfeifer, G. P. (2010). Environmental exposures and mutational patterns of cancer genomes. *Genome Med, 2*(8), 54. doi: 10.1186/gm175

Piccart-Gebhart, M. J., Procter, M., Leyland-Jones, B., Goldhirsch, A., Untch, M., Smith, I., . . . Herceptin Adjuvant Trial Study, T. (2005). Trastuzumab after adjuvant chemotherapy in HER2-positive breast cancer. *N Engl J Med, 353*(16), 1659-1672. doi: 10.1056/NEJMoa052306

Pilla, L., Rivoltini, L., Patuzzo, R., Marrari, A., Valdagni, R., & Parmiani, G. (2009). Multipeptide vaccination in cancer patients. *Expert Opin Biol Ther, 9*(8), 1043-1055. doi: 10.1517/14712590903085109

Porter, D. L., Levine, B. L., Kalos, M., Bagg, A., & June, C. H. (2011). Chimeric antigen receptor-modified T cells in chronic lymphoid leukemia. *N Engl J Med, 365*(8), 725-733. doi: 10.1056/NEJMoa1103849

Qiu, Q., Wang, R. Y., Jiao, X., Jin, B., Sugauchi, F., Grandinetti, T., . . . Shih, J. W. (2008). Induction of multispecific Th-1 type immune response against HCV in mice by protein immunization using CpG and Montanide ISA 720 as adjuvants. *Vaccine, 26*(43), 5527-5534. doi: 10.1016/j.vaccine.2008.07.034

Quezada, S. A., Simpson, T. R., Peggs, K. S., Merghoub, T., Vider, J., Fan, X., . . . Allison, J. P. (2010). Tumor-reactive CD4(+) T cells develop cytotoxic activity and eradicate large established melanoma after transfer into lymphopenic hosts. *J Exp Med, 207*(3), 637-650. doi: 10.1084/jem.20091918

Qureshi, O. S., Zheng, Y., Nakamura, K., Attridge, K., Manzotti, C., Schmidt, E. M., . . . Sansom, D. M. (2011). Trans-endocytosis of CD80 and CD86: a molecular basis for the cell-extrinsic function of CTLA-4. *Science, 332*(6029), 600-603. doi: 10.1126/science.1202947

Rahma, O. E., Ashtar, E., Czystowska, M., Szajnik, M. E., Wieckowski, E., Bernstein, S., . . . Khleif, S. N. (2012). A gynecologic oncology group phase II trial of two p53 peptide vaccine approaches: subcutaneous injection and intravenous pulsed dendritic cells in high recurrence risk ovarian cancer patients. *Cancer Immunol Immunother, 61*(3), 373-384. doi: 10.1007/s00262-011-1100-9

Rahma, O. E., Hamilton, J. M., Wojtowicz, M., Dakheel, O., Bernstein, S., Liewehr, D. J., . . . Khleif, S. N. (2014). The immunological and clinical effects of mutated ras peptide vaccine in combination with IL-2, GM-CSF, or both in patients with solid tumors. *J Transl Med, 12*, 55. doi: 10.1186/1479-5876-12-55

Rahma, O. E., & Khleif, S. N. (2011). Therapeutic vaccines for gastrointestinal cancers. *Gastroenterol Hepatol (N Y), 7*(8), 517-564.

Rammensee, H., Bachmann, J., Emmerich, N. P., Bachor, O. A., & Stevanovic, S. (1999). SYFPEITHI: database for MHC ligands and peptide motifs. *Immunogenetics, 50*(3-4), 213-219.

Ressing, M. E., Sette, A., Brandt, R. M., Ruppert, J., Wentworth, P. A., Hartman, M., . . . Kast, W. M. (1995). Human CTL epitopes encoded by human papillomavirus type 16 E6 and E7 identified through in vivo and in vitro immunogenicity studies of HLA-A*0201-binding peptides. *J Immunol, 154*(11), 5934-5943.

Restifo, N. P., Dudley, M. E., & Rosenberg, S. A. (2012). Adoptive immunotherapy for cancer: harnessing the T cell response. *Nat Rev Immunol, 12*(4), 269-281. doi: 10.1038/nri3191

Robbins, P. F., Lu, Y. C., El-Gamil, M., Li, Y. F., Gross, C., Gartner, J., . . . Rosenberg, S. A. (2013). Mining exomic sequencing data to identify mutated antigens recognized by adoptively transferred tumor-reactive T cells. *Nat Med, 19*(6), 747-752. doi: 10.1038/nm.3161

Roberts, P. J., & Der, C. J. (2007). Targeting the Raf-MEK-ERK mitogen-activated protein kinase cascade for the treatment of cancer. *Oncogene, 26*(22), 3291-3310. doi: 10.1038/sj.onc.1210422

Robinson, J., Halliwell, J. A., McWilliam, H., Lopez, R., Parham, P., & Marsh, S. G. (2013). The IMGT/HLA database. *Nucleic Acids Res, 41*(Database issue), D1222-1227. doi: 10.1093/nar/gks949

Romond, E. H., Perez, E. A., Bryant, J., Suman, V. J., Geyer, C. E., Jr., Davidson, N. E., . . . Wolmark, N. (2005). Trastuzumab plus adjuvant chemotherapy for operable HER2-positive breast cancer. *N Engl J Med, 353*(16), 1673-1684. doi: 10.1056/NEJMoa052122

Ropke, M., Hald, J., Guldberg, P., Zeuthen, J., Norgaard, L., Fugger, L., . . . Claesson, M. H. (1996). Spontaneous human squamous cell carcinomas are killed by a human cytotoxic T lymphocyte clone recognizing a wild-type p53-derived peptide. *Proc Natl Acad Sci U S A, 93*(25), 14704-14707.

Rosenberg, S. A. (2011). Cell transfer immunotherapy for metastatic solid cancer--what clinicians need to know. *Nat Rev Clin Oncol, 8*(10), 577-585. doi: 10.1038/nrclinonc.2011.116

Rosenberg, S. A., Lotze, M. T., Muul, L. M., Leitman, S., Chang, A. E., Ettinghausen, S. E., . . . et al. (1985). Observations on the systemic administration of autologous lymphokine-activated killer cells and recombinant interleukin-2 to patients with metastatic cancer. *N Engl J Med, 313*(23), 1485-1492. doi: 10.1056/NEJM198512053132327

Rosenberg, S. A., Yang, J. C., Schwartzentruber, D. J., Hwu, P., Marincola, F. M., Topalian, S. L., . . . White, D. E. (1998). Immunologic and therapeutic evaluation of a synthetic peptide vaccine for the treatment of patients with metastatic melanoma. *Nat Med, 4*(3), 321-327.

Rosenberg, S. A., Yang, J. C., Sherry, R. M., Kammula, U. S., Hughes, M. S., Phan, G. Q., . . . Dudley, M. E. (2011). Durable complete responses in heavily pretreated patients with metastatic melanoma using T-cell transfer immunotherapy. *Clin Cancer Res, 17*(13), 4550-4557. doi: 10.1158/1078-0432.CCR-11-0116

Rothenberg, E. V. (2014). Transcriptional control of early T and B cell developmental choices. *Annu Rev Immunol, 32*, 283-321. doi: 10.1146/annurev-immunol-032712-100024

Rowley, J. D. (1973). Letter: A new consistent chromosomal abnormality in chronic myelogenous leukaemia identified by quinacrine fluorescence and Giemsa staining. *Nature, 243*(5405), 290-293.

Sakaguchi, S. (2004). Naturally arising CD4+ regulatory t cells for immunologic self-tolerance and negative control of immune responses. *Annu Rev Immunol, 22*, 531-562. doi: 10.1146/annurev.immunol.21.120601.141122

Sallusto, F., Geginat, J., & Lanzavecchia, A. (2004). Central memory and effector memory T cell subsets: function, generation, and maintenance. *Annu Rev Immunol, 22*, 745-763. doi: 10.1146/annurev.immunol.22.012703.104702

Sallusto, F., Lenig, D., Forster, R., Lipp, M., & Lanzavecchia, A. (1999). Two subsets of memory T lymphocytes with distinct homing potentials and effector functions. *Nature, 401*(6754), 708-712. doi: 10.1038/44385

Salmond, R. J., Filby, A., Qureshi, I., Caserta, S., & Zamoyska, R. (2009). T-cell receptor proximal signaling via the Src-family kinases, Lck and Fyn, influences T-cell activation, differentiation, and tolerance. *Immunol Rev, 228*(1), 9-22. doi: 10.1111/j.1600-065X.2008.00745.x

Santarosa, M., & Ashworth, A. (2004). Haploinsufficiency for tumour suppressor genes: when you don't need to go all the way. *Biochim Biophys Acta, 1654*(2), 105-122. doi: 10.1016/j.bbcan.2004.01.001

Schliehe, C., Redaelli, C., Engelhardt, S., Fehlings, M., Mueller, M., van Rooijen, N., . . . Groettrup, M. (2011). CD8- dendritic cells and macrophages cross-present poly(D,L-lactate-co-glycolate) acid microsphere-encapsulated antigen in vivo. *J Immunol, 187*(5), 2112-2121. doi: 10.4049/jimmunol.1002084

Schmidt, H. H., Ge, Y., Hartmann, F. J., Conrad, H., Klug, F., Nittel, S., . . . Beckhove, P. (2013). HLA Class II tetramers reveal tissue-specific regulatory T cells that suppress T-cell responses in breast carcinoma patients. *Oncoimmunology, 2*(6), e24962. doi: 10.4161/onci.24962

Schmitz-Winnenthal, F. H., Escobedo, L. V., Beckhove, P., Schirrmacher, V., Bucur, M., Ziouta, Y., . . . Z'Graggen, K. (2006). Specific immune recognition of pancreatic carcinoma by patient-derived CD4 and CD8 T cells and its improvement by interferon-gamma. *Int J Oncol, 28*(6), 1419-1428.

Schmitz-Winnenthal, F. H., Volk, C., Z'Graggen, K., Galindo, L., Nummer, D., Ziouta, Y., . . . Beckhove, P. (2005). High frequencies of functional tumor-reactive T cells in bone marrow and blood of pancreatic cancer patients. *Cancer Res, 65*(21), 10079-10087. doi: 10.1158/0008-5472.CAN-05-1098

Schreiber, R. D., Old, L. J., & Smyth, M. J. (2011). Cancer immunoediting: integrating immunity's roles in cancer suppression and promotion. *Science, 331*(6024), 1565-1570. doi: 10.1126/science.1203486

Schreiber, T. H., Wolf, D., Bodero, M., & Podack, E. (2012). Tumor antigen specific iTreg accumulate in the tumor microenvironment and suppress therapeutic vaccination. *Oncoimmunology, 1*(5), 642-648. doi: 10.4161/onci.20298

Schubbert, S., Shannon, K., & Bollag, G. (2007). Hyperactive Ras in developmental disorders and cancer. *Nat Rev Cancer, 7*(4), 295-308. doi: 10.1038/nrc2109

Schulz, O., Diebold, S. S., Chen, M., Naslund, T. I., Nolte, M. A., Alexopoulou, L., . . . Reis e Sousa, C. (2005). Toll-like receptor 3 promotes cross-priming to virus-infected cells. *Nature, 433*(7028), 887-892. doi: 10.1038/nature03326

Schumacher, T., Bunse, L., Pusch, S., Sahm, F., Wiestler, B., Quandt, J., . . . Platten, M. (2014). A vaccine targeting mutant IDH1 induces antitumour immunity. *Nature, 512*(7514), 324-327. doi: 10.1038/nature13387

Schwartzentruber, D. J., Lawson, D. H., Richards, J. M., Conry, R. M., Miller, D. M., Treisman, J., . . . Hwu, P. (2011). gp100 peptide vaccine and interleukin-2 in patients with advanced melanoma. *N Engl J Med, 364*(22), 2119-2127. doi: 10.1056/NEJMoa1012863

Seeburg, P. H., Colby, W. W., Capon, D. J., Goeddel, D. V., & Levinson, A. D. (1984). Biological properties of human c-Ha-ras1 genes mutated at codon 12. *Nature, 312*(5989), 71-75.

Seliger, B. (2012). Novel insights into the molecular mechanisms of HLA class I abnormalities. *Cancer Immunol Immunother, 61*(2), 249-254. doi: 10.1007/s00262-011-1153-9

Shankaran, V., Ikeda, H., Bruce, A. T., White, J. M., Swanson, P. E., Old, L. J., & Schreiber, R. D. (2001). IFNgamma and lymphocytes prevent primary tumour development and shape tumour immunogenicity. *Nature, 410*(6832), 1107-1111. doi: 10.1038/35074122

Sharkey, M. S., Lizee, G., Gonzales, M. I., Patel, S., & Topalian, S. L. (2004). CD4(+) T-cell recognition of mutated B-RAF in melanoma patients harboring the V599E mutation. *Cancer Res, 64*(5), 1595-1599.

Sheiness, D., & Bishop, J. M. (1979). DNA and RNA from uninfected vertebrate cells contain nucleotide sequences related to the putative transforming gene of avian myelocytomatosis virus. *J Virol, 31*(2), 514-521.

Shiao, S. L., & Coussens, L. M. (2010). The tumor-immune microenvironment and response to radiation therapy. *J Mammary Gland Biol Neoplasia, 15*(4), 411-421. doi: 10.1007/s10911-010-9194-9

Slifka, M. K., & Whitton, J. L. (2000). Antigen-specific regulation of T cell-mediated cytokine production. *Immunity, 12*(5), 451-457.

Smith, C. M., Wilson, N. S., Waithman, J., Villadangos, J. A., Carbone, F. R., Heath, W. R., & Belz, G. T. (2004). Cognate CD4(+) T cell licensing of dendritic cells in CD8(+) T cell immunity. *Nat Immunol, 5*(11), 1143-1148. doi: 10.1038/ni1129

Smith, F. O., Downey, S. G., Klapper, J. A., Yang, J. C., Sherry, R. M., Royal, R. E., . . . Rosenberg, S. A. (2008). Treatment of metastatic melanoma using interleukin-2 alone or in conjunction with vaccines. *Clin Cancer Res, 14*(17), 5610-5618. doi: 10.1158/1078-0432.CCR-08-0116

Soerjomataram, I., Lortet-Tieulent, J., Parkin, D. M., Ferlay, J., Mathers, C., Forman, D., & Bray, F. (2012). Global burden of cancer in 2008: a systematic analysis of disability-adjusted life-years in 12 world regions. *The Lancet, 380*(9856), 1840-1850. doi: 10.1016/s0140-6736(12)60919-2

Solomon, H., Madar, S., & Rotter, V. (2011). Mutant p53 gain of function is interwoven into the hallmarks of cancer. *J Pathol, 225*(4), 475-478. doi: 10.1002/path.2988

Somasundaram, R., Swoboda, R., Caputo, L., Otvos, L., Weber, B., Volpe, P., . . . Herlyn, D. (2006). Human leukocyte antigen-A2-restricted CTL responses to mutated BRAF peptides in melanoma patients. *Cancer Res, 66*(6), 3287-3293. doi: 10.1158/0008-5472.CAN-05-1932

Sommerfeldt, N., Beckhove, P., Ge, Y., Schutz, F., Choi, C., Bucur, M., . . . Schirrmacher, V. (2006). Heparanase: a new metastasis-associated antigen recognized in breast cancer patients by spontaneously induced memory T lymphocytes. *Cancer Res, 66*(15), 7716-7723. doi: 10.1158/0008-5472.CAN-05-2363

Sommerfeldt, N., Schutz, F., Sohn, C., Forster, J., Schirrmacher, V., & Beckhove, P. (2006). The shaping of a polyvalent and highly individual T-cell repertoire in the bone marrow of breast cancer patients. *Cancer Res, 66*(16), 8258-8265. doi: 10.1158/0008-5472.CAN-05-4201

Soto, C. M., Stone, J. D., Chervin, A. S., Engels, B., Schreiber, H., Roy, E. J., & Kranz, D. M. (2013). MHC-class I-restricted CD4 T cells: a nanomolar affinity TCR has improved anti-tumor efficacy in vivo compared to the micromolar wild-type TCR. *Cancer Immunol Immunother, 62*(2), 359-369. doi: 10.1007/s00262-012-1336-z

Speetjens, F. M., Kuppen, P. J., Welters, M. J., Essahsah, F., Voet van den Brink, A. M., Lantrua, M. G., . . . van der Burg, S. H. (2009). Induction of p53-specific immunity by a p53 synthetic long peptide vaccine in patients treated for metastatic colorectal cancer. *Clin Cancer Res, 15*(3), 1086-1095. doi: 10.1158/1078-0432.CCR-08-2227

Srivastava, S., Zou, Z. Q., Pirollo, K., Blattner, W., & Chang, E. H. (1990). Germ-line transmission of a mutated p53 gene in a cancer-prone family with Li-Fraumeni syndrome. *Nature, 348*(6303), 747-749. doi: 10.1038/348747a0

Stehelin, D., Varmus, H. E., Bishop, J. M., & Vogt, P. K. (1976). DNA related to the transforming gene(s) of avian sarcoma viruses is present in normal avian DNA. *Nature, 260*(5547), 170-173.

Stratton, M. R., Campbell, P. J., & Futreal, P. A. (2009). The cancer genome. *Nature, 458*(7239), 719-724. doi: 10.1038/nature07943

Swanton, C. (2012). Intratumor heterogeneity: evolution through space and time. *Cancer Res, 72*(19), 4875-4882. doi: 10.1158/0008-5472.CAN-12-2217

Szymczak-Workman, A. L., Workman, C. J., & Vignali, D. A. (2009). Cutting edge: regulatory T cells do not require stimulation through their TCR to suppress. *J Immunol, 182*(9), 5188-5192. doi: 10.4049/jimmunol.0803123

Teijaro, J. R., Turner, D., Pham, Q., Wherry, E. J., Lefrancois, L., & Farber, D. L. (2011). Cutting edge: Tissue-retentive lung memory CD4 T cells mediate optimal protection to respiratory virus infection. *J Immunol, 187*(11), 5510-5514. doi: 10.4049/jimmunol.1102243

Theobald, M., Biggs, J., Hernandez, J., Lustgarten, J., Labadie, C., & Sherman, L. A. (1997). Tolerance to p53 by A2.1-restricted cytotoxic T lymphocytes. *J Exp Med, 185*(5), 833-841.

Thornton, A. M., Korty, P. E., Tran, D. Q., Wohlfert, E. A., Murray, P. E., Belkaid, Y., & Shevach, E. M. (2010). Expression of Helios, an Ikaros transcription factor family member, differentiates thymic-derived from peripherally induced Foxp3+ T regulatory cells. *J Immunol, 184*(7), 3433-3441. doi: 10.4049/jimmunol.0904028

Tian, J., Gregori, S., Adorini, L., & Kaufman, D. L. (2001). The Frequency of High Avidity T Cells Determines the Hierarchy of Determinant Spreading. *The Journal of Immunology, 166*(12), 7144-7150. doi: 10.4049/jimmunol.166.12.7144

Toubaji, A., Achtar, M., Provenzano, M., Herrin, V. E., Behrens, R., Hamilton, M., . . . Khleif, S. N. (2008). Pilot study of mutant ras peptide-based vaccine as an adjuvant treatment in pancreatic and colorectal cancers. *Cancer Immunol Immunother, 57*(9), 1413-1420. doi: 10.1007/s00262-008-0477-6

Tran, E., Turcotte, S., Gros, A., Robbins, P. F., Lu, Y. C., Dudley, M. E., . . . Rosenberg, S. A. (2014). Cancer immunotherapy based on mutation-specific CD4+ T cells in a patient with epithelial cancer. *Science, 344*(6184), 641-645. doi: 10.1126/science.1251102

Tveita, A. A., Schjesvold, F. H., Sundnes, O., Haabeth, O. A., Haraldsen, G., & Bogen, B. (2014). Indirect CD4 T-cell-mediated elimination of MHC II tumor cells is spatially restricted and fails to prevent escape of antigen-negative cells. *Eur J Immunol*. doi: 10.1002/eji.201444659

Vacchelli, E., Galluzzi, L., Fridman, W. H., Galon, J., Sautes-Fridman, C., Tartour, E., & Kroemer, G. (2012). Trial watch: Chemotherapy with immunogenic cell death inducers. *Oncoimmunology, 1*(2), 179-188. doi: 10.4161/onci.1.2.19026

van der Bruggen, P., Traversari, C., Chomez, P., Lurquin, C., De Plaen, E., Van den Eynde, B., . . . Boon, T. (1991). A gene encoding an antigen recognized by cytolytic T lymphocytes on a human melanoma. *Science, 254*(5038), 1643-1647.

van Hall, T., & van der Burg, S. H. (2012). Mechanisms of peptide vaccination in mouse models: tolerance, immunity, and hyperreactivity. *Adv Immunol, 114*, 51-76. doi: 10.1016/B978-0-12-396548-6.00003-2

van Rooij, N., van Buuren, M. M., Philips, D., Velds, A., Toebes, M., Heemskerk, B., . . . Schumacher, T. N. (2013). Tumor exome analysis reveals neoantigen-specific T-cell reactivity in an ipilimumab-responsive melanoma. *J Clin Oncol, 31*(32), e439-442. doi: 10.1200/JCO.2012.47.7521

Vesely, M. D., Kershaw, M. H., Schreiber, R. D., & Smyth, M. J. (2011). Natural innate and adaptive immunity to cancer. *Annu Rev Immunol, 29*, 235-271. doi: 10.1146/annurev-immunol-031210-101324

Vignali, D. A., Collison, L. W., & Workman, C. J. (2008). How regulatory T cells work. *Nat Rev Immunol, 8*(7), 523-532. doi: 10.1038/nri2343

Vigneron, N., Stroobant, V., Van den Eynde, B. J., & van der Bruggen, P. (2013). Database of T cell-defined human tumor antigens: the 2013 update. *Cancer Immun, 13*, 15.

Vincent, A., Herman, J., Schulick, R., Hruban, R. H., & Goggins, M. (2011). Pancreatic cancer. *The Lancet, 378*(9791), 607-620. doi: 10.1016/s0140-6736(10)62307-0

Vlad, A. M., Kettel, J. C., Alajez, N. M., Carlos, C. A., & Finn, O. J. (2004). MUC1 immunobiology: from discovery to clinical applications. *Adv Immunol, 82*, 249-293. doi: 10.1016/S0065-2776(04)82006-6

Vogelstein, B., Papadopoulos, N., Velculescu, V. E., Zhou, S., Diaz, L. A., Jr., & Kinzler, K. W. (2013). Cancer genome landscapes. *Science, 339*(6127), 1546-1558. doi: 10.1126/science.1235122

von Herrath, M. G., & Harrison, L. C. (2003). Antigen-induced regulatory T cells in autoimmunity. *Nat Rev Immunol, 3*(3), 223-232. doi: 10.1038/nri1029

Wakita, D., Chamoto, K., Ohkuri, T., Narita, Y., Ashino, S., Sumida, K., . . . Nishimura, T. (2009). IFN-gamma-dependent type 1 immunity is crucial for immunosurveillance against squamous cell

carcinoma in a novel mouse carcinogenesis model. *Carcinogenesis, 30*(8), 1408-1415. doi: 10.1093/carcin/bgp144

Walter, S., Weinschenk, T., Stenzl, A., Zdrojowy, R., Pluzanska, A., Szczylik, C., . . . Singh-Jasuja, H. (2012). Multipeptide immune response to cancer vaccine IMA901 after single-dose cyclophosphamide associates with longer patient survival. *Nat Med, 18*(8), 1254-1261. doi: 10.1038/nm.2883

Weaver, C. T., Hatton, R. D., Mangan, P. R., & Harrington, L. E. (2007). IL-17 family cytokines and the expanding diversity of effector T cell lineages. *Annu Rev Immunol, 25*, 821-852. doi: 10.1146/annurev.immunol.25.022106.141557

Weber, J. S., Kahler, K. C., & Hauschild, A. (2012). Management of immune-related adverse events and kinetics of response with ipilimumab. *J Clin Oncol, 30*(21), 2691-2697. doi: 10.1200/JCO.2012.41.6750

Weden, S., Klemp, M., Gladhaug, I. P., Moller, M., Eriksen, J. A., Gaudernack, G., & Buanes, T. (2011). Long-term follow-up of patients with resected pancreatic cancer following vaccination against mutant K-ras. *Int J Cancer, 128*(5), 1120-1128. doi: 10.1002/ijc.25449

Weijzen, S., Meredith, S. C., Velders, M. P., Elmishad, A. G., Schreiber, H., & Kast, W. M. (2001). Pharmacokinetic Differences Between a T Cell-Tolerizing and a T Cell-Activating Peptide. *The Journal of Immunology, 166*(12), 7151-7157. doi: 10.4049/jimmunol.166.12.7151

Welters, M. J., Bijker, M. S., van den Eeden, S. J., Franken, K. L., Melief, C. J., Offringa, R., & van der Burg, S. H. (2007). Multiple CD4 and CD8 T-cell activation parameters predict vaccine efficacy in vivo mediated by individual DC-activating agonists. *Vaccine, 25*(8), 1379-1389. doi: 10.1016/j.vaccine.2006.10.049

Wherry, E. J., & Ahmed, R. (2004). Memory CD8 T-cell differentiation during viral infection. *J Virol, 78*(11), 5535-5545. doi: 10.1128/JVI.78.11.5535-5545.2004

Williams, M. A., Tyznik, A. J., & Bevan, M. J. (2006). Interleukin-2 signals during priming are required for secondary expansion of CD8+ memory T cells. *Nature, 441*(7095), 890-893. doi: 10.1038/nature04790

Willis, A., Jung, E. J., Wakefield, T., & Chen, X. (2004). Mutant p53 exerts a dominant negative effect by preventing wild-type p53 from binding to the promoter of its target genes. *Oncogene, 23*(13), 2330-2338. doi: 10.1038/sj.onc.1207396

Wing, K., & Sakaguchi, S. (2010). Regulatory T cells exert checks and balances on self tolerance and autoimmunity. *Nat Immunol, 11*(1), 7-13. doi: 10.1038/ni.1818

Wirnsberger, G., Hinterberger, M., & Klein, L. (2011). Regulatory T-cell differentiation versus clonal deletion of autoreactive thymocytes. *Immunol Cell Biol, 89*(1), 45-53. doi: 10.1038/icb.2010.123

Wood, L. D., Parsons, D. W., Jones, S., Lin, J., Sjoblom, T., Leary, R. J., . . . Vogelstein, B. (2007). The genomic landscapes of human breast and colorectal cancers. *Science, 318*(5853), 1108-1113. doi: 10.1126/science.1145720

Wu, C., Thalhamer, T., Franca, R. F., Xiao, S., Wang, C., Hotta, C., . . . Kuchroo, V. K. (2014). Galectin-9-CD44 Interaction Enhances Stability and Function of Adaptive Regulatory T Cells. *Immunity, 41*(2), 270-282. doi: 10.1016/j.immuni.2014.06.011

Wu, L., & Shortman, K. (2005). Heterogeneity of thymic dendritic cells. *Semin Immunol, 17*(4), 304-312. doi: 10.1016/j.smim.2005.05.001

Yadav, M., Louvet, C., Davini, D., Gardner, J. M., Martinez-Llordella, M., Bailey-Bucktrout, S., . . . Bluestone, J. A. (2012). Neuropilin-1 distinguishes natural and inducible regulatory T cells among regulatory T cell subsets in vivo. *J Exp Med, 209*(10), 1713-1722, S1711-1719. doi: 10.1084/jem.20120822

Yamada, A., Sasada, T., Noguchi, M., & Itoh, K. (2013). Next-generation peptide vaccines for advanced cancer. *Cancer Sci, 104*(1), 15-21. doi: 10.1111/cas.12050

Yanuck, M., Carbone, D. P., Pendleton, C. D., Tsukui, T., Winter, S. F., Minna, J. D., & Berzofsky, J. A. (1993). A mutant p53 tumor suppressor protein is a target for peptide-induced CD8+ cytotoxic T-cells. *Cancer Res, 53*(14), 3257-3261.

Yap, T. A., Gerlinger, M., Futreal, P. A., Pusztai, L., & Swanton, C. (2012). Intratumor heterogeneity: seeing the wood for the trees. *Sci Transl Med, 4*(127), 127ps110. doi: 10.1126/scitranslmed.3003854

Yazdanbakhsh, M., Kremsner, P. G., & van Ree, R. (2002). Allergy, parasites, and the hygiene hypothesis. *Science, 296*(5567), 490-494. doi: 10.1126/science.296.5567.490

Zaunders, J. J., Dyer, W. B., Wang, B., Munier, M. L., Miranda-Saksena, M., Newton, R., . . . Kelleher, A. D. (2004). Identification of circulating antigen-specific CD4+ T lymphocytes with a CCR5+, cytotoxic phenotype in an HIV-1 long-term nonprogressor and in CMV infection. *Blood, 103*(6), 2238-2247. doi: 10.1182/blood-2003-08-2765

Zehn, D., Lee, S. Y., & Bevan, M. J. (2009). Complete but curtailed T-cell response to very low-affinity antigen. *Nature, 458*(7235), 211-214. doi: 10.1038/nature07657

Zeng, G., Li, Y., El-Gamil, M., Sidney, J., Sette, A., Wang, R. F., . . . Robbins, P. F. (2002). Generation of NY-ESO-1-specific CD4+ and CD8+ T cells by a single peptide with dual MHC class I and class II specificities: a new strategy for vaccine design. *Cancer Res, 62*(13), 3630-3635.

Zhang, H., Hong, H., Li, D., Ma, S., Di, Y., Stoten, A., . . . Jiang, S. (2009). Comparing pooled peptides with intact protein for accessing cross-presentation pathways for protective CD8+ and CD4+ T cells. *J Biol Chem, 284*(14), 9184-9191. doi: 10.1074/jbc.M809456200

Zhang, Y., Joe, G., Hexner, E., Zhu, J., & Emerson, S. G. (2005). Host-reactive CD8+ memory stem cells in graft-versus-host disease. *Nat Med, 11*(12), 1299-1305. doi: 10.1038/nm1326

Zhou, X. Y., Yashiro-Ohtani, Y., Nakahira, M., Park, W. R., Abe, R., Hamaoka, T., . . . Fujiwara, H. (2002). Molecular mechanisms underlying differential contribution of CD28 versus non-CD28 costimulatory molecules to IL-2 promoter activation. *J Immunol, 168*(8), 3847-3854.

Zhu, J., & Paul, W. E. (2008). CD4 T cells: fates, functions, and faults. *Blood, 112*(5), 1557-1569. doi: 10.1182/blood-2008-05-078154

Zhu, J., & Paul, W. E. (2010). Heterogeneity and plasticity of T helper cells. *Cell Res, 20*(1), 4-12. doi: 10.1038/cr.2009.138

Zom, G. G., Khan, S., Britten, C. M., Sommandas, V., Camps, M. G., Loof, N. M., . . . Ossendorp, F. (2014). Efficient Induction of Antitumor Immunity by Synthetic Toll-like Receptor Ligand-Peptide Conjugates. *Cancer Immunol Res*. doi: 10.1158/2326-6066.CIR-13-0223

Zorn, E., Nelson, E. A., Mohseni, M., Porcheray, F., Kim, H., Litsa, D., . . . Ritz, J. (2006). IL-2 regulates FOXP3 expression in human CD4+CD25+ regulatory T cells through a STAT-dependent mechanism and induces the expansion of these cells in vivo. *Blood, 108*(5), 1571-1579. doi: 10.1182/blood-2006-02-004747

Zwaveling, S., Mota, S. C. F., Nouta, J., Johnson, M., Lipford, G. B., Offringa, R., . . . Melief, C. J. M. (2002). Established Human Papillomavirus Type 16-Expressing Tumors Are Effectively Eradicated Following Vaccination with Long Peptides. *The Journal of Immunology, 169*(1), 350-358. doi: 10.4049/jimmunol.169.1.350

## 6. Abbreviations and Definitions

| | |
|---|---|
| [$^3$H] | Tritium-hydrogen 3 |
| µg | µmicrogram |
| µl | µmicroliter |
| µm | µmicrometer |
| $A_{260}$ | Absorbance at 260nm |
| aa | amino acid |
| Ab | Antibody |
| Ag | Antigen |
| APC | Antigen Presenting Cells |
| BM | Bone marrow |
| bp | base pairs |
| Braf | Serine/threonine-protein kinase Braf |
| BSA | Bovine Serum Albumin |
| °C | Degree Celsius |
| cAMP | cyclic Adenosine Monophosphate |
| cpm | counts per minute |
| CCR | Chemokine Receptor |
| CD | Cluster of Differentiation |
| cDNA | complementary DNA |
| Ci | Curie |
| cTECs | cortical Thymic Epithelial Cells |
| CTLA-4 | cytotoxic T lymphocyte antigen 4 |
| CTLs | Cytotoxic T cells |
| d | Day |
| DBD | DNA binding domain |
| DC | Dendritic cell |
| dd$H_2O$ | double distilled water |
| DN | Double Negative |
| DNA | deoxyribonucleic acid |
| DNase | Deoxyribonuclease |
| dNTPs | deoxyribonucleoside triphosphate |
| DP | Double Positive |
| EDTA | Ethylenediaminetetraacetic acid |
| EGFR | Epidermal growth factor receptor |
| ELISpot | Enzyme-linked immunosorbent assay |
| ETPs | Early Thymic Progenitors |
| FACS | Fluorescent Activated Cell Sorting |
| FCS | Fetal Calf Serum |
| FITC | Fluorescein isothiocyanate |
| FMO | Fluorescence Minus One |
| Foxp3 | Forkhead box p3 |
| FACS | Flow Cytometric Analysis and Cell Sorting |
| FSC | Forward Side Scatter |
| G | Gate |
| GM-CSF | Granulocyte macrophage-colony stimulating factor |
| Gy | gray |
| h | hours |
| HA | influenza hemaglutinin |

| | |
|---|---|
| HEPES | 4-(2-hydroxyethyl)-1-piperazineethanesulfonic acid |
| Her2/neu | Human epidermal growth factor receptor 2 |
| HLA | Human Leukocyte Antigen |
| HPLC | High-performance liquid chromatography |
| HSCs | Hematopoietic Stem Cells |
| ICAM1 | intercellular adhesion molecule 1 |
| ICOS | Inducible Costimulator |
| IDO | indoleamine 2,3-dioxygenase |
| IFA | Incomplete Freund's Adjuvant |
| IFN-γ | Interferon gamma |
| IgG | Immunoglobulin |
| IL | Interleukin |
| Iono | Ionomycin |
| iTreg | Induced Treg |
| J | Joining region |
| kDA | Kilo Dalton |
| Kras | GTPase Kras<br>V-Ki-ras2 Kirsten rat sarcoma viral oncogene homolog |
| l | Liter |
| LAG3 | Lymphocyte-Activation Gene 3 |
| LFA1 | leukocyte function-associated antigen |
| LB medium | Luria Broth medium |
| mAb | Monoclonal Antibody |
| MACS | Magnetically Activated Cell Sorting |
| MAGE | Melanoma-associated antigen |
| max | maximum |
| MH | Morisita-Horn index |
| MHC | Major Histocompatibility Complex |
| min | minutes |
| ml | milliliter |
| mM | Millimolarity |
| mRNA | messenger RNA |
| mTEC | medullary Thymic Epithelial Cells |
| MUC | Mucin 1 |
| ns | Not significant |
| NK | Natural Killer Cells |
| nM | nanomolarity |
| nt | nucleotide |
| nTreg | Natural Treg |
| ON | Overnight (~12h) |
| p53 | Tumor suppressor p53 |
| PB | Peripheral Blood |
| PBMC | Peripheral Blood Mononuclear Cells |
| PBS | Phosphate Buffer Saline |
| PCR | Polymerase Chain Reaction |
| PD-1 | Programmed Death-1 |
| PE | Phycoerythrin |
| PE-Cy5.5 | Phycoerythrin-cyanine5.5 |
| PE-Cy7 | Phycoerythrin-cyanine7 |
| PerCP | Peridinin-chlorophyl-protein-complex |
| PI | Propidium Iodide |

| | |
|---|---|
| PI3K | phosphatidylinositol 3-kinase |
| PMA | Phorbol-12-myristat-13-acetat |
| RA | Retinoic Acid |
| RNA | Ribonucleic acid |
| (ROR)γt | retinoid-related orphan receptor γt |
| rpm | round per minute |
| RT | Room Temperature |
| RT | Reverse Transcription |
| SB | Strong binder |
| SDS-PAGE | Sodium dodecylsulfat polyacrylamide gel electrophoresis |
| SEB | Staphylococcal enterotoxin B |
| SEM | Standard error of the mean |
| SHP2 | SRC homology 2-domain-containing protein tyrosine phosphatase 2 |
| SP | Single positive |
| TAA | Tumor Associated Antigen |
| TAE | Tris-Acetate EDTA |
| TC | T lymphocytes/T cell |
| $T_{CM}$ | Central memory T cells |
| $T_{con}$ | Conventional T cells |
| TCR | T Cell Receptor |
| TCRα | T Cell Receptor α chain |
| TCRβ | T Cell Receptor β chain |
| Teff | Effector T cells |
| $T_{EM}$ | Effector memory T cells |
| Tfh | follicular helper TC |
| TGF-β | Transforming growth factor β |
| TIL | Tumor infiltrating lymphocyte |
| $T_H$ | $CD4^+$ T helper cells |
| TLR | Toll like receptor |
| TNF | Tumor necrosis factor |
| TNF-R | Tumor necrosis factor receptor |
| $T_{reg}$ | Regulatory T cells |
| TSA | Tumor specific antigen |
| TSPs | Thymic Seeding Progenitors |
| U | Units |
| UV | ultraviolet |
| V | Volts |
| v/v | Volume per volume |
| W | Watt |
| WB | Weak binder |
| WHO | World Health Organization |
| w/o | without |
| w/v | Weight per volume |
| wt | Wild-type |

# 7. Appendix

## 7.1. Chimeric (mutated) Tp53/Kras transgene sequences

**Mu_wt_tag (with HA-tag)**

```
   1  accatgttcc acctgggctt cctgcagtct gggacagcca agtctgttat gtgcacgtac
  61  tctcctcccc tcaataagct attctgccag ctggcgaaga cgtgccctgt gcagttgtgg
 121  gtcagcgcca cacctccagc tgggagccgt gtccgcgcca tggccatcta caagaagtca
 181  cagcacatga cggaggtcgt gagacgctgc ccccaccatg agcgctgctc cgatggtgat
 241  ggcctggctc ctccccagca tcttatccgg gtggaaggaa atttgtatcc cgagtatctg
 301  gaagacaggc agacttttcg ccacagcgtg gtggtacctt atgagccacc cgaggccggc
 361  tctgagtata ccaccatcca ctacaagtac atgtgtaata gctcctgcat gggggggcatg
 421  aaccgccgac ctatccttac catcatcaca ctggaagact ccagtgggaa ccttctggga
 481  cgggacagct ttgaggttcg tgtttgtgcc tgccctggga gagaccgccg tacagaagaa
 541  gaaaatggta gcggcagcgg tagcatgact gagtataaac ttgtggtggt tggagctggt
 601  ggcgtaggca agagcgcctt gacgatacag ctaattcaga atcactttgt ggatgagtat
 661  gaccctacga tagaggactc ctacaggaaa caagtagtaa ttgatggaga aacctgtctc
 721  ttggatattc tcgacacagc aggtcaagag gagtacagtg caatgaggga ccagtacatg
 781  agaactgggg agggctttct ttgtgtattt gccataaata atactaaatc atttgaagat
 841  attcaccatt atagagaaca aattaaaaga gtaaaggact ctgaagatgt gcctatggtc
 901  ctggtaggga ataagtgtga tttgccttct agaacagtag acacgaaaca ggctcaggag
 961  ttagcaagga gttacgggat tccgttcatt gagacctcag caaagacaag atatccgtat
1021  gacgtgcccg actatgcctg a
```

**Mu_mut (without tag)**

```
   1  accatgttcc acctgggctt cctgcagtct gggacagcca agtctgttat gtgcacgtac
  61  tctcctcccc tcaataagct attctgccag ctggcgaaga cgtgccctgt gcagttgtgg
 121  gtcagcgcca cacctccagc tgggagccgt gtccgcgcca tggccatcta caagaagtca
 181  cagcacatga cggaggtcgt gagacgctgc ccccaccatg agcgctgctc cgatggtgat
 241  ggcctggctc ctccccagca tcttatccgg gtggaaggaa atttgtatcc cgagtatctg
 301  gaagacaggc agacttttcg ccacagcgtg gtggtacctt atgagccacc cgaggccggc
 361  tctgagtata ccaccatcca ctacaagtac atgtgtaata gctcctgcat gggggggcatg
 421  aactggcgac ctatccttac catcatcaca ctggaagact ccagtgggaa ccttctggga
 481  cgggacagct ttgaggttcg tgtttgtgcc tgccctggga gagaccgccg tacagaagaa
 541  gaaaatggta gcggcagcgg tagcatgact gagtataaac ttgtggtggt tggagctgtg
 601  ggcgtaggca agagcgcctt gacgatacag ctaattcaga atcactttgt ggatgagtat
 661  gaccctacga tagaggactc ctacaggaaa caagtagtaa ttgatggaga aacctgtctc
 721  ttggatattc tcgacacagc aggtcaagag gagtacagtg caatgaggga ccagtacatg
 781  agaactgggg agggctttct ttgtgtattt gccataaata atactaaatc atttgaagat
 841  attcaccatt atagagaaca aattaaaaga gtaaaggact ctgaagatgt gcctatggtc
 901  ctggtaggga ataagtgtga tttgccttct agaacagtag acacgaaaca ggctcaggag
 961  ttagcaagga gttacgggat tccgttcatt gagacctcag caaagacaag atga
```

**Mu_mut_tag (with HA-tag)**

```
   1  accatgttcc acctgggctt cctgcagtct gggacagcca agtctgttat gtgcacgtac
  61  tctcctcccc tcaataagct attctgccag ctggcgaaga cgtgccctgt gcagttgtgg
 121  gtcagcgcca cacctccagc tgggagccgt gtccgcgcca tggccatcta caagaagtca
 181  cagcacatga cggaggtcgt gagacgctgc ccccaccatg agcgctgctc cgatggtgat
 241  ggcctggctc ctccccagca tcttatccgg gtggaaggaa atttgtatcc cgagtatctg
 301  gaagacaggc agacttttcg ccacagcgtg gtggtacctt atgagccacc cgaggccggc
 361  tctgagtata ccaccatcca ctacaagtac atgtgtaata gctcctgcat gggggggcatg
 421  aactggcgac ctatccttac catcatcaca ctggaagact ccagtgggaa ccttctggga
 481  cgggacagct ttgaggttcg tgtttgtgcc tgccctggga gagaccgccg tacagaagaa
 541  gaaaatggta gcggcagcgg tagcatgact gagtataaac ttgtggtggt tggagctgtg
 601  ggcgtaggca agagcgcctt gacgatacag ctaattcaga atcactttgt ggatgagtat
 661  gaccctacga tagaggactc ctacaggaaa caagtagtaa ttgatggaga aacctgtctc
 721  ttggatattc tcgacacagc aggtcaagag gagtacagtg caatgaggga ccagtacatg
 781  agaactgggg agggctttct ttgtgtattt gccataaata atactaaatc atttgaagat
 841  attcaccatt atagagaaca aattaaaaga gtaaaggact ctgaagatgt gcctatggtc
 901  ctggtaggga ataagtgtga tttgccttct agaacagtag acacgaaaca ggctcaggag
 961  ttagcaagga gttacgggat tccgttcatt gagacctcag caaagacaag atatccgtat
1021  gacgtgcccg actatgcctg a
```

**Hu_wt_tag (with HA-tag)**

```
   1  accatgttcc gtctgggctt cttgcattct gggacagcca agtctgtgac ttgcacgtac
  61  tcccctgccc tcaacaagat gttttgccaa ctggccaaga cctgccctgt gcagctgtgg
 121  gttgattcca cacccccgcc cggcacccgc gtccgcgcca tggccatcta caagcagtca
 181  cagcacatga cggaggttgt gaggcgctgc ccccaccatg agcgctgctc agatagcgat
 241  ggtctggccc ctcctcagca tcttatccga gtggaaggaa atttgcgtgt ggagtatttg
 301  gatgacagaa acacttttcg acatagtgtg gtggtgccct atgagccgcc tgaggttggc
 361  tctgactgta ccaccatcca ctacaactac atgtgtaaca gttcctgcat gggcggcatg
 421  aaccggaggc ccatcctcac catcatcaca ctggaagact ccagtggtaa tctactggga
 481  cggaacagct ttgaggtgcg tgtttgtgcc tgtcctggga gagaccggcg cacagaggaa
 541  gagaatggta gcggcagcgg tagcatgact gaatataaac ttgtggtagt tggagctggt
 601  ggcgtaggca agagtgcctt gacgatacag ctaattcaga atcattttgt ggacgaatat
 661  gatccaacaa tagaggattc ctacaggaag caagtagtaa ttgatggaga aacctgtctc
 721  ttggatattc tcgacacagc aggtcaagag gagtacagtg caatgaggga ccagtacatg
 781  aggactgggg agggctttct ttgtgtattt gccataaata atactaaatc atttgaagat
 841  attcaccatt atagagaaca aattaaaaga gttaaggact ctgaagatgt acctatggtc
 901  ctagtaggaa ataaatgtga tttgccttct agaacagtag acacaaaaca ggctcaggac
 961  ttagcaagaa gttatggaat tccttttatt gaaacatcag caaagacaag acagtatccg
1021  tatgacgtgc ccgactatgc ctga
```

**Hu_mut_tag (with HA-tag)**

```
   1  accatgttcc gtctgggctt cttgcattct gggacagcca agtctgtgac ttgcacgtac
  61  tcccctgccc tcaacaagat gttttgccaa ctggccaaga cctgccctgt gcagctgtgg
 121  gttgattcca cacccccgcc cggcacccgc gtccgcgcca tggccatcta caagcagtca
 181  cagcacatga cggaggttgt gaggcgctgc ccccaccatg agcgctgctc agatagcgat
 241  ggtctggccc ctcctcagca tcttatccga gtggaaggaa atttgcgtgt ggagtatttg
 301  gatgacagaa acacttttcg acatagtgtg gtggtgccct atgagccgcc tgaggttggc
 361  tctgactgta ccaccatcca ctacaactac atgtgtaaca gttcctgcat gggcggcatg
 421  aactggaggc ccatcctcac catcatcaca ctggaagact ccagtggtaa tctactggga
 481  cggaacagct ttgaggtgcg tgtttgtgcc tgtcctggga gagaccggcg cacagaggaa
 541  gagaatggta gcggcagcgg tagcatgact gaatataaac ttgtggtagt tggagctgtg
 601  ggcgtaggca agagtgcctt gacgatacag ctaattcaga atcattttgt ggacgaatat
 661  gatccaacaa tagaggattc ctacaggaag caagtagtaa ttgatggaga aacctgtctc
 721  ttggatattc tcgacacagc aggtcaagag gagtacagtg caatgaggga ccagtacatg
 781  aggactgggg agggctttct ttgtgtattt gccataaata atactaaatc atttgaagat
 841  attcaccatt atagagaaca aattaaaaga gttaaggact ctgaagatgt acctatggtc
 901  ctagtaggaa ataaatgtga tttgccttct agaacagtag acacaaaaca ggctcaggac
 961  ttagcaagaa gttatggaat tccttttatt gaaacatcag caaagacaag acagtatccg
1021  tatgacgtgc ccgactatgc ctga
```

**Hu_mut_tag (with HA-tag) codon-optimized for expression in mice**

```
   1  ACAATGTTCA GACTGGGCTT CCTGCACAGC GGCACCGCCA AGAGCGTGAC CTGTACCTAC
  61  AGCCCTGCCC TGAACAAGAT GTTCTGTCAG CTGGCCAAGA CCTGCCCCGT GCAGCTGTGG
 121  GTGGACAGCA CACCTCCTCC AGGCACAAGA GTGCGCGCCA TGGCCATCTA CAAGCAGAGC
 181  CAGCACATGA CCGAGGTCGT GCGGAGATGC CCCCACCACG AGAGATGTAG CGACAGCGAC
 241  GGACTGGCCC CTCCCCAGCA CCTGATTAGA GTGGAAGGCA ACCTGAGAGT GGAATACCTG
 301  GACGACAGAA ACACCTTCAG ACACAGCGTG GTGGTGCCCT ACGAGCCCCC TGAAGTGGGC
 361  AGCGACTGTA CCACCATCCA CTACAACTAC ATGTGCAACA GCAGCTGCAT GGGCGGCATG
 421  AACTGGCGGC CCATCCTGAC CATCATCACC CTGGAAGATA GCAGCGGCAA CCTGCTGGGC
 481  AGAAACAGCT TCGAAGTGCG CGTGTGCGCC TGCCCTGGCA GAGACAGAAG AACCGAGGAA
 541  GAGAACGGCA GCGGCTCCGG CAGCATGACA GAGTACAAGC TGGTGGTCGT GGGCGCTGTG
 601  GGCGTGGGAA AGTCTGCCCT GACAATCCAG CTGATCCAGA ACCACTTCGT GGACGAGTAC
 661  GACCCCACCA TCGAGGACAG CTACAGAAAA CAGGTCGTGA TCGACGGCGA GACATGCCTG
 721  CTGGACATCC TGGATACAGC CGGCCAGGAA GAGTACAGCG CCATGAGGGA CCAGTACATG
 781  AGAACCGGCG AGGGCTTTCT GTGCGTGTTC GCCATCAACA ACACCAAGAG CTTCGAGGAC
 841  ATCCACCACT ACCGCGAGCA GATCAAGAGA GTGAAGGACA GCGAGGACGT GCCCATGGTG
 901  CTCGTGGGAA ACAAGTGCGA CCTGCCTAGC AGAACCGTGG ACACCAAGCA GGCCCAGGAC
 961  CTGGCCAGAA GCTACGGCAT CCCCTTCATC GAGACAAGCG CCAAGACCAG ACAGTACCCC
1021  TACGACGTGC CCGACTACGC CTGA
```

Red = mutated codons
Green = Linker
Blue = p53 and Kras backbone sequences
Purple = HA tag
**aca atg** = Koazk consensus sequence with start codon
**tga** = Stop codon

## 7.2. Vector charts

**pDONOR Gateway vector chart**

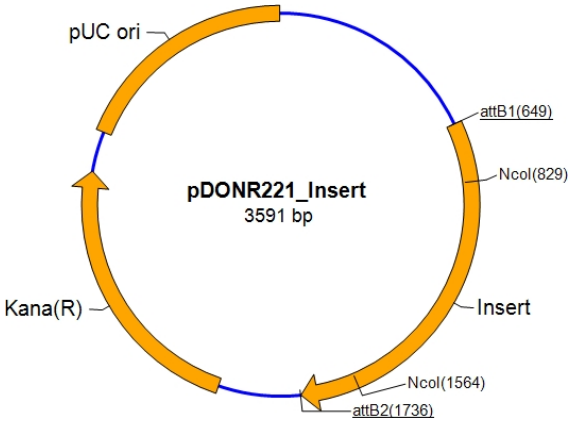


**pDEST-N-eGFP Gateway vector chart**

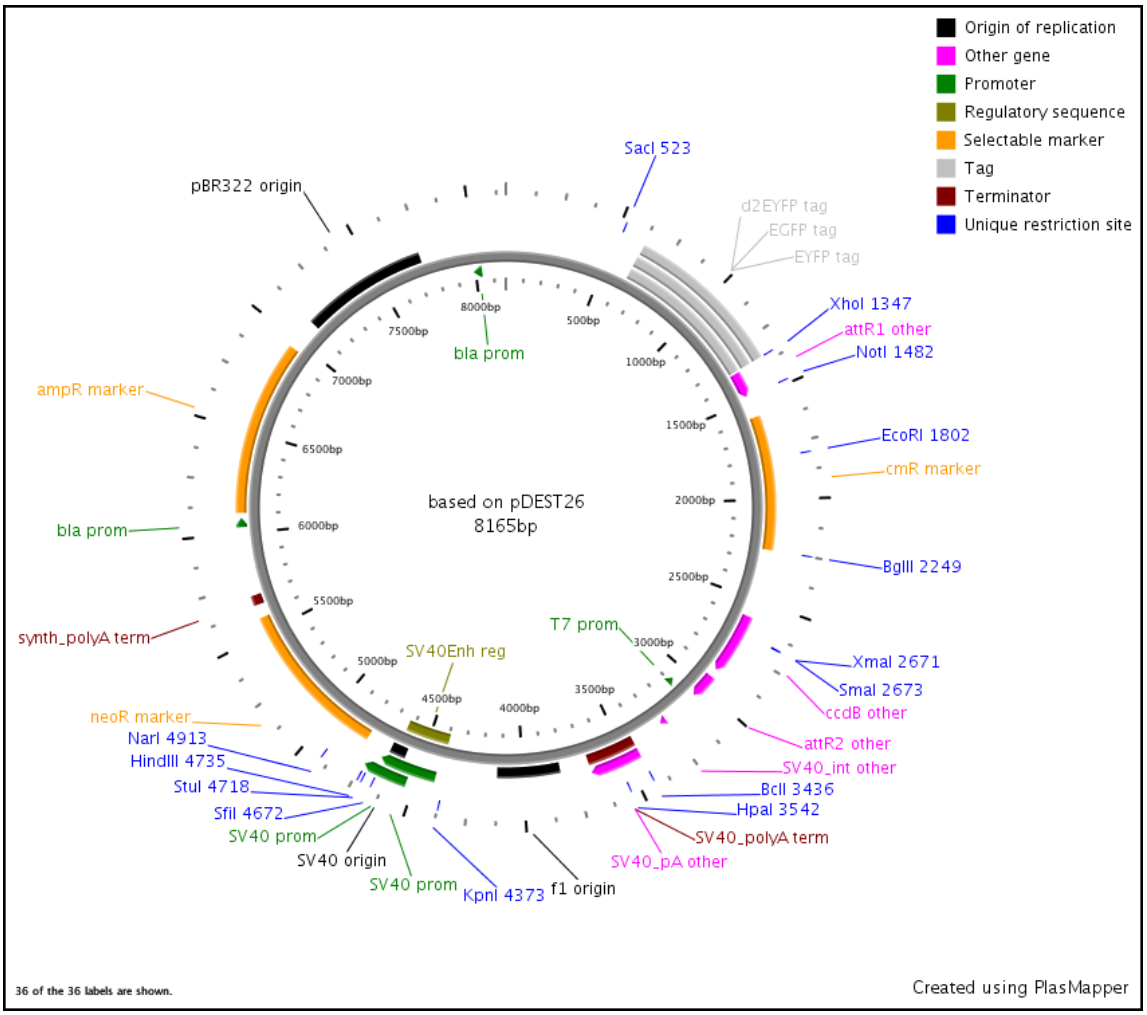
Origin of replication
Other gene
Promoter
Regulatory sequence
Selectable marker
Tag
Terminator
Unique restriction site
based on pDEST26
8165bp
SacI 523
d2EYFP tag
EGFP tag
EYFP tag
XhoI 1347
attR1 other
NotI 1482
EcoRI 1802
cmR marker
BglII 2249
XmaI 2671
SmaI 2673
ccdB other
attR2 other
SV40_int other
BclI 3436
HpaI 3542
SV40_polyA term
SV40_pA other
f1 origin
KpnI 4373
SV40 prom
SV40 origin
SV40 prom
SfiI 4672
StuI 4718
HindIII 4735
NarI 4913
neoR marker
synth_polyA term
bla prom
ampR marker
pBR322 origin
bla prom
SV40Enh reg
T7 prom
500bp
1000bp
1500bp
2000bp
2500bp
3000bp
3500bp
4000bp
4500bp
5000bp
5500bp
6000bp
6500bp
7000bp
7500bp
8000bp
36 of the 36 labels are shown.
Created using PlasMapper